UNIVERSITAT DE BARCELONA

Nueva generación de biomarcadores epigenéticos y transcriptómicos en el cáncer de tiroides bien diferenciado

Raquel Buj Gómez

Nueva generación de biomarcadores epigenéticos y transcriptómicos en el cáncer de tiroides bien diferenciado

Memoria presentada por

Raquel Buj Gómez

Para optar al título de

Doctora por la Universitat de Barcelona

Programa de doctorado en Genética, Departamento de Genética, Microbiología y Estadística

Tesis realizada bajo la dirección de la Dra. Mireia Jordà Ramos y el Dr. Miguel A. Peinado Morales en el Programa de Medicina Predictiva y Personalizada del Cáncer (PMPPC) del Instituto Germans Trias i Pujol (IGTP)

Directora	Director	Tutor	Doctoranda
Dra. Mireia Jordà Ramos	Dr. Miguel A. Peinado Morales	Dr. Bru Cormand Rifà	Raquel Buj Gómez

Barcelona, diciembre 2016

Esta tesis doctoral ha sido realizada en el laboratorio de mecanismos epigenéticos del cáncer y de la diferenciación celular (Dr. Miguel A. Peinado Morales) y en el laboratorio de tumores endocrinos (Dra. Mireia Jordà Ramos), ambos incluidos dentro del Programa de Medicina Predictiva y Personalizada del Cáncer (PMPPC) del Instituto Germans Trias i Pujol (IGTP). Este trabajo ha sido posible gracias a la beca predoctoral para la Formación de Personal Investigador (FPI) del Ministerio de Economía y Competitividad de España (BES-2012-055368), los proyectos FIS PI14/00308, del Instituto de Salud Carlos III cofinanciado por FEDER *una manera de hacer Europa*, Fundación Olga Torres (FOT), SAF2011-23638 y SAF2015-64251-R.

Dicen que un poco de conocimiento es peligroso,
pero no tanto como mucha ignorancia.

Terry Pratchett (Ritos iguales, 1987)

A Fran

A Ana

A mis padres

Agradecimientos

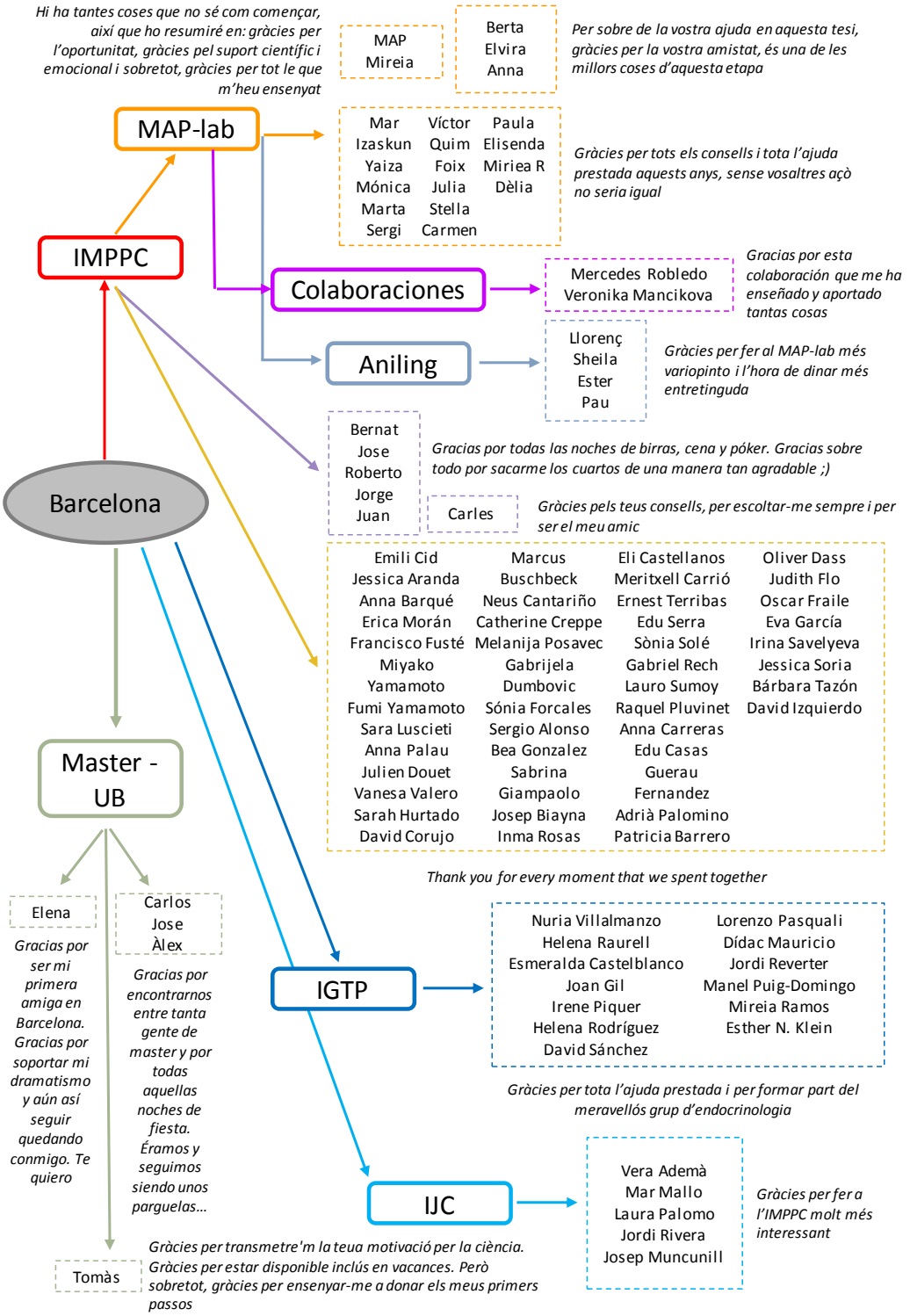

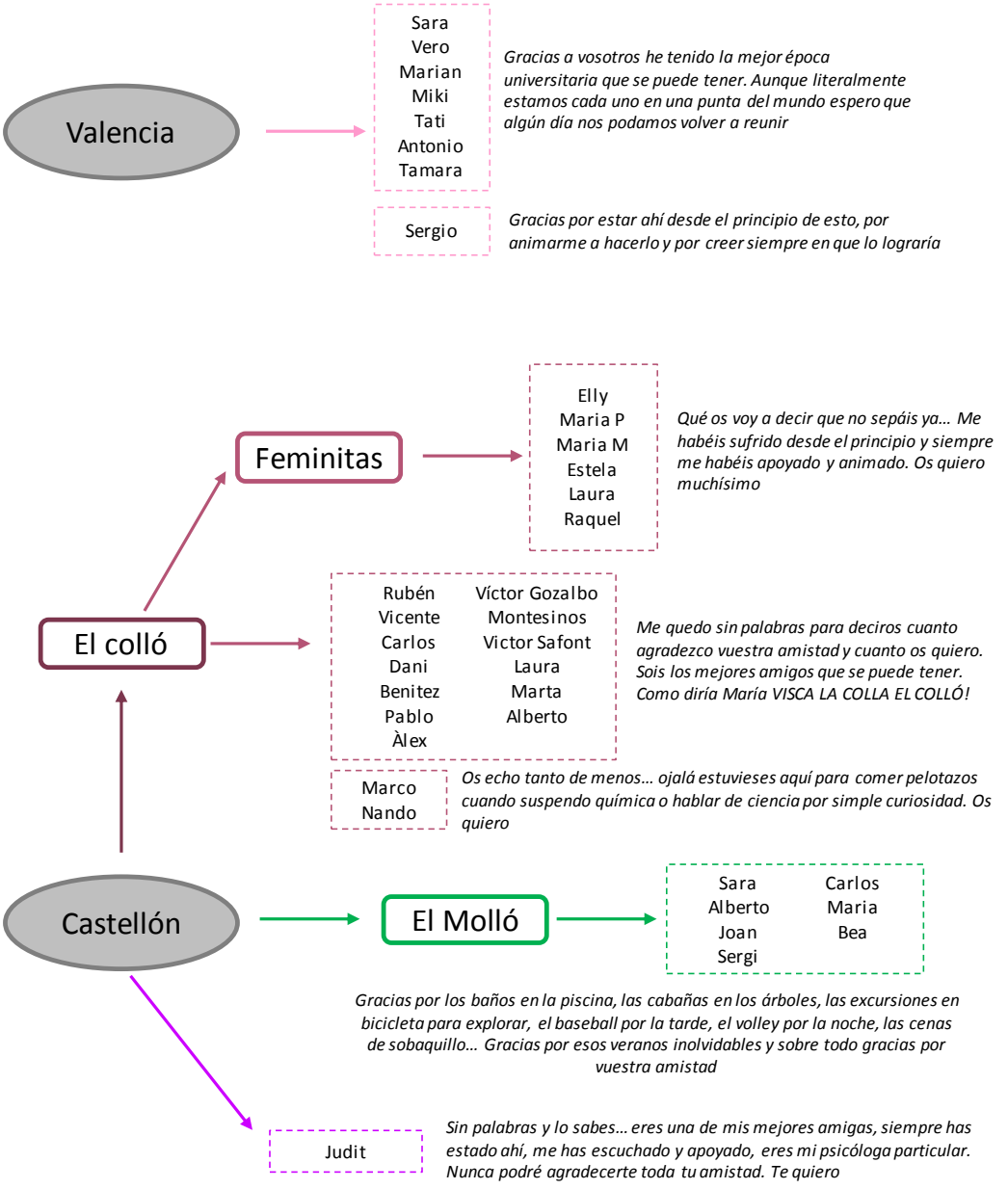
Valencia
Sara
Vero
Marian
Miki
Tati
Antonio
Tamara
Gracias a vosotros he tenido la mejor época universitaria que se puede tener. Aunque literalmente estamos cada uno en una punta del mundo espero que algún día nos podamos volver a reunir
Sergio
Gracias por estar ahí desde el principio de esto, por animarme a hacerlo y por creer siempre en que lo lograría
Feminitas
Elly
Maria P
Maria M
Estela
Laura
Raquel
Qué os voy a decir que no sepáis ya… Me habéis sufrido desde el principio y siempre me habéis apoyado y animado. Os quiero muchísimo
El colló
Rubén
Vicente
Carlos
Dani
Benitez
Pablo
Àlex
Víctor Gozalbo
Montesinos
Victor Safont
Laura
Marta
Alberto
Me quedo sin palabras para deciros cuanto agradezco vuestra amistad y cuanto os quiero. Sois los mejores amigos que se puede tener. Como diría María VISCA LA COLLA EL COLLÓ!
Marco
Nando
Os echo tanto de menos… ojalá estuvieses aquí para comer pelotazos cuando suspendo química o hablar de ciencia por simple curiosidad. Os quiero
Castellón
El Molló
Sara
Alberto
Joan
Sergi
Carlos
Maria
Bea
Gracias por los baños en la piscina, las cabañas en los árboles, las excursiones en bicicleta para explorar, el baseball por la tarde, el volley por la noche, las cenas de sobaquillo… Gracias por esos veranos inolvidables y sobre todo gracias por vuestra amistad
Judit
Sin palabras y lo sabes… eres una de mis mejores amigas, siempre has estado ahí, me has escuchado y apoyado, eres mi psicóloga particular. Nunca podré agradecerte toda tu amistad. Te quiero

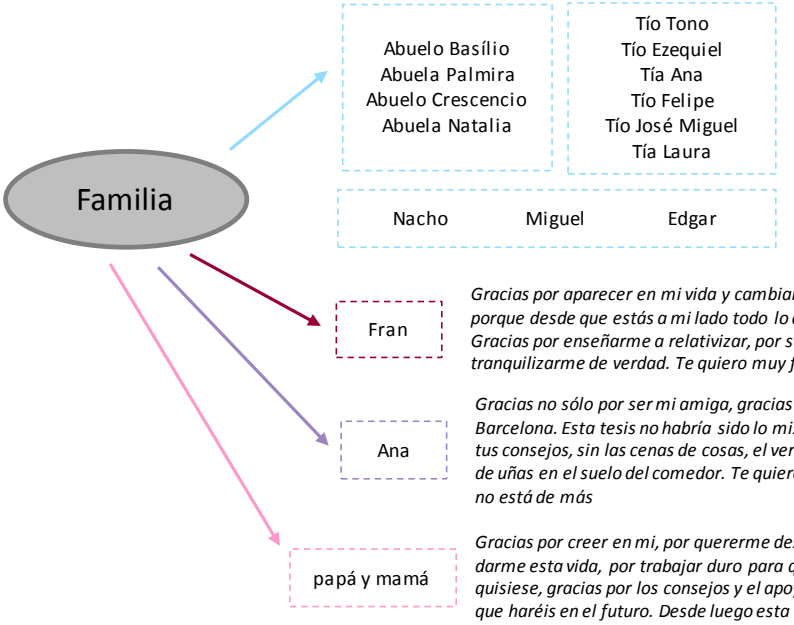

Gracias por animarme y apoyarme desde que nací. Estoy muy orgullosa de tener una familia como la nuestra. Os quiero a todos

Gracias por aparecer en mi vida y cambiarla por completo, gracias porque desde que estás a mi lado todo lo demás no es tan importante. Gracias por enseñarme a relativizar, por ser la única persona capaz de tranquilizarme de verdad. Te quiero muy fuerte

Gracias no sólo por ser mi amiga, gracias por ser mi familia en Barcelona. Esta tesis no habría sido lo mismo sin ti en casa, sin tu apoyo, tus consejos, sin las cenas de cosas, el vermut en la Barceloneta y la laca de uñas en el suelo del comedor. Te quiero mucho, se que lo sabes pero no está de más

Gracias por creer en mi, por quererme desde que nací, gracias por darme esta vida, por trabajar duro para que yo pudiese hacer lo que quisiese, gracias por los consejos y el apoyo. Gracias también por todo lo que haréis en el futuro. Desde luego esta tesis no habría sido posible sin vosotros. Os quiero mucho.

índice

Lista de abreviaturas

Abreviatura	*En inglés*	En Español
ASCO	American Society of Clinical Oncology	Sociedad americana de oncología clínica
ATA	American Thyroid Association	Asociación americana de tiroides
ATC	Anaplastic Thyroid Carcinoma	Carcinoma anaplásico de tiroides
AUS	Atypia of Undetermined Significance	Atipia de significado indeterminado
BRU	BRAF / RAS Unlike tumors	Tumores no similares a BRAF- o RAS-*like*
DNA:	*Deoxyriboucleic Acid*	Ácido desoxirribonucleico
cDMRs	*Cancer-specific Differentially DNA-Methylated Regions*	Regiones metiladas diferencialmente específicas de cáncer
CpG	*Cytosine-Guanine dinucleotide*	Dinucleótido citosina-guanina
CGI	*Cytosine-Guanine dinucleotide Island*	Isla citosina-guanina
CT	*Computed Tomography*	Tomografía computarizada
DIT	*3,5- Diiodotyrosine*	3,5-Diyodotirosina
ENCODE	*Encyclopedia of DNA Elements*	Enciclopedia de elementos del DNA
ELISA	*Enzyme-Linked Immunosorbent Assay*	Ensayo por inmunoabsorción ligado a enzimas
FFPE	*Formalin-Fixed, Paraffin-Embedded*	Fijado con formol y embebidos en parafina
FLUS	*Follicular Lesion of Undetermined Significance*	Lesión folicular de significado indeterminado
FN	*Follicular Neoplasm*	Neoplasia folicular
FNAB	*Fine-Needle Aspiration Biopsy*	Biopsia por punción con aguja fina
FTA	*Follicular Thyroid Adenoma*	Adenoma folicular tiroideo
FTC	*Follicular Thyroid Carcinoma*	Carcinoma folicular tiroideo
FVPTC	*Follicular Variant of Papillary Thyroid Carcinoma*	Variante folicular del carcinoma papilar de tiroides
GDP	*Guanosine Diphosphate*	Guanosín difosfato
GTP	*Guanosine Triphosphate*	Guanosín trifosfato
GWAS	*Genome-Wide Association Study*	Estudios de asociación del genoma completo
H3K27ac	*Acethylation of lysine 27 of histone H3*	Acetilación de la lisina 27 de la histona H3
H3K4ac	*Acethylation of lysine 4 of histone H3*	Acetilación de la lisina 27 de la histona H3
H3K27me3	*Trimethylation of lysine 27 of histone H3*	Trimetilación de la lisina 27 de la histona H3
H3K36me3	*Trimethylation of lysine 36 of histone H3*	Trimetilación de la lisina 36 de la histona H3

Abreviatura	*En inglés*	En Español
H3K4me1	*Monomethylation of lysine 4 of histone H3*	Monometilación de la lisina 4 de la histona H3
H3K4me2	*Dimethylation of lysine 4 of histone H3*	Dimetilación de la lisina 4 de la histona H3
H3K4me3	*Trimethylation of lysine 4 of histone H3*	Trimetilación de la lisina 4 de la histona H3
H3K9me3	*Trimethylation of lysine 4 of histone H3*	Trimetilación de la lisina 9 de la histona H3
HCC	*Hürthle Cell Carcinoma*	Carcinoma de la célula de Hürthle
HDAC	*Histone Deacetylase*	Histona deacetilasa
HPLC	*High Performance Liquid Chromatography*	Cromatografía líquida de alta eficacia
KLK	*Human tissue Kallikrein family*	Familia de las calicreínas tisulares humanas
LINE	*Long-Interpresed Nucleolar Elements*	Elementos dispersos largos
lncRNA	*Long non-coding Ribonucleic Acid*	Ácido ribonucleico no codificante largo
LOH	*Loss Of Heterozygosity*	Pérdida de heterozigosidad
LREA	*Long-Range Epigenetic Activation*	Activación epigenética a larga distancia
LTR	*Long Terminal-Repeats*	Repeticiones terminales largas
MAPK	*Mitogen-Activated Protein Kinases*	Proteínas cinasas activadas por mitógeno
MEN 1	*Multiple Endocrine Neoplasia type 1*	Neoplasia endocrina múltiple tipo 1
MEN 2	*Multiple Endocrine Neoplasia type 2*	Neoplasia endocrina múltiple tipo 2
miRNA	*micro Ribonucleic Acid*	Micro ácido ribonucleico
MIT	*3-Monoiodotyrosine*	3-nonoyodotirosina
MNasa	*Micrococcal nuclease*	Nucleasa micrócica
mRNA	*Messenger Ribonucleic Acid*	Ácido ribonucleico mensajero
MTC	*Medullary Thyroid Carcinoma*	Cáncer medular de tiroides
NADPH	*Nicotinamide Adenine Dinucleotide Phosphate*	Nicotinamida adenina dinucleótido fosfato
NGS	*Next Generation Sequencing*	Secuenciación de segunda generación
NT	*Normal Tissue*	Tejido normal
OMS	*World Health Organization*	Organización Mundial de la Salud
PET	*Positron Emission Tomography*	Tomografía por emisión de positrones
PDS	*Pendred Syndrome*	Síndrome de Pendred
PDTC	*Poorly Differentiated Thyroid Carcinoma*	Carcinoma de tiroides pobremente diferenciado
PI3K-AKT	*Phosphoinositide 3-Kinase / protein kinase B*	Fosfoinositol 3-cinasa / proteína cinasa B

Abreviatura	*En inglés*	En Español
PMC	*Papillary Microcarcinoma*	Microcarcinoma papilar
PPFP	*Rearrangement PAX8/PPARγ*	Reordenamiento PAX8/PPARγ
PSA	*Prostate Specific Antigen*	Antígeno prostático específico
PTC	*Papillary Thyroid Carcinoma*	Carcinoma papilar tiroideo
PUMA	*Percentage of Unmethylated Alu elements*	Porcentaje de elementos *Alu* no metilados
QUAlu	*Quantification of Unmethylated Alu elements*	Cuantificación de elementos *Alu* no metilados
RAI	*Radioactive Iodine*	Yodo radioactivo
RAI-R-WDTC	*Radioiodine Refractory Well Differentiated Thyroid Carcinoma*	Carcinoma de tiroides bien diferenciado refractario al tratamiento con yodo radioactivo
RefSeq.	*Reference Sequence database*	Base de datos de secuencias de referencia
RNA	*Ribonucleic Acid*	Ácido ribonucleico
ROC	*Receiver Operating Characteristic*	Característica Operativa del Receptor
SAM	*S-Adenosyl-L-Methionine*	S-adenosil-L-metionina
SCNA	*Somatic Copy Number Alterations*	Alteraciones del número de copias
SEEN	*Spanish Society of Endocrinology and Nutrition*	Sociedad Española de Endocrinología y Nutrición
SEER	*Surveillance, Epidemiology, and End Results*	Programa de vigilancia, epidemiología y resultados finales
SFN	*Suspicious for Follicular Neoplasm*	Lesión sospechosa de neoplasia folicular
SINE	*Short Interspersed-Nuclear Elements*	Elementos dispersos cortos
SM	*Suspicious of Malignancy*	Lesión sospechosa de malignidad
T3	*Triiodothyronine*	Triyodotironina
T3r	*Triiodothyronine reverse*	Triyodotironina reversa
T4	*Tetraiodothyronine (thyroxine)*	Tetrayodotironina (tiroxina)
TCGA	*The Cancer Genome Atlas*	Atlas genómico del cáncer
TNM	*Tumor, Node, Methastasis*	Tumor, Nódulo, Metástasis
TSA	*Trichostatin A*	Tricostatina A
TSS	*Transcription Start Sites*	Sitios de inicio de la transcripción
TTF	*Thyroid Transcription Factor*	Factor de transcripción tiroideo
WDTC	*Well-Differentiated Thyroid Carcinoma*	Carcinoma de tiroides bien diferenciado

Lista de anglicismos

Anglicismo	Traducción y definición.
Beads-on-a-string	Fibra de 10 nm formada como consecuencia del enrollamiento del DNA alrededor de las histonas. Recibe este nombre debido a que en las microfotografías electrónicas, la cromatina desplegada tienen apariencia de cuentas de un collar en la que cada cuenta es un nucleosoma y el hilo del collar es el DNA de unión.
Branch-type evolution	Evolución ramificada. Escisión de una reserva génica en dos o más reservas separadas que darán lugar a dos genomas tumorales diferentes que a su vez pueden volver a escindirse.
Cancer hallmark	Huella distintiva del cáncer. Conjunto de alteraciones propias de las células cancerosas.
CGI shore	Orillas CGI. Regiones del DNA que se extienden 2 Kb a ambos lados de la isla CpG.
Dark matter cases	Casos opacos. En el estudio de PTCs del TCGA, casos en los que se desconoce el factor oncogénico iniciador del tumor.
Driver mutation	Mutación conductora. Mutación causativamente implicada en la aparición de un tumor. Aquella que da una ventaja selectiva a un clon en su microambiente ya sea a través de un aumento de su supervivencia o de su reproducción.
Enhancer	Intensificador génico. Secuencia de DNA a la que se pueden unir factores de transcripción que aumentan la expresión de un gen o grupo de genes localizados, incluso, a varias kilobases de distancia.
Gene Imprinting	Impronta génica. Fenómeno epigenético por el cual ciertos genes se expresan de manera diferencial de acuerdo al origen parental.
Genome-wide analysis	Análisis del genoma completo. Término que se utiliza para referirse a todos aquellos estudios en los que se analiza alguna característica molecular simultáneamente sobre todo el genoma.
Insulator	Aislante. Secuencia genética que establece una frontera entre dos zonas genómicas.
Knudson's two-hit hypothesis	Hipótesis de dos eventos de Knudson. Hipótesis según la cual para que tenga lugar el desarrollo de un tumor es necesario que los dos alelos de un gen conductor sufran alguna alteración genética y/o epigenética.
Machine learning	Aprendizaje automático. Creación de programas capaces de generar comportamientos a partir de una información no estructurada suministrada en forma de ejemplos.
Passenger mutation	Mutación pasajera. Aquella que no interviene activamente en la formación de un tumor. No tienen efecto sobre la capacidad proliferativa o de supervivencia de un clon, pero puede estar asociada a la expansión del mismo.
Splicing	Empalme. Proceso de maduración del RNA en el que se eliminan los intrones y se ensamblan los exones.

Índice de figuras

Figuras de la introducción

Figuras del trabajo I

Figuras del trabajo II

Figuras del trabajo III

Figuras de la discusión

Índice de tablas

Tablas de la introducción

Tablas del trabajo I

Tablas del trabajo II

Tablas del trabajo III

Introducción

1. Del genotipo al fenotipo a través del epigenotipo

A mediados del siglo XIX, Gregor J. Mendel estableció, gracias a sus estudios con la planta del guisante, tres principios conocidos como las *leyes de la herencia de Mendel* (Mendel, 1865). Estos trabajos fueron los primeros en los que se puso de manifiesto el genotipo subyacente bajo los rasgos observados en un organismo (Bowler, 2003). Unos años después, Walther Flemming proponía el término «cromatina» para referirse a aquella estructura nuclear de naturaleza refractante y teñida con colorantes basófilos; mientras que Albrecht Kossel descubría la presencia de las proteínas histonas en el núcleo celular (Olins and Olins, 2003).

Sin embargo, no fue hasta el 25 de abril de 1953 cuando la revista *Nature* publica una serie de tres artículos firmados por James Watson y Francis Crick (Watson and Crick, 1953), Maurice Wilkins *et al.* (Wilkins et al., 1953) y Rosalind Franklin y Raymond Gosling (Franklin and Gosling, 1953), que se detalla la estructura en doble hélice del DNA (*Deoxyribonucleic Acid*). Es en este momento cuando surgió la idea de que la secuencia de DNA, residente en el núcleo y empaquetada en la cromatina, es el vehículo de la información genética de cada una de las células de un organismo. Cinco años después, el mismo Crick proponía el *dogma central de la biología molecular* en el que se establecía, por primera vez, un modelo de síntesis de proteínas a partir del DNA (Crick, 1958).

Así pues, el **genotipo**, se refiere a la información genética, almacenada en la molécula de DNA y empaquetada en la cromatina, que posee un organismo en particular y que pude transmitir a su descendencia (Figura I1). En un sentido más estricto, se refiere al conjunto de alelos o variantes de un gen que porta un organismo y que se transcribirán a moléculas de RNA (*Ribonucleic Acid*) y estas a su vez, se traducirán a proteínas, que conferirán al organismo unas características morfológicas, fisiológicas y de comportamiento determinadas (**fenotipo**).

Sin embargo, hoy en día sabemos que el subconjunto final de proteínas que expresa una célula y que darán lugar a su fenotipo, no solo dependen de la secuencia de DNA, sino que existe una compleja red de regulación que actúa a todos los niveles: transcripcional, postranscripcional y postraduccional. Entre los actores que participan en la regulación transcripcional encontramos factores de transcripción, intensificadores (*enhancers*) génicos y mecanismos epigenéticos. Por otro lado, la regulación postranscripcional comprende procesos tales como el empalme (*splicing*) alternativo, la poliadenilación alternativa o la regulación por micro RNAs (miRNAs). Finalmente, la

adición de grupos químicos a los residuos aminoacídicos de las proteínas (fosforilación, metilación, glicosilación, etc.) o la adición de pequeñas proteínas (ubiquitinización y sumoilación) se consideran modificaciones postraduccionales.

Por ser uno de los temas centrales de esta tesis, a continuación, pasaremos a describir los aspectos más importantes de la regulación génica a nivel epigenético.

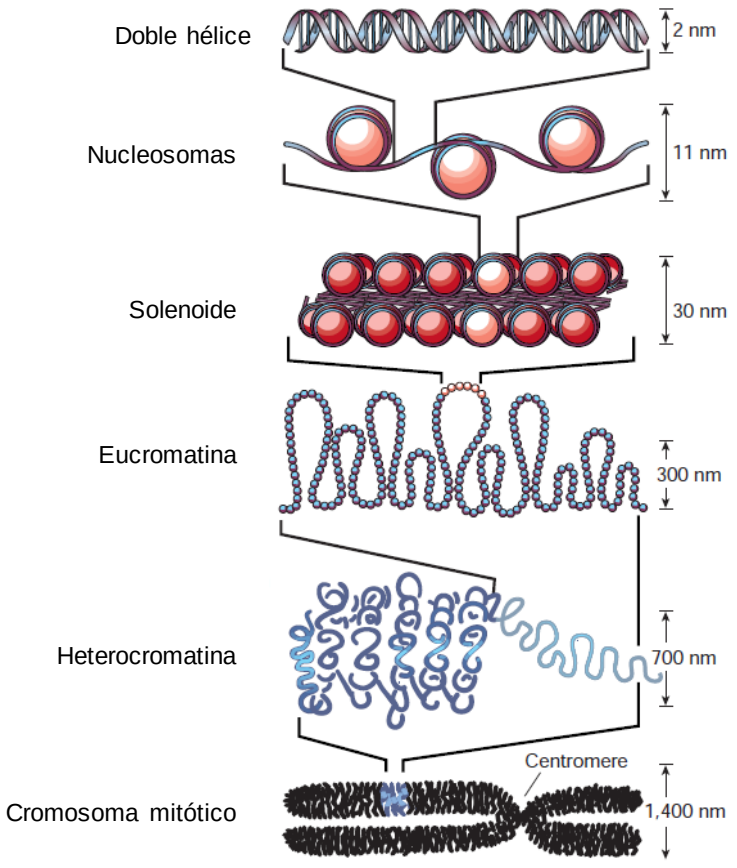

Figura I1 | Compactación del DNA. La acomodación de la doble hélice de DNA (2 m de longitud) dentro del núcleo celular (5-10 µm) involucra a una serie de proteínas que ayudan al DNA a plegarse de manera secuencial, resultando en una estructura altamente organizada llamada cromatina. Típicamente, los nucleosomas (unidades funcionales de la cromatina), están espaciados por unos ~200 bp de DNA. No obstante, el posicionamiento es dinámico no solo entre tipos y momentos celulares sino también a lo largo de una misma molécula de DNA (Schones et al., 2008). La unión de los nucleosomas entre sí gracias a la histona H1 forma la fibra de 10 nm también llamada "cuentas de collar" (*beads-on-a-string)* (Locklear et al., 1990). El siguiente nivel estructural lleva a la formación de la fibra de 30 nm o solenoide. Aunque se han propuesto diferentes modelos estructurales, se desconoce la organización exacta e incluso algunos autores cuestionan su existencia (Fussner et al., 2011; Razin and Gavrilov, 2014). Estas fibras, forman una amplia variedad de estructuras más complejas cuya naturaleza está sujeta a un intenso debate (Grigoryev and Woodcock, 2012). Normalmente, en la mayor parte de las células de mamíferos, la cromatina altamente compactada o heterocromatina se localiza hacia la periferia, mientras que la más relajada o eucromatina se localiza hacia el interior (de Nooijer et al., 2009). Figura extraída de (Felsenfeld and Groudiner, 2003).

1.1. Epigenética

En principio, y a excepción de los gametos, todas las células de un organismo multicelular comparten un mismo genotipo. No obstante, presentan un amplio abanico morfológico y funcional derivado de una expresión génica diferencial. Por lo tanto, la identidad de una célula individual no sólo depende de su componente genético, sino también, de la interpretación del mismo. Esta ciencia que constituye el puente entre el genotipo y el fenotipo, siendo capaz de alterar el resultado final del genoma sin cambiar la secuencia subyacente de DNA se conoce como **epigenética**.

El concepto de epigenética (del griego *epi*, *en* o *sobre*, y –genética) fue establecido en 1942 por Conrad H. Waddington (Waddington, 1942) quien la definió como la rama de la biología que estudia las interacciones causales entre los genes y sus productos que dan lugar al fenotipo (Goldberg et al., 2007; Waddington, 2012). Hoy en día se entiende como el estudio de los cambios heredables en la expresión génica que ocurren de manera independiente a los cambios en la secuencia de DNA (Sharma et al., 2010).

Estos cambios se regulan por modificaciones químicas del DNA y de las proteínas asociadas. En conjunto se conocen como **mecanismos epigenéticos** e incluyen: la metilación del DNA, las modificaciones de las colas de las histonas, la incorporación de variantes de histonas y el posicionamiento de nucleosomas (Sharma et al., 2010). Se denomina **epigenoma o epigenotipo** al conjunto de todas las modificaciones epigenéticas de una célula que en última instancia determinan y mantienen la arquitectura global y local de la cromatina en cada célula individual, permitiendo la expresión de un subconjunto específico de genes (Suzuki and Bird, 2008). Dado su papel de regulador estructural y de la expresión génica, no es de extrañar que distorsiones del epigenoma se hayan demostrado asociadas a diversas enfermedades entre las que se encuentra el cáncer (Jones and Baylin, 2002; Sandoval and Esteller, 2012).

1.2. Mecanismos epigenéticos

1.2.1. Metilación del DNA

La **metilación del DNA** es, con toda seguridad, la modificación epigenética más estudiada. Si bien se tenía constancia previa de la existencia de un quinto nucleótido diferente de los previamente descritos por Phoebus Levene (Levene and London, 1905), no fue hasta 1948 cuando Rollin Hotchkiss consigue aislar la 5-metilcitosina (él la llamó epicitosina) a partir de una cromatografía en papel de ácidos nucleicos de timo de ternera (Hotchkiss, 1948). Sin embargo, hubo que esperar casi tres décadas para ver los primeros

estudios que demostraban el papel de la metilación del DNA en la regulación de la expresión génica (Compere and Palmiter, 1981; Holliday and Pugh, 1975). Además, hoy en día sabemos que este mecanismo epigenético está involucrado en el mantenimiento de la conformación e integridad de los cromosomas, así como en la defensa del genoma frente al daño potencial que puedan causar los elementos móviles del genoma conocidos con el nombre de transposones (Bestor, 1998; Herceg and Vaissière, 2011; O'Neill et al., 1998).

La metilación del DNA consiste en la adición covalente de un grupo metilo (-CH_3) al carbono 5 del anillo pirimidínico de la citosina (Figura I2), siendo este, el proceso de metilación del DNA mayoritario descubierto en eucariotas (Jeltsch, 2002). Más concretamente, hoy en día sabemos que en mamíferos, la 5-metilcitosina tienen lugar casi exclusivamente en el contexto del dinucleótido citosina-guanina (CpG) y de manera simétrica en ambas hebras (Marx, 2012). Empero, y aunque la metilación fuera de CpGs es muy poco frecuente en células somáticas (0.02%), se ha encontrado como un fenómeno relativamente común tanto en células pluripotentes como en neuronas (25%) (He and Ecker, 2015).

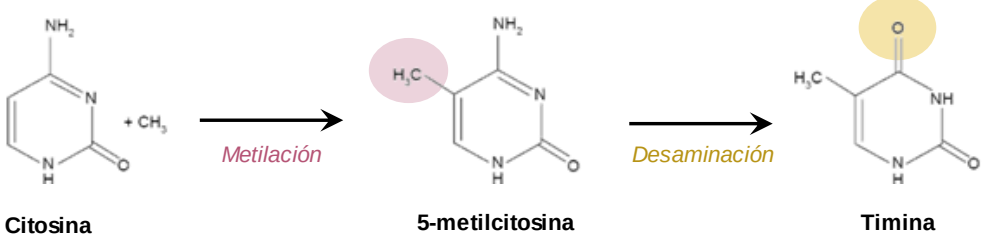

Figura I2 | Metilación de citosinas y desaminación de 5-metilcitosinas. La metilación de citosinas mediante la adición de un grupo metilo (-CH3) al carbono 5 del anillo pirimidínico da lugar a la 5-metilcitosina y esta, por desaminación del carbono 4, da lugar al nucleótido timina. Figura modificada de (Osamor et al., 2016).

Cabe destacar que las CpGs son puntos calientes de mutaciones puntuales debido a la relativamente alta propensión de la 5-metilcitosina a desaminarse mutando a timina tanto en células somáticas como en la línea germinal (Figura I2) (Bestor et al., 1993). Esto hace que la proporción de CpGs en el genoma esté por debajo de lo esperado (Bird, 1980). De hecho, el contenido GC del genoma humano es del 42%, por lo tanto, la probabilidad esperada de encontrar un dinucleótido CpG debería ser del 4.41% (0.21 G x 0.21 C = 0.0441). En cambio, la frecuencia observada es del 1% (~28 millones de CpGs) de las que el 60-80% están permanentemente metiladas (Duret and Galtier, 2000;

Saxonov et al., 2005; Suzuki and Bird, 2008). Así mismo, su distribución no es homogénea, sino que existen zonas ricas en CpGs entre las que encontramos islas CpG (CGI) y elementos repetitivos transponibles como las repeticiones terminales largas (*Long Terminal Repeats*, LTRs), los elementos dispersos largos (*Long Interspersed Nuclear Elements*, LINEs) o elementos dispersos cortos (*Short Interspersed Nuclear Elements*, SINEs) (Figura I3a).

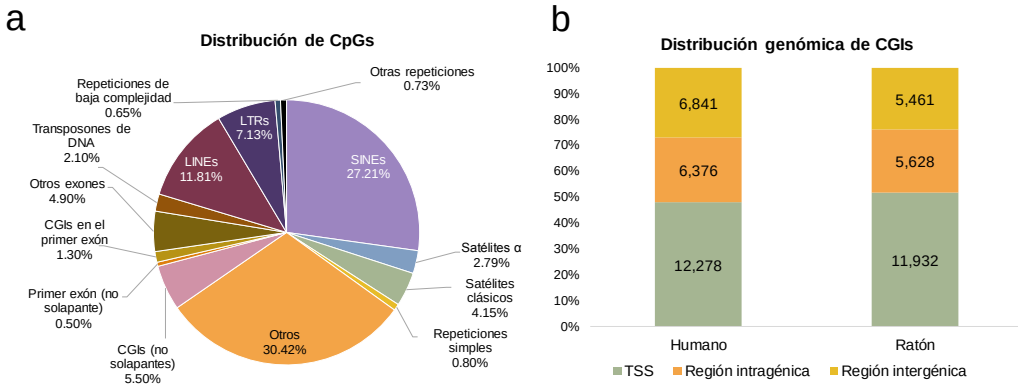

Figura I3 | Porcentaje de CpGs por compartimento genómico y distribución de islas CpG (CGIs). (a) El contenido en CpGs por compartimento genómico en humanos muestra elevados porcentajes de CpGs en elementos repetitivos transponibles. Figura modificada de (Rollins et al., 2006). **(b)** La distribución genómica de CGIs comparada entre humano y ratón pone de manifiesto la alta conservación en la distribución de CGIs por compartimento genómico. La categorización de las CGIs se ha realizado respecto a los genes anotados en RefSeq. Figura modificada de (Deaton and Bird, 2011).

Las CGIs fueron identificadas por primera vez gracias a digestiones del DNA genómico de varios vertebrados con el enzima *Hpa*II, el cual es capaz de reconocer y digerir sitios C/CGG no metilados; se dice pues, que es un enzima sensible a metilación. En estas digestiones, se observó que se generaba una población de pequeños fragmentos de DNA que procedían de grupos de CpGs no metiladas, y que, en su conjunto, constituían aproximadamente el 1% del genoma de mamífero (Bird et al., 1985; Cooper, 1983).

Aunque la definición de CGI ha ido variando a lo largo de las últimas décadas, se pueden definir como aquellas regiones del genoma de entre 200 bp y 3,000 bp (1,000 bp de media) en las que el porcentaje de CpGs supera el 50% y el promedio entre CpGs observadas y esperadas es mayor al 0.6 (Deaton and Bird, 2011). El elevado contenido en CpGs de las CGIs, se debe principalmente a su resistencia a la metilación, lo que impide la desanimación espontánea a la que están sometidas el resto de citosinas del genoma. Además, su distribución no es homogénea, sino que se localizan

preferentemente en la región promotora del 60-70% de los genes (Sharma et al., 2010; Suzuki and Bird, 2008). Los estudios de Illingworth *et al.* demostraron, no solo que el número de CGIs por genoma haploide entre humanos y ratones era muy similar (25,495 y 23,021, respectivamente), sino que la distribución entre diferentes localizaciones genómicas también estaba conservada (Figura I3b), lo que demostraba la importancia funcional de estas regiones (Illingworth et al., 2010).

Como se menciona en el parágrafo anterior, el ~70% de los promotores génicos se asocian a CGIs. Entre estos genes se incluyen casi todos los de expresión constitutiva, así como el ~50% de genes con expresión específica de tejido. También se sabe, que las CGIs asociadas a promotores, suelen caracterizarse por presentar un estado laxo y activo de la cromatina, principalmente debido al empobrecimiento en nucleosomas en la región y a las marcas de histona activa en las colas de las histonas de los nucleosomas colindantes (Jones, 2012). Estos dos hechos apuntan a que las CGIs podrían estar involucradas en la regulación de la transcripción génica. En contraposición, aproximadamente la mitad de las CGIs se encuentran en regiones intra- o intergénicas (Figura I3b). Estudios recientes han demostrado que estas CGIs, llamadas CGIs huérfanas poseen en su mayoría características de promotores funcionales; esto es, reclutan RNA polimerasa II, presentan marcas de histona asociadas a activación génica y/o poseen inicios de transcripción (*Transcription Start Sites,* TSS) activos en algún tejido (Illingworth et al., 2010; Maunakea et al., 2010).

Existen algunos casos en los que la metilación de CGIs ocurre de manera fisiológica. Así pues, la inactivación del cromosoma X y la impronta génica (*gene imprinting*) constituyen los ejemplos más clásicos de metilación normal de islas CpG durante el desarrollo (Bird, 2002). Así mismo, los análisis de metilación a escala genómica, han demostrado la existencia de patrones de metilación específicos de tejido, establecidos principalmente por CGIs no asociadas a promotores (Illingworth and Bird, 2009; Rakyan et al., 2008) y por las regiones colindantes a las CGIs asociadas a promotores, llamadas ***CGI shores*** (2 Kb a ambos lados de la CGI) (Irizarry et al., 2009; Sandoval and Esteller, 2012).

Como hemos comentado anteriormente el caso de las CGIs es único, ya que la mayoría de las CpGs del genoma humano se encuentran metiladas. Esto incluye también, a CpGs localizadas en genes, *enhancers* y aislantes (*insulators*). Se sabe que, así como la metilación del DNA en regiones promotoras reprime el inicio de la transcripción, esta parece ejercer un efecto sinérgico sobre la elongación cuando está presente en **regiones**

génicas (exones e intrones) (Aran et al., 2011; Hellman and Chess, 2007; Jones, 1999; Lister et al., 2009; Varley et al., 2013). Esto excluye al primer exón cuyo estado de metilación sí parece influir en el inicio de transcripción del mismo modo en que lo hace el del promotor (Brenet et al., 2011). Aunque el papel de la metilación de los genes (exones e intrones) permanece sin resolver, trabajos recientes han establecido un nexo de unión entre la metilación y el *splicing* alternativo a través de CTCF (*CCCTC-binding factor*), MECP2 (*methyl-CpG binding protein 2*) y HP1 (*heterochromatin protein 1*) (Maunakea et al., 2013; Piacentini et al., 2009; Shukla et al., 2011). Las dos primeras modulan la tasa de elongación de la RNA polimerasa II, mientras que HP1 recluta factores de *splicing* desde el DNA metilado hasta el mRNA (RNA mensajero) precursor (Lev Maor et al., 2015). Por otro lado, parece que la metilación del DNA también podría estar implicada en otros procesos como el uso de TSS alternativos (Cheong et al., 2006; Maunakea et al., 2010; Shmelkov et al., 2004), la regulación de RNAs no codificantes[1] (ncRNAs) como miRNAS o lncRNAs (*long non-coding RNAs*) (Lujambio et al., 2010; Lyle et al., 2000) o la regulación de *enhancers* embebidos en genes (Kulis et al., 2013).

Los ***enhancers*** se definen como regiones reguladoras que pueden aumentar la expresión de un gen asociado situado, incluso, a varias kilobases de distancia. Pese a que la mayoría de estas regiones son pobres en CpGs, se sabe que la metilación juega un papel importante en la unión de factores de transcripción que son, en última instancia, los que producen el efecto intensificador. Finalmente, sabemos que en el genoma existen ***insulators*****,** zonas limítrofes establecidas por la unión de diversas proteínas entre ellas CTCF. Debido a la sensibilidad de CTCF por la metilación, alteraciones del perfil de metilación del DNA pueden llevar a la pérdida o ganancia de CTCF lo que conlleva una pérdida de los límites estructurales normales (Jones, 2012).

1.2.2. Modificaciones postraduccionales de las histonas

Las **histonas** son proteínas estructurales que juegan un papel importante en la organización y función del DNA dentro del núcleo eucariótico. Permiten el empaquetamiento del DNA en los nucleosomas, unidad básica de la cromatina, con el objetivo de acomodarlo en el pequeño espacio nuclear. El nucleosoma está formado por un octámero de histonas, que contiene dos copias de cada histona H2A, H2B, H3 y H4, rodeado por DNA (Figura I4). Estas pequeñas proteínas de carga positiva coordinan los

[1] Los RNAs no codificantes (ncRNAs) son moléculas de RNA que no se traducen a proteínas, sino que su función está desempeñada por la propia molécula de RNA. Según su biogénesis, función y mecanismo, los ncRNAs se clasifican en diferentes familias (micro RNAs, RNAs no codificantes largos, piwi RNAs, etc.) que pueden estar codificados en locis diferentes a sus secuencias diana y funcionar a partir de una hibridación imperfecta de bases [revisado en (Zhou et al., 2010)].

cambios entre la heterocromatina, altamente compactada e inaccesible a la maquinaria transcripcional y la eucromatina, que por encontrarse menos compactada posibilita la unión de proteínas (principalmente factores de transcripción) que permiten y regulan la transcripción (Bannister and Kouzarides, 2011).

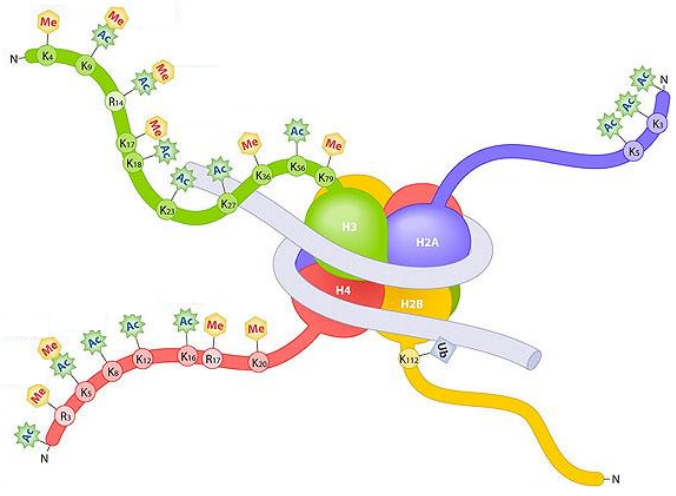

Figura I4 | Nucleosoma y modificaciones postraduccionales de las colas de las histonas. Metilación (Me), acetilación (Ac), ubiquitinación (Ub). Figura extraída de AMS Biotechnology (www.amsbio.com).

En su extremo C-terminal, las histonas tienen un dominio globular que forma parte del corazón del octámero, mientras que su parte N-terminal forma una cola que sobresale del nucleosoma y cuyos aminoácidos están sujetos a diversas **modificaciones postraduccionales** (acetilación, metilación, fosforilación, ubiquitinización, isomerización, sumorilación, ADP ribosilación y citrulinación). De todas ellas, las más comunes son la metilación y acetilación de los residuos de lisina de las histonas H3 y H4 (Strahl and Allis, 2000). La adición y eliminación de estas modificaciones está catalizada por un conjunto de enzimas modificadoras de las colas de las histonas (histona acetiltransferasas, deacetilasas, metiltransferasas, demetilasas, fosforilasas, etc.) que hacen de este un proceso dinámico y reversible (Falkenberg and Johnstone, 2014).

Si tenemos en cuenta que las colas de histonas cuentan con decenas de residuos susceptibles de ser modificados de diferentes maneras, que cada nucleosoma tiene ocho histonas y que aproximadamente cada 200 pb encontramos un nucleosoma, las posibles combinaciones a lo largo del genoma son innumerables. Sin embargo, hay ciertas modificaciones que tienden a localizarse juntas, mientras que otras raramente coinciden. Por ejemplo, las marcas activadoras H3K4me3 (trimetilación de la lisina 4 de la histona

H3) y H3K4ac (acetilación de la lisina 4 de la histona H3) y las marcas represoras H3K9me3 (trimetilación de la lisina 9 de la histona H3) y H3K27me3 (trimetilación de la lisina 27 de la histona H3) suelen colocalizar en regiones de cromatina activa o inactiva respectivamente (Kim et al., 2005; Nielsen et al., 2001; Noma K et al., 2001; Schübeler et al., 2004). De esta forma, mientras que H3K4me1 (monometilación de la lisina 4 de la histona H3) es una marca de *enhancers* activos, H3K4me2 (dimetilación de la lisina 4 de la histona H3) y H3K4me3 lo son de promotores activos. Así mismo, H3K27ac (acetilación de la lisina 27 de la histona H3), se ha encontrado tanto en *enhancers* como en promotores activos y H3K36me3 (trimetilación de la lisina 36 de la histona H3) está enriquecida en exones e intrones (Kolasinska-zwierz et al., 2009).

Por otro lado, y mientras que H3K27me3 es una señal que controla proteínas reguladoras del desarrollo y que suele encontrarse en regiones ricas en genes, H3K9me3 se encuentra en zonas con poca densidad génica actuando como una señal estable para la formación de heterocromatina en regiones cromosómicas con repeticiones en tándem (telómeros y regiones pericentroméricas) (Hon et al., 2009; Kouzarides, 2007). H3K9me3 y H3K27me3 constituyen las dos principales marcas de silenciamiento génico en mamíferos. Más aún, se sabe que la H3K9me3 trabaja conjuntamente con la metilación del DNA mientras que la H3K27me3 no (Sharma et al., 2010).

Todo esto llevó a pensar en la existencia de un código de histonas en el que la coexistencia de ciertas modificaciones podría predecir el estado o la susceptibilidad de algunos genes a ser expresados o reprimidos (Jenuwein and Allis, 2001). Además, ya que muchas de estas modificaciones se asocian a diferentes elementos funcionales del genoma, su presencia nos puede ayudar a mapear diferentes compartimentos genómicos como exones, intrones, TSS o *enhancers* entre otros (Heintzman et al., 2009).

1.2.3. Variantes de histona

Además de las modificaciones covalentes de las colas de las histonas, sabemos que existen algunas **variantes no alélicas de histonas**, capaces de sustituir a las canónicas asumiendo diferentes funciones en la célula (Maze et al., 2014). A diferencia de las canónicas (H2A, H2B, H3 y H4), que son sintetizadas y ensambladas en los nucleosomas únicamente durante la fase S de la replicación del DNA, las variantes de histona carecen de esta restricción pudiendo ser sintetizadas e incorporadas a los nucleosomas en cualquier momento del ciclo celular (Kamakaka and Biggins, 2005). Aunque altamente conservadas, estas variantes poseen diferentes características biofísicas capaces de alterar las propiedades de los nucleosomas portadores afectando

tanto a su estabilidad como al reclutamiento de complejos modificadores de la cromatina (Talbert and Henikoff, 2010; Weber and Henikoff, 2014).

1.2.4. Posicionamiento de nucleosomas

Como hemos mencionado anteriormente, el nucleosoma es la unidad básica y funcional de la cromatina. La definición incluye el término funcional, pues, modificaciones de sus proteínas constituyentes, afectan a la organización y estructura de la cromatina, que es justo donde radica su función principal. Por ello, no es de extrañar que la posición específica de estas unidades básicas afecte igualmente a la estructura de la cromatina, regulando la expresión génica a través de la modulación del acceso de los factores de transcripción a las secuencias reguladoras del DNA (Jiang and Pugh, 2009).

Los estudios de posicionamiento nucleosomal se iniciaron en los 80, a partir de la digestión de pequeños fragmentos de DNA (<1 Kb) con enzimas como la MNasa (*micrococcal nuclease*) y la DNasaI (Keene and Elgin, 1981; Wu, 1980). Hoy en día, gracias a la mejora de las enzimas y de los protocolos de digestión y al acople de las nuevas metodologías de secuenciación masiva y/o análisis por *microarrays* (Lieleg et al., 2015), se han obtenido mapas completos de varios organismos eucariotas. En los tejidos estudiados se ha observado, de manera generalizada, un posicionamiento muy preciso de los nucleosomas alrededor de los promotores génicos, mientras que la disposición tiende a ser más arbitraria en los genes. Además, su relación con la activación/represión de la transcripción es bastante clara en tanto que promotores activos o que necesitan activarse de manera rápida están libres de nucleosomas, mientras que promotores inactivos están obstruidos por estas unidades (Radman-Livaja and Rando, 2010).

2. El cáncer y su epigenoma

El **cáncer** se define como un conjunto de enfermedades caracterizadas por la transformación maligna de las células que proliferan de manera anormal e incontrolada (Real Academia Española, 2014). Actualmente concebimos el cáncer como un proceso evolutivo caracterizado por la acumulación de alteraciones genéticas y epigenéticas que llevan a la aparición y progresión tumoral así como a la adquisición de resistencias frente al tratamiento (Toyota and Suzuki, 2010). Este complejo proceso requiere esquivar una serie de barreras entre las células normales y tumorales que reflejan el modo de operar de la evolución descrita por Charles Darwin (Darwin, 1859).

En 1976, Peter C. Nowell propuso un modelo de inicio y progresión tumoral que combinaba los conocimientos de la biología evolutiva con los de la biología tumoral (Nowell, 1976). Hoy en día este modelo se conoce como *modelo de evolución clonal* y propone que los tumores se inician a partir de alteraciones genéticas y epigenéticas en una sola célula. Seguidamente, la acumulación progresiva de alteraciones, aseguran la progresión tumoral. Además, durante este proceso tienen lugar un breve periodo de heterogeneidad celular seguido de una expansión de múltiples subpoblaciones celulares llamadas subclones. Cada uno de estos subclones se encontrarían bajo presión de selección darwiniana, de manera que estarían sometidos a selección positiva o negativa dependiendo de las ventajas o desventajas que sus alteraciones (epi-)genéticas les confiriesen (Greaves and Maley, 2012). En los subclones se dan dos tipos de alteraciones, las ventajosas o conductoras (*drivers*), que constituyen las principales fuerzas de expansión, y las pasajeras (*passengers*), simples polizones que parecen no estar bajo la presión de selección (De Carvalho et al., 2012; Kalari and Pfeifer, 2010).

A diferencia del modelo lineal de evolución tumoral propuesta por Erik R. Fearon y Bert Volgestein en cáncer colorrectal (Fearon and Vogelstein, 1990), en el que la aparición secuencial de mutaciones conductoras acaba originando un tumor homogéneo, una visión más moderna sugiere un mecanismo de evolución ramificada (*branch-type evolution*) (Figura I5). En este tipo de evolución, los diferentes subclones pueden coexistir de manera separada o entremezclados dentro del mismo tumor dando lugar a una heterogeneidad tumoral (Swanton, 2014). La evolución tumoral ramificada ha sido ampliamente demostrada en diferentes tipos de cáncer como: leucemias (Anderson et al., 2011), cáncer de mama (Nik-Zainal et al., 2012), cáncer renal (Gerlinger et al., 2012), cáncer de próstata (Haffner et al., 2013) o cáncer pancreático (Yachida et al., 2010) entre otros.

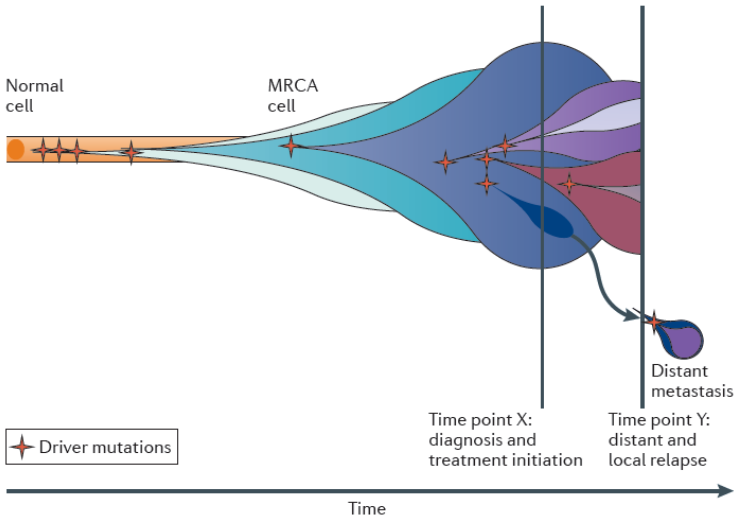

Figura I5 | Evolución ramificada. Los cánceres son entidades dinámicas y genómica y epigenómicamente diversas. Al igual que en la evolución de las especies, las diferentes poblaciones subclonales (representadas con diferentes colores) emergen como consecuencia de la acumulación de diversas alteraciones conductoras (estrellas rojas) en la progenie de la célula ancestral común más cercana. La evolución ramificada origina múltiples subclones que de manera individual pueden dar lugar a episodios de recaída o metástasis. La arquitectura clonal es dinámica y está modelada por la presión de selección tanto del ambiente tumoral como de los posibles tratamientos oncológicos recibidos. Figura extraída de (Yates and Campbell, 2012).

Las investigaciones oncológicas en el último cuarto de siglo, indican que prácticamente todas las células tumorales estudiadas adquieren un conjunto bastante bien determinado de características responsables de la transformación tumoral (Kreeger and Lauffenburger, 2010). Esto se debe a que la regulación de los procesos celulares básicos (división, diferenciación y apoptosis) es casi idéntica en todos los tipos celulares. Por ello, no es de sorprender que existan ciertas reglas básicas que gobiernan la transformación de una célula normal a una tumoral (Hanahan and Weinberg, 2000). Estas reglas, que fueron definidas a finales del siglo XX por Douglas Hanahan y Robert A. Weinberg (Hanahan and Weinberg, 2000) y redefinidas doce años más tarde por estos mismos autores, incluyen: el mantenimiento de las señales proliferativas, la evasión de la supresión del crecimiento y de la destrucción inmune, la resistencia a la apoptosis, la permisividad a la inmortalidad replicativa, la estimulación de la angiogénesis, la activación de la invasión y la metástasis y la desregulación energética celular (Hanahan and Weinberg, 2011).

Como hemos comentado anteriormente, el cáncer es un proceso **multietapa** que involucra tanto a alteraciones genéticas (mutaciones, alteraciones del número de copias, inserciones, deleciones y recombinaciones, etc.) como alteraciones en los previamente

descritos mecanismos epigenéticos (Hatzimichael and Crook, 2013). Es más, ambos tipos de alteraciones no son eventos separados, sino que se entrelazan aprovechándose unos de otros durante el proceso tumoral. Así, alteraciones epigenéticas pueden dar lugar a mutaciones (desaminación de la 5-metilcitosina a timina), mientras que mutaciones en las enzimas efectoras de las modificaciones epigenéticas, pueden dar lugar a alteraciones del epigenoma (You and Jones, 2012).

Por su función en el control de la expresión génica y en la estabilidad de la arquitectura de la cromatina, las alteraciones del patrón de metilación del DNA son unas de las más importantes durante los procesos tumorales (Esteller, 2008), pudiendo ser más o menos agresivas dependiendo del tipo tumoral (Fernandez et al., 2012). Los genomas tumorales suelen caracterizarse por una pérdida de metilación (hipometilación) global acompañada de un incremento de metilación (hipermetilación) local que afecta especialmente a CGIs y otras regiones reguladoras (Sandoval and Esteller, 2012). Estos cambios alteran la estructura de la cromatina y la función del DNA, contribuyendo enormemente a la inestabilidad génica y al fenotipo de las células tumorales. Dado que la hipometilación global y las hipermetilaciones locales se han observado en todas las neoplasias estudiadas, se les considera como un sello distintivo del cáncer (*cancer hallmark*).

La **hipometilación** del DNA fue descrita por primera vez en 1983 por Melanie Ehrlich (Gama-Sosa et al., 1983), Andrew P. Feinberg y Bert Vogelstein (Feinberg and Vogelstein, 1983). Hoy por hoy sabemos que es un evento temprano y sostenido en la tumorogénesis y que muchas veces se da, incluso antes de que tenga lugar la transformación tumoral (Ehrlich, 2009; Sheaffer et al., 2016). La hipometilación suele ocurrir en grandes dominios (*cancer-specific Differentially DNA-Methylated Regions*, cDMRs) que pueden llegar a cubrir la mitad del genoma y que se asocian a replicación tardía y anclaje a la lámina nuclear (Berman et al., 2011). Además, estos cDMRs, están enriquecidos en genes con expresión variable y asociados a heterogeneidad y progresión tumoral (Hansen et al., 2011). Aunque clásicamente se había asociado la desmetilación de las secuencias repetitivas con el aumento de la hipometilación global durante los procesos cancerosos (Itano et al., 2002; Jackson et al., 2004; Widschwendter et al., 2004), Hansen *et al*., demostraron que es la hipometilación de las cDMRs la verdadera responsable de la hipometilación global del genoma (Hansen et al., 2011).

Se cree que, entre otras cosas, esta pérdida de metilación que provoca la pérdida del *imprinting* génico y la reexpresión de secuencias repetitivas como LINEs o elementos

Alu, acaba por desestabilizar el genoma favoreciendo las recombinaciones mitóticas que llevan a deleciones, inserciones y translocaciones (Eden et al., 2003). De hecho, Karpf *et al.* observaron que la reducción de la metilación del DNA *in vitro*, mediante mutaciones inactivadoras de las DNA metiltransferasas[2] (DNMTs), era capaz de causar aneuploidía en líneas celulares tumorales humanas (Karpf and Matsui, 2005). Por otro lado, la alteración de la impronta del locus *IGF-2*/*H19* parece ser un evento clave en el desarrollo y progresión del tumor de Wilms (Ludgate et al., 2013) y se ha visto como un factor de riesgo en el cáncer colorrectal y de mama (Cui et al., 2002; Ito et al., 2008; Murrell et al., 2008).

Así mismo, la reactivación ectópica o extemporánea de genes o ncRNAs, debida a la pérdida de la metilación de sus CGIs, contribuyen a la tumorogénesis (Berdasco and Esteller, 2010; Brueckner et al., 2007; Jeter et al., 2015). Finalmente, cabe destacar que en los últimos años, esta *hallmark* ha atraído mucho interés desde el punto de vista clínico ya que numerosos estudios han establecido una relación directa entre el nivel de hipometilación y el grado o estadio tumoral (Choi et al., 2009; Frigola et al., 2005; Lin et al., 2001; Matsuda et al., 2012; Moore et al., 2008; Rodriguez et al., 2006; Toraño et al., 2012; Zelic et al., 2014) .

Por su parte, la hipermetilación ocurre principalmente en regiones concretas, particularmente en CGIs asociadas a promotores de genes supresores de tumores y genes de reparación del DNA (Feinberg and Tycko, 2004; Jones and Baylin, 2002b). Así pues, la represión génica mediada por metilación del DNA podría considerarse como un segundo evento en la hipótesis de dos eventos de Alfred G. Knudson (Knudson's *two-hit hypothesis*) (Knudson, 2001, 1971). Por lo tanto, la hipermetilación y consecuente silenciamiento de genes supresores de tumores provoca una pérdida de heterocigosidad (*Loss Of Hetorezygosity*, LOH) que da lugar a una proliferación incontrolada en innumerables tipos de cáncer. Entre los genes silenciados por hipermetilación del DNA se encuentran genes supresores de tumores clásicos como el *RB* (retinoblastoma) y el *APC* (*adenomoatous polyposis coli*) en cáncer de colon o el *BRCA1* (*breast* cancer 1) en cáncer de mama, así como genes involucrados en la reparación del DNA como *MLH1* (*mutL homolog 1*) y *MGMT* (*O-6-methylguanine-DNA methyltransferase*) o en la adhesión molecular como *CDH1* (*cadherin 1*) (Esteller, 2008). Aunque muchos de estos eventos se consideran como biomarcadores tumorales, ninguno se utiliza de manera sistemática en

[2] Las DNA metiltransferasas son una familia de enzimas que catalizan la transferencia de un grupo metilo desde el S-adenosil-L-metionina al carbono 5 del anillo pirimidínico de una citosina [revisado en (Jin and Robertson, 2013)].

la práctica clínica. No obstante, recientemente, Manel Esteller y sus colaboradores han sacado al mercado un test epigenético que, basándose en el perfil de metilación específico de una muestra, es capaz de asignar un origen primario a una muestra de un tumor desconocido (Gracia et al., 2015; Moran et al., 2016).

Pero no solamente la metilación del DNA es importante durante el inicio y la progresión tumoral. La desorganización de la estructura local y global normal de la cromatina como consecuencia de alteraciones en el resto de mecanismos epigenéticos también juegan un papel muy importante en el desarrollo tumoral (Ferraro, 2016). Por ejemplo, la expresión anómala de diferentes enzimas modificadoras de las colas de las histonas es un evento común en múltiples tipos de cáncer (Füllgrabe et al., 2011). Por otro lado, investigaciones recientes sugieren que, mutaciones genéticas en las proteínas histonas, así como en las proteínas chaperonas que median la incorporación de las variantes de histona en los nucleosomas, están directamente implicadas en numerosos cánceres (Hondele and Ladurner, 2011; Schwartzentruber et al., 2012; Wu et al., 2012). Finalmente, en los últimos años tenemos una clara constancia de la función de los ncRNA en el control de la expresión de otros genes, por lo tanto, expresiones anómalas de estos ncRNAs llevan a expresiones anómalas de sus genes diana (Huarte, 2015).

3. Glándula tiroides

3.1. Anatomía e histología

La **tiroides** (del griego *thyreoeides*; propiamente 'en forma de escudo') es una glándula endocrina que en humanos adultos se sitúa en el espacio visceral de la porción infrahioidea del cuello. Está formada por dos lóbulos que flanquean la tráquea justo por debajo de la prominencia laríngea o nuez de Adán (Figura I6a). Ambos lóbulos se encuentran unidos en la línea media por el istmo, una banda de tejido que se extiende de uno a otro lóbulo por delante de la tráquea entre su primer y tercer anillo (Mohebati and Shaha, 2012). Los lóbulos de la glándula tiroides adulta miden de 4 a 6 cm en sentido craneocaudal y de 2 a 3 cm en sentido sagital y transversal. Así mismo, el istmo mide alrededor de 1.25 cm en ambos sentidos (craneocaudal y transversal). El volumen medio de la glándula en mujeres es de 18 mL mientras que en hombres es de 25 mL con un peso aproximado de 20 g (Bliss et al., 2000; Ghervan, 2011).

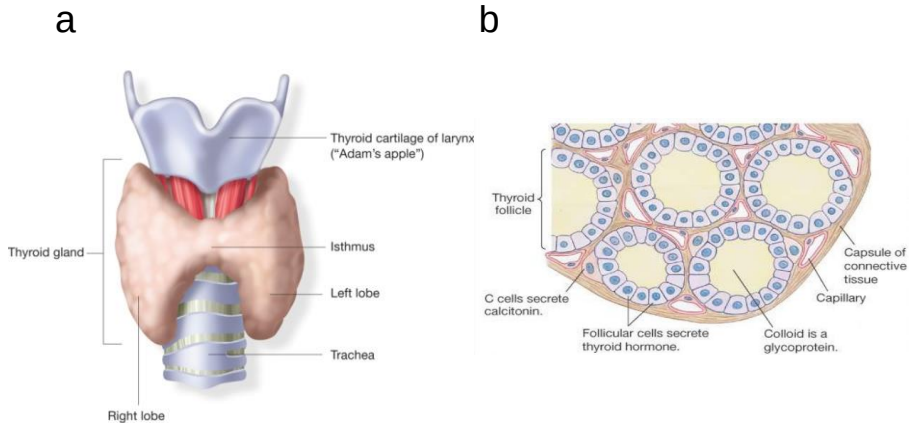

Figura I6 | Diagrama de la anatomía e histología de la glándula tiroides. (a) La glándula tiroides se localiza delante de la tráquea y está formada por dos lóbulos unidos por un istmo. **(b)** El folículo tiroideo consiste en una esfera de células foliculares que delimitan el lumen en el que se almacena la tiroglobulina. Adosadas a la pared de células foliculares se encuentran las células parafoliculares y todo el conjunto se envuelve en una membrana basal. El folículo está altamente irrigado por capilares sanguíneos a los que se secretan las hormonas tiroideas. Todo el conjunto está envuelto por una cápsula de tejido conectivo. Figura extraída de www.healthythyro.com.

La tiroides está altamente vascularizada y cuenta con una amplia red de capilares y arterias que rodean y abastecen a los **folículos tiroideos**, unidades funcionales y estructurales de la glándula (Figura I6b). Estas estructuras de entre 0.2 a 0.9 mm de diámetro consisten en un epitelio simple y cúbico de **células foliculares**. Las células están polarizadas de tal manera que la parte basolateral de la membrana contacta con el

flujo sanguíneo, mientras que la apical lo hace con el lumen (Mondal et al., 2016). El lumen está repleto de un coloide compuesto principalmente por la tiroglobulina secretada por las propias células foliculares. En condiciones de baja actividad glandular (p.ej. hipotiroidismo) los folículos se agrandan aumentando el contenido coloidal mientras que las células foliculares se aplanan reduciendo considerablemente su citoplasma. Por el contrario, cuando aumenta la actividad glandular, los folículos se empequeñecen y las células se alargan adquiriendo un aspecto de columna. Bajo el microscopio electrónico estas células presentan un núcleo basal con un retículo endoplasmático bien formado, múltiples vesículas secretoras apicales y pequeñas mitocondrias. Adheridas a los folículos tiroideos se encuentran las células **parafoliculares** o células C. Estas pequeñas células de citoplasma granuloso son las encargadas de la síntesis y secreción de calcitonina. El conjunto formado por el folículo y las células parafoliculares está rodeado por una membrana basal (Gartner, 2007; Villacorte et al., 2016).

3.2. Embriogénesis

La tiroides es la primera glándula endocrina que se desarrolla en el embrión humano. Comienza hacia el final de la tercera semana a partir de una proliferación del endodermo en el suelo de la faringe primitiva, que más adelante en el desarrollo embrionario se le conocerá como *foramen cecum* (agujero ciego). La evaginación de esta protuberancia celular origina el primordio tiroideo, el cual se alarga y bifurca desenganchándose de la faringe y formando los lóbulos de la tiroides. Hacia el final de la séptima semana de gestación y a medida que el embrión crece longitudinalmente, la glándula tiroides desciende hacia su posición final en la parte anterior de la tráquea pasando por delante del hueso hioides y los cartílagos laríngeos (Kirsten, 2000). Durante esta migración la glándula permanece unida a la lengua primigenia por el conducto tirogloso, la parte lingual del cual es visible hasta el final del desarrollo fetal (Mohebati and Shaha, 2012). En algunos casos, el conducto tirogloso persiste en el adulto y crece formando el denominado lóbulo piramidal (Kim et al., 2013; Takanashi et al., 2015).

A nivel genético sabemos que la proliferación, migración y supervivencia del primordio tiroideo está orquestada por cuatro factores de transcripción (NKX2-1, FOXE1, PAX8 y HHEX) conocidos como factores de transcripción tiroideos o TTFs de su acrónimo en inglés *Thyroid Transcription Factors* (Figura I7). En un primer momento la expresión de los TTFs es simultánea y mutuamente independiente, excepto FOXE1 cuya expresión está regulada por PAX8 (Parlato et al., 2004). No obstante, experimentos con mutaciones deletéreas de los TTFs en modelos murinos, concluyeron que ninguno de los TTFs es

imprescindible para el desarrollo del primordio tiroideo (Fernández et al., 2015; Parlato et al., 2004). A continuación, se observa el establecimiento de una red de relaciones transcripcionales en la que HHEX regula la expresión del resto de TTFs y a su vez está regulado por PAX8 y NKX2-1 el cual, adquiere la capacidad de regular a FOXE1 (Antonica et al., 2012; Fernández et al., 2015; Ma et al., 2015; Parlato et al., 2004).

Sólo cuando las células precursoras llegan a su posición final empieza su diferenciación hacia células foliculares con la expresión de tiroglobulina (*TG*) y finaliza con la expresión de genes específicos de tiroides como el receptor de tirotropina (*TSHR*), la peroxidasa tiroidea (*TPO*) y el *solute carrier family 5, member 5* (*SLC5A5*) también conocido como simportador de sodio/yodo (*NIS*) (Figura I7). Cabe destacar que, aunque la tirotropina (TSH) es el principal estímulo de crecimiento de la glándula tiroides adulta y la señalización vía TSH/TSHR es necesaria para completar la diferenciación correcta de la tiroides, no parece imprescindible para el desarrollo de la glándula (Fagman and Nilsson, 2010; Fernández et al., 2015). Modelos murinos demuestran que aunque, si bien, tanto el tamaño de la glándula como los niveles de slc5a5 y tpo se ven reducidos, no se observan alteraciones estructurales considerables (Marians et al., 2002; Postiglione et al., 2002; Szinnai et al., 2014).

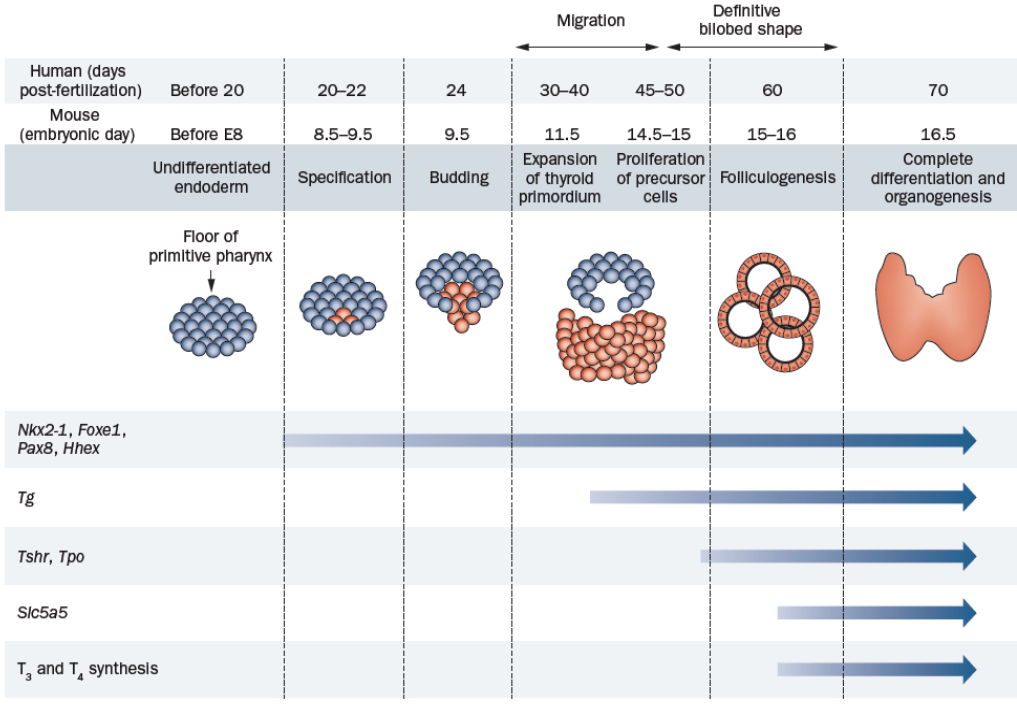

Figura I7 | Factores de transcripción involucrados en los diferentes estadios de la diferenciación de la glándula tiroides. Figura extraída de (Fernández et al., 2015).

3.3. Función y biosíntesis de hormonas tiroideas

La función principal de la glándula tiroides es la síntesis y secreción de las dos hormonas tiroideas, la triyodotironina (T3) y su precursora la tetrayodotironina o tiroxina (T4). Ambas hormonas desempeñan un papel clave en la regulación y control del sistema endocrino, así como del metabolismo general del cuerpo participando en la síntesis de proteínas y carbohidratos (Chung, 2014; Mondal et al., 2016). Regulan la termogénesis (Solmonson and Mills, 2016) y las funciones cardíaca (Vargas-Uricoechea et al., 2014) y renal (Szymański et al., 2016). También están involucradas en la maduración ósea (Cardoso et al., 2014; Desjardin et al., 2014) y en el funcionamiento del sistema nervioso central fetal (de Escobar et al., 2007) y adulto (Kapoor et al., 2015; Wirth et al., 2014). Por otro lado, las células parafoliculares de la glándula tiroides producen calcitonina, que junto con la hormona paratiroidea producida por la glándula paratiroides controlan la homeostasis del calcio (Noordin and Glowacki, 2016).

Como hemos mencionado anteriormente, el lumen de los folículos tiroideos se encuentra repleto de **tiroglobulina**, esta glicoproteína dimérica de 660 KDa constituye el mayor reservorio de yodo del cuerpo y a partir de ella se sintetizan las hormonas tiroideas. La transcripción de *TG* está controlada principalmente por NKX2-1, FOXE1 y PAX8 cuya transcripción está a su vez estimulada por otras hormonas como la TSH, la insulina o el factor de crecimiento insulínico tipo 1 (IGF-1) (Jacobson and Tomer, 2007; Santisteban et al., 1992; Suzuki et al., 2011, 2000; Van Heuverswyn et al., 1985). Tras su traducción, la TG sufre un intenso proceso de modificación postraduccional que la transportarán desde el retículo endoplasmático rugoso al aparato de Golgi y a la membrana apical de la célula folicular, para acabar en el lumen del folículo. Estas modificaciones postraduccionales incluyen: el ensamblaje de los dos homodímeros que forman la hormona, la incorporación de ácido siálico, la sulfatación, fosforilación, yodación, multimerización y la formación de puentes disulfuro (Mondal et al., 2016; Spiro and Gorski, 1986; Targovnik et al., 2011, 2010).

El proceso de biosíntesis de la tiroxina y la triyodotiroxina consta de tres pasos principales en los que la tiroglobulina tiene un papel central como precursora de ambas hormonas (Mondal et al., 2016). El primer paso es la captación del yoduro diluido en el plasma sanguíneo a través de SLC5A5 (Dai et al., 1996; Smanik et al., 1996). A continuación, el yoduro es transportado desde el citoplasma hacia el lumen folicular presumiblemente mediante algún transportador. Numerosos estudios han detectado varios transportadores en la membrana apical de las células foliculares con la capacidad

de transportar yoduro. Entre ellos, el más estudiado es el transportador de cloro/yodo independiente de sodio pendrina, codificado por el gen *SLC26A4* (Mount and Romero, 2004). Se sabe que mutaciones en este gen son las causantes del Síndrome de Pendred (PDS), enfermedad hereditaria autosómica recesiva que cursa con una amplia gama de síntomas, entre ellos, hipotiroidismo, bocio y defectos en la organificación del yoduro (Kopp et al., 2008). Sin embargo, otros transportadores como CLCN5, SLC5A8, CFTR o ANO1 han sido igualmente reconocidos como posibles transportadores apicales de yoduro (Fong, 2011; Mondal et al., 2016). Todos estos trabajos evidencian la existencia de una compleja red de transportadores apicales interrelacionados que permitirían el influjo de yoduro desde el citoplasma hacia el lumen folicular.

El segundo paso en la biosíntesis de las hormonas tiroideas es la obtención de peróxido de hidrógeno (H_2O_2), sustrato imprescindible para la actividad enzimática de la enzima TPO. La producción de peróxido de hidrógeno tiene lugar en la membrana apical de las células foliculares gracias a la acción de dos NADPH oxidasas, DUOX1 y DUOX2 (Ameziane-El-Hassani et al., 2005; Miot et al., 2000). En la tercera etapa, el peróxido de hidrógeno producido en el paso anterior es utilizado por la enzima TPO para oxidar el ion yoduro a yodo e incorporarlo a la TG en un proceso conocido como **organificación del yodo** (Luo et al., 2014; Miot et al., 2000). En este proceso, la TPO cataliza la yodación de los residuos de tirosina de la TG formando las yodotirosinas MIT (3-monoyodotirosina) y DIT (3,5-diyodotirosina) que permanecen unidas a la TG. Seguidamente la misma TPO cataliza el acoplamiento entre dos moléculas DIT, formando la T4, o entre una molécula DIT y otra MIT formando la T3. Al unirse las dos yodotirosinas, una pierde la cadena lateral de alanina quedando la estructura básica de las tironinas: dos anillos (fenólico y tirosílico) con tres (T3) o cuatro (T4) átomos de yodo y una cadena lateral de alanina (Miot et al., 2000; Miralles García and Leiva Hidalgo, 2001) (Figura I8). Todo esto ocurre en la misma TG que actúa como un andamiaje sobre el que tienen lugar todas estas reacciones químicas.

La molécula madura de TG que contiene MIT, DIT, T4 y T3, es almacenada en el lumen folicular hasta su liberación. El contenido de TG en el lumen depende de muchos factores tales como la concentración de yoduro, la actividad enzimática de las proteínas implicadas en la producción de TG o la concentración y estado físico y químico de la TG. Cuando la concentración plasmática de TSH aumenta, la TG es internalizada en las células foliculares mediante endocitosis y sufre una proteólisis lisosomal que libera las hormonas tiroideas. En este momento, las moléculas DIT y MIT que no han sido acopladas sufren un proceso de desyodación gracias a la flavoproteína yodotirosina desyodasa

(*iodotyrosine deiodinase*, IYD) (Marinò and McCluskey, 2000; Miot et al., 2000). Una vez liberadas al torrente circulatorio las hormonas tiroideas se unen a diversas proteínas transportadoras como la globulina fijadora de tirosina (*thyroxine-binding globulin*, TBG), la transterritina (*transthyretin*, TTR) o la albúmina sérica humana (*human serum albumin*, HSA) que las acompañarán hasta sus tejidos diana (Schussler, 2000).

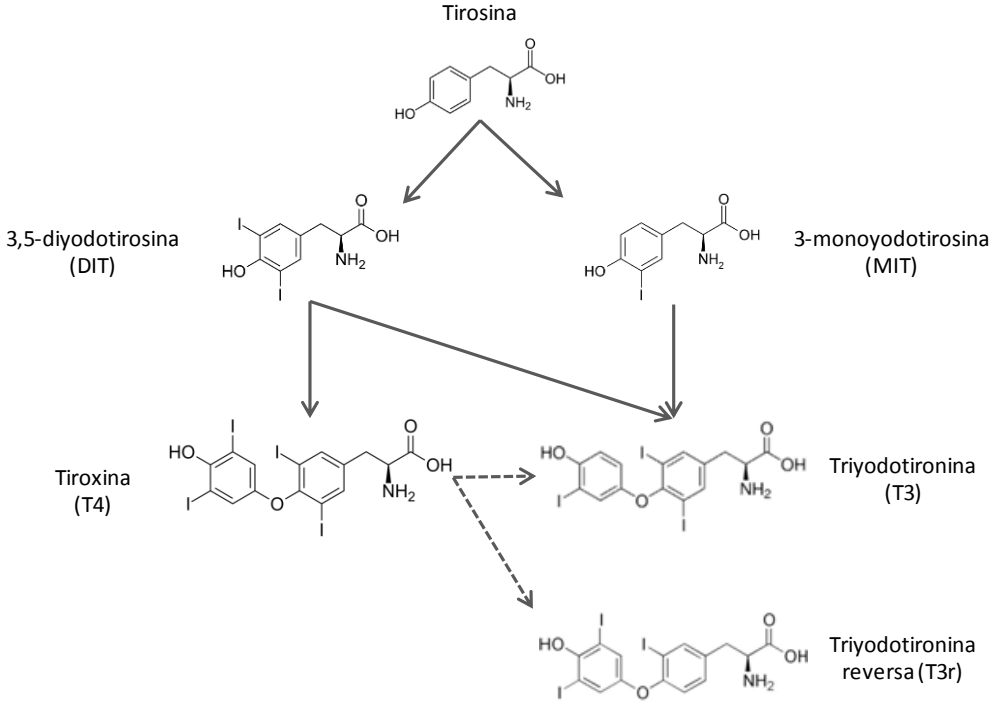

Figura I8 | Biosíntesis de las hormonas tiroideas a partir de los residuos de tirosinas de la tiroglobulina. La TPO cataliza la adición de uno o dos iones yodo al carbono 3 o 3 y 5 del anillo fenólico de la tirosina formando la 3-monoyodotirosina (MIT) y la 3,5-diyodotirosina (DIT) respectivamente. El acoplamiento dentro de la misma tiroglobulina entre dos moléculas DIT o una molécula DIT y otra MIT, catalizado por la TPO, resulta en la obtención de la tiroxina (T4) o la triyodotiroxina (T3). Eventualmente, en sus tejidos diana, la tiroxina puede transformarse en triyodotironina mediante la acción de la IYD 1/2 o al metabolito alternativo y metabólicamente inactivo triyodotironina reversa (T3r) por la IYD 3. Figura modificada de (Miralles García and Leiva Hidalgo, 2001).

4. Cáncer de tiroides

4.1. Epidemiología

La prevalencia de los **nódulos tiroideos** en la población humana es extremadamente elevada, dependiendo, en gran manera del método de detección utilizado (Castro and Gharib, 2015; Tufano et al., 2015). Así, la prevalencia es del 4-7% en exploraciones físicas (palpación), mientras que la utilización de sistemas de imagen (p.ej. ultrasonografía, tomografía computarizada, etc.) incrementan este porcentaje hasta el 67% (Guth et al., 2009; Tan and Gharib, 1997). Si bien la gran mayoría de los nódulos tiroideos son benignos, el 8-16% de ellos puede malignizar y desembocar en cáncer (Burman and Wartofsky, 2016; Hegedüs, 2009; Huang et al., 2013; Tunbridge et al., 1977).

A diferencia de los nódulos, el cáncer de tiroides es un evento poco común en la población, representando el 1-2% de todos los tumores humanos (Conzo et al., 2016). Al igual que en la presencia de nódulos, existe un sesgo en la incidencia con respecto al sexo, afectando a 3 mujeres por cada hombre, siendo el quinto tumor más frecuente en mujeres (Fortuny et al., 2015; Huang et al., 2013; Vanderpump, 2011). De acuerdo con los datos obtenidos en el programa de vigilancia, epidemiología y resultados finales (*Surveillance, Epidemiology, and End Results*, SEER), se estima que, en Estados Unidos, 64,300 personas desarrollarán cáncer de tiroides y 1,980 morirán a causa de esta enfermedad en el año 2016. Las estadísticas españolas no son mucho más halagüeñas. Según los datos de la Sociedad Española de Endocrinología y Nutrición (SEEN) Cada año se diagnostican 2.1 casos por cada 100,000 habitantes, una cifra que se triplica entre las mujeres, colectivo que registra 6 casos por cada 100,000 habitantes.

Los datos recogidos por el programa SEER en el periodo 2004-2013, revelan un incremento anual de la incidencia del 4.7%, convirtiéndose en el cáncer humano con la mayor tasa de incidencia independientemente del sexo o la edad (Figura I9a-b). Afortunadamente, el porcentaje de supervivencia a los 5 años es muy elevado en aquellos pacientes que presentan lesiones localizadas en el foco tumoral o con metástasis regionales (nodales) (99.9% y 97.8%, respectivamente), los cuales representan el 95% de los casos de cáncer de tiroides. Por otro lado, en el 7% de los pacientes se observa recurrencia de la enfermedad (Hoang et al., 2015) y en el 4% metástasis a distancia, con una supervivencia a los 5 años del 55.3% (Figura I9c-d).

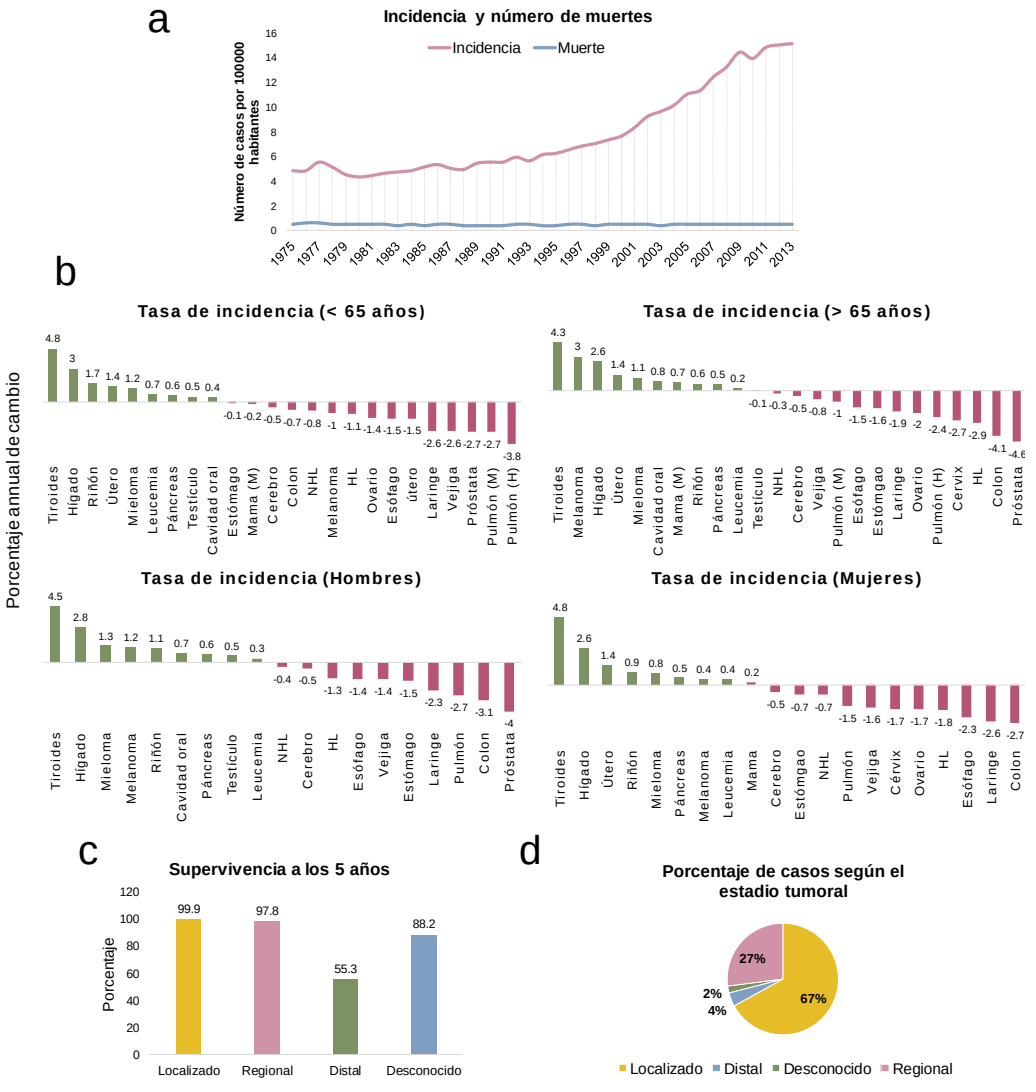

Figura I9 | Características epidemiológicas del cáncer de tiroides. (a) La incidencia del cáncer de tiroides ha aumentado drásticamente en el periodo 1975-2013, sin embargo, el número de muertes se mantiene por debajo de 1 por cada 100,000 habitantes. **(b)** La incidencia del cáncer de tiroides protagoniza el mayor incremento anual independientemente del grupo de edad y el sexo. **(c)** Más del 97% de los pacientes con tumores de tiroides localizados o con metástasis regionales (nodales) sobreviven a los 5 años mientras que este porcentaje se reduce al 55.3% en los pacientes con metástasis a distancia. **(d)** El 94% de los pacientes de cáncer de tiroides se encuentran en los grupos con mayor probabilidad de supervivencia a los 5 años. Datos extraídos del programa SEER.

Actualmente, parece que la causa del incremento en la incidencia mundial del cáncer de tiroides se debe principalmente a la difusión y mejora en la sensibilidad de detección de sistemas de imagen como la tomografía por emisión de positrones (*Positron Emission Tomography*, PET), la tomografía computarizada (*Computed Tomography,* CT) o la ultrasonografía. Estas mejoras han permitido la detección casual (incidentalomas) de

microcarcinomas (<1 cm) asintomáticos, principalmente de tipo papilar, que no contribuyen al aumento en el número de muertes, lo que explicaría por qué este parámetro se mantiene constantemente bajo (0.5 por cada 100,000 habitantes en el periodo 2009-2013) (Brito and Davies, 2014; Hoang et al., 2015). No obstante, algunos investigadores proponen que no todo se debe a las mejoras en los sistemas de detección ya que [revisado en (Pellegriti et al., 2013)]: (1) la incidencia de tumores grandes (>1 cm) ha aumentado tanto como la de los microcarcinomas (Rego-Iraeta et al., 2009), (2) se da tanto en tumores localizados como regionales (nodales) que cursan con sintomatología evidente (Simard et al., 2012) y (3) si bien la incidencia de los tumores foliculares de la tiroides parece haber aumentado discretamente no es en absoluto comparable al aumento de los tumores papilares de tiroides (Aschebrook-Kilfoy et al., 2013). En principio, las mejoras técnicas deberían conllevar un incremento de la incidencia en ambos tipos histológicos.

4.2. Factores de riesgo

La Organización Mundial de la Salud (OMS), define factor de riesgo como cualquier rasgo, característica o exposición de un individuo que aumenta su probabilidad de sufrir una enfermedad o lesión.

Como hemos comentado en el apartado anterior, la incidencia del cáncer de tiroides es más elevada en mujeres que en hombres (al igual que casi todas las enfermedades de la tiroides), lo que convierte al **sexo** en un claro factor de riesgo en esta neoplasia. Aunque se desconocen las razones exactas de esta disparidad sexual, numerosos estudios apuntan hacia el papel regulador de las hormonas sexuales (p.ej. estrógeno y progesterona) y sus receptores en la aparición y desarrollo del cáncer de tiroides (Libutti, 2005). Al igual que en muchos tumores humanos (DePinho, 2000), la **edad** es un factor de riesgo en el cáncer de tiroides. No obstante, a diferencia de otros cánceres en los que el pico de incidencia se encuentra a edades avanzadas (>60 años), en tiroides la incidencia máxima se registra entre los 45 y los 54 años, siendo 51 años la media de edad de diagnóstico de esta neoplasia (Figura I10a). Por otro lado, y al igual que en la mayoría de tumores, la muerte asociada a la enfermedad aumenta claramente con la edad (Figura I10b) (McLeod et al., 2015).

Varios autores apuntan a que, si bien la incidencia del cáncer ha aumentado en todas las **etnias** estudiadas, no en todas ha aumentado con la misma intensidad ni se ha producido en los mismos tipos histológicos (Enewold et al., 2009; Finlayson et al., 2014;

Magreni et al., 2015). Esto sugiere que tanto factores externos como factores genéticos juegan un papel importante en el desarrollo del cáncer de tiroides.

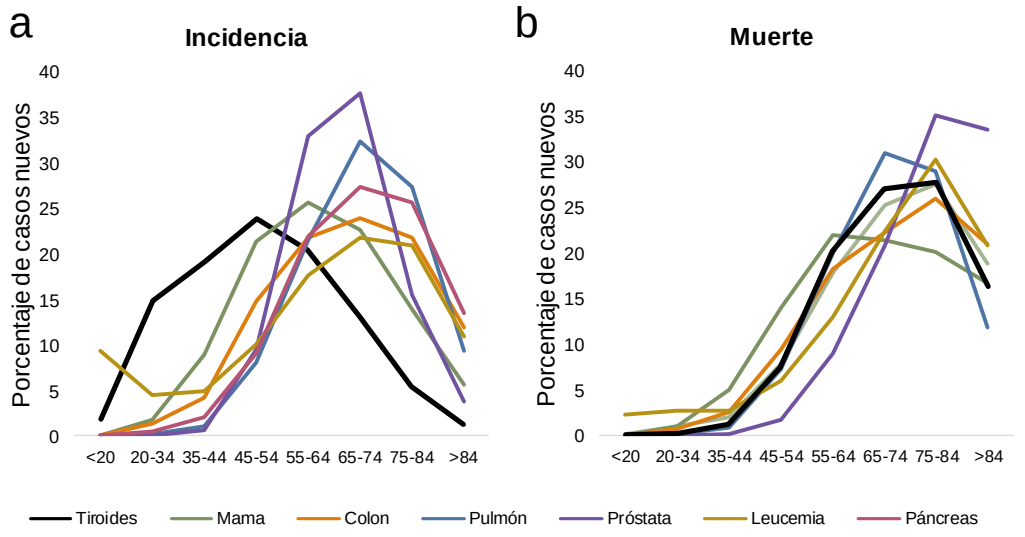

Figura I10 | Incidencia y mortalidad asociada a diversos tipos de cáncer. (a) La distribución de la incidencia por franja de edad muestra que el cáncer de tiroides tiene un máximo más temprano (45-54 años). que el resto de tumores (>60 años). **(b)** la mortalidad aumenta de manera exponencial al aumentar la edad en todos los tumores representados. Datos extraídos del programa SEER durante el periodo 2009-2013.

Varios factores ambientales han sido clasificados como factores de riesgo en el desarrollo de esta enfermedad, entre ellos el principal es la exposición a **radiación ionizante**. Debido a su posición y a su gran capacidad para captar y concentrar yodo, la tiroides es la principal glándula afectada por la radiación ionizante. Además, parece afectar más durante la niñez, como se demostró en el accidente de Chernóbil en el que la glándula tiroides recibió una dosis entre 500 a 1000 veces superior a la del resto del cuerpo, lo que acarreó un total de 4000 nuevos casos (Pellegriti et al., 2013; D Williams, 2008). Así mismo, diversos procedimientos de diagnóstico radiológicos (CT, yodo radioactivo, Rayos-X) han sido considerados como potenciales factores de riesgo especialmente en niños (Berrington de González et al., 2009; Hieu et al., 2012; Linton et al., 2003; Memon et al., 2010; Pearce et al., 2012).

La **deficiencia en yodo** también es un factor de riesgo ya que favorece la hipersecreción de TSH por parte de la hipófisis lo que provoca una hiperestimulación de la glándula tiroides (Feldt-Rasmussen, 2001). Modelos animales sugieren que la deficiencia en yodo no es un factor iniciador del cáncer de tiroides pero sí un factor promotor de la enfermedad (Zimmermann and Galetti, 2015). Además, estudios retrospectivos en los que se administró yodo de manera profiláctica demuestran que el

déficit de yodo está asociado a un incremento del cáncer folicular, y posiblemente anaplásico, con respecto al papilar de tiroides (Feldt-Rasmussen, 2001).

Algunos estudios apuntan hacia la **obesidad** como un factor de riesgo en el desarrollo de cáncer de tiroides. Esto es debido a que dos de los trastornos metabólicos más importantes asociados a la obesidad (hiperinsulinémia y resistencia a la insulina), promueven altos niveles de insulina en la sangre la que, como se ha comentado antes, regula la expresión de TG estimulando la proliferación y diferenciación de las células foliculares (Almquist et al., 2011; Renehan et al., 2008; Rezzónico et al., 2009; Rinaldi et al., 2012).

Aunque no se ha establecido una relación causal clara, algunos **contaminantes medioambientales** como nitratos, amianto, benceno, formaldehido, bisfenol A, bifenilos policlorados o polibromodifenil éteres entre otros se han postulado como agentes cancerígenos (Pellegriti et al., 2013). Concretamente se ha visto que los polibromodifenil éteres pueden inducir una proliferación anormal de las células foliculares favoreciendo un estado precanceroso (Zhang et al., 2008). El mecanismo de acción de estos compuestos sobre el organismo va desde la activación anormal de receptores esteroideos a cambios en la metilación del DNA o daño del DNA (Maqbool et al., 2016).

Mutaciones hereditarias en el protoncogén *RET* se han asociado con el desarrollo de cáncer medular de tiroides esporádico o familiar. En algunos casos, la mutación en *RET* viene asociada con otras alteraciones endocrinas (p.ej. feocromocitoma, adenoma o hiperplasia de la paratiroides) en cuyo caso el síndrome se conoce como neoplasia endocrina múltiple 1/2 (MEN1 y MEN2) (Raue and Frank-Raue, 2015; Sanso et al., 2002). Otros trastornos genéticos tales como: poliposis adenomatosa familiar, síndrome de Gardner, síndrome del complejo de Carney tipo I o la enfermedad de Cowden, han sido reconocidos como factores de riesgo en el desarrollo de tumores foliculares y papilares de la tiroides (Gara et al., 2015; Moses et al., 2011; Vriens et al., 2009).

4.3. Tipos histopatológicos

El 90% de los tumores de tiroides se desarrollan a partir de las células foliculares mientras que el otro 10% deriva de las células parafoliculares y se denomina Cáncer Medular de Tiroides (*Medullary Thyroid Carcinoma*, MTC) (resumen en Anexo 1.1). El 70-80% de los casos de MTC son esporádicos, sin embargo un 20-30% son casos hereditarios en los que la mutación autosómica dominante en el protoncogén *RET* es la principal causante (Figlioli et al., 2013). Aunque histológicamente diversos (Schmid,

2015), el MTC típico presenta un patrón de crecimiento compacto de células poligonales o fusiformes que se agrupan en nidos, trabéculas o folículos. En el 60–85% de los casos se observan depósitos de amiloide acelular en el estroma adyacente y también infiltraciones hacia el tejido no tumoral. Bajo microscopía electrónica el citoplasma de las células parafoliculares tumorales presenta gránulos densos rodeados de membrana presumiblemente repletos de calcitonina (Pacini et al., 2010).

Clásicamente, los tumores tiroideos derivados de las células foliculares se clasifican de acuerdo al grado de diferenciación y agresividad (Hedinger et al., 1989; Katoh et al., 2015; Scopa, 2004). En primer lugar, encontramos los **adenomas foliculares** (*Follicular Thyriod Adenoma*, FTA), tumores benignos y encapsulados de tamaño variable (2-3 cm de media), sin presencia de invasión vascular o capsular (McHenry and Phitayakorn, 2011). Por otro lado, los tumores malignos poco agresivos y altamente diferenciados se conocen como tumores bien diferenciados de la tiroides (*Well-Differentiated Thyroid Carcinoma*, WDTC). Dentro de este concepto se engloban los tumores foliculares (*Follicular Thyroid Carcinoma*, FTC) y papilares (*Papillary Thyroid Carcinoma*, PTC). Aunque existen algunos casos en los que el WDTC se presenta como una enfermedad de agregación familiar (carcinoma familiar de tiroides no medular), más del 95% de los casos de WDTC son esporádicos (Kebebew, 2008; Nosé, 2011).

Dependiendo de la bibliografía consultada, entre un 5% y un 15% de los tumores de tiroides son diagnosticados como **FTC** (Bose and Walts, 2012; D'Avanzo et al., 2004; Phitayakorn R1, 2006), sin embargo, en regiones con dietas pobres en yodo este porcentaje asciende hasta el 30-40% (Scopa, 2004). El FTC se define como un tumor maligno epitelial que muestra diferenciación folicular con ausencia de las características nucleares típicas del PTC y que, a diferencia del FTA, presenta invasión capsular y/o vascular (Schlumberger, 1998). A menudo acostumbra a ser unicéntrico y con poca tendencia a recurrir tras una tiroidectomía, no obstante y dado a su capacidad invasiva, tiene propensión a metastatizar a distancia (hueso, pulmones, cerebro o hígado) (Haigh, 2002; Sobrinho-Simões et al., 2011). Dependiendo del grado de invasión, los FTCs se clasifican en FTC mínimamente invasivos y FTC invasivos. La diferencia entre ambos radica en que la invasión capsular y/o vascular de los mínimamente invasivos sólo puede ser detectada bajo microscopía mientras que en los invasivos se observa macroscópicamente (Ito et al., 2007; Scopa, 2004; Sobrinho-Simões et al., 2011). Con fines pronósticos y terapéuticos, algunos autores han considerado importante subdividir los FTC mínimamente invasivos entre aquellos con o sin invasión vascular (Collini et al., 2004; Goffredo et al., 2016; H.J. et al., 2014; Lang et al., 1986; Stenson et al., 2016).

El **carcinoma de la célula de Hürthle** (*Hürthle Cell Carcinoma*, HCC), también llamado, carcinoma de células oxifílicas o carcinoma de células oncocíticas, es una variante poco común del FTC (3-8%) que algunos autores han considerado como una tercera entidad dentro de los WDTC (Barnabei et al., 2009; Mills et al., 2009; Parameswaran et al., 2010). Más del 75% de las células en el HCC presentan características oncocíticas, esto es: derivadas de células foliculares con forma poligonal y alargada (10-15 μm) y bordes bien diferenciados, un gran núcleo redondeado e hipercromático y un citoplasma acidofílico y granular debido al alto número de mitocondrias (Cannon, 2011; Zavitsanos et al., 2015). Parece ser que la acumulación de mitocondrias es el resultado de diversas alteraciones genéticas (deleciones y mutaciones) en enzimas de la cadena de transporte de electrones que producen una disminución en la actividad mitocondrial lo que lleva a la estimulación de la proliferación de este orgánulo (Montone et al., 2008). Esta variedad de FTC se considera la más agresiva de todos los WDTC ya que estos pacientes tienen más propensión a desarrollar metástasis nodales y a distancia, recurren más y decrece su capacidad de captar I^{131}.

El **PTC** es el tipo más común de cáncer de tiroides suponiendo el 80-85% de los diagnósticos con una media de edad de entre 40 y 45 años. A diferencia del FTC, el PTC tiende a la diseminación intraglandular con metástasis nodales e invasión local (40-60% de los casos) y menos predisposición a la diseminación hematológica, siendo poco frecuentes, pero más agresivas las metástasis fuera del cuello (5-7% de los casos). El tamaño medio de estos tumores es de 2-3 cm y se define como un tumor maligno epitelial que muestra evidencias de diferenciación folicular y presenta rasgos nucleares distintivos tales como: aspecto esmerilado, pálido y/o vacío, tamaño grande, contorno irregular, hendiduras profundas, nucléolo pequeño y pseudoinclusiones (LiVolsi, 2011; Teijeiro and Sobrinho-Simoes, 2003). Aproximadamente, en el 50% de los casos se observan presencia de cuerpos de psamoma en la lesión, estructuras con calcificaciones concéntricas que se producen por la degeneración de las células neoplásicas (Slough et al., 2006). Dado que no suelen aparecer en FTC o en MTC, su identificación, sobretodo en ganglios linfáticos o tejido peritiroideo, es una característica diagnóstica diferencial del PTC (Hunt and Barnes, 2003; LiVolsi, 2011).

Aun teniendo en cuenta el generalizado buen pronóstico de los pacientes con PTC, en los últimos años se han descrito numerosas variantes histológicas que exhiben un amplio rango de agresividad (Sadow and Hunt, 2011) (Tabla I1). A continuación, comentaremos algunas de las variantes más importantes bien por su grado de agresividad o por su alta incidencia.

La variante menos agresiva es el microcarcinoma papilar (*Papillary Microcarcinoma*, PMC), antes conocido como carcinoma papilar esclerosante oculto, tumor esclerosante no encapsulado o carcinoma papilar oculto (Scopa, 2004). Esta variedad de PTC se caracteriza por su pequeño tamaño (<1 cm), por ser un tumor no encapsulado y por su excelente pronóstico aun cursando, ocasionalmente, con metástasis nodales. A menudo son descubiertos de manera accidental (incidentalomas) durante cirugías o escáneres de cuello (Siddiqui et al., 2016) siendo la causa principal del aumento de la incidencia de PTCs en las últimas décadas.

La variante folicular del carcinoma papilar (*Follicular Variant of PTC*, FVPTC), representa el 9-22% de todos los diagnósticos de PTC. Está formada por folículos de tamaño variable y borde dentado que presentan un patrón de crecimiento multifocal reteniendo las características nucleares típicas del PTC, aunque en muchos casos se presenten total o parcialmente encapsulados (Braunstein, 2012).

Tabla I1 | Variantes del PTC según su pronóstico. Adaptado de (Scopa, 2004).

Bueno	Variable	Malo
• Microcarcinoma • Encapsulado • Macrofolicular	• Folicular • Células oncocíticas • Sólido esclerosante • Sólido trabecular	• Esclerosante difuso • Folicular difuso • Células altas • Células columnares

Por otro lado, dentro de las variantes más agresivas, pero también menos comunes encontramos la variante de células altas (3.8 –10.4%) y la variante de células columnares (0.15 – 0.2%). Como su nombre indica, la principal característica de la variante de células altas es la longitud de las células de la monocapa del folículo siendo como mínimo el doble de una célula folicular normal. Además, el citoplasma suele ser abundante y eosinófilo. Generalmente se suele observar diferenciación oncocítica, crecimiento celular sincitial e invasión capsular o vascular (Gonzalez-Gonzalez et al., 2011). Por su parte y aun presentando células alargadas, la variante de células columnares se diferencia por la estratificación nuclear, una marcada vacuolización subnuclear y un citoplasma claro (Sadow and Hunt, 2011; Scopa, 2004). Ambas variantes se han asociado con la presencia de extensión extratiroidea, recurrencia y metástasis nodales y a distancia (Adeniran and Chhieng, 2016; Kazaure et al., 2012).

En cuanto a los tipos histológicos más agresivos dentro del carcinoma de tiroides encontramos el **carcinoma de tiroides pobremente diferenciado** (*Poorly Differentiated Thyroid Carcinoma*, PDTC) y el carcinoma anaplásico de tiroides (*Anaplastic Thyroid Carcinoma*, ATC). El primero de ellos supone un 4-7% de los casos de cáncer de tiroides y tanto morfológica como funcionalmente, ocupa una posición intermedia (pero sesgada hacia la agresividad) entre el WDTC y el tipo histológico más agresivo, el ATC. Macroscópicamente son tumores grandes (>5 cm), sólidos, no encapsulados, nodulares o multinodulares con tendencia a la invasión de tejidos peritiroideos. Microscópicamente presentan un patrón de crecimiento insular con células hipercromáticas pequeñas, con núcleo de contorno irregular y nucléolo indistinguible (Bongiovanni et al., 2009; Kane and Sharma, 2015).

Finalmente, aun con una baja incidencia (3% de los casos), el **ATC** es la forma más agresiva de cáncer de tiroides siendo responsable de la tercera parte de las muertes debidas a esta enfermedad, con una supervivencia media menor a los 6 meses (Adeniran and Chhieng, 2016; Pinchot et al., 2008; Smallridge et al., 2009). Son tumores muy desdiferenciados, de crecimiento muy rápido con invasión local masiva y tempranas metástasis a distancia, sobre todo a pulmones, glándula adrenal y hueso (Scopa, 2004). Se suelen identificar tres patrones de crecimiento celular (de células fusiformes, gigantes o epidermoides) de manera individual o combinada, con una alta capacidad mitótica, necrótica e invasiva tanto dentro como fuera de la tiroides. Algunos autores han postulado que la aparición de los ATC se debe a una lesión WDTC previa que se desdiferenció y adquirió características más agresivas ya que en muchos casos de ATC se encuentran en zonas con características típicas de los FTC o PTC. Además, muchos ATC se desarrollan como recidivas de un WDTC previamente operado (Giuffrida and Gharib, 2000; Khairy, 2009; Rosai et al., 1985; Wiseman et al., 2007).

De todos los tipos histológicos expuestos, en esta tesis nos centraremos en los FTA y WDTC. Aun habiendo mencionado la importancia de la distinción entre FTC mínimamente invasivo y FTC invasivo, por cuestiones técnicas y estadísticas (reducción drástica del número de pacientes por grupo tumoral), no haremos tal distinción. En cuanto a las variantes histológicas de PTC en este trabajo se utilizarán muestras de PTC clásicos, variante folicular y de células altas. Las características histológicas de las muestras incluidas en cada una de las series utilizadas se detallan en el apartado de materiales y métodos de cada artículo de este compendio.

4.4. Manejo del cáncer de tiroides bien diferenciado

Desde que en los años 60 un grupo de médicos escandinavos introdujeran la **biopsia por punción con aguja fina** (*Fine-Needle Aspiration Biopsy*, FNAB) como sistema para obtener muestras citológicas sobre las que determinar la potencial tumorogénesis de un nódulo tiroideo (Einhorn et al., 1962), su uso se ha extendido por todo el mundo (Bäckdahl et al., 1987). Generalmente hoy en día, cuando el médico endocrinólogo sospecha de la posibilidad de un tumor tiroideo, se realiza una FNAB guiada con ultrasonografía. La biopsia, recogida y extendida en un portaobjetos, es fijada, teñida e inspeccionada por el médico patólogo quien, a partir de la cantidad y morfología de las células, de la presencia de material hemático y de la apariencia, cantidad y distribución del coloide, clasificará la muestra en una de las categorías diagnósticas del sistema Bethesda, véase: insatisfactoria/indeterminada, benigna, atipia de significado indeterminado (AUS)/lesión folicular de significado indeterminado (FLUS), neoplasia folicular (FN)/sospechosa de neoplasia folicular (SFN), lesión sospechosa de malignidad (SM) o maligna (Cibas and Ali, 2009) (Figura I11).

En caso de necesitarlo y con el objetivo de determinar la extensión de la resección quirúrgica, todos los pacientes deben someterse a una evaluación preoperatoria tanto de la tiroides como de los ganglios linfáticos centrales y laterales del cuello mediante ultrasonografía (Kouvaraki et al., 2003; Stulak et al., 2006). El tratamiento inicial general para los pacientes con WDTC suele ser la **tiroidectomía total**, aunque existen otras modalidades dependiendo de la cantidad de resección quirúrgica (tiroidectomía parcial y hemitiroidectomía). La tiroidectomía puede ir acompañada de un vaciamiento ganglionar cervical central o lateral del cuello en el caso de sospecha o confirmación de una metástasis nodal (Cooper et al., 2009; Pacini et al., 2006).

La tiroidectomía total se refiere a la extirpación completa de la tiroides (ambos lóbulos, el istmo y el lóbulo piramidal) mientras que la tiroidectomía subtotal o parcial consiste en una tiroidectomía en la que se deja >1 g de tejido con la cápsula posterior en el lado no comprometido. Finalmente, la hemitiroidectomía se refiere a la resección quirúrgica del lóbulo afectado y del istmo. Hoy en día, a pesar de las pruebas contradictorias acerca de la superioridad oncológica de la tiroidectomía total y de las complicaciones quirúrgicas resultantes de la hemitiroidectomía, ha habido un aumento constante de la proporción de tiroidectomías totales (Mitchell et al., 2007). De hecho, se estima que entorno al 90% de los pacientes con WDTC mayor o superior a 1 cm son tratados con tiroidectomía total en los Estados Unidos (Bilimoria et al., 2007).

Los principales **problemas derivados de la cirugía tiroidea** son el cambio de la voz como consecuencia del daño en la rama externa del nervio laríngeo y el hipoparatiroidismo como consecuencia de lesiones de las glándulas paratiroides o de sus vasos sanguíneos. Igualmente pueden ocurrir infecciones y hemorragias, y en casos extremos obstrucciones de las vías respiratorias (Filho and Kowalski, 2005; Zambudio et al., 2004).

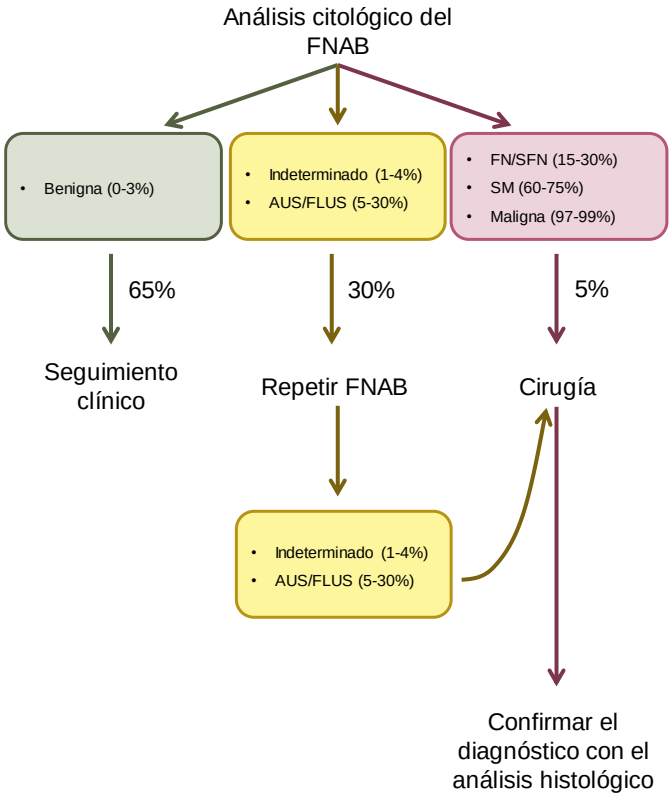

Figura I11 | Manejo de los resultados obtenidos del análisis citológico del FNAB. Las 6 categorías diagnósticas Bethesda están agrupadas de acuerdo al modo de actuación. Junto a cada categoría aparece el porcentaje de casos que malignizan, mientras que el porcentaje de casos de cada grupo aparece debajo de cada grupo. Atipia de significado indeterminado (AUS)/lesión folicular de significado indeterminado (FLUS), neoplasia folicular (FN)/Sospechosa de neoplasia folicular (SFN), Figura modificada de (Cibas and Ali, 2009).

En el **postoperatorio** se determina el estadio tumoral (TNM) y en consecuencia el tratamiento adyuvante más adecuado (Sobin et al., 2009). Los tratamientos más comunes son la ablación con yodo radioactivo (*Radioactive Iodine*, RAI) y/o supresión de TSH, el objetivo es evitar la proliferación del posible tejido tiroideo remanente. El **tratamiento con RAI** empieza a partir de la cuarta o sexta semana después de la cirugía. Siempre y cuando NIS funcione correctamente, las células remanentes y/o las metastáticas absorberán y concentrarán RAI, muriendo como consecuencia de la radiación emitida. Sin embargo existe un porcentaje de pacientes (~5%) que son refractarios al RAI, es decir, que no responden a dicho tratamiento (Ricarte-Filho et al., 2009). El WDTC refractario a RAI (*Radioiodine Refractory Well-Differentiated Thyroid Carcinoma*, RAI-R-WDTC) es un

desafío ya que el pronóstico es limitado y las opciones de tratamiento escasas. Recientemente, los ensayos clínicos con terapias dirigidas han mejorado las perspectivas de estos pacientes mediante la inhibición de VEGF (*vascular endothelial growth factor*) a partir de inhibidores de tirosina quinasa entre los que se encuentran los famosos Sorafenib y Lenvatinib (Narayanan and Colevas, 2016).

Por otro lado, tras el tratamiento con RAI, y dado que la glándula tiroidea ha sido extirpada total o parcialmente, se inicia el tratamiento con L-tiroxina (L-T4 sintética o 3,5,3',5'-tetrayodo-L-tironina) con dos objetivos: (1) la sustitución hormonal, para corregir el hipotiroidismo inducido por la cirugía; y (2) la supresión hormonal, para reducir los niveles séricos de TSH, la cual puede estimular el crecimiento del tejido tumoral remanente (Biondi et al., 2005). Dado los efectos adversos que puede producir el tratamiento prolongado con L-T4, la administración de dosis supresivas es necesaria solamente cuando hay evidencia de recurrencia o persistencia de la enfermedad. En cambio, en los pacientes con WDTC de bajo riesgo (sin recurrencia, persistencia o metástasis), el tratamiento sirve para mantener unos niveles normales de TSH (Biondi et al., 2005). Es importante, además, adaptar la dosis de L-T4 a cada paciente en particular (Mistry et al., 2011).

Tabla I2 | Clasificación según el riesgo de recurrencia inicial de la ATA. Adaptado de (Martínez et al., 2014).

Bajo	Intermedio	Alto
Todos los siguientes están presentes • Ausencia de metástasis locales o a distancia • Resección de todo el tumor macroscópico • Ausencia de invasión loco-regional de tejidos o vascular • Tumor sin histología agresiva • Ausencia de captación de yodo fuera del lecho tiroideo tras el tratamiento con RAI	Alguno de los siguientes está presente • Invasión microscópica de tejido peritiroideos blandos • Metástasis en ganglios linfáticos cervicales • Captación de yodo fuera del lecho tiroideo tras el tratamiento con RAI • Tumor con histología agresiva	Alguno de los siguientes está presente • Invasión tumoral macroscópica de tejidos peritiroideos blandos • Resección tumoral incompleta • Metástasis a distancia

Finalmente, y tras la remisión total del tejido tumoral, se inicia un **periodo de seguimiento** que será más o menos extenso dependiendo del nivel de riesgo de recurrencia de los pacientes (Tabla I2) (Martínez et al., 2014). El reto actual en el manejo del cáncer de tiroides radica en la detección precisa de aquellos pacientes que no responderán correctamente a los tratamientos adyuvantes existentes o que desarrollarán metástasis y/o recidivas. Como se ha comentado anteriormente, estos casos complicados

son los menos frecuentes en cáncer de tiroides. Por lo tanto, para mantener en todo lo posible la calidad de vida del paciente, así como para evitar las molestias postquirúrgicas, sería conveniente detectar este tipo de complicaciones en las biopsias previas a la cirugía (FNAB). En consecuencia, la aplicación de las nuevas técnicas de biología molecular (GWAS, secuenciación masiva, *arrays* de expresión y metilación, etc.) que han demostrado su sutilidad en muchos tipos tumorales (Bock, 2009; Friedman et al., 2015; Simon and Roychowdhury, 2013), podrían ser de gran ayuda en el descubrimiento de biomarcadores de pronóstico y de respuesta a tratamiento más eficientes. En el apartado 5.2 se comentarán en profundidad los tipos de biomarcadores moleculares actuales en WDTC.

4.5. Alteraciones moleculares

El cáncer de tiroides esporádico está estrechamente relacionado con la desregulación, tanto genética como epigenética, de dos de las vías de señalización centrales en la supervivencia, diferenciación, proliferación, metabolismo y movilidad celular: la vía de las MAP cinasas o MAPK (*mitogen-activated protein kinases*) y la de la PI3K-AKT (*phosphoinositide 3-kinase/protein kinase B*) (Brehar et al., 2013; Nikiforov and Nikiforova, 2011). Dado el papel central de ambas vías en el control de la homeostasis celular, la consecuencia de su desregulación es la alteración de multitud de procesos celulares que llevan a la adquisición de las capacidades necesarias para el desarrollo de un tumor descritas por Hanahan y Weinberg y comentadas en el apartado 2 (Dhillon et al., 2007; Hanahan and Weinberg, 2011, 2000).

Si bien la frecuencia media de mutaciones somáticas encontradas en el WDTC es relativamente baja (<1 mutación somática/MB) en comparación con otros tumores (Alexandrov et al., 2013; Lawrence et al., 2013) sabemos que las mutaciones puntuales y reordenamientos génicos en efectores clave de estas vías de señalización (*BRAF*, *RAS*, *RET*/*PTC*) son capaces de iniciar un proceso tumoral por sí mismas (mutaciones conductoras) y de manera excluyente, es decir, muy rara vez (<0.1%) encontramos un tumor con más de una mutación conductora (Kimura et al., 2003; Soares et al., 2003). Es importante destacar que las diferentes mutaciones están asociadas no solamente a características clínicas y biológicas determinadas, sino que se asocian a tipos histopatológicos específicos. Así, la mutación $BRAF^{V600E}$ y la translocación *RET*/*PTC* se asocian a PTC mientras que las mutaciones en los genes *RAS* lo hacen a FTC (Adeniran et al., 2006).

La prevalencia de las mutaciones de ***BRAF*** en PTC es del 40-45%, mientras que en FTC es inferior al 2% (Kebebew et al., 2007). Sin embargo, de entre todas las mutaciones descritas en el gen *BRAF* (Wan et al., 2004), más del 90% consisten en la transversión T1799A que conlleva la sustitución del aminoácido neutro valina por ácido glutámico (carga negativa) en la posición 600 ($BRAF^{V600E}$) (Rebaï and Rebaï, 2016). La consecuencia molecular de esta mutación es la mimetización de la fosforilación Thr599/Ser602 requerida durante la activación normal de $BRAF^{WT}$. Esto hace que la proteína codificada por $BRAF^{V600E}$ esté constitutivamente activa, lo que, a su vez, mantiene activa la vía de las MAPK independientemente de señalización extracelular (Figura I12a-b). El resultado es la expresión descontrolada de genes relacionados con el crecimiento, supervivencia y diferenciación celular (Lito et al., 2013; Puxeddu et al., 2003; Zhang and Liu, 2002). Más recientemente se han identificado algunos casos (2.7%) en los que *BRAF* se fusiona con diferentes genes tales como *HOOK3, SND1* o *MKRN1*, adquiriendo la capacidad de activar la vía de las MAPK (Cancer Genome Atlas Research Network et al., 2014; Ciampi et al., 2005; Lee et al., 2012).

Por otro lado, se ha observado la presencia de mutaciones puntuales activadoras de los genes ***RAS*** (*HRAS, KRAS, NRAS*) tanto en FTA (20-40%) como en FTC (25-45%) y en la variante folicular de PTC (15-45%) apoyando el argumento de que estas mutaciones son un evento temprano en el desarrollo de tumores tiroideos (Tavares et al., 2015; Vasko et al., 2003; Vu-Phan and Koenig, 2014). Curiosamente, las mutaciones descritas en estos genes siempre se dan en los codones 61, 12 o 13, siendo las mutaciones en $NRAS^{Q61}$ las más frecuentes (51.2%), seguidas por $KRAS^{G12}$ (19%), $HRAS^{Q61}$ y $KRAS^{G13}$ (~8% ambas) (Howell et al., 2013; Prior et al., 2012). La consecuencia de todas estas mutaciones es la evasión de la inactivación de RAS lo que provoca que dicha proteína permanezca permanentemente activa (Anexo 1.2).

RAS es capaz de activar una amplia colección de vías de señalización basadas en cascadas de fosforilación, entre las que encontramos la vía de las MAPK y la de la PI3K-AKT. Del mismo modo en el que RAS inicia la cascada de las MAPK mediante la activación de BRAF por fosforilación, es capaz de fosforilar y activar la subunidad catalítica p110 de PI3K (clase I) iniciando la cascada de fosforilaciones en esta vía (Castellano and Downward, 2011) (Figura I13). Cabe destacar que, así como KRAS activa la vía de las MAPK de manera preferencial, NRAS y sobre todo HRAS activan la de la PI3K-AKT (Caró et al., 2005; Haigis et al., 2008; Whitwam et al., 2007). Esto parece ser debido a diferencias en el tipo de anclaje de las proteínas RAS a la membrana plasmática lo que comporta una compartimentalización de sus actividades (Prior and Hancock, 2001).

Hasta el momento, no existe ninguna publicación que ponga de manifiesto este hecho en cáncer de tiroides. No obstante, se sabe que, en la gran mayoría de WDTC con mutación en *RAS*, mayoritariamente se desregula la vía PI3K-AKT, lo que concuerda con el hecho de que, como hemos comentado anteriormente, la mutación mayoritaria es la de *NRAS*^{Q61}.

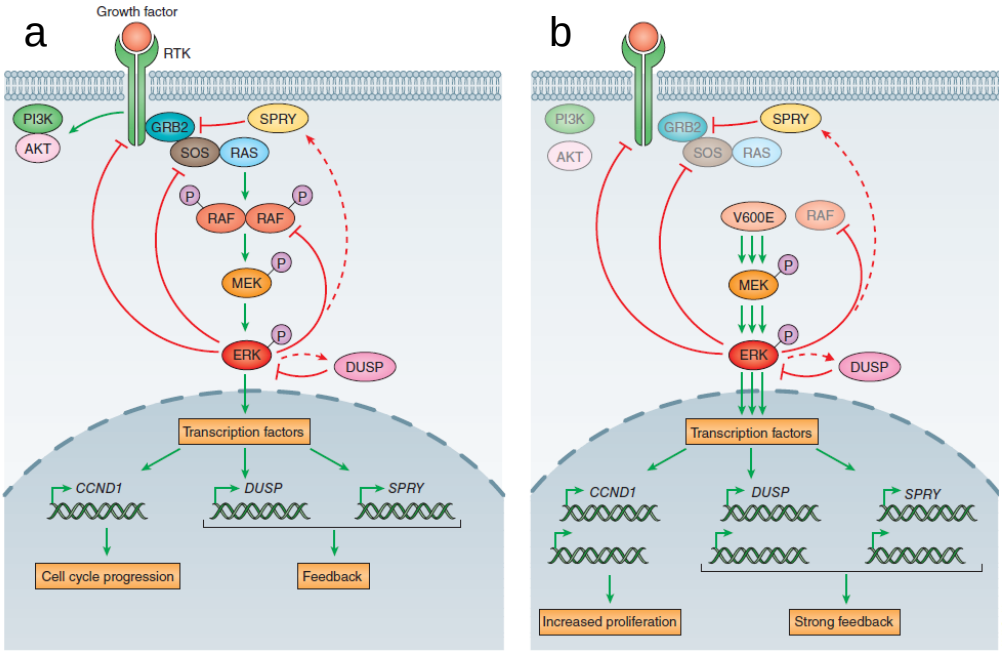

Figura I12 | Regulación de la vía de las MAPK en condiciones fisiológicas y en células mutantes *BRAF*^{V600E}. (a) En condiciones fisiológicas, la unión de ligandos a la fracción extracelular del receptor de tirosina cinasa (RTK) provoca la autofosforilación de su fracción intracelular, lo que conlleva el reclutamiento de complejos proteicos como GRB2-SOS a la membrana plasmática (Puxeddu et al., 2003). A su vez, SOS activa RAS mediante el intercambio del GDP unido a RAS por GTP lo que desencadena la activación de la cascada de fosforilación de la vía de las MAPK. RAS-GTP promueve la dimerización y activación de RAF la cual fosforila y activa a MEK1-2 y estas a ERK1-2, la que es capaz de activar a numerosos sustratos citoplasmáticos y nucleares (incluyendo factores de transcripción) que regulan a su vez la expresión de genes responsables de múltiples procesos celulares tales como proliferación, diferenciación y supervivencia. Además, ERK activa puede regular la vía mediante un ciclo de retroalimentación negativa que le inhibe de manera directa (DUSP) o indirecta, inhibiendo algunos efectores de la vía (RTK, GRB2, SOS, RAF). **(b)** En células con la mutación *BRAF*^{V600E}, la vía se mantiene constantemente activa independientemente de la presencia de ligando extracelular, ERK activa es incapaz de inhibir a BRAF^{V600E} debido a la conformación mutante que la mantiene constitutivamente activa de manera que desaparece la retroalimentación negativa lo que conlleva una sobreactivación de los genes diana de ERK estimulando la proliferación y la evasión de la apoptosis. Figura extraída de (Lito et al., 2013).

En cuanto a la reordenación génica ***RET/PTC***, sabemos que puede ser clonal, distribuyéndose de manera más o menos homogénea y afectando a la mayor parte de las células tumorales, o no clonal, afectando a pequeñas fracciones del tumor. La prevalencia media en PTC de ambas formas de esta reordenación es del 10-20% mientras que en FTA y otras lesiones tiroideas no neoplásicas sólo ocurre la forma no clonal con una

prevalencia media de 10-45%. Sin embargo, estos porcentajes varían bastante dependiendo de la sensibilidad de los métodos de detección y del sesgo que pueden tener las series estudiadas debidas a factores tales como la exposición a radiación ionizante (50-80%) o PTCs pediátricos (40-70%) (Nikiforov, 2011; Romei and Elisei, 2012).

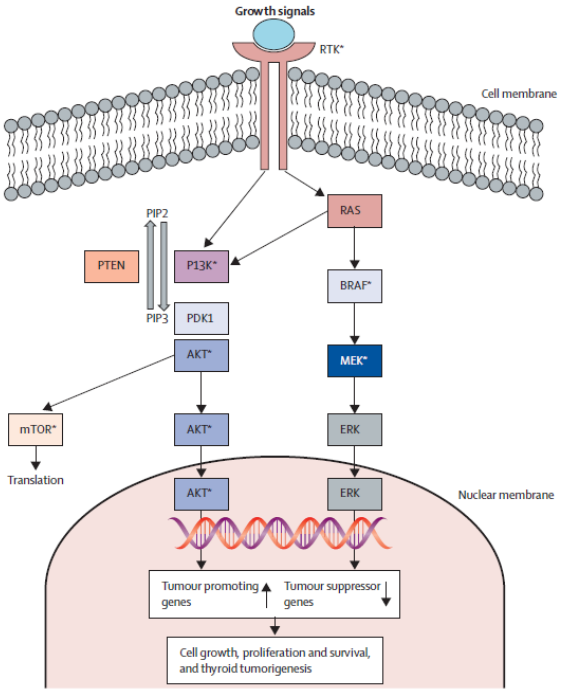

Figura I13 | Principales vías de señalización afectadas en WDTC. Los receptores tirosina cinasa (RTK) de la membrana plasmática transducen la información de las señales extracelulares (factores de crecimiento, supervivencia, diferenciación, etc.) en señales intracelulares a través de dos cascadas de señalización: la vía de las MAPK (derecha) y la de la PI3K-AKT (izquierda). El gen *RAS* actúa como un acoplador dual de señales pudiendo recoger la información transmitida por RTK y enviarla tanto a la vía MAPK como a PI3K-AKT. Figura extraída de (Xing et al., 2013b).

Esta translocación se debe a la fusión del dominio 3' catalítico tirosina cinasa del protoncogén *RET* (*rearranged during transfection*), localizado en 10q11.2 y la región 5' de varios genes no relacionados (Anexo 1.3). De entre todas las translocaciones encontradas, las más comunes (60-70%) son *RET/PTC1* que involucra a *CCDC6* (*coiled-coil domain-containig gene 6*) y *RET/PTC3* (20-30%) que implica a *NCOA4* (*nuclear receptor co-activator 4*) y está altamente relacionada con exposiciones a radiación ionizante (Nikiforov, n.d.; Dillwyn Williams, 2008). Estas translocaciones no sólo provocan la expresión ectópica del gen *RET* sino que proporcionan un dominio de dimerización que, mediante la autofosforilación de diversos residuos tirosina, permite la activación de RET independiente de sustrato (Jhiang, 2000; Tong et al., 1997). La activación de las vías de señalización (principalmente MAPK y PI3K-AKT) depende en gran medida de la posición de los residuos de tirosina que se autofosforilan ya que en cada uno de ellos se acoplan efectores diferentes de dichas vías (Willem de Groot et al., 2006).

Menos frecuente es el reordenamiento *PAX8*/*PPARγ* llamado **PPFP**. Se da en un 30-40% de FTCs y en un 2-13% de FTAs, siendo extremadamente raro en PTCs (1%) y ligeramente más frecuente en la variante folicular de PTC (1-5%) (Rebaï and Rebaï, 2016). Este reordenamiento, al igual que el *RET/PTC*, parece estar asociado a edades tempranas, pero también a invasión vascular y tumores pequeños (Omur and Baran, 2014).

Como se comentó en el apartado 3.2, *PAX8* (*paired box 8*) es uno de los factores de transcripción tiroideos importantes en el desarrollo de la glándula tiroides. La translocación t(2;3)(q13;p25) tiene lugar entre la región codificante 5' de *PAX8* con prácticamente todo el gen que codifica el receptor de peroxisoma-proliferador-activo gamma (*nuclear receptor peroxisome proliferator-activated receptor-gamma*, *PPARγ* (Kroll, 2000; Kroll et al., 2000). Se cree que PPFP podría actuar, dependiendo de su gen diana y del contexto celular, bien como un inhibidor dominante negativo de PPARγ o bien como un factor de transcripción similar a PPARγ (Raman and Koenig, 2014).

Recientemente Mingzhao Xing y sus colaboradores han descrito la frecuencia, relativamente elevada en cáncer de tiroides, de mutaciones en el promotor del gen que codifica para la **transcriptasa telomérica reversa** (*telomerase reverse transcriptase*, *TERT*) (X. Liu et al., 2013). La frecuencia de estas mutaciones está claramente asociada a la agresividad del tumor, siendo nula en lesiones benignas, algo mayor en WDTC (12-14%) y bastante elevada en PDTC y ATC (38-46%) (Liu and Xing, 2016).

La proteína codificada por este gen es la subunidad catalítica de la telomerasa, cuya función consiste en la adición en tándem de la secuencia TTAGGG al final de los cromosomas manteniendo su integridad y por extensión estabilizando el genoma (Moyzis et al., 1988). Tal y como descubrieron los ganadores del premio Nobel de medicina de 2009 Elizabeth H. Blackburn, Carol W. Greider y Jack W. Szostak, la telomerasa se va agotando con cada ciclo celular. Esto hace que los telómeros se vayan acortando hasta llegar a un punto crítico a partir del cual la célula entra en senescencia y muere. No obstante, se ha encontrado una reactivación de la telomerasa en muchos tipos de cáncer, hecho que permitiría a las células tumorales sortear la senescencia y continuar ciclando (Blackburn et al., 2006). Parece ser que mutaciones en el promotor del gen *TERT* (principalmente C2228T y C250T) generarían un lugar de unión para el factor de transcripción ETS (*E-twenty-six*) responsable de la reactivación transcripcional del gen.

Finalmente, mucho menos frecuentes son las mutaciones en los genes supresores de tumores *PTEN* y *TP53*, en el gen que codifica para la proteína de adhesión celular catenina beta (CTNNB1), en el receptor de neurotrópico de tirosina quinasa (NTRK1), en el recientemente descubierto gen conductor *EIF1AX* o en genes mitocondriales como *NDUFA13* (Brehar et al., 2013; Cancer Genome Atlas Research Network et al., 2014). Hasta la publicación del estudio integral del consorcio TCGA (*The Cancer Genome Atlas*) se desconocía los factores iniciadores oncogénicos del 25-30% de los casos de PTC, eran los llamados «casos opacos» (*dark matter cases)*. Gracias al profundo estudio realizado por el TCGA se ha podido reducir el porcentaje de opacidad al 3.5% (Figura I14). Más aún, en 9 de los 14 casos opacos, se detectaron mutaciones potencialmente conductoras en genes como *APC*, *ATM*, *NF1*, *SPOP* o *MLL* (Cancer Genome Atlas Research Network et al., 2014).

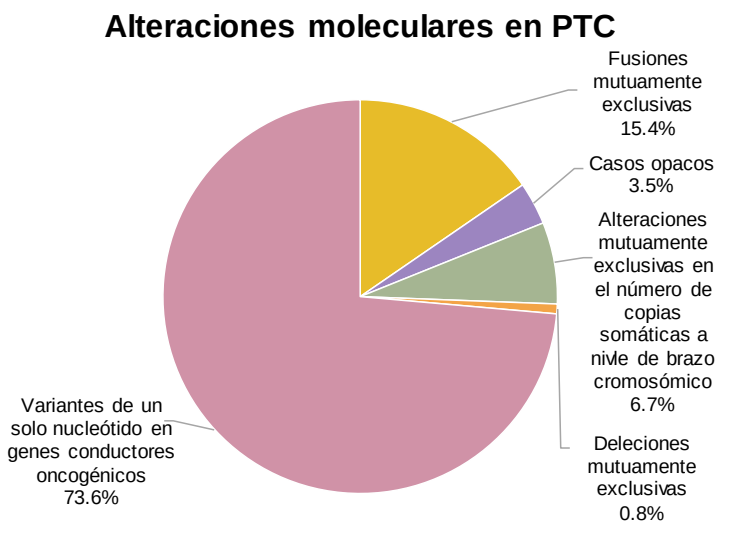

Figura I14 | Resumen de las alteraciones moleculares en la serie PTC del TCGA. Extraído de (Cancer Genome Atlas Research Network et al., 2014).

En los últimos años, numerosas publicaciones han demostrado el papel central de la epigenética en WDTC (Cancer Genome Atlas Research Network et al., 2014; Kikuchi et al., 2013; Rodríguez-Rodero et al., 2013). No es de extrañar que muchas de las alteraciones encontradas afecten a efectores de las vías MAPK y PI3K-AKT subrayando el papel central de estas cascadas de señalización en el desarrollo y progresión del WDTC (D. Liu et al., 2013; Russo et al., 2011; Schagdarsurengin et al., 2010; White et al., 2016).

La metilación del DNA es una de las marcas epigenéticas más estudiadas en cáncer de tiroides. Concretamente se ha observado la hipermetilación de las regiones promotoras y el consecuente silenciamiento de múltiples genes (Tabla I3) relacionados

con la función tiroidea (*TG*, *TPO*, *NIS* y *TSHR*) cuyo silenciamiento se ha postulado que podría influir en la captación y almacenamiento normal de yodo, haciendo inefectivo el tratamiento de ablación con RAI (J. A. Smith et al., 2007; Xing et al., 2003b). También se han encontrado reprimidos, por metilación de sus promotores, genes supresores de tumores como *PTEN* involucrado en la desfosforilación de PIP3 en la vía de la PI3K-AKT (Alvarez-Nuñez et al., 2006), *RASSF1A* que, entre otras funciones inhibe la acumulación de ciclina D1 bloqueando la progresión del ciclo celular (Xing et al., 2004) o el regulador del crecimiento celular *RAPβ2* (Hu et al., 2006). Asimismo la represión transcripcional del inhibidor de metaloproteinasas 3 (*TIMP3*), involucrado en invasión y migración tumoral, también es un evento común en cáncer de tiroides (Anania et al., 2011).

Tabla I3 | Prevalencia de genes hipermetilados en WDTC. Adaptado de (Faam et al., 2015).

Gen	Prevalencia	Referencia
PTEN	• 50% PTC • 100% FTC	(Alvarez-Nuñez et al., 2006)
RASSF1A	• 30% WDTC	(Xing et al., 2004)
TIMP3	• 53% PTC	(Hu et al., 2006)
DAPK	• 34% PTC	(Hu et al., 2006)
RAPβ2	• 22% PTC	(Hu et al., 2006)
RAP1GAP	• 72% PTC • 38% FTC	(Zuo et al., 2010)
NIS	• 53.8% WDTC	(Stephen et al., 2011)
TSHR	• 59% PTC • 47% FTC	(Xing et al., 2003b)

Por otro lado, y gracias a las nuevas tecnologías de análisis global (*genome-wide analysis*) de la metilación del DNA mediante *arrays* de metilación, se han publicado varios estudios en los que se han determinado los diferentes perfiles de metilación asociados no solo a los diferentes tipos histológicos de cáncer de tiroides sino también a la mutación conductora subyacente (Cancer Genome Atlas Research Network et al., 2014; Ellis et al., 2014; Kikuchi et al., 2013; Rodríguez-Rodero et al., 2013). Entre ellos destaca nuestro trabajo llevado a cabo sobre 83 muestras tumorales y 8 muestras de tejido normal adyacente al tumor que forma parte de los resultados de esta tesis (Mancikova et al., 2014).

Aunque existen pocos trabajos sobre el papel que juegan las modificaciones de las histonas en la tumorogénesis tiroidea, se ha observado que el tratamiento de varias líneas celulares de cáncer de tiroides con inhibidores de histona deacetilasas (*histone*

deacethylases, HDACs) provoca un aumento de la acetilación de histonas promoviendo la expresión de *NIS*, *TPO* y *TG*, aumentando así la captación de yodo (Furuya et al., 2004; Kitazono et al., 2001). Igualmente, este tipo de tratamientos inhiben el crecimiento de las células cancerosas, promoviendo la apoptosis, a través de la activación de la cadena de caspasas y la detención del ciclo celular, a partir de la reducción de las ciclinas dependientes de quinasa (CDK-2 y CDK-1) (Greenberg et al., 2001). También se ha observado la capacidad de los inhibidores de HDACs para inducir la expresión de cadherin-E contribuyendo a la disminución de la invasión y migración celular (Catalano et al., 2012). Recientemente, se ha demostrado que la sobreexpresión de la histona-lisina metiltransferasa *EZH2*, perteneciente al grupo de proteínas Policomb[3] (PcG), contribuye directamente al silenciamiento de *PAX8* en ATC (Borbone et al., 2011).

Por lo que respecta a los ncRNAs numerosos trabajos han señalado la importancia de los miRNAs en el desarrollo y progresión tumoral. Así pues, la sobreexpresión de miR-146b, miR-221 y miR-222 en PTC se ha asociado a la pérdida de expresión de c-Kit, un receptor de tirosina quinasa con un importante papel en la regulación y diferenciación del PTC (He et al., 2005). Por otro lado mientras que miR-197 y miR-346 parecen estar involucrados en la transición entre FTA y FTC (Weber et al., 2006), Mancikova *et al.*, propusieron un modelo en el que la disminución de la expresión de miR-192 junto con la sobreexpresión de let-7a se asociaba a un aumento del riesgo de recidiva en pacientes con WDTC (Mancikova et al., 2015). Finalmente, se ha demostrado que la desregulación de algunos lncRNAs como THCAT126, NR_036575.1, MEG3 o PVT1, entre otros, están activamente involucrados en la tumorogénesis tiroidea (Iyer et al., 2015; Sun et al., 2016; Wang et al., 2015; Zhou et al., 2016).

[3] Las proteínas del grupo Policomb (PcG) son un conjunto de proteínas estructual y funcionalmente diversas que forman grandes complejos multiméricos. Se cree que estos complejos, agrupados principalmente en PRC1 y PRC2, son capaces de reconocer y mediar la deposición de múltiples modificaciones postraductionales de las colas de las histonas, colaborando no solo en la represión transcripcional de múltiples genes mediante alteración local de la cromatina sino también en procesos de remodelación de la compactación de orden superior de la cromatina (Whitcomb et al., 2007).

5. Marcadores moleculares

5.1. Definición y utilidad de los marcadores moleculares

"Si el médico entiende los males que está padeciendo el enfermo y conoce los que han de venir durante su enfermedad, dirigirá con acierto la curación"

(El libro de los pronósticos. Hipócrates, 400 a.C.)

Uno de los principales desafíos de la medicina desde hace cientos de años es el perfeccionamiento de la capacidad de predecir el resultado final de un paciente dada la observación del estado actual del mismo (Burke, 2016). Esta inferencia debe realizarse en base al análisis de una serie de características informativas que nos den la probabilidad empírica del resultado futuro de un paciente a partir del estado presente del mismo. Por ello, desde hace siglos se vienen utilizando los llamados marcadores biológicos o **biomarcadores**, características o cambios fisiológicos, bioquímicos o morfológicos medibles y evaluables a nivel molecular bioquímico o celular, que actúan como indicadores de un proceso biológico normal o patológico o como respuesta a una intervención terapéutica (Atkinson A.J. et al., 2001). Por ejemplo, altos niveles de glucosa, en suero tras 12 horas de ayuno es un biomarcador de diagnóstico de diabetes, un elevado nivel de troponina sérica es un biomarcador de daño cardiovascular y el alto nivel de tirotropina es la principal característica de hipotiroidismo (Diamandis, 2010).

Los biomarcadores se pueden clasificar de acuerdo a muchas características, sin embargo, en esta tesis hablaremos en términos de dos de ellas: según la información que proporcionan y según su naturaleza. Así, dentro de la primera clasificación encontramos en primer lugar, a los biomarcadores de riesgo, aquellos que informan sobre la predisposición de padecer una patología, en segundo lugar, a los biomarcadores diagnósticos, que revelan la naturaleza del estado de un paciente (enfermedad, síndrome, exposición atóxicos, etc.), en tercer lugar, a los biomarcadores de pronóstico, que informan sobre la progresión de dicho paciente, y finalmente, a los biomarcadores de respuesta a tratamiento que predicen la mejora o empeoramiento de un paciente tras un tratamiento dado (Braunwald, 2009; Ludwig and Weinstein, 2005; Mayeux, 2004).

En cuanto a la clasificación según su naturaleza, los biomarcadores pueden ser genéticos (p.ej. mutaciones, translocaciones o polimorfismos), transcriptómicos o proteómicos [p.ej. análisis del antígeno prostático específico en cáncer de próstata (Saini, 2016)], metabólicos [p.ej. medida de SAM y ácido pipecólico en la saliva en cáncer oral

(Ishikawa et al., 2016)] o epigenéticos [p.ej. metilación del promotor del MGMT (Zhang et al., 2013)].

Un **biomarcador molecular ideal** debe ser detectado y cuantificado de manera objetiva con un riesgo nulo o muy bajo para el paciente. Para facilitar su análisis rutinario debe ser bioquímicamente estable, económico y clínicamente impactante. Finalmente, debe aportar nueva información diagnóstica, pronóstica y terapéutica a la obtenida a partir de los datos clínicos (Ask et al., 2015). Este último punto es crucial dado que en los últimos años estamos intentando avanzar hacia una medicina predictiva y personalizada. Esto implica el desarrollo de biomarcadores individuales o paneles de biomarcadores que señalen tanto las causas de la enfermedad como el tipo de tratamiento y la dosis más adecuados para cada paciente en particular.

Los avances en las tecnologías de biología molecular han permitido el desarrollo de toda una serie de ciencias conocidas como **ómicas**, neologismo proveniente del inglés que en biología hace referencia al estudio de la totalidad o del conjunto de algo (genómica, proteómica, transcriptómica, metabolómica, epigenómica, etc.). Gracias a la aplicación de estas técnicas ha habido una explosión en el número de biomarcadores descubiertos en ensayos preclínicos, con el potencial para mejorar el tratamiento y reducir los costes de la asistencia sanitaria. De hecho, la Sociedad Americana de Oncología Clínica (ASCO) recomendó en 2009 el análisis rutinario de la mutación *KRAS* en todos aquellos pacientes con cáncer de colon metastático, candidatos para el tratamiento con anti-EGFR. Esto se debe a que los pacientes con dicha mutación no responden a esta terapia, lo que ahorraría aproximadamente 7500$ por paciente (Kircher et al., 2014). Sin embargo, la explosión de biomarcadores no ha ido acompañada de un aumento en su uso clínico (Figura I15) (Drucker and Krapfenbauer, 2013). Esto se debe a que, la transferencia de biomarcadores desde su descubrimiento en los laboratorios de biología molecular, hasta su aplicación en la práctica clínica, está sujeta a numerosos obstáculos tanto estructurales como científicos [revisado en (Diamandis, 2010)].

Los requisitos que debe cumplir un biomarcador para considerarse apto son muy exigentes. Por ejemplo, un biomarcador de diagnóstico temprano de cáncer, debe poder ser fácilmente detectado en tumores asintomáticos para evitar falsos negativos, lo que muchas veces constituye un oxímoron. Debe ser específico de tejido para evitar falsos positivos y para no ver comprometida su utilidad, no debería estar afectado por otras enfermedades. Además, el flujo de acontecimientos desde el diseño experimental (correcta selección de los grupos experimentales y controles, de sus características

clínicas, de las técnicas utilizadas, etc.), pasando por la logística de transporte, almacenamiento y manipulación de las muestras, hasta los análisis estadísticos e interpretación de los datos, están sujetos a alteraciones que pueden provocar sesgos en los resultados finales. Es pues, responsabilidad tanto de los investigadores como de los revisores de las revistas científicas, el percatarse de los posibles puntos débiles de la investigación e intentar mejorar la eficiencia en la identificación y validación de potenciales biomarcadores (Diamandis, 2010).

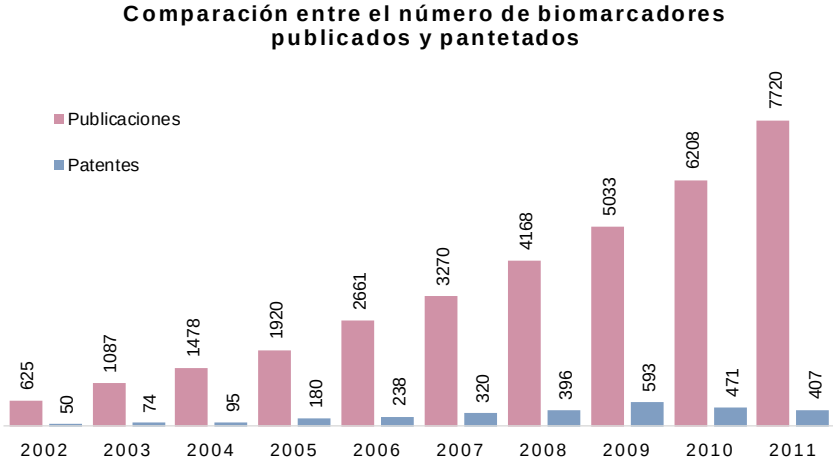

Figura I15 | Relación entre el número de biomarcadores publicados y patentados en el periodo 2002–2011. Figura modificada de (Drucker and Krapfenbauer, 2013).

5.2. Marcadores moleculares en cáncer de tiroides

Idealmente, un biomarcador individual o un panel de biomarcadores de cáncer tiroideo debería poder distinguir entre un nódulo benigno y los diferentes tipos de nódulos malignos. Además, debería ser capaz de diferenciar entre aquellos tumores malignos que cursarán con metástasis nodales o a distancia, así como aquellos casos con alta probabilidad de recurrencia o, menos probable en cáncer de tiroides, muerte. Igualmente, debería poder ser detectado en muestras preoperatorias como suero o FNAB.

Muchas de las alteraciones comentadas en el apartado 4.5 han sido propuestas como biomarcadores de diagnóstico o pronóstico. La posibilidad de analizar algunas de estas alteraciones en muestras prequirúrgicas como FNABs es una realidad que puede mejorar el diagnóstico, especialmente en aquellos casos con biopsias indeterminadas. En este sentido, Nikiforov *et al.* fueron los primeros en proponer la aplicación sistemática de los análisis de las **mutaciones oncológicas conductoras** en los aspirados tiroideos

(Nikiforov et al., 2011, 2009; Yip et al., 2012). Desde entonces numerosos trabajos han revelado su utilidad. Concretamente, la mutación *BRAF*^{V600E} se ha alzado como un buen marcador diagnóstico de la presencia de PTC, con valores medios de sensibilidad, especificidad, precisión, valor predictivo positivo y valor predictivo negativo especialmente buenos (52.4%, 97.9%, 70.5%, 99.9% y 51.6%, respectivamente) (Rodrigues et al., 2012). Sin embargo y aunque numerosas publicaciones han apuntado a que la mutación *BRAF*^{V600E} está asociada a mal pronóstico (invasión extratiroidea, tumores multicéntricos, presencia de metástasis ganglionares, recidiva y persistencia de la enfermedad) (Howell et al., 2011; Rinaldi et al., 2012; Xing et al., 2013a), otras muchas no indican tal asociación (Fugazzola et al., 2006; Li et al., 2012; Zoghlami et al., 2014), por lo que su utilidad como marcador de pronóstico aún está por determinar. No obstante, recientemente, Xing *et al.*, han descrito una gran asociación entre las mutaciones en el promotor del gen *TERT* y características de mal pronóstico, especialmente en aquellos tumores donde la mutación *BRAF*^{V600E} está presente (Xing et al., 2014). Por otro lado, ni *RAS* ni *PAX8*/*PPAR*γ se consideran biomarcadores tumorales específicos en tanto que pueden encontrarse en adenomas. Aun así, adenomas con estas alteraciones se han considerado como lesiones premalignas y la tiroidectomía está mayoritariamente aceptada (Melillo and Santoro, 2012).

Los **marcadores inmunohistoquímicos** solos o combinados en paneles, parecen aportar una buena información diagnóstica y pronóstica siendo, además, fácilmente incorporables en los laboratorios de anatomía patológica. Así pues, la sobreexpresión de CK19 y RET o la infraexpresión de P27 son característicos de PTC (De Matos et al., 2005; Dunderovic et al., 2015; Mai et al., 2001), mientras que un aumento de Ki67 y BCL2 y una disminución de cadherin-E están asociados a FTC (Brecelj et al., 2005; De Matos et al., 2005; Hoos et al., 2002; Kato et al., 2002; Khoo et al., 2002).

Por lo que respecta a **marcadores basados en la expresión génica**, en los últimos años, ha salido al mercado Afirma®, un test preoperatorio en formato de *microarray* que analiza la expresión de más de 100 genes y que está pensado para facilitar la toma de decisión sobre la necesidad o no, de realizar una tiroidectomía (Chudova et al., 2010). El test identifica la firma transcripcional de nódulos benignos con un 95% de valor predictivo negativo en los FNABs clasificados como atipia de significado indeterminado/lesión folicular de significado indeterminado (AUS/FLUS), un 94% en los clasificados como neoplasia folicular (FN) y un 85% en los sospechosos de malignidad (SM) (Alexander et al., 2012; Lastra et al., 2014). Aunque algunos autores afirman la gran utilidad de Afirma® (Alexander et al., 2012; Harrell and Bimston, 2014; Lastra et al., 2014) muchos otros la

desmienten, debido a discrepancias en el valor predictivo positivo de esta firma (McIver et al., 2014; Villabona et al., 2016).

En cuanto a los **biomarcadores epigenéticos**, el silenciamiento mediado por hipermetilación de los genes supresores de tumores *TIMP3*, *SLC5A8* y *DAPK* se ha asociado a mal pronóstico en PTCs, debido a un aumento en la invasión extratiroidea, metástasis nodal y a distancia, multifocalidad y angiogénesis (Xing, 2007). Así mismo, aunque no existe una evidencia completa, diversos autores apuntan a que el silenciamiento por metilación del DNA, tanto de *NIS* como de *TSHR*, podría estar detrás de los casos de tumores refractarios al tratamiento con RAI (Venkataraman et al., 1999; Xing et al., 2003b). Por lo tanto, su detección tanto en muestras pre- como postquirúrgicas podría indicar la utilidad de los tratamientos adyuvantes clásicos. Así mismo, varios trabajos han demostrado el valor de los miRNAs como biomarcadores diagnósticos y pronósticos tanto en muestras histológicas como en FNABs (Chen et al., 2008; Chou et al., 2010; Pallante et al., 2006). Entre estos trabajos cabe destacar el modelo basado en la expresión de dos miRNAs (miR-192 y let-7a) publicado por Mancikova *et al.*, capaz de detectar aquellos pacientes con alto riesgo de recurrencia (Mancikova et al., 2015) mencionado en el apartado anteriormente (apartado 4.5).

Desde hace varios años, existe en el conocimiento colectivo de los investigadores del cáncer de tiroides la idea de que estos tumores pueden clasificarse de acuerdo a su similitud molecular a los tumores *BRAF* o *RAS* mutados, independientemente de si son o no son mutantes. Durante el curso de esta tesis, el consorcio TCGA ha propuesto un panel basado en la expresión de 71 genes con la capacidad de clasificar las muestras postquirúrgicas en BRAF- o RAS-similares (BRAF- o RAS-*like*) (Cancer Genome Atlas Research Network et al., 2014). Hoy por hoy esta firma constituye un panel de clasificadores ya que no se ha podido demostrar su valor diagnóstico, pronóstico o de respuesta a tratamiento. No obstante, Popovici *et al.,* revelaron la existencia de un grupo de tumores BRAF-*like* en cáncer de colon (Popovici et al., 2012) demostrando que esto no es un evento exclusivo del WDTC.

5.3. Hipometilación de Elementos *Alu* como biomarcador

Los elementos o **secuencias *Alu***, son transposones pertenecientes a la familia de las SINEs y específicos de primates, descubiertos en los años 90 por Carl W. Schmid, Prescott L. Deininger y Catherine M. Houck (Houck et al., 1979; Schmid and Deininger, 1975). A pesar de que estas secuencias no codificantes de ~300 bp, necesitan la maquinaria de las LINEs para su retrotransposición, son las más activas del genoma,

produciéndose una inserción *de novo* cada 21 nacimientos (Xing et al., 2009). Se estima que hay 1.1 millón de secuencias *Alu* por genoma haploide, lo que constituye algo más del 10% del genoma humano, encontrando de media, una secuencia *Alu* cada 3 Kb (Lander et al., 2001). Numerosas publicaciones han demostrado que la inserción de secuencias *Alu* contribuyen tanto al aumento de la diversidad genética como al desarrollo de enfermedades dado su destacado papel en la preservación de la estabilidad genética (Deininger, 2011). Por lo tanto, su alteración (epi-)genética puede dar lugar a disrupciones génicas, translocaciones o recombinaciones (Sen et al., 2006), modificaciones de lugares de *splicing* (Stower, 2013), generación de nuevos sitios de poliadenilación (Chen et al., 2009), reactivación o represión de la expresión de genes cercanos (Liang et al., 2013) o alteración de los límites de los dominios activos e inactivos del genoma (Edwards et al., 2010).

Resulta interesante la observación de que el compartimento genómico de las secuencias *Alu*, no sólo es el que más CpGs concentra de todo el genoma (>25%), sino que está localizado en regiones ricas en genes y se encuentra altamente metilado, especialmente en tejidos somáticos (Kochanek et al., 1993; Lander et al., 2001). De hecho, la forma en la que la célula sortea la inestabilidad cromosómica debida a la transposición descontrolada, no solo de elementos *Alu*, sino de otros transposones, es la metilación del DNA (Liu et al., 1994).

Al poner sobre la mesa estas características, junto con el hecho de que, como hemos comentado en el apartado 2, la hipometilación global del genoma es una *hallmark* temprana y mantenida del cáncer, es fácil de entender por qué se puede utilizar el estado de metilación de las secuencias *Alu* como reporteras del estado de metilación global de la célula tumoral [revisado en (Jordà and Peinado, 2010; Toraño et al., 2012)]. En este sentido, numerosas investigaciones han asociado la hipometilación de los elementos *Alu* a progresión tumoral y mal pronóstico en cáncer gástrico (Bae et al., 2012), epitelial de ovario (Akers et al., 2014), adenocarcinoma de pulmón (Lee et al., 2009) o mieloma (Walker et al., 2011). Recientemente, se ha observado el papel de la hipometilación, tanto de elementos *Alu* como de LINEs en la inestabilidad cromosómica asociada al subtipo enriquecido en HER2 de cáncer de mama, en el que además, la hipometilación de elementos *Alu* es un biomarcador de supervivencia libre de enfermedad (Park et al., 2014). La hipometilación de secuencias *Alu*, también se ha visto como un posible marcador de riesgo de padecer cáncer de mama, ya que en varios estudios se ha observado su hipometilación en leucocitos de niñas con antecedentes familiares (Delgado-Cruzata et al., 2014; Wu et al., 2011).

5.4. Familia de las calicreínas tisulares como biomarcador

La familia de las calicreínas tisulares humanas (*human tissue kallikrein family*, KLKs) está formada por 15 proteasas extracelulares de serina que se localizan juntas en una pequeña región (265 Kb) del cromosoma 19 (19q13.4), conformando la agrupación génica de proteasas más grande del genoma humano (Yousef and Diamandis, 2001). Reciben este nombre, ya que, en un primer momento y aunque la calicreína tisular humana 1 (*KLK1*) había sido previamente descrita como parte de la orina humana, Heinrich Kraunt *et al.* observaron altos niveles de esta proteína en páncreas (*Kallikreas* en griego) (Borgoño et al., 2004). Desde entonces se han descubierto otros 14 genes (y un pseudogén) que codifican proteasas de serina homólogas a *KLK1* y que se ha convenido en llamar calicreínas tisulares humanas relacionadas (*human tissue kallikrein-related peptidases*) (Figura I16).

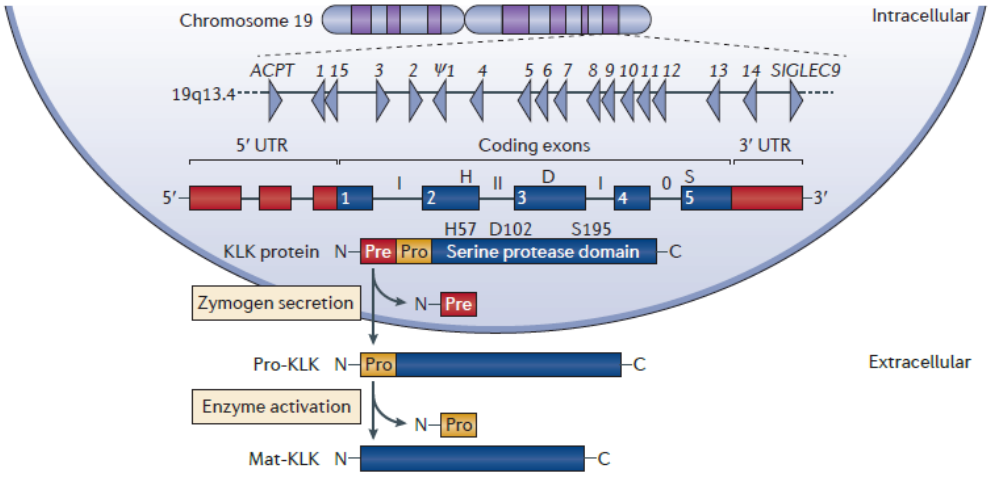

Figura I16: Locus, estructura génica y secreción de las calicreínas. La familia de las calicreínas tisulares se localiza en la región 19q13.4 y está flanqueada por los genes *ACPT* y *SIGLEC9*. Cada uno de los 15 genes *KLK* está representado por una flecha cuya dirección indica la dirección de transcripción de dicha *KLK*. Todos los genes *KLK* comparten una misma estructura génica compuesta por 5 exones codificantes (cajas azules) y cinco intrones en fase (I-II-I-0). Las regiones 5' y 3' UTR varían en longitud entre cada *KLK*. Las letras H, D y S indican la localización de los aminoácidos histidina, ácido aspártico y serina, respectivamente, que forman parte del bolsillo catalítico de todas las KLKs. Las KLKs son traducidas por los ribosomas directamente al interior del retículo endoplasmático en forma de preprozimógenos inactivos. En el interior de este orgánulo se lleva a cabo la hidrólisis de la señal pre y el prozimógeno es secretado al medio extracelular, donde permanecerá inactivo hasta que una proteasa hidrolize la señal pro y la KLK pueda adquirir la conformación funcionalmente apropiada. Figura adaptada de (Prassas et al., 2015).

De entre todas las KLKs, las más estudiadas son la KLK1, por ser la primera en descubrirse y por participar activamente en el sistema cinina-calicreína (Bryant and Shariat-Madar, 2009) y la KLK3, también conocida como antígeno prostático específico (*prostate specific antigen*, *PSA*), uno de los biomarcadores más utilizados en cáncer de próstata (Lilja et al., 2008). Sin embargo, en las últimas dos décadas, numerosas investigaciones han puesto de manifiesto la importancia de estas proteínas en procesos fisiológicos tan diversos como: la regulación renal, la descamación cutánea, la formación del esmalte dental, la licuefacción seminal, la plasticidad de la sinapsis neuronal o diversas funciones cerebrales (Prassas et al., 2015).

La coexpresión, tanto a nivel de mRNA como de proteína, de varias *KLKs* se ha detectado en un sinfín de tejidos. Por ejemplo, *KLK2-KLK4*, *KLK11* y *KLK15* se coexpresan en la próstata de hombres sanos, mientras que *KLK5-KLK6*, *KLK10* y *KLK13* se coexpresan en la glándula mamaria de mujeres sanas (Borgoño et al., 2004).Pero, es en las glándulas salivares donde podemos encontrar el mayor número de *KLKs* coexpreadas, todas menos la *KLK9* se expresan a niveles detectables por la técnica ELISA (*Enzyme-Linked ImmunoSorbent Assay*). Shaw *et al*. fueron los primeros en analizar sistemáticamente la expresión de las 15 *KLKs* en una amplia colección de tejidos humanos adultos y fetales, así como en diversos fluidos corporales (Shaw and Diamandis, 2007). De los resultados obtenidos cabe destacar las diferencias encontradas entre tejido adulto y tejido fetal en prácticamente todas las muestras analizadas, sugiriendo la posible implicación de los mecanismos epigenéticos en la regulación de la expresión de esta región.

No es de extrañar que la actividad anormal de estas proteínas se haya asociado a diversas patologías entre las que se encuentra el cáncer. La evidencia experimental indica que, dada la actividad proteasa de las KLKs, estas pueden influir directamente en el microambiente tumoral mediante la proteólisis de componentes de la matriz extracelular o el procesamiento de diversos factores de crecimiento u hormonas, promoviendo el crecimiento tumoral, la invasión y la metástasis y/o la angiogénesis (Yousef and Diamandis, 2002). Sin embargo, no podemos hablar de estas proteínas como una familia oncogénica, porque, si bien se ha observado una asociación entre la sobreexpresión de las *KLKs* y el mal pronóstico de los pacientes en determinados tipos tumorales, algunas *KLKs* (*KLK10*, *KLK3*, *KLK6* y *KLK13*) han demostrado su capacidad para inhibir la carcinogénesis en ciertos tipos tumorales (Fortier et al., 1999; Liu et al., 1996; Roman-Gomez et al., 2004; Sotiropoulou et al., 2003). De hecho, numerosos trabajos apuntan hacia el doble papel oncogénico/supresor de tumores especialmente de *KLK10*. Por

ejemplo, se sabe que su sobreexpresión en ratones inmunodeprimidos puede suprimir la formación de tumores en la glándula mamaria (Goyal et al., 1998) y puede reducir el crecimiento tumoral y promover la apoptosis, así como aumentar la sensibilidad a ciertos fármacos en cáncer de esófago (Li et al., 2015). Sin embargo, se ha encontrado sobreexpresado y en algunos casos asociado a mal pronóstico en cáncer de la cavidad oral (Wang et al., 2013), colon (Talieri et al., 2011), útero (Santin et al., 2006) o páncreas (Rückert et al., 2008). En la tabla I4 se muestran algunos ejemplos en los que el análisis de expresión génica o proteica se ha relacionado con buen o mal pronóstico en diferentes tipos de cáncer.

Tabla I4 | Las *KLKs* como biomarcadores de pronóstico. Adaptado de (Kryza et al., 2016)

Cáncer	Gen KLK	Material de partida	Supervivencia[a]
Cerebro	*KLK7*	mRNA	
Mama	*KLK5, KLK7, KLK14*	mRNA	
	KLK3, KLK9, KLK12, KLK13, KLK15	mRNA	
Colon	*KLK5, KLK6, KLK7, KLK10, KLK11, KLK14*	mRNA y proteína	
Gástrico	*KLK6, KLK10, KLK12*	mRNA y proteína	
	KLK11, KLK13	mRNA y proteína	
Laringe	*KLK11*	mRNA	
Pulmón	*KLK6, KLK12*	mRNA	
	KLK8, KLK11, KLK13	mRNA	
Ovario	*KLK4, KLK5, KLK6, KLK7, KLK15*	mRNA y proteína	
	KLK8, KLK9, KLK10, KLK11, KLK13, KLK14, KLK15	mRNA y proteína	
Páncreas	*KLK7*	proteína	
Próstata	*KLK15*	mRNA	

[a]Expresión asociada al aumento (rojo) o descenso (verde) de la supervivencia.

Hipótesis y objetivos

El cáncer de tiroides y más concretamente el cáncer de tiroides bien diferenciado es la neoplasia más común del sistema endocrino afectando mayoritariamente a mujeres. Aunque el WDTC es uno de los tumores con mejor pronóstico de los que se conocen, con más del 90% de los pacientes alcanzando valores de supervivencia superiores a los 10 años, el tratamiento rutinario actual, la tiroidectomía total, es altamente agresivo. Esto ha llevado a la comunidad científico-clínica a plantearse si los actuales sistemas de estratificación del riesgo en WDTC son verdaderamente eficientes.

Si bien durante mucho tiempo se ha tratado de establecer el valor pronóstico de las diferentes alteraciones genéticas del WDTC (mutaciones en *BRAF*, *RAS*, *PTEN*, *P53*, translocación *RET*/*PTC*, etc.) ninguna parece ser totalmente resolutiva. En este sentido, los biomarcadores epigenéticos, concretamente la metilación del DNA, ha demostrado ser de mucha utilidad en otros tipos tumorales como el cáncer de colon, de mama o de pulmón entre otros (Mikeska and Craig, 2014). Al empezar esta tesis existían algunos trabajos en los que, a través del análisis del estado de metilación del DNA de genes específicos, se demostraba la implicación de la desregulación de esta marca epigenética en el desarrollo y progresión del WDTC (Xing, 2007). Nuestra **hipótesis** es que, el estudio de la metilación del DNA en WDTC nos permitirá detectar cambios globales y/o específicos asociados a diferentes características diagnósticas (tipos histopatológicos) y pronósticas (riesgo de recurrencia, metástasis, refracción del tratamiento con yodo radioactivo, etc.) que nos ayudarán a mejorar la actual estratificación de riesgo de los pacientes con WDTC. En base a esta hipótesis, el **objetivo general** de esta tesis es la identificación de alteraciones de la metilación del DNA asociados a características diagnósticas y/o pronósticas que nos permitan mejorar los sistemas actuales de estratificación del riesgo en WDTC. A continuación, se detallan los **objetivos específicos** mediante los que pretendemos abordar nuestra hipótesis y alcanzar el objetivo general.

- Evaluar la hipometilación global de los elementos *Alu* como aproximación al estudio de la hipometilación global del genoma y su utilidad como biomarcador en WDTC.

- Estudiar los patrones de metilación del DNA de las regiones promotoras en el WDTC e identificar nuevos biomarcadores epigenéticos.

- Caracterizar la familia génica de las calicreínas a nivel epigenético (metilación del DNA) y transcriptómico para investigar su contribución a la estratificación molecular del WDTC.

Compendio de publicaciones

Por la presente, Mireia Jordà y Miguel A. Peinado, directores de esta tesis, certificamos que Raque Buj presentará la tesis doctoral en forma de compendio de tres artículos.

Raquel Buj, cumple la normativa de la Comisión de Doctorado de la facultad de Biología de la Universitat de Barcelona según la cual se requiere un mínimo de dos artículos aceptados, en uno de los cuales, el doctorando debe ser el primer firmante. En este caso Raquel Buj es la primera firmante de los dos artículos publicados y presentados en esta tesis (Trabajo I y Trabajo II). Así mismo, es la primera firmante del tercer trabajo (Trabajo III) que se encuentra actualmente en preparación.

Atendiendo al artículo 37 de la normativa reguladora de doctorado de la Universitat de Barcelona, certificamos que el trabajo II ha sido realizado en coautoría de Raquel Buj y Veronika Mancikova tal y como consta explícitamente en la publicación. De acuerdo al apartado 2.*b* de este mismo artículo, hacemos constar que los datos de este trabajo han sido utilizados en la tesis de Veronika Mancikova leída en la Universidad Autónoma de Madrid en 2015. A continuación, se procede a especificar la referencia y factor de impacto de los dos artículos (Trabajo I y Trabajo II), así como la contribución de Raquel Buj a cada uno de estos trabajos.

Trabajo I:

Buj, R., Mallona, I., Diez-Villanueva, A., Barrera, V., Mauricio, D., Puig-Domingo, M., Reverter, J.L., Matias-Guiu, X., Azuara, D., Ramirez, J.L., Alonso, S., Rosell, R., Capella, G., Perucho, M., Robledo, M., Peinado, M.A., Jorda, M., 2016. Quantification of Unmethylated *Alu* (QUAlu): a tool to assess global hypomethylation in routine clinical samples. Oncotarget 7, 10536–10546. doi:10.18632/oncotarget.7233

Factor de impacto (2015/2016): 5.008

Junto con Mireia Jordà y Miguel A. Peinado, Raquel Buj diseñó los experimentos de este proyecto y llevó a cabo la puesta a punto de la técnica. Realizó todos los ensayos necesarios para validar cada uno de los parámetros de QUAlu, así como la concentración de cada componente, los tiempos de digestión y ligación y el programa de qPCR más adecuado. Junto con Mireia Jordà y Miguel A. Peinado, realizó la selección de los tipos de tumores y de las muestras más adecuadas. En los casos necesarios realizó la extracción del DNA (FFPEs y FNABs) y llevó a cabo la técnica QUAlu en las 300 muestras de este trabajo. Junto con Anna Díez-Villanueva e Izaskun Mallona desarrolló el método

de normalización de los resultados. Bajo la supervisión de Anna Díez- Villanueva (estadística) e Izaskun Mallona (bioinformática) realizó los análisis estadísticos y la representación de los resultados. En colaboración con Mireia Jordà y Miguel A. Peinado, Raquel Buj interpretó los resultados obtenidos y fue la encargada de escribir el primer manuscrito de este artículo que posteriormente fue revisado por el resto de colaboradores.

Trabajo II:

Mancikova, V., Buj, R., Castelblanco, E., Inglada-Pérez, L., Diez, A., De Cubas, A.A., Curras-Freixes, M., Maravall, F.X., Mauricio, D., Matias-Guiu, X., Puig-Domingo, M., Capel, I., Bella, M.R., Lerma, E., Castella, E., Reverter, J.L., Peinado, M.Á., Jorda, M., Robledo, M., 2014. DNA methylation profiling of well-differentiated thyroid cancer uncovers markers of recurrence free survival. Int. J. Cancer 135, 598–610. doi:10.1002/ijc.28703

Factor de impacto (2015/2016): 5.531

Junto con Veronika Mancikova, Lucía Inglada-Pérez y Anna Diez-Villanueva, Raquel Buj participó activamente en el análisis de metilación diferencial de los resultados del *array*. Llevó a cabo el análisis y representación de los datos mediante diagramas de barras y puntos, *volcano plots*, *heatmaps* y análisis de componentes principales además del análisis de los datos del TCGA. Bajo la supervisión de Mireia Jordà, Raquel Buj seleccionó los genes candidatos derivados del análisis de metilación para su posterior validación. Realizó dicha validación mediante la técnica alternativa de tratamiento con bisulfito y secuenciación Sanger tanto en las muestras de la serie de descubrimiento (*discovery series*) como en las de validación. Del mismo modo, junto con Veronika Mancikova, Miguel A. Peinado, Mireia Jordà y Mercedes Robledo participó en la interpretación de los resultados y en colaboración con Veronika Mancikova redactó el primer manuscrito.

Trabajo III:

Buj, R., Mallona, I., Diez-Villanueva, A., Roca, M., Puig-Domingo, M., Reverter, J.L., Zafón C., Mauricio, D., Peinado, M.Á., Jordà. M. An algorithm based on kallikreins defines a novel good prognosis subtype in papillary thyroid cancer.

Manuscrito en preparación

Mireia Jordà y Raquel Buj describieron la hipótesis y objetivos planteados en este trabajo y junto con Miguel A. Peinado e Izaskun Mallona diseñaron los experimentos

necesarios. Mireia Roca y Raquel Buj realizaron los ensayos de expresión mediante qPCR Bajo la supervisión de Izaskun Mallona (bioinformática), Raquel Buj llevó a cabo todos los análisis estadísticos de este trabajo, así como la obtención del algoritmo de las KLKs mediante técnicas de *machine learning* y representó los datos en los múltiples gráficos incluidos en el trabajo. Junto con Mireia Jordà, Miguel A. Peinado e Izaskun Mallona, Raquel Buj participó en la interpretación de los resultados y la obtención de las conclusiones. Raquel Buj escribió la primera versión de este manuscrito que ha sido posteriormente revisada por Mireia Jordà y el resto de coautores.

Y para que así conste a todos los efectos firmamos la presente en Badalona, Barcelona a 1 de noviembre de 2016.

Mireia Jordà

Investigadora principal del grupo de tumores endocrinos del Instituto Germans Trias i Pujol (IGTP)

Miguel A. Peinado

Investigador principal del grupo de mecanismos epigenéticos del cáncer y de la diferenciación celular del Instituto Germans Trias i Pujol (IGTP)

1. Trabajo I

A continuación, se presenta el artículo I (*Quantification of Unmethylated Alu (QUAlu): a tool to assess global hypomethylation in routine clinical samples*) publicado en la revista *Oncotarget* en marzo de 2016. El artículo en su formato original y el material suplementario asociado puede encontrarse en el Anexo 2.1 y/o en la versión digital de esta tesis.

Resumen en castellano

La hipometilación global del DNA es una marca característica del cáncer, y muchos autores han propuesto su análisis como biomarcador tumoral. No obstante, debido a la falta de una metodología estandarizada, su implementación en laboratorios clínicos ha sido dificultosa. En este trabajo presentamos la técnica QUAlu (*Quantification of Unmethylated Alu*), un nuevo método capaz de estimar el porcentaje de elementos *Alu* no metilados (PUMA, *Percentage of UnMethylated Alu*) como medida de la hipometilación global del DNA.

QUAlu consiste en la digestión del DNA genómico con un par de isoesquizómeros (*Hpa*II/*Msp*I) con sensibilidad diferencial por la metilación, cuya diana (C/CGG) contiene el dinucleótido CpG susceptible de ser interrogado y está presente de manera significativa en las secuencias *Alu* (32.3%). Los fragmentos de restricción resultantes son ligados a un adaptador y cuantificados mediante PCR cuantitativa. El rendimiento de esta técnica ha sido evaluado obteniendo altos valores de reproducibilidad, sensibilidad y especificidad, validando los resultados obtenidos mediante secuenciación masiva. Para demostrar su utilidad, QUAlu ha sido aplicado a una amplia variedad de tipos de muestras patológicas de cinco tipos de cáncer.

Los principales resultados de la aplicación preliminar de QUAlu son: (1) todos los tejidos normales presentan PUMA similares; (2) los PUMA de los tumores son variables encontrando los niveles más altos en pulmón y colon y los más bajos en cáncer de tiroides; (3) el DNA proveniente de heces de pacientes con cáncer de colon presentan PUMA más elevados que los de los controles sanos; (4) el carcinoma escamoso de pulmón tiene PUMA mucho más alto que el adenocarcinoma de pulmón. En relación a esto último, hemos encontrado una asociación entre la hipometilación global de los tumores de pulmón y el tabaquismo, siendo significativamente más altos en los pacientes fumadores que en los exfumadores y no fumadores.

En conclusión, QUAlu permite cuantificar la hipometilación de los elementos *Alu* y ofrece una serie de ventajas con respecto a otras técnicas alternativas que la hacen especialmente sensible, específica, rápida, y económica por lo que fácilmente se podría introducir en los laboratorios de anatomía patológica. Los estudios preliminares indican su potencial aplicabilidad en oncología, aunque es necesario ampliar el número de muestras para confirmar su utilidad.

Oncotarget: 7(9), 10536-105346 (2016)

Quantification of Unmethylated *Alu* (QUAlu): a tool to assess global hypomethylation in routine clinical samples

Raquel Buj[1,2], Izaskun Mallona[1,2], Anna Díez-Villanueva[1,2], Víctor Barrera[1], Dídac Mauricio[2,3,4], Manel Puig-Domingo[2,3,4], Jordi L. Reverter[2,3], Xavier Matias-Guiu[5], Daniel Azuara[6], Jose L. Ramírez[2,7], Sergio Alonso[1,2], Rafael Rosell[2,7], Gabriel Capellà[6], Manuel Perucho[1,2,8], Mercedes Robledo[9,10], Miguel A. Peinado[1,2] and Mireia Jordà[1,2]

[1]Institute of Predictive and Personalized Medicine of Cancer (IMPPC), Badalona, Barcelona, Spain. [2]Germans Trias i Pujol Health Sciences Research Institute (IGTP), Badalona, Barcelona, Spain. [3]Department of Endocrinology and Nutrition, University Hospital Germans Trias i Pujol, Badalona, Barcelona, Spain. [4]ISCIII Center for Biomedical Research on Diabetes and Metabolic Associated Diseases (CIBERDEM), Madrid, Spain. [5]Department of Pathology and Molecular Genetics, University Hospital Arnau de Vilanova and University of Lleida, Biomedical Research Institute of Lleida (IRBLLEIDA), Lleida, Spain. [6]Catalan Institute of Oncology (ICO-IDIBELL), L'Hospitalet de Llobregat, Barcelona, Spain. [7]Catalan Institute of Oncology (ICO), Hospital Germans Trias i Pujol, Badalona, Barcelona, Spain. [8]Catalan Institution for Research and Advanced Studies (ICREA), Barcelona, Spain. [9]Hereditary Endocrine Cancer Group, Spanish National Cancer Research Center (CNIO), Madrid, Spain. [10]ISCIII Center for Biomedical Research on Rare Diseases (CIBERER), Madrid, Spain.

Keywords: DNA hypomethylation, *Alu* repeats, human cancer, biomarker, routine

Abbreviations: AUC: area under the curve; BRAF: v-raf murine sarcoma viral oncogene homolog B1; Cq: quantification cycle; DIEXF: digestive organ expansion factor homolog (zebrafish); E: efficiency; FFPE: formalin-fixed paraffin-embedded; FNAB: fine-needle aspiration biopsy; HPLC: High performance liquid chromatography; LAD: lung adenocarcinoma; LINEs: Long interspersed elements; LUMA: Luminometric-Based Assay; LSCC: lung squamous cell carcinoma; QUAlu: quantification of unmethylated *Alu* elements; N: normal tissue adjacent to tumor; PUMA: percentage of unmethylated *Alu* elements; QUAlu: quantification of unmethylated *Alu* elements; QUMA: quantification of unmethylated *Alu*s, qAlu H: Alu elements qPCR with DNA digested with *Hpa*II; qAlu M: *Alu* elements qPCR with DNA digested with *Msp*I; qL1PA H: L1PA qPCR with DNA digested with *Hpa*II; qL1PA M: L1PA qPCR with DNA digested with *Msp*I; RAS association domain family protein 1; ROC: receiver operating characteristic; SINEs: short interspersed elements; T: tumor.

DOI: 10.18632/oncotarget.723

History: Received 23 Nov 2015; Accepted 25 Jan 2016; Published 07 Feb 2016

Correspondence to: Mireia Jordà, Institute of Predictive and Personalized Medicine of Cancer (IMPPC), Badalona, Barcelona, Spain, Tel.: 134-935-543-050, Fax: 134-934-651-472, E-mail: mjorda@imppc.org or Miguel A. Peinado, Institute of Predictive and Personalized Medicine of Cancer (IMPPC), Badalona, Barcelona, Spain, Tel.: 134-935-572-832, Fax: 134-934-651-472, E-mail: map@imppc.org.

Abstract

Hypomethylation of DNA is a hallmark of cancer and its analysis as tumor biomarker has been proposed, but its determination in clinical settings is hampered by lack of standardized methodologies. Here, we present QUAlu (Quantification of Unmethylated *Alu*), a new technique to estimate the Percentage of UnMethylated *Alu* (PUMA) as a surrogate for global hypomethylation.

QUAlu consists in the measurement by qPCR of *Alu* repeats after digestion of genomic DNA with isoschizomers with differential sensitivity to DNA methylation. QUAlu performance has been evaluated for reproducibility, trueness and specificity, and validated by deep sequencing. As a proof of use, QUAlu has been applied to a broad variety of pathological examination specimens covering five cancer types.

Major findings of the preliminary application of QUAlu to clinical samples include: (1) all normal tissues displayed similar PUMA; (2) tumors showed variable PUMA with the highest levels in lung and colon and the lowest in thyroid cancer; (3) stools from colon cancer patients presented higher PUMA than those from control individuals; (4) lung squamous cell carcinomas showed higher PUMA than lung adenocarcinomas, and an increasing hypomethylation trend associated with smoking habits.

In conclusion, QUAlu is a simple and robust method to determine *Alu* hypomethylation in human biospecimens and may be easily implemented in research and clinical settings

Introduction

Extensive evidence describes cancer as a combination of genetic and epigenetic alterations which cooperate at every step of the tumor progression [reviewed in (Sandoval et al., 2012)]. DNA methylation is the most well-characterized epigenetic mark in mammals and consists in the covalent addition of a methyl group to the cytosine located within the CpG dinucleotide. It is frequently associated with silenced chromatin and transcriptional repression [reviewed in (Ehrlich et al., 2009; Feinberg et al., 2007)]. Among all the epigenetic alterations that delineate cancer genomes, loss of global DNA methylation has been considered a hallmark. Numerous works have demonstrated that DNA hypomethylation is an early and sustained event in tumorigenesis. Besides, it promotes a permissive landscape for cancer development and progression by encouraging chromosomal instability, imprinting loss, aberrant gene expression and transposon activation [reviewed in (Ehrlich et al., 2009; Feinberg et al., 2007)]. More importantly, it has been reported a strong association between the degree of DNA hypomethylation and the tumor grade and stage, which has attracted great interest for its potential clinical value, not only in cancer diagnosis and prognosis (Li et al., 2014; Fabris et al., 2011; Igarashi et al., 2010; Saito et al., 2010; Frigola et al., 2005; Torano et al., 2012), but also as a marker of cancer risk (Torano et al., 2012; Moore et al., 2008; Choi et al., 2009; Matsuda et al., 2010).

A wide variety of techniques have been designed to measure global DNA methylation, some of which quantify the overall levels of 5-methylcytosine in the genome compared with unmethylated cytosines (e.g. HPLC, immunochemical assay, etc.), while others assess the methylation levels of specific genome compartments [reviewed in (Torano et al., 2012; Jordà et al., 2010)]. Among the second group, the most widely used methods are those based on repeat elements, as they exhibit a high copy number and are widespread throughout the human genome. Nevertheless, none of them has been established in the clinical practice due in part to technical, economical and time shortcomings, which preclude a standardized alternative.

Here we present a new method, Quantification of Unmethylated *Alu* (QUAlu), which uses *Alu* repeats as surrogate reporter of global DNA methylation. *Alu* repeats are primate-specific transposable elements that belong to the Short Interspersed Elements (SINEs) family and represent the most abundant class of repetitive sequences in the human genome (1.1 million copies per haploid genome) (Deininger, 2011). *Alu* elements contain

up to 25% of the overall CpG sites in the genome (Table 1) and are highly methylated in somatic tissues. Interestingly, they are located in gene-rich regions (Lander et al., 2001).

Table 1 | *Alu* repeats content in the human genome and representativeness in the virtual QUALuome

Sequence	No of elements[a]	Base pairs	No of CpGs	No of *Hpa*II/*Msp*I sites	AACCCGG hits	QUALuome[d]
Alu[b]	1,194,734	305,076,148 (9.7%)	7,173,987 (25.4%)	742,725 (32.3%)	172,574 (79,1%)	155,878
LINE[c]	1,498,690	638,481,131 (20.4%)	3,412,416 (12.1%)	155,813 (6.8%)	6,881 (3.2%)	0
CpG Island	28,691	21,842,742 (0.7%)	2,089,537 (7.4%)	270,622 (11.8%)	4,470 (2.1%)	0
Genome	-	~3,200 million (100%)	28,217,009 (100%)	2,297,221 (100%)	218,131 (100%)	0

[a]Data based on GRCH37/hg19 human genome assembly
[b]RepeatMasker's *Alu* repFamily members discarding FLAMS and FRAMS
[c]RepeatMasker's LINE repClass members
[d]Virtual QUAlu amplicons

QUAlu is a simple and rapid method based on the digestion of genomic DNA with the methylation-sensitive and insensitive isoschizomers *Hpa*II/*Msp*I, the ligation of an adaptor and a qPCR using primers specific for the *Alu* consensus sequence. We have applied this technique to a broad variety of pathological examination samples including fresh frozen tissues, Formalin-Fixed Paraffin Embedded (FFPE) sections, Fine-Needle Aspiration Biopsies (FNAB), stools and liquid biopsies. Our preliminary results underscore the potential clinical utility of the assessment of unmethylated *Alu* elements by QUAlu.

Results

QUAlu design and technical evaluation

According to the reference human assembly hg19, there are over 28 million of CpG dinucleotides in the human genome and more than half are located within repeat elements, being *Alu* elements those containing the highest fraction, namely 25.4% (Table 1). Therefore, we selected *Alu* elements as the most adequate surrogate reporter of global methylation and developed QUAlu technique, a method to identify unmethylated *Alu* repeats which shares the quantitative nature of the related technique LUMA (Karimi et al., 2006) and the specificity of QUMA (Rodriguez et al., 2008). Fundamentals of QUAlu assay are outlined in Figure 1 and Supplementary Figure S1. QUAlu is based on the different

methylation sensitivity of the isoschizomers *Hpa*II/*Msp*I (see Materials and Methods and Supplementary Material), whose recognition site is C/CGG, located in the Alu consensus sequence AACCCGG present in 14.4% of Alu elements (Table 1). Noteworthy, analysis of whole genome bisulfite sequencing data (Lister et al., 2009) showed that the *Hpa*II/*Msp*I sites embedded in CpG islands may be used as reporters of the overall methylation of these genomic elements (Barrera et al., 2012). In this regard, we also confirmed that this postulate may be also applied to Alu repeats: more than 90% of the *Hpa*II/ *Msp*I sites within the Alu consensus sequence AACCCGG showed concordant methylation levels with the whole Alu sequence (Supplementary Table S4). To determine the virtual representativeness of QUAlu (QUAluome), an electronic qPCR simulation was performed showing a theoretical coverage of 155,878 Alu elements (see Supplementary Material), which corresponded to the 13.65% of the Aluome, with a bias toward amplification of young subfamilies (Supplementary Figure S2).

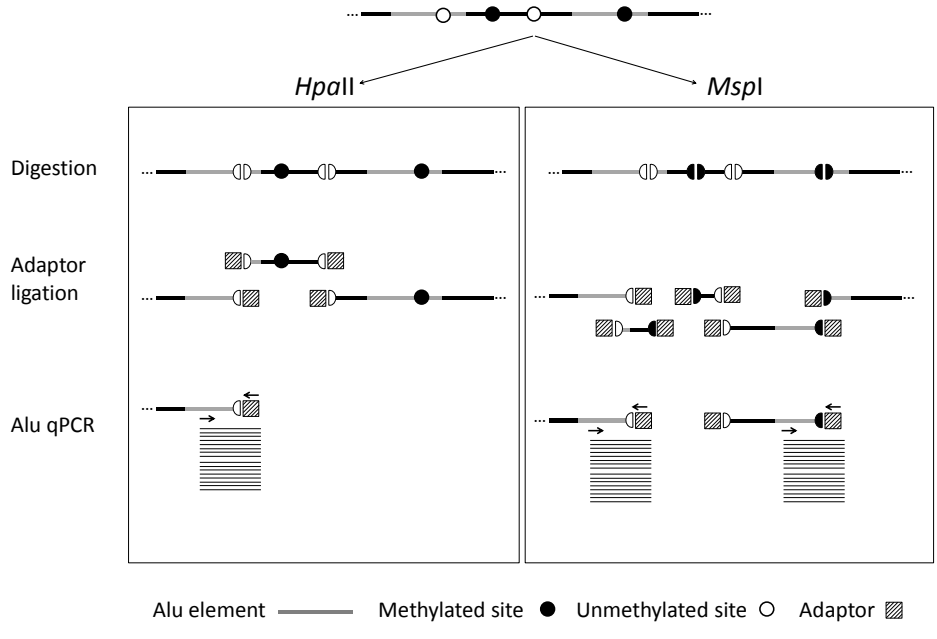

Figure 1 | QUAlu technique diagram. Genomic DNA is digested using *Hpa*II and *Msp*I isoschizomers (DNA methylation sensitive and insensitive, respectively), ligated to a synthetic adaptor, and *Alu* elements are specifically amplified by qPCR in two separated reactions. The ratio between the two reactions gives the percentage of unmethylated *Alu* elements (PUMA). DNA normalization is performed by parallel amplification of L1PA.

To assess the linearity of QUAlu, different starting amounts of HCT116 genomic DNA, ranging from 0.3 to 80 ng, were used. As it can be observed in Figure 2A, all quantifications showed excellent linearity (R2 > 0.98 in all cases). Moreover, similar percentages of unmethylated *Alu* elements were obtained, being the overall average 8.8 ± 2.2 (Supplementary Figure S3A). The same assay was done with clinical samples from normal tissues of lung, colon and thyroid, obtaining an excellent linearity in all cases (Supplementary Table S5).

The inter-assay repeatability was assessed by analyzing the same HCT116 genomic DNA in 39 independent QUAlu assays. The mean of all the analyses was 9.9% and the standard deviation ± 1.6. Furthermore, replicates of tumor and normal clinical samples were measured in different plates confirming that the technique is reproducible (R2 = 0.981) (Figure 2B). Importantly, the feasibility of QUAlu in samples containing partially degraded DNA was verified (Supplementary Material and Supplementary Figure S3B-S3C).

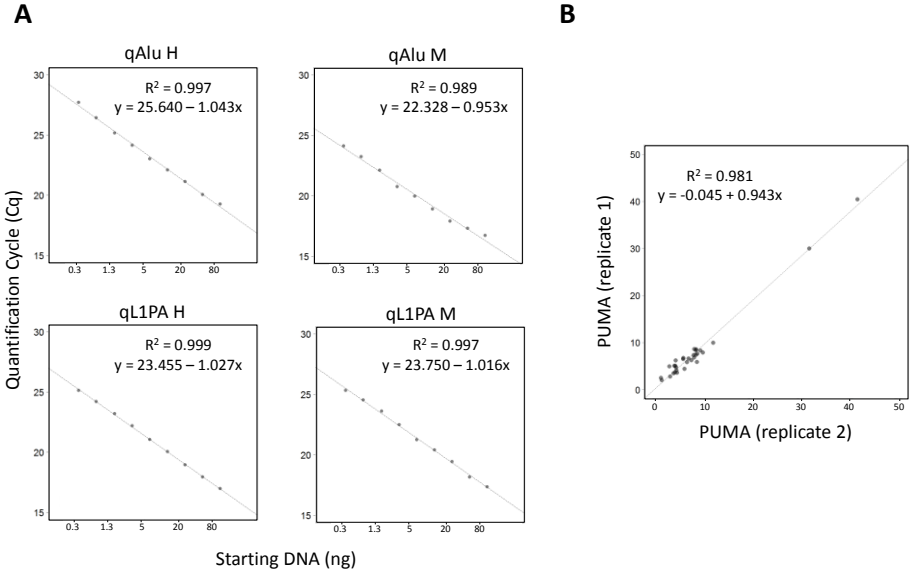

Figure 2 | Evaluation of QUAlu technique. (A) Standard curves showing the linear range of the different qPCRs performed in a QUAlu assay. HCT116 genomic DNA amounts ranging from 0.3 to 80 ng were used. **(B)** Correlation of the percentage of unmethylated *Alu* elements (PUMA) determined by QUAlu in two independent experiments.

It is of note that consistent QUAlu results may be achieved with DNA amounts well below one haploid genome. In fact, linear range response was reached with as little as 0.005 pg of DNA per PCR tube (equivalent to 0.002 haploid genomes) (Supplementary Figure S4). The low requirements of QUAlu are due to the multiplex nature of its target (a large pool of more than one hundred thousand *Alu* repeats), reaching sensitivity detection 4 to 5 orders of magnitude higher than a single copy locus [e.g. promoter region of Digestive organ expansion factor homolog (zebrafish) -DIEXF- gene] (Supplementary Figure S4 and Supplementary Material). Noteworthy, the complexity of the QUAlu product is visualized as a broad melting peak for both the *Hpa*II and the *Msp*I samples, contrasting with the narrower peak of a single PCR product (Supplementary Figure S5).

Finally, the specificity of QUAlu to amplify *Alu* elements was validated by next-generation sequencing of five QUAlu determinations. The results showed that 97% of the reads (range 96.6-98.1%) obtained from the sequenced samples aligned with *Alu* repeats (Supplementary Table S6) and confirmed the complex composition of QUAlu product composed of multiple different *Alu* elements with similar distributions among all the analyzed samples (Supplementary Figure S6).

QUAlu application to fresh frozen human cancer samples

QUAlu technique was applied to analyze the levels of unmethylated *Alu* elements in different cancer types and their normal counterparts (Table 2 and Supplementary Table S7). Interestingly, the different normal tissue types showed similar values of Percentage of UnMethylated *Alu* elements (PUMA) (Table 2) (Kruskal Wallis test, p-value = 0.308), being the average PUMA 6.0 ± 2.1 (range 1.8-14.8). However, PUMA showed a broad variation in tumors, ranging from 0.9 to 40.5 (average = 10.7 ± 6.8). Furthermore, important differences were observed between cancer types (Table 2 and Figure 3A) (Kruskal Wallis test, p-value < 0.05), with colon and lung exhibiting 2-3 fold higher levels of unmethylated *Alu* repeats as compared with thyroid, prostate and breast cancer (Supplementary Tables S7 and S8). The comparison between normal and tumor samples showed statistically significant differences in most cancer types, except in prostate cancer (Mann-Whitney U test, p-value = 0.357) (Figure 3A and Table 2).

Since there were no differences among normal tissues in the proportion of unmethylated *Alu* elements, the 99th percentile (PUMA = 12%) was taken as a cutoff value to consider a tumor as hypomethylated. Thus, particular analysis of each tumor type revealed that 62.5% of colon and 64.1% of lung tumors were hypomethylated, while in

breast and prostate tumors this figure was 20% and 16.7%, respectively. Otherwise, only 11.9% of thyroid tumors had percentages of unmethylated *Alu* elements above the reference value (Supplementary Figure S7). When considering only the matched normal-tumor pairs of all cancer types (n = 81), the difference among them was evident in most cases (paired Mann-Whitney U test p-value< 0.001). About one third of colon (5/16) and lung (13/37) tumors displayed a high hypomethylation as compared with the paired normal tissue (fold change greater than 3). Contrarily, this big difference was uncommon in breast (2/14), prostate (1/7) or thyroid (0/7) cancer (Supplementary Tables S7 and S9).

Table 2. Percentage of Unmethylated *Alu* repeats (PUMA) in different human tissues and tumors

	Thyroid	Prostate	Breast	Colon	Lung
Normal tissue	6.2 ± 1.6 (n = 9)	4.8 ± 2.6 (n = 7)	5.6 ± 2.66 (n = 14)	6.9 ± 2.0 (n = 16)	5.9 ± 2.0 (n = 37)
Tumor tissue	8.2 ± 3.1 (n = 59)	8.5 ± 8.8 (n = 18)	10.0 ± 5.9 (n = 20)	14.6 ± 5.2 (n = 16)	14.6 ± 8.3 (n = 39)
p-value[a]	0.032	0.357	0.002	< 0.001	< 0.001

[a]Normal Vs Tumor, Mann-Whitney U test

Evaluation of PUMA as biomarker in specific cancers

To estimate the potential value of the percentage of unmethylated *Alu* elements to discriminate between normal and tumoral tissue we performed ROC analyses (Figure 3B). Area Under the Curve (AUC) values confirmed that PUMA was a good biomarker (AUC > 0.8) for breast, colon and lung cancer, with sensitivities and specificities >80%, except for breast cancer, whose sensitivity reached 92.9% but the specificity was lower (60%). Otherwise, for both prostate and thyroid cancer, although the sensitivity reached 100%, the specificity was low (44.4% and 27.3%, respectively). The cut-off values varied from tissue to tissue (Figure 3B), with the lowest levels in lung (6.97) and the highest in thyroid (9.54). Moreover, to evaluate the clinical value of the QUAlu assay, we performed additional statistical analyses in two cancer types with the highest and the lowest PUMA, namely lung and thyroid cancer.

As described above, lung cancers exhibited high levels of hypomethylated *Alu* elements, but differences were also detected among lung cancer subtypes. Specifically, lung squamous cell carcinoma showed the highest PUMA (16.8 ± 8.8) compared with lung adenocarcinomas (12.2 ± 6.1) (Mann-Whitney U test p-value = 0.001) (Figure 4A and Supplementary Table S10). On the other hand, while no significant differences were observed in PUMA among lung normal tissue from never smokers, former smokers (more than 10 years) and current smokers (Kruskal Wallis test p-value >0.05), there was a

significant increasing trend (Mann-Whitney U test, p-value = 0.006) of lung tumors to become more unmethylated in current smokers compared to former smokers (Figure 4B).

As regard to thyroid cancer, there were no significant differences in the percentage of unmethylated *Alu* elements in relation to histology subtype (Kruskal Wallis test, p-value = 0.231) or genetic alteration (*RAS* or *BRAF* mutations) (Kruskal Wallis test p-value = 0.147).

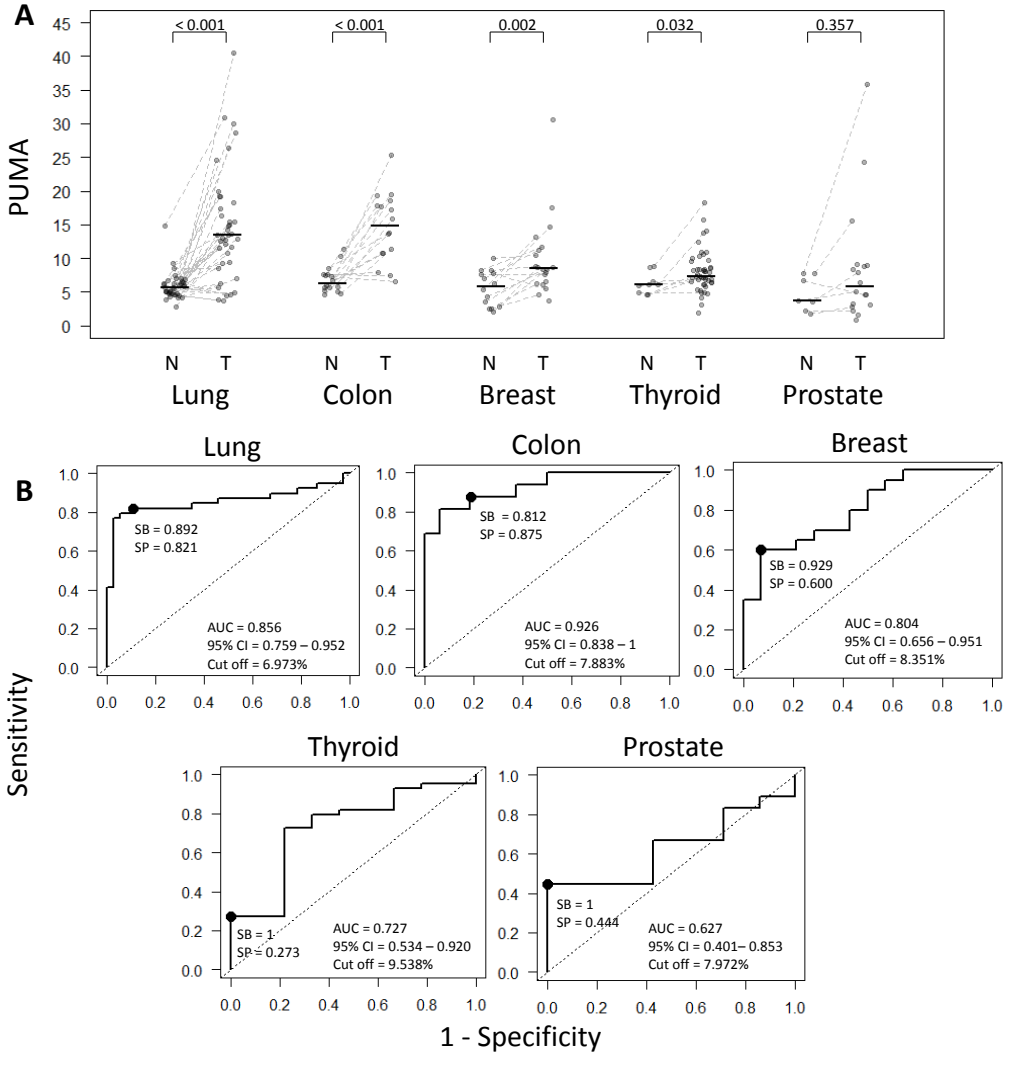

Figure 3 | Comparison and diagnostic value of QUAlu among different cancer types. (A) PUMA in different cancer types [normal tissue (N) and tumor (T)]; the median of each group is represented by a black line. **(B)** Receiver Operating Characteristic curves for the diagnosis of lung, colon, breast, thyroid and prostate cancer according to the percentage of unmethylated *Alu* (PUMA) elements determined by QUAlu.

QUAlu application to diverse pathological examination biospecimens

Next, we evaluated the applicability of QUAlu to biospecimens obtained in standard pathological procedures often containing low amount of poor quality DNA (FFPE, FNAB, liquid biopsies and stools). Due to the low amount of starting material, DNA was not quantified and 1 ul of the extracted DNA was used for QUAlu analysis (see Supplementary Material). All samples produced detectable levels of amplified *Alu* elements (qAlu M Cq range: 16 to 30, qAlu H Cq range: 19 to 34) (Supplementary Figure S8), with the exception of plasma samples obtained from healthy individuals and one stool sample from one colon cancer patient.

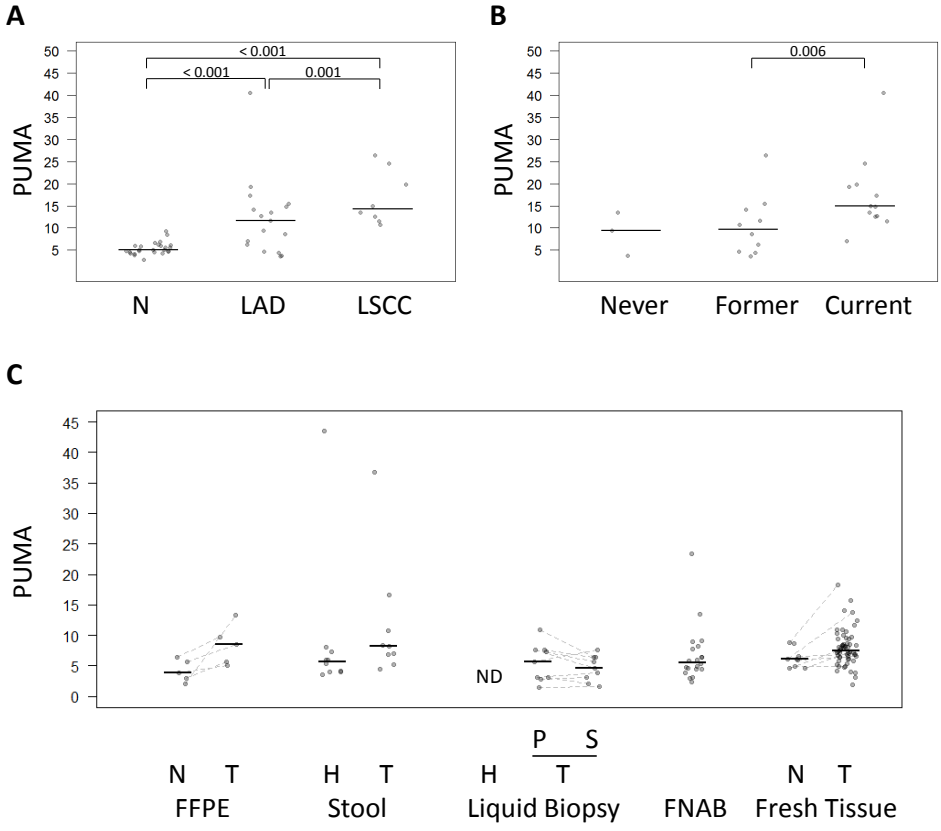

Figure 4. Comparison of QUAlu among different clinical characteristics and simple types. (A) PUMA in normal and lung tissue, lung adenocarcinoma (LAD) and lung squamous cell carcinoma (LSCC) and **(B)** in lung cancer patients according to their smoking habits. **(C)** PUMA in different sample types: FFPE (colon cancer patients), stool (healthy donors and colon cancer patients), liquid biopsy (plasma from healthy donors and plasma and serum from lung cancer patients), FNAB (thyroid goiter patients), fresh tissue (thyroid cancer patients). The median of each group is represented by a black line. Normal (N), tumor (T), healthy donors (H), plasma (P), serum (S), no detectable samples (ND).

The low number of samples precluded a robust comparison of the results, but some insightful trends were observed (Figure 4C). FFPE colon tumors showed higher PUMA than the matching normal samples (paired Mann-Whitney U test p-value = 0.062). Moreover, elevated *Alu* hypomethylation in the stools was more frequent in colon cancer patients than in control individuals (Mann-Whitney U test p-value = 0.079). Interestingly, liquid biopsies produced similar PUMA in plasma and serum from lung cancer patients, but did not amplify in cancer-free controls, which is consistent with the common absence of circulating free DNA in healthy individuals (Schwarzenbach et al., 2011).

Finally, thyroid goiters FNABs showed a PUMA in the same range than normal tissues with some exceptions: four cases presented a PUMA above 8.8, the highest value in normal thyroid tissue (Figure 4C).

Discussion

Most of human genome is methylated, but in a wide range of pathologies, including cancer, a global DNA hypomethylation occurs affecting in large extent repetitive elements, which constitute ~45% of the genome. Weisenberger *et al.* (Weisenberger et al., 2005) demonstrated that the methylation of different repetitive sequences, namely, LINE-1, *Alu* and satellite 2 (Sat2), significantly correlated with global methylation levels measured by high performance liquid chromatography (HPLC), and proposed the use of these repeats as surrogate reporters of global methylation. LINEs have been broadly used to estimate the global levels of hypomethylation (Tajuddin et al., 2014; Salas et al., 2014; Inamura et al., 2014), but *Alu* elements display some features that make them more suited for this purpose. Namely, *Alu* repeats constitute the most abundant retrotransposon and contain 25% of all the CpGs in the human genome. Moreover, due to their prevalent localization in gene-rich regions (Deininger 2011) epigenetic variations in *Alu* repeats may have direct implications in gene regulation, and by extension, in tumor biology.

Here we present QUAlu, a new technique to measure the levels of DNA unmethylation in *Alu* repeats, with several features that facilitate a direct implementation in clinical and research settings. These include a 100-fold higher sensitivity than other related methods (Lisanti et al., 2013), as accurate determinations can be performed with as little as 300 pg of DNA (corresponding to approximately 150 diploid cells). QUAlu specificity for *Alu* elements is extremely high, as demonstrated by deep sequencing of its products, where 97% of the reads mapped in *Alu* repeats.

Moreover, thanks to the calibration with internal controls (L1PA simultaneously with *Alu* repeats), QUAlu is relatively unaffected by the quantity and quality of the starting material in artificially degraded DNA. Furthermore, we have demonstrated that this technique is amenable to be applied to a broad spectrum of pathological examination specimens routinely collected in clinical settings (frozen tissues, FFPE, liquid biopsies, stools and FNAB). In spite of the low number of samples analyzed, preliminary results are promising, especially for FFPE and stools. Nevertheless, direct applicability of QUAlu in different clinical settings requires the analysis of large series of cases to define the threshold, sensitivities and specificities.

With clinical practice in mind, technical benefits of QUAlu include the small number of steps (digestion-ligation, real time PCR and analysis), the short time required to complete the determination (less than 5 hours from the DNA to the final result, even without automation of the process), and the low cost (about 6.3 US$ per sample, including technician labor).

As mentioned above, several techniques have been developed to estimate global methylation, and many of them target repeat elements as surrogate reporters [reviewed in (Torano et al., 2012; Moore et al., 2008; Choi et al., 2009; Matsuda et al., 2012; Jordà et al., 2010)]. While most of these methods may constitute good alternatives to compare global methylation levels among a few samples, their implementation as a clinical tool is not a straightforward approach due to either technical complexity or exquisite sample necessities. QUAlu simplicity and limited equipment requirements facilitate its implementation in most laboratories.

To assess the clinical potential of QUAlu, we determined the extent of *Alu* hypomethylation in different human cancers by analyzing normal and tumor tissues. In a first analysis we compared the different normal tissues and different individuals, showing that the levels of unmethylated *Alu* elements were very consistent from tissue to tissue and from individual to individual. This result was in agreement with previous studies analyzing global DNA methylation by MethyLight and HPLC (Weisenberger et al., 2005) or targeting *Alu* elements (Choi et al., 2009; Wu et al., 2011), but not with other works reporting tissue-associated global methylation differences targeting LINE-1 (Chalitchagorn et al., 2004).

Our data suggests that the degree of hypomethylation is variable among different cancer types, with thyroid, prostate and breast cancer exhibiting low levels of

hypomethylation, while cancers of colon and lung displayed the highest levels. Chalitchagorn *et al.* (Chalitchagorn et al., 2004) analyzed LINE-1 methylation using bisulfite based PCR in several cancers, and although they found high levels of hypermethylation in some types (e.g. esophagus cancer), no hypomethylation was observed among the ones analyzed in our study. This might be explained by the low sensitivity of their technique or the low number of samples analyzed.

It is interesting to note that the low-hypomethylation cancer group included hormone-related tissues (thyroid, prostate and breast) with no direct interaction with external factors, while the high-hypomethylation group (colon and lung) was composed by tumors with a high exposure to environmental factors (e.g. diet, air). While we do not know the reason for this association, there are evidences supporting the impact of certain environmental factors (drugs, chemicals, pollutants and other agents) in the deregulation of epigenetic enzymes, which will eventually generate epigenetic changes, including DNA hypomethylation, that may accumulate over the time causing alterations in key cellular processes and promoting cancer (Herceg et al., 2011; Mathers et al., 2010). Noteworthy, it has been reported that *Alu* hypomethylation (but not LINE-1 hypomethylation) in esophageal mucosa may reflect an epigenetic field for cancerization in esophageal carcinogenesis (Matsuda et al., 2012). Other alternative explanations may be related with the dynamics of tumor progression in different tumor types and the role of DNA hypomethylation behind specific deregulation of biological pathways, including genomic stability (Rodriguez et al., 2006; Eden et al., 2003).

Confirming previous reports (Suzuki et al., 2013) we found significant differences in the levels of hypomethylation among the two types of lung cancers considered here. Lung adenocarcinomas, the histological subtype most frequently associated with never-smokers and former smokers, were less hypomethylated than lung squamous cell carcinomas. Many studies have suggested a strong correlation between loss of DNA methylation and smoking habit in cancer patients (Smith et al., 2007; Andreotti et al., 2014; Liu et al., 2010), but also in healthy people (Shigaki et al., 2012; Tajuddin et al., 2013). In this regard, we found a significant increase of hypomethylation in current smokers compared to former smokers, but this trend was not observed in the adjacent normal tissue. This result may indicate different mechanisms of tumor progression in ex-smokers as compared with current smokers.

In summary, we have demonstrated that QUAlu is a feasible approach to analyze global DNA methylation in almost any type of biospecimen routinely collected in ordinary

clinical settings. DNA hypomethylation is a hallmark of cancer but, as we have shown, its degree is highly variable. Its determination with a technique as QUAlu may have a broad spectrum of applications including diagnostic and prognostic evaluations.

Materials and methods

Samples

This study included a total of 300 pathological examination samples of different sources: 220 fresh frozen tissue samples (Supplementary Tables S1 and S2), 10 FFPE samples, 31 liquid biopsies, 19 stool samples and 20 thyroid goiter FNAB samples. Regarding fresh frozen tissues, 16 colorectal carcinomas and their paired normal adjacent tissues were obtained from Hospital Universitari de Bellvitge (Barcelona, Spain). Forty-four thyroid carcinomas and 9 paired adjacent thyroid tissues were obtained as described in our previous study (Mancikova et al., 2014). DNA of 20 breast carcinomas and 14 paired normal adjacent tissues, 18 prostate carcinomas and 7 paired normal adjacent tissues, and 39 lung carcinomas and 37 normal adjacent tissues were obtained from the Spanish National DNA Bank (BNADN, Salamanca, Spain). Patient characteristics are shown in Supplementary Tables S1 and S2. Five normal and tumoral paired colorectal carcinoma FFPE samples were obtained from Cooperative Human Tissue Network (CHTN). Nine stool samples from colorectal carcinoma patients and 10 from healthy donors were obtained from Hospital Universitari de Bellvitge (Barcelona, Spain). Finally, nine plasma and serum paired lung carcinoma liquid biopsies, 13 plasma liquid biopsies from healthy donors and 20 thyroid goiter FNAB samples were obtained from Hospital Universitari Germans Trias i Pujol (Badalona, Spain). The study was approved by the Hospital Germans Trias i Pujol Ethics Committee. Informed consent was obtained before surgery.

The colorectal carcinoma cell line HCT116 was obtained from the American Type Culture Collection (ATCC) and was authenticated on 3rd March 2014 by using the AmpFLSTR® Identifiler® Plus PCR Amplification Kit (Applied Biosystems). Cells were cultured in D-MEM/ F12, supplemented with sodium pyruvate, L-glutamine and 10% fetal bovine serum (Life Technologies, MD, USA) and were maintained at 37ºC in a 5% CO_2 atmosphere. Genomic DNA was isolated using different methods as described in the Supplementary Material.

Human genome sequence data sets

We used the GRCh37/hg19 human genome assembly. Genomic positions of *Alu* elements, LINE sequences, CpG islands and CpG dinucleotides were retrieved from the UCSC MySQL repository (genomemysql.cse.ucsc.edu). Motif search was performed with EMBOSS (http://emboss.sourceforge.net/). To count the number of overlapping features (Table 1) we used the BEDTools package (v2.19.1, (Quinlan et al., 2010)). For more technical details, see Supplementary Material.

Quantification of Unmethylated *Alu* (QUAlu) assay

The principle underlying this technique is the selective amplification of *Alu* repeats containing an unmethylated CpG site within the consensus sequence AACCCGG. Briefly, genomic DNA was digested in parallel in two separated tubes with *Hpa*II and *Msp*I methylation-sensitive and -insensitive isoschizomers, respectively, which leave identical sticky ends (C/CGG). Next, a synthetic adaptor was ligated to the digested DNA fragments. Quantification was performed by qPCR using a primer complementary to the chimeric sequence of the adaptor plus the consensus *Alu* sequence after *Hpa*II digestion (AACC + synthetic adaptor) and another one complementary to the *Alu* consensus sequence and located ~20 nucleotides upstream of the *Hpa*II cutting site (Supplementary Figure S1). Thereby, qPCR of *Msp*I digestion (qAlu M) allowed the quantification of all the amplifiable *Alu* elements (irrespective of the methylation status), while qPCR of *Hpa*II digestion (qAlu H) only quantified the subset of amplifiable *Alu* elements containing an unmethylated CpG. Thus, the final result corresponded to the fraction of unmethylated *Alu* elements respect the total number of amplifiable *Alu* elements calculated according to the equation described below. Furthermore, two specific qPCRs for L1PA (a Long Interspersed Nuclear Element-1, LINE-1 subfamily) were performed to normalize the DNA input for both *Msp*I (qL1PA M) and *Hpa*II digestions (qL1PA H). For more technical details, see Supplementary Material.

QUAlu data analysis

Statistical analyses were performed using R version 3.1.0. The Percentage of UnMethylated *Alu* elements (PUMA) for each sample was assigned according to this equation:

$$\mathrm{PUMA} = \frac{\frac{E_{qAlu\ H}^{-Cq_{qAlu\ H}}}{E_{qL1PA\ H}^{-Cq_{qAlu\ H}}}}{\frac{E_{qAlu\ M}^{-Cq_{qAlu\ M}}}{E_{qL1PA\ M}^{-Cq_{qL1PA\ M}}}} \mathrm{X}\ 100$$

The relative amount of unmethylated *Alu* elements (given by qAlu H normalized by the reference sequence qL1PA (qL1PA H)) and the relative amount of total amplifiable *Alu* elements (given by qAlu M normalized by qL1PA M) were calculated as a ratio of exponential functions in which the base was the qPCR efficiency (E) and the variable was the quantification cycle (Cq). To tackle the qPCR error propagation, permutation tests were done to obtain a final PUMA and its variation using the qPCR R package [v1.4-0, (Ritz et al., 2008)]. Mann-Whitney U test and Kruskal Wallis tests were used, as appropriate, to assess the significance among the different groups of samples. Correlation analyses were conducted using two-tailed Kendall tests. The significance level was established at $p < 0.05$ for all analyses. Receiver operating characteristic (ROC) curves were generated using the pROC R package [v1.7.3, (Robin et al., 2011)] to assess the cut-off value that best discriminated between tumor and normal tissue according to the PUMA.

Characterization of QUAlu product by Next Generation Sequencing

To determine the specificity of the technique, the products generated by qAlu H and qAlu M from 5 samples (the colorectal cancer cell line HCT116, a lung squamous carcinoma with its normal matching tissue and a papillary thyroid carcinoma with its normal matching tissue) were sequenced using Ion Torrent technology (Life Technologies). For more technical details, see Supplementary Material and Supplementary Table S3.

Acknowledgments

We thank Mar Muñoz, Esmeralda Castelblanco and Veronica Mancikova for excellent technical support. We also thank all the patients and control donors for making this study possible.

Conflicts of interests

MAP is cofounder and equity holder of Aniling, a biotech company with no interests in this paper. The other authors declare no conflict of interest.

Grant support

RB was supported by a FPI fellowship from Ministerio de Economía y Competitividad. AD-V was supported in part by a contract PTC2011-1091 from Ministerio de Economía y Competitividad. This work was supported by grants from FEDER, the Ministerio de Economía y Competitividad (SAF2011/23638 to MAP), the Instituto de Salud Carlos III (FIS PI11/02421 to JR, FIS PI11/01359 and FIS PI14/00240 to MR, FIS PI14/00308 to MJ, FIS PI12/00511 to MP), and Fundació Olga Torres (to MJ).

References

Andreotti, G., Karami, S., Pfeiffer, R.M., Hurwitz, L., Liao, L.M., Weinstein, S.J., Albanes, D., Virtamo, J., Silverman, D.T., Rothman, N., Moore, L.E., 2013. LINE1 methylation levels associated with increased bladder cancer risk in pre-diagnostic blood DNA among US (PLCO) and European (ATBC) cohort study participants. Epigenetics 9, 404–415. doi:10.4161/epi.27386

Barrera, V., Peinado, M.A., 2012. Evaluation of single CpG sites as proxies of CpG island methylation states at the genome scale. Nucleic Acids Res. 40, 11490–11498. doi:10.1093/nar/gks928

Chalitchagorn, K., Shuangshoti, S., Hourpai, N., Kongruttanachok, N., Tangkijvanich, P., Thong-ngam, D., Voravud, N., Sriuranpong, V., Mutirangura, A., 2004. Distinctive pattern of LINE-1 methylation level in normal tissues and the association with carcinogenesis. Oncogene 23, 8841–8846. doi:10.1038/sj.onc.1208137

Choi, J.-Y., James, S.R., Link, P. a, McCann, S.E., Hong, C.-C., Davis, W., Nesline, M.K., Ambrosone, C.B., Karpf, A.R., 2009. Association between global DNA hypomethylation in leukocytes and risk of breast cancer. Carcinogenesis 30, 1889–1897. doi:10.1093/carcin/bgp143

Choi, S., Worswick, S., Byun, H.-M., Shear, T., Soussa, J.C., Wolff, E.M., Douer, D., Garcia-Manero, G., Liang, G., Yang, A.S., 2009. Changes in DNA methylation of tandem DNA repeats are different from interspersed repeats in cancer. Int. J. cancer 125, 723–9. doi:10.1002/ijc.24384

Deininger, P., 2011. Alu elements: know the SINEs. Genome Biol 12, 236. doi:10.1186/gb-2011-12-12-236

Eden, A., Gaudet, F., Waghmare, A., Jaenisch, R., 2003. Chromosomal Instability and Tumors Promoted by DNA Hypomethylation. Science (80). 300, 2003. doi:10.1126/science.1083557

Ehrlich, M., 2009. DNA hypomethylation in cancer cells. Epigenomics 1, 239–59. doi:10.2217/epi.09.33

Fabris, S., Bollati, V., Agnelli, L., Morabito, F., Motta, V., Cutrona, G., Matis, S., Recchia, A.G., Gigliotti, V., Gentile, M., Deliliers, G.L., Bertazzi, P.A., Ferrarini, M., Neri, A., Baccarelli, A., 2011. Biological and clinical relevance of quantitative global methylation of repetitive DNA sequences in chronic lymphocytic leukemia. Epigenetics 6, 188–194. doi:10.4161/epi.6.2.13528

Feinberg, A.P., 2007. Phenotypic plasticity and the epigenetics of human disease. Nature 447, 433–440. doi:10.1038/nature05919

Frigola, J., Solé, X., Paz, M.F., Moreno, V., Esteller, M., Capellà, G., Peinado, M.A., 2005. Differential DNA hypermethylation and hypomethylation signatures in colorectal cancer. Hum. Mol. Genet. 14, 319–326. doi:10.1093/hmg/ddi028

Herceg, Z., Vaissière, T., 2011. Epigenetic mechanisms and cancer an interface between the environment and the genome. Epigenetics 6, 804–819. doi:10.4161/epi.6.7.16262

Igarashi, S., Suzuki, H., Niinuma, T., Shimizu, H., Nojima, M., Iwaki, H., Nobuoka, T., Nishida, T., Miyazaki, Y., Takamaru, H., Yamamoto, E., Yamamoto, H., Tokino, T., Hasegawa, T., Hirata, K., Imai, K., Toyota, M., Shinomura, Y., 2010. A novel correlation between LINE-1 hypomethylation and the malignancy of gastrointestinal stromal tumors. Clin. Cancer Res. 16, 5114–5123. doi:10.1158/1078-0432.CCR-10-0581

Inamura, K., Yamauchi, M., Nishihara, R., Lochhead, P., Qian, Z.R., Kuchiba, A., Kim, S.A., Mima, K., Sukawa, Y., Jung, S., Zhang, X., Wu, K., Cho, E., Chan, A.T., Meyerhardt, J.A., Harris, C.C., Fuchs, C.S., Ogino, S., 2014. Tumor LINE-1 methylation level and microsatellite instability in relation to colorectal cancer prognosis. J. Natl. Cancer Inst. 106. doi:10.1093/jnci/dju195

Jordà, M., Peinado, M. a, 2010. Methods for DNA methylation analysis and applications in colon cancer. Mutat. Res. 693, 84–93. doi:10.1016/j.mrfmmm.2010.06.010

Karimi, M., Johansson, S., Ekström, T.J., 2006. Using LUMA: A luminometric-based assay for global DNA-methylation. Epigenetics 1, 45–48. doi:10.4161/epi.1.1.2587

Lander, E.S., Linton, L.M., Birren, B., Nusbaum, C., Zody, M.C., Baldwin, J., Devon, K., Dewar, K., Doyle, M., FitzHugh, W., Funke, R., Gage, D., Harris, K., Heaford, A., Howland, J., Kann, L., Lehoczky, J., LeVine, R., McEwan, P., McKernan, K., Meldrim, J., Mesirov, J.P., Miranda, C., Morris, W., Naylor, J., Raymond, C., Rosetti, M., Santos, R., Sheridan, A., Sougnez, C., Stange-Thomann, N., Stojanovic, N., Subramanian, A., Wyman, D., Rogers, J., Sulston, J., Ainscough, R., Beck, S., Bentley, D., Burton, J., Clee, C., Carter, N., Coulson, A., Deadman, R., Deloukas, P., Dunham, A., Dunham, I., Durbin, R., French, L., Grafham, D., Gregory, S.,

Hubbard, T., Humphray, S., Hunt, A., Jones, M., Lloyd, C., McMurray, A., Matthews, L., Mercer, S., Milne, S., Mullikin, J.C., Mungall, A., Plumb, R., Ross, M., Shownkeen, R., Sims, S., Waterston, R.H., Wilson, R.K., Hillier, L.W., McPherson, J.D., Marra, M.A., Mardis, E.R., Fulton, L.A., Chinwalla, A.T., Pepin, K.H., Gish, W.R., Chissoe, S.L., Wendl, M.C., Delehaunty, K.D., Miner, T.L., Delehaunty, A., Kramer, J.B., Cook, L.L., Fulton, R.S., Johnson, D.L., Minx, P.J., Clifton, S.W., Hawkins, T., Branscomb, E., Predki, P., Richardson, P., Wenning, S., Slezak, T., Doggett, N., Cheng, J.F., Olsen, A., Lucas, S., Elkin, C., Uberbacher, E., Frazier, M., Gibbs, R.A., Muzny, D.M., Scherer, S.E., Bouck, J.B., Sodergren, E.J., Worley, K.C., Rives, C.M., Gorrell, J.H., Metzker, M.L., Naylor, S.L., Kucherlapati, R.S., Nelson, D.L., Weinstock, G.M., Sakaki, Y., Fujiyama, A., Hattori, M., Yada, T., Toyoda, A., Itoh, T., Kawagoe, C., Watanabe, H., Totoki, Y., Taylor, T., Weissenbach, J., Heilig, R., Saurin, W., Artiguenave, F., Brottier, P., Bruls, T., Pelletier, E., Robert, C., Wincker, P., Smith, D.R., Doucette-Stamm, L., Rubenfield, M., Weinstock, K., Lee, H.M., Dubois, J., Rosenthal, A., Platzer, M., Nyakatura, G., Taudien, S., Rump, A., Yang, H., Yu, J., Wang, J., Huang, G., Gu, J., Hood, L., Rowen, L., Madan, A., Qin, S., Davis, R.W., Federspiel, N.A., Abola, A.P., Proctor, M.J., Myers, R.M., Schmutz, J., Dickson, M., Grimwood, J., Cox, D.R., Olson, M. V, Kaul, R., Raymond, C., Shimizu, N., Kawasaki, K., Minoshima, S., Evans, G.A., Athanasiou, M., Schultz, R., Roe, B.A., Chen, F., Pan, H., Ramser, J., Lehrach, H., Reinhardt, R., McCombie, W.R., de la Bastide, M., Dedhia, N., Blocker, H., Hornischer, K., Nordsiek, G., Agarwala, R., Aravind, L., Bailey, J.A., Bateman, A., Batzoglou, S., Birney, E., Bork, P., Brown, D.G., Burge, C.B., Cerutti, L., Chen, H.C., Church, D., Clamp, M., Copley, R.R., Doerks, T., Eddy, S.R., Eichler, E.E., Furey, T.S., Galagan, J., Gilbert, J.G., Harmon, C., Hayashizaki, Y., Haussler, D., Hermjakob, H., Hokamp, K., Jang, W., Johnson, L.S., Jones, T.A., Kasif, S., Kaspryzk, A., Kennedy, S., Kent, W.J., Kitts, P., Koonin, E. V, Korf, I., Kulp, D., Lancet, D., Lowe, T.M., McLysaght, A., Mikkelsen, T., Moran, J. V, Mulder, N., Pollara, V.J., Ponting, C.P., Schuler, G., Schultz, J., Slater, G., Smit, A.F., Stupka, E., Szustakowski, J., Thierry-Mieg, D., Thierry-Mieg, J., Wagner, L., Wallis, J., Wheeler, R., Williams, A., Wolf, Y.I., Wolfe, K.H., Yang, S.P., Yeh, R.F., Collins, F., Guyer, M.S., Peterson, J., Felsenfeld, A., Wetterstrand, K.A., Patrinos, A., Morgan, M.J., de Jong, P., Catanese, J.J., Osoegawa, K., Shizuya, H., Choi, S., Chen, Y.J., International Human Genome Sequencing, C., 2001. Initial sequencing and analysis of the human genome. Nature 409, 860–921. doi:10.1038/35057062

Li, J., Huang, Q., Zeng, F., Li, W., He, Z., Chen, W., Zhu, W., Zhang, B., 2014. The prognostic value of global DNA hypomethylation in cancer: a meta-analysis. PLoS One 9, e106290. doi:10.1371/journal.pone.0106290\rPONE-D-14-10144 [pii]

Lisanti, S., Omar, W.A.W., Tomaszewski, B., De Prins, S., Jacobs, G., Koppen, G., Mathers, J.C., Langie, S.A.S., 2013. Comparison of methods for quantification of global DNA methylation in human cells and tissues. PLoS One 8. doi:10.1371/journal.pone.0079044

Lister, R., Pelizzola, M., Dowen, R.H., Hawkins, R.D., Hon, G., Tonti-Filippini, J., Nery, J.R., Lee, L., Ye, Z., Ngo, Q.-M., Edsall, L., Antosiewicz-Bourget, J., Stewart, R., Ruotti, V., Millar, A.H., Thomson, J.A., Ren, B., Ecker, J.R., 2009. Human DNA methylomes at base resolution show widespread epigenomic differences. Nature, Publ. online 14 Oct. 2009; | doi10.1038/10.1038/nature08514 462, 315. doi:10.1038/NATURE08514

Liu, F., Killian, J.K., Yang, M., Walker, R.L., Hong, J. a, Zhang, M., Davis, S., Zhang, Y., Hussain, M., Xi, S., Rao, M., Meltzer, P. a, Schrump, D.S., 2010. Epigenomic alterations and gene expression profiles in respiratory epithelia exposed to cigarette smoke condensate. Oncogene 29, 3650–64. doi:10.1038/onc.2010.129

Mancikova, V., Buj, R., Castelblanco, E., Inglada-Pérez, L., Diez, A., De Cubas, A.A., Curras-Freixes, M., Maravall, F.X., Mauricio, D., Matias-Guiu, X., Puig-Domingo, M., Capel, I., Bella, M.R., Lerma, E., Castella, E., Reverter, J.L., Peinado, M.Á., Jorda, M., Robledo, M., 2014. DNA methylation profiling of well-differentiated thyroid cancer uncovers markers of recurrence free survival. Int. J. Cancer 135, 598–610. doi:10.1002/ijc.28703

Mathers, J.C., Strathdee, G., Relton, C.L., 2010. Induction of Epigenetic Alterations by Dietary and Other Environmental Factors, Advances in Genetics. doi:10.1016/B978-0-12-380864-6.00001-8

Matsuda, Y., Yamashita, S., Lee, Y.C., Niwa, T., Yoshida, T., Gyobu, K., Igaki, H., Kushima, R., Lee, S., Wu, M.S., Osugi, H., Suehiro, S., Ushijima, T., 2012. Hypomethylation of Alu repetitive elements in esophageal mucosa, and its potential contribution to the epigenetic field for cancerization. Cancer Causes Control 23, 865–873. doi:10.1007/s10552-012-9955-4

Moore, L.E., Pfeiffer, R.M., Poscablo, C., Real, F.X., Kogevinas, M., Silverman, D., Garc??a-Closas, R., Chanock, S., Tard??n, A., Serra, C., Carrato, A., Dosemeci, M., Garc??a-Closas, M., Esteller, M., Fraga, M., Rothman, N., Malats, N., 2008. Genomic DNA hypomethylation as a biomarker for bladder cancer susceptibility in the Spanish Bladder Cancer Study: a case-control study. Lancet Oncol. 9, 359–366. doi:10.1016/S1470-2045(08)70038-X

Quinlan, A.R., Hall, I.M., 2010. BEDTools: A flexible suite of utilities for comparing genomic features. Bioinformatics 26, 841–842. doi:10.1093/bioinformatics/btq033

Ritz, C., Spiess, A.-N., 2008. qpcR: an R package for sigmoidal model selection in quantitative real-time polymerase chain reaction analysis. Bioinformatics 24, 1549–51. doi:10.1093/bioinformatics/btn227

Robin, X., Turck, N., Hainard, A., Tiberti, N., Lisacek, F., Sanchez, J.-C., Müller, M., 2011. pROC: an open-source package for R and S+ to analyze and compare ROC curves. BMC Bioinformatics 12, 77. doi:10.1186/1471-2105-12-77

Rodriguez, J., Frigola, J., Vendrell, E., Risques, R.-A., Fraga, M.F., Morales, C., Moreno, V., Esteller, M., Capellà, G., Ribas, M., Peinado, M. a, 2006. Chromosomal instability correlates with genome-wide DNA demethylation in human primary colorectal cancers. Cancer Res. 66, 8462–9468. doi:10.1158/0008-5472.CAN-06-0293

Rodriguez, J., Vives, L., Jordà, M., Morales, C., Muñoz, M., Vendrell, E., Peinado, M.A., 2008. Genome-wide tracking of unmethylated DNA Alu repeats in normal and cancer cells. Nucleic Acids Res. 36, 770–784. doi:10.1093/nar/gkm1105

Saito, K., Kawakami, K., Matsumoto, I., Oda, M., Watanabe, G., Minamoto, T., 2010. Long interspersed nuclear element 1 hypomethylation is a marker of poor prognosis

in stage IA non-small cell lung cancer. Clin. Cancer Res. 16, 2418–2426. doi:10.1158/1078-0432.CCR-09-2819

Salas, L.A., Villanueva, C.M., Tajuddin, S.M., Amaral, A.F.S., Fernandez, A.F., Moore, L.E., Carrato, A., Tardón, A., Serra, C., García-Closas, R., Basagaña, X., Rothman, N., Silverman, D.T., Cantor, K.P., Kogevinas, M., Real, F.X., Fraga, M.F., Malats, N., 2014. LINE-1 methylation in granulocyte DNA and trihalomethane exposure is associated with bladder cancer risk. Epigenetics 9, 1532–1539. doi:10.4161/15592294.2014.983377

Sandoval, J., Esteller, M., 2012. Cancer epigenomics: Beyond genomics. Curr. Opin. Genet. Dev. doi:10.1016/j.gde.2012.02.008

Schwarzenbach, H., Hoon, D.S.B., Pantel, K., 2011. Cell-free nucleic acids as biomarkers in cancer patients. Nat Rev Cancer 11, 426–437. doi:10.1038/nrc3066

Shigaki, H., Baba, Y., Watanabe, M., Iwagami, S., Miyake, K., Ishimoto, T., Iwatsuki, M., Baba, H., 2012. LINE-1 Hypomethylation in Noncancerous Esophageal Mucosae is Associated with Smoking History. Ann. Surg. Oncol. 19, 4238–4243. doi:10.1245/s10434-012-2488-y

Smith, I.M., Mydlarz, W.K., Mithani, S.K., Califano, J.A., 2007. DNA global hypomethylation in squamous cell head and neck cancer associated with smoking, alcohol consumption and stage. Int. J. Cancer 121, 1724–8. doi:10.1002/ijc.22889

Suzuki, M., Shiraishi, K., Eguchi, A., Ikeda, K., Mori, T., Yoshimoto, K., Ohba, Y., Yamada, T., Ito, T., Baba, Y., Baba, H., 2013. Aberrant methylation of LINE-1, SLIT2, MAL and IGFBP7 in non-small cell lung cancer. Oncol. Rep. 29, 1308–1314. doi:10.3892/or.2013.2266

Tajuddin, S.M., Amaral, A.F.S., Fernández, A.F., Chanock, S., Silverman, D.T., Tardón, A., Carrato, A., García-Closas, M., Jackson, B.P., Toraño, E.G., Márquez, M., Urdinguio, R.G., García-Closas, R., Rothman, N., Kogevinas, M., Real, F.X., Fraga, M.F., Malats, N., Sala, M., Castaño, G., Torà, M., Puente, D., Villanueva, C., Murta-Nascimento, C., Fortuny, J., López, E., Hernández, S., Jaramillo, R., Vellalta, G., Palencia, L., Fermández, F., Amorós, A., Alfaro, A., Carretero, G., Lloreta, J., Serrano, S., Ferrer, L., Gelabert, A., Carles, J., Bielsa, O., Villadiego, K., Cecchini, L., Saladié, J.M., Ibarz, L., Céspedes, M., Serra, C., García, D., Pujadas, J., Hernando, R., Cabezuelo, A., Abad, C., Prera, A., Prat, J., Domènech, M., Badal, J., Malet, J., Rodríguez de Vera, J., Martín, A.I., Taño, J., Cáceres, F., García-López, F., Ull, M., Teruel, A., Andrada, E., Bustos, A., Castillejo, A., Soto, J.L., Guate, J.L., Lanzas, J.M., Velasco, J., Fernández, J.M., Rodríguez, J.J., Herrero, A., Abascal, R., Manzano, C., Miralles, T., Rivas, M., Arguelles, M., Díaz, M., Sánchez, J., González, O., Mateos, A., Frade, V., Asturias, M., Muntañola, P., Pravia, C., Huescar, A.M., Huergo, F., Mosquera, J., Fernandez, A.F., Tardon, A., Garcia-Closas, M., Torano, E.G., Marquez, M., Garcia-Closas, R., Investigators, for the S.B.C.S., 2014. LINE-1 methylation in leukocyte DNA, interaction with phosphatidylethanolamine N-methyltransferase variants and bladder cancer risk. Br J Cancer 110, 2123–2130. doi:10.1038/bjc.2014.67

Tajuddin, S.M., Amaral, A.F.S., Fernández, A.F., Rodríguez-Rodero, S., Rodríguez, R.M., Moore, L.E., Tardón, A., Carrato, A., García-Closas, M., Silverman, D.T., Jackson, B.P., García-Closas, R., Cook, A.L., Cantor, K.P., Chanock, S., Kogevinas, M., Rothman, N., Real, F.X., Fraga, M.F., Malats, N., Spanish Bladder Cancer/EPICURO Study Investigators, 2013. Genetic and non-genetic predictors of LINE-1 methylation in leukocyte DNA. Environ. Health Perspect. 121, 650–6. doi:10.1289/ehp.1206068

Toraño, E.G., Petrus, S., Fernandez, A.F., Fraga, M.F., 2012. Global DNA hypomethylation in cancer: review of validated methods and clinical significance. Clin. Chem. Lab. Med. 50, 1733–42. doi:10.1515/cclm-2011-0902

Weisenberger, D.J., Campan, M., Long, T.I., Kim, M., Woods, C., Fiala, E., Ehrlich, M., Laird, P.W., 2005. Analysis of repetitive element DNA methylation by MethyLight. Nucleic Acids Res. 33, 6823–6836. doi:10.1093/nar/gki987

Wu, H.-C., Delgado-Cruzata, L., Flom, J.D., Kappil, M., Ferris, J.S., Liao, Y., Santella, R.M., Terry, M.B., 2011. Global methylation profiles in DNA from different blood cell types. Epigenetics 6, 76–85. doi:10.4161/epi.6.1.13391

2. Trabajo II

A continuación, se presenta el artículo II (*DNA methylation profiling of well-differentiated thyroid cancer uncovers markers of recurrence free survival*) publicado en la revista *International Journal of Cancer* en diciembre de 2013. El artículo en su formato original y el material suplementario asociado puede encontrarse en el Anexo 3 y/o en la versión digital de esta tesis.

Resumen en castellano

El cáncer de tiroides es una neoplasia heterogénea con diferentes tipos histológicos caracterizados por diferencias citológicas, histológicas y por diferentes alteraciones genéticas. Sin embargo, se desconoce en gran medida la contribución de la desregulación del epigenoma en el desarrollo y progresión de este tipo de tumor. Es por ello que en este trabajo quisimos estudiar el papel que juega la alteración de la metilación del DNA en el tipo más común de cáncer de tiroides, el cáncer de tiroides bien diferenciado (WDTC).

Con este objetivo, realizamos un análisis a escala genómica de la metilación del DNA mediante el *Illumina Infinium 27K array* en la serie más larga de WDTC publicada hasta el momento (83 tumores primarios y 8 tejidos tiroideos normales adyacentes al tumor). Los resultados obtenidos revelaron que el perfil de metilación del DNA no sólo estaba asociado a los tipos histológicos estudiados (FTA, FTC y PTC), sino también. a la mutación conductora subyacente (*BRAF*^{V600E} y *RAS*). Además, los genomas FTC estaban mucho más hipermetilados que los PTC, compartiendo muchos de los cambios con los FTA, lo que respalda la teoría de progresión tumoral desde adenomas a carcinomas debido a la acumulación progresiva de cambios en la metilación del DNA. Seguidamente, los cambios de metilación encontrados en algunos genes candidatos potencialmente implicados en la tumorogénesis del WDTC (*DLEC1*, *COL4A2*, *KLK10*) fueron validados en una serie alternativa independiente. Gracias a la integración de estos resultados con análisis de expresión previamente publicados en WDTC, identificamos una serie de genes cuya expresión está asociada con la metilación de sus secuencias promotoras. Por último, estudiamos el valor pronóstico de la hipermetilación de *EI24* y *WT1* como biomarcadores de riesgo de recurrencia tumoral.

En conjunto los resultados de este artículo confirman que la alteración de la metilación del DNA es un mecanismo a tener en cuenta en el estudio del WDTC y que la

caracterización de estos cambios puede contribuir enormemente a la búsqueda de biomarcadores que mejoren la estratificación del riesgo en esta neoplasia.

International Journal of Cancer: 135, 598-610 (2014)

DNA methylation profiling of well-differentiated thyroid cancer uncovers markers of recurrence free survival

Veronika Mancikova[1]*, Raquel Buj[2]*, Esmeralda Castelblanco[3], Lucıa Inglada-Perez[1,4], Anna Diez-Villanueva[2], Aguirre A. de Cubas[1], Maria Curras-Freixes[1], Francisco Xavier Maravall[3], Didac Mauricio[5,6,7], Xavier Matias-Guiu[8], Manel Puig-Domingo[5,6,7], Ismael Capel[9], Marıa Rosa Bella[10], Enrique Lerma[11], Eva Castella[12], Jordi Lluis Reverter[5,6,7], Miguel Angel Peinado[2], Mireia Jorda[2] and Mercedes Robledo[1,4]

[1]Hereditary Endocrine Cancer Group, Spanish National Cancer Research Centre (CNIO), Madrid, Spain. [2]Institute of Predictive and Personalized Medicine of Cancer (IMPPC), Badalona, Barcelona, Spain. [3]Department of Endocrinology and Nutrition, University Hospital Arnau de Vilanova, IRBLLEIDA, Lleida, Spain. [4]ISCIII Center for Biomedical Research on Rare Diseases (CIBERER), Madrid, Spain. [5]Germans Trias i Pujol Health Sciences Research Institute (IGTP), Badalona, Spain. [6]Department of Endocrinology and Nutrition, University Hospital Germans Trias i Pujol, Barcelona, Spain. [7]Department of Medicine, Autonomous University of Barcelona, Barcelona, Spain. [8]Department of Pathology, University Hospital Arnau de Vilanova, University of Lleida, IRBLLEIDA, Lleida, Spain. [9]Department of Endocrinology and Nutrition, Hospital de Sabadell, Sabadell, Spain. [10]Department of Pathology, Hospital de Sabadell, Sabadell, Barcelona, Spain. [11]Department of Pathology, Hospital Santa Creu i Sant Pau, Barcelona, Spain. [12]Department of Pathology, University Hospital Germans Trias i Pujol, Badalona, Spain.

Key words: well-differentiated thyroid cancer, methylation, BRAF, RAS, prognostic markers.

Abbreviations: *AKT3*: v-akt murine thymoma viral oncogene homolog 3; *BRAF*: v-raf murine sarcoma viral oncogene homolog B1; CIMP: CpG island methylator phenotype; *COL4A2*: collagen type IV alpha 2; *DLEC1*: deleted in lung and esophageal cancer 1; *EI24*: etoposide induced 2.4 mRNA; FA: follicular adenoma; FDR: false discovery rate; FTC: follicular thyroid carcinoma; fvPTC: papillary thyroid carcinoma follicular variant; *KLK10*: kallikrein-related peptidase 10; *NIS*: sodium-iodine symporter; PcG: PolyComb Group; PTC: papillary thyroid carcinoma; *RARb2*: retinoic acid receptor b2; *RASSF1*: RAS association domain family protein 1; *RET*: rearranged during transfection protooncogene; RFS: recurrence-free survival; *TIMP3*: tissue inhibitor of metalloproteinase-3; *TSHR*: thyroid-stimulating hormone receptor; *WT1*: Wilms tumor 1.

*V.M. and R.B. contributed equally to this work.

DOI: 10.1002/ijc.28703

History: Received 14 Oct 2013; Accepted 19 Dec 2013; Online 31 Dec 2013.

Correspondence to: Mercedes Robledo, Spanish National Cancer Center (CNIO), Madrid, Spain, Tel.: 134-917-328-000, Fax: 134-912-246- 972, E-mail: mrobledo@cnio.es or Mireia Jorda, Institute of Predictive and Personalized Medicine of Cancer (IMPPC), Badalona, Barcelona, Spain, Tel.: 134-935-543-050, Fax: 134-934-651-472, E-mail: mjorda@imppc.org.

Abstract

Thyroid cancer is a heterogeneous disease with several subtypes characterized by cytological, histological and genetic alterations, but the involvement of epigenetics is not well understood. Here, we investigated the role of aberrant DNA methylation in the development of well-differentiated thyroid tumors. We performed genome-wide DNA methylation profiling in the largest well-differentiated thyroid tumor series reported to date, comprising 83 primary tumors as well as 8 samples of adjacent normal tissue. The epigenetic profiles were closely related to not only tumor histology but also the underlying driver mutation; we found that follicular tumors had higher levels of methylation, which seemed to accumulate in a progressive manner along the tumorigenic process from adenomas to carcinomas. Furthermore, tumors harboring a *BRAF* or *RAS* mutation had a larger number of hypo- or hypermethylation events, respectively. The aberrant methylation of several candidate genes potentially related to thyroid carcinogenesis was validated in an independent series of 52 samples. Furthermore, through the integration of methylation and transcriptional expression data, we identified genes whose expression is associated with the methylation status of their promoters. Finally, by integrating clinical follow-up information with methylation levels we propose etoposide induced 2.4 and Wilsm tumor 1 as novel prognostic markers related to recurrence-free survival. This comprehensive study provides insights into the role of DNA methylation in well-differentiated thyroid cancer development and identifies novel markers associated with recurrence-free survival.

Introduction

Follicular cell-derived carcinoma arises from the main cell population of the thyroid gland and is the most common endocrine malignancy, accounting for more than 95% cases. This general term represents a highly heterogeneous entity composed of a spectrum of differentiation stages, ranging from benign lesions such as follicular adenoma (FA), to well-differentiated but mostly indolent carcinomas such as papillary thyroid carcinoma (PTC) or follicular thyroid carcinoma (FTC), through to undifferentiated, more invasive and lethal human malignancies, such those classified as poorly differentiated thyroid carcinoma and anaplastic thyroid carcinoma. Most well-differentiated carcinomas can be effectively clinically managed and have an excellent prognosis. However, a subset of these tumors behave aggressively, and there is currently no effective treatment for them (Kondo et al., 2006). As all these malignancies arise from the same cell type, it is of great interest to understand the molecular alterations giving rise to the observed heterogeneity.

Genetics has been shown to play an important role in the development of this disease. The most recurrent point mutations and rearrangements tend to affect the effector genes of the MAPK pathway, such as v-raf murine sarcoma viral oncogene homolog B1 (*BRAF*), the *RAS* family and the “rearranged during transfection” protooncogene *RET*. These early alterations have been shown to be exclusive, subtype-specific and to a certain extent prognostic. Virtually all tumors bearing *RAS* mutations present a follicular pattern of growth [FA, FTC or PTC follicular variant (fvPTC)], while *BRAF* mutations and rearrangements in the *RET* gene are characteristic of PTC (Nikiforov et al., 2011). It is widely accepted that *BRAF*-positive tumors tend to have a worse prognosis (Lupi et al., 2007; Xing et al., 2005). Conversely, *RAS* mutations are detected among both follicular carcinomas and adenomas, thus having diagnostic value but not prognostic value, and leaving many clinical questions to be answered.

At present, high-throughput techniques are being used to identify altered pathways related to the development of specific tumor types or clinical features. In thyroid cancer, it has been demonstrated that aberrant expression patterns can predict a patient’s prognosis (Montero-Conde et al., 2008). Moreover, these patterns have been closely linked to the presence of particular mutations and shown to be specific to each (Montero-Conde et al., 2008; Giordano et al., 2005; Malixzewska et al., 2013). Although it might be expected that other genomic features such as methylation are also closely related to the particular mutated gene that leads to carcinogenesis, little is known about aberrant epigenetic profiles specific to individual thyroid cancer subtypes. Studies published to date have

followed either a strict candidate gene-based approach or have used a limited number of samples (Rodriguez-Rodero et al., 2013). Therefore, the genes identified so far as repressed by aberrant methylation are either involved in thyroid gland function [e.g., thyroid-stimulating hormone receptor (*TSHR*) (Xing et al., 2003), sodium-iodine symporter (*NIS*) (Venkataraman et al., 2003)] or have a tumor suppressor gene function [e.g., tissue inhibitor of metalloproteinase-3 (*TIMP3*), retinoic acid receptor b2 (*RARb2*) (Hu et al., 2006; Brait et al., 2012), *RAS* association domain family protein 1 (*RASSF1*) (Schagdarsurengin et al., 2002)]. A global view of genome-wide aberrant methylation in thyroid cancer is still lacking.

In this study, we quantitatively profiled the genome-wide DNA methylation of 83 primary thyroid tumors (18 FA, 18 FTC and 47 PTC) and 8 samples of adjacent normal thyroid tissue using the 27K Infinium Methylation Array. We identified disease subtype and mutation-specific DNA methylation patterns and propose novel markers related to recurrence free survival (RFS). Moreover, by integrating methylation data with mRNA expression, we were able to identify genes whose expression is associated with the methylation status of their promoter regions, thereby adding new insights into thyroid carcinogenesis.

Materials and methods

Sample collection and patient follow-up

One hundred and thirty-two thyroid tumors were snap frozen following surgery at Hospital Sant Pau and Hospital Sabadell in Barcelona (Spain) and at Hospital Arnau de Vilanova in Lleida (Spain), and stored at -80ºC. Of these, 83 primary thyroid tumors (42 PTC, 5 fvPTC, 18 FA and 18 FTC) not previously profiled at the genome-wide DNA methylation level (Rodriguez-Rodero et al., 2013) were used in the discovery phase of the study, and the remaining 49 tumor samples (24 PTC, 9 fvPTC, 12 FA and 4 FTC) in the replication phase. Sections of each sample were evaluated by a pathologist and, when necessary, non-tumoral tissue was dissected. We studied eight adjacent normal thyroid tissues in the discovery and three in the replication series. At least 80% of the cells were cancerous in all tumor samples, while non-tumor samples had no observable tumor epithelium. Tumors were classified as PTC, fvPTC, FA and FTC according to the criteria proposed by WHO classification of tumors of the endocrine system, by three pathologists with experience on thyroid pathology (XM, MRB and EL). All cases in the PTC group exhibited the typical cytological and architectural features of the classical variant. Strict

criteria were used for fvPTC; tumors showed unquestionable cytological features together with a follicular pattern of growth. For FA, presence of capsule and absence of hyperplasic changes in the adjacent thyroid tissue was required. For FTC, obvious evidence of vascular and capsular invasion was also required. Genomic DNA was extracted from all samples using the DNeasy Blood and Tissue kit (QIAGEN) according to the manufacturer's protocol.

The clinical follow-up of the patients was performed by physical examination, neck ultrasonography, simultaneous determination of serum anti-tiroglobulin antibodies with tiroglobulin (basal, or after thyrotropin stimulation by thyroid hormone withdrawal or the administration of recombinant human thyrotropin) and whole-body iodine scanning. If there was a suspicion of local or distant disease, other imaging techniques such as CT, MRI, PET-CT or scintigraphy were used. The frequency and the type of technique used depended on the postoperative staging, which was also used to assess prognosis and to guide adjunctive therapy.

Mutation analysis

All PTCs were screened by Sanger sequencing for BRAF mutations at codon 600 in exon 15, while FA, FTC and fvPTC samples were screened for mutations in *H-, N-* and *K-RAS* at mutational hotspots on codons 12 and 13 of exon 2 and codon 61 of exon 3. When available, cDNA from PTC samples was also screened for *RET*/*PTC1* and *RET*/*PTC3* rearrangements as previously described (Montero-Conde et al., 2008).

DNA methylation assay, data processing and data analysis

Briefly, genomic DNA was bisulfite-converted using the EZ DNA Methylation Kit (Zymo Research, Orange, CA) following the manufacturer's recommended procedures. Genome wide promoter DNA methylation profiling was performed at the Spanish "Centro Nacional de Genotipado (CEGENISCIII)" (www.cegen.org) using the Illumina Infinium HumanMethylation 27K Platform (Illumina, San Diego, CA) as described previously (Biblikova et al., 2009). This assay generates DNA methylation data for 27,578 CpG dinucleotides covering 14,473 unique genes. The raw intensity data were quartile normalized using the R package, HumMeth27QCReport (Mancuso et al., 2011). For each CpG site, methylation levels were quantified using β-values, which represent the proportion of methylation, calculated as M/(M + U), where M is the methylated probe intensity and U the unmethylated probe intensity. β-values range from 0 to 1, with 0 being

completely unmethylated and 1 being completely methylated. M-Values, defined as log2(M/U), were used for statistical analyses; negative values indicate less than 50% methylation and positive values indicate more than 50% methylation (Du et al., 2010). We excluded probes that were detected in less than 95% of the samples (16 probes), probes designed for sequences on either the X or the Y chromosome (1,084 or 7 probes, respectively) as well as probes that potentially hybridized to more than one genomic locus (538 probes). The data discussed in this publication have been deposited in NCBI's Gene Expression Omnibus and are accessible through GEO Series accession number GSE51090 (http://www.ncbi.nlm.nih.gov/geo/query/acc.cgi?acc=GSE51090).

Unsupervised hierarchical clustering was performed using Cluster 3.0 software with "complete linkage" (Pearson correlation, uncentered metrics). The clusters were subsequently visualized using Treeview (http://rana.stanford.edu/software), and Principal Component Analysis (PCA) was performed using R CRAN version 2.15.3 (R, 2013).

Differences in DNA methylation status between normal thyroid tissue and specific subtypes were tested using POMELLO II, applying either a t-test with 200,000 permutations or linear models (limma) (Morrissey et al., 2009). To account for multiple hypotheses testing, p-values were adjusted using Benjamini's false discovery rate (FDR) correction. We defined a probe to be hypomethylated or hypermethylated when it displayed a mean M-value difference (ΔM-value) < 21.4 or >1.4, respectively, between a particular tumor group and normal tissue, and had a FDR < 0.05.

Methylation status validation: selection of candidate genes and bisulfite sequencing

Three of the most differentially methylated probes, all with a high fold-change across the experimental groups, were selected for validation. Biological functions were considered as additional criteria to select candidate promoter regions. Technical validation of microarray results was performed using bisulfite sequencing, first in a subset of the original discovery series (comprising 4 FA, 7 FTC, 13 PTC and 8 adjacent normal thyroid tissue samples). The candidate markers were then validated in 52 independent samples (24 PTC, 9 fvPTC, 12 FA, 4 FTC and 3 adjacent normal thyroid tissue samples).

From the bisulfite-treated DNA, at least two independent nested PCRs (for each sequence to be studied) were performed using two sets of primers specifically designed to contain no CpG sites (Supporting Information Table S1). The pooled PCR products were

purified (High Pure PCR product Purification Kit, Roche) and analyzed by Sanger sequencing (BigDye Terminator v3.1 Cycle Sequencing Kit, Applied Biosystems). Primary tumors were classified as hyper- or hypomethylated when the studied locus showed an increase or a decrease, respectively, in methylation level of over 20% relative to the average methylation of normal thyroid samples.

Integration of gene expression and DNA methylation

To identify genes whose expression is associated with methylation of their promoters, we assessed correlations between methylation and mRNA expression using two approaches. First, mRNA expression was compared to DNA methylation using the 31 primary thyroid tumors (Montero-Conde et al., 2008) for which data were available. Expression of all the available genes identified as differentially methylated (FDR <0.05, ΔM-value > |1.4|) was examined in this study. For genes with multiple probes included in the methylation array, the probe with the highest variance was selected, as previously described (Selamat et al., 2012). Correlation was measured using the Spearman coefficient. Second, we used an independent mRNA expression dataset available from GEO (http://www.ncbi.nlm.nih.gov/geo; GEO data base GSE27155) (Giordano et al., 2013). This database contains both histopathological and genetic information on the samples included. We merged the list of genes with differential methylation (FDR < 0.05, ΔM-value > |1.4|) with that of those identified as differentially expressed (t-test, FDR < 0.05).

Identification of genes whose methylation is of potential prognostic value

To identify methylation changes that could serve as potential prognostic markers, we integrated available clinical follow-up data of 60 patients with the methylation profiles. First, we performed supervised analysis with the POMELO II tool using methylation data for carcinoma samples from individuals free of the disease for at least 5 years and those with recurrence within 5 years after the appearance of the disease. Next, we chose probes with the most significant changes in methylation (FDR < 0.05, ΔM-value > |1.4|), and using SPSS (IBM SPSS Statistics version 19) we conducted an univariate Cox regression analysis to determine the impact of methylation status on RFS. RFS was defined as the time between initial diagnosis and relapse or death by the disease, with observations censored at last follow-up if no event had occurred. P-values were adjusted using Benjamini’s FDR correction.

Results

DNA methylation profiles reflect histology and *RAS*/*BRAF* mutational status in well-differentiated thyroid cancer

The main clinical and pathological characteristics, as well as the somatic tumoral mutation status, of the patients included in the study are summarized in Table 1 (more detailed information is available in Supporting Information Table S2). The prevalence of the mutations found among our samples is similar to that previously described (Nikiforov et al., 2006). We excluded probes that appeared to be constitutively unmethylated (*M*-value <-2.0, corresponding to a β-value <2.0; 8,657 probes) or methylated (*M*-value >2.0, corresponding to a β-value >0.8; 717 CpGs) in all samples. The vast majority of the unmethylated probes were in CpG islands (97.8%); DAVID functional annotation analysis (Huang et al., 2009) returned GO terms such as primary metabolic processes (Benjamini–Hochberg-adjusted p-value = 1.8 X 10^{-18}) and cellular metabolic processes (Benjamini-Hochberg-adjusted pvalue = 4.8 X 10^{-24}) as best hits (Supporting Information Fig. S1), suggesting an enrichment of housekeeping genes. Most of the methylated probes were located at non-CpG islands (63.6%), and no functional enrichment of the genes involved was observed. Further analyses were performed with the remaining 17,274 probes.

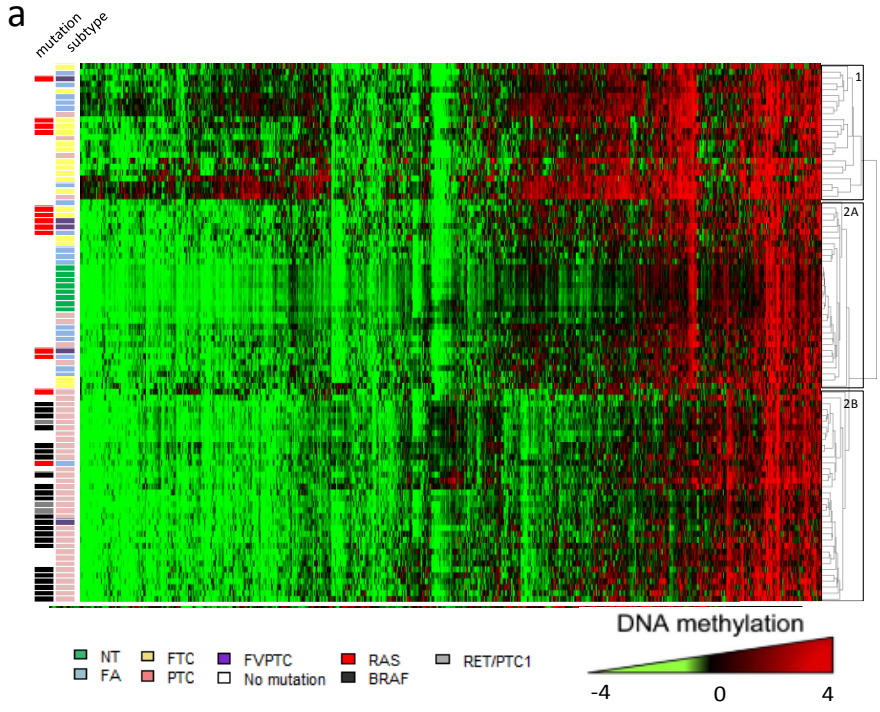

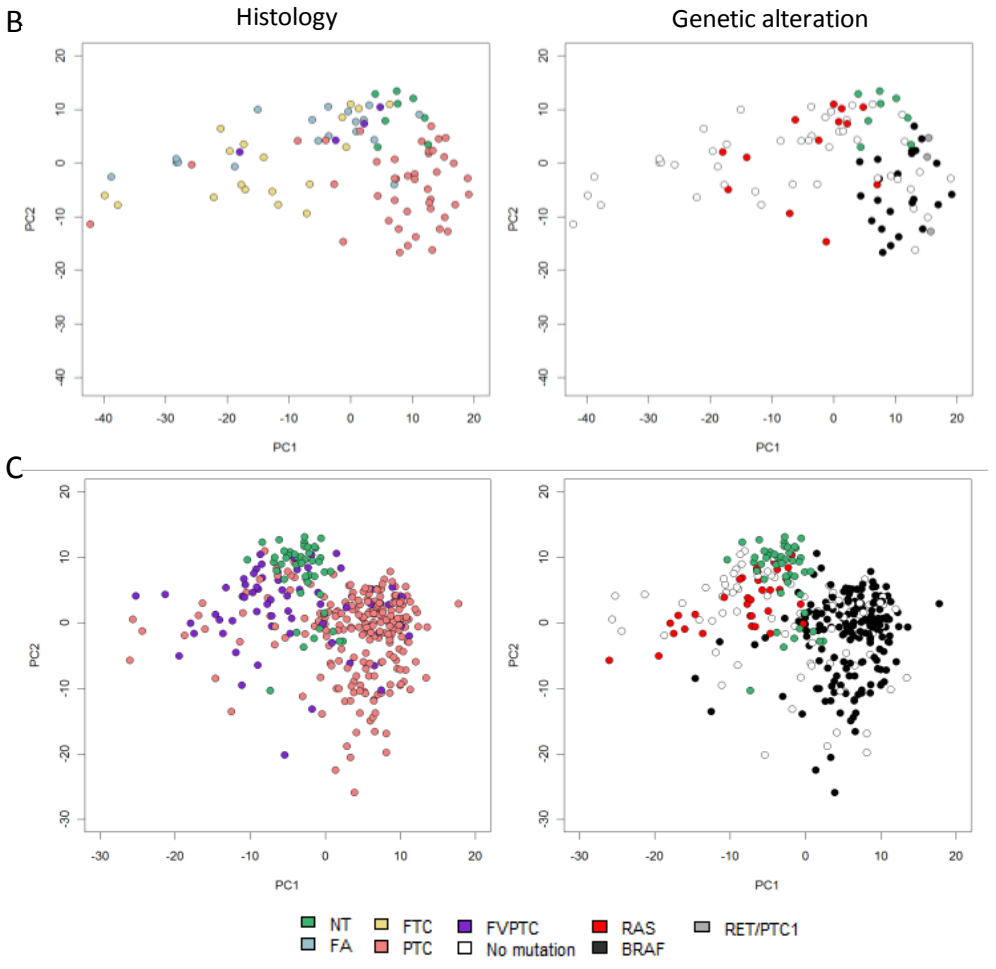

Figure 1 | (a) Unsupervised hierarchical cluster analysis. Hierarchical cluster analysis of 83 primary thyroid tumors and 8 adjacent normal tissue samples based on the 912 CpGs with the greatest variability (SD > 1.2). The analysis divided the sample set into two main clusters. "Cluster 1" was statistically significantly enriched with FTC samples. In "cluster 2B" the majority of PTC was gathered, while in "cluster 2A" normal tissues, showing a very homogeneous profile, were localized together with the majority of FA. **(b)** Principal component analysis. PCA analysis of 83 primary thyroid tumors and 8 adjacent normal tissue samples based on the 912 CpGs with the greatest variability (SD > 1.2). PCA analysis showed a clear relationship between DNA methylation and histology as well as genetic alterations. The three tumors containing a RET/PTC rearrangement group with BRAF-positive samples. **(c)** Principal component analysis. PCA analysis using DNA methylation data from the TCGA project (including 304 primary thyroid tumors and 50 adjacent normal tissue samples) based on the same CpGs with the greatest variability (SD > 1.2) identified in our study.

An unsupervised hierarchical cluster analysis of the 912 CpGs with standard deviation >1.2 identified two distinct clusters based on histological subtype and the underlying mutation (Fig. 1a). More specifically, "cluster 1" was enriched with FTC (p-value <0.0001) and showed statistically significantly higher levels of methylation when compared

to normal tissue samples grouped in “cluster 2” (p-value = 2.7 X 10^{-7}). “Cluster 2” comprised two sub-clusters. “Cluster 2A” consisted of tumors with substantial histological heterogeneity, including, among others, the majority of FA samples (11 out of 18 FA) and all the normal thyroid tissue samples. Of note, the branch lengths between the normal thyroid samples were shorter than those between the tumor samples, indicating greater heterogeneity in methylation profiles among the latter. The tumors grouped in this sub-cluster also showed higher levels of methylation compared to normal tissue (p-value = 4.6 X 10^{-3}). Finally, “cluster 2B” showed a robust methylation profile and comprised 36 tumors, 35 of which were PTCs; this sub-cluster included all those with the *BRAF*^{V600E} mutation and *RET*/*PTC1* rearrangement. The methylation levels of samples in “cluster 2B” showed no statistical difference compared with normal tissue samples, suggesting methylation profiles differences between tumors with follicular and papillary growth patterns.

Table 1 | Summary of the main clinical and pathological characteristics of samples used in this study.

Clinical characteristics		Discovery series (n=83). Number (%)[1]	Replication series (n=49). Number (%)[1]
Gender			
	Male	17 (20.5)	13 (26.5)
	Female	66 (79.5)	35 (71.5)
	Missing	0 (0)	1 (2.0)
Age			
	Median	47	45
	Min-Max	13-78	20 – 84
Histology		42 (50.6)	24 (49.0)
	PTC	5 (6.0)	9 (18.4)
	fvPTC	18 (21.7)	4 (8.2)
	FA	18 (21.7)	12 (24.4)
	NT	8	3
Recurrence[2]			
	Yes	14 (21.5)	7 (18.69)
	No	47 (72.3)	24 (64.9)
	Missing	4 (6.2)	6 (16.2)
Follow-up (months)			
	Median	36	46.5
	IQR	13.5 – 84	21 – 73.25
Mutation			
	BRAF^{V600E}	23 (27.7)	13 (26.5)
	RAS	13 (15.7)	2 (4.1)
	RET/*PTC1*	3 (3.6)	0 (0)
	Negative	44 (53.0)	44 (69.4)

A total number of 132 tumor samples and 11 normal adjacent tissues were used in this study, divided in the discovery series (83 tumors and 8 normal thyroid tissues) and replication series (49 tumors and 3 normal samples).
IQR, interquartile range
[1]The percentage is calculated taking into account only the total number of tumors (normal tissues were not included)
[2]The data on recurrence are only included for the malignant tumors (adenomas were not taking into account).

Although no clustering of samples harboring *RAS* mutations was observed using unsupervised analysis, it is noteworthy that those fvPTC bearing a *RAS* mutation were grouped in clusters 1 and 2A, together with *RAS*-FTC and *RAS*-FA, while the only tumor bearing a *BRAF* mutation clustered with *BRAF*-PTC tumors. Therefore, we applied a principal component analysis (PCA) using the 912 CpGs with highest methylation variability, and confirmed the grouping of samples according to their mutational status (Fig. 1b). Using publically available data from The Cancer Genome Atlas (TCGA) project (87%

of the 912 probes used for the unsupervised analysis were also included in the 450K platform), we were able to confirm the robust clustering of thyroid tumors according to primary mutation, *BRAF versus RAS* (Fig. 1c).

Identification of differentially methylated regions in well differentiated thyroid cancer

We identified 9 hypomethylated probes (9 genes) in FA, 83 (77 genes) in FTC and 53 (51 genes) in PTC. We also observed 89 hypermethylated CpGs (83 genes) in FA, 460 (416 genes) in FTC and 39 (31 genes) in PTC. A Venn diagram analysis revealed that a substantial proportion of differentially methylated regions identified in FA was also altered in FTC. Sixty-nine (83%) hypermethylated and six (67%) hypomethylated probes in FA were also hyper- and hypomethylated, respectively, in FTC (Figs. 2a and 2b and Supporting Information Fig. S2). Table 2 summarizes the 20 most significant subtype specific probes identified as well as their corresponding Δβ-values. An extended list of all differentially methylated probes is listed in Supporting Information Table S3. After dividing FA and FTC samples according to their mutational status, we assessed associations of individual probes with each of the genetic subgroups. For *RAS*-positive tumors, we identified 72 probes (70 genes) and 203 probes (181 genes) to be hypomethylated in FA and FTC, respectively. Hypermethylated were 263 probes (258 genes) and 454 probes (426 genes) in FA and FTC, respectively. In tumors with no mutations, we identified on one hand 11 hypomethylated probes (11 genes) in FA and 77 (71 genes) in FTC, and on the other hand 105 hypermethylated probes (97 genes) in FA and 587 (528 genes) in FTC (Figs. 2c and 2d upper and Supporting Information Fig. S2).

After dividing PTC samples according to the genetic alterations they harbored, we identified 126 hypomethylated probes (121 genes) in *BRAF*-positive tumors, 74 (72 genes) in *RAS*-positive tumors and 7 (7 genes) in tumors with no detectable mutations (16 tumors); we found 78 hypermethylated probes (70 genes) in *BRAF*-related tumors, 141 (132 genes) *RAS*-mutated tumors and 84 (78 genes) in tumors with no mutations. No probes were found to be specific to PTC tumors harboring the *RET*/*PTC1* rearrangement (Figs. 2c and 2d lower and Supporting Information Fig. S2). All hypo- and hypermethylated genes for each tumor subtype are listed in Supporting Information Table S3.

Furthermore, we aimed to identify the differentially methylated probes specifically associated with mutational status, independently of histology, by separately comparing with normal tissue all *RAS*-tumors, all *BRAF*-tumors and all non-mutated tumors. We

obtained 450 probes from these analyses (Supporting Information Table S3) that, when used to perform PCA, resulted in a robust separation of mutated samples into two main groups: *BRAF*-positive samples together with *RET*/*PTC1* samples and samples harboring *RAS* mutations (Fig. 3).

Table 2 | Top 20 subtype-specific probes for FA, FTC and PTC

Probe ID	Gene ID	FDR	ΔM-value	Δβ-value	Chr.	CpG Island
Top 20 FA specific probes						
cg06367117	*ALDOC*	2.00E-07	2.71093869	0.3926528	17	TRUE
cg08047457	*RASSF1*	9.00E-07	2.29675986	0.40019958	3	TRUE
cg21554552	*RASSF1*	2.40E-06	2.44631867	0.36554431	3	TRUE
cg17568996	*NFAM1*	2.42E-05	2.25126535	0.33678735	22	FALSE
cg06821120	*RASSF1*	0.0001938	1.7311015	0.33777293	3	TRUE
cg27219973	*GNRHR*	0.0008154	1.54777294	0.22217650	4	FALSE
cg13926569	*PAPSS2*	0.0013162	1.72337985	0.27635483	10	FALSE
cg09606564	*MFAP4*	0.0013598	1.4726875	0.25294503	17	FALSE
cg16393207	*GDPD5*	0.0013598	1.54616899	0.22478436	11	TRUE
cg14129786	*MGMT*	0.0014039	1.66225486	0.22401578	10	TRUE
cg14973995	*TETRAN*	0.0014039	2.07575889	0.30959818	4	TRUE
cg18055007	*DDAH2*	0.0014133	1.88659804	0.25590677	6	TRUE
cg17582777	*EFNA3*	0.0017439	-1.53694597	-0.23233439	1	FALSE
cg05656364	*VAMP8*	0.0021883	-1.55332458	-0.16488351	2	FALSE
cg22995106	*COG4*	0.0022767	1.40257423	0.1805763	16	TRUE
cg15692239	*ALDOC*	0.0022767	2.53820971	0.20161756	17	TRUE
cg21402071	*CHRNB4*	0.0028915	1.82059373	0.20535253	15	FALSE
cg26365553	*MADD*	0.0031854	1.42934142	0.24722019	11	FALSE
cg12783776	*SERPING1*	0.0033165	1.9289042	0.27738869	11	TRUE
Top 20 FTC specific probes						
cg21554552	*RASSF1*	7.00E-07	2.98852759	0.45417166	3	TRUE
cg08047457	*RASSF1*	9.00E-07	2.72818463	0.47218605	3	TRUE
cg14679230	*LIPE*	3.80E-06	1.45037569	0.1459732	19	FALSE
cg04972979	*C20orf54*	5.50E-06	1.61451484	0.30256229	20	FALSE
cg16517394	*TNFSF4*	9.60E-06	1.8536169	0.23950413	1	FALSE
cg00804392	*RHOH*	1.11E-05	1.85216994	0.29420054	4	TRUE
cg05467458	*SLC7A9*	1.52E-05	1.70161824	0.28134819	19	FALSE
cg20802392	*CTSK*	1.52E-05	1.98033411	0.27687162	1	TRUE
cg26218269	*MAB21L2*	1.58E-05	1.72450003	0.21028063	4	TRUE
cg06367117	*ALDOC*	1.58E-05	3.13695217	0.45480542	17	TRUE
cg16779976	*BLNK*	1.58E-05	-1.5932182	-0.17493057	10	FALSE
cg04629204	*EXTL1*	1.68E-05	1.4815062	0.24451418	1	FALSE
cg14120436	*GNB5*	2.62E-05	1.59384173	0.20025587	15	FALSE
cg20592700	*WIPI2*	2.62E-05	-1.50386259	-0.13059051	7	TRUE
cg00777121	*RASSF1*	4.72E-05	1.4952662	0.24566678	3	TRUE
cg10861599	*TNFSF4*	4.72E-05	1.57521415	0.19950722	1	FALSE
cg20356482	*FBP2*	5.00E-05	1.40957532	0.20331262	9	TRUE
cg09538582	*KRTHA5*	5.45E-05	1.47233264	0.09209393	17	FALSE
cg20394284	*JAK2*	6.48E-05	1.69088777	0.22587538	9	TRUE
Top 20 PTC specific probes						
cg13019092	*PDZK1*	<0.0000001	1.4330228	0.15003065	1	FALSE
cg07763768	*C9orf45*	<0.0000001	1.85389182	0.22681097	9	TRUE
cg02423618	*SPATA8*	<0.0000001	-1.56480549	-0.20065839	15	FALSE
cg18302652	*IL8*	2.58E-05	-1.69117713	-0.22868075	4	FALSE
cg17568996	*NFAM1*	7.01E-05	1.87197435	0.24967876	22	FALSE
cg24497819	*SELPLG*	0.0001279	-2.22238036	-0.3194521	12	FALSE
cg19385139	*COL4A2*	0.0002352	1.95997347	0.2680565	13	FALSE
cg03001305	*STAT5A*	0.000285	-2.54273891	-0.31643091	17	FALSE
cg15262516	*COL4A2*	0.0004566	1.40539859	0.16244608	13	FALSE
cg04057858	*UNQ9391*	0.0008376	-1.40846284	-0.18092863	8	FALSE
cg02523400	*SERPIND1*	0.0009559	2.57803439	0.31279995	22	FALSE
cg27105123	*EPS8L1*	0.0009877	-1.60910587	-0.23177057	19	FALSE
cg03733371	*LIPH*	0.0012087	-2.5252893	-0.35653317	3	FALSE
cg18752880	*C1QTNF3*	0.0014062	1.47593113	0.26132674	5	FALSE
cg04756629	*LOC400696*	0.0015227	-1.8391597	-0.21467597	19	FALSE
cg12385643	*UGT1A6*	0.0016378	-1.65626606	-0.18292765	2	FALSE
cg12530080	*PMCHL1*	0.0016882	-1.81689239	-0.26447097	5	FALSE
cg18343292	*MS4A7*	0.0016882	-1.49789853	-0.18361614	11	FALSE
cg27009703	*HOXA9*	0.0017272	1.75344159	0.18988395	7	TRUE
cg10236239	*SULT1C2*	0.001969	1.48508253	0.23764054	2	FALSE

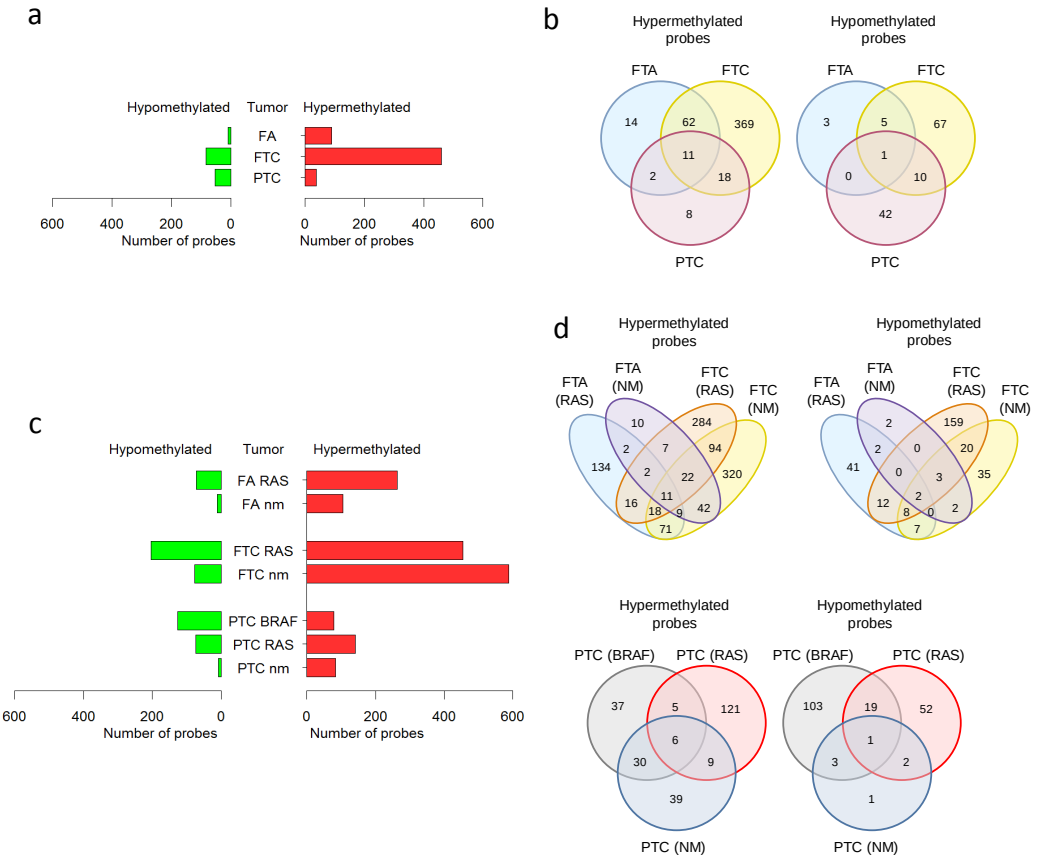

Figure 2 | Differentially methylated probes. (a) Subtype-specific probes identified using POMELO II based on FDR<0.05 and ΔM-value>|1.4| **(b)** Venn diagram showing the overlap between the identified subtype-specific hyper- and hypomethylated probes. **(c)** Mutation-specific probes identified using POMELO II and the criteria listed above. **(d)** Venn diagram analysis showing overlap between the identified mutation-specific hypermethylated and hypomethylated probes, respectively. Format of figures b and d have been modified from the original article, the original ones are at the Anexo 3.1.

For all differentially methylated probes identified (both mutation- and subtype-related), we also investigated the genomic context of their location, as it is well-known that hypo- and hypermethylation target different genomic regions in cancer (Supporting Information Fig. S3). We observed that hypermethylation in thyroid tumors occurred preferentially within a CpG island, whereas hypomethylation tended to affect probes outside of CpG islands (p-value < 0.0001). In addition, and as previously reported (Zhuang et al., 2012), hypermethylation occurred preferentially at stem cell Polycomb Group (PcG) target genes (p-value < 0.0001), while hypomethylated probes were highly enriched with CpGs that are heavily methylated in Embryonic Stem Cells (p-value < 0.0001).

Validation and replication of differentially methylated loci

We chose the promoter regions of three genes for validation using bisulfite sequencing; hypermethylation of two of them (*COL4A2* and *DLEC1*) was more common in thyroid neoplasias in general than in normal tissues, while hypomethylation of *KLK10* was specific to PTC tumors harboring the *BRAF*^{V600E} mutation. Comparison of quantitative methylation values at these three CpG sites from the HumanMethylation 27K Platform and bisulfite sequencing in 32 samples confirmed the accuracy of the array-based measurement (Supporting Information Fig. S4). The analysis by bisulfite sequencing assessed not only the methylation state of the CpG within the probe but also the flanking CpGs, revealing that the differential methylation affected a larger region (Supporting Information Fig. S4). These results validate the use of the single CpG sites interrogated by Illumina Infinium HumanMethylation 27K Platform as surrogate reporters of regional methylation. In addition, we replicated the findings for the three candidate genes in an independent series of 24 PTC, 9 fvPTC, 12 FA, 4 FTC and 3 normal thyroid tissues (Supporting Information Table S2).

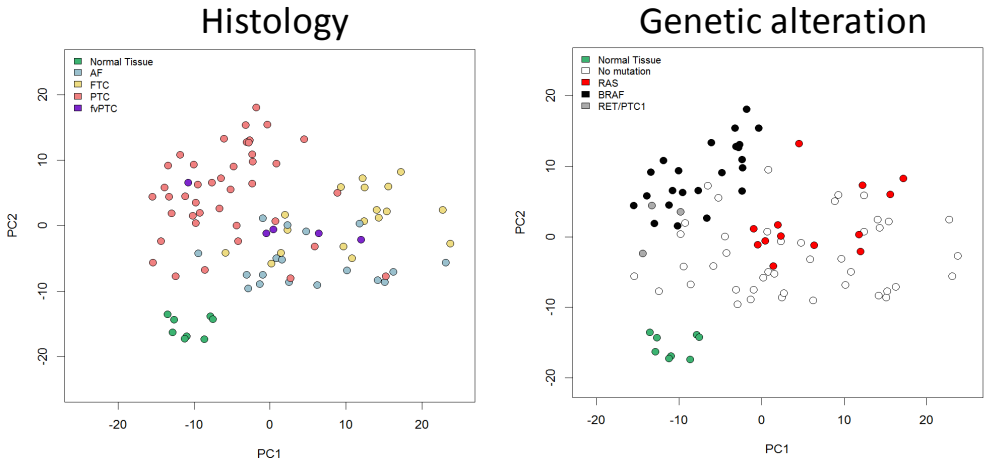

Figure 3 | PCA analysis using 450 mutation-specific probes. PCA analysis using 450 probes identified to be differentially methylated in supervised cluster analysis. The probes were identified to be specifically associated with the mutational status and independent of the histology and their usage resulted in a robust separation of samples into two main groups: *BRAF*- and *RET/PTC*-positive tumors and *RAS*-positive tumors.

In the discovery series, as measured by the array, *COL4A2* was hypermethylated in 66% of PTC, 21% of FA and in 56% of FTC samples; in the independent replication series hypermethylation was observed in 41% of PTC and 33% of FA samples. The lack of *COL4A2* hypermethylation among FTC samples could be due to the fact that only four

samples were available. Conversely, *DLEC1* showed hypermethylation in the discovery series in 23% of PTC, 42% of FA and 56% of FTC samples, compared to 23% of PTC, 8% of FA and 75% of FTC samples in the replication series. In the replication series, we confirmed the *KLK10* hypomethylation in all *BRAF*-positive samples (Supporting Information Fig. S4).

Correlation between DNA methylation and mRNA expression

The integration of methylation and expression data available (Montero-Conde et al., 2008) from 31 thyroid tumors allowed us to examine gene expression levels of a limited number of genes (4,029 genes on both platforms that represent 27.8% of the genes included on the methylation array). We examined the correlation between DNA methylation and mRNA expression in all histological groups where at least five samples were available for the analysis. In PTCs with the *BRAF*^{V600E} mutation, we observed an inverse correlation with expression for 13.3% (6 out of 45 genes available for integration) of genes with significant changes in methylation. Among FTC, 10.4% (16/153) of genes showed a similar trend, while in the case of FA it was 11.6% (5/43).

Additionally, we identified differentially expressed genes using an mRNA expression data from an independent case series (Giordano et al., 2005). After comparing these genes with the lists of differentially methylated genes we found that 10% (7 out of 70 differentially methylated genes) and 2.9% (12/416) of the genes hypermethylated in PTC (*BRAF*-related) and FTC, respectively, were down-regulated. Moreover, we found that 20.7% (25/121) of the hypomethylated genes in PTC (*BRAF*-related) and 1.9% (1/77) in FTC were up-regulated. We did not, however, find any association between changes in methylation and gene expression in FA.

A substantial portion of the genes whose expression we observed to be inversely correlated with the methylation level of their corresponding promoters has been already described to play a role in the tumorigenic process (*CTSF, KLK10, PHLDA2, RUNX1, TACSTD2, BAALC, CTSF, HMGA1, RASSF2, IMPDH1* and *TNFRSF10C*). Moreover, for *BRAF*-related PTC they also included genes from the MAPK pathway (*MAPK13, DUSP5 and RAP1GA1*) and genes involved in apoptosis (*LCN2, RIPK1* and *LGALS1*), whereas for FTC we observed a down-regulation by hypermethylation of several genes involved in innate immune response (*C7, SERPING1, TRAF3, PYCARD* and *CFH*). All genes identified in this analysis are listed in Supporting Information Table S4.

Identification of methylation-related prognostic markers

The analysis of 34 samples (PTC and FTC) with available follow-up information identified 32 probes differentially methylated among patients with and without recurrence (Supporting Information Table S3). We performed survival analysis of 60 patients to evaluate the impact of methylation levels of these genes on RFS, obtaining significant associations with risk of recurrence for etoposide induced 2.4 (*EI24*) and Wilms tumor 1 (*WT1*) (Fig. 4). Among all known risk factors associated with poor prognosis (sex, age of onset, mutation in *BRAF*, FTC and tumor size), only the latter showed statistical significance in our study (p = 0.016). After including tumor size as a covariable, the association of *EI24* and *WT1* methylation levels with prognosis remained significant (p = 0.004; HR = 2.08; CI = 1.262–3.445 and p = 0.006; HR = 1.64; IC = 1.149–2.335, respectively); results from the univariate analysis are shown in Figure 4. In addition, the association of *EI24* and *WT1* methylation level with recurrence remained significant in multivariable analysis including separately each of the remaining clinical variables known to be related to poor prognosis.

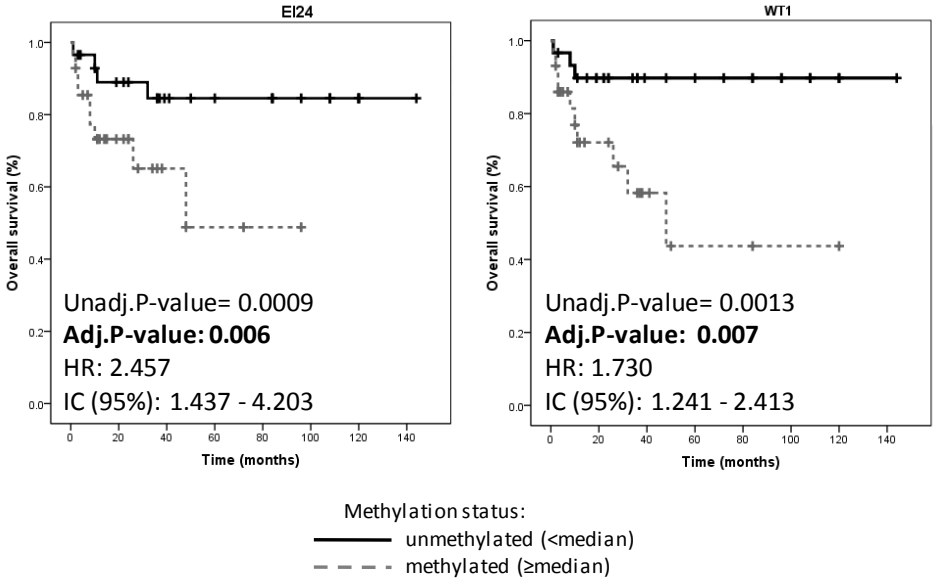

Figure 4 | Prognostic value of the methylation status of *EI24* and *WT1* genes. RFS of 60 thyroid cancer patients based on the methylation levels, considered as a continuous variable, of each of the proposed prognostic factors. RFS was defined as the time between initial diagnosis and recurrence or death due to the disease, with follow-up censored at last contact if no event had occurred. The unadjusted p-values (Unadj. p-value) were obtained from Cox regression analysis, and were corrected for multiple testing (adj. p-value, shown in bold).

Discussion

Alterations in DNA methylation have been shown to play a role in tumorigenesis and disease progression in many malignancies, including thyroid cancer. Until recently, technical limitations have restricted methylation studies to the characterization of a handful of candidate loci (Xing et al., 2003; Venkataraman et al., 1999; Hu et al., 2006; Schagdarsurengin et al., 2002) and one genome-wide exploratory study, mainly focused on identification of subtype specific methylation patterns (Rodriguez-Rodero et al., 2013). Here, we describe quantitative DNA methylation levels at more than 26,000 loci across 14,000 gene promoters. By assaying the largest collection of thyroid tumors described so far, we were able to not only confirm methylation changes seen in previously published candidate loci studied but also identify novel recurrent ones. Our results suggested that in thyroid cancer, aberrant methylation targets specific genomic regions, particularly PcG-associated stem cell genes and sequences that are highly methylated in stem cells, which are also commonly epigenetically deregulated in other cancer types (Zhuang et al., 2012). Moreover, according to our results, the methylation patterns in thyroid cancer are specific to the follicular and papillary patterns of growth as well as to the underlying mutational event. Furthermore, by comparing DNA methylation with mRNA expression data, we further confirmed that the relationship between methylation and expression is complex and context dependent (Varley et al., 2013). Finally, by integrating methylation data with clinical information we were able to propose novel prognostic markers in well-differentiated thyroid cancer.

Alterations in DNA methylation have been observed in early cancers and precursor lesions, suggesting that they play an important role in malignant initiation (Zhuang et al., 2012; Belinsky et al., 2013; Fernandez et al., 2012), and our observations are largely consistent with this hypothesis. It has been proposed that follicular adenoma is a precursor lesion for follicular thyroid carcinoma, as evidenced by both the simultaneous presence of carcinomas in benign lesions and the similarity in the molecular alterations observed in FA and FTC (Arora et al., 2008). The few differences in methylation between FA and normal thyroid tissue samples that were also observed in FTC could represent the initiating changes, providing an additional piece of evidence that FA may give rise to FTC, and new insights about the critical steps in follicular cell neoplastic transformation. We also observed a progressive gain of promoter CpG-island hypermethylation between benign- (83 probes) and malignant-stage tumors (460 probes), which confirms previous findings (Zhuang et al., 2012; Fernandez et al., 2012).

Although in other cancer types distinct methylation patterns have been found to be associated with the presence of specific mutations (Michaloglou et al., 2005; Weisenberger et al., 2006; Shen et al., 2007; Hinoue et al., 2009; Hinoue, et al., 2012), to our knowledge, ours is the first study to assess this in thyroid cancer. We observed a robust separation of mutated samples, especially evident for fvPTC, where the mutation apparently was tightly associated with their methylation pattern and subsequent clustering. These findings are consistent with those from a recent genome-wide methylation study in two thyroid cancer cell lines showed they undergo hypermethylation in an important proportion of genes upon the knockdown of *BRAF* (Hou et al., 2011). Given that TCGA project's methylation data validated the pattern according to the mutation, it seems reasonable to conclude that methylation pattern is specific to the particular mutation involved in thyroid cancer. However, the biological mechanism explaining this remains unknown, and further experiments are needed.

We found it particularly striking that PTCs had a higher proportion of hypomethylated probes. In cancer, hypomethylation is more prominent in large inter-genic satellite regions and has been related to genomic instability (Rodriguez et al., 2006, Li et al., 2012), whereas PTC has been described as the thyroid cancer subtype with least structural rearrangements (Ward et al., 1998). As the platform used in the study was biased towards gene promoters, it is likely that the observed hypomethylation events on unique sequences could cause increased expression of cancer-promoting genes, rather than genomic instability. An integrative study applying various OMICs approaches to a common series of PTC tumors is required to shed light on the relationship between hypomethylation and genomic instability.

The results for PTC tumors harboring the *BRAF*^{V600E} mutation specifically caught our attention. The presence of *BRAF*^{V600E} has been strongly associated with the "CpG island methylator phenotype" (CIMP) in colorectal cancer (Weisenberger et al., 2006; Hinoue et al., 2012), but it has been suggested that this mutation is not sufficient to induce CIMP in a colorectal cell line (Hinoue et al., 2009). Rather, to promote its oncogenic effects, it requires additional cooperative events, often of an epigenetic nature (Hinoue et al., 2009; Suzuki et al., 2010), which bypass the senescence and apoptosis that this mutation induces in cells (Zhu et al., 1998; Michaloglou et al., 2005). Importantly, this tumor suppressor mechanism has been recently described in thyroid carcinogenesis (Vizioli et al., 2011) even though it remains to be established which events are associated with its impairment. Concomitant activation of v-akt murine thymoma viral oncogene homolog 3 (*AKT3*) was reported to overcome *BRAF*-induced senescence in melanoma cells (Cheung

et al., 2008). Indeed, in our experimental setting, we observed strong *AKT3* promoter hypomethylation (FDR = 6.6 x 10^{-6}, ΔM-value = -2.26). However, we did not observe a correlation between *AKT3* methylation and expression, probably due to the fact that the corresponding CpG dinucleotide arrayed did not lie within a CpG island. Nevertheless, a tendency towards elevated expression of *AKT3* specifically in PTC has been reported by others (Ringel et al., 2001). In addition, the over-activation of the mTOR pathway, which is classically regulated through the phosphatidylinositol-3-kinase (*PI3K*)/ AKT pathway, has been recently reported to be strongly associated with *BRAF* mutation-positive PTC (Faustino et al., 2012). Further studies are necessary to decipher the precise role of *AKT3* in the development of *BRAF*-related thyroid tumors.

In both case series considered, the hypermethylation of the promoter regions of *COL4A2* and *DLEC1* was confirmed in follicular cell-derived tumors, while the hypomethylation of *KLK10* was strongly associated with *BRAF* mutation positive PTC. *KLK10* is a member of the kallikrein family of genes, which are secreted serine proteases that have been extensively studied in cancer due to their involvement in extracellular matrix degradation as well as their promising role as disease biomarkers (Borgoño et al., 2004). Hypomethylation of *KLK10* has been recently associated with biochemical recurrence in prostate cancer (Olkhov-Mitsel et al., 2012). Conversely, *COL4A2* encodes one of the six subunits of type IV collagen, the major structural component of basement membranes. The C-terminal portion of the protein, known as canstatin, is an inhibitor of angiogenesis and tumor growth (Roth et al., 2005). Finally, *DLEC1* is a candidate tumor suppressor gene, which is commonly deleted in various carcinomas; more importantly, it has been reported to be epigenetically repressed in many tumor types (Seng et al., 2008; Wang et al., 2012).

To gain insights into the functional implications of epigenetic changes, we integrated the DNA methylation data with gene expression profiling data. The integration with an independent series of samples identified a relatively lower proportion of correlated genes in FTC, and we observed no correlations for FA, which was probably due to the small number of samples included in the original study (Giordano et al., 2005). Nevertheless, in general, we observed similar proportions of genes showing correlation to those reported in previous studies (Selamat et al., 2012; Hinoue et al., 2012). The products of some of the correlated genes in PTC samples harboring the *BRAF*^{V600E} mutation were clustered in the MAP kinase cascade, which further confirms the importance of impairment of this pathway in the development of this tumor subtype. In FTC samples, we observed an

enrichment of genes involved in innate immunity response mechanisms, known for a long time to promote carcinogenesis (Dunn et al., 2002).

We found that elevated levels of methylation of at least two genes known to participate in carcinogenesis were associated with increased risk of recurrence of thyroid cancer. Interestingly, both genes, *EI24* and *WT1*, exhibited a significant association with poor prognosis even after adjustment for relevant clinical variables. Although preliminary, the associations of these novel markers with disease recurrence could potentially serve to better stratify patients. Specifically, *EI24* is a putative tumor-suppressor gene, the expression of which is impaired in several types of cancer by either aberrant methylation or deletion (Mazumder et al., 2011). More importantly, this impairment has been found to be associated with tumor invasiveness (Mazumder et al., 2011) and poor response to treatment (Mork et al., 2007). *WT1* encodes a transcription factor, mutated in a small subset of patients with Wilm's tumors, and whose expression has been suggested to be indicative of minimal residual disease in leukemias (Trka et al., 2002; Weisser et al., 2005). Furthermore, its methylation status has been recently proposed to be correlated with time to recurrence in prostate cancer (Kobayashi et al., 2011).

To summarize, the assessment of genome-wide DNA methylation profiles in the largest series of well differentiated thyroid tumors described so far allowed us to identify and replicate distinct epigenetic signatures that reflect the underlying tumor histology as well as the mutation status. Specific aberrant methylation associated with the early development of this disease was found, and DNA methylation events associated with changes in gene expression were identified. We proposed novel prognostic markers, which according to our data are independent of the already established ones.

Acknowledgments

The authors would like to thank Mario Fraga and Agustin Fernandez for their invaluable suggestions about methylation data analyses. The authors used data generated by The Cancer Genome Atlas managed by the NCI and NHGRI; information about TCGA can be found at http://cancergenome. nih.gov.

Conflicts of interests

All authors declare no conflict of interest.

Grant support

Fondo de Investigaciones Sanitarias; Grant numbers: PI11/01359; FIS PI11/02421 and PI11/01354; Grant sponsor: The Fundación Mutua Madrileña; Grant number: AP2775/2008; Grant sponsors: the Comunidad de Madrid S2011/BMD-2328 TIRONET, “la Caixa”/CNIO international PhD programme (V.M. and A.A.d.C.), CIBERER (L.I.-P.) and Spanish Ministry of Economy and Competitiveness (FPI program) (R.B.); Grant sponsor: Spanish Ministry of Economy and Competitiveness; Grant number: SAF2011/23638; Grant sponsor: Fondo de Investigaciones Sanitarias; Grant number: PI12/00236 (M.C.); Grant sponsor: Technical Support Staff program of the Spanish. Ministry of Economy and Competitiveness; Grant number: PTA2011-5655-I (A.D.)

References

Arora, N., Scognamiglio, T., Zhu, B., Fahey, T.J., 2008. Do benign thyroid nodules have malignant potential? An evidence-based review, in: World Journal of Surgery. pp. 1237–1246. doi:10.1007/s00268-008-9484-1

Belinsky, S.A., Nikula, K.J., Palmisano, W.A., Michels, R., Saccomanno, G., Gabrielson, E., Baylin, S.B., Herman, J.G., 1998. Aberrant methylation of p16(INK4a) is an early event in lung cancer and a potential biomarker for early diagnosis. Proc. Natl. Acad. Sci. U. S. A. 95, 11891–11896. doi:10.1073/pnas.95.20.11891

Bibikova, M., Le, J., Barnes, B., Saedinia-Melnyk, S., Zhou, L., Shen, R., Gunderson, K.L., 2009. Genome-wide DNA methylation profiling using Infinium ® assay. Epigenomics 1, 177–200. doi:10.2217/epi.09.14

Borgono, C.A., Diamandis, E.P., 2004. The emerging roles of human tissue kallikreins in cancer. Nat Rev Cancer 4, 876–890. doi:10.1038/nrc1474

Brait, M., Loyo, M., Rosenbaum, E., Ostrow, K.L., Markova, A., Papagerakis, S., Zahurak, M., Goodman, S.N., Zeiger, M., Sidransky, D., Umbricht, C.B., Hoque, M.O., 2012. Correlation between BRAF mutation and promoter methylation of TIMP3, RAR??2 and RASSF1A in thyroid cancer. Epigenetics 7, 710–719. doi:10.4161/epi.205248

Cheung, M., Sharma, A., Madhunapantula, S. V., Robertson, G.P., 2008. Akt3 and mutant V600EB-Raf cooperate to promote early melanoma development. Cancer Res. 68, 3429–3439. doi:10.1158/0008-5472.CAN-07-5867

Du, P., Zhang, X., Huang, C.-C., Jafari, N., Kibbe, W.A., Hou, L., Lin, S.M., 2010. Comparison of Beta-value and M-value methods for quantifying methylation levels by microarray analysis. BMC Bioinformatics 11, 587. doi:10.1186/1471-2105-11-587

Dunn, G.P., Bruce, A.T., Ikeda, H., Old, L.J., Schreiber, R.D., 2002. Cancer immunoediting: from immunosurveillance to tumor escape. Nat Immunol 3, 991–998. doi:10.1038/ni1102-991

Faustino, A., Couto, J.P., Pópulo, H., Rocha, A.S., Pardal, F., Cameselle-Teijeiro, J.M., Lopes, J.M., Sobrinho-Simões, M., Soares, P., 2012. mTOR pathway overactivation in BRAF mutated papillary thyroid carcinoma. J. Clin. Endocrinol. Metab. 97. doi:10.1210/jc.2011-2748

Fernandez, A.F., Assenov, Y., Martin-Subero, J.I., Balint, B., Siebert, R., Taniguchi, H., Yamamoto, H., Hidalgo, M., Tan, A.C., Galm, O., Ferrer, I., Sanchez-Cespedes, M., Villanueva, A., Carmona, J., Sanchez-Mut, J. V., Berdasco, M., Moreno, V., Capella, G., Monk, D., Ballestar, E., Ropero, S., Martinez, R., Sanchez-Carbayo, M., Prosper, F., Agirre, X., Fraga, M.F., Gra??a, O., Perez-Jurado, L., Mora, J., Puig, S., Prat, J., Badimon, L., Puca, A.A., Meltzer, S.J., Lengauer, T., Bridgewater, J., Bock, C., Esteller, M., 2012. A DNA methylation fingerprint of 1628 human samples. Genome Res. 22, 407–419. doi:10.1101/gr.119867.110

Giordano, T.J., Kuick, R., Thomas, D.G., Misek, D.E., Vinco, M., Sanders, D., Zhu, Z., Ciampi, R., Roh, M., Shedden, K., Gauger, P., Doherty, G., Thompson, N.W., Hanash, S., Koenig, R.J., Nikiforov, Y.E., 2005. Molecular classification of papillary thyroid carcinoma: distinct BRAF, RAS, and RET/PTC mutation-specific gene expression profiles discovered by DNA microarray analysis. Oncogene 24, 6646–56. doi:10.1038/sj.onc.1208822

Hinoue, T., Weisenberger, D.J., Lange, C.P.E., Shen, H., Byun, H.M., Van Den Berg, D., Malik, S., Pan, F., Noushmehr, H., Van Dijk, C.M., Tollenaar, R.A.E.M., Laird, P.W., 2012. Genome-scale analysis of aberrant DNA methylation in colorectal cancer. Genome Res. 22, 271–282. doi:10.1101/gr.117523.110

Hinoue, T., Weisenberger, D.J., Pan, F., Campan, M., Kim, M., Young, J., Whitehall, V.L., Leggett, B.A., Laird, P.W., 2009. Analysis of the association between CIMP and BRAF in colorectal cancer by DNA methylation profiling. PLoS One 4, e8357. doi:10.1371/journal.pone.0008357

Hou, P., Liu, D., Xing, M., 2011. Genome-wide alterations in gene methylation by the BRAF V600E mutation in

papillary thyroid cancer cells. Endocr Relat Cancer 18, 687–697. doi:ERC-11-0212 [pii]\r10.1530/ERC-11-0212

Hu, S., Liu, D., Tufano, R.P., Carson, K.A., Rosenbaum, E., Cohen, Y., Holt, E.H., Kiseljak-Vassiliades, K., Rhoden, K.J., Tolaney, S., Condouris, S., Tallini, G., Westra, W.H., Umbricht, C.B., Zeiger, M.A., Califano, J.A., Vasko, V., Xing, M., 2006. Association of aberrant methylation of tumor suppressor genes with tumor aggressiveness and BRAF mutation in papillary thyroid cancer. Int. J. Cancer 119, 2322–2329. doi:10.1002/ijc.22110

Huang, D.W., Lempicki, R. a, Sherman, B.T., 2009. Systematic and integrative analysis of large gene lists using DAVID bioinformatics resources. Nat. Protoc. 4, 44–57. doi:10.1038/nprot.2008.211

Kobayashi, Y., Absher, D.M., Gulzar, Z.G., Young, S.R., McKenney, J.K., Peehl, D.M., Brooks, J.D., Myers, R.M., Sherlock, G., 2011. DNA methylation profiling reveals novel biomarkers and important roles for DNA methyltransferases in prostate cancer. Genome Res. 21, 1017–1027. doi:10.1101/gr.119487.110

Kondo, T., Ezzat, S., Asa, S.L., 2006. Pathogenetic mechanisms in thyroid follicular-cell neoplasia. Nat. Rev. Cancer 6, 292–306. doi:10.1038/nrc1836

Li, J., Harris, R.A., Cheung, S.W., Coarfa, C., Jeong, M., Goodell, M.A., White, L.D., Patel, A., Kang, S.-H., Shaw, C., Chinault, A.C., Gambin, T., Gambin, A., Lupski, J.R., Milosavljevic, A., 2012. Genomic hypomethylation in the human germline associates with selective structural mutability in the human genome. PLoS Genet. 8, e1002692. doi:10.1371/journal.pgen.1002692

Lupi, C., Giannini, R., Ugolini, C., Proietti, A., Berti, P., Minuto, M., Materazzi, G., Elisei, R., Santoro, M., Miccoli, P., Basolo, F., 2007. Association of BRAF V600E Mutation with Poor Clinicopathological Outcomes in 500 Consecutive Cases of Papillary Thyroid Carcinoma. J. Clin. Endocrinol. Metab. 92, 4085–4090. doi:10.1210/jc.2007-1179

Maliszewska, A., Leandro-Garcia, L.J., Castelblanco, E., Macià, A., de Cubas, A., Goméz-López, G., Inglada-Pérez, L., Alvarez-Escolá, C., De la Vega, L., Letón, R., Gómez-Graña, A., Landa, I., Cascón, A., Rodríguez-Antona, C., Borrego, S., Zane, M., Schiavi, F., Merante-Boschin, I., Pelizzo, M.R., Pisano, D.G., Opocher, G., Matias-Guiu, X., Encinas, M., Robledo, M., 2013. Differential gene expression of medullary thyroid carcinoma reveals specific markers associated with genetic conditions. Am. J. Pathol. 182, 350–62. doi:10.1016/j.ajpath.2012.10.025

Mancuso, F.M., Montfort, M., Carreras, A., Alibes, A., Roma, G., 2011. HumMeth27QCReport: an R package for quality control and primary analysis of Illumina Infinium methylation data. BMC Res Notes 4, 546. doi:10.1186/1756-0500-4-546

Mazumder ' Indra, D., Mitra, S., Singh, R.K., Dutta, S., Roy, A., Mondal, R.K., Basu, P.S., Roychoudhury, S., Panda, C.K., 2010. Inactivation of CHEK1 and EI24 are associated with the development of invasive cervical carcinoma: Clinical and prognostic implications. Int J Cancer. doi:10.1002/ijc.25849

Michaloglou, C., Vredeveld, L.C.W., Soengas, M.S., Denoyelle, C., Kuilman, T., van der Horst, C.M. a M., Majoor, D.M., Shay, J.W., Mooi, W.J., Peeper, D.S., 2005. BRAFE600-associated senescence-like cell cycle arrest of human naevi. Nature 436, 720–724. doi:10.1038/nature03890

Montero-Conde, C., Martín-Campos, J.M., Lerma, E., Gimenez, G., Martínez-Guitarte, J.L., Combalía, N., Montaner, D., Matías-Guiu, X., Dopazo, J., de Leiva, A., Robledo, M., Mauricio, D., 2008. Molecular profiling related to poor prognosis in thyroid carcinoma. Combining gene expression data and biological information. Oncogene 27, 1554–1561. doi:10.1038/sj.onc.1210792

Mork, C.N., Faller, D. V., Spanjaard, R.A., 2007. Loss of putative tumor suppressor EI24/PIG8 confers resistance to etoposide. FEBS Lett. 581, 5440–5444. doi:10.1016/j.febslet.2007.10.046

Morrissey, E.R., Diaz-Uriarte, R., 2009. Pomelo II: Finding differentially expressed genes. Nucleic Acids Res. 37. doi:10.1093/nar/gkp366

Nikiforov, Y.E., Nikiforova, M.N., 2011. Molecular genetics and diagnosis of thyroid cancer. Nat. Rev. Endocrinol. 7, 569–580. doi:10.1038/nrendo.2011.142

Olkhov-Mitsel, E., Van der Kwast, T., Kron, K.J., Ozcelik, H., Briollais, L., Massey, C., Recker, F., Kwiatkowski, M., Fleshner, N.E., Diamandis, E.P., Zlotta, A.R., Bapat, B., 2012. Quantitative DNA methylation analysis of genes coding for kallikrein-related peptidases 6 and 10 as biomarkers for prostate cancer. Epigenetics 7, 1037–1045. doi:10.4161/epi.21524

Ringel, M.D., Hayre, N., Saito, J., Saunier, B., Schuppert, F., Burch, H., Bernet, V., Burman, K.D., Kohn, L.D., Saji, M., 2001. Overexpression and Overactivation of Akt in Thyroid Carcinoma Overexpression and Overactivation of Akt in Thyroid Carcinoma 1. Cancer Res. 61, 6105–6111.

Rodriguez, J., Frigola, J., Vendrell, E., Risques, R.-A., Fraga, M.F., Morales, C., Moreno, V., Esteller, M., Capellà, G., Ribas, M., Peinado, M. a, 2006. Chromosomal instability correlates with genome-wide DNA demethylation in human primary colorectal cancers. Cancer Res. 66, 8462–9468. doi:10.1158/0008-5472.CAN-06-0293

Rodríguez-Rodero, S., Fernández, A.F., Fernández-Morera, J.L., Castro-Santos, P., Bayon, G.F., Ferrero, C., Urdinguio, R.G., Gonzalez-Marquez, R., Suarez, C., Fernández-Vega, I., Fresno Forcelledo, M.F., Martínez-Camblor, P., Mancikova, V., Castelblanco, E., Perez, M., Marrón, P.I., Mendiola, M., Hardisson, D., Santisteban, P., Riesco-Eizaguirre, G., Matías-Guiu, X., Carnero, A., Robledo, M., Delgado-Álvarez, E., Menéndez-Torre, E., Fraga, M.F., 2013. DNA methylation signatures identify biologically distinct thyroid cancer subtypes. J. Clin. Endocrinol. Metab. 98, 2811–21. doi:10.1210/jc.2012-3566

Roth, J.M., Akalu, A., Zelmanovich, A., Policarpio, D., Ng, B., MacDonald, S., Formenti, S., Liebes, L., Brooks, P.C., 2005. Recombinant alpha2(IV)NC1 domain inhibits tumor cell-extracellular matrix interactions, induces cellular senescence, and inhibits tumor growth in vivo. Am. J. Pathol. 166, 901–911. doi:10.1016/S0002-9440(10)62310-3

Schagdarsurengin, U., Richter, A.M., Hornung, J., Lange, C., Steinmann, K., Dammann, R.H., 2010. Frequent epigenetic inactivation of RASSF2 in thyroid cancer and functional consequences. Mol. Cancer 9, 264. doi:10.1186/1476-4598-9-264

Selamat, S.A., Chung, B.S., Girard, L., Zhang, W., Zhang, Y., Campan, M., Siegmund, K.D., Koss, M.N., Hagen, J.A., Lam, W.L., Lam, S., Gazdar, A.F., Laird-Offringa, I.A., 2012. Genome-scale analysis of DNA methylation in lung adenocarcinoma and integration with mRNA expression. Genome Res. 22, 1197–1211. doi:10.1101/gr.132662.111

Seng, T.J., Currey, N., Cooper, W. a, Lee, C.-S., Chan, C., Horvath, L., Sutherland, R.L., Kennedy, C., McCaughan, B., Kohonen-Corish, M.R.J., 2008. DLEC1 and MLH1 promoter methylation are associated with poor prognosis in non-small cell lung carcinoma. Br. J. Cancer 99, 375–382. doi:10.1038/sj.bjc.6604452

Shen, L., Toyota, M., Kondo, Y., Lin, E., Zhang, L., Guo, Y., Hernandez, N.S., Chen, X., Ahmed, S., Konishi, K., Hamilton, S.R., Issa, J.-P.J., 2007. Integrated genetic and epigenetic analysis identifies three different subclasses of colon cancer. Proc. Natl. Acad. Sci. U. S. A. 104, 18654–9. doi:10.1073/pnas.0704652104

Suzuki, H., Igarashi, S., Nojima, M., Maruyama, R., Yamamoto, E., Kai, M., Akashi, H., Watanabe, Y., Yamamoto, H., Sasaki, Y., Itoh, F., Imai, K., Sugai, T., Shen, L., Issa, J.P., Shinomura, Y., Tokino, T., Toyota, M., 2009. IGFBP7 is a p53 Responsive Gene Specifically Silenced in Colorectal Cancer with CpG Island Methylator Phenotype. Carcinogenesis.

Trka, J., Kalinova, M., Hrusak, O., Zuna, J., Krejci, O., Madzo, J., Sedlacek, P., Vavra, V., Michalova, K., Jarosova, M., Stary, J., 2002. Real-time quantitative PCR detection of WT1 gene expression in children with AML: prognostic significance, correlation with disease status and residual disease detection by flow cytometry. Leukemia 16, 1381–9. doi:10.1038/sj.leu.2402512

Varley, K.E., Gertz, J., Bowling, K.M., Parker, S.L., Reddy, T.E., Pauli-Behn, F., Cross, M.K., Williams, B.A., Stamatoyannopoulos, J.A., Crawford, G.E., Absher, D.M., Wold, B.J., Myers, R.M., 2013. Dynamic DNA methylation across diverse human cell lines and tissues. Genome Res. 23, 555–567. doi:10.1101/gr.147942.112

Venkataraman, G.M., Yatin, M., Marcinek, R., Ain, K.B., 1999. Restoration of iodide uptake in dedifferentiated thyroid carcinoma: relationship to human Na+/I-symporter gene methylation status. J. Clin. Endocrinol. Metab. 84, 2449–57. doi:10.1210/jcem.84.7.5815

Vizioli, M.G., Possik, P.A., Tarantino, E., Meissl, K., Borrello, M.G., Miranda, C., Anania, M.C., Pagliardini, S., Seregni, E., Pierotti, M.A., Pilotti, S., Peeper, D.S., Greco, A., 2011. Evidence of oncogene-induced senescence in thyroid carcinogenesis. Endocr. Relat. Cancer 18, 743–757. doi:10.1530/ERC-11-0240

Wang, Z., Li, L., Su, X., Gao, Z., Srivastava, G., Murray, P.G., Ambinder, R., Tao, Q., 2012. Epigenetic silencing of the 3p22 tumor suppressor DLEC1 by promoter CpG methylation in non-Hodgkin and Hodgkin lymphomas. J. Transl. Med. 10, 209. doi:10.1186/1479-5876-10-209

Ward, L.S., Brenta, G., Medvedovic, M., Fagin, J.A., 1998. Studies of allelic loss in thyroid tumors reveal major differences in chromosomal instability between papillary and follicular carcinomas. J. Clin. Endocrinol. Metab. 83, 525–530. doi:10.1210/jc.83.2.525

Weisenberger, D.J., Siegmund, K.D., Campan, M., Young, J., Long, T.I., Faasse, M. a, Kang, G.H., Widschwendter, M., Weener, D., Buchanan, D., Koh, H., Simms, L., Barker, M., Leggett, B., Levine, J., Kim, M., French, A.J., Thibodeau, S.N., Jass, J., Haile, R., Laird, P.W., 2006. CpG island methylator phenotype underlies sporadic microsatellite instability and is tightly associated with BRAF mutation in colorectal cancer. Nat. Genet. 38, 787–93. doi:10.1038/ng1834

Weisser, M., Kern, W., Rauhut, S., Schoch, C., Hiddemann, W., Haferlach, T., Schnittger, S., 2005. Prognostic impact of RT-PCR-based quantification of WT1 gene expression during MRD monitoring of acute myeloid leukemia. Leukemia 19, 1416–23. doi:10.1038/sj.leu.2403809

Xing, M., Westra, W.H., Tufano, R.P., Cohen, Y., Rosenbaum, E., Rhoden, K.J., Carson, K.A., Vasko, V., Larin, A., Tallini, G., Tolaney, S., Holt, E.H., Hui, P., Umbricht, C.B., Basaria, S., Ewertz, M., Tufaro, A.P., Califano, J.A., Ringel, M.D., Zeiger, M.A., Sidransky, D., Ladenson, P.W., 2005. BRAF mutation predicts a poorer clinical prognosis for papillary thyroid cancer. J. Clin. Endocrinol. Metab. 90, 6373–9. doi:10.1210/jc.2005-0987

Zhu, J., Woods, D., McMahon, M., Bishop, J.M., 1998. Senescence of human fibroblasts induced by oncogenic Raf. Genes Dev. 12, 2997–3007. doi:10.1101/gad.12.19.2997

Zhuang, J., Jones, A., Lee, S.H., Ng, E., Fiegl, H., Zikan, M., Cibula, D., Sargent, A., Salvesen, H.B., Jacobs, I.J., Kitchener, H.C., Teschendorff, A.E., Widschwendter, M., 2012. The dynamics and prognostic potential of DNA methylation changes at stem cell gene loci in women's Cancer. PLoS Genet. 8. doi:10.1371/journal.pgen.1002517

3. Trabajo III

A continuación, se presenta el trabajo III (*An algorithm based on kallikreins defines a novel good prognosis subtype in papillary thyroid cancer*) el cual se encuentra en preparación. El material suplementario asociado puede encontrarse en el Anexo 4 y/o en la versión digital de esta tesis.

Resumen en castellano

El cáncer papilar de tiroides (PTC), es una neoplasia de bajo riesgo cuya incidencia ha aumentado exponencialmente en las últimas décadas, a diferencia de su mortalidad que se ha mantenido constantemente baja. Muchos investigadores aseguran que esta "epidemia diagnóstica" se debe a la mejora en los sistemas de rastreo de nódulos tiroideos que llevan a un aumento del número de diagnósticos de PTC asintomáticos (incidentalomas). Al aumentar los diagnósticos también aumenta el número de tiroidectomías totales (tratamiento estándar) que pueden ocasionar daños como hipoparatiroidismo o afectación de las cuerdas vocales entre otros. Por lo tanto, es necesaria la búsqueda de biomarcadores de pronóstico capaces de estratificar el riesgo y mejorar así el manejo de estos pacientes.

Recientemente, se ha demostrado que el PTC puede clasificarse de acuerdo a la distorsión de la señalización ejercida por *BRAF* o *RAS*, ya sea por mutación o por otras causas, la cual está asociada a las características clinicopatológicas de los pacientes. En este sentido, nuestros estudios previos demuestran la hipometilación recurrente y específica del promotor de *KLK10* en tumores *BRAF* mutados y en un subconjunto de tumores no mutados. *KLK10* es un miembro de la familia génica de las calicreínas tisulares (*KLKs*) humanas, las cuales comprenden un total de 15 peptidasas extracelulares que recientemente han sido clasificadas como biomarcadores en muchos tipos tumorales. Sin embargo, nada se sabe sobre su papel en el cáncer de tiroides.

El objetivo de este trabajo es el estudio de esta familia a nivel epigenético (metilación del DNA) y transcripcional para investigar su posible contribución en la estratificación molecular del cáncer de tiroides. Nuestros resultados revelan que el clúster génico de las *KLKs* está altamente desregulado en PTC mostrando perfiles epigenéticos y transcripcionales asociados con la mutación conductora subyacente (*BRAF*^{V600E} y *RAS*). Esto nos ha permitido desarrollar un árbol de decisión capaz de clasificar las muestras según su perfil molecular (BRAF- o RAS-*like*) con altos valores de especificidad y

sensibilidad (>95% y >80%, respectivamente). Además, gracias a la aplicación de este algoritmo al total de las muestras (tejido normal, tumores *BRAF* y *RAS* mutados y tumores no mutados) hemos podido describir un subconjunto de tumores de buen pronóstico con características clinicopatológicas definidas.

En conclusión, el algoritmo KLK es una aproximación simple y robusta capaz de estratificar el riesgo de los pacientes con PTC. Por lo tanto, su implementación en la práctica clínica puede mejorar el manejo de los pacientes optimizando el siempre complicado balance entre los riesgos y los beneficios del tratamiento actual.

Manuscrito en preparación

An algorithm based on kallikreins defines a novel good prognosis subtype in papillary thyroid cancer

Raquel Buj[1], Izaskun Mallona[1], Anna Díez-Villanueva[1], Mireia Roca[1], Manel Puig-Domingo[1,2,3], Jordi L. Reverter[2,3], Carles Zafón[2,4], Dídac Mauricio[2,3], Miguel A. Peinado[1] and Mireia Jordà[1]

[1]Program of Predictive and Personalized Medicine of Cancer (PMPPC), at Germans Trias i Pujol Health Sciences Research Institute (IGTP), Badalona, Barcelona, Spain. [2]ISCIII Center for Biomedical Research on Diabetes and Metabolic Associated Diseases (CIBERDEM), Madrid, Spain; [3]Department of Endocrinology and Nutrition, University Hospital Germans Trias i Pujol, Badalona, Barcelona, Spain.[4]University Hospital Vall d'Hebron and Autonomous University of Barcelona, Diabetes and Metabolism Research Unit (VHIR) and Department of Endocrinology, Barcelona, Spain;

Key words: BRAF- and RAS-like, cancer molecular stratification, DNA methylation, kallikrein-related peptidases, papillary thyroid cancer.

Correspondence to: Mireia Jorda, Institute of Predictive and Personalized Medicine of Cancer (IMPPC), Badalona, Barcelona, Spain, Tel.: 134-935-543-050, Fax: 134-934-651-472, E-mail: mjorda@imppc.org.

Abstract

The increasing incidence of papillary thyroid carcinoma (PTC) mainly due to improved diagnosis has led to an overtreatment of occult clinically irrelevant PTC. Conversely, the lack of prognostic markers often drives to undertreatment. Recent evidence suggests that the underlying *BRAF* or *RAS* signaling is associated with clinicopathological characteristics. We previously identified the hypomethylation of Kallikrein-10 promoter specifically associated with $BRAF^{V600E}$ mutation. Kallikreins (KLK) are emergent biomarkers in cancer but little is known in thyroid cancer. Here we show that the entire KLK family was deregulated in PTC and displayed a specific epigenetic and transcriptional profile strongly associated with $BRAF^{V600E}$ or *RAS* mutation, allowing the development of a 3-features decision tree with >80% sensitivity and >95% specificity identifying *BRAF* and *RAS* mutated tumors. Its application to tumors lacking these mutations classified them as BRAF- or RAS-like. Most importantly, KLK algorithm uncovered a novel good-prognosis PTC subtype. In summary, KLK algorithm is a robust and simple approach to stratify PTC and its implementation in clinical settings may improve patient management and optimize the sometimes difficult risk-benefit balance.

Introduction

Papillary thyroid carcinoma (PTC) is the most common thyroid malignancy (80-85%), and its incidence has increased steadily in recent years all over the world mainly due to the use of advanced diagnostic techniques (Dralle et al., 2015). Fortunately, PTC is an uncommon cause of death, and the vast majority of patients have an excellent prognosis with long-term survival rates. As a consequence, the current management strategies lead to overdiagnosis and overtreatment of clinically irrelevant nodules (Morris et al., 2013). On the other hand, despite the general indolent course of this malignancy, a small percentage of patients show poor outcomes with presence of extrathyroidal extension, recurrence and/or distant metastases (Verbug et al., 2013), but their early identification is limited due to the lack of markers. Therefore, fine-tuning the preoperative risk stratification of thyroid cancer would help in tailoring the management of patients to provide the most effective but least aggressive approach.

A better understanding of the molecular architecture of PTC could provide a useful tool to personalize the treatment. In this regard, several genetic molecular biomarkers have been proposed. Among them, *BRAF*^{V600E} mutation, which occurs in 40 to 45% of PTC, has been strongly associated with tumor aggressiveness (Kim et al., 2012). On the other hand, point mutations in RAS genes are also present in thyroid tumors, but there is controversy about its prognostic value due to their presence along all thyroid cancer spectrum from benign follicular adenomas to the most aggressive forms (Tavares et al., 2015). These and other mutations and rearrangements (*TERT*, *TP53*, *RET/PTC*, *PAX8/PPARγ*) are included as diagnostic markers in multigene mutational panel (Nikiforov et al., 2015).

It is already apparent that classic genetics alone cannot explain human cancer. Accordingly, epigenetics offers a partial explanation that together with genetics could shed light on cancer development and progression. Among all epigenetic mechanisms, the best characterized is DNA methylation which occurs almost exclusively at cytosines in the context of CpG dinucleotides. Noteworthy, CpG dinucleotides are not randomly distributed in the human genome but there are CpG-rich regions, known as CpG islands, commonly located in gene promoters whose methylation is associated with gene silencing (Suzuki and Bird, 2008). It is extensively documented that during cancer development there is a global loss of DNA methylation concomitantly with specific gene promoter hypermethylation (Portela and Esteller, 2010). Different genome-wide studies performed in recent years have revealed that methylomes in thyroid cancer are specifically associated not only with histology but also with *BRAF*^{V600E} and *RAS* mutations (Kikuchi et al., 2013;

Cancer Genome Atlas Research Network et al., 2014; Ellis et al., 2014; Mancikova et al., 2014).

The Cancer Genome Atlas (TCGA) study (Cancer Genome Atlas Research Network et al., 2014) was especially interesting because of the large cohort size and the deep high-throughput analysis. One of their major contributions to PTC knowledge was the development of a *BRAF*^{V600E}*-RAS* score (BRS) based on the gene expression signature of 71 genes that accurately identified *BRAF*^{V600E} and *RAS* mutated tumors (BRAF and RAS tumors from now on). Most importantly, its application to tumors lacking these mutations (non-mutated tumors from now on) revealed that their gene expression pattern was close to BRAF or RAS tumors. As a result, this allowed the classification of PTC in BRAF- and RAS-like tumors.

These findings pave the way to improve the patient staging system and to identify molecules and signaling pathways that could be used as biomarkers. Accordingly, in our previous genome-wide DNA methylation analysis (Mancikova et al., 2014), we identified Kallikrein 10 (*KLK10*) gene as being specifically hypomethylated in BRAF tumors and, interestingly, in a subset of non-mutated tumors. *KLK10* is a member of the human tissue Kallikreins (KLKs) family, the largest contiguous cluster (15 genes within 265 Kb) of secreted serine proteases in the human genome located in the chromosome 19q13.4. As secreted endopeptidases, KLKs have been shown to process several substrates such as growth factors, hormones and extracellular matrix components, and to control many vital processes (Prassas et al., 2015). Interestingly, in recent years KLKs have emerged as an important family of cancer biomarkers, with *KLK3* encoding for *Prostate Specific Antigen* (*PSA*) being the most recognized (Kirby, 2016). However, their clinical significance in thyroid cancer is completely unknown.

The aim of the present study was the molecular characterization of KLK gene cluster in PTC to investigate their potential contribution to the improvement of risk stratification and patient management. Our findings showed the deregulation of the entire KLK family in PTC and the existence of distinct KLK expression profiles specifically associated with the mutational state of the tumor. Most importantly, we developed a simple 3-features binary decision tree based on the DNA methylation and the expression of KLK genes, whose application to a large series of PTC uncovered a novel good prognosis molecular subgroup. These results underscore the potential of KLKs to improve thyroid cancer management as well as the easy implementation in pathology laboratories.

Material and methods

Patients and data sets

We used three independent and previously published data sets which included thyroid cancer samples and normal adjacent tissues: Mancikova series (Mancikova et al., 2014), Smallridge series (Smallridge et al., 2014) and TCGA series (http://cancergenome.nih.gov/) (Cancer Genome Atlas Research Network et al., 2014). Baseline characteristics of each series are shown in Supplementary Table S1.

From our previous study (Mancikova et al., 2014), consisting of 8 normal adjacent tissues and 65 well differentiated thyroid carcinomas, we used the β-value of the cg06130787 probe, located within *KLK10* promoter (Illumina infinium HumanMethylation 27K array). Expression data from Smallridge series, kindly provided by Dr. E. Aubrey. Thompson from Mayo Clinic (Jacksonville, Florida, USA), consisted in Log_2 transformed RPKM+1 of the 15 Kallikrein genes for 12 $BRAF^{V600E}$ and 8 $BRAF^{WT}$ PTC tumors. Finally, data from TCGA series were generated by the TCGA Research Network and included the β-value of the 208 probes (Illumina Infinium HumanMethylation 450K array) covering the KLK cluster and the whole RNASeq from 50 normal adjacent tissues and 437 PTCs fulfilling four requirements: >60% tumoral nuclei, availability of RNASeq data, DNA methylation data and mutational analysis for *BRAF* and *RAS* genes. HiSeq exon and gene quantifications computed by the RNASeq version 2 pipeline were downloaded with TCGA-Assembler (Zhu et al., 2014), and RPKM+1 were Log_2 transformed. On the other hand, mutational information as well as clinical data were downloaded from cBioportal (Cerami et al., 2012).

In addition, RNASeq data from 11 different cancer types from TCGA were obtained through Wanderer (Diez-Villanueva et al., 2015). These series included data from normal-tumor pairs of 19 bladder urothelial carcinomas (BLCA), 113 breast invasive carcinomas (BRCA), 26 colon adenocarcinomas (COAD), 41 head and neck squamous cell carcinomas (HNSC), 72 kidney renal clear cell carcinomas (KIRC), 30 kidney renal papillary cell carcinomas (KIRP), 25 chromophobe renal cell carcinomas (KICH), 50 liver hepatocellular carcinomas (LIHC), 57 lung adenocarcinomas (LUAD), 50 lung squamous cell carcinomas (LUSC) and 52 prostate adenocarcinomas (PRAD).

RNA isolation and quantitative reverse transcription PCR

Total RNA (kindly provided by Dra. M. Robledo from CNIO, Madrid, Spain) from 7 normal tissues and 14 thyroid tumors (1 non-mutated tumor, 3 *RAS* and 10 *BRAF* tumors) were isolated and reverse transcribed to analyze the expression of *KLK4*, *KLK6*, *KLK7* and *KLK10.* For more technical details, see Supplementary Methods.

Decision tree development

TCGA series was randomly divided in training and validation series and the latter, in turn, was divided in a high pure validation (HPV) and low pure validation (LPV) series regarding the percentage of tumoral nuclei (PTN). Thus, training series included a total of 92 samples [16 normal tissues (NT), 56 *BRAF* and 19 *RAS* tumors] with PTNs varying from 65% to 100%. HPV series enclosed 17 NT and 94 (74 *BRAF* and 20 *RAS*) high pure tumors (PTN >85%), while LPV series contained 17 NT and 94 (85 *BRAF* and 9 *RAS*) low pure tumors (PTN varying from 60 to 85).

The training series was used to train the C4.5 algorithm implemented in RWeka [v0.4-24, (Hornik et al., 2009; Witten et al., 2011)] including as attributes the expression data [Log_2(RPKM+1)] of the 15 *KLK* genes and the DNA methylation of the 208 probes included in Illumina Infinum HumanMethylation 450K array covering KLK region (Chr9: 51,307,734 – 51,598,009). The resulting decision tree was used to perform the validation with both HPV and LPV series, and finally it was applied to non-mutated tumors.

Differential DNA methylation and expression analysis

Differential DNA methylation between NT and *BRAF*, *RAS* and non-mutated tumors was analyzed using linear models by the R Bioconductor package limma [v3.28-17, (Ritchie et al., 2015)] and p-values were adjusted according to Benjamini and Hochberg's false discovery rate (FDR). Probes accomplishing an adjusted p-value <0.05 and a Δβ-value (T_{mean}-NT_{mean}) >0.2 or <0.2 were considered as hyper- or hypomethylated, respectively.

The Log_2(RPKM+1) of the 15 *KLK* genes was used to perform a gene supervised hierarchical clustering of thyroid cancer from TCGA series and another 11 additional cancer types as specified in the Supplementary Methods.

Statistical analysis

All analyses were performed using R version 3.1.0 (R Development Core Team, 2011). ANOVA, Kruskall Wallis, Mann-Whitney U, Fisher's exact test and Pearson correlation tests were applied as appropriated and the significance level was established at $p < 0.05$ for all analyses. Kruskall Wallis test were performed with kruskal function from the agricolae R package [v1.2-3, (De Mendiburu, 2014)]. The adjusted p-values in post-hoc analyses were calculated with FDR and TukeyHSD (confidence level = 0.95) methods for Kruskal Wallis and ANOVA respectively.

Kaplan-Meier method was used to estimate survival curves and the hazard ratio (HR) and 95% confidence intervals (95% CI) were estimated by the Cox proportional hazard model. The functions survfit and coxph from survival [v2.39-2 (Therneau and Foundation, 1999)] R-package were used. The end-point was defined as the time (in months) between initial diagnosis and recurrence of the malignancy, with follow-up censored at last contact if no event had occurred.

Significance p-values (<0.05, <0.01 and <0.001) where indicated with increasing number of stars.

Results

KLK10 hypomethylation and gene overexpression are characteristic of *BRAF* tumors

In our previous methylation genome-wide analysis we identified a small region (~190 bp) within 1500 bp upstream of the transcription start site of *KLK10* gene which was specifically hypomethylated in *BRAF* and in a subset of non-mutated tumors (Figure 1A-B and F) (Mancikova et al., 2014)**.** This finding was validated using an independent series from TCGA (Figure 1C), and moreover we demonstrated its association with the upregulation of *KLK10* at mRNA level (Figure 1D-E), suggesting the implication of DNA methylation in the regulation of this gene.

It is noteworthy that this region, comprising 4 CpG sites, was located within a CpG island shore which displayed a progressive gain of methylation the further away from the CpG island (Figure 1A). Interestingly, the methylation boundary in *BRAF* and non-mutated tumors was shifted as compared with normal tissues and *RAS* tumors (Supplemental figure S1).

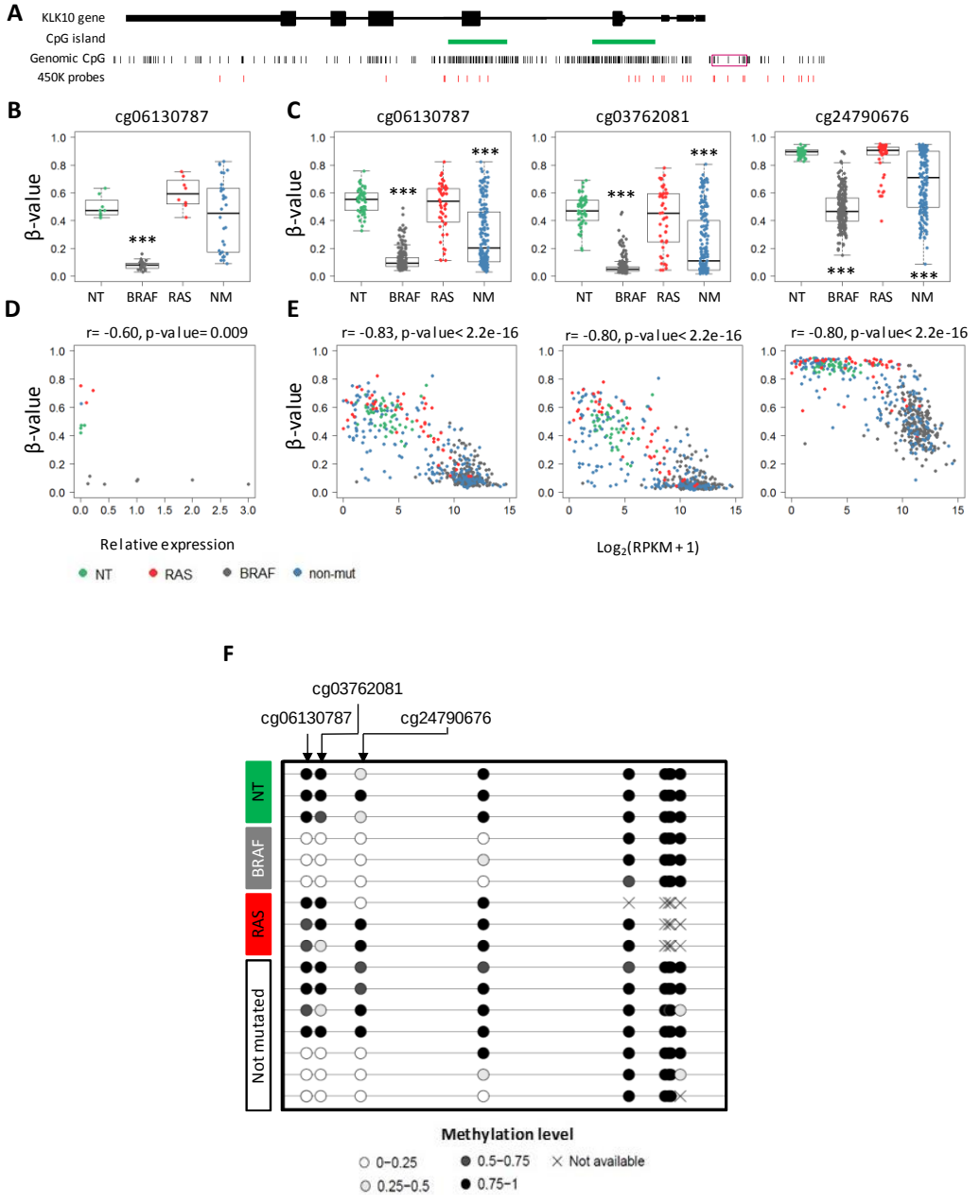

Figure 1 | DNA methylation and RNA expression of *KLK10* in thyroid cancer. (A) Diagram of *KLK10* gene region; black bars represent the CpG sites within the region and red bars represent the CpG sites covered by the Infinium HumanMethylation450K array. **(B, C)** β-values of 3 CpG sites in the promoter region of *KLK10* in tumors from Mancikova series (analyzed by Infinium HumanMethylation 27K array) and TCGA series (analyzed by Infinium HumanMethylation 450K array), respectively. NM (non-mutated). **(D, E)** Correlation between *KLK10* mRNA expression and DNA methylation in Mancikova series (expression analyzed by RT-qPCR relative to *PUM1* and *PPIA*) and TCGA series (expression analyzed by RNA-Seq), respectively. **(F)** Lollipop diagram showing the methylation level of the CpG sites (circles) within the promoter region of *KLK10* assessed by bisulphite sequencing in a subset of samples from Mancikova series; the region analyzed is indicated as a magenta square in (A). (B) and (F) were modified from (Mancikova et al., 2014).

The expression profile of the entire KLK cluster is dysregulated in thyroid cancer

Taking into account that *KLK10* is a member of the human tissue Kallikrein (KLK) family and given that most *KLK* genes are altered in multiple cancer types, we extended our study to the rest of KLKs using TCGA data. Among the 208 CpG sites analyzed within the region, only 7 in *BRAF* and 3 in non-mutated tumors were hypomethylated compared to normal tissues, while no hypomethylations were identified in *RAS* tumors (Supplementary Table S2). Not surprisingly, the 3 hypomethylated CpGs in non-mutated tumors were also present in *BRAF* tumors pointing out their similarity. Regarding *RAS* mutated tumors, 3 CpGs in the promoter region of *KLK13* were hypermethylated in comparison with normal tissues, while no hypermethylations were detected in *BRAF* and non-mutated tumors (Supplementary Table S2). Next, we investigated the association of these differentially methylated CpGs with the expression of their related *KLK*, and found a statistically significant correlation in all hypomethylations (but not in hypermethylations (Supplementary Table S2).

Although not many methylation changes were found in *KLK* cluster, the expression profile of the whole family was highly dysregulated. As shown in Figure 2A, three domains (A to C) were defined in accordance to *KLK* expression profile in the different tumor groups (*BRAF, RAS* and non-mutated) regarding normal tissues. Thus, domain A (from *KLK1* to *KLK4*) was characterized by a significant overall downregulation of *KLK* expression in all tumor groups while domains B (from *KLK5* to *KLK8*) and C (from *KLK10* to *KLK13*) were characterized by a specific upregulation in *BRAF* and non-mutated tumors. As regard *RAS* mutated tumors, no significant differences compared to normal tissues were observed in domains B and C except for *KLK10* and *KLK13* which were slightly and clearly upregulated, respectively (Supplementary Figure S2A and Supplementary Table S3). Reinforcing this result, *BRAF*-associated profile of *KLK*s was validated in an independent series from Smallridge *et al.* (Smallridge et al., 2014) (Supplemental Figure S2B). Furthermore, we validated the expression pattern of *KLK4*, *KLK6*, *KLK7* and *KLK10*, as representative of the different domains, by RT-qPCR in a subset of samples from Mancikova series (Supplementary Figure S2C and supplementary Methods).

To further confirm that KLK expression profile could provide a differential signature specifically associated with the mutational state of PTC we run a supervised hierarchical clustering analysis. As a result, Figure 2B shows that thyroid tumors clustered in two groups. Group 1 (G1) was characterized by an increased expression of KLKs in domains

B and C and contained virtually all BRAF tumors (98.6%) and about half of non-mutated ones (52.3%). On the other hand, group 2 was subdivided in two subgroups. Subgroup 2A (G2A) was made up of most normal tissues (96%) together with some non-mutated (19%) and RAS (10.4%) tumors, while subgroup 2B (G2B) included the majority of RAS (79.2%) and the remaining non-mutated (28.7%) tumors. Subgroup 2A was defined by the upregulation of KLK domain A, whereas subgroup 2B displayed a generalized low expression of KLKs. Thus, KLK signature of G1 non-mutated tumors was similar to BRAF tumors, while G2B non-mutated tumors were close to RAS tumors. Interestingly, G2A tumors showed a KLK profile similar to normal tissue.

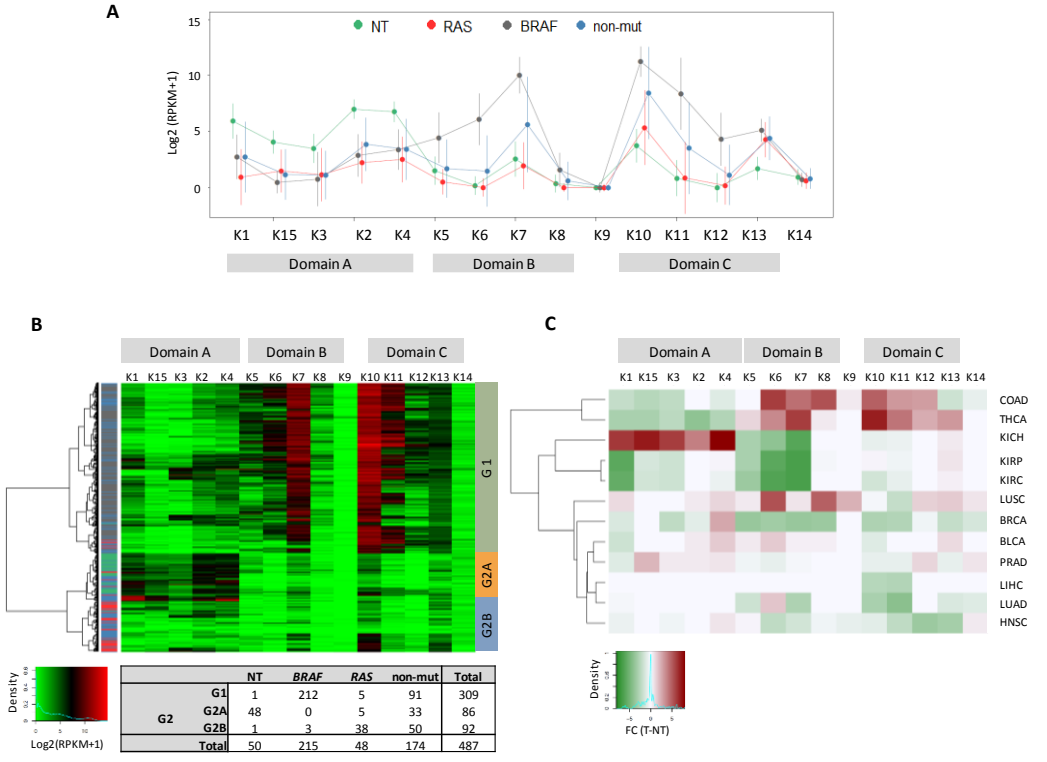

		NT	*BRAF*	*RAS*	non-mut	Total
G2	G1	1	212	5	91	309
	G2A	48	0	5	33	86
	G2B	1	3	38	50	92
	Total	50	215	48	174	487

Figure 2 | Expression profile of KLK cluster. TCGA RNA-Seq data of the 15 members (K1 to K15) comprised in *KLK* cluster were used. **(A)** Expression profile of the 15 *KLKs* in normal thyroid tissues (NT), *BRAF*, *RAS* and non-mutated (non-mut) tumors. The cluster can be divided in 3 domains (A to C) based on the differential expression between NT and tumors. **(B)** *KLK* gene supervised hierarchical clustering using Log_2(RPKM+1) data. Samples grouped in 3 clusters (G1, G2A and G2B) as summarized in the table. **(C)** *KLK* gene supervised hierarchical clustering using fold change (FC) values ($T_{mean} - NT_{mean}$) from 12 different cancer types.

Additionally, we investigated the expression profile of *KLK* in a broad variety of cancer types. Due to the low prevalence of *BRAF* and *RAS* mutations in these cancers and the high interindividual variability observed in some normal tissues such as bladder or breast (Supplementary Figure S3), we used the average of paired normal-tumor samples for the clustering analysis (Figure 2C). It is noteworthy that the three domains (A to C) were maintained in all analyzed normal tissues but showed a tissue-specific pattern (e.g. thyroid was completely different from kidney or prostate) (Supplementary Figure S3). When comparing tumors with their normal counterparts we observed expression differences in most cancer types being COAD, THCA, KICH, KIRP and KIRC those showing the most drastic deregulation (Figure 2C). Conversely, *KLK* cluster expression was not affected in BLCA and PRAD. In general, the differential expression profile of *KLKs* was characteristic of each cancer type with some exceptions, e.g. THCA and COAD exhibited domain A downregulated, specially THCA, and domains B and C upregulated.

Contribution of KLK gene cluster to the molecular classification of thyroid cancer

The finding that *KLK* expression and, to a lesser extent, DNA methylation profiles of non-mutated tumors resembled those harboring *BRAF* or *RAS* mutation prompted us to study the contribution of *KLKs* to the stratification of thyroid cancer. Thus, TCGA series was used to develop a decision tree based on the expression level of the 15 Kallikrein genes and the methylation value of 208 CpG sites within the *KLK* cluster. As a result, we obtained a simple dichotomic tree with 3 features (Figure 3A): the methylation level of the *KLK10* promoter-associated CpG cg06130787, and the expression of *KLK7* and *KLK4*. Samples lowly methylated in *KLK10* CpG (β-value ≤0.204) with high levels of *KLK7* [Log_2(RPKM+1) >3.98] were assigned to BRAF class whereas if *KLK7* expression was low [Log_2(RPKM+1) ≤3.98] were classified as RAS. On the other hand, samples highly methylated in *KLK10* CpG (β-value >0.204) with *KLK4* highly expressed [Log_2(RPKM+1) >4.91) were assigned to normal tissue (NT) class whereas if *KLK4* expression was low [Log_2(RPKM+1) ≤4.91] were classified as RAS. Validation was performed with a high pure and a low pure validation (HPV and LPV, respectively) series (Materials and Methods and Supplementary Table S4). As expected, HPV series showed the highest accuracy (87.39%) while in LPV series was 81.82%. Both series showed fairly good kappa statistics (0.77 and 0.62, respectively) accordingly to Viera *et al.* (Viera and Garret, 2005) (Supplementary Table S4) and very good sensitivity (HPV = 0.87, LPV = 0.82) and specificity (HPV = 0.96, LPV = 0.97) values (Figure 3B and Supplementary Table S4).

Moreover, ROC areas were excellent (ranging from 0.90 to 0.93) in all groups of both series (Supplementary Table S4).

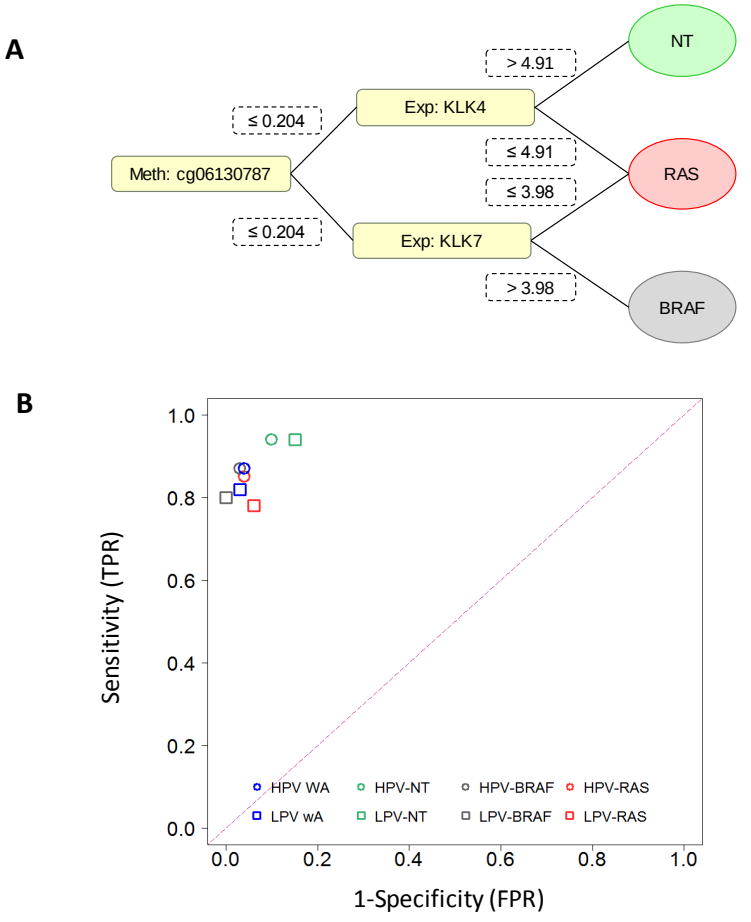

Figure 3 | KLK Algorithm. (A) KLK decision tree obtained with the training series using the expression of the 15 KLK genes and the B-value of 208 CpG sites within KLK region (Chr9: 51,307,734 – 51,598,009). Meth: DNA methylation level; Exp: mRNA expression level. **(B).** Sensitivity and specificity of the considered mutational tumors groups in HPV and LPV series.

Next, we applied the KLK decision tree to non-mutated tumors, among which 78 were classified as BRAF and 58 as RAS. Given that the KLK algorithm could not determine the mutational state of *BRAF* or *RAS* by itself but predicted the BRAF- or RAS-associated phenotype, we called BRAF- or RAS-like those tumors classified as BRAF or RAS, respectively, and independently of the underlying mutation. Strikingly, from the complete TCGA series 19 *BRAF*, 5 *RAS* and 38 non-mutated tumors were classified as normal tissues. Accordingly, we called them “BRAF/RAS Unlike” (BRU) tumors. We discarded an

enrichment of normal cells in BRU tumors (Supplementary Figure S4B). Since TCGA developed a *BRAF*^{V600E}-*RAS* score (BRS) based on an expression signature of 71 genes, we compared both classifications showing a large overlap (78.6%). It is important to note that BRU contributed with a 14.7% to non-overlapping samples (Supplementary Figure S4C).

BRU tumors constitute a good prognosis PTC subtype with specific molecular and clinicopathological features

Since our findings suggested that BRU tumors represented a differential PTC group, we further investigated their specific features. First, we performed a differential expression analysis (Supplementary Methods) between BRU tumors and the other groups (BRAF-like, RAS-like and normal tissue). A total of 3416 genes were found to be differentially expressed (adjusted p-value <0.05 and $|FC_{T\text{-}NT}| \geq 2$). More specifically, BRU showed 2119, 795 and 1881 differentially expressed genes regarding BRAF-like, RAS-like and normal tissue groups, respectively. Of those, only 189 genes (5.5%) were common in all three comparisons while 2226 genes (65.2%) were exclusive of one comparison: 1048 (30.7%) in BRAF-like, 279 (8.2%) in RAS-like and 889 (26.3%) in normal tissue regarding BRU (Figure 4A).

To further characterize BRU tumors, some molecular characteristics were analyzed (Figure 4B). In this regard, ploidity and somatic copy number alterations (SCNA) were higher than in BRU than in BRAF-and RAS-like tumors. Additionally, BRU tumors had a higher level of differentiation and a lower MAPK overactivation [based on differentiation and ERK scores from TCGA (Cancer Genome Atlas Research Network et al., 2014)] than BRAF-like tumors. Most importantly, BRU tumors showed distinctive clinicopathological features. We found statistically significant differences (Fisher's exact test p-value <0.05) in the histological subtype, tumor size, extrathyroidal extension, risk, stage, pathological T and N, recurrence and radiation therapy (Table 1). More specifically, BRU tumors mostly included the classical and the follicular variants, unlike BRAF-like tumors, and a higher proportion of microcarcinomas. Moreover, they showed neither moderate nor advanced extrathyroidal extension, none of them were high-risk and only one was assigned to IV stage. The frequency of high pathological T (T3-T4) was lower than in BRAF-like tumors and similar to RAS-like group, but pathological N1 was less frequent in BRU group. All these analyses suggested that BRU tumors might constitute a good prognostic PTC subtype.

To further confirm the prognostic value of KLK algorithm, we generated Kaplan-Meier curves using recurrence as end-point. Results showed that disease free survival (DFS) was longest in patients with a BRU tumor and shortest in those with BRAF-like tumor (Figure 4C). Cox regression analysis was significant for KLK algorithm (likelihood ratio test p-value = 0.041) unlike mutational status and BRS (likelihood ratio test p-value = 0.159 and 0.054, respectively) (Figure 4C). Interestingly, and although the capacity of KLK algorithm to discriminate between BRU and BRAF-like or RAS-like tumors was not significant (p-value = 0.066 and 0.363, respectively), the hazard ratio of BRU tumors versus BRAF-like and RAS-like where fairly good [HR (95% CI) = 3.8 (0.91 – 15.85), 2.08 (0.43 – 10.00), respectively].

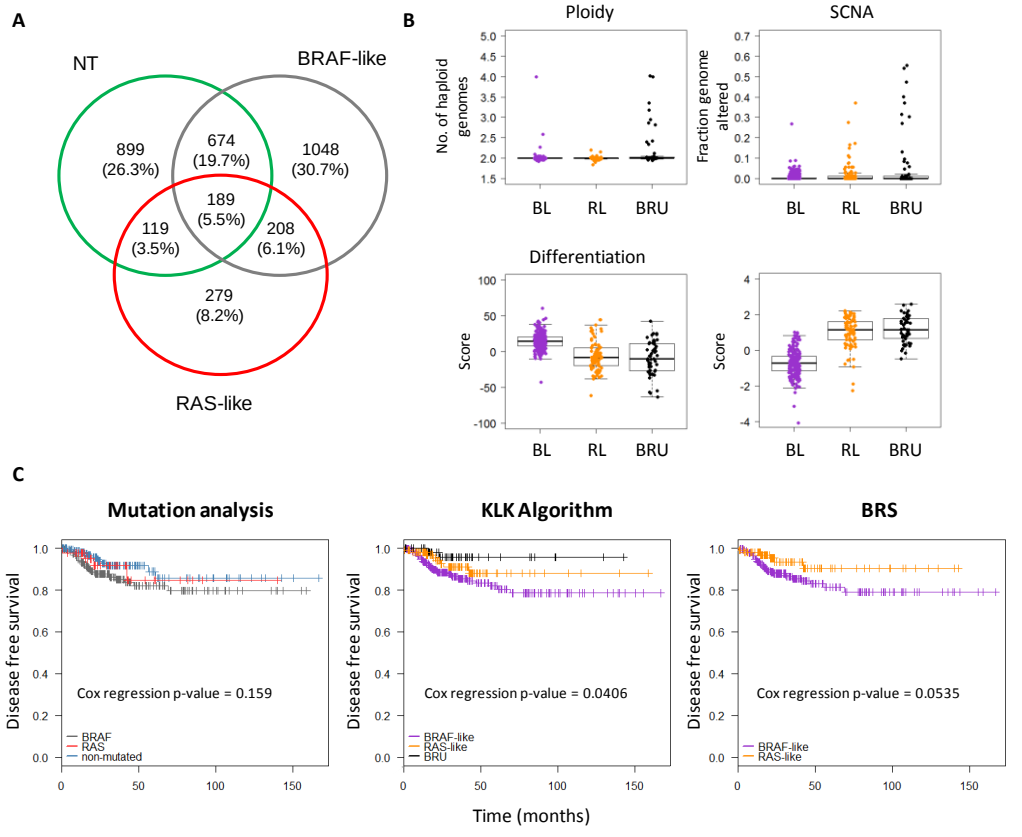

Figure 4 | Molecular, clinicopathological features and prognostic value of the different PTC groups according to KLK algorithm. (A) Differentially expressed genes between BRU tumors and normal tissue (NT), BRAF-like and RAS-like groups (adjusted p-value <0.05 and $|FC_{T\text{-}NT}| \geq 2$). **(B)** Molecular features of the different tumoral groups: BRU, BRAF-like (BL) and RAS-like (RL). **(C)** Disease free survival curves for the different molecular classifications of tumors according to their mutational status, KLK algorithm or BRS (*BRAF*^{V600E}-*RAS* Score).

Table 1 | Clinicobiologic features of TCGA series according to the KLK classification.

Parameter	BRAF-like n (%)	RAS-like n (%)	BRU n (%)	p-value
Age (n = 437)				
Under 45	128 (29.3%)	45 (10.3%)	27 (6.2%)	0.4603
Over 45	138 (31.6%)	64 (14.6%)	35 (8.0%)	
Gender (n = 437)				
Female	196 (44.9%)	75 (17.2%)	50 (11,4%)	0.2540
Male	70 (16.0%)	34 (7.8%)	12 (2.7%)	
Ethnicity (n = 341)				
Hispanic or latino	25 (7.3%)	8 (2.3%)	0 (0.0%)	0.0578
Not hispanic or latino	194 (56.9%)	39 (11.4%)	75 (22%)	
Histology (n = 437)				
Classical	219 (50.4%)	58 (13.3%)	33 (7.6%)	< 2.2e-16
Follicular	19 (4.3%)	49 (11.2%)	25 (5.7%)	
Tall cell	28 (6.4%)	2 (0.5%)	4 (0.9%)	
Tumor size (n = 425)				
Microcarcinoma (<1cm)	4 (0.9%)	4 (0.9%)	5 (1.2%)	0.01658
Macrocarcinoma (<1cm)	258 (60.7%)	101 (23.8%)	53 (12.5%)	
Extrathyroidal extension (n = 424)				
None or minimal	247 (58.3%)	101 (23.8%)	61 (14.4%)	0.040
Moderate or advanced	14 (3.3%)	1 (0.2%)	0 (0.0%)	
Risk (n = 350)				
Low	58 (16.6%)	47 (13.4%)	32 (9.1%)	1.08E-06
Intermediate	139 (39.7%)	37 (10.6%)	20 (5.7%)	
High	14 (4.0%)	3 (0.9%)	0 (0.0%)	
Stage (n = 438)				
Low (I-III)	231 (52.7%)	101 (23.1%)	60 (13.7%)	0.0118
High (IV)	35 (8.0%)	10 (2.3%)	1 (0.2%)	
Pathological T (n = 435)				
T1-T2	149 (34.3%)	81 (18.6%)	44 (10.1%)	0.0007
T3-T4	117 (26.9%)	27 (6.2%)	17 (3.9%)	
Pathological N (n = 342)				
N0	99 (25.3%)	62 (15.8%)	37 (9,4%)	2.50E-07
N1	148 (37.8%)	33 (8.4%)	13 (3.3%)	
Pathological M (n = 239)				
M0	144 (60.3%)	56 (23.4%)	31 (13 %)	0.7612
M1	6 (2.5%)	2 (0.8%)	0 (0.0%)	
Disease status (n = 424)				
Disease free	225 (53.1%)	98 (23.1%)	58 (13.8%)	0.0321
Recurred	34 (8.0%)	7 (1.7%)	2 (1.5%)	
Radiation therapy (n = 424%)				
Yes	171 (40.3%)	68 (16.0%)	26 (6.1%)	0.0304
No	90 (21.2%)	39 (9.2%)	30 (7.1%)	
Tumor Laterality (n = 432)				
Bilateral	42 (9.7%)	21 (4.9%)	14 (3.2%)	0.1929
Unilateral	205 (47.5%)	85 (19.7%)	47 (10.9%)	
Isthmus	15 (3.5%)	3 (0.7%)	0 (0.0%)	
Tumor Focality (n = 445)				
Unifocal	141 (31.7%)	64 (14.4%)	26 (5.8%)	0.0892
Multifocal	119 (26.7%)	42 (9.4%)	35 (11.9%)	
MACIS (n = 341)				
Low (C1-C2)	172 (50.4%)	72 (21.1%)	47 (13.8%)	0.3891
High (C3-C4)	35 (10.3%)	10 (2.9%)	5 (1.5%)	

Percentages are calculated regarding the total number of samples with available data (indicated for each clinicopathological feature).

Discussion

KLKs constitute a family of 15 extracellular secreted trypsin- or chymotrypsin-like serine proteases that cluster together in the chromosome 19 and are known to be involved in a wide range of physiological and pathological processes. In recent years, KLKs have emerged as promising biomarkers, especially in cancer (Prassas et al., 2015). They have been reported to be altered in different tumor types but their functional and clinical implications in THCA are poorly known. In the present study we show for the first time the aberrant expression of the entire *KLK* family in PTC which is partly regulated by DNA methylation. Moreover, we have developed a simple algorithm based on three KLKs which classifies PTC in BRAF- and RAS-like tumors and, most importantly, defines a novel good prognosis PTC subtype.

Although some specific *KLKs* (*KLK2*, *KLK3*, *KLK7*) have been reported to be altered in THCA (Ishikawa et al., 1998; Magklara et al., 2000; Roddiger et al., 2003, Kim et al., 2010), there is scarce data on the expression of *KLKs* in this neoplasia. Our results show the overexpression of *KLK10*, due at least in part to DNA hypomethylation. *KLK10* is also deregulated in other cancer types and has even been proposed as a diagnostic, prognostic and therapy response biomarker (Paliouras et al., 2007). Conversely to THCA, in some cancer types it is downregulated and hypermethylated, and interestingly, while hypermethylation occurs in the CpG island in exon 3 (Pasic et al., 2012), the hypomethylation we identified affects 3 CpGs located in a CpG island shore within the promoter. This is consistent with Hansen *et al.* findings demonstrating that hypomethylated cancer-specific differentially regions (cDMRs) are enriched in CpG islands, whereas hypomethylated cDMRs are enriched in CpG island shores (Hansen et al., 2011).

But not only *KLK10* is altered. To the best of our knowledge this is the first study showing the deregulation of the whole *KLK* cluster in PTC. Moreover, our results reveal the presence of three domains (A to C) whose expression is distinctive and specific of the *BRAF* and *RAS* mutational state. Domain A is downregulated in all tumors while domains B (comprising *KLK10*) and C are upregulated in *BRAF* and a fraction of non-mutated tumors. Further investigation is required to elucidate the mechanism linking *BRAF* mutation and the upregulation of domains B and C. Interestingly, it has been reported that colorectal tumors harboring *BRAF* mutation also overexpress *KLK6* and *KLK10* (Popovici et al., 2012) suggesting a common underlying *BRAF*-dependent regulation.

Taking advantage of TCGA data we analyzed other neoplasias. Our findings reveal, on the one hand, and accordingly to previous studies (Shaw and Diamandis, 2007), that *KLKs* are coexpressed in different tissues, being some of them tissue-specific while others are ubiquitously expressed. On the other hand, we show that the aberrant expression of the entire *KLK* cluster is a widespread phenomenon in cancer. Most importantly, the three expression domains identified in PTC are maintained in all analyzed normal and tumoral tissues although displaying different profiles.

Regulation of *KLKs* is little understood. In the last decade there has been an increasing body of data demonstrating their regulation by DNA methylation (Pasic et al., 2012), but while the expression of *KLK* cluster is dramatically altered in PTC, we have just identified some few CpGs aberrantly methylated. Therefore, other mechanisms must be involved in the regulation of *KLKs*. The identification of three expression domains suggests a regional co-regulation. In this regard, Bert *et al.* reported that KLK cluster was deregulated by a coordinated Long-Range Epigenetic Activation (LREA) in prostate cancer through the gain and loss of active and repressive histone marks, respectively (Bert et al., 2013).

Although most PTC patients are cured, there is a need of new preoperative markers for early diagnosis and prognosis assessment. Recent studies have proposed the mutagenic analysis, especially in relation to *BRAF* and *RAS*, as an important tool to stratify the risk and to determine the extent of surgery in PTC patients (Miccoli, 2014). On the other hand, TCGA has introduced the BRAF- and RAS-like phenotypes (Cancer Genome Atlas Research Network et al., 2014). Accordingly, in the present study we have developed a simpler classifier that stratifies PTC in BRAF- and RAS-like tumors, but instead of using an expression signature of 71 genes as TCGA does it consists in a binary decision tree based on the DNA methylation of a CpG associated with *KLK10* and the expression of *KLK7* and *KLK4*. Moreover, the inclusion of normal thyroid tissues in the training series has allowed us the identification of a novel group of tumors associated with a KLK profile similar to normal tissue which we refer to as BRAF/RAS unlike (BRU) tumors.

Importantly, such BRU group comprises about 13% of all cases analyzed and do not seem to represent misclassified samples, but a distinct subgroup with differential molecular and clinicopathological features. The analysis of the transcriptome indicated that BRU tumors have a specific expression profile consisting of 3416 genes differentially expressed regarding BRAF-like, RAS-like and normal tissue. Interestingly, 54.68% of these genes are included in the. prognostic signature defined by Brennan *et al* to

distinguish between extreme good and extreme poor prognosis patients (Brennan et al., 2016). On the other hand, the analysis of both molecular and clinicopathological features indicates that BRU tumors represent a low risk PTC subtype, which may require a less aggressive treatment. In the case of BRU microcarcinomas, unless they show high-risk features, an active observation could be an alternative therapy to the immediate surgery, as Ito *et al*. (Ito et al., 2010) already proposed. KLK algorithm would provide molecular data to the inclusion criteria of candidates for observation.

KLK algorithm performance in *BRAF* and *RAS* tumors has been evaluated reaching high sensitivities (>80%) and specificities (>85%) values. This validation assumed that BRAF tumors should show a BRAF-like phenotype and *RAS* tumors should show a RAS-like phenotype, thus those *BRAF* tumors classified as RAS-like and vice versa were considered misclassifications. Curiously, this phenomenon was also noticed by Popovici *et al.* in colorectal cancer and they suggested a common biology between these tumors independently of their mutational status (Popovici et al., 2012). Thus, further validation in independent series is required. It should be noted that in the validation of the algorithm using mutated tumors we did not consider the BRU group, which leads to an underestimation of the sensitivity and the specificity.

This study has been performed in PTC but it would be interesting to assess whether it can be extended to the rest of thyroid cancer histological subtypes derived from follicular cell. Preliminary results from our lab analyzing some few adenomas and follicular carcinomas confirmed it (Mancikova et al., 2014, data not show). Since KLK algorithm is based on the measurement of the DNA methylation of a CpG and the expression of two genes, future implementation in clinical practices requires the use of simple and cheap techniques (bisulphite conversion, PCR, sequencing, RT-qPCR and/or immunohistochemistry) easily available in routine anatomopathological laboratories. In addition, and most importantly, the stratification of patients according to KLK algorithm could be applied to preoperative specimens such as fine-needle aspiration biopsies (FNAB), allowing the tailoring of surgery extension and treatment.

In summary, we report the aberrant expression of *KLK* cluster in PTC regulated partly by DNA methylation. Moreover, we show their clinical significance by developing a simple and clinically applicable decision tree classifier that stratifies PTC tumors in BRAF-like, RAS-like and BRU tumors, being the latter a novel good prognosis subtype. Thus, the stratification of PTC patients with KLK algorithm may have a broad spectrum of applications including diagnostic and prognostic preoperative evaluation.

Acknowledgments

RB was supported by a FPI fellowship from Spanish Ministerio de Economía y Competitividad. AD-V was supported in part by a contract PTC2011-1091 from Spanish Ministerio de Economía y Competitividad. This work was supported by grants from the Spanish Ministerio de Economía y Competitividad (SAF2011/23638) and from the Instituto de Salud Carlos III, co-funded by ERDF/ESF, “Investing in your future” (FIS PI11/02421 and FIS PI14/00308).

Conflicts of interests

MAP is cofounder and equity holder of Aniling, a biotech company with no interests in this paper. The other authors have nothing to disclose.

References

Bert, S.A., Robinson, M.D., Strbenac, D., Statham, A.L., Song, J.Z., Hulf, T., et al. 2013. Regional Activation of the Cancer Genome by Long-Range Epigenetic Remodeling. Cancer Cell 23: 9–22.

Brennan, K., Holsinger, C., Dosiou, C., Sunwoo, J.B., Akatsu, H., Haile, R., et al. 2016. Development of prognostic signatures for intermediate-risk papillary thyroid cancer. BMC Cancer 16: 736. BioMed Central.

Cancer Genome Atlas Research Network, N., Akbani, R., Aksoy, B.A., Ally, A., Arachchi, H., Asa, S.L., et al. 2014. Integrated genomic characterization of papillary thyroid carcinoma. Cell 159: 676–90. Elsevier.

Cerami, E., Gao, J., Dogrusoz, U., Gross, B.E., Sumer, S.O., Aksoy, B.A., et al. 2012. The cBio Cancer Genomics Portal: An open platform for exploring multidimensional cancer genomics data. Cancer Discov. 2: 401–404.

De Mendiburu, F. 2014. Agricolae: Statistical procedures for agricultural research. R Packag. version 1: 1–6.

Diez-Villanueva, A., Mallona, I. & Peinado, M.A. 2015. Wanderer, an interactive viewer to explore DNA methylation and gene expression data in human cancer. Epigenetics Chromatin 8: 22.

Dralle, H., Machens, A., Basa, J., Fatourechi, V., Franceschi, S., Hay, I.D., et al. 2015. Follicular cell-derived thyroid cancer. Nat. Rev. Dis. Prim. 1: 15077.

Ellis, R.J., Wang, Y., Stevenson, H., Boufraqech, M., Patel, D., Nilubol, N., et al. 2014. Genome-wide methylation patterns in papillary thyroid cancer are distinct based on histological subtype and tumor genotype. J. Clin. Endocrinol. Metab. 99.

Hansen, K.D., Timp, W., Bravo, H.C., Sabunciyan, S., Langmead, B., Mcdonald, O.G., et al. 2011. Increased methylation variation in epigenetic domains across cancer types. Nat. Genet. 43: 768–775.

Hornik, K., Buchta, C. & Zeileis, A. 2009. Open-source machine learning: R meets Weka. Comput. Stat. 24: 225–232.

Howell, G.M., Hodak, S.P. & Yip, L. 2013. RAS mutations in thyroid cancer. Oncologist 18: 926–32.

Ishikawa, T., Kashiwagi, H., Iwakami, Y., Hirai, M., Kawamura, T., Aiyoshi, Y., et al. 1998. Expression of alpha-fetoprotein and prostate-specific antigen genes in several tissues and detection of mRNAs in normal circulating blood by reverse transcriptase-polymerase chain reaction. Jpn. J. Clin. Oncol. 28: 723–8.

Ito, Y., Miyauchi, A., Inoue, H., Fukushima, M., Kihara, M., Higashiyama, T., et al. 2010. An observational trial for papillary thyroid microcarcinoma in Japanese patients. World J. Surg. 34: 28–35.

Kikuchi, Y., Tsuji, E., Yagi, K., Matsusaka, K., Tsuji, S., Kurebayashi, J., et al. 2013. Aberrantly methylated genes in human papillary thyroid cancer and their association with BRAF/RAS mutation. Front. Genet. 4: 271.

Kim, H.S., Kim, D.H., Kim, J.Y., Jeoung, N.H., Lee, I.K., Bong, J.G., et al. 2010. Microarray analysis of papillary thyroid cancers in Korean. Korean J. Intern. Med. 25: 399–407.

Kim, T.H., Park, Y.J., Lim, J.A., Ahn, H.Y., Lee, E.K., Lee, Y.J., et al. 2012. The association of the BRAFV600E mutation with prognostic factors and poor clinical outcome in papillary thyroid cancer: A meta-analysis. Cancer 118: 1764–1773.

Kirby, R. 2016. The role of PSA in detection and management of prostate cancer. Practitioner 260: 17–21, 3.

Magklara, A., Cheung, C.C., Asa, S.L. & Diamandis, E.P. 2000. Expression of prostate-specific antigen and human glandular kallikrein 2 in the thyroid gland. Clin. Chim. Acta 300: 171–180.

Mancikova, V., Buj, R., Castelblanco, E., Inglada-Pérez, L., Diez, A., De Cubas, A.A., et al. 2014. DNA methylation profiling of well-differentiated thyroid cancer uncovers markers of recurrence free survival. Int. J. Cancer 135: 598–610.

Maxime, A., Maintainer, H. & Hervé, M. 2016. Package "RVAideMemoire" Title Diverse Basic Statistical and Graphical Functions.

Miccoli, P. 2014. Application of molecular diagnostics to the evaluation of the surgical approach to thyroid cancer. Curr. Genomics 15: 184–9.

Mogensen, U.B., Ishwaran, H. & Gerds, T.A. 2012. Evaluating Random Forests for Survival Analysis using Prediction Error Curves. J. Stat. Softw. 50: 1–23.

Morris, L.G.T., Sikora, A.G., Tosteson, T.D. & Davies, L. 2013. The Increasing Incidence of Thyroid Cancer: The Influence of Access to Care. Thyroid 23: 885–891.

Nikiforov, Y.E., Carty, S.E., Chiosea, S.I., Coyne, C., Duvvuri, U., Ferris, R.L., Gooding, W.E., LeBeau, S.O., Ohori, N.P., Seethala, R.R., Tublin, M.E., Yip, L., Nikiforova, M.N., 2015. Impact of the Multi-Gene ThyroSeq Next-Generation Sequencing Assay on Cancer Diagnosis in Thyroid Nodules with Atypia of Undetermined Significance/Follicular Lesion of Undetermined Significance Cytology. Thyroid 25, 1217–1223. doi:10.1089/thy.2015.0305

Paliouras, M., Borgono, C. & Diamandis, E.P. 2007. Human tissue kallikreins: The cancer biomarker family.

Pasic, M.D., Olkhov, E., Bapat, B. & Yousef, G.M. 2012. Epigenetic regulation of kallikrein-related peptidases: there is a whole new world out there. Biol. Chem. 393.

Popovici, V., Budinska, E., Tejpar, S., Weinrich, S., Estrella, H., Hodgson, G., et al. 2012. Identification of a poor-prognosis BRAF-mutant-like population of patients with colon cancer. J. Clin. Oncol. 30: 1288–95.

Portela, A. & Esteller, M. 2010. Epigenetic modifications and human disease. Nat Biotechnol 28: 1057–1068.

Prassas, I., Eissa, A., Poda, G. & Diamandis, E.P. 2015. Unleashing the therapeutic potential of human kallikrein-related serine proteases. Nat. Rev. Drug Discov. 14: 183–202.

R Development Core Team, R. 2011. R: A Language and Environment for Statistical Computing.

Roddiger, S.J., Renneberg, H., Martin, T., Tunn, U.W., Zamboglou, N. & Kurek, R. 2003. Human kallikrein 2 (hK2) mRNA in peripheral blood of patients with thyroid cancer: a novel molecular marker? J Cancer Res Clin Oncol 129: 29–34.

Shaw, J.L. V & Diamandis, E.P. 2007. Distribution of 15 human kallikreins in tissues and biological fluids. Clin. Chem. 53: 1423–1432.

Smallridge, R.C., Chindris, A.M., Asmann

, Y.W., Casler, J.D., Serie, D.J., Reddi, H. V., et al. 2014. RNA sequencing identifies multiple fusion transcripts, differentially expressed genes, and reduced expression of immune function genes in BRAF (V600E) mutant vs BRAF wild-type papillary thyroid carcinoma. J. Clin. Endocrinol. Metab. 99.

Suzuki, M.M. & Bird, A. 2008. DNA methylation landscapes: provocative insights from epigenomics. Nat. Rev. Genet. 9: 465–76.

Tavares, C., Melo, M., Cameselle Teijeiro, J.M., Soares, P. & Sobrinho-Simoes, M. 2015. ENDOCRINE TUMOURS: Genetic predictors of thyroid cancer outcome. Eur J Endocrinol 174: 117–26.

Therneau, T.M. & Foundation, M. 1999. A Package for Survival Analysis in S.

Verburg, F.A., Mäder, U., Tanase, K., Thies, E.-D., Diessl, S., Buck, A.K., et al. 2013. Life expectancy is reduced in differentiated thyroid cancer patients ≥ 45 years old with extensive local tumor invasion, lateral lymph node, or distant metastases at diagnosis and normal in all other DTC patients. J. Clin. Endocrinol. Metab. 98: 172–80.

Viera, A.J. & Garrett, J.M. 2005. Understanding interobserver agreement: The kappa statistic. Fam. Med., doi: Vol. 37, No. 5.

Witten, I.H., Frank, E. & Hall, M. a. 2011. Data Mining: Practical Machine Learning Tools and Techniques (Google eBook).

Zevallos, J.P., Hartman, C.M., Kramer, J.R., Sturgis, E.M. & Chiao, E.Y. 2015. Increased thyroid cancer incidence corresponds to increased use of thyroid ultrasound and fine-needle aspiration: A Study of the veterans affairs health care system. Cancer 121: 741–746.

Zhu, Y., Qiu, P. & Ji, Y. 2014. TCGA-Assembler: Pipeline for TCGA Data Downloading, Assembling, and Processing. Health.Bsd.Uchicago.Edu 1–8.

Resumen global y discusión de los resultados

1. La necesidad de biomarcadores en el WDTC

La incidencia del cáncer de tiroides bien diferenciado ha ido aumentando de manera constante en las últimas décadas, siendo actualmente el cáncer humano con mayor incremento de la incidencia (5.3% en mujeres y 4.5% en hombres) (Siegel et al., 2015). Aunque buena parte de este aumento puede atribuirse a las mejoras en los métodos de rastreo, principalmente aquellos basados en la identificación por ultrasonografía de tumores subclínicos, parece que podrían existir otro tipo de causas de carácter ambiental, nutricional y genético (Pellegriti et al., 2013). Aun así, poco sabemos acerca de la etiología de esta enfermedad.

Por otro lado, cabe señalar el general buen pronóstico de estos pacientes, más del 90% de los cuales alcanzan supervivencias superiores a los 10 años (Figura D1). Hoy en día sabemos que la progresión del WDTC depende tanto de la biología del tumor (tamaño, infiltración, tipo histológico, etc.) como del paciente (sexo, edad, etnia, etc.). Se ha visto, además, que el tratamiento inicial, que suele consistir en una tiroidectomía total con posterior ablación con RAI del remanente de tejido, también influye en la supervivencia global (Duntas and Grab-Duntas, 2006). No obstante y dado el bajo porcentaje de casos que derivan en mal pronóstico (~4%) (Goffredo et al., 2013; Lee and Soh, 2010; Schlumberger, 1998), muchos investigadores han apuntado hacia la posibilidad de reducir el número de cirugías, sustituyéndolas por un seguimiento más intenso de los pacientes, especialmente en los casos de microcarcinoma papilar (Leboulleux et al., 2016).

Con este nuevo paradigma de seguimiento clínico del paciente es importante el desarrollo de biomarcadores capaces de detectar de manera fehaciente aquellos casos que, con toda probabilidad, cursarán con mal pronóstico o, por el contrario, aquellos casos con un riesgo ínfimo de metástasis, recurrencia y/o persistencia de la enfermedad. Indudablemente, para que los futuros biomarcadores sean de utilidad, deben poder detectarse de manera inequívoca en las muestras prequirúrgicas (FNAB, sangre, saliva, etc.). Por ello, el primer paso para el establecimiento de biomarcadores fiables es su descubrimiento y caracterización en tejidos tumorales, para continuar con la puesta a punto en muestras preoperatorias.

Ya que los biomarcadores epigenéticos han demostrado su gran utilidad diagnóstica, pronóstica y de respuesta a tratamiento en múltiples tipos tumorales, y dado que el estudio del papel de la metilación del DNA no ha sido extensamente explorado en el WDTC, el objetivo de esta tesis se focalizó justamente en este punto, la utilidad de los

cambios en la metilación del DNA como biomarcadores en el cáncer de tiroides bien diferenciado.

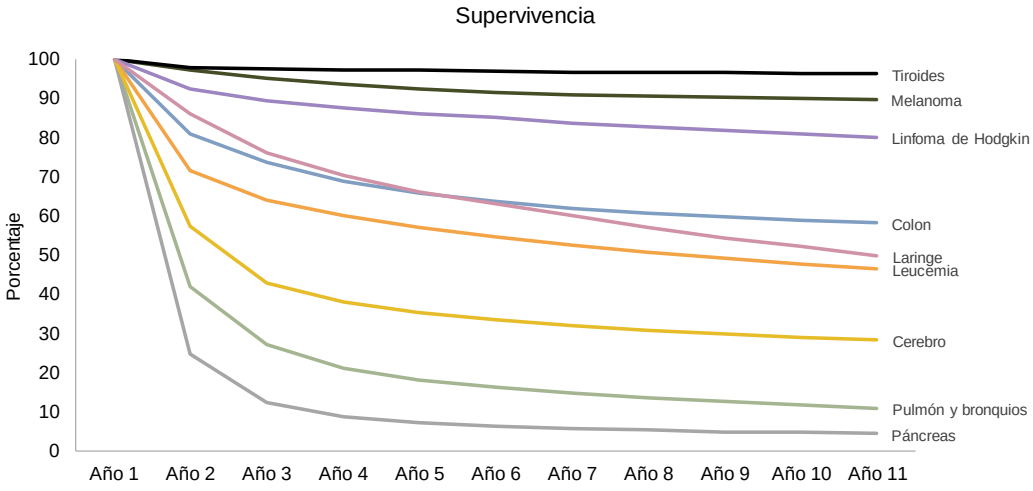

Figura D1 | Supervivencia por tipo tumoral. Porcentaje de supervivencia relativa (quedan excluidos los pacientes que han fallecido debido a causas distintas al cáncer en estudio) por tiempo durante el periodo 1988 – 2012. Datos extraídos del programa SEER.

El diseño experimental para alcanzar este objetivo se ha basado en dos estrategias, por un lado, el estudio de la hipometilación global como biomarcador de diagnóstico y/o pronóstico (trabajo I) y, por el otro, la caracterización de los perfiles de metilación del WDTC y la identificación de alteraciones de metilación específicas susceptibles de ser utilizadas como biomarcadores (trabajo II). Derivado de este rastreo o *screening* surge el trabajo III en el que se caracterizaron los cambios transcripcionales y de metilación del DNA del clúster génico de las calicreínas y su utilidad como biomarcadores en WDTC.

A continuación, se discutirán los resultados obtenidos en cada uno de estos trabajos.

1.1. Cuantificación de la hipometilación global

Típicamente, el patrón de metilación del DNA de los genomas de mamífero consiste en pequeños dominios (<4 Kb) no metilados, embebidos en grandes regiones metiladas donde residen numerosas repeticiones en tándem y elementos repetitivos dispersos (Ehrlich, 2002; Rollins et al., 2006; Suzuki and Bird, 2008). Los elementos repetitivos constituyen aproximadamente el 45% del genoma y albergan más del 50% de las CpGs del genoma (Xie et al., 2010), por lo tanto, su estado de metilación contribuye enormemente al patrón de metilación global del DNA (Yang et al., 2004). En personas

jóvenes y sanas, estas CpGs están altamente metiladas reprimiendo así su capacidad para replicarse y moverse dentro del genoma. Sin embargo, con la edad y/o con diversos procesos patológicos entre los que se encuentra el cáncer, tiene lugar una desmetilación global que afecta, entre otros compartimentos genómicos, a las secuencias repetitivas (Ehrlich, 2009). La consecuencia de esta hipometilación global es la alteración generalizada de la expresión génica así como el control del empaquetamiento de la cromatina, lo que provoca un aumento de la inestabilidad genómica (Dean et al., 2005). Recientemente, el estudio de la hipometilación global ha atraído mucho interés como biomarcador de diagnóstico, pronóstico y de riesgo, ya que numerosas investigaciones han asociado el nivel de metilación global del DNA con el estadio y grado tumoral (Choi et al., 2009; Li et al., 2014; Mendoza- Pérez et al., 2016; Moore et al., 2008; Saito et al., 2010).

Dada la abundancia y dispersión genómica de los elementos repetitivos, numerosos investigadores han coincidido en cuantificar sus niveles de metilación como medida de la hipometilación global del genoma, siendo las LINEs una de las claras favoritas (Inamura et al., 2014; Salas et al., 2014; Tajuddin et al., 2014; Weisenberger et al., 2005). No obstante, los elementos *Alu* tienen ciertas características que las hacen más interesantes como marcadores del estado de metilación global. En primer lugar, son los elementos repetitivos más abundantes y con mayor porcentaje de sitios CpG (25.4%) y, en segundo lugar, aunque se encuentran dispersos por todo el genoma, tienden a localizarse en regiones ricas en genes (Lander et al., 2001), pudiendo actuar como barreras que delimitan las regiones promotoras (Willoughby et al., 2000). Esta última característica es especialmente interesante ya que alteraciones epigenéticas en estas secuencias podrían afectar directamente a la regulación de la expresión genética tal y como demuestran estudios recientes de nuestro laboratorio (Jorda et al., aceptado para publicación.; Martín et al.,a,b, en preparación).

No obstante, y a pesar de la amplia gama de técnicas que analizan tanto LINEs como elementos *Alu* (Jordà and Peinado, 2010; Toraño et al., 2012), ninguna ha sido establecida en la práctica clínica debido a problemas técnicos (principalmente a la baja calidad y cantidad del DNA en las muestras de anatomía patológica), y económicos (como protocolos largos y complejos que necesitan de personal altamente cualificado y equipamientos sofisticados). Con el objetivo de sortear los obstáculos que impiden que la hipometilación global sea una variable más a tener en cuenta en los laboratorios de anatomía patológica, y dado que nunca se ha estudiado la hipometilación global como biomarcador en cáncer de tiroides, hemos desarrollado la técnica QUAlu (*Quantification*

of Unmethylated Alu). Al mismo tiempo y para demostrar la amplia utilidad de QUAlu, no sólo la hemos aplicado a cáncer de tiroides, sino a otros tipos tumorales como colon, pulmón, mama y próstata, partiendo de diferentes tipos de muestras (FNABs, biopsias líquidas, FFPEs y heces).

Como objeto de medida de la metilación global, QUAlu estima el porcentaje de secuencias *Alu* no metiladas en una muestra. QUAlu consiste en la digestión del DNA genómico con un par de isoesquizómeros (*Hpa*II/*Msp*I) con sensibilidad diferencial por la metilación, cuya diana (C/CGG) contiene el dinucleótido CpG susceptible de ser interrogado y está presente de manera significativa en las secuencias *Alu* (32.3%). Finalmente, los fragmentos de restricción resultantes son ligados a un adaptador y cuantificados mediante qPCR. QUAlu ha demostrado ser 100 veces más sensible que otras técnicas que miden hipometilación, siendo capaz de obtener determinaciones precisas de la metilación global con sólo 300 pg de DNA (equivalente a unas 50 células humanas[4]). Además, la alta especificidad de la técnica ha sido validada mediante secuenciación masiva de los productos de PCR (>97% de *mapajes* sobre secuencias *Alu*). Así mismo, es una técnica sencilla (digestión-ligación, qPCR y análisis), rápida (entre 5 y 6 horas dependiendo del número de muestras a procesar) y barata (~5 € / muestra) (Figura D2).

El potencial de la técnica se ha demostrado con el análisis de una serie heterogénea de 300 muestras de diferente naturaleza. Los resultados obtenidos demostraron una baja variabilidad en el estado de metilación global de los diferentes tipos de tejidos normales analizados (promedio = 6.8 ± 2.1), lo que está en consonancia con lo publicado por otras técnicas alternativas como HPLC, MethyLight (Weisenberger et al., 2005) o pirosecuenciación específica de elementos *Alu* (S. Choi et al., 2009; Wu et al., 2011). No obstante, Chalitchagorn *et al.*, basándose en la técnica COBRA-LINE-1, encontraron diferencias estadísticamente significativas entre diversos tipos de tejidos normales no asociadas al sexo o la edad (Chalitchagorn et al., 2004). La explicación de este fenómeno puede deberse a la diferente distribución genómica entre elementos *Alu* y LINEs (Lander et al., 2001). Podemos pensar que los elementos *Alu*, por encontrarse en regiones importantes en la regulación génica, se hallan bajo una presión más estricta que las LINEs de manera que toleran menos los cambios de metilación. Curiosamente, de los 12 tejidos normales que analizaron, entre los que se encuentran los 5 tejidos estudiados

[4] En el artículo (trabajo I, (Buj et al., 2016a)) se indica que el número aproximado de células que contienen 300 pg de DNA es de 150. Se trata de un error que hemos subsanado en esta tesis, ya que se estima que una célula humana contienen aproximadamente 6 pg de DNA (Morton, 1991).

en nuestro trabajo, fueron los niveles de hipometilación del tejido normal de tiroides y de esófago los que mostraron mayor variabilidad interindividual (42.612 – 73.71% y 34.42 – 68.49%, respectivamente) (Chalitchagorn et al., 2004).

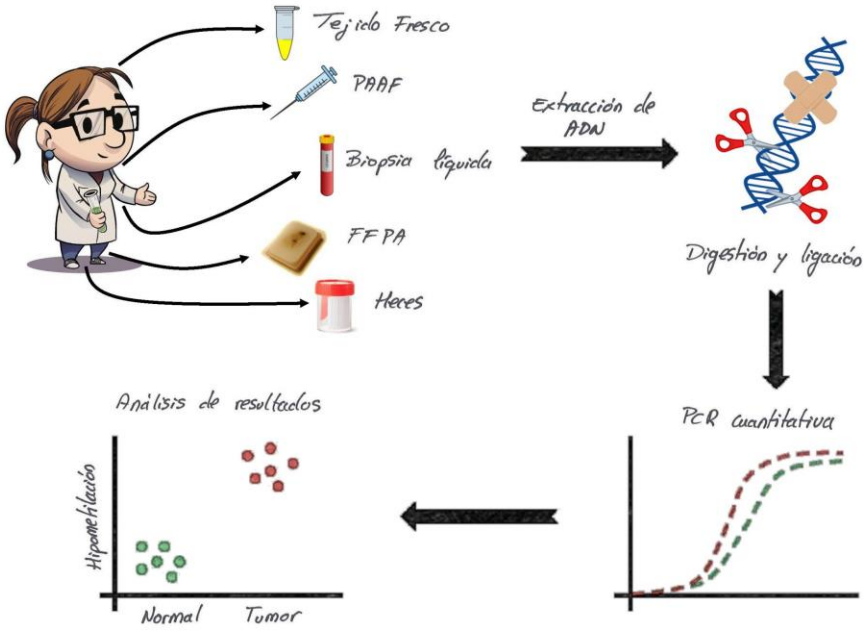

Figura D2 | Esquema de los pasos para la cuantificación de la hipometilación global mediante la técnica QUAlu. Figura extraída (Buj et al., 2016b)**.**

Por el contrario, los niveles de hipometilación de los tumores fueron mucho más variables tanto a nivel interindividual como entre los diferentes tipos tumorales. El cáncer de colon y pulmón presentaron los mayores niveles de hipometilación seguidos de los de mama, próstata y tiroides. De hecho, a excepción del cáncer de próstata, todos los tumores mostraron diferencias estadísticamente significativas con su tejido normal de referencia. Contrariamente, en el estudio de Chalitchagorn *et al.*, no solo se encontró que el carcinoma de próstata era uno de los más hipometilados por encima del de pulmón y el de colon, sino que no se observaron diferencias significativas entre el carcinoma de tiroides y su tejido normal adyacente (Chalitchagorn et al., 2004). Los resultados de Chalitchagorn *et al.*, van en sintonía con los publicados por Lee *et al.* (Lee et al., 2008) cuatro años más tarde, en los que no se encontraron diferencias significativas en el nivel de hipometilación global de las 21 parejas normal-tumor de FTCs analizadas por dos técnicas alternativas: LUMA (Karimi et al., 2006) y PyroMark™ LINE-1 assay. Las discrepancias entre los trabajos pueden deberse, como hemos comentado anteriormente,

a la naturaleza del compartimento genómico analizado, a las diferencias en la sensibilidad de las técnicas utilizadas y/o al bajo tamaño muestra de Chalitchagorn *et al.* (7 parejas normal-tumor) y a la homogeneidad histopatológica de la serie de Lee *et al.* (21 parejas normal-FTC), con respecto a la nuestra (7 parejas normal-tumor más 2 tejidos normales adyacentes y 37 tejidos tumorales independientes en los que se incluyen tanto PTCs como FTCs). No obstante, y de acuerdo con nuestros hallazgos, otros investigadores, basándose en el marcaje específico de heterocromatina metilada con anticuerpo anti-5mC y posterior análisis con técnicas de imagen computarizadas, observaron una hipometilación significativa en tumores tiroideos. Además, fueron capaces de detectar una pérdida de metilación asociada tanto al grado del tumor como al tipo histológico (de Capoa et al., 2004; Galusca et al., 2005).

En relación a los tipos histológicos del WDTC, aunque obtuvimos diferencias estadísticamente significativas entre tejido tiroideo normal y WDTC, la significación se perdió cuando se analizaron los diferentes tipos histológicos por separado (PTCs y FTCs). No obstante, se observó una tendencia en la que los PTC estaban ligeramente más hipometilados que los FTC, estos más que los FTAs, y estos más que el tejido normal (Figura D3). Ahora bien, cabe destacar que, aunque no es significativo, el PUMA de los PTCs es mucho más variable que el del resto (desviación estándar = 1.6 en NT, 2.3 en FTA, 2.5 en FTC y 3.4 en PTC), con varios tumores con PUMA muy por encima del tejido normal.

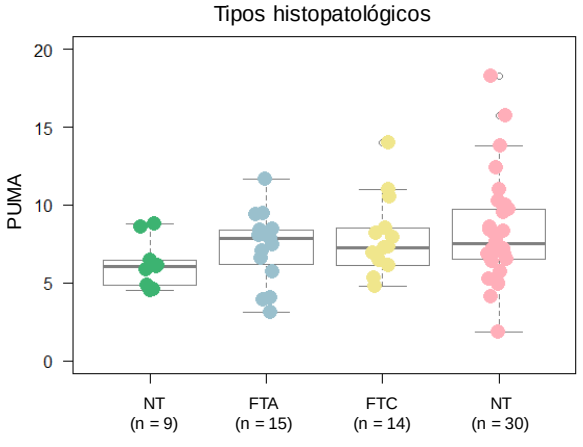

Figura D3 | Valores de hipometilación global obtenidos mediante QUAlu en los diferentes tipos histológicos del cáncer de tiroides. En esta gráfica se han incluido los resultados de 15 FTAs que no aparecen en el trabajo I.

Más recientemente, los estudios basados en las plataformas de *microarrays* de metilación, entre los que se encuentra nuestro trabajo II (Mancikova et al., 2014), han arrojado luz sobre el estado global de metilación del cáncer de tiroides. De hecho, tanto

el trabajo de Ellis *et al.* (Ellis et al., 2014), como el nuestro, señalan a la hipometilación global del DNA como un mecanismo importante asociado al desarrollo del WDTC, especialmente del PTC.

Aunque en nuestro primer estudio no se encontraron diferencias significativas en la hipometilación de los elementos *Alu* entre los grupos histopatológicos ni tampoco entre los grupos mutacionales de WDTC, resultados recientes del laboratorio en una serie retrospectiva de muestras histológicas FFPE de cáncer de tiroides, demuestran un aumento significativo en los tumores de alto riesgo (PDTC, ATC y WDTC metastático a distancia) con respecto al tejido normal y WDTC de bajo riesgo (Figura D4a) (Klein Hesselink et al., en preparación). No solo eso, sino que el análisis de supervivencia demostró que la hipometilación de los elementos *Alu* estaba asociada a un aumento en la mortalidad relacionada con cáncer de tiroides independientemente de la edad (Figura D4b). Estos resultados sugieren la implicación de la hipometilación global del DNA en la progresión tumoral y en la desdiferenciación celular en cáncer de tiroides, respaldando el potencial de la técnica QUAlu y el PUMA como biomarcador de pronóstico.

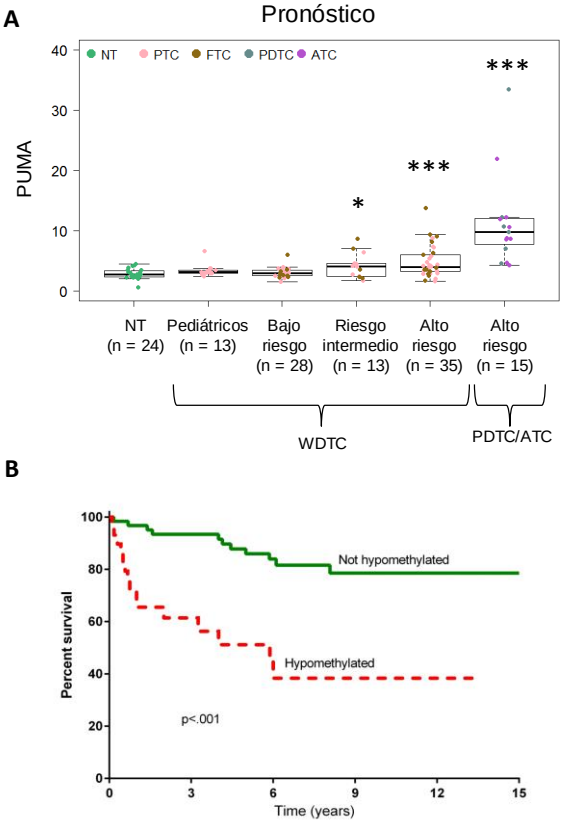

Figura D4 | Comparación de los PUMA en cáncer de tiroides y su valor como biomarcador de pronóstico. (a) Tanto los casos de WDTC de riesgo intermedio como los de alto riesgo y los casos desdiferenciados de cáncer de tiroides presentan diferencias estadísticamente significativas con respecto al tejido tiroideo normal**. (b)** Las curvas de Kaplan-Meier muestran un porcentaje de supervivencia significativamente mayor en los casos no hipometilados con respecto a los hipometilados (regresión COX con p-valor ajustado por la edad) con valores de HR (95% CI) = 1.02 (0.96 – 1.09). Figura modificada de (Klein Hesselink et al. en preparación).

Por otro lado, en el caso del cáncer de pulmón, en el que también contábamos con las dos principales histologías patológicas (adenocarcinoma de pulmón y carcinoma escamoso de pulmón), sí que encontramos diferencias asociadas al tipo histológico, confirmando resultados previos (Suzuki et al., 2013). El adenocarcinoma de pulmón, tipo histológico no asociado al tabaquismo, estaba significativamente menos hipometilado que el carcinoma escamoso de pulmón, asociado a tabaquismo.

Curiosamente, los cánceres menos hipometilados (tiroides, próstata y mama) se desarrollan a partir de glándulas donde la regulación hormonal juega un papel muy importante, mientras que en los cánceres más hipometilados (pulmón y colon) la exposición a factores ambientales (dieta, polución, etc.) es claramente más alta. Aunque no hemos indagado en esta asociación, numerosas evidencias sostienen que ciertas drogas, químicos o contaminantes están directamente implicados en la desregulación de enzimas epigenéticas contribuyendo a la hipometilación del DNA (Herceg and Vaissière, 2011; Hou et al., 2012; Mathers et al., 2010). En relación a esto último, hemos encontrado una asociación entre la hipometilación global de los tumores de pulmón y el tabaquismo, siendo significativamente más altos en los pacientes fumadores que en los exfumadores y no fumadores, confirmando los resultados de otros investigadores, tanto en pacientes con cáncer (Andreotti et al., 2013; Liu et al., 2010; I. M. Smith et al., 2007) como en personas sanas (Shigaki et al., 2012; Tajuddin et al., 2014). Confirmando el efecto del tabaquismo en la metilación global, Guerrero-Preston *et al.*, observaron que los niveles de metilación obtenidos a partir de suero sanguíneo de cordón umbilical eran menores en neonatos de madres fumadoras en comparación con los neonatos de madres fumadoras pasivas y no fumadoras (Figura D5) (Guerrero-Preston et al., 2010).

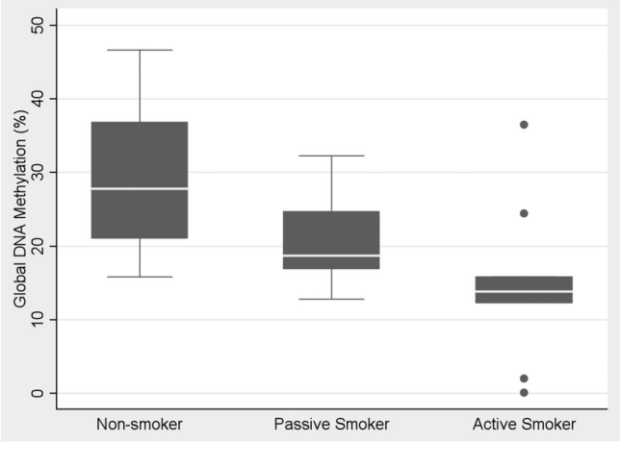

Figura D5 | Niveles de metilación global en suero sanguíneo de neonatos cuyas madres estaban expuestas a diferentes niveles de tabaquismo. Figura extraída (Guerrero-Preston et al., 2010).

Pero, para poder demostrar la utilidad del QUAlu como técnica para estratificar el riesgo de enfermedad, sería necesario realizar un ensayo prospectivo largo (varias décadas) y contar con muestras preclínicas (preferiblemente saliva o esputos) de pacientes sanos (fumadores, exfumadores y no fumadores) tomadas en diferentes momentos. De esta manera podríamos estudiar la progresión de la hipometilación y su asociación a los eventuales tumores de pulmón que se puedan desarrollar en esta cohorte.

Por último, con el objetivo de verificar la utilidad de QUAlu como biomarcador en la práctica clínica, esta técnica fue aplicada a diferentes tipos de muestras habituales en el trabajo diario de los laboratorios de anatomía patológica. Eso incluye DNA extraído de: cortes histológicos fijados en formol e incluidos en parafina de tejido tumoral y normal de colon, heces de personas sanas y pacientes con cáncer de colon, biopsias líquidas procedente de suero de personas sanas y suero y plasma de personas con cáncer de pulmón, y, finalmente, punciones con aguja fina de nódulos de tiroides en los que la presencia de patología tiroidea era desconocida. Aunque en ninguno de los casos en los que existía el equivalente normal (parafinas) o sano (heces y biopsias líquidas) se encontró una diferencia significativa con respecto al tejido tumoral, pudimos extraer algunas conclusiones que nos aventuran a especular que en series más largas el resultado podría ser significativo. Por ejemplo, en todos los casos, los PUMA de los cortes histológicos de pacientes con cáncer de colon fueron mayores que los de su respectivo tejido normal adyacente (p-valor = 0.062), y el PUMA medio del DNA extraído de heces de personas sanas era menor que el de personas con cáncer de colon (p-valor = 0.079). En cuanto a las biopsias líquidas, el hecho de no detectar valores de metilación en el DNA de personas sanas, pero sí en el de pacientes con cáncer de pulmón ya tiene valor diagnóstico dado que el aumento de la concentración de DNA libre en sangre ha sido demostrado en múltiples tumores como mama, próstata, colon y pulmón (Frattini et al., 2006; Kamat et al., 2006; Papadopoulou et al., 2006; Yoon et al., 2009).

En conclusión, QUAlu ofrece una serie de ventajas con respecto a las técnicas alternativas que la hacen especialmente sensible, específica, rápida, y económica por lo que fácilmente se podría introducir en los laboratorios de anatomía patológica. Los estudios preliminares indican su potencial aplicabilidad como biomarcador de pronóstico, diagnóstico e incluso riesgo oncológico, aunque sería conveniente ampliar este estudio en series más largas.

1.2. Caracterización de perfiles de metilación del DNA asociados a WDTC

Podemos decir que la segunda década del siglo XX ha sido la década de los estudios epigenéticos a escala genómica. Aunque en los últimos dos años se han incrementado los análisis de metilación del DNA basados en secuenciación de nueva generación o *Next Generation Sequencing* (NGS), los análisis mediante *arrays* de metilación han estado y siguen estando entre las plataformas favoritas para el estudio de la metilación del DNA (Figura D6) (Soto et al., 2016).

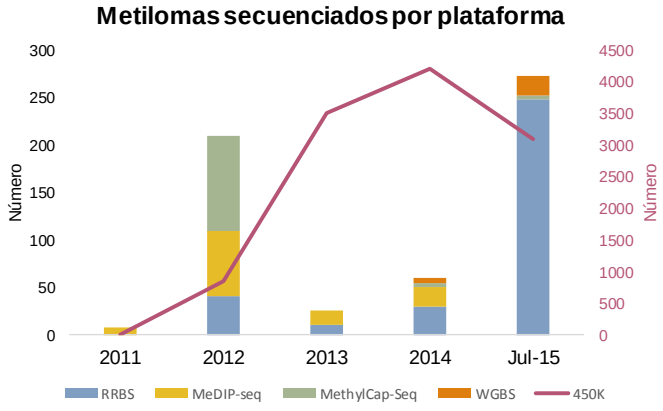

Figura D6 | Perspectiva general del número de metilomas analizados por diferentes plataformas durante el periodo 2011-2015. *Whole-genome bisulfite sequencing* (WGBS), MethylCap-Seq (Brinkman et al., 2010), *Methyl DNA Immunoprecipitation Sequencing* (MeDIP-Seq), Reduced Representation Bisulfite Sequencing (RRBS), *Illumina infinium 450K array* (450K). Figura adaptada de (Soto et al., 2016).

Concretamente, a partir del año 2008, la casa comercial Illumina lanza su *Illumina Infinium 27K array* capaz de determinar el estado de metilación de 27,578 CpGs en la región promotora de 14,495 genes (Bibikova et al., 2009). Cuatro años después esta misma casa sacó al mercado una versión ampliada, *Illumina Infinium 450K array*, que analizaba 485,577 CpGs incorporando el 96% de las CpGs incluidas en la versión anterior (Bibikova et al., 2011). La cobertura de este *array* abarca el 99% de los genes anotados en RefSeq y el 96% de las CGI anotadas en la base de datos de UCSC, además de otros compartimentos reguladores como CGI *shores* y *enhancers*. En 2016, Illumina vuelve a lanzar un nuevo *microarray*, el *Illumina Infinium EPIC array*, que cubre 853,307 sitios CpG y que, entre otras mejoras técnicas, incorpora 333,265 CpGs dentro de regiones *enhancer* identificadas en ENCODE (Moran et al., 2016).

Gracias a estos avances ha sido posible hacer el salto desde el estudio de un número limitado de genes y/o secuencias candidatas al análisis del estado de metilación de todo el genoma en un solo experimento, lo que ahorra tiempo, dinero y sobre todo muestra. Gracias a estos estudios se han podido determinar los perfiles de metilación del

DNA de diversos tipos de cáncer (The Cancer Genome Atlas Network, 2014; Rhee et al., 2013; Tahara et al., 2014), pero también de multitud de tejidos de personas sanas (Fernandez et al., 2012) o con diversas enfermedades neurodegenerativas (Lu et al., 2013) o endocrinas (Almén et al., 2014; Howard et al., 2014; Stefan et al., 2014), entre otras.

En este trabajo hemos utilizado la plataforma *Illumina Infinium 27K array* para analizar la que, hasta ese momento fue la mayor serie de WDTC estudiada. Teniendo en cuenta que esta plataforma cubre, en especial, regiones promotoras, no es de sorprender que el 97.8% de las CpGs constitutivamente desmetiladas se encontrasen en CGIs de genes de mantenimiento celular (*housekeeping genes*), algunos genes específicos de tejido y varios genes reguladores del desarrollo embrionario, coincidiendo con resultados previamente publicados (Deaton and Bird, 2011). En consecuencia, los resultados obtenidos del análisis de ontologías genéticas mostraron un enriquecimiento en procesos metabólicos primarios. Por el contrario, el 63.6% de las CpGs constitutivamente hipermetiladas se encontraban fuera de CGIs sin enriquecimiento significativo en ningún término de ontología genética.

Por otro lado, el análisis no supervisado de conglomerados jerárquicos y de componentes principales con las sondas más variables (SD > 1.2) reveló la existencia de patrones de metilación asociados no solo a la histología tumoral sino a la mutación conductora subyacente. Este resultado fue confirmado además, con una serie alternativa mucho más amplia (304 tumores y 50 tejidos normales) proveniente del consorcio TCGA (Cancer Genome Atlas Research Network et al., 2014). Por lo tanto, los análisis de metilación diferencial del DNA fueron realizados teniendo en cuenta tanto la histopatología como el estado mutacional de los tumores.

Las diferencias más claras en el perfil de metilación del DNA se observaron entre PTC y FTC. En nuestro trabajo, encontramos que los PTCs, a diferencia de los FTCs, presentan más hipometilaciones que hipermetilaciones. No obstante, en el trabajo previo de Rodríguez-Rodero *et al.*, se reportó un mayor porcentaje de sondas hipermetiladas que hipometiladas en ambos tipos histológicos (PTC y FTC) (Rodríguez-Rodero et al., 2013) (Figura D7). Esta discrepancia podría atribuirse al bajo número muestral analizado por Rodríguez-Rodero *et al.*, (2 NTs, 2 FTCs, 2 PTCs) en comparación con nuestro trabajo (8 NTs, 18 FTAs, 47 PTCs, 18 FTCs). Posteriormente, Ellis *et al.* analizando una serie de PTCs mediante la versión *Illumina Infinium 450K array* corroboraron nuestros resultados (Figura D7).

En muchos tipos tumorales se ha podido observar como el patrón de metilación del DNA se va alterando conforme aumenta la malignidad tumoral desde lesiones precancerosas benignas hasta carcinomas (Yamanoi et al., 2015) e incluso entre diferentes estadios tumorales (Brock et al., 2008; Sandoval et al., 2013) y/o metastáticos y recurrentes (Maier et al., 2004; Marzese et al., 2012). Nuestros resultados, en los que el 83% de las CpGs hipermetiladas y el 67% de las hipometiladas en FTA también fueron halladas en FTC respaldan esta hipótesis de progresión tumoral previamente descrita por otros trabajos en WDTC (Brown et al., 2014; Xing et al., 2003a). Si bien, a nivel clínico no parece existir una evolución clara del FTA a FTC, parece que a nivel histológico es frecuente encontrar carcinomas heterogéneos con características celulares adenomatosas mezcladas con las cancerosas (Baloch and LiVolsi, 2002). Una de las posibles razones que explicarían por qué la progresión tumoral que parece real a nivel histológico y molecular no puede visualizarse a nivel clínico, sería la existencia de dos tipos de FTA, los de no progresión y los de progresión rápida. Dado que muchos FTA son asintomáticos, los FTA de progresión rápida podrían evolucionar a FTC sin que ni el paciente ni el endocrino se percatasen. No obstante, es necesario realizar más investigaciones para poder determinar lo acertado de esta hipótesis.

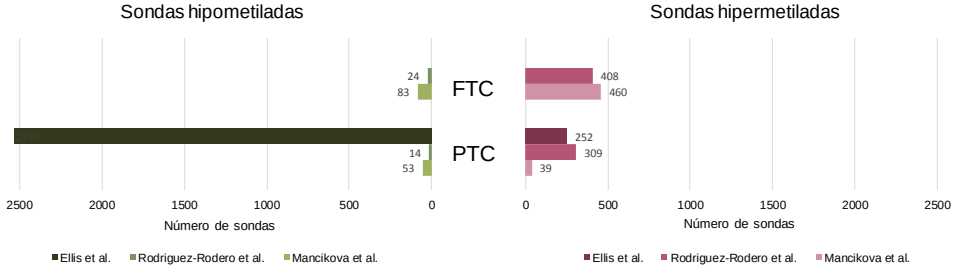

Figura D7 | Comparación del número de sondas hiper- e hipometiladas en tres trabajos. Los resultados muestran una ratio hipermetilación/hipometilación menor en PTC tanto en el estudio de Ellis *et al.* (0.10) como en el nuestro (Mancikova et al., 0.74) pero no en el de Rodríguez-Rodero *et al.* (22.07). Por otro lado, la hipermetilación de FTCs fue un evento común en nuestro trabajo (Mancikova et al.) y en el de Rodríguez-Rodero *et al.*

Aunque la asociación entre el estado mutacional y el perfil de metilación del DNA había sido previamente descrito en otros cánceres (Hinoue et al., 2012, 2009; Shen et al., 2007; Weisenberger et al., 2006), este ha sido el primer trabajo en demostrar esta asociación en WDTC. Los tumores *BRAF* mutados estaban mucho más hipometilados que los *RAS* mutados y aquellos tumores sin mutación en *BRAF* o *RAS* (“no mutados” a partir de ahora). Este resultado no debería sorprendernos ya que, como se explica en la introducción de esta tesis, las mutaciones conductoras en WDTC están muy asociadas al

tipo histológico. Por tanto, que los tumores *BRAF* mutados, la mayoría de los cuales son PTCs, sean los más hipometilados y que los tumores *RAS* mutados, asociados a una histología FTC, sean los más hipermetilados no es extraño. Sin embargo, esta separación dependiente de la mutación se hizo especialmente evidente en el tipo histológico FVPTC en el que se observó una agrupación robusta con respecto a la mutación y no al tipo histológico. Nuestros resultados no solo confirman los experimentos de Hou *et al.* en los que el silenciamiento de *BRAF*^{V600E} en líneas celulares va asociada a numerosas hipermetilaciones (Hou et al., 2011), sino que también han sido confirmados en tejido tumoral (Ellis et al., 2014; Kikuchi et al., 2013). Estos artículos revelan que la desregulación de la metilación del DNA como consecuencia de la mutación *BRAF*^{V600E} es un mecanismo importante en la tumorogénesis de PTC.

Para entender la posible repercusión funcional de los cambios de metilación obtenidos, se realizó una integración de los datos de metilación con datos de expresión de dos trabajos (Giordano et al., 2005; Montero-Conde et al., 2008). Los resultados obtenidos demuestran que numerosos genes implicados en el proceso tumoral (*CTSF*, *KLK10*, *FHLDA2*, *RUNX1*, *TACSTD2*, *BAALC*, *HMGA1*, *RASSF2*, *IMPDH1* y *TNFRSF10C*) presentan una correlación negativa entre la expresión y el estado de metilación de sus promotores tanto en PTC como en FTC. Cabe mencionar que, de todos estos genes, *KLK10* es particularmente interesante ya que tanto su estado de metilación como de expresión se asociaba al estado mutacional y fueron el punto de partida para el trabajo III. Así mismo, en PTC *BRAF* mutados, se observó una correlación negativa significativa entre la expresión y metilación de genes involucrados en la vía de las MAPK (*MAPK13*, *DUSP5* y *RAP1GA1*) y en apoptosis (*LCN2*, *RIPK1* y *LGALS1*), mientras que en FTC fue en genes relacionados con la respuesta inmune (*C7*, *SERPING1*, *TRAF3*, *PYCARD* y *CFH*).

Finalmente, demostramos que el estado de metilación de dos genes involucrados en la carcinogénesis (*EI24* y *WT1*) podía utilizarse para determinar el riesgo de recurrencia en WDTC. Más concretamente, se ha descrito que *EI24* es un supresor de tumores putativo, cuyo silenciamiento por metilación de su promotor o por deleción génica, se ha visto asociada a un aumento en la invasión y a la falta de respuesta a tratamiento (Mazumder ’ Indra et al., 2010; Mork et al., 2007). Igualmente, *WT1* codifica un factor de transcripción implicado en diversos tumores como tumor de Wilms, leucemia y próstata (Kobayashi et al., 2011; Trka et al., 2002; Weisser et al., 2005).

En conclusión, el estudio a escala genómica que hemos realizado en este trabajo, con una amplia serie de WDTC teniendo en cuenta no solo los tipos histológicos sino también la mutación conductora subyacente, nos ha permitido demostrar que los perfiles de metilación del DNA se asocian tanto al perfil histológico como al mutacional. En conjunto, estos descubrimientos han reafirmado la importancia de la regulación epigenética en el mantenimiento del correcto funcionamiento celular y cómo los patrones de metilación del DNA pueden ser buenos indicadores no sólo de diagnóstico sino también de pronóstico.

1.3. Papel de los genes *KLK* en la estratificación del riesgo de WDTC

De todas las sondas diferencialmente metiladas entre los tres grupos mutacionales (*BRAF*, *RAS* y no mutados) y el tejido normal obtenidas en el trabajo II, la sonda asociada al promotor del gen *KLK10* nos llamó especialmente la atención por tres motivos. En primer lugar, fue la segunda CpG con mayor diferencia de metilación del DNA entre los tumores *BRAF* mutados y el tejido normal. En segundo lugar, porque esta CpG exhibía un perfil de metilación del DNA bimodal en los tumores no mutados, esto es, algunos tumores no mutados presentaban valores de metilación del DNA similares a los *BRAF* mutados, mientras que otros tenían valores de metilación similares al tejido normal y a los tumores *RAS* mutados. Finalmente, el estudio de la bibliografía asociada al gen *KLK10* nos sirvió para descubrir el largo historial como biomarcador tumoral no solo de *KLK10* sino de toda la familia de genes KLK (Yousef and Diamandis, 2002).De hecho, *KLK3*, también conocido como *PSA* (*Prostate Specific Antigen*), no sólo es uno de los primeros biomarcadores descritos, sino que es uno de los más utilizados, concretamente en cáncer de próstata (De Angelis et al., 2007).

Hoy en día se conocen 15 calicreínas tisulares humanas las cuales conforman la mayor familia de proteasas extracelulares que se agrupan juntas en el genoma humano (Borgoño et al., 2004). A través del procesamiento de diferentes sustratos como componentes de la matriz extracelular, hormonas o factores de crecimiento, modulan múltiples procesos fisiológicos: licuefacción seminal, formación del esmalte dental, descamación de la piel, etc. (Prassas et al., 2015). Se sabe que alteraciones en la regulación de esta familia génica están implicadas en procesos cancerígenos favoreciendo el crecimiento tumoral, la invasión y la angiogénesis (Yousef and Diamandis, 2002). Es más, en muchos tumores, en especial aquellos con una fuerte regulación hormonal, la desregulación, tanto postraduccional como transcripcional, de alguno o

varios de los miembros de las KLKs tiene implicaciones clínicas, pudiendo ser utilizados como biomarcadores de pronóstico, riesgo y/o respuesta a tratamiento (Kryza et al., 2016).

Aunque la alteración de algunos de los miembros de esta familia (*KLK2*, *KLK3* y *KLK7*) ha sido relacionada con el WDTC, todavía no existe una descripción completa del estado de expresión y metilación de las *KLKs* en esta enfermedad. En este trabajo descubrimos por primera vez la desregulación epigenética y transcriptómica de las calicreínas en PTC. Además, gracias al uso de herramientas de minería de datos y aprendizaje automático (*machine learning*) hemos podido desarrollar un algoritmo basado en la expresión de dos calicreínas (*KLK4* y *KLK7*) y en el estado de metilación del promotor de la *KLK10*, capaz de clasificar los PTC de acuerdo a su perfil molecular, definiendo un nuevo subgrupo de buen pronóstico.

Si bien la desregulación de *KLK10* se ha postulado como un biomarcador de diagnóstico, pronóstico y de respuesta a tratamiento (Oikonomopoulou et al., 2008; Schmitt et al., 2013), actualmente no solo se desconocen sus sustratos, sino que su papel durante los procesos tumorales se ha descrito como dual, comportándose como oncogén y supresor de tumores dependiendo del tipo de cáncer (Borgoño et al., 2004). Pese a que su desregulación epigenética está descrita, hasta el momento todos los artículos publicados asocian la regulación de su expresión con cambios de metilación del DNA en la CGI asociada al exón 3 y su hipermetilación en cáncer. No obstante, en este trabajo hemos observado en dos series diferentes de muestras que, al menos en PTC, la desmetilación de una región en el promotor de *KLK10* dentro de una CGI *shore* está asociada a la expresión aberrante de *este gen* en tumores BRAF-*like*. Estos resultados, concuerdan con los obtenidos por Hansen *et al.*, en los que demostraron que, así como la hipermetilación cDMR suelen coincidir con CGIs, las cDMRs hipometiladas están enriquecidas en CGI *shores*.

Al extender nuestro estudio al resto de los miembros de esta familia, observamos no solo que la expresión de esta región estaba alterada en PTC, sino que su desregulación estaba asociada con la mutación conductora subyacente. Se describieron tres dominios de acuerdo al perfil de expresión de las calicreínas en los diferentes grupos tumorales. Así la expresión de los genes del domino A (*KLK1* a *KLK5*) estaban silenciados con respecto al tejido normal, mientras que la expresión de los dominios B (*KLK6* a *KLK8*) y C (*KLK10* a *KLK13*) en tumores *BRAF* mutados y en un subgrupo de tumores no mutados estaba incrementada con respecto al tejido normal y a los *RAS* mutados. Curiosamente,

se ha descrito que *KLK6* y *KLK10*, pertenecientes a los dominos B y C respectivamente, también están sobreexpresados en carcinoma de colon *BRAF* mutados (Popovici et al., 2012). Gracias a la aportación de datos públicos del TCGA, hemos descrito la alteración de esta familia en otros 11 tumores demostrando que la alteración de esta familia es un evento común en cáncer; y que, si bien los perfiles pueden cambiar, los límites de los tres dominios descritos en PTC se mantienen tanto en el tejido normal como en el tumoral. Además, confirmamos resultados anteriores en los que se demostraba la ubicuidad de expresión de algunos *KLKs* y la expresión específica de tejido de otros (Shaw and Diamandis, 2007).

Por otro lado, aunque los cambios de expresión fueron muy evidentes en toda la región, los cambios de metilación del DNA no fueron tan exacerbados, sugiriendo la implicación de otros mecanismos reguladores. En este sentido, el estudio reciente de Bert *et al.* demuestra la desregulación de la familia de las KLKs en células tumorales de próstata y asocia estos cambios a un proceso de activación epigenética de larga distancia (*Long-Range Epigenetic Activation*, LREA), en el que la ganancia y pérdida de marcas de histona parece ser el principal mecanismo subyacente. Estos resultados apoyan la hipótesis de un mecanismo de regulación regional el cual podría explicar el mantenimiento de los tres dominos de expresión (A-C) en todos los tejidos analizados.

Aunque se necesita explorar más en profundidad estos mecanismos epigenéticos, en esta tesis hicimos una pequeña aproximación mediante el estudio *in vitro* con células tumorales de cáncer de tiroides. Utilizamos la línea TPC-1, derivada de un PTC, la FTC133, derivada de FTC y la HTH83, derivada de ATC para llevar a cabo un experimento de inhibición de HDACs mediante el inhibidor tricostatina A (TSA). Esta droga provocó un aumento de la expresión de *KLK4*, *KLK7* y *KLK10* en todas las líneas celulares excepto de *KLK7* en HTH83, cuya expresión se vio reducida (Figura D8). Concretamente, las HDACs son enzimas reclutadas a sitios CpG metilados mediante proteínas de unión a CpGs, que promueven la eliminación del grupo acetilo de los residuos de lisina de las colas de las histonas (p.ej. H3K9), lo que favorece la condensación de la cromatina y la represión transcripcional. Por lo tanto, la inhibición de estas enzimas se ha asociado a una hipoacetilación de histonas asociada al aumento de transcripción génica (Pokholok et al., 2005). Nuestros resultados han sido confirmados recientemente en un estudio con líneas celulares pancreáticas y cervicales (Panc-1 y HeLa) en las que se demostró que la reactivación de *KLK7* inducida por TSA estaba mediada por el factor de transcripción Sp1 y la marca de activación cromatínica H3K4me3 (Raju et al., 2016).

En los últimos años, dos estudios nos dieron la clave de la importancia que podían tener las KLKs como biomarcadores en cáncer de tiroides. Por un lado, se ha propuesto el análisis de las mutaciones *RAS*, y sobre todo *BRAF*, en la evaluación no solo del riesgo sino como contribución a la toma de decisión acerca del tipo de cirugía (total o parcial) en pacientes de WDTC (Miccoli, 2014). Por el otro, la reciente publicación del trabajo sobre PTC realizado por el TCGA, demostró que los tumores PTC podían clasificarse de acuerdo a su fenotipo BRAF- o RAS-*like*, independientemente de la presencia de la mutación, en base a una firma de expresión de 71 genes (Cancer Genome Atlas Research Network et al., 2014).

De acuerdo con estos dos estudios, en esta tesis hemos desarrollado un algoritmo clasificador más simple que el propuesto por el TCGA, capaz de estratificar el PTC en BRAF- o RAS-*like*. Además, la acertada decisión de incluir el tejido normal en el desarrollo de este algoritmo nos ha permitido identificar un nuevo grupo de tumores (*BRAF/RAS Unlike tumors*, BRU) cuyo perfil de *KLKs* es similar al tejido normal y que presentan características de pronóstico favorable.

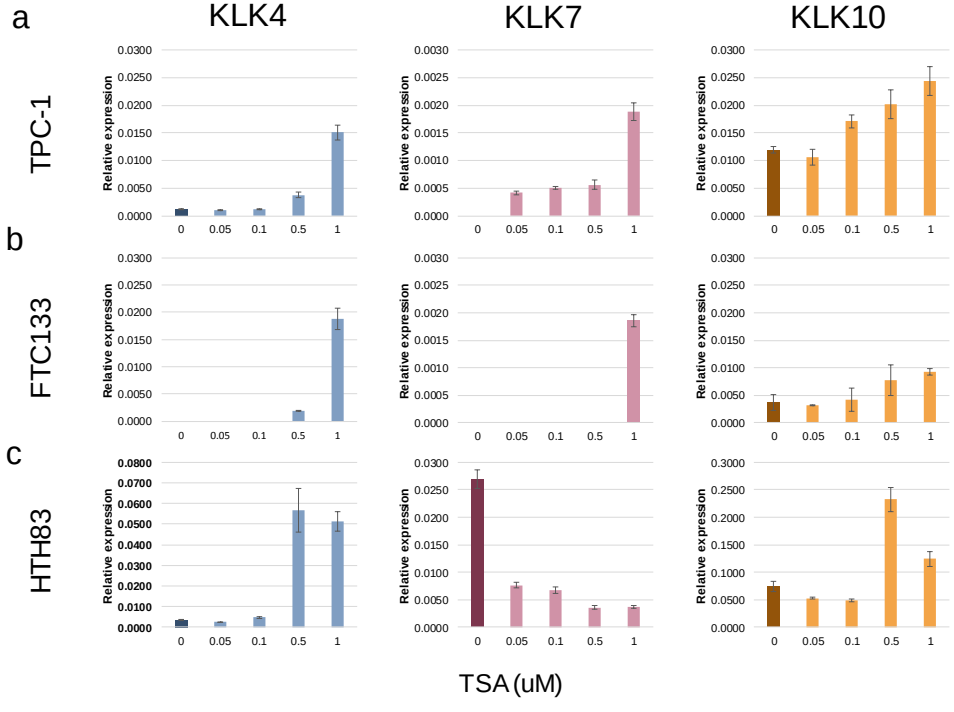

Figura D8 | Expresión de *KLK4*, *KLK7* y *KLK10* en 3 líneas tumorales de cáncer de tiroides tras un tratamiento con TSA. La expresión del *KLK4*, *KLK7* y *KLK10* se vio incrementada en TPC-1 **(a)** y FTC133 **(b)**, especialmente a altas dosis de TSA. **(c)** La expresión de *KLK4* y *KLK10* a altas dosis de TSA aumentó en HTH83, mientras que la de *KLK7* disminuyó. Expresión relativa a ciclofilina y *PUM1*, datos obtenidos mediante RT-qPCR.

El algoritmo ha sido evaluado en dos series de validación que diferían en el porcentaje de pureza tumoral. En ambas series se obtuvieron resultados óptimos en los que la sensibilidad y la especificidad del algoritmo estaba por encima del 80% y del 85%, respectivamente, con valores superiores a 0.90 en la curva de ROC. Tanto las series de entrenamiento como las de validación incluían únicamente casos *BRAF* o *RAS* positivos, encontrando que, tras la aplicación de nuestro algoritmo, algunos tumores quedaban clasificados en el grupo opuesto; esto es, 8 tumores *BRAF* mutados fueron clasificados en el grupo RAS-*like* y un tumor *RAS* mutado fue clasificados en el grupo BRAF-*like*. Aunque este hecho ha sido recientemente descrito por Popovici *et al.* en cáncer de colon, sugiriendo una desregulación similar de las vías de señalización independientemente del estado mutacional (Popovici et al., 2012), son necesarios más estudios para descartar errores de clasificación. Además, y dado que en la validación no tuvimos en cuenta el grupo BRU, y los tumores clasificados como tejido normal se consideraron errores, subestimando la sensibilidad y la especificidad.

El análisis transcriptómico de BRU, que constituye el 13% de los tumores analizados en este trabajo, indica que este nuevo grupo presenta 3,416 genes diferencialmente expresados con respecto a los tumores BRAF- y RAS-*like* y con el tejido normal. Esta firma incluye el 54.68% de los genes del perfil de Brennan *et al.*, en el que se comparó el transcriptoma de PTC de buen pronóstico con PTC de mal pronóstico (Brennan et al., 2016), indicando que los genes diferencialmente expresados en BRU parecen implicados en el pronóstico de los pacientes con PTC. Por otro lado, los tumores BRU están significativamente enriquecidos en muestras con una mayor ploidía y SNCA, así como un alto grado de diferenciación celular y poca sobreactivación de la vía de las MAPK. Curiosamente, de acuerdo a los resultados obtenidos por el TCGA, la mayoría de los tumores con un alto grado de alteraciones del número de copias somático (*Somatic Copy Number Alterations*, SCNA) no poseen ninguna de las mutaciones conductoras, sugiriendo que, en estos tumores, las SCNAs podrían ser el mecanismo conductor de la tumorogénesis (Cancer Genome Atlas Research Network et al., 2014). Desde el punto de vista clínico, los tumores BRU se caracterizan por presentar claras diferencias con respecto a BRAF-*like,* pero no tantas con RAS-*like*. Así pues, BRU se asocia a parámetros de buen pronóstico como son: el bajo número de casos con histología de células altas, estadios tumorales bajos, extensión extratiroidea nula o mínima, enriquecimiento en casos de bajo riesgo y microcarcinomas y pocos pacientes tratados con RAI. Además, las curvas de Kaplan-Meier muestran un mejor pronóstico (menor porcentaje de pacientes con recurrencia de la enfermedad) de los pacientes del grupo BRU con respecto a los pacientes clasificados como BRAF- o RAS-*like*.

Nuestros resultados sugieren que los tumores BRU son de bajo riesgo y podrían seguir un tratamiento menos agresivo. En especial, en el caso de los microcarcinomas que no presentan factores de alto riesgo (metástasis, invasión extratiroidea, etc.). Tal y como propuso Ito *et al* (Ito et al., 2010)., sería conveniente realizar un cambio en la práctica clínica sustituyendo el agresivo tratamiento actual (tiroidectomía total) por una vigilancia más activa del paciente. En este sentido, nuestro algoritmo podría ayudar a encontrar aquellos pacientes candidatos a renunciar a la tiroidectomía y entrar en un programa de seguimiento intenso.

Aunque nuestro trabajo ha sido realizado en PTC, cabría la posibilidad de extender los análisis tanto a FTA y FTC como a PDTC y ATC. De hecho, nuestros resultados de metilación y expresión de *KLK10* obtenidos en el trabajo II apuntan a que el algoritmo KLK podría ser utilizado igualmente en FTA y FTC. Además, y dado que nuestro algoritmo se basa en el análisis de la expresión de *KLK4* y *KLK7* y el estado de metilación del DNA de una CpG asociada a la expresión del gen *KLK10*, su implementación en la práctica clínica a través de técnicas simples y económicas (conversión por bisulfito, RT-qPCR, inmunohistoquímica, etc.) ponen de manifiesto la utilidad del algoritmo KLK en el manejo del WDTC. Además, su puesta a punto en FNABs podría ahorrar cirugías innecesarias y ayudar a determinar el tratamiento más adecuado.

Por otro lado, también nos intensa conocer la función de las KLKs en la progresión tumoral. Recientemente hemos utilizado la técnica CRISPR/Cas9 SAM (*CRISPR/Cas9 Synergistic Activation Mediator*) para sobreexpresar *KLK10* y *KLK7* en la línea celular TPC-1. Resultados preliminares demuestran que *KLK7*, pero no *KLK10* están implicados en el aumento de la migración celular (Figura D9a), mientras que ninguna de estas calicreínas produjo un cambio significativo de la proliferación celular (Figura D9b). En este sentido, varios trabajos funcionales han relacionado activamente a *KLK7* con procesos de invasión y proliferación (Johnson et al., 2007; Mo et al., 2010; Ramani et al., 2011). Por su parte, como se ha comentado anteriormente, *KLK10* puede tener un papel dual como supresor tumoral y como oncogén (Dhar et al., 2001; Feng et al., 2006; Yousef and Diamandis, 2002).

En conclusión, en este trabajo hemos descrito las alteraciones a nivel epigenético y transcriptómico de la familia de proteasas extracelulares calicreínas, conocidas por su papel como biomarcadoras en numerosos tipos de cáncer (Yousef and Diamandis, 2002). Además, hemos desarrollado un algoritmo simple capaz de estratificar el riesgo de PTC con potencial para ser utilizado de manera rápida en los laboratorios de anatomía

patológica. Gracias a la aplicación preliminar del mismo, hemos descrito un nuevo grupo de tumores con características de buen pronóstico (BRU) que podría mejorar la práctica clínica actual permitiendo tratamientos menos agresivos y más personalizados.

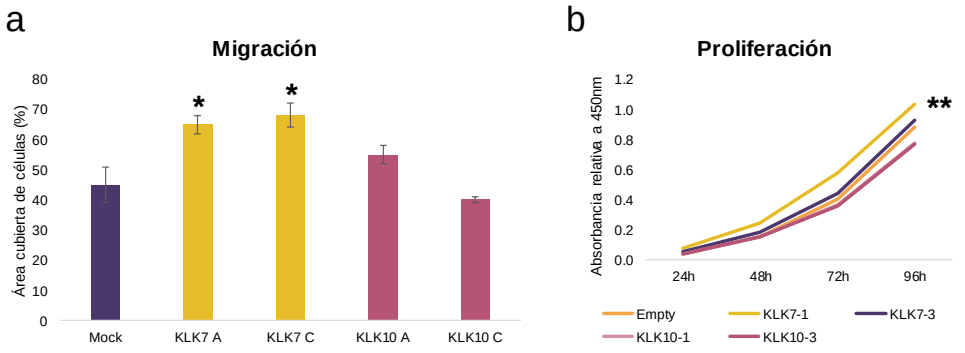

Figura D9 | Ensayos de migración y proliferación de TPC-1 sobreexpresando *KLK7* y *KLK10*. (a) La migración celular medida a las 24h en un ensayo de reparación de heridas (*wound healling*) demostró un aumento significativo únicamente en las células con sobreexpresión de *KLK7*, pero no de *KLK10*. **(b)** No se observaron diferencias significativas en la proliferación celular de las células TPC-1 con sobreexpresión de *KLK7* o *KLK10* a ninguno de los tiempos estudiados mediante el ensayo CCK8 (*Cell Counting Kit-8*).

2. Observaciones finales

En conjunto, en esta tesis hemos abierto el camino al estudio de una serie de biomarcadores de nueva generación epigenéticos y transcriptómicos, cuya puesta a punto en muestras prequirúrgicas puede representar un avance muy significativo en la medicina predictiva y personalizada del WDTC.

La metodología seguida para alcanzar este objetivo se ha basado en dos estrategias. Por un lado, hemos estudiado la hipometilación global como biomarcador de diagnóstico y/o pronóstico en cáncer de tiroides. Para ello nos centramos en el desarrollo de un método simple y económico capaz de cuantificar la hipometilación global en muestras habituales en los laboratorios de anatomía patológica (trabajo I). Por el otro, hemos caracterizado los perfiles de metilación del WDTC y hemos identificado cambios específicos de metilación susceptibles de ser utilizados como biomarcadores (trabajo II). Además, y derivado de los descubrimientos de esta última estrategia, hemos caracterizado la desregulación transcripcional y epigenética de toda una familia de genes previamente descritos como biomarcadores en otros tipos de cáncer, especialmente de aquellos tejidos con una alta implicación endocrina (trabajo III). No solo eso, sino que gracias al desarrollo de un algoritmo basado en el estado de metilación y el nivel de expresión de tres miembros de esta familia hemos sido capaces de mejorar la estratificación del WDTC describiendo un nuevo grupo de tumores con características clinicopatológicas de buen pronóstico.

Salvando la necesidad de realizar estudios de validación más completos, creemos que, la futura incorporación en los laboratorios patológicos de las dos metodologías propuestas en esta tesis de manera combinada (QUAlu y algoritmo KLK) podría ser de mucha utilidad en la estratificación del WDTC. Así pues, en la figura D10 se esquematiza el procedimiento analítico pre- y postquirúrgico actual y en qué puntos se podría introducir los biomarcadores propuestos en esta tesis.

A partir de los resultados de esta tesis, nuestro interés inmediato es la puesta a punto de ambas técnicas en series más complejas que cuenten con casos de buen y mal pronóstico, que incluyan no solo tumores metastáticos, sino también casos con diferentes grados de extensión extratiroidea, infiltración capsular y/o vascular, microcarcinomas, etc. El objetivo es, por un lado validar los resultados recientemente obtenidos en el laboratorio por en tumores de alto riesgo de metástasis a distancia (Klein Hesselink et al. en preparación) e intentar asociar el aumento de hipometilación con otras variables de mal

pronóstico. Por otro, validar los resultados obtenidos en el trabajo III para afirmar con total seguridad que los tumores BRU son de buen pronóstico y, por lo tanto, en especial si son microcarcinomas, sustituir la tiroidectomía total por un seguimiento más exhaustivo. En consecuencia, la aplicación tanto del QUAlu como del algoritmo KLK permitiría un manejo más adecuado de estos tumores facilitando la toma de decisiones a los endocrinos y mejorando significativamente la calidad de vida de los pacientes de WDTC.

a

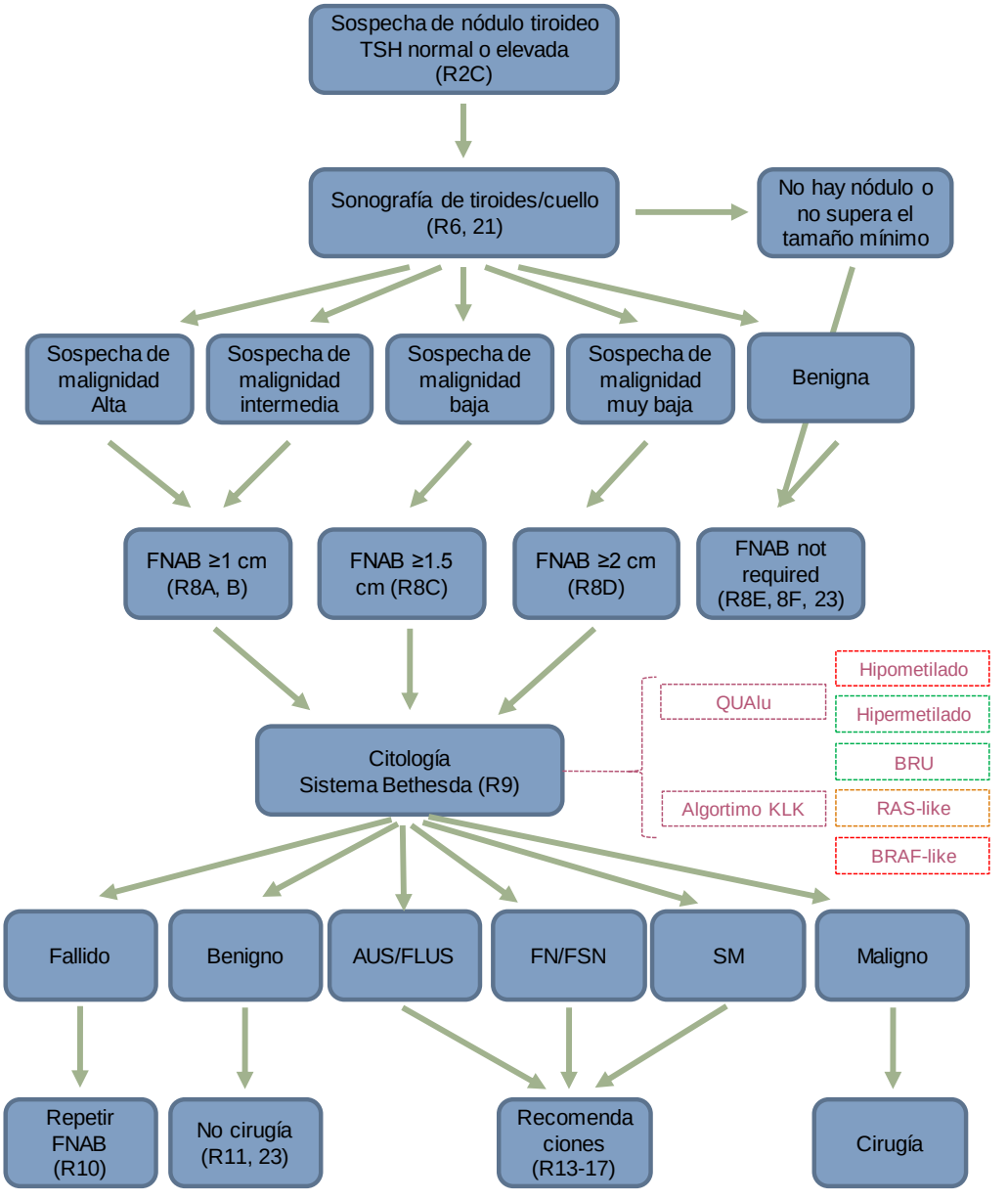

b

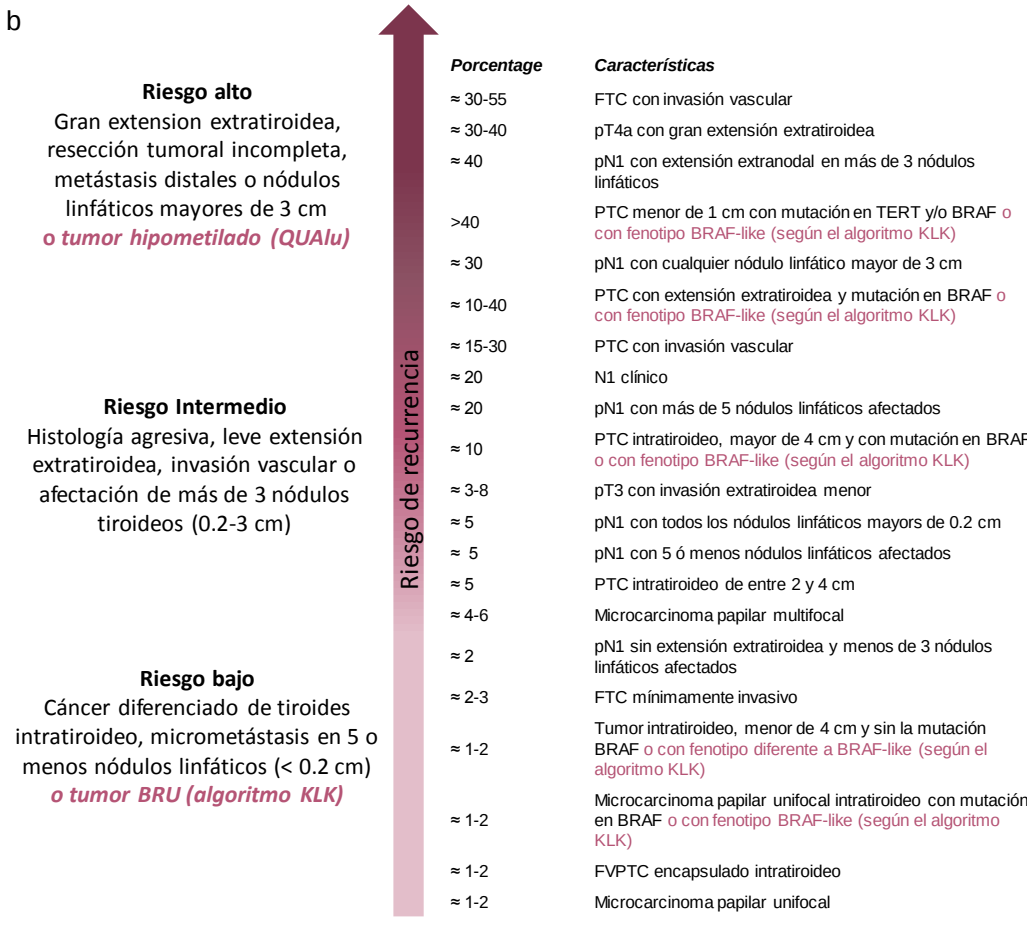

Figura D10 | Modificaciones propuestas para el procedimiento pre- y postquirúrgico establecido en la guía de la ATA 2015. (a) Algoritmo para el manejo y evaluación prequirúrgico de los pacientes con nódulos tiroideos. En el esquema se propone la implementación de los exámenes citológicos mediante la técnica QUAlu y el algoritmo KLK a fin de detectar niveles altos de hipometilación (mal pronóstico) o tumores clasificados como BRU (buen pronóstico). El color de las cajas de los resultados del QUAlu y del algoritmo KLK indican el nivel de riesgo: alto (rojo), intermedio (naranja), bajo (verde). **(b)** Esquema del riesgo de recurrencia en el examen postquirúrgico. En magenta se señalan las aportaciones de esta tesis. Figuras modificadas de (Haugen et al., 2015); R (recomendación en el texto del artículo).

Conclusiones

De acuerdo a los objetivos presentados y a los resultados obtenidos en esta tesis, las conclusiones son:

Objetivo I:

Evaluar la hipometilación global de los elementos Alu como aproximación al estudio de la hipometilación global del genoma y su utilidad como biomarcador en WDTC.

1. QUAlu es una técnica simple, rápida y económica que permite cuantificar la hipometilación global del genoma en un amplio espectro de tipos muestrales de rutina en los laboratorios de anatomía patológica.

2. Los tejidos no tumorales presentan niveles de hipometilación homogéneamente bajos mientras que los tejidos tumorales están heterogéneamente más hipometilados, siendo los carcinomas de pulmón y colon los más hipometilados y los de tiroides los menos hipometilados.

3. Aunque la hipometilación de elementos *Alu* no parece ser una marca distintiva del cáncer de tiroides bien diferenciado, algunos tumores presentan valores muy por encima del tejido normal.

4. QUAlu ha demostrado ser especialmente útil en cáncer de colon ya que el DNA extraído de heces de pacientes está más hipometilado que el de las personas sanas. Asimismo, en cáncer de pulmón se ha visto que el carcinoma escamoso está significativamente más hipometilado que el adenocarcinoma encontrando una asociación con el tabaquismo.

Objetivo II:

Estudiar los patrones de metilación del DNA de las regiones promotoras en el WDTC e identificar nuevos biomarcadores epigenéticos.

5. El 83% de las CpGs hipermetiladas y el 67% de las hipometiladas en adenoma folicular también fueron encontradas en carcinoma folicular, respaldando la hipótesis de progresión tumoral desde adenomas a carcinomas.

6. Los perfiles de metilación del DNA a escala genómica en cáncer de tiroides bien diferenciado se asocian no solo al tipo histológico sino también a la mutación conductora subyacente *BRAF* y *RAS*.

7. La hipermetilación de los genes *EI24* (*etoposide induced 2.4*) y *WT1* (*Wilms tumor 1*) se asocia a un mayor riesgo de recurrencia siendo buenos candidatos como biomarcadores de pronóstico.

Objetivo III:

Caracterizar la familia génica de las calicreínas (KLKs) a nivel epigenético (metilación del DNA) y transcriptómico para investigar su contribución a la estratificación molecular del WDTC.

8. La hipometilación y la sobreexpresión de KLK10 son característicos de los tumores BRAF-*like*

9. La familia de las calicreínas tisulares está desregulada a nivel transcripcional en el cáncer papilar de tiroides, de manera que los perfiles de expresión se asocian específicamente al estado mutacional de *BRAF* y *RAS*.

10. La desregulación transcripcional de las calicreínas tisulares es un evento generalizado en otros tipos de cáncer incluyendo cáncer de colon, pulmón, mama o próstata entre otros.

11. El algoritmo KLK supone un sistema simple, eficiente y clínicamente aplicable para la estratificación del cáncer papilar de tiroides en los ya conocidos grupos BRAF- y RAS-*like*, además de un nuevo grupo de tumores BRU con características clínicas de buen pronóstico.

Referencias

Adeniran, A.J., Chhieng, D., 2016. Variants of Papillary Thyroid Carcinoma, in: Common Diagnostic Pitfalls in Thyroid Cytopathology. Springer International Publishing, Cham, pp. 137–180. doi:10.1007/978-3-319-31602-4_10

Adeniran, A.J., Zhu, Z., Gandhi, M., Steward, D.L., Fidler, J.P., Giordano, T.J., Biddinger, P.W., Nikiforov, Y.E., 2006. Correlation between genetic alterations and microscopic features, clinical manifestations, and prognostic characteristics of thyroid papillary carcinomas. Am. J. Surg. Pathol. 30, 216–22.

Akers, S.N., Moysich, K., Zhang, W., Collamat Lai, G., Miller, A., Lele, S., Odunsi, K., Karpf, A.R., 2014. LINE1 and Alu repetitive element DNA methylation in tumors and white blood cells from epithelial ovarian cancer patients. Gynecol. Oncol. 132, 462–467. doi:10.1016/j.ygyno.2013.12.024

Alexander, E.K., Kennedy, G.C., Baloch, Z.W., Cibas, E.S., Chudova, D., Diggans, J., Friedman, L., Kloos, R.T., Livolsi, V. a, Mandel, S.J., Raab, S.S., Rosai, J., Steward, D.L., Walsh, P.S., Wilde, J.I., Zeiger, M. a, Lanman, R.B., Haugen, B.R., Ph, D., 2012. Preoperative diagnosis of benign thyroid nodules with indeterminate cytology. N. Engl. J. Med. 367, 705–15. doi:10.1056/NEJMoa1203208

Alexandrov, L.B., Nik-Zainal, S., Wedge, D.C., Aparicio, S. a J.R., Behjati, S., Biankin, A. V, Bignell, G.R., Bolli, N., Borg, A., Børresen-Dale, A.-L., Boyault, S., Burkhardt, B., Butler, A.P., Caldas, C., Davies, H.R., Desmedt, C., Eils, R., Eyfjörd, J.E., Foekens, J. a, Greaves, M., Hosoda, F., Hutter, B., Ilicic, T., Imbeaud, S., Imielinski, M., Imielinsk, M., Jäger, N., Jones, D.T.W., Jones, D., Knappskog, S., Kool, M., Lakhani, S.R., López-Otín, C., Martin, S., Munshi, N.C., Nakamura, H., Northcott, P. a, Pajic, M., Papaemmanuil, E., Paradiso, A., Pearson, J. V, Puente, X.S., Raine, K., Ramakrishna, M., Richardson, A.L., Richter, J., Rosenstiel, P., Schlesner, M., Schumacher, T.N., Span, P.N., Teague, J.W., Totoki, Y., Tutt, A.N.J., Valdés-Mas, R., van Buuren, M.M., van 't Veer, L., Vincent-Salomon, A., Waddell, N., Yates, L.R., Zucman-Rossi, J., Futreal, P.A., McDermott, U., Lichter, P., Meyerson, M., Grimmond, S.M., Siebert, R., Campo, E., Shibata, T., Pfister, S.M., Campbell, P.J., Stratton, M.R., 2013. Signatures of mutational processes in human cancer. Nature 500, 415–21. doi:10.1038/nature12477

Almén, M.S., Nilsson, E.K., Jacobsson, J.A., Kalnina, I., Klovins, J., Fredriksson, R., Schiöth, H.B., 2014. Genome-wide analysis reveals DNA methylation markers that vary with both age and obesity. Gene 548, 61–67. doi:10.1016/j.gene.2014.07.009

Almquist, M., Johansen, D., Bj??rge, T., Ulmer, H., Lindkvist, B., Stocks, T., Hallmans, G., Engeland, A., Rapp, K., Jonsson, H., Selmer, R., Diem, G., H??ggstr??m, C., Tretli, S., Stattin, P., Manjer, J., 2011. Metabolic factors and risk of thyroid cancer in the Metabolic syndrome and Cancer project (Me-Can). Cancer Causes Control 22, 743–751. doi:10.1007/s10552-011-9747-2

Alvarez-Nuñez, F., Bussaglia, E., Mauricio, D., Ybarra, J., Vilar, M., Lerma, E., de Leiva, A., Matias-Guiu, X., 2006. PTEN promoter methylation in sporadic thyroid carcinomas. Thyroid 16, 17–23. doi:10.1089/thy.2006.16.17

American Thyroid Association (ATA) Guidelines Taskforce on Thyroid Nodules and Differentiated Thyroid Cancer, Cooper, D.S., Doherty, G.M., Haugen, B.R., Hauger, B.R., Kloos, R.T., Lee, S.L., Mandel, S.J., Mazzaferri, E.L., McIver, B., Pacini, F., Schlumberger, M., Sherman, S.I., Steward, D.L., Tuttle, R.M., 2009. Revised American Thyroid Association management guidelines for patients with thyroid nodules and differentiated thyroid cancer. Thyroid 19, 1167–214. doi:10.1089/thy.2009.0110

Ameziane-El-Hassani, R., Morand, S., Boucher, J.-L., Frapart, Y.-M., Apostolou, D., Agnandji, D., Gnidehou, S., Ohayon, R., Noël-Hudson, M.-S., Francon, J., Lalaoui, K., Virion, A., Dupuy, C., 2005. Dual oxidase-2 has an intrinsic Ca2+-dependent H2O2-generating activity. J. Biol. Chem. 280, 30046–54. doi:10.1074/jbc.M500516200

Anania, M.C., Sensi, M., Radaelli, E., Miranda, C., Vizioli, M.G., Pagliardini, S., Favini, E., Cleris, L., Supino, R., Formelli, F., Borrello, M.G., Pierotti, M. a, Greco, a, 2011. TIMP3 regulates migration, invasion and in vivo tumorigenicity of thyroid tumor cells. Oncogene 30, 3011–23. doi:10.1038/onc.2011.18

Anderson, K., Lutz, C., van Delft, F.W., Bateman, C.M., Guo, Y., Colman, S.M., Kempski, H., Moorman, A. V., Titley, I., Swansbury, J., Kearney, L., Enver, T., Greaves, M., 2011. Genetic variegation of clonal architecture and propagating cells in leukaemia. Nature 469, 356–61. doi:10.1038/nature09650

Andreotti, G., Karami, S., Pfeiffer, R.M., Hurwitz, L., Liao, L.M., Weinstein, S.J., Albanes, D., Virtamo, J., Silverman, D.T., Rothman, N., Moore, L.E., 2013. LINE1 methylation levels associated with increased bladder cancer risk in pre-diagnostic blood DNA among US (PLCO) and European (ATBC) cohort study participants. Epigenetics 9, 404–415. doi:10.4161/epi.27386

Antonica, F., Kasprzyk, D.F., Opitz, R., Iacovino, M., Liao, X.-H., Dumitrescu, A.M., Refetoff, S., Peremans, K., Manto, M., Kyba, M., Costagliola, S., 2012. Generation of functional thyroid from embryonic stem cells. Nature 491, 66–71. doi:10.1038/nature11525

Aran, D., Toperoff, G., Rosenberg, M., Hellman, A., 2011. Replication timing-related and gene body-specific methylation of active human genes. Hum. Mol. Genet. 20, 670–680. doi:10.1093/HMG/DDQ513

Aschebrook-Kilfoy, B., Grogan, R.H., Ward, M.H., Kaplan, E., Devesa, S.S., 2013. Follicular thyroid cancer incidence patterns in the United States, 1980-2009. Thyroid 23, 1015–1021. doi:10.1089/thy.2012.0356

Ask, K., Hambly, N., Kolb, M.R.J., 2015. Biomarkers in interstitial lung disease: moving towards composite indexes and multimarkers? Curr. Pulmonol. Reports 4, 125–129. doi:10.1007/s13665-015-0123-7

Atkinson A.J., J., Colburn, W.A., DeGruttola, V.G., DeMets, D.L., Downing, G.J., Hoth, D.F., Oates, J.A., Peck, C.C., Schooley, R.T., Spilker, B.A., Woodcock, J., Zeger, S.L., 2001. Biomarkers and surrogate endpoints: Preferred definitions and conceptual framework. Clin. Pharmacol. Ther. doi:10.1067/mcp.2001.113989

Bäckdahl, M., Wallin, G., Löwhagen, T., Auer, G., Granberg, P.O., 1987. Fine-needle biopsy cytology and DNA

analysis. Their place in the evaluation and treatment of patients with thyroid neoplasms. Surg. Clin. North Am. 67, 197–211.

Bae, J.M., Shin, S.H., Kwon, H.J., Park, S.Y., Kook, M.C., Kim, Y.W., Cho, N.Y., Kim, N., Kim, T.Y., Kim, D., Kang, G.H., 2012. ALU and LINE-1 hypomethylations in multistep gastric carcinogenesis and their prognostic implications. Int. J. Cancer 131, 1323–1331. doi:10.1002/ijc.27369

Baloch, Z.W., LiVolsi, V.A., 2002. Follicular-patterned lesions of the thyroid: The bane of the pathologist. Am. J. Clin. Pathol. doi:10.1309/8VL9-ECXY-NVMX-2RQF

Bannister, A.J., Kouzarides, T., 2011. Regulation of chromatin by histone modifications. Cell Res. 21, 381–95. doi:10.1038/cr.2011.22

Barnabei, A., Ferretti, E., Baldelli, R., Procaccini, A., Spriano, G., Appetecchia, M., 2009. Hurthle cell tumours of the thyroid. Personal experience and review of the literature. Acta Otorhinolaryngol. Ital. organo Uff. della Soc. Ital. di Otorinolaringol. e Chir. Cerv.-facc. 29, 305–11.

Berdasco, M., Esteller, M., 2010. Aberrant Epigenetic Landscape in Cancer: How Cellular Identity Goes Awry. Dev. Cell. doi:10.1016/j.devcel.2010.10.005

Berman, B.P., Weisenberger, D.J., Aman, J.F., Hinoue, T., Ramjan, Z., Liu, Y., Noushmehr, H., E Lange, C.P., van Dijk, C.M., E M Tollenaar, R.A., Van Den Berg, D., Laird, P.W., 2011. Regions of focal DNA hypermethylation and long-range hypomethylation in colorectal cancer coincide with nuclear lamina–associated domains. Nat. Genet. 44. doi:10.1038/ng.969

Berrington de González, A., Mahesh, M., Kim, K.-P., Bhargavan, M., Lewis, R., Mettler, F., Land, C., 2009. Projected cancer risks from computed tomographic scans performed in the United States in 2007. Arch. Intern. Med. 169, 2071–7. doi:10.1001/archinternmed.2009.440

Bestor, T.H., 1998. The host defence function of genomic methylation patterns. Novartis Found. Symp. 214, 187–189,228–232.

Bestor, T.H., Coxon, A., Li, E., Bestor, T.H., Jaenisch, R., Shen, J.-C., Rideout, W.M., Jones, P.A., Steinberg, R.A., Gorman, K.B., Hodges, P., Scott, J., Selker, E.U., Bestor, T.H., Jahner, D., Jaenisch, R., Kricker, M.C., Drake, J.W., Radman, M., Paulien, S., Turc-Carel, C., Cin, P.D., Jani-Sait, S., Sreetanaiah, C., Leong, S.P., Vogelstein, B., Kinzler, K.W., Sandberg, A.A., Gemmill, R.M., Sutcliffe, J.S., Nelson, D.L., Zhang, F., Pierretti, M., Caskey, S.T., Saxe, D., Warren, S.T., Matzke, M., Matzke, A.J.M., Riggs, A.D., Pfeiffer, G.D., Turker, M.S., Swisshelm, K., Smith, A.C., Martin, G.M., Holliday, R., Ho, T., Sakai, T., Toguchida, J., Ohtani, N., Yandell, D.W., Rapaport, F.M., Dryja, T.P., Royer-Pokora, B., Schneider, S., Ono, T., Yamamoto, S., Kurishita, A., Yamamoto, K., Yamamoto, Y., Ujeno, Y., Sagisaka, K., Fukui, Y., Miyamoto, M., Tawa, R., Hirose, S., Okada, S., Rainier, S., Johnson, L.A., Dobry, C.J., Ping, A.J., Grundy, P.E., Feinberg, A.P., Ogawa, O., Eccles, M.R., Szeto, J., McNoe, L.A., Yun, K., Maw, M.A., Smith, P.J., Reeve, A.E., 1993. Cytosine methylation The pros and cons of DNA methylation. Curr. Biol. 3, 384–386. doi:10.1016/0960-9822(93)90209-7

Bibikova, M., Barnes, B., Tsan, C., Ho, V., Klotzle, B., Le, J.M., Delano, D., Zhang, L., Schroth, G.P., Gunderson, K.L., Fan, J.-B., Shen, R., 2011. High density DNA methylation array with single CpG site resolution. Genomics 98, 288–295. doi:10.1016/j.ygeno.2011.07.007

Bibikova, M., Le, J., Barnes, B., Saedinia-Melnyk, S., Zhou, L., Shen, R., Gunderson, K.L., 2009. Genome-wide DNA methylation profiling using Infinium ® assay. Epigenomics 1, 177–200. doi:10.2217/epi.09.14

Bilimoria, K.Y., Bentrem, D.J., Linn, J.G., Freel, A., Yeh, J.J., Stewart, A.K., Winchester, D.P., Ko, C.Y., Talamonti, M.S., Sturgeon, C., 2007. Utilization of total thyroidectomy for papillary thyroid cancer in the United States. Surgery 142, 906–913. doi:10.1016/j.surg.2007.09.002

Biondi, B., Filetti, S., Schlumberger, M., 2005. Thyroid-hormone therapy and thyroid cancer: a reassessment. Nat. Clin. Pract. Endocrinol. Metab. 1, 32–40. doi:10.1038/ncpendmet0020

Bird, A., 2002. DNA methylation patterns and epigenetic memory. Genes Dev. doi:10.1101/gad.947102

Bird, A., Taggart, M., Frommer, M., Miller, O.J., Macleod, D., 1985. A fraction of the mouse genome that is derived from islands of nonmethylated, CpG-rich DNA. Cell 40, 91–9.

Bird, A.P., 1980. DNA methylation and the frequency of CpG in animal DNA. Nucleic Acids Res. 8, 1499.

Blackburn, E.H., Greider, C.W., Szostak, J.W., 2006. Telomeres and telomerase: the path from maize, Tetrahymena and yeast to human cancer and aging. Nat. Med. 12, 1133–1138. doi:10.1038/nm1006-1133

Bliss, R.D., Gauger, P.G., Delbridge, L.W., 2000. Surgeon's approach to the thyroid gland: Surgical anatomy and the importance of technique. World J. Surg. 24, 891–897. doi:10.1007/s002680010173

Bock, C., 2009. Epigenetic biomarker development. Epigenomics 1, 99–110. doi:10.2217/epi.09.6

Bongarzone, I., Butti, M.G., Coronelli, S., Borrello, M.G., Santoro, M., Mondellini, P., Pilotti, S., Fusco, A., Della Porta, G., 1994. Frequent activation of ret protooncogene by fusion with a new activating gene in papillary thyroid carcinomas. Cancer Res. 54, 2979–2985.

Bongarzone, I., Monzini, N., Borrello, M.G., Carcano, C., Ferraresi, G., Arighi, E., Mondellini, P., Della Porta, G., Pierotti, M.A., 1993. Molecular characterization of a thyroid tumor-specific transforming sequence formed by the fusion of ret tyrosine kinase and the regulatory subunit RI alpha of cyclic AMP-dependent protein kinase A. Mol. Cell. Biol. 13, 358–66.

Bongiovanni, M., Sadow, P.M., Faquin, W.C., 2009. Poorly differentiated thyroid carcinoma: a cytologic-histologic review. Adv. Anat. Pathol. 16, 283–9. doi:10.1097/PAP.0b013e3181b50640

Borbone, E., Troncone, G., Ferraro, A., Jasencakova, Z.,

Stojic, L., Esposito, F., Hornig, N., Fusco, A., Orlando, V., 2011. Enhancer of zeste homolog 2 overexpression has a role in the development of anaplastic thyroid carcinomas. J. Clin. Endocrinol. Metab. 96, 1029–1038. doi:10.1210/jc.2010-1784

Borgoño, C. a, Michael, I.P., Diamandis, E.P., 2004. Human tissue kallikreins: physiologic roles and applications in cancer. Mol. Cancer Res. 2, 257–280. doi:2/5/257 [pii]

Bose, S., Walts, A.E., 2012. Thyroid fine needle aspirate: a post-Bethesda update. Adv. Anat. Pathol. 19, 160–9. doi:10.1097/PAP.0b013e3182534610

Bowler, P.J., 2003. Evolution : the history of an idea. University of California Press.

Braunstein, G.D. (Ed.), 2012. Thyroid Cancer, Endocrine Updates. Springer US, Boston, MA. doi:10.1007/978-1-4614-0875-8

Braunwald, E., 2009. Biomarkers in Heart Failure. http://dx.doi.org/10.1056/NEJMra0800239.

Brecelj, E., Frkovic Grazio, S., Auersperg, M., Bracko, M., 2005. Prognostic value of E-cadherin expression in thyroid follicular carcinoma. Eur J Surg Oncol 31, 544–548. doi:10.1016/j.ejso.2005.02.003

Brehar, A.C., Brehar, F.M., Bulgar, A.C., Dumitrache, C., 2013. Genetic and epigenetic alterations in differentiated thyroid carcinoma. J. Med. Life 6, 403–408.

Brenet, F., Moh, M., Funk, P., Feierstein, E., Viale, A.J., Socci, N.D., Scandura, J.M., 2011. DNA methylation of the first exon is tightly linked to transcriptional silencing. PLoS One 6. doi:10.1371/journal.pone.0014524

Brennan, K., Holsinger, C., Dosiou, C., Sunwoo, J.B., Akatsu, H., Haile, R., Gevaert, O., 2016. Development of prognostic signatures for intermediate-risk papillary thyroid cancer. BMC Cancer 16, 736. doi:10.1186/s12885-016-2771-6

Brinkman, A.B., Simmer, F., Ma, K., Kaan, A., Zhu, J., Stunnenberg, H.G., 2010. Whole-genome DNA methylation profiling using MethylCap-seq. Methods 52, 232–236. doi:10.1016/j.ymeth.2010.06.012

Brito, J.P., Davies, L., 2014. Is there really an increased incidence of thyroid cancer? Curr. Opin. Endocrinol. Diabetes. Obes. 21, 405–408. doi:10.1097/MED.0000000000000094

Brock, M. V, Hooker, C.M., Ota-Machida, E., Han, Y., Guo, M., Ames, S., Glöckner, S., Piantadosi, S., Gabrielson, E., Pridham, G., Pelosky, K., Belinsky, S. a, Yang, S.C., Baylin, S.B., Herman, J.G., 2008. DNA methylation markers and early recurrence in stage I lung cancer. N. Engl. J. Med. 358, 1118–28. doi:10.1056/NEJMoa0706550

Brown, T.C., Juhlin, C.C., Healy, J.M., Prasad, M.L., Korah, R., Carling, T., 2014. Frequent silencing of RASSF1A via promoter methylation in follicular thyroid hyperplasia: a potential early epigenetic susceptibility event in thyroid carcinogenesis. JAMA Surg. 149, 1146–52. doi:10.1001/jamasurg.2014.1694

Brueckner, B., Stresemann, C., Kuner, R., Mund, C., Musch, T., Meister, M., S??ltmann, H., Lyko, F., 2007. The human let-7a-3 locus contains an epigenetically regulated microRNA gene with oncogenic function. Cancer Res. 67, 1419–1423. doi:10.1158/0008-5472.CAN-06-4074

Bryant, J.W., Shariat-Madar, Z., 2009. Human plasma kallikrein-kinin system: physiological and biochemical parameters. Cardiovasc. Hematol. Agents Med. Chem. 7, 234–250. doi:10.2174/187152509789105444

Buj, R., Mallona, I., Diez-Villanueva, A., Barrera, V., Mauricio, D., Puig-Domingo, M., Reverter, J.L., Matias-Guiu, X., Azuara, D., Ramirez, J.L., Alonso, S., Rosell, R., Capella, G., Perucho, M., Robledo, M., Peinado, M.A., Jorda, M., 2016a. Quantification of Unmethylated Alu (QUAlu): a tool to assess global hypomethylation in routine clinical samples. Oncotarget 7, 10536–10546. doi:10.18632/oncotarget.7233

Buj, R., Peinado, M.A., Jorda, M., 2016b. QUAlu, un nuevo método para detectar cambios epigenéticos globales en muestras clínicas. Genética Médica News.

Burke, H.B., 2016. Predicting Clinical Outcomes Using Molecular Biomarkers. Biomark. Cancer 8, 89–99. doi:10.4137/BIC.S33380

Burman, K.D., Wartofsky, L., 2016. Thyroid Nodules. N. Engl. J. Med. 374, 1294–5. doi:10.1056/NEJMc1600493

Cancer Genome Atlas Research Network, N., Akbani, R., Aksoy, B.A., Ally, A., Arachchi, H., Asa, S.L., Auman, J.T., Balasundaram, M., Balu, S., Baylin, S.B., Behera, M., Bernard, B., Beroukhim, R., Bishop, J.A., Black, A.D., Bodenheimer, T., Boice, L., Bootwalla, M.S., Bowen, J., Bowlby, R., Bristow, C.A., Brookens, R., Brooks, D., Bryant, R., Buda, E., Butterfield, Y.S.N., Carling, T., Carlsen, R., Carter, S.L., Carty, S.E., Chan, T.A., Chen, A.Y., Cherniack, A.D., Cheung, D., Chin, L., Cho, J., Chu, A., Chuah, E., Cibulskis, K., Ciriello, G., Clarke, A., Clayman, G.L., Cope, L., Copland, J.A., Covington, K., Danilova, L., Davidsen, T., Demchok, J.A., DiCara, D., Dhalla, N., Dhir, R., Dookran, S.S., Dresdner, G., Eldridge, J., Eley, G., El-Naggar, A.K., Eng, S., Fagin, J.A., Fennell, T., Ferris, R.L., Fisher, S., Frazer, S., Frick, J., Gabriel, S.B., Ganly, I., Gao, J., Garraway, L.A., Gastier-Foster, J.M., Getz, G., Gehlenborg, N., Ghossein, R., Gibbs, R.A., Giordano, T.J., Gomez-Hernandez, K., Grimsby, J., Gross, B., Guin, R., Hadjipanayis, A., Harper, H.A., Hayes, D.N., Heiman, D.I., Herman, J.G., Hoadley, K.A., Hofree, M., Holt, R.A., Hoyle, A.P., Huang, F.W., Huang, M., Hutter, C.M., Ideker, T., Iype, L., Jacobsen, A., Jefferys, S.R., Jones, C.D., Jones, S.J.M., Kasaian, K., Kebebew, E., Khuri, F.R., Kim, J., Kramer, R., Kreisberg, R., Kucherlapati, R., Kwiatkowski, D.J., Ladanyi, M., Lai, P.H., Laird, P.W., Lander, E., Lawrence, M.S., Lee, D., Lee, E., Lee, S., Lee, W., Leraas, K.M., Lichtenberg, T.M., Lichtenstein, L., Lin, P., Ling, S., Liu, J., Liu, W., Liu, Y., LiVolsi, V.A., Lu, Y., Ma, Y., Mahadeshwar, H.S., Marra, M.A., Mayo, M., McFadden, D.G., Meng, S., Meyerson, M., Mieczkowski, P.A., Miller, M., Mills, G., Moore, R.A., Mose, L.E., Mungall, A.J., Murray, B.A., Nikiforov, Y.E., Noble, M.S., Ojesina, A.I., Owonikoko, T.K., Ozenberger, B.A., Pantazi, A., Parfenov, M., Park, P.J., Parker, J.S., Paull, E.O., Pedamallu, C.S., Perou, C.M., Prins, J.F., Protopopov, A., Ramalingam, S.S., Ramirez, N.C., Ramirez, R., Raphael, B.J., Rathmell, W.K., Ren, X., Reynolds, S.M., Rheinbay, E., Ringel, M.D., Rivera, M., Roach, J., Robertson, A.G., Rosenberg, M.W., Rosenthal, M.,

Sadeghi, S., Saksena, G., Sander, C., Santoso, N., Schein, J.E., Schultz, N., Schumacher, S.E., Seethala, R.R., Seidman, J., Senbabaoglu, Y., Seth, S., Sharpe, S., Shaw, K.R.M., Shen, J.P., Shen, R., Sherman, S., Sheth, M., Shi, Y., Shmulevich, I., Sica, G.L., Simons, J.V., Sinha, R., Sipahimalani, P., Smallridge, R.C., Sofia, H.J., Soloway, M.G., Song, X., Sougnez, C., Stewart, C., Stojanov, P., Stuart, J.M., Sumer, S.O., Sun, Y., Tabak, B., Tam, A., Tan, D., Tang, J., Tarnuzzer, R., Taylor, B.S., Thiessen, N., Thorne, L., Thorsson, V., Tuttle, R.M., Umbricht, C.B., Van Den Berg, D.J., Vandin, F., Veluvolu, U., Verhaak, R.G.W., Vinco, M., Voet, D., Walter, V., Wang, Z., Waring, S., Weinberger, P.M., Weinhold, N., Weinstein, J.N., Weisenberger, D.J., Wheeler, D., Wilkerson, M.D., Wilson, J., Williams, M., Winer, D.A., Wise, L., Wu, J., Xi, L., Xu, A.W., Yang, L., Yang, L., Zack, T.I., Zeiger, M.A., Zeng, D., Zenklusen, J.C., Zhao, N., Zhang, H., Zhang, J., Zhang, J. (Julia), Zhang, W., Zmuda, E., Zou, L., Adeniran, A.J., Zhu, Z., Gandhi, M., Steward, D.L., Fidler, J.P., Giordano, T.J., Biddinger, P.W., Nikiforov, Y.E., Alexander, E.K., Kennedy, G.C., Baloch, Z.W., Cibas, E.S., Chudova, D., Diggans, J., Friedman, L., Kloos, R.T., LiVolsi, V.A., Mandel, S.J., al., et, Cooper, D.S., Doherty, G.M., Haugen, B.R., Kloos, R.T., Lee, S.L., Mandel, S.J., Mazzaferri, E.L., McIver, B., Pacini, F., Schlumberger, M., Cancer, A.T.A. (ATA) G.T. on T.N. and D.T., al., et, Bischoff, L.A., Curry, J., Ahmed, I., Pribitkin, E., Miller, J.L., Network, C.G.A.R., Carter, S.L., Cibulskis, K., Helman, E., McKenna, A., Shen, H., Zack, T., Laird, P.W., Onofrio, R.C., Winckler, W., Weir, B.A., al., et, Chakravarty, D., Santos, E., Ryder, M., Knauf, J.A., Liao, X.H., West, B.L., Bollag, G., Kolesnick, R., Thin, T.H., Rosen, N., al., et, Charles, R.P., Iezza, G., Amendola, E., Dankort, D., McMahon, M., Chen, A.Y., Jemal, A., Ward, E.M., Chou, C.K., Yang, K.D., Chou, F.F., Huang, C.C., Lan, Y.W., Lee, Y.F., Kang, H.Y., Liu, R.T., Chu, J., Sadeghi, S., Raymond, A., Jackman, S.D., Nip, K.M., Mar, R., Mohamadi, H., Butterfield, Y.S., Robertson, A.G., Birol, I., Ciampi, R., Knauf, J.A., Kerler, R., Gandhi, M., Zhu, Z., Nikiforova, M.N., Rabes, H.M., Fagin, J.A., Nikiforov, Y.E., Ciriello, G., Cerami, E., Sander, C., Schultz, N., Cohen, Y., Xing, M., Mambo, E., Guo, Z., Wu, G., Trink, B., Beller, U., Westra, W.H., Ladenson, P.W., Sidransky, D., Leva, G. Di, Garofalo, M., Croce, C.M., Durante, C., Puxeddu, E., Ferretti, E., Morisi, R., Moretti, S., Bruno, R., Barbi, F., Avenia, N., Scipioni, A., Verrienti, A., al., et, Ellis, R.J., Wang, Y., Stevenson, H.S., Boufraqech, M., Patel, D., Nilubol, N., Davis, S., Edelman, D.C., Merino, M.J., He, M., al., et, Forbes, S.A., Bindal, N., Bamford, S., Cole, C., Kok, C.Y., Beare, D., Jia, M., Shepherd, R., Leung, K., Menzies, A., al., et, Franco, A.T., Malaguarnera, R., Refetoff, S., Liao, X.H., Lundsmith, E., Kimura, S., Pritchard, C., Marais, R., Davies, T.F., Weinstein, L.S., al., et, Ghossein, R.A., Katabi, N., Fagin, J.A., Giordano, T.J., Kuick, R., Thomas, D.G., Misek, D.E., Vinco, M., Sanders, D., Zhu, Z., Ciampi, R., Roh, M., Shedden, K., al., et, Grieco, M., Santoro, M., Berlingieri, M.T., Melillo, R.M., Donghi, R., Bongarzone, I., Pierotti, M.A., Porta, G. Della, Fusco, A., Vecchio, G., Groenewoud, M.J., Zwartkruis, F.J., Guerra, A., Sapio, M.R., Marotta, V., Campanile, E., Rossi, S., Forno, I., Fugazzola, L., Budillon, A., Moccia, T., Fenzi, G., Vitale, M., Hay, I.D., Bergstralh, E.J., Goellner, J.R., Ebersold, J.R., Grant, C.S., Hay, I.D., Thompson, G.B., Grant, C.S., Bergstralh, E.J., Dvorak, C.E., Gorman, C.A., Maurer, M.S., McIver, B., Mullan, B.P., Oberg, A.L., al., et, Ho, A.L., Grewal, R.K., Leboeuf, R., Sherman, E.J., Pfister, D.G., Deandreis, D., Pentlow, K.S., Zanzonico, P.B., Haque, S., Gavane, S., al., et, Hofree, M., Shen, J.P., Carter, H., Gross, A., Ideker, T., Hutchinson, K.E., Lipson, D., Stephens, P.J., Otto, G., Lehmann, B.D., Lyle, P.L., Vnencak-Jones, C.L., Ross, J.S., Pietenpol, J.A., Sosman, J.A., al., et, Imam, J.S., Plyler, J.R., Bansal, H., Prajapati, S., Bansal, S., Rebeles, J., Chen, H.I., Chang, Y.F., Panneerdoss, S., Zoghi, B., al., et, Jung, C.K., Little, M.P., Lubin, J.H., Brenner, A.V., Wells, S.A., Sigurdson, A.J., Nikiforov, Y.E., Kelly, L.M., Barila, G., Liu, P., Evdokimova, V.N., Trivedi, S., Panebianco, F., Gandhi, M., Carty, S.E., Hodak, S.P., Luo, J., al., et, Kimura, E.T., Nikiforova, M.N., Zhu, Z., Knauf, J.A., Nikiforov, Y.E., Fagin, J.A., Kjellman, P., Lagercrantz, S., Höög, A., Wallin, G., Larsson, C., Zedenius, J., Kleiblova, P., Shaltiel, I.A., Benada, J., Ševčík, J., Pecháčková, S., Pohlreich, P., Voest, E.E., Dundr, P., Bartek, J., Kleibl, Z., al., et, Kostic, A.D., Ojesina, A.I., Pedamallu, C.S., Jung, J., Verhaak, R.G., Getz, G., Meyerson, M., Kroll, T.G., Sarraf, P., Pecciarini, L., Chen, C.J., Mueller, E., Spiegelman, B.M., Fletcher, J.A., Lawrence, M.S., Stojanov, P., Polak, P., Kryukov, G.V., Cibulskis, K., Sivachenko, A., Carter, S.L., Stewart, C., Mermel, C.H., Roberts, S.A., al., et, Lawrence, M.S., Stojanov, P., Mermel, C.H., Robinson, J.T., Garraway, L.A., Golub, T.R., Meyerson, M., Gabriel, S.B., Lander, E.S., Getz, G., Lee, N.V., Lira, M.E., Pavlicek, A., Ye, J., Buckman, D., Bagrodia, S., Srinivasa, S.P., Zhao, Y., Aparicio, S., Rejto, P.A., al., et, Lemoine, N.R., Mayall, E.S., Wyllie, F.S., Farr, C.J., Hughes, D., Padua, R.A., Thurston, V., Williams, E.D., Wynford-Thomas, D., Mardente, S., Mari, E., Consorti, F., Gioia, C. Di, Negri, R., Etna, M., Zicari, A., Antonaci, A., Martin, M., Maßhöfer, L., Temming, P., Rahmann, S., Metz, C., Bornfeld, N., Nes, J. van de, Klein-Hitpass, L., Hinnebusch, A.G., Horsthemke, B., al., et, Melo, M., Rocha, A.G. da, Vinagre, J., Batista, R., Peixoto, J., Tavares, C., Celestino, R., Almeida, A., Salgado, C., Eloy, C., al., et, Mermel, C.H., Schumacher, S.E., Hill, B., Meyerson, M.L., Beroukhim, R., Getz, G., Minamiya, Y., Saito, H., Ito, M., Imai, K., Konno, H., Takahashi, N., Motoyama, S., Ogawa, J., Mitsutake, N., Miyagishi, M., Mitsutake, S., Akeno, N., Mesa, C., Knauf, J.A., Zhang, L., Taira, K., Fagin, J.A., Nikiforov, Y.E., Ohori, N.P., Hodak, S.P., Carty, S.E., LeBeau, S.O., Ferris, R.L., Yip, L., Seethala, R.R., Tublin, M.E., Stang, M.T., al., et, Nikiforov, Y.E., Yip, L., Nikiforova, M.N., Nucera, C., Lawler, J., Parangi, S., Oliva-Trastoy, M., Berthonaud, V., Chevalier, A., Ducrot, C., Marsolier-Kergoat, M.C., Mann, C., Leteurtre, F., Park, J.Y., Kim, W.Y., Hwang, T.S., Lee, S.S., Kim, H., Han, H.S., Lim, S.D., Kim, W.S., Yoo, Y.B., Park, K.S., Paull, E.O., Carlin, D.E., Niepel, M., Sorger, P.K., Haussler, D., Stuart, J.M., Pierotti, M.A., Bongarzone, I., Borrello, M.G., Mariani, C., Miranda, C., Sozzi, G., Greco, A., Poulikakos, P.I., Zhang, C., Bollag, G., Shokat, K.M., Rosen, N., Pratilas, C.A., Taylor, B.S., Ye, Q., Viale, A., Sander, C., Solit, D.B., Rosen, N., Qiu, Y.H., Wei, Y.P., Shen, N.J., Wang, Z.C., Kan, T., Yu, W.L., Yi, B., Zhang, Y.J., Ricarte-Filho, J.C., Li, S., Garcia-Rendueles, M.E., Montero-Conde, C., Voza, F., Knauf, J.A., Heguy, A., Viale, A., Bogdanova, T., Thomas, G.A., al., et, Roberts, S.A., Lawrence, M.S., Klimczak, L.J., Grimm, S.A., Fargo, D., Stojanov, P., Kiezun, A., Kryukov, G.V., Carter, S.L., Saksena, G., al., et, Sabra, M.M., Dominguez, J.M., Grewal, R.K., Larson, S.M., Ghossein, R.A., Tuttle, R.M., Fagin, J.A., Soares, P., Trovisco, V., Rocha, A.S., Lima, J., Castro, P., Preto, A., Máximo, V., Botelho, T., Seruca, R., Sobrinho-Simões, M., Streit, M., Lex, A., Gratzl, S., Partl, C., Schmalstieg, D., Pfister, H., Park, P.J., Gehlenborg, N., Suárez, H.G., Villard, J.A. Du, Caillou, B., Schlumberger, M., Tubiana, M., Parmentier, C., Monier, R., Woiwode, A., Johnson, S.A., Zhong, S., Zhang, C., Roeder, R.G., Teichmann, M., Johnson, D.L., Wreesmann, V.B., Ghossein, R.A., Hezel, M., Banerjee, D., Shaha, A.R., Tuttle, R.M., Shah, J.P., Rao, P.H., Singh, B., Wreesmann, V.B., Sieczka, E.M., Socci, N.D., Hezel, M., Belbin, T.J., Childs, G., Patel, S.G., Patel, K.N., Tallini, G., Prystowsky, M., al., et, Xing, M., Xing, M., Alzahrani, A.S., Carson, K.A., Viola, D., Elisei, R.,

Bendlova, B., Yip, L., Mian, C., Vianello, F., Tuttle, R.M., al., et, Xing, M., Liu, R., Liu, X., Murugan, A.K., Zhu, G., Zeiger, M.A., Pai, S., Bishop, J., Yip, L., Wharry, L.I., Armstrong, M.J., Silbermann, A., McCoy, K.L., Stang, M.T., Ohori, N.P., LeBeau, S.O., Coyne, C., Nikiforova, M.N., al., et, Zhu, S., Wu, H., Wu, F., Nie, D., Sheng, S., Mo, Y.Y., Altschul, S.F., Madden, T.L., Schäffer, A.A., Zhang, J., Zhang, Z., Miller, W., Lipman, D.J., Ashburner, M., Ball, C.A., Blake, J.A., Botstein, D., Butler, H., Cherry, J.M., Davis, A.P., Dolinski, K., Dwight, S.S., Eppig, J.T., Consortium, T.G.O., al., et, Benjamini, Y., Hochbeg, Y., Berger, M.F., Hodis, E., Heffernan, T.P., Deribe, Y.L., Lawrence, M.S., Protopopov, A., Ivanova, E., Watson, I.R., Nickerson, E., Ghosh, P., al., et, Bibikova, M., Barnes, B., Tsan, C., Ho, V., Klotzle, B., Le, J.M., Delano, D., Zhang, L., Schroth, G.P., Gunderson, K.L., al., et, Byers, L.A., Diao, L., Wang, J., Saintigny, P., Girard, L., Peyton, M., Shen, L., Fan, Y., Giri, U., Tumula, P.K., al., et, Atlas, N.C.G., Network, C.G.A., Network, C.G.A.R., Network, C.G.A.R., Chen, K., Wallis, J.W., McLellan, M.D., Larson, D.E., Kalicki, J.M., Pohl, C.S., McGrath, S.D., Wendl, M.C., Zhang, Q., Locke, D.P., al., et, Chiang, D.Y., Getz, G., Jaffe, D.B., O'Kelly, M.J., Zhao, X., Carter, S.L., Russ, C., Nusbaum, C., Meyerson, M., Lander, E.S., Cibulskis, K., Lawrence, M.S., Carter, S.L., Sivachenko, A., Jaffe, D., Sougnez, C., Gabriel, S., Meyerson, M., Lander, E.S., Getz, G., Cibulskis, K., McKenna, A., Fennell, T., Banks, E., DePristo, M., Getz, G., Cingolani, P., Platts, A., Wang, L., Coon, M., Nguyen, T., Wang, L., Land, S.J., Lu, X., Ruden, D.M., Costello, M., Pugh, T.J., Fennell, T.J., Stewart, C., Lichtenstein, L., Meldrim, J.C., Fostel, J.L., Friedrich, D.C., Perrin, D., Dionne, D., al., et, Dabney, A.R., Das, J., Yu, H., Hoon, M.J. de, Imoto, S., Nolan, J., Miyano, S., Drier, Y., Lawrence, M.S., Carter, S.L., Stewart, C., Gabriel, S.B., Lander, E.S., Meyerson, M., Beroukhim, R., Getz, G., Dulak, A.M., Stojanov, P., Peng, S., Lawrence, M.S., Fox, C., Stewart, C., Bandla, S., Imamura, Y., Schumacher, S.E., Shefler, E., al., et, Forbes, S.A., Tang, G., Bindal, N., Bamford, S., Dawson, E., Cole, C., Kok, C.Y., Jia, M., Ewing, R., Menzies, A., al., et, Gaujoux, R., Seoighe, C., Getz, G., Höfling, H., Mesirov, J.P., Golub, T.R., Meyerson, M., Tibshirani, R., Lander, E.S., Gonzalez-Angulo, A.M., Hennessy, B.T., Meric-Bernstam, F., Sahin, A., Liu, W., Ju, Z., Carey, M.S., Myhre, S., Speers, C., Deng, L., al., et, Helwak, A., Kudla, G., Dudnakova, T., Tollervey, D., Hennessy, B.T., Lu, Y., Gonzalez-Angulo, A.M., Carey, M.S., Myhre, S., Ju, Z., Davies, M.A., Liu, W., Coombes, K., Meric-Bernstam, F., al., et, Hennessy, B.T., Lu, Y., Poradosu, E., Yu, Q., Yu, S., Hall, H., Carey, M.S., Ravoori, M., Gonzalez-Angulo, A.M., Birch, R., al., et, Hollants, S., Redeker, E.J., Matthijs, G., Hsu, S.D., Tseng, Y.T., Shrestha, S., Lin, Y.L., Khaleel, A., Chou, C.H., Chu, C.F., Huang, H.Y., Lin, C.M., Ho, S.Y., al., et, Hu, J., He, X., Baggerly, K.A., Coombes, K.R., Hennessy, B.T., Mills, G.B., Huang, da W., Sherman, B.T., Zheng, X., Yang, J., Imamichi, T., Stephens, R., Lempicki, R.A., Huang, F.W., Hodis, E., Xu, M.J., Kryukov, G.V., Chin, L., Garraway, L.A., Kanehisa, M., Goto, S., Korn, J.M., Kuruvilla, F.G., McCarroll, S.A., Wysoker, A., Nemesh, J., Cawley, S., Hubbell, E., Veitch, J., Collins, P.J., Darvishi, K., al., et, Landau, D.A., Carter, S.L., Stojanov, P., McKenna, A., Stevenson, K., Lawrence, M.S., Sougnez, C., Stewart, C., Sivachenko, A., Wang, L., al., et, Lee, I., Blom, U.M., Wang, P.I., Shim, J.E., Marcotte, E.M., Lee, W.P., Stromberg, M.P., Ward, A., Stewart, C., Garrison, E.P., Marth, G.T., Lex, A., Streit, M., Schulz, H.-J., Partl, C., Schmalstieg, D., Park, P.J., Gehlenborg, N., Li, B., Dewey, C.N., Li, H., Durbin, R., Li, J., Tibshirani, R., Liang, J., Shao, S.H., Xu, Z.X., Hennessy, B., Ding, Z., Larrea, M., Kondo, S., Dumont, D.J., Gutterman, J.U., Walker, C.L., al., et, Liu, Y., Hayes, D.N., Nobel, A., Marron, J.S., Lohr, J.G., Stojanov, P., Lawrence, M.S., Auclair, D., Chapuy, B., Sougnez, C., Cruz-Gordillo, P., Knoechel, B., Asmann, Y.W., Slager, S.L., al., et, Luc, P.V., Tempst, P., McCarroll, S.A., Kuruvilla, F.G., Korn, J.M., Cawley, S., Nemesh, J., Wysoker, A., Shapero, M.H., Bakker, P.I. de, Maller, J.B., Kirby, A., al., et, Mullokandov, G., Baccarini, A., Ruzo, A., Jayaprakash, A.D., Tung, N., Israelow, B., Evans, M.J., Sachidanandam, R., Brown, B.D., Neeley, E.S., Kornblau, S.M., Coombes, K.R., Baggerly, K.A., Olshen, A.B., Venkatraman, E.S., Lucito, R., Wigler, M., R-Core-Team, Robinson, M.D., McCarthy, D.J., Smyth, G.K., Saldanha, A.J., Saunders, C.T., Wong, W.S., Swamy, S., Becq, J., Murray, L.J., Cheetham, R.K., Smigielski, E.M., Sirotkin, K., Ward, M., Sherry, S.T., Stransky, N., Egloff, A.M., Tward, A.D., Kostic, A.D., Cibulskis, K., Sivachenko, A., Kryukov, G.V., Lawrence, M.S., Sougnez, C., McKenna, A., al., et, Subramanian, A., Tamayo, P., Mootha, V.K., Mukherjee, S., Ebert, B.L., Gillette, M.A., Paulovich, A., Pomeroy, S.L., Golub, T.R., Lander, E.S., Mesirov, J.P., Tay, Y., Rinn, J., Pandolfi, P.P., Thorvaldsdóttir, H., Robinson, J.T., Mesirov, J.P., Tibes, R., Qiu, Y., Lu, Y., Hennessy, B., Andreeff, M., Mills, G.B., Kornblau, S.M., Torres-García, W., Zheng, S., Sivachenko, A., Vegesna, R., Wang, Q., Yao, R., Berger, M.F., Weinstein, J.N., Getz, G., Verhaak, R.G., Tusher, V.G., Tibshirani, R., Chu, G., Vandin, F., Clay, P., Upfal, E., Raphael, B.J., Vaske, C.J., Benz, S.C., Sanborn, J.Z., Earl, D., Szeto, C., Zhu, J., Haussler, D., Stuart, J.M., Wang, K., Singh, D., Zeng, Z., Coleman, S.J., Huang, Y., Savich, G.L., He, X., Mieczkowski, P., Grimm, S.A., Perou, C.M., al., et, Wilkerson, M.D., Hayes, D.N., Yang, L., Luquette, L.J., Gehlenborg, N., Xi, R., Haseley, P.S., Hsieh, C.H., Zhang, C., Ren, X., Protopopov, A., Chin, L., al., et, Zack, T.I., Schumacher, S.E., Carter, S.L., Cherniack, A.D., Saksena, G., Tabak, B., Lawrence, M.S., Zhang, C.Z., Wala, J., Mermel, C.H., al., et, 2014. Integrated genomic characterization of papillary thyroid carcinoma. Cell 159, 676–90. doi:10.1016/j.cell.2014.09.050

Cannon, J., 2011. The Significance of Hurthle Cells in Thyroid Disease. Oncologist. doi:10.1634/theoncologist.2010-0253

Cardoso, L.F., Maciel, L.M.Z., Paula, F.J.A. de, 2014. The multiple effects of thyroid disorders on bone and mineral metabolism. Arq. Bras. Endocrinol. Metabol. 58, 452–63.

Caró, R.W., Yacoub, A., Li, M., Zhu, X., Mitchell, C., Hong, Y., Hawkins, W., Sasazuki, T., Shirasawa, S., Kozikowski, A.P., Dennis, P.A., Hagan, M.P., Grant, S., Dent, P., 2005. Activated forms of H-RAS and K-RAS differentially regulate membrane association of PI3K, PDK-1, and AKT and the effect of therapeutic kinase inhibitors on cell survival. Mol. Cancer Ther. 4, 254–270.

Castellano, E., Downward, J., 2011. RAS Interaction with PI3K: More Than Just Another Effector Pathway. Genes Cancer 2, 261–74. doi:10.1177/1947601911408079

Castro, M.R., Gharib, H., 2015. Thyroid nodules and cancer. http://dx.doi.org/10.3810/pgm.2000.01.808.

Catalano, M.G., Fortunati, N., Pugliese, M., Marano, F., Ortoleva, L., Poli, R., Asioli, S., Bandino, A., Palestini, N., Grange, C., Bussolati, B., Boccuzzi, G., 2012. Histone deacetylase inhibition modulates E-cadherin expression and suppresses migration and invasion of anaplastic thyroid cancer cells. J. Clin. Endocrinol.

Metab. 97, E1150–9. doi:10.1210/jc.2011-2970

Chalitchagorn, K., Shuangshoti, S., Hourpai, N., Kongruttanachok, N., Tangkijvanich, P., Thong-ngam, D., Voravud, N., Sriuranpong, V., Mutirangura, A., 2004. Distinctive pattern of LINE-1 methylation level in normal tissues and the association with carcinogenesis. Oncogene 23, 8841–8846. doi:10.1038/sj.onc.1208137

Chen, C., Ara, T., Gautheret, D., 2009. Using Alu elements as polyadenylation sites: A case of retroposon exaptation. Mol. Biol. Evol. 26, 327–334. doi:10.1093/molbev/msn249

Chen, Y.-T., Kitabayashi, N., Zhou, X.K., Fahey, T.J., Scognamiglio, T., 2008. MicroRNA analysis as a potential diagnostic tool for papillary thyroid carcinoma. Mod. Pathol. 21, 1139–1146. doi:10.1038/modpathol.2008.105

Cheong, J., Yamada, Y., Yamashita, R., Irie, T., Kanai, A., Wakaguri, H., Nakai, K., Ito, T., Saito, I., Sugano, S., Suzuki, Y., 2006. Diverse DNA methylation statuses at alternative promoters of human genes in various tissues. DNA Res. 13, 155–167. doi:10.1093/dnares/dsl008

Choi, J.-Y., James, S.R., Link, P. a, McCann, S.E., Hong, C.-C., Davis, W., Nesline, M.K., Ambrosone, C.B., Karpf, A.R., 2009. Association between global DNA hypomethylation in leukocytes and risk of breast cancer. Carcinogenesis 30, 1889–1897. doi:10.1093/carcin/bgp143

Choi, S., Worswick, S., Byun, H.-M., Shear, T., Soussa, J.C., Wolff, E.M., Douer, D., Garcia-Manero, G., Liang, G., Yang, A.S., 2009. Changes in DNA methylation of tandem DNA repeats are different from interspersed repeats in cancer. Int. J. cancer 125, 723–9. doi:10.1002/ijc.24384

Chou, C.-K., Chen, R.-F., Chou, F.-F., Chang, H.-W., Chen, Y.-J., Lee, Y.-F., Yang, K.D., Cheng, J.-T., Huang, C.-C., Liu, R.-T., 2010. miR-146b is highly expressed in adult papillary thyroid carcinomas with high risk features including extrathyroidal invasion and the BRAF(V600E) mutation. Thyroid 20, 489–494. doi:10.1089/thy.2009.0027

Chudova, D., Wilde, J.I., Wang, E.T., Wang, H., Rabbee, N., Egidio, C.M., Reynolds, J., Tom, E., Pagan, M., Rigl, C.T., Friedman, L., Wang, C.C., Lanman, R.B., Zeiger, M., Kebebew, E., Rosai, J., Fellegara, G., LiVolsi, V.A., Kennedy, G.C., 2010. Molecular classification of thyroid nodules using high-dimensionality genomic data. J. Clin. Endocrinol. Metab. 95, 5296–5304. doi:10.1210/jc.2010-1087

Chung, H.R., 2014. Iodine and thyroid function. Ann. Pediatr. Endocrinol. Metab. 19, 8–12. doi:10.6065/apem.2014.19.1.8

Ciampi, R., Giordano, T.J., Wikenheiser-Brokamp, K., Koenig, R.J., Nikiforov, Y.E., 2007. HOOK3-RET: a novel type of RET/PTC rearrangement in papillary thyroid carcinoma. Endocr. Relat. Cancer 14, 445–452. doi:10.1677/ERC-07-0039

Ciampi, R., Knauf, J.A., Kerler, R., Gandhi, M., Zhu, Z., Nikiforova, M.N., Rabes, H.M., Fagin, J.A., Nikiforov, Y.E., 2005. Oncogenic AKAP9-BRAF fusion is a novel mechanism of MAPK pathway activation in thyroid cancer. J. Clin. Invest. 115, 94–101. doi:10.1172/JCI200523237

Cibas, E.S., Ali, S.Z., 2009. The Bethesda System for Reporting Thyroid Cytopathology. Am J Clin Pathol 132, 658–665. doi:10.1309/AJCPPHLWMI3JV4LA

Collini, P., Sampietro, G., Pilotti, S., 2004. Extensive vascular invasion is a marker of risk of relapse in encapsulated non-Hurthle cell follicular carcinoma of the thyroid gland: a clinicopathological study of 18 consecutive cases from a single institution with a 11-year median follow-up. Histopathology 44, 35–39. doi:10.1111/j.1365-2559.2004.01729.x

Compere, S.J., Palmiter, R.D., 1981. DNA methylation controls the inducibility of the mouse metallothionein-I gene in lymphoid cells. Cell 25, 233–240. doi:10.1016/0092-8674(81)90248-8

Conzo, G., Tartaglia, E., Avenia, N., Calò, P.G., de Bellis, A., Esposito, K., Gambardella, C., Iorio, S., Pasquali, D., Santini, L., Sinisi, M.A., Sinisi, A.A., Testini, M., Polistena, A., Bellastella, G., 2016. Role of prophylactic central compartment lymph node dissection in clinically N0 differentiated thyroid cancer patients: analysis of risk factors and review of modern trends. World J. Surg. Oncol. 14, 149. doi:10.1186/s12957-016-0879-4

Cooper, D.N., 1983. Eukaryotic DNA methylation. Hum. Genet. 64, 315–33.

Corvi, R., Berger, N., Balczon, R., Romeo, G., n.d. RET/PCM-1: a novel fusion gene in papillary thyroid carcinoma.

Cox, A.D., Fesik, S.W., Kimmelman, A.C., Luo, J., Der, C.J., 2014. Drugging the undruggable RAS: Mission Possible? Nat. Rev. Drug Discov. 13, 828–51. doi:10.1038/nrd4389

CRICK, F.H., 1958. On protein synthesis. Symp. Soc. Exp. Biol. 12, 138–63.

Cui, H., Onyango, P., Brandenburg, S., Wu, Y., Hsieh, C.-L., Feinberg, A.P., 2002. Loss of imprinting in colorectal cancer linked to hypomethylation of H19 and IGF2. Cancer Res. 62, 6442–6.

D'Avanzo, A., Treseler, P., Ituarte, P.H.G., Wong, M., Streja, L., Greenspan, F.S., Siperstein, A.E., Duh, Q.Y., Clark, O.H., 2004. Follicular Thyroid Carcinoma: Histology and Prognosis. Cancer 100, 1123–1129. doi:10.1002/cncr.20081

Dai, G., Levy, O., Carrasco, N., 1996. Cloning and characterization of the thyroid iodide transporter. Nature 379, 458–60. doi:10.1038/379458a0

Darwin, C., 1859. On the Origin of the Species, Darwin. doi:10.1016/S0262-4079(09)60380-8

De Angelis, G., Rittenhouse, H.G., Mikolajczyk, S.D., Blair Shamel, L., Semjonow, A., 2007. Twenty Years of PSA: From Prostate Antigen to Tumor Marker. Rev. Urol. 9, 113–23.

de Capoa, A., Grappelli, C., Volpino, P., Bononi, M., Musolino, A., Ciardi, A., Cavallaro, A., Cangemi, V., 2004. Nuclear methylation levels in normal and cancerous

thyroid cells. Anticancer Res 24, 1495–1500.

De Carvalho, D., Sharma, S., You, J.S., Su, S.F., Taberlay, P.C., Kelly, T.K., Yang, X., Liang, G., Jones, P.A., 2012. DNA Methylation Screening Identifies Driver Epigenetic Events of Cancer Cell Survival. Cancer Cell 21, 655–667. doi:10.1016/j.ccr.2012.03.045

de Escobar, G.M., Obregón, M.J., del Rey, F.E., 2007. Iodine deficiency and brain development in the first half of pregnancy. Public Health Nutr. 10, 1554–70. doi:10.1017/S1368980007360928

De Matos, P.S., Ferreira, A.P., De Oliveira Facuri, F., Assump????o, L.V.M., Metze, K., Ward, L.S., 2005. Usefulness of HBME-1, cytokeratin 19 and galectin-3 immunostaining in the diagnosis of thyroid malignancy. Histopathology 47, 391–401. doi:10.1111/j.1365-2559.2005.02221.x

Dean, W., Lucifero, D., Santos, F., 2005. DNA methylation in mammalian development and disease. Birth Defects Res. C. Embryo Today 75, 98–111. doi:10.1002/bdrc.20037

Deaton, A.M., Bird, A., 2011. CpG islands and the regulation of transcription. Genes Dev. 25, 1010–1022. doi:10.1101/gad.2037511

Deininger, P., 2011. Alu elements: know the SINEs. Genome Biol 12, 236. doi:10.1186/gb-2011-12-12-236

Delgado-Cruzata, L., Wu, H.C., Liao, Y., Santella, R.M., Terry, M.B., 2014. Differences in DNA methylation by extent of breast cancer family history in unaffected women. Epigenetics 9, 243–248. doi:10.4161/epi.26880

DePinho, R. a, 2000. The age of cancer. Nature 408, 248–54. doi:10.1038/35041694

Desjardin, C., Charles, C., Benoist-Lasselin, C., Riviere, J., Gilles, M., Chassande, O., Morgenthaler, C., Laloé, D., Lecardonnel, J., Flamant, F., Legeai-Mallet, L., Schibler, L., 2014. Chondrocytes play a major role in the stimulation of bone growth by thyroid hormone. Endocrinology 155, 3123–3135. doi:10.1210/en.2014-1109

Dhar, S., Bhargava, R., Yunes, M., Li, B., Goyal, J., Naber, S.P., Wazer, D.E., Band, V., 2001. Analysis of normal epithelial cell specific-1 (NES1)/kallikrein 10 mRNA expression by in situ hybridization, a novel marker for breast cancer. Clin. Cancer Res. 7, 3393–8.

Dhillon, A.S., Hagan, S., Rath, O., Kolch, W., 2007. MAP kinase signalling pathways in cancer. Oncogene 26, 3279–90. doi:10.1038/sj.onc.1210421

Diamandis, E.P., 2010. Cancer biomarkers: can we turn recent failures into success? J. Natl. Cancer Inst. 102, 1462–7. doi:10.1093/jnci/djq306

Drucker, E., Krapfenbauer, K., 2013. Pitfalls and limitations in translation from biomarker discovery to clinical utility in predictive and personalised medicine. EPMA J. 4, 7. doi:10.1186/1878-5085-4-7

Dunderovic, D., Lipkovski, J.M., Boricic, I., Soldatovic, I., Bozic, V., Cvejic, D., Tatic, S., 2015. Defining the value of CD56, CK19, Galectin 3 and HBME-1 in diagnosis of follicular cell derived lesions of thyroid with systematic review of literature. Diagn Pathol 10, 196. doi:10.1186/s13000-015-0428-4

Duntas, L., Grab-Duntas, B.M., 2006. Risk and prognostic factors for differentiated thyroid cancer. Hell. J. Nucl. Med. 9, 156–62.

Duret, L., Galtier, N., 2000. The Covariation Between TpA Deficiency, CpG Deficiency, and GC Content of Human Isochores Is Due to a Mathematical Artifact. Mol. Biol. Evol 17, 1620–1625.

Eden, A., Gaudet, F., Waghmare, A., Jaenisch, R., 2003. Chromosomal Instability and Tumors Promoted by DNA Hypomethylation. Science (80-.). 300, 2003. doi:10.1126/science.1083557

Edwards, J.R., O'Donnell, A.H., Rollins, R.A., Peckham, H.E., Lee, C., Milekic, M.H., Chanrion, B., Fu, Y., Su, T., Hibshoosh, H., Gingrich, J.A., Haghighi, F., Nutter, R., Bestor, T.H., 2010. Chromatin and sequence features that define the fine and gross structure of genomic methylation patterns. Genome Res. 20, 972–80. doi:10.1101/gr.101535.109

Ehrlich, M., 2009. DNA hypomethylation in cancer cells. Epigenomics 1, 239–59. doi:10.2217/epi.09.33

Ehrlich, M., 2002. DNA methylation in cancer: too much, but also too little. Oncogene 21, 5400–5413. doi:10.1038/sj.onc.1205651

Einhorn, J., Franzbn, S., Radiumhemmet Director, F., Hultberg, S., Sjukhuset, K., n.d. THIN-NEEDLE BIOPSY IN THE DIAGNOSIS OF THYROID DISEASE. Acta radiol. 58.

Ellis, R.J., Wang, Y., Stevenson, H., Boufraqech, M., Patel, D., Nilubol, N., Davis, S., Edelman, D.C., Merino, M.J., He, M., Zhang, L., Meltzer, P.S., Kebebew, E., 2014. Genome-wide methylation patterns in papillary thyroid cancer are distinct based on histological subtype and tumor genotype. J. Clin. Endocrinol. Metab. 99. doi:10.1210/jc.2013-2749

Enewold, L., Zhu, K., Ron, E., Marrogi, A.J., Stojadinovic, A., Peoples, G.E., Devesa, S.S., 2009. Rising thyroid cancer incidence in the United States by demographic and tumor characteristics, 1980-2005. Cancer Epidemiol. Biomarkers Prev. 18, 784–91. doi:10.1158/1055-9965.EPI-08-0960

Esteller, M., 2008. Epigenetics in cancer. N. Engl. J. Med. 358, 1148–59. doi:10.1056/NEJMra072067

Faam, B., Ghaffari, M.A., Ghadiri, A., Azizi, F., 2015. Epigenetic modifications in human thyroid cancer. Biomed. reports 3, 3–8. doi:10.3892/br.2014.375

Fagman, H., Nilsson, M., 2010. Morphogenesis of the thyroid gland. Mol. Cell. Endocrinol. doi:10.1016/j.mce.2009.12.008

Falkenberg, K.J., Johnstone, R.W., 2014. Histone deacetylases and their inhibitors in cancer, neurological diseases and immune disorders. Nat. Rev. Drug Discov. 13, 673–91. doi:10.1038/nrd4360

Fearon, E.R., Vogelstein, B., 1990. A genetic model for colorectal tumorigenesis. Cell. doi:10.1016/0092-8674(90)90186-I

Feinberg, A.P., Tycko, B., 2004. The history of cancer epigenetics. Nat. Rev. Cancer 4, 143–53. doi:10.1038/nrc1279

Feinberg, A.P., Vogelstein, B., 1983. Hypomethylation distinguishes genes of some human cancers from their normal counterparts. Nature 301, 89–92.

Feldt-Rasmussen, U., 2001. Iodine and cancer. Thyroid 11, 483–486. doi:10.1089/105072501300176435

Feng, B., Xu, W.-B., Zheng, M.-H., Ma, J.-J., Cai, Q., Zhang, Y., Ji, J., Lu, A.-G., Qu, Y., Li, J.-W., Wang, M.-L., Hu, W.-G., Liu, B.-Y., Zhu, Z.-G., 2006. Clinical significance of human kallikrein 10 gene expression in colorectal cancer and gastric cancer. J. Gastroenterol. Hepatol. 21, 1596–1603. doi:10.1111/j.1440-1746.2006.04228.x

Fernandez, A.F., Assenov, Y., Martin-Subero, J.I., Balint, B., Siebert, R., Taniguchi, H., Yamamoto, H., Hidalgo, M., Tan, A.C., Galm, O., Ferrer, I., Sanchez-Cespedes, M., Villanueva, A., Carmona, J., Sanchez-Mut, J. V., Berdasco, M., Moreno, V., Capella, G., Monk, D., Ballestar, E., Ropero, S., Martinez, R., Sanchez-Carbayo, M., Prosper, F., Agirre, X., Fraga, M.F., Gra??a, O., Perez-Jurado, L., Mora, J., Puig, S., Prat, J., Badimon, L., Puca, A.A., Meltzer, S.J., Lengauer, T., Bridgewater, J., Bock, C., Esteller, M., 2012. A DNA methylation fingerprint of 1628 human samples. Genome Res. 22, 407–419. doi:10.1101/gr.119867.110

Fernández, L.P., López-Márquez, A., Santisteban, P., 2015. Thyroid transcription factors in development, differentiation and disease. Nat. Rev. Endocrinol. 11, 29–42. doi:10.1038/nrendo.2014.186

Ferraro, A., 2016. Altered primary chromatin structures and their implications in cancer development. Cell. Oncol. 1–16. doi:10.1007/s13402-016-0276-6

Figlioli, G., Landi, S., Romei, C., Elisei, R., Gemignani, F., 2013. Medullary thyroid carcinoma (MTC) and RET proto-oncogene: Mutation spectrum in the familial cases and a meta-analysis of studies on the sporadic form. Mutat. Res. - Rev. Mutat. Res. doi:10.1016/j.mrrev.2012.09.002

Filho, J.G., Kowalski, L.P., 2005. Surgical complications after thyroid surgery performed in a cancer hospital. Otolaryngol. - Head Neck Surg. 132, 490–494. doi:10.1016/j.otohns.2004.09.028

Finlayson, A., Barnes, I., Sayeed, S., McIver, B., Beral, V., Ali, R., 2014. Incidence of thyroid cancer in England by ethnic group, 2001-2007. Br J Cancer 110, 1322–1327. doi:10.1038/bjc.2014.4

Fong, P., 2011. Thyroid iodide efflux: a team effort? J. Physiol. 589, 5929–39. doi:10.1113/jphysiol.2011.218594

Fortier, A.H., Nelson, B.J., Grella, D.K., Holaday, J.W., 1999. Antiangiogenic activity of prostate-specific antigen. J. Natl. Cancer Inst. 91, 1635–40. doi:10.1093/jnci/91.19.1635

Fortuny, J.V., Guigard, S., Karenovics, W., Triponez, F., 2015. Surgery of the thyroid: recent developments and perspective. Swiss Med. Wkly. 145, w14144. doi:10.4414/smw.2015.14144

Franklin, R.E., Gosling R G, 1953. Molecular configuration in sodium thymonucleate. Nature 171, 740–1.

Frattini, M., Gallino, G., Signoroni, S., Balestra, D., Battaglia, L., Sozzi, G., Leo, E., Pilotti, S., Pierotti, M.A., 2006. Quantitative Analysis of Plasma DNA in Colorectal Cancer Patients: A Novel Prognostic Tool. Ann. N. Y. Acad. Sci. 1075, 185–190. doi:10.1196/annals.1368.025

Friedman, A. a., Letai, A., Fisher, D.E., Flaherty, K.T., 2015. Precision medicine for cancer with next-generation functional diagnostics. Nat. Rev. Cancer 15, 747–756. doi:10.1038/nrc4015

Frigola, J., Solé, X., Paz, M.F., Moreno, V., Esteller, M., Capellà, G., Peinado, M.A., 2005. Differential DNA hypermethylation and hypomethylation signatures in colorectal cancer. Hum. Mol. Genet. 14, 319–326. doi:10.1093/hmg/ddi028

Fugazzola, L., Pierotti, M.A., Vigano, E., Pacini, F., Vorontsova, T. V, Bongarzone, I., 1996. Molecular and biochemical analysis of RET/PTC4, a novel oncogenic rearrangement between RET and ELE1 genes, in a post-Chernobyl papillary thyroid cancer. Oncogene 13, 1093–7.

Fugazzola, L., Puxeddu, E., Avenia, N., Romei, C., Cirello, V., Cavaliere, A., Faviana, P., Mannavola, D., Moretti, S., Rossi, S., Sculli, M., Bottici, V., Beck-Peccoz, P., Pacini, F., Pinchera, A., Santeusanio, F., Elisei, R., 2006. Correlation between B-RAFV600E mutation and clinico-pathologic parameters in papillary thyroid carcinoma: Data from a multicentric Italian study and review of the literature. Endocr. Relat. Cancer 13, 455–464. doi:10.1677/erc.1.01086

Füllgrabe, J., Kavanagh, E., Joseph, B., 2011. Histone onco-modifications. Oncogene 30, 3391–403. doi:10.1038/onc.2011.121

Furuya, F., Shimura, H., Suzuki, H., Taki, K., Ohta, K., Haraguchi, K., Onaya, T., Endo, T., Kobayashi, T., 2004. Histone Deacetylase Inhibitors Restore Radioiodide Uptake and Retention in Poorly Differentiated and Anaplastic Thyroid Cancer Cells by Expression of the Sodium/Iodide Symporter Thyroperoxidase and Thyroglobulin. Endocrinology 145, 2865–2875. doi:10.1210/en.2003-1258

Galusca, B., Dumollard, J.M., Lassandre, S., Niveleau, A., Prades, J.M., Estour, B., Peoc'h, M., 2005. Global DNA methylation evaluation: Potential complementary marker in differential diagnosis of thyroid neoplasia. Virchows Arch. 447, 18–23. doi:10.1007/s00428-005-1268-5

Gama-Sosa, M.A., Slagel, V.A., Trewyn, R.W., Oxenhandler, R., Kuo, K.C., Gehrke, C.W., Ehrlich, M., 1983. The 5-methylcytosine content of DNA from human tumors. Nucleic Acids Res. 11, 6883–94.

Gara, S.K., Jia, L., Merino, M.J., Agarwal, S.K., Zhang, L., Cam, M., Patel, D., Kebebew, E., 2015. Germline HABP2 Mutation Causing Familial Nonmedullary Thyroid Cancer. N. Engl. J. Med. 373, 448–55. doi:10.1056/NEJMoa1502449

Gartner, L.P., 2007. Textbook of histology.

Gerlinger, M., Rowan, A.J., Horswell, S., Larkin, J.,

Endesfelder, D., Gronroos, E., Martinez, P., Matthews, N., Stewart, A., Tarpey, P., Varela, I., Phillimore, B., Begum, S., McDonald, N.Q., Butler, A., Jones, D., Raine, K., Latimer, C., Santos, C.R., Nohadani, M., Eklund, A.C., Spencer-Dene, B., Clark, G., Pickering, L., Stamp, G., Gore, M., Szallasi, Z., Downward, J., Futreal, P.A., Swanton, C., 2012. Intratumor Heterogeneity and Branched Evolution Revealed by Multiregion Sequencing. N. Engl. J. Med. 366, 883–892. doi:10.1056/NEJMoa1113205

Ghervan, C., 2011. Thyroid and parathyroid ultrasound. Med. Ultrason. 13, 80–84. doi:10.1007/0-387-31056-8_55

Giordano, T.J., Kuick, R., Thomas, D.G., Misek, D.E., Vinco, M., Sanders, D., Zhu, Z., Ciampi, R., Roh, M., Shedden, K., Gauger, P., Doherty, G., Thompson, N.W., Hanash, S., Koenig, R.J., Nikiforov, Y.E., 2005. Molecular classification of papillary thyroid carcinoma: distinct BRAF, RAS, and RET/PTC mutation-specific gene expression profiles discovered by DNA microarray analysis. Oncogene 24, 6646–56. doi:10.1038/sj.onc.1208822

Giuffrida, D., Gharib, H., 2000. Anaplastic thyroid carcinoma: current diagnosis and treatment. Ann. Oncol. 11, 1083–1089. doi:11061600

Goffredo, P., Jillard, C., Thomas, S., Scheri, R.P., Sosa, J.A., Roman, S., 2016. Minimally invasive follicular carcinoma: predictors of vascular invasion and impact on patterns of care. Endocrine 51, 123–30. doi:10.1007/s12020-015-0649-z

Goffredo, P., Sosa, J.A., Roman, S.A., 2013. Differentiated thyroid cancer presenting with distant metastases: A population analysis over two decades. World J. Surg. 37, 1599–1605. doi:10.1007/s00268-013-2006-9

Goldberg, A.D., Allis, C.D., Bernstein, E., 2007. Epigenetics: A Landscape Takes Shape. Cell. doi:10.1016/j.cell.2007.02.006

Gonzalez-Gonzalez, R., Bologna-Molina, R., Carreon-Burciaga, R.G., Gómezpalacio-Gastelum, M., Molina-Frechero, N., Salazar-Rodríguez, S., Gonzalez-Gonzalez, R., Bologna-Molina, R., Carreon-Burciaga, R.G., Gómezpalacio-Gastelum, M., Molina-Frechero, N., Salazar-Rodríguez, S., Gil, n, G&#xf3, mezpalacio-Gastelum, M., Molina-Frechero, N., Salazar-Rodr&#xed, guez, S., 2011. Papillary thyroid carcinoma: differential diagnosis and prognostic values of its different variants: review of the literature. ISRN Oncol. 2011, 915925. doi:10.5402/2011/915925

Goyal, J., Smith, K.M., Cowan, J.M., Wazer, D.E., Lee, S.W., Band, V., 1998. The role for NES1 serine protease as a novel tumor suppressor. Cancer Res. 58, 4782–4786.

Gracia, A., Balañá, C., Kaskens, L., Chiavenna, S., Matias-Guiu, X., Rubio-Rodríguez, D., Rubio-Terrés, C., Iglesias, L., Esteller, M., 2015. Economic Analysis Of Epicup, An Epigenetic Test To Predict The Tissue Of Origin In Cancer Of Unknown Primary Site, From The Spanish Nhs Perspective. Value Heal. 18, A356–A357. doi:10.1016/j.jval.2015.09.672

Greaves, M., Maley, C.C., 2012. Clonal evolution in cancer. Nature 481, 306–13. doi:10.1038/nature10762

Greenberg, V.L., Williams, J.M., Cogswell, J.P., Mendenhall, M., Zimmer, S.G., 2001. Histone Deacetylase Inhibitors Promote Apoptosis and Differential Cell Cycle Arrest in Anaplastic Thyroid Cancer Cells. THYROID 11.

Grieco, M., Santoro, M., Berlingieri, M.T., Melillo, R.M., Donghi, R., Bongarzone, I., Pierotti, M.A., Della Porta, G., Fusco, A., Vecchio, G., Besmer, P., Murphy, J.E., George, P.C., Qui, F., Bergold, P.J., Lederman, L., Snyder, H.W., Brodeur, D., Zuckerman, E.E., Hardy, W.D., Biggin, M.D., Gibson, T.J., Hong, G.F., Bongarzone, I., Pierotti, M.A., Monzini, N., Modellini, P., Manenti, G., Donghi, R., Pilotti, S., Gríeco, M., Santoro, M., Fusco, A., Vecchio, G., Porta, G.D., Donghi, R., Sozzi, G., Pierotti, M.A., Biunno, I., Miozzo, M., Fusco, A., Grieco, M., Santoro, M., Vecchio, G., Spurr, N.K., Porta, G.D., Downward, J., Yarden, Y., Meyes, E., Scrace, G., Totty, N., Stockwell, P., Ullrich, A., Schlessinger, J., Waterfield, M.D., Feinberg, A.P., Vogelstein, B., Fusco, A., Grieco, M., Santoro, M., Berlingieri, M.T., Pilotti, S., Pierotti, M.A., Porta, G.D., Vecchio, G., Graham, F.L., Eb, A.J. van der, Grieco, M., Santoro, M., Berlingieri, M.T., Donghi, R., Pierotti, M.A., Porta, G.D., Fusco, A., Vecchio, G., Heitz, P., Moser, H., Staub, J.J., Huynh, T.V., Young, R.A., Davis, R.W., Ishikawa, F., Takaku, F., Nagao, M., Sugimura, T., Ishizaka, Y., Ochiai, M., Tahira, T., Sugimura, T., Nagao, M., Koda, T., Kozak, M., Lemoine, N.R., Mayall, E.S., Wyllie, F.S., Farr, C.J., Hughes, D., Padua, R.A., Thurston, V., Williams, E.D., Wynford-Thomas, D., Maniatis, T., Fritsch, E.F., Sambrook, J., Martin-Zanca, D., Hughes, S.H., Barbacid, M., Neckameyer, W.S., Wang, L.H., Park, M., Dean, M., Cooper, C.S., Schmidt, M., O'Brien, S.J., Blair, D.G., Woude, G.F. Vande, Parker, M.H., Seis, J.M., Stringer, B.M., Ingemansson, S., Woodhouse, N., Goyns, M.H., Sanger, F., Nicklen, S., Coulson, A.R., Stanton, V.P., Cooper, G.M., Suarez, H.G., Villard, J.A. Du, Caillou, B., Schlumberger, M., Tubiana, M., Parmentier, C., Monier, R., Takahashi, M., Cooper, G.M., Takahashi, M., Ritz, J., Cooper, G.M., Takahashi, M., Inaguma, Y., Hiai, H., Hirose, F., Takahashi, M., Burma, Y., Iwamoto, T., Inaguma, Y., Ikeda, H., Hiai, H., Takahashi, M., Burma, Y., Hiai, H., Terrier, P., Sheng, Z.M., Schlumberger, M., Tubiana, M., Caillou, B., Travagli, J.P., Fragu, P., Parmentier, C., Riou, G., Watson, C.J., Jackson, J.F., 1990. PTC is a novel rearranged form of the ret proto-oncogene and is frequently detected in vivo in human thyroid papillary carcinomas. Cell 60, 557–63. doi:10.1016/0092-8674(90)90659-3

Guerrero-Preston, R., Goldman, L.R., Brebi-Mieville, P., Ili-Gangas, C., LeBron, C., Hernández-Arroyo, M., Witter, F.R., Apelberg, B.J., Roystacher, M., Jaffe, A., Halden, R.U., Sidransky, D., 2010. Global DNA hypomethylation is associated with in utero exposure to cotinine and perfluorinated alkyl compounds. Epigenetics 5, 539–546. doi:10.4161/epi.5.6.12378

Guth, S., Theune, U., Aberle, J., Galach, A., Bamberger, C.M., 2009. Very high prevalence of thyroid nodules detected by high frequency (13 MHz) ultrasound examination. Eur. J. Clin. Invest. 39, 699–706. doi:10.1111/j.1365-2362.2009.02162.x

H.J., K., J.-Y., S., Y.L., O., J.H., K., Y.-I., S., Y.-K., M., S.W., K., 2014. Association of vascular invasion with increased mortality in patients with minimally invasive follicular thyroid carcinoma but not widely invasive follicular thyroid carcinoma. Head Neck.

Haffner, M.C., Mosbruger, T., Esopi, D.M., Fedor, H., Heaphy,

C.M., Walker, D.A., Adejola, N., G??rel, M., Hicks, J., Meeker, A.K., Halushka, M.K., Simons, J.W., Isaacs, W.B., De Marzo, A.M., Nelson, W.G., Yegnasubramanian, S., 2013. Tracking the clonal origin of lethal prostate cancer. J. Clin. Invest. 123, 4918–4922. doi:10.1172/JCI70354

Haigh, P.I., 2002. Follicular thyroid carcinoma. Curr. Treat. Options Oncol. 3, 349–54.

Haigis, K.M., Kendall, K.R., Wang, Y., Cheung, A., Haigis, M.C., Glickman, J.N., Niwa-Kawakita, M., Sweet-Cordero, A., Sebolt-Leopold, J., Shannon, K.M., Settleman, J., Giovannini, M., Jacks, T., 2008. Differential effects of oncogenic K-Ras and N-Ras on proliferation, differentiation and tumor progression in the colon. Nat. Genet. 40, 600–8. doi:10.1038/ng.115

Hanahan, D., Weinberg, R.A., 2011. Hallmarks of Cancer: The Next Generation. Cell 144, 646–674. doi:10.1016/j.cell.2011.02.013

Hanahan, D., Weinberg, R.A., 2000. The Hallmarks of Cancer Review evolve progressively from normalcy via a series of pre. Cell 100, 57–70.

Hansen, K.D., Timp, W., Bravo, H.C., Sabunciyan, S., Langmead, B., Mcdonald, O.G., Wen, B., Wu, H., Liu, Y., Diep, D., Briem, E., Zhang, K., Irizarry, R.A., Feinberg, A.P., 2011. Increased methylation variation in epigenetic domains across cancer types. Nat. Genet. 43, 768–775. doi:10.1038/ng.865

Harrell, R.M., Bimston, D.N., 2014. Surgical utility of Afirma: effects of high cancer prevalence and oncocytic cell types in patients with indeterminate thyroid cytology. Endocr Pr. 20, 364–369. doi:10.4158/EP13330.OR

Hatzimichael, E., Crook, T., 2013. Cancer epigenetics: new therapies and new challenges. J. Drug Deliv. 2013, 529312. doi:10.1155/2013/529312

Haugen, B.R., Alexander, E.K., Bible, K.C., Doherty, G., Mandel, S.J., Nikiforov, Y.E., Pacini, F., Randolph, G., Sawka, A., Schlumberger, M., Schuff, K.G., Sherman, S.I., Sosa, J.A., Steward, D., Tuttle, R.M., Wartofsky, L., 2015. 2015 American Thyroid Association Management Guidelines for Adult Patients with Thyroid Nodules and Differentiated Thyroid Cancer. Thyroid 26, thy.2015.0020. doi:10.1089/thy.2015.0020

He, H., Jazdzewski, K., Li, W., Liyanarachchi, S., Nagy, R., Volinia, S., Calin, G.A., Liu, C.-G., Franssila, K., Suster, S., Kloos, R.T., Croce, C.M., de la Chapelle, A., 2005. The role of microRNA genes in papillary thyroid carcinoma. Proc. Natl. Acad. Sci. U. S. A. 102, 19075–80. doi:10.1073/pnas.0509603102

He, Y., Ecker, J.R., 2015. Non-CG Methylation in the Human Genome. Annu. Rev. Genomics Hum. Genet 16, 55–77. doi:10.1146/annurev-genom-090413-025437

Hedinger, C., Williams, E.D., Sobin, L.H., 1989. The WHO histological classification of thyroid tumors: a commentary on the second edition. Cancer 63, 908–11. doi:10.1002/1097-0142(19890301)63:5<908::AID-CNCR2820630520>3.0.CO;2-I

Hegedüs, L., 2009. The Thyroid Nodule. http://dx.doi.org/10.1056/NEJMcp031436.

Heintzman, N.D., Hon, G.C., Hawkins, R.D., Kheradpour, P., Stark, A., Harp, L.F., Ye, Z., Lee, L.K., Stuart, R.K., Ching, C.W., Ching, K. a, Antosiewicz-Bourget, J.E., Liu, H., Zhang, X., Green, R.D., Lobanenkov, V. V, Stewart, R., Thomson, J. a, Crawford, G.E., Kellis, M., Ren, B., 2009. Histone modifications at human enhancers reflect global cell-type-specific gene expression. Nature 459, 108–112. doi:10.1038/nature07829

Hellman, A., Chess, A., 2007. Gene body-specific methylation on the active X chromosome. Science 315, 1141–3. doi:10.1126/science.1136352

Herceg, Z., Vaissière, T., 2011. Epigenetic mechanisms and cancer an interface between the environment and the genome. Epigenetics 6, 804–819. doi:10.4161/epi.6.7.16262

Hieu, T.T., Russell, A.W., Cuneo, R., Clark, J., Kron, T., Hall, P., Doi, S.A.R., 2012. Cancer risk after medical exposure to radioactive iodine in benign thyroid diseases: A meta-analysis. Endocr. Relat. Cancer 19, 645–655. doi:10.1530/ERC-12-0176

Hinoue, T., Weisenberger, D.J., Lange, C.P.E., Shen, H., Byun, H.M., Van Den Berg, D., Malik, S., Pan, F., Noushmehr, H., Van Dijk, C.M., Tollenaar, R.A.E.M., Laird, P.W., 2012. Genome-scale analysis of aberrant DNA methylation in colorectal cancer. Genome Res. 22, 271–282. doi:10.1101/gr.117523.110

Hinoue, T., Weisenberger, D.J., Pan, F., Campan, M., Kim, M., Young, J., Whitehall, V.L., Leggett, B.A., Laird, P.W., 2009. Analysis of the association between CIMP and BRAF in colorectal cancer by DNA methylation profiling. PLoS One 4, e8357. doi:10.1371/journal.pone.0008357

Hoang, J.K., Nguyen, X. V., Davies, L., 2015. Overdiagnosis of Thyroid Cancer. Answers to Five Key Questions. Acad. Radiol. doi:10.1016/j.acra.2015.01.019

Holliday, R., Pugh, J.E., 1975. DNA modification mechanisms and gene activity during development. Science 187, 226–232. doi:10.1126/science.1111098

Hon, G.C., Hawkins, R.D., Ren, B., 2009. Predictive chromatin signatures in the mammalian genome. Hum. Mol. Genet. 18. doi:10.1093/hmg/ddp409

Hondele, M., Ladurner, A.G., 2011. The chaperone-histone partnership: For the greater good of histone traffic and chromatin plasticity. Curr. Opin. Struct. Biol. doi:10.1016/j.sbi.2011.10.003

Hoos, A., Stojadinovic, A., Singh, B., Dudas, M.E., Leung, D.H.Y., Shaha, A.R., Shah, J.P., Brennan, M.F., Cordon-Cardo, C., Ghossein, R., 2002. Clinical significance of molecular expression profiles of Hürthle cell tumors of the thyroid gland analyzed via tissue microarrays. Am. J. Pathol. 160, 175–183. doi:10.1016/S0002-9440(10)64361-1

HOTCHKISS, R.D., 1948. The quantitative separation of purines, pyrimidines, and nucleosides by paper chromatography. J. Biol. Chem. 175, 315–32.

Hou, L., Zhang, X., Wang, D., Baccarelli, A., 2012. Environmental chemical exposures and human epigenetics. Int. J. Epidemiol. 41, 79–105. doi:10.1093/ije/dyr154

Hou, P., Liu, D., Xing, M., 2011. Genome-wide alterations in gene methylation by the BRAF V600E mutation in papillary thyroid cancer cells. Endocr Relat Cancer 18, 687–697. doi:ERC-11-0212 [pii]\r10.1530/ERC-11-0212

Houck, C.M., Rinehart, F.P., Schmid, C.W., 1979. A ubiquitous family of repeated DNA sequences in the human genome. J. Mol. Biol. 132, 289–306.

Howard, B., Wang, Y., Xekouki, P., Faucz, F.R., Jain, M., Zhang, L., Meltzer, P.G., Stratakis, C.A., Kebebew, E., 2014. Integrated analysis of genome-wide methylation and gene expression shows epigenetic regulation of CYP11B2 in aldosteronomas. J. Clin. Endocrinol. Metab. 99. doi:10.1210/jc.2013-3495

Howell, G.M., Carty, S.E., Armstrong, M.J., LeBeau, S.O., Hodak, S.P., Coyne, C., Stang, M.T., McCoy, K.L., Nikiforova, M.N., Nikiforov, Y.E., Yip, L., 2011. Both BRAF V600E Mutation and Older Age (≥65 Years) are Associated with Recurrent Papillary Thyroid Cancer. Ann. Surg. Oncol. 18, 3566–3571. doi:10.1245/s10434-011-1781-5

Howell, G.M., Hodak, S.P., Yip, L., 2013. RAS mutations in thyroid cancer. Oncologist 18, 926–32. doi:10.1634/theoncologist.2013-0072

Hu, S., Liu, D., Tufano, R.P., Carson, K.A., Rosenbaum, E., Cohen, Y., Holt, E.H., Kiseljak-Vassiliades, K., Rhoden, K.J., Tolaney, S., Condouris, S., Tallini, G., Westra, W.H., Umbricht, C.B., Zeiger, M.A., Califano, J.A., Vasko, V., Xing, M., 2006. Association of aberrant methylation of tumor suppressor genes with tumor aggressiveness and BRAF mutation in papillary thyroid cancer. Int. J. Cancer 119, 2322–2329. doi:10.1002/ijc.22110

Huang, T.-W., Lai, J.-H., Wu, M.-Y., Chen, S.-L., Wu, C.-H., Tam, K.-W., 2013. Systematic review of clinical practice guidelines in the diagnosis and management of thyroid nodules and cancer. BMC Med. 11, 191. doi:10.1186/1741-7015-11-191

Huarte, M., 2015. The emerging role of lncRNAs in cancer. Nat. Med. 21, 1253–61. doi:10.1038/nm.3981

Hunt, J.L., Barnes, E.L., 2003. Non-tumor-associated psammoma bodies in the thyroid. Am. J. Clin. Pathol. 119, 90–4. doi:10.1309/RWPP-YCBY-T2JV-A023

Illingworth, R.S., Bird, A.P., 2009. CpG islands - "A rough guide." FEBS Lett. doi:10.1016/j.febslet.2009.04.012

Illingworth, R.S., Gruenewald-Schneider, U., Webb, S., Kerr, A.R.W., James, K.D., Turner, D.J., Smith, C., Harrison, D.J., Andrews, R., Bird, A.P., 2010. Orphan CpG Islands Identify numerous conserved promoters in the mammalian genome. PLoS Genet. 6. doi:10.1371/journal.pgen.1001134

Inamura, K., Yamauchi, M., Nishihara, R., Lochhead, P., Qian, Z.R., Kuchiba, A., Kim, S.A., Mima, K., Sukawa, Y., Jung, S., Zhang, X., Wu, K., Cho, E., Chan, A.T., Meyerhardt, J.A., Harris, C.C., Fuchs, C.S., Ogino, S., 2014. Tumor LINE-1 methylation level and microsatellite instability in relation to colorectal cancer prognosis. J. Natl. Cancer Inst. 106. doi:10.1093/jnci/dju195

Irizarry, R.A., Ladd-Acosta, C., Wen, B., Wu, Z., Montano, C., Onyango, P., Cui, H., Gabo, K., Rongione, M., Webster, M., Ji, H., Potash, J.B., Sabunciyan, S., Feinberg, A.P., 2009. The human colon cancer methylome shows similar hypo- and hypermethylation at conserved tissue-specific CpG island shores. Nat. Genet. 41, 178–86. doi:10.1038/ng.298

Itano, O., Ueda, M., Kikuchi, K., Hashimoto, O., Hayatsu, S., Kawaguchi, M., Seki, H., Aiura, K., Kitajima, M., 2002. Correlation of postoperative recurrence in hepatocellular carcinoma with demethylation of repetitive sequences. Oncogene 21, 789–797. doi:10.1038/sj.onc.1205124

Ito, Y., Hirokawa, M., Higashiyama, T., Takamura, Y., Miya, A., Kobayashi, K., Matsuzuka, F., Kuma, K., Miyauchi, A., 2007. Prognosis and prognostic factors of follicular carcinoma in Japan: Importance of postoperative pathological examination. World J. Surg. 31, 1417–1424. doi:10.1007/s00268-007-9095-2

Ito, Y., Koessler, T., Ibrahim, A.E.K., Rai, S., Vowler, S.L., Abu-amero, S., Silva, A.L., Maia, A.T., Huddleston, J.E., Uribe-lewis, S., Woodfine, K., Jagodic, M., Nativio, R., Dunning, A., Moore, G., Klenova, E., Bingham, S., Pharoah, P.D.P., Brenton, J.D., Beck, S., Sandhu, M.S., Murrell, A., 2008. Somatically acquired hypomethylation of IGF2 in breast and colorectal cancer. Hum. Mol. Genet. 17, 2633–2643. doi:10.1093/hmg/ddn163

Ito, Y., Miyauchi, A., Inoue, H., Fukushima, M., Kihara, M., Higashiyama, T., Tomoda, C., Takamura, Y., Kobayashi, K., Miya, A., 2010. An observational trial for papillary thyroid microcarcinoma in Japanese patients. World J. Surg. 34, 28–35. doi:10.1007/s00268-009-0303-0

Iyer, M.K., Niknafs, Y.S., Malik, R., Singhal, U., Sahu, A., Hosono, Y., Barrette, T.R., Prensner, J.R., Evans, J.R., Zhao, S., Poliakov, A., Cao, X., Dhanasekaran, S.M., Wu, Y.-M., Robinson, D.R., Beer, D.G., Feng, F.Y., Iyer, H.K., Chinnaiyan, A.M., 2015. The landscape of long noncoding RNAs in the human transcriptome. Nat. Publ. Gr. 47. doi:10.1038/ng.3192

Jackson, K., Yu, M.C., Arakawa, K., Fiala, E., Youn, B., Fiegl, H., Müller-Holzner, E., Widschwendter, M., Ehrlich, M., 2004. DNA hypomethylation is prevalent even in low-grade breast cancers. Cancer Biol. Ther. 3, 1225–1231. doi:1222 [pii]

Jacobson, E.M., Tomer, Y., 2007. The CD40, CTLA-4, thyroglobulin, TSH receptor, and PTPN22 gene quintet and its contribution to thyroid autoimmunity: back to the future. J. Autoimmun. 28, 85–98. doi:10.1016/j.jaut.2007.02.006

Jeltsch, A., 2002. Beyond Watson and Crick: DNA methylation and molecular enzymology of DNA methyltransferases. Chembiochem 3, 274–93. doi:10.1002/1439-7633(20020402)3:4<274::AID-CBIC274>3.0.CO;2-S

Jenuwein, T., Allis, C.D., 2001. Translating the histone code. Science (80-.). 293, 1074–1080. doi:10.1126/science.1063127

Jeter, C.R., Yang, T., Wang, J., Chao, H.-P., Tang, D.G., 2015. NANOG in Cancer Stem Cells and Tumor Development: An Update and Outstanding Questions. Stem Cells 1–12. doi:10.1002/stem.2007

Jhiang, S.M., 2000. The RET proto-oncogene in human cancers. Oncogene 19, 5590–7. doi:10.1038/sj.onc.1203857

Jiang, C., Pugh, B.F., 2009. Nucleosome positioning and gene regulation: advances through genomics. Nat. Rev. Genet. 10, 161–72. doi:10.1038/nrg2522

Jin, B., Robertson, K.D., 2013. DNA methyltransferases, DNA damage repair, and cancer. Adv. Exp. Med. Biol. doi:10.1007/978-1-4419-9967-2-1

Johnson, S.K., Ramani, V.C., Hennings, L., Haun, R.S., 2007. Kallikrein 7 enhances pancreatic cancer cell invasion by shedding E-cadherin. Cancer 109, 1811–1820. doi:10.1002/cncr.22606

Jones, P. a, Baylin, S.B., 2002a. The fundamental role of epigenetic events in cancer. Nat. Rev. Genet. 3, 415–28. doi:10.1038/nrg816

Jones, P. a, Baylin, S.B., 2002b. The fundamental role of epigenetic events in cancer. Nat. Rev. Genet. 3, 415–28. doi:10.1038/nrg816

Jones, P.A., 2012. Functions of DNA methylation: islands, start sites, gene bodies and beyond. Nat. Rev. Genet. 13, 484–92. doi:10.1038/nrg3230

Jones, P.A., 1999. The DNA methylation paradox. Trends Genet. doi:10.1016/S0168-9525(98)01636-9

Jorda, M., Diez-Villanueva, A., Mallona, I., Martin, B., Lois, S., Barrera, V., Esteller, M., Vavouri, T., Peinado, M.., n.d. The epigenetic landscape of Alu repeats delineates the structural and functional genomic architecture of colon cancer cells. Genome Res.

Jordà, M., Peinado, M. a, 2010. Methods for DNA methylation analysis and applications in colon cancer. Mutat. Res. 693, 84–93. doi:10.1016/j.mrfmmm.2010.06.010

Kalari, S., Pfeifer, G.P., 2010. Identification of Driver and Passenger DNA Methylation in Cancer by Epigenomic Analysis, Advances in Genetics. doi:10.1016/B978-0-12-380866-0.60010-1

Kamakaka, R.T., Biggins, S., 2005. Histone variants: deviants? Genes Dev. 19, 295–310. doi:10.1101/gad.1272805

Kamat, A.A., Sood, A.K., Dang, D., Gershenson, D.M., Simpson, J.L., Bischoff, F.Z., 2006. Quantification of Total Plasma Cell-Free DNA in Ovarian Cancer Using Real-Time PCR. Ann. N. Y. Acad. Sci. 1075, 230–234. doi:10.1196/annals.1368.031

Kane, S. V, Sharma, T.P., 2015. Cytologic diagnostic approach to poorly differentiated thyroid carcinoma: a single-institution study. Cancer Cytopathol. 123, 82–91. doi:10.1002/cncy.21500

Kapoor, R., Fanibunda, S.E., Desouza, L.A., Guha, S.K., Vaidya, V.A., 2015. Perspectives on thyroid hormone action in adult neurogenesis. J. Neurochem. doi:10.1111/jnc.13093

Karimi, M., Johansson, S., Ekström, T.J., 2006. Using LUMA: A luminometric-based assay for global DNA-methylation. Epigenetics 1, 45–48. doi:10.4161/epi.1.1.2587

Karpf, A.R., Matsui, S.I., 2005. Genetic disruption of cytosine DNA methyltransferase enzymes induces chromosomal instability in human cancer cells. Cancer Res. 65, 8635–8639. doi:10.1158/0008-5472.CAN-05-1961

Kato, N., Tsuchiya, T., Tamura, G., Motoyama, T., 2002. E-cadherin expression in follicular carcinoma of the thyroid. Pathol. Int. 52, 13–18. doi:10.1046/j.1440-1827.2002.01310.x

Katoh, H., Yamashita, K., Enomoto, T., Watanabe, M., 2015. Annals of Clinical Pathology Classification and General Considerations of Thyroid Cancer. Ann Clin Pathol 3.

Kazaure, H.S., Roman, S. a., Sosa, J. a., 2012. Aggressive Variants of Papillary Thyroid Cancer: Incidence, Characteristics and Predictors of Survival among 43,738 Patients. Ann. Surg. Oncol. 19, 1874–1880. doi:10.1245/s10434-011-2129-x

Kebebew, E., 2008. Hereditary non-medullary thyroid cancer. World J. Surg. doi:10.1007/s00268-007-9312-z

Kebebew, E., Weng, J., Bauer, J., Ranvier, G., Clark, O.H., Duh, Q.-Y., Shibru, D., Bastian, B., Griffin, A., 2007. The Prevalence and Prognostic Value of BRAF Mutation in Thyroid Cancer. Ann surg 246, 466–470. doi:10.1097/SLA.0b013e318148563d

Keene, M.A., Elgin, S.C., 1981. Micrococcal nuclease as a probe of DNA sequence organization and chromatin structure. Cell 27, 57–64.

Khairy, G., 2009. Anaplastic Transformation of Differentiated Thyroid Carcinoma. Int. J. Heal. Sci. Qassim Univ. 3.

Khoo, M.L.C., Beasley, N.J.P., Ezzat, S., Freeman, J.L., Asa, S.L., 2002. Overexpression of cyclin D1 and underexpression of p27 predict lymph node metastases in papillary thyroid carcinoma. J. Clin. Endocrinol. Metab. 87, 1814–1818. doi:10.1210/jc.87.4.1814

Kikuchi, Y., Tsuji, E., Yagi, K., Matsusaka, K., Tsuji, S., Kurebayashi, J., Ogawa, T., Aburatani, H., Kaneda, A., 2013. Aberrantly methylated genes in human papillary thyroid cancer and their association with BRAF/RAS mutation. Front. Genet. 4, 271. doi:10.3389/fgene.2013.00271

Kim, D.W., Jung, S.L., Baek, J.H., Kim, J., Ryu, J.H., Na, D.G., Park, S.-W., Kim, J., Sung, J.Y., Lee, Y., Rho, M.H., 2013. The prevalence and features of thyroid pyramidal lobe, accessory thyroid, and ectopic thyroid as assessed by computed tomography: a multicenter study. Thyroid 23, 84–91. doi:10.1089/thy.2012.0253

Kim, T.H., Barrera, L.O., Zheng, M., Qu, C., Singer, M.A., Richmond, T.A., Wu, Y., Green, R.D., Ren, B., 2005. A high-resolution map of active promoters in the human genome. Nature 436, 876–80. doi:10.1038/nature03877

Kimura, E.T., Nikiforova, M.N., Zhu, Z., Knauf, J.A., Nikiforov, Y.E., Fagin, J.A., 2003. High prevalence of BRAF mutations in thyroid cancer: Genetic evidence for constitutive activation of the RET/PTC-RAS-BRAF

signaling pathway in papillary thyroid carcinoma. Cancer Res. 63, 1454–1457.

Kircher, S.M., Mohindra, N., Nimeiri, H., 2014. Cost Estimates and Economic Implications of Expanded RAS Testing in Metastatic Colorectal Cancer. Oncologist 14–18. doi:10.1634/theoncologist.2014-0252

Kirsten, D., 2000. The thyroid gland: physiology and pathophysiology. Neonatal Netw. 19, 11–26. doi:10.1891/0730-0832.19.8.11

Kitazono, M., Robey, R., Zhan, Z., Sarlis, N.J., Skarulis, M.C., Aikou, T., Bates, S., Fojo, T., 2001. Low concentrations of the histone deacetylase inhibitor, depsipeptide (FR901228), increase expression of the Na(+)/I(-) symporter and iodine accumulation in poorly differentiated thyroid carcinoma cells. J. Clin. Endocrinol. Metab. 86, 3430–5. doi:10.1210/jcem.86.7.7621

Klein Hesselink, E.N., Zafón, C., Buj, R., Villalmanzo, N., Iglesias, C., van Hemel, B.M., Klein Hesselink, M.S., Mate, J.L., Mauricio, D., Montero, C., Puig-Domingo, M., Reverter, J.L., Riesco-Eizaguirre, G., Peinado, M.A., Robledo, M., Links, T.P., Jorda, M., n.d. Increased global DNA hypomethylation in metastatic and dedifferentiated thyroid cancer. Press.

Klugbauer, S., Jauch, A., Lengfelder, E., Demidchik, E., Rabes, H.M., 2000. A novel type of RET rearrangement (PTC8) in childhood papillary thyroid carcinomas and characterization of the involved gene (RFG8). Cancer Res. 60, 7028–7032.

Klugbauer, S., Rabes, H., n.d. The transcription coactivator HTIF1 and a related protein are fused to the RET receptor tyrosine kinase in childhood papillary thyroid carcinomas.

Knudson, a G., 2001. Two genetic hits (more or less) to cancer. Nat. Rev. Cancer 1, 157–162. doi:10.1038/35101031

Knudson, A.G., 1971. Mutation and cancer: statistical study of retinoblastoma. Proc. Natl. Acad. Sci. U. S. A. 68, 820–3. doi:10.1073/pnas.68.4.820

Kobayashi, Y., Absher, D.M., Gulzar, Z.G., Young, S.R., McKenney, J.K., Peehl, D.M., Brooks, J.D., Myers, R.M., Sherlock, G., 2011. DNA methylation profiling reveals novel biomarkers and important roles for DNA methyltransferases in prostate cancer. Genome Res. 21, 1017–1027. doi:10.1101/gr.119487.110

Kochanek, S., Renz, D., Doerfler, W., 1993. DNA methylation in the Alu sequences of diploid and haploid primary human cells. EMBO J. 12, 1141–51.

Kolasinska-zwierz, P., Down, T., Latorre, I., Liu, T., Liu, X.S., Ahringer, J., 2009. Differential chromatin marking of introns and expressed exons by H3K36me3. Nat. Genet. 41, 376–381. doi:10.1038/ng.322.Differential

Kopp, P., Pesce, L., Solis-S, J.C., Pendred, V., Morgans, M.E., Trotter, W.R., Fraser, G.R., al., et, Medeiros-Neto, G., Stanbury, J.B., Everett, L.A., al., et, Kopp, P., Reardon, W., al., et, Campbell, C., al., et, Cremers, C.W.R.J., al., et, Phelps, P.D., al., et, Fugazzola, L., al., et, Pryor, S.P., al., et, Hartley, G.J., Phelps, P.D., Nilsson, L.R., al., et, Fraser, G.R., Gausden, E., al., et, Sato, E., al., et, Usami, S., al., et, Baschieri, L., al., et, Gillam, M.P., al., et, Kopp, P., Trotter, W.R., Kopp, P., al., et, Trevino, O.G., al., et, Everett, L.A., Green, E.D., Mount, D.B., Romero, M.F., Dawson, P.A., Markovich, D., Zheng, J., al., et, Oliver, D., al., et, Scott, D.A., al., et, Soleimani, M., al., et, Royaux, I.E., al., et, Yoshida, A., al., et, Taylor, J.P., al., et, Royaux, I.E., al., et, Aravind, L., Koonin, E.V., Ko, S.B., al., et, Ko, S.B., al., et, Shcheynikov, N., al., et, Gillam, M.P., al., et, Dossena, S., al., et, Rotman-Pikielny, P., al., et, Everett, L.A., al., et, Everett, L.A., al., et, Wangemann, P., al., et, Wangemann, P., al., et, Nakaya, K., al., et, Dohan, O., al., et, Wolff, J., Arvan, P., Jeso, B. Di, Moreno, J.C., Golstein, P., al., et, Bidart, J.M., al., et, Yoshida, A., al., et, Weiss, S.J., al., et, Nilsson, M., al., et, Nilsson, M., al., et, Dentice, M., al., et, Suzuki, K., al., et, Suzuki, K., al., et, Suzuki, K., al., et, Suzuki, K., Kohn, L.D., Kohn, L.D., al., et, Wolff, J., Andros, G., Wollman, S.H., Rodriguez, A.M., al., et, Paroder, V., al., et, Hove, M.F. van den, al., et, Wall, S.M., Scott, D.A., Karniski, L.P., Verlander, J.W., al., et, Verlander, J.W., al., et, Kim, Y.H., al., et, Delange, F., al., et, Rillema, J.A., Hill, M.A., Lacroix, L., al., et, Pedemonte, N., al., et, 2008. Pendred syndrome and iodide transport in the thyroid. Trends Endocrinol. Metab. 19, 260–8. doi:10.1016/j.tem.2008.07.001

Kouvaraki, M.A., Shapiro, S.E., Fornage, B.D., Edeiken-Monro, B.S., Sherman, S.I., Vassilopoulou-Sellin, R., Lee, J.E., Evans, D.B., 2003. Role of preoperative ultrasonography in the surgical management of patients with thyroid cancer. Surgery 134, 946–54; discussion 954–5. doi:10.1016/S0039

Kouzarides, T., 2007. Chromatin Modifications and Their Function. Cell. doi:10.1016/j.cell.2007.02.005

Kreeger, P.K., Lauffenburger, D.A., 2010. Cancer systems biology: a network modeling perspective. Carcinogenesis 31, 2–8. doi:10.1093/carcin/bgp261

Kroll, T.G., 2000. PAX8-PPARgamma 1 Fusion in Oncogene Human Thyroid Carcinoma. Science (80-.). 289, 1357–1360. doi:10.1126/science.289.5483.1357

Kroll, T.G., Sarraf, P., Pecciarini, L., Chen, C.J., Mueller, E., Spiegelman, B.M., Fletcher, J. a, 2000. PAX8-PPARgamma1 fusion oncogene in human thyroid carcinoma [corrected]. Science (80-.). 289, 1357–1360. doi:8756 [pii]

Kryza, T., Silva, M.L., Loessner, D., Heuzé-Vourc'h, N., Clements, J.A., 2016. The kallikrein-related peptidase family: Dysregulation and functions during cancer progression. Biochimie 122, 283–299. doi:10.1016/j.biochi.2015.09.002

Kulis, M., Queirós, A.C., Beekman, R., Martín-Subero, J.I., 2013. Intragenic DNA methylation in transcriptional regulation, normal differentiation and cancer. Biochim. Biophys. Acta - Gene Regul. Mech. doi:10.1016/j.bbagrm.2013.08.001

Lander, E.S., Linton, L.M., Birren, B., Nusbaum, C., Zody, M.C., Baldwin, J., Devon, K., Dewar, K., Doyle, M., FitzHugh, W., Funke, R., Gage, D., Harris, K., Heaford, A., Howland, J., Kann, L., Lehoczky, J., LeVine, R., McEwan, P., McKernan, K., Meldrim, J., Mesirov, J.P., Miranda, C., Morris, W., Naylor, J., Raymond, C., Rosetti, M., Santos, R., Sheridan, A., Sougnez, C., Stange-Thomann, N., Stojanovic, N., Subramanian, A., Wyman, D., Rogers, J., Sulston, J., Ainscough, R., Beck, S., Bentley, D., Burton, J., Clee,

C., Carter, N., Coulson, A., Deadman, R., Deloukas, P., Dunham, A., Dunham, I., Durbin, R., French, L., Grafham, D., Gregory, S., Hubbard, T., Humphray, S., Hunt, A., Jones, M., Lloyd, C., McMurray, A., Matthews, L., Mercer, S., Milne, S., Mullikin, J.C., Mungall, A., Plumb, R., Ross, M., Shownkeen, R., Sims, S., Waterston, R.H., Wilson, R.K., Hillier, L.W., McPherson, J.D., Marra, M.A., Mardis, E.R., Fulton, L.A., Chinwalla, A.T., Pepin, K.H., Gish, W.R., Chissoe, S.L., Wendl, M.C., Delehaunty, K.D., Miner, T.L., Delehaunty, A., Kramer, J.B., Cook, L.L., Fulton, R.S., Johnson, D.L., Minx, P.J., Clifton, S.W., Hawkins, T., Branscomb, E., Predki, P., Richardson, P., Wenning, S., Slezak, T., Doggett, N., Cheng, J.F., Olsen, A., Lucas, S., Elkin, C., Uberbacher, E., Frazier, M., Gibbs, R.A., Muzny, D.M., Scherer, S.E., Bouck, J.B., Sodergren, E.J., Worley, K.C., Rives, C.M., Gorrell, J.H., Metzker, M.L., Naylor, S.L., Kucherlapati, R.S., Nelson, D.L., Weinstock, G.M., Sakaki, Y., Fujiyama, A., Hattori, M., Yada, T., Toyoda, A., Itoh, T., Kawagoe, C., Watanabe, H., Totoki, Y., Taylor, T., Weissenbach, J., Heilig, R., Saurin, W., Artiguenave, F., Brottier, P., Bruls, T., Pelletier, E., Robert, C., Wincker, P., Smith, D.R., Doucette-Stamm, L., Rubenfield, M., Weinstock, K., Lee, H.M., Dubois, J., Rosenthal, A., Platzer, M., Nyakatura, G., Taudien, S., Rump, A., Yang, H., Yu, J., Wang, J., Huang, G., Gu, J., Hood, L., Rowen, L., Madan, A., Qin, S., Davis, R.W., Federspiel, N.A., Abola, A.P., Proctor, M.J., Myers, R.M., Schmutz, J., Dickson, M., Grimwood, J., Cox, D.R., Olson, M. V, Kaul, R., Raymond, C., Shimizu, N., Kawasaki, K., Minoshima, S., Evans, G.A., Athanasiou, M., Schultz, R., Roe, B.A., Chen, F., Pan, H., Ramser, J., Lehrach, H., Reinhardt, R., McCombie, W.R., de la Bastide, M., Dedhia, N., Blocker, H., Hornischer, K., Nordsiek, G., Agarwala, R., Aravind, L., Bailey, J.A., Bateman, A., Batzoglou, S., Birney, E., Bork, P., Brown, D.G., Burge, C.B., Cerutti, L., Chen, H.C., Church, D., Clamp, M., Copley, R.R., Doerks, T., Eddy, S.R., Eichler, E.E., Furey, T.S., Galagan, J., Gilbert, J.G., Harmon, C., Hayashizaki, Y., Haussler, D., Hermjakob, H., Hokamp, K., Jang, W., Johnson, L.S., Jones, T.A., Kasif, S., Kaspryzk, A., Kennedy, S., Kent, W.J., Kitts, P., Koonin, E. V, Korf, I., Kulp, D., Lancet, D., Lowe, T.M., McLysaght, A., Mikkelsen, T., Moran, J. V, Mulder, N., Pollara, V.J., Ponting, C.P., Schuler, G., Schultz, J., Slater, G., Smit, A.F., Stupka, E., Szustakowski, J., Thierry-Mieg, D., Thierry-Mieg, J., Wagner, L., Wallis, J., Wheeler, R., Williams, A., Wolf, Y.I., Wolfe, K.H., Yang, S.P., Yeh, R.F., Collins, F., Guyer, M.S., Peterson, J., Felsenfeld, A., Wetterstrand, K.A., Patrinos, A., Morgan, M.J., de Jong, P., Catanese, J.J., Osoegawa, K., Shizuya, H., Choi, S., Chen, Y.J., International Human Genome Sequencing, C., 2001. Initial sequencing and analysis of the human genome. Nature 409, 860–921. doi:10.1038/35057062

Lang, W., Choritz, H., Hundeshagen, H., 1986. Risk factors in follicular thyroid carcinomas. A retrospective follow-up study covering a 14-year period with emphasis on morphological findings. Am. J. Surg. Pathol. 10, 246–55.

Lastra, R.R., Pramick, M.R., Crammer, C.J., LiVolsi, V.A., Baloch, Z.W., 2014. Implications of a suspicious afirma test result in thyroid fine-needle aspiration cytology: an institutional experience. Cancer Cytopathol. 122, 737–744. doi:10.1002/cncy.21455

Lawrence, M.S., Stojanov, P., Polak, P., Kryukov, G. V, Cibulskis, K., Sivachenko, A., Carter, S.L., Stewart, C., Mermel, C.H., Roberts, S.A., Kiezun, A., Hammerman, P.S., Mckenna, A., Drier, Y., Zou, L., Ramos, A.H., Pugh, T.J., Stransky, N., Helman, E., Kim, J., Sougnez, C., Ambrogio, L., Nickerson, E., Shefler, E., Cortés, M.L., Auclair, D., Saksena, G., Voet, D., Noble, M., Dicara, D., Lin, P., Lichtenstein, L., Heiman, D.I., Fennell, T., Imielinski, M., Hernandez, B., Hodis, E., Baca, S., Dulak, A.M., Lohr, J., Landau, D.-A., Wu, C.J., Melendez-Zajgla, J., Hidalgo-Miranda, A., Koren, A., Mccarroll, S.A., Mora, J., Lee, R.S., Crompton, B., Onofrio, R., Parkin, M., Winckler, W., Ardlie, K., Gabriel, S.B., Roberts, C.W.M., Biegel, J.A., Stegmaier, K., Bass, A.J., Garraway, L.A., Meyerson, M., Golub, T.R., Gordenin, D.A., Sunyaev, S., Lander, E.S., Getz, G., 2013. Mutational heterogeneity in cancer and the search for new cancer-associated genes. Nature 499. doi:10.1038/nature12213

Leboulleux, S., Tuttle, R.M., Pacini, F., Schlumberger, M., 2016. Papillary thyroid microcarcinoma: time to shift from surgery to active surveillance? Lancet Diabetes Endocrinol. 0, 2072–2076. doi:10.1016/S2213-8587(16)30180-2

Lee, N. V., Lira, M.E., Pavlicek, A., Ye, J., Buckman, D., Bagrodia, S., Srinivasa, S.P., Zhao, Y., Aparicio, S., Rejto, P.A., Christensen, J.G., Ching, K.A., 2012. A novel SND1-BRAF fusion confers resistance to c-Met inhibitor PF-04217903 in GTL16 cells though MAPK activation. PLoS One 7. doi:10.1371/journal.pone.0039653

Lee, H.S., Kim, B.H., Cho, N.Y., Yoo, E.J., Choi, M., Shin, S.H., Jang, J.J., Suh, K.S., Kim, Y.S., Kang, G.H., 2009. Prognostic implications of and relationship between CpG island hypermethylation and repetitive DNA hypomethylation in hepatocellular carcinoma. Clin. Cancer Res. 15, 812–820. doi:10.1158/1078-0432.CCR-08-0266

Lee, J., Soh, E.-Y., 2010. Differentiated thyroid carcinoma presenting with distant metastasis at initial diagnosis clinical outcomes and prognostic factors. Ann. Surg. 251, 114–9. doi:10.1097/SLA.0b013e3181b7faf6

Lee, J.J., Geli, J., Larsson, C., Wallin, G., Karimi, M., Zedenius, J., Höög, A., Foukakis, T., 2008. Gene-specific promoter hypermethylation without global hypomethylation in follicular thyroid cancer. Int. J. Oncol. 33, 861–869. doi:10.3892/ijo_00000074

Lev Maor, G., Yearim, A., Ast, G., 2015. The alternative role of DNA methylation in splicing regulation. Trends Genet. doi:10.1016/j.tig.2015.03.002

Levene, P.A., London, E.S., 1905. THE STRUCTURE OF THYMONUCLEIC ACID. J. Biol. Chem. Z. physiol. Chem. Z. physiol. Chem. J. Biol. Chem 41.

Li, C., Lee, K.C., Schneider, E.B., Zeiger, M. a, 2012. BRAF V600E mutation and its association with clinicopathological features of papillary thyroid cancer: a meta-analysis. J. Clin. Endocrinol. Metab. 97, 4559–70. doi:10.1210/jc.2012-2104

Li, J., Huang, Q., Zeng, F., Li, W., He, Z., Chen, W., Zhu, W., Zhang, B., 2014. The prognostic value of global DNA hypomethylation in cancer: a meta-analysis. PLoS One 9, e106290. doi:10.1371/journal.pone.0106290\rPONE-D-14-10144 [pii]

Li, L., Xu, N., Fan, N., Meng, Q., Luo, W., Lv, L., Ma, W., Liu, X., Liu, L., Xu, F., Wang, H., Mao, W., Li, Y., 2015. Upregulated KLK10 inhibits esophageal cancer

proliferation and enhances cisplatin sensitivity in vitro. Oncol. Rep. 34, 2325–2332. doi:10.3892/or.2015.4211

Liang, K.-H., Yeh, C.-T., Cordaux, R., Batzer, M., Price, A., Eskin, E., Pevzner, P., Batzer, M., Deininger, P., Häsler, J., Strub, K., Burns, K., Boeke, J., Umylny, B., Presting, G., Efird, J., Bennett, E., Keller, H., Mills, R., Lander, E., Linton, L., Birren, B., Chu, W., Liu, W., Schimd, C., Kaneko, H., Dridi, S., Tarallo, V., Tsirigos, A., Rigoutsos, I., Shen, S., Lin, L., Shen, S., Tye, A., Smalheiser, N., Torvik, V., Gong, C., Maquat, L., Grover, D., Majumder, P., Rao, C., Muotri, A., Carthew, R., Sontheimer, E., Tomari, Y., Zamore, P., Kumar, M., Carmichael, G., Poliseno, L., Salmena, L., Zhang, J., Salmena, L., Poliseno, L., Tay, Y., Vidal, F., Mougneau, E., Glaichenhaus, N., Kertesz, M., Iovino, N., Unnerstall, U., Gaul, U., Segal, E., Pruitt, K., Tatusova, T., Brown, G., Maglott, D., Mootha, V., Lindgren, C., Eriksson, K., Subramanian, A., Tamayo, P., Mootha, V., Rubin, C., Hofacker, I., Hofacker, I., Noe, L., Kucherov, G., Thomas, P., Kejariwal, A., Campbell, M., Bolstad, B., Irizarry, R., Astrand, M., Irizarry, R., Bolstad, B., Collin, F., Irizarry, R., Hobbs, B., Collin, F., Hoon, M. de, Imoto, S., Nolan, J., Eisen, M., Spellman, P., Brown, P., Botstein, D., Saldanha, A., 2013. A gene expression restriction network mediated by sense and antisense Alu sequences located on protein-coding messenger RNAs. BMC Genomics 14, 325. doi:10.1186/1471-2164-14-325

Libutti, S.K., n.d. Understanding the role of gender in the incidence of thyroid cancer. Cancer J. 11, 104–5.

Lieleg, C., Krietenstein, N., Walker, M., Korber, P., 2015. Nucleosome positioning in yeasts: methods, maps, and mechanisms. Chromosoma. doi:10.1007/s00412-014-0501-x

Lilja, H., Ulmert, D., Vickers, A.J., 2008. Prostate-specific antigen and prostate cancer: prediction, detection and monitoring. Nat. Rev. Cancer 8, 268–78. doi:10.1038/nrc2351

Lin, C.H., Hsieh, S.Y., Sheen, I.S., Lee, W.C., Chen, T.C., Shyu, W.C., Liaw, Y.F., 2001. Genome-wide hypomethylation in hepatocellular carcinogenesis. Cancer Res. 61, 4238–4243.

Linton, O.W., Mettler, F.A., National Council on Radiation Protection and Measurements, 2003. National conference on dose reduction in CT, with an emphasis on pediatric patients. AJR. Am. J. Roentgenol. 181, 321–9. doi:10.2214/ajr.181.2.1810321

Lister, R., Pelizzola, M., Dowen, R.H., Hawkins, R.D., Hon, G., Tonti-Filippini, J., Nery, J.R., Lee, L., Ye, Z., Ngo, Q.-M., Edsall, L., Antosiewicz-Bourget, J., Stewart, R., Ruotti, V., Millar, A.H., Thomson, J.A., Ren, B., Ecker, J.R., 2009. Human DNA methylomes at base resolution show widespread epigenomic differences. Nature, Publ. online 14 Oct. 2009; | doi10.1038/10.1038/nature08514 462, 315. doi:10.1038/NATURE08514

Lito, P., Rosen, N., Solit, D.B., 2013. Tumor adaptation and resistance to RAF inhibitors. Nat. Med. 19, 1401–1409. doi:10.1038/nm.3392

Liu, D., Yang, C., Bojdani, E., Murugan, A.K., Xing, M., Xing, M.M., 2013. identification of RASAL1 as a Major tumor Suppressor Gene in thyroid cancer. doi:10.1093/jnci/djt249

Liu, F., Killian, J.K., Yang, M., Walker, R.L., Hong, J. a, Zhang, M., Davis, S., Zhang, Y., Hussain, M., Xi, S., Rao, M., Meltzer, P. a, Schrump, D.S., 2010. Epigenomic alterations and gene expression profiles in respiratory epithelia exposed to cigarette smoke condensate. Oncogene 29, 3650–64. doi:10.1038/onc.2010.129

Liu, R., Xing, M., 2016. TERT promoter mutations in thyroid cancer. Endocr. Relat. Cancer. doi:10.1530/ERC-15-0533

Liu, W.M., Maraia, R.J., Rubin, C.M., Schmid, C.W., 1994. Alu transcripts: cytoplasmic localisation and regulation by DNA methylation. Nucleic Acids Res. 22, 1087–1095. doi:10.1093/nar/22.6.1087

Liu, X., Bishop, J., Shan, Y., Pai, S., Liu, D., Murugan, A.K., Sun, H., El-Naggar, A., Xing, M., 2013. Highly prevalent TERT promoter mutations in aggressive thyroid cancers. Endocr. Relat. Cancer 20, 603–610. doi:10.1530/ERC-13-0210

Liu, X.L., Wazer, D.E., Watanabe, K., Band, V., 1996. Identification of a novel serine protease-like gene, the expression of which is down-regulated during breast cancer progression. Cancer Res. 56, 3371–3379.

LiVolsi, V. a, 2011. Papillary thyroid carcinoma: an update. Mod. Pathol. 24 Suppl 2, S1–S9. doi:10.1038/modpathol.2010.129

Lu, H., Liu, X., Deng, Y., Qing, H., 2013. DNA methylation, a hand behind neurodegenerative diseases. Front. Aging Neurosci. doi:10.3389/fnagi.2013.00085

Ludgate, J.L., Le Mée, G., Fukuzawa, R., Rodger, E.J., Weeks, R.J., Reeve, A.E., Morison, I.M., 2013. Global demethylation in loss of imprinting subtype of wilms tumor. Genes, Chromosom. Cancer 52, 174–184. doi:10.1002/gcc.22017

Ludwig, J.A., Weinstein, J.N., 2005. Biomarkers in cancer staging, prognosis and treatment selection. Nat. Rev. Cancer 5, 845–856. doi:Doi 10.1038/Nrc1739

Lujambio, A., Portela, A., Liz, J., Melo, S.A., Rossi, S., Spizzo, R., Croce, C.M., Calin, G.A., Esteller, M., 2010. CpG island hypermethylation-associated silencing of non-coding RNAs transcribed from ultraconserved regions in human cancer. Oncogene 29, 6390–401. doi:10.1038/onc.2010.361

Luo, Y., Ishido, Y., Hiroi, N., Ishii, N., Suzuki, K., Luo, Y., Ishido, Y., Hiroi, N., Ishii, N., Suzuki, K., 2014. The Emerging Roles of Thyroglobulin. Adv. Endocrinol. 2014, 1–7. doi:10.1155/2014/189194

Lyle, R., Watanabe, D., te Vruchte, D., Lerchner, W., Smrzka, O.W., Wutz, A., Schageman, J., Hahner, L., Davies, C., Barlow, D.P., 2000. The imprinted antisense RNA at the Igf2r locus overlaps but does not imprint Mas1. Nat. Genet. 25, 19–21. doi:10.1038/75546

Ma, R., Latif, R., Davies, T.F., 2015. Human embryonic stem cells form functional thyroid follicles. Thyroid 25, 455–61. doi:10.1089/thy.2014.0537

Magreni, A., Bann, D. V, Schubart, J.R., Goldenberg, D., 2015. The effects of race and ethnicity on thyroid

cancer incidence. JAMA Otolaryngol Head Neck Surg 141, 319–323. doi:10.1001/jamaoto.2014.3740

Mai, K.T., Vaccani, J.P., Thomas, J., Odell, P.F., 2001. Immunostaining for ret oncogene proteins in papillary thyroid carcinoma: a correlation of ret immunoreactivity and potential of lymph node metastasis. Thyroid 11, 859–863. doi:10.1089/105072501316973118

Maier, S., Nimmrich, I., Marx, A., Eppenberger-Castori, S., Jaenicke, F., Paradiso, A., Spyratos, F., Foekens, J., Schmitt, M., Harbeck, N., 2004. DNA methylation profile predicts risk of recurrence in tamoxifen-treated, node-negative breast cancer patients. ASCO Meet. Abstr. 22, 525.

Malumbres, M., Barbacid, M., 2003. RAS oncogenes: the first 30 years. Nat. Rev. Cancer 3, 459–465. doi:10.1038/nrc1193

Mancikova, V., Buj, R., Castelblanco, E., Inglada-Pérez, L., Diez, A., De Cubas, A.A., Curras-Freixes, M., Maravall, F.X., Mauricio, D., Matias-Guiu, X., Puig-Domingo, M., Capel, I., Bella, M.R., Lerma, E., Castella, E., Reverter, J.L., Peinado, M.Á., Jorda, M., Robledo, M., 2014. DNA methylation profiling of well-differentiated thyroid cancer uncovers markers of recurrence free survival. Int. J. Cancer 135, 598–610. doi:10.1002/ijc.28703

Mancikova, V., Castelblanco, E., Pineiro-Yanez, E., Perales-Paton, J., de Cubas, A.A., Inglada-Perez, L., Matias-Guiu, X., Capel, I., Bella, M., Lerma, E., Riesco-Eizaguirre, G., Santisteban, P., Maravall, F., Mauricio, D., Al-Shahrour, F., Robledo, M., 2015. MicroRNA deep-sequencing reveals master regulators of follicular and papillary thyroid tumors. Mod. Pathol. 28, 748–57. doi:10.1038/modpathol.2015.44

Maqbool, F., Mostafalou, S., Bahadar, H., Abdollahi, M., 2016. Review of endocrine disorders associated with environmental toxicants and possible involved mechanisms. Life Sci. 145, 265–273. doi:10.1016/j.lfs.2015.10.022

Marians, R.C., Ng, L., Blair, H.C., Unger, P., Graves, P.N., Davies, T.F., 2002. Defining thyrotropin-dependent and -independent steps of thyroid hormone synthesis by using thyrotropin receptor-null mice. Proc. Natl. Acad. Sci. U. S. A. 99, 15776–81. doi:10.1073/pnas.242322099

Marinò, M., McCluskey, R.T., 2000. Role of thyroglobulin endocytic pathways in the control of thyroid hormone release. Am. J. Physiol. Cell Physiol. 279, C1295–C1306. doi:10.2528/pier13111003

Martín, B., Barrero, M.J., Peinado, M.A., Jordà, M., n.d. The epigenetic landscape of GLDC regulation in cell differentiation and cancer. Under Prep.

Martín, B., Pappa, S., Diez-Villanueva, A., Mallona, I., Barrero, M.J., Peinado, M.A., Jordà, M., n.d. Alu-mediated epigenetic regulation of. Under Prep.

Martínez, M., Lozano Bullrich, M., Rey, M., Ridruejo, M., Bomarito, M., Claus Hermberg, H., Pozzo, M., 2014. Carcinoma diferenciado de tiroides: reclasificación del riesgo de recurrencia según la respuesta al tratamiento inicial. Rev. Argent. Endocrinol. Metab. 51, 8–14.

Marx, V., 2012. Epigenetics: Reading the second genomic code. Nature 491, 143. doi:10.1038/491143a

Marzese, D.M., Hoon, D.S.B., Chong, K.K., Gago, F.E., Orozco, J.I., Tello, O.M., Vargas-Roig, L.M., Roqué, M., 2012. DNA methylation index and methylation profile of invasive ductal breast tumors. J. Mol. Diagnostics 14, 613–622. doi:10.1016/j.jmoldx.2012.07.001

Mathers, J.C., Strathdee, G., Relton, C.L., 2010. Induction of Epigenetic Alterations by Dietary and Other Environmental Factors, Advances in Genetics. doi:10.1016/B978-0-12-380864-6.00001-8

Matsuda, Y., Yamashita, S., Lee, Y.C., Niwa, T., Yoshida, T., Gyobu, K., Igaki, H., Kushima, R., Lee, S., Wu, M.S., Osugi, H., Suehiro, S., Ushijima, T., 2012. Hypomethylation of Alu repetitive elements in esophageal mucosa, and its potential contribution to the epigenetic field for cancerization. Cancer Causes Control 23, 865–873. doi:10.1007/s10552-012-9955-4

Maunakea, A.K., Chepelev, I., Cui, K.R., Zhao, K.J., 2013. Intragenic DNA methylation modulates alternative splicing by recruiting MeCP2 to promote exon recognition. Cell Res. 23, 1256–1269. doi:10.1038/cr.2013.110

Maunakea, A.K., Nagarajan, R.P., Bilenky, M., Ballinger, T.J., D'Souza, C., Fouse, S.D., Johnson, B.E., Hong, C., Nielsen, C., Zhao, Y., Turecki, G., Delaney, A., Varhol, R., Thiessen, N., Shchors, K., Heine, V.M., Rowitch, D.H., Xing, X., Fiore, C., Schillebeeckx, M., Jones, S.J.M., Haussler, D., Marra, M. a, Hirst, M., Wang, T., Costello, J.F., 2010. Conserved role of intragenic DNA methylation in regulating alternative promoters. Nature 466, 253–257. doi:10.1038/nature09165

Mayeux, R., 2004. Biomarkers: potential uses and limitations. NeuroRx 1, 182–8. doi:10.1602/neurorx.1.2.182

Maze, I., Noh, K.-M., Soshnev, A.A., Allis, C.D., 2014. Every amino acid matters: essential contributions of histone variants to mammalian development and disease. Nat. Rev. Genet. 15, 259–71. doi:10.1038/nrg3673

Mazumder ' Indra, D., Mitra, S., Singh, R.K., Dutta, S., Roy, A., Mondal, R.K., Basu, P.S., Roychoudhury, S., Panda, C.K., 2010. Inactivation of CHEK1 and EI24 are associated with the development of invasive cervical carcinoma: Clinical and prognostic implications. Int J Cancer. doi:10.1002/ijc.25849

McHenry, C.R., Phitayakorn, R., 2011. Follicular adenoma and carcinoma of the thyroid gland. Oncologist 16, 585–593. doi:10.1634/theoncologist.2010-0405

McIver, B., Castro, M.R., Morris, J.C., Bernet, V., Smallridge, R., Henry, M., Kosok, L., Reddi, H., 2014. An independent study of a gene expression classifier (Afirma) in the evaluation of cytologically indeterminate thyroid nodules. J. Clin. Endocrinol. Metab. 99, 4069–4077. doi:10.1210/jc.2013-3584

McLeod, D.S.A., Carruthers, K., Kevat, D.A.S., 2015. Optimal differentiated thyroid cancer management in the elderly. Drugs Aging 32, 283–94. doi:10.1007/s40266-015-0256-y

Melillo, R.M., Santoro, M., 2012. Molecular Biomarkers in Thyroid FNA Samples. J. Clin. Endocrinol. Metab. 97, 4370–4373. doi:10.1210/jc.2012-3730

Memon, A., Godward, S., Williams, D., Siddique, I., Al-Saleh, K., 2010. Dental x-rays and the risk of thyroid cancer: a case-control study. Acta Oncol 49, 447–453. doi:10.3109/02841861003705778

Mendel, G., 1865. Verhandlungen des naturforschenden Vereines in Brünn, Bd. IV für das Jahr, 1865, Abhandlungen, in: Versuche Über Pflanzenhybriden. pp. 3–47.

Mendoza- Pérez, J., Gu, J., Herrera, L.A., Tannir, N.M., Matin, S.F., Karam, J.A., Huang, M., Chang, D.W., Wood, C.G., Wu, X., 2016. Genomic DNA Hypomethylation and Risk of Renal Cell Carcinoma: A Case–Control Study. Clin. Cancer Res. 22.

Miccoli, P., 2014. Application of molecular diagnostics to the evaluation of the surgical approach to thyroid cancer. Curr. Genomics 15, 184–9. doi:10.2174/1389202915999140404101257

Mikeska, T., Craig, J.M., 2014. DNA methylation biomarkers: Cancer and beyond. Genes (Basel). doi:10.3390/genes5030821

Mills, S.C., Haq, M., Smellie, W.J.B., Harmer, C., 2009. H??rthle cell carcinoma of the thyroid: Retrospective review of 62 patients treated at the Royal Marsden Hospital between 1946 and 2003. Eur. J. Surg. Oncol. 35, 230–234. doi:10.1016/j.ejso.2008.06.007

Miot, F., Dupuy, C., Dumont, J., Rousset, B., 2000. Chapter 2 Thyroid Hormone Synthesis And Secretion, Endotext.

Miralles García, J.M., Leiva Hidalgo, A. de, 2001. Enfermedades del sistema endocrino y de la nutrición. Ediciones Universidad de Salamanca.

Mistry, D., Atkin, S., Atkinson, H., Gunasekaran, S., Sylvester, D., Rigby, A.S., England, R.J., 2011. Predicting thyroxine requirements following total thyroidectomy. Clin. Endocrinol. (Oxf). 74, 384–387. doi:10.1111/j.1365-2265.2010.03940.x

Mitchell, I., Livingston, E.H., Chang, A.Y., Holt, S., Snyder, W.H., Lingvay, I., Nwariaku, F.E., 2007. Trends in thyroid cancer demographics and surgical therapy in the United States. Surgery 142, 823–828. doi:10.1016/j.surg.2007.09.011

Mo, L., Zhang, J., Shi, J., Xuan, Q., Yang, X., Qin, M., Lee, C., Klocker, H., Li, Q.Q., Mo, Z., 2010. Human kallikrein 7 induces epithelial-mesenchymal transition-like changes in prostate carcinoma cells: A role in prostate cancer invasion and progression. Anticancer Res. 30, 3413–3420. doi:30/9/3413 [pii]

Mohebati, A., Shaha, A.R., 2012. Anatomy of thyroid and parathyroid glands and neurovascular relations. Clin. Anat. doi:10.1002/ca.21220

Mondal, S., Raja, K., Schweizer, U., Mugesh, G., 2016. Chemistry and Biology in the Biosynthesis and Action of Thyroid Hormones. Angew. Chemie Int. Ed. 55, 7606–7630. doi:10.1002/anie.201601116

Montero-Conde, C., Martín-Campos, J.M., Lerma, E., Gimenez, G., Martínez-Guitarte, J.L., Combalía, N., Montaner, D., Matías-Guiu, X., Dopazo, J., de Leiva, A., Robledo, M., Mauricio, D., 2008. Molecular profiling related to poor prognosis in thyroid carcinoma. Combining gene expression data and biological information. Oncogene 27, 1554–1561. doi:10.1038/sj.onc.1210792

Montone, K.T., Baloch, Z.W., LiVolsi, V.A., 2008. The thyroid H??rthle (oncocytic) cell and its associated pathologic conditions: A surgical pathology and cytopathology review. Arch. Pathol. Lab. Med. doi:10.1043/1543-2165(2008)132[1241:TTHOCA]2.0.CO;2

Moore, L.E., Pfeiffer, R.M., Poscablo, C., Real, F.X., Kogevinas, M., Silverman, D., Garc??a-Closas, R., Chanock, S., Tard??n, A., Serra, C., Carrato, A., Dosemeci, M., Garc??a-Closas, M., Esteller, M., Fraga, M., Rothman, N., Malats, N., 2008. Genomic DNA hypomethylation as a biomarker for bladder cancer susceptibility in the Spanish Bladder Cancer Study: a case-control study. Lancet Oncol. 9, 359–366. doi:10.1016/S1470-2045(08)70038-X

Moran, S., Martínez-Cardús, A., Sayols, S., Musulén, E., Balañá, C., Estival-Gonzalez, A., Moutinho, C., Heyn, H., Diaz-Lagares, A., Castro De Moura, M., Stella, G.M., Comoglio, P.M., Ruiz-Miró, M., Matias-Guiu, X., Pazo-Cid, R., Antón, A., Lopez-Lopez, R., Soler, G., Longo, F., Guerra, I., Fernandez, S., Assenov, Y., Plass, C., Morales, R., Carles, J., Bowtell, D., Mileshkin, L., Sia, D., Tothill, R., Tabernero, J., Llovet, J.M., Esteller, M., 2016. Articles Epigenetic profi ling to classify cancer of unknown primary: a multicentre, retrospective analysis. Funding Eur. Res. Counc. doi:10.1016/S1470-2045(16)30297-2

Mork, C.N., Faller, D. V., Spanjaard, R.A., 2007. Loss of putative tumor suppressor EI24/PIG8 confers resistance to etoposide. FEBS Lett. 581, 5440–5444. doi:10.1016/j.febslet.2007.10.046

Morton, N.E., 1991. Parameters of the human genome. Proc. Natl. Acad. Sci. U. S. A. 88, 7474–7476. doi:10.1073/pnas.88.17.7474

Moses, W., Weng, J., Kebebew, E., 2011. Prevalence, clinicopathologic features, and somatic genetic mutation profile in familial versus sporadic nonmedullary thyroid cancer. Thyroid 21, 367–371. doi:10.1089/thy.2010.0256

Mount, D.B., Romero, M.F., 2004. The SLC26 gene family of multifunctional anion exchangers. Pflügers Arch. Eur. J. Physiol. 447, 710–21. doi:10.1007/s00424-003-1090-3

Moyzis, R.K., Buckingham, J.M., Cram, L.S., Dani, M., Deaven, L.L., Jones, M.D., Meyne, J., Ratcliff, R.L., Wu, J.R., 1988. A highly conserved repetitive DNA sequence, (TTAGGG)n, present at the telomeres\rof human chromosomes. Proc. Natl. Acad. Sci. U S A.

Murrell, A., Ito, Y., Verde, G., Huddleston, J., Woodfine, K., Silengo, M.C., Spreafico, F., Perotti, D., De Crescenzo, A., Sparago, A., Cerrato, F., Riccio, A., 2008. Distinct methylation changes at the IGF2-H19 locus in congenital growth disorders and cancer. PLoS One 3. doi:10.1371/journal.pone.0001849

Nakata, T., Yokota, T., Emi, M., Minami, S., 2002. Differential expression of multiple isoforms of theELKS mRNAs involved in a papillary thyroid carcinoma. Genes,

Chromosom. Cancer 35, 30–37. doi:10.1002/gcc.10095

Narayanan, S., Colevas, A.D., 2016. Current Standards in Treatment of Radioiodine Refractory Thyroid Cancer. Curr. Treat. Options Oncol. 17, 30. doi:10.1007/s11864-016-0404-6

Network, T.C.G.A.R., Cancer, T., Atlas, G., 2014. Comprehensive molecular characterization of urothelial bladder carcinoma. Nature 507, 315–22. doi:10.1038/nature12965

Nielsen, S.J., Schneider, R., Bauer, U.M., Bannister, A.J., Morrison, A., O'Carroll, D., Firestein, R., Cleary, M., Jenuwein, T., Herrera, R.E., Kouzarides, T., 2001. Rb targets histone H3 methylation and HP1 to promoters. Nature 412, 561–5. doi:10.1038/35087620

Nikiforov, Y.E., 2011. Molecular analysis of thyroid tumors. doi:10.1038/modpathol.2010.167

Nikiforov, Y.E., n.d. MOLECULAR " REFLEX TESTING " OF THYROID FNA.

Nikiforov, Y.E., Nikiforova, M.N., 2011. Molecular genetics and diagnosis of thyroid cancer. Nat. Rev. Endocrinol. 7, 569–580. doi:10.1038/nrendo.2011.142

Nikiforov, Y.E., Ohori, N.P., Hodak, S.P., Carty, S.E., LeBeau, S.O., Ferris, R.L., Yip, L., Seethala, R.R., Tublin, M.E., Stang, M.T., Coyne, C., Johnson, J.T., Stewart, A.F., Nikiforova, M.N., 2011. Impact of mutational testing on the diagnosis and management of patients with cytologically indeterminate thyroid nodules: a prospective analysis of 1056 FNA samples. J. Clin. Endocrinol. Metab. 96, 3390–7. doi:10.1210/jc.2011-1469

Nikiforov, Y.E., Steward, D.L., Robinson-Smith, T.M., Haugen, B.R., Klopper, J.P., Zhu, Z., Fagin, J. a, Falciglia, M., Weber, K., Nikiforova, M.N., 2009. Molecular testing for mutations in improving the fine-needle aspiration diagnosis of thyroid nodules. J. Clin. Endocrinol. Metab. 94, 2092–2098. doi:10.1210/jc.2009-0247

Nikiforova, M.N., Nikiforov, Y.E., 2008. Molecular genetics of thyroid cancer: implications for diagnosis, treatment and prognosis. Expert Rev. Mol. Diagn. 8, 83–95. doi:10.1586/14737159.8.1.83

Nik-Zainal, S., Alexandrov, L.B., Wedge, D.C., Van Loo, P., Greenman, C.D., Raine, K., Jones, D., Hinton, J., Marshall, J., Stebbings, L.A., Menzies, A., Martin, S., Leung, K., Chen, L., Leroy, C., Ramakrishna, M., Rance, R., Lau, K.W., Mudie, L.J., Varela, I., McBride, D.J., Bignell, G.R., Cooke, S.L., Shlien, A., Gamble, J., Whitmore, I., Maddison, M., Tarpey, P.S., Davies, H.R., Papaemmanuil, E., Stephens, P.J., McLaren, S., Butler, A.P., Teague, J.W., Jönsson, G., Garber, J.E., Silver, D., Miron, P., Fatima, A., Boyault, S., Langerod, A., Tutt, A., Martens, J.W.M., Aparicio, S.A.J.R., Borg, Å., Salomon, A.V., Thomas, G., Borresen-Dale, A.L., Richardson, A.L., Neuberger, M.S., Futreal, P.A., Campbell, P.J., Stratton, M.R., 2012. Mutational processes molding the genomes of 21 breast cancers. Cell 149, 979–993. doi:10.1016/j.cell.2012.04.024

Noma K, Allis, C.D., Grewal, S.I., 2001. Transitions in distinct histone H3 methylation patterns at the heterochromatin domain boundaries. Science 293, 1150–5. doi:10.1126/science.1064150

Noordin, S., Glowacki, J., 2016. Parathyroid hormone and its receptor gene polymorphisms: implications in osteoporosis and in fracture healing. Rheumatol. Int. 36, 1–6. doi:10.1007/s00296-015-3319-9

Nosé, V., 2011. Familial thyroid cancer: a review. Mod. Pathol. 24. doi:10.1038/modpathol.2010.147

Nowell, P.C., 1976. The clonal evolution of tumor cell populations. Science. doi:10.1126/science.959840

O'Neill, R.J., O'Neill, M.J., Graves, J.A., 1998. Undermethylation associated with retroelement activation and chromosome remodelling in an interspecific mammalian hybrid. Nature 393, 68–72. doi:10.1038/29985

Oikonomopoulou, K., Li, L., Zheng, Y., Simon, I., Wolfert, R.L., Valik, D., Nekulova, M., Simickova, M., Frgala, T., Diamandis, E.P., 2008. Prediction of ovarian cancer prognosis and response to chemotherapy by a serum-based multiparametric biomarker panel. Br. J. Cancer 99, 1103–13. doi:10.1038/sj.bjc.6604630

Olins, D.E., Olins, A.L., 2003. Chromatin history: our view from the bridge. Nat. Rev. Mol. Cell Biol. 4, 809–14. doi:10.1038/nrm1225

Omur, O., Baran, Y., 2014. An update on molecular biology of thyroid cancers. Crit. Rev. Oncol. Hematol. doi:10.1016/j.critrevonc.2013.12.007

Osamor, V.C., Chinedu, S.N., Azuh, D.E., Iweala, E.J., Ogunlana, O.O., 2016. The interplay of post-translational modification and gene therapy. Drug Des. Devel. Ther. doi:10.2147/DDDT.S80496

Pacini, F., Castagna, M.G., Cipri, C., Schlumberger, M., 2010. Medullary thyroid carcinoma. Clin. Oncol. (R. Coll. Radiol). 22, 475–85. doi:10.1016/j.clon.2010.05.002

Pacini, F., Schlumberger, M., Dralle, H., Elisei, R., Smit, J.W.A., Wiersinga, W., 2006. European consensus for the management of patients with differentiated thyroid carcinoma of the follicular epithelium. Eur. J. Endocrinol. 154, 787–803. doi:10.1530/eje.1.02158

Pallante, P., Visone, R., Ferracin, M., Ferraro, A., Berlingieri, M.T., Troncone, G., Chiappetta, G., Liu, C.G., Santoro, M., Negrini, M., Croce, C.M., Fusco, A., 2006. MicroRNA deregulation in human thyroid papillary carcinomas. Endocr. Relat. Cancer 13, 497–508. doi:10.1677/erc.1.01209

Papadopoulou, E., Davilas, E., Sotiriou, V., Georgakopoulos, E., Georgakopoulou, S., Koliopanos, A., Aggelakis, F., Dardoufas, K., Agnanti, N.J., Karydas, I., Nasioulas, G., 2006. Cell-free DNA and RNA in Plasma as a New Molecular Marker for Prostate and Breast Cancer. Ann. N. Y. Acad. Sci. 1075, 235–243. doi:10.1196/annals.1368.032

Parameswaran, R., Brooks, S., Sadler, G.P., 2010. Molecular pathogenesis of follicular cell derived thyroid cancers. Int. J. Surg. doi:10.1016/j.ijsu.2010.01.005

Park, S.Y., Seo, A.N., Jung, H.Y., Gwak, J.M., Jung, N., Cho, N.Y., Kang, G.H., 2014. Alu and LINE-1

hypomethylation is associated with HER2 enriched subtype of breast cancer. PLoS One 9. doi:10.1371/journal.pone.0100429

Parlato, R., Rosica, A., Rodriguez-Mallon, A., Affuso, A., Postiglione, M.P., Arra, C., Mansouri, A., Kimura, S., Di Lauro, R., De Felice, M., 2004. An integrated regulatory network controlling survival and migration in thyroid organogenesis. Dev. Biol. 276, 464–475. doi:10.1016/j.ydbio.2004.08.048

Pearce, M.S., Salotti, J.A., Little, M.P., McHugh, K., Lee, C., Kim, K.P., Howe, N.L., Ronckers, C.M., Rajaraman, P., Sir Craft, A.W., Parker, L., Berrington de Gonzalez, A., 2012. Radiation exposure from CT scans in childhood andsubsequent risk of leukaemia and brain tumours:a retrospective cohort study. Lancet 380, 499–505. doi:10.1016/S0140-6736(12)60815-0

Pellegriti, G., Frasca, F., Regalbuto, C., Squatrito, S., Vigneri, R., 2013. Worldwide increasing incidence of thyroid cancer: Update on epidemiology and risk factors. J. Cancer Epidemiol. doi:10.1155/2013/965212

Phitayakorn R1, M.C., 2006. Follicular and Hürthle cell carcinoma of the thyroid gland. Surg Oncol Clin N Am 3, 603–23. doi:10.1016/j.soc.2006.05.011

Piacentini, L., Fanti, L., Negri, R., Del Vescovo, V., Fatica, A., Altieri, F., Pimpinelli, S., 2009. Heterochromatin Protein 1 (HP1a) positively regulates euchromatic gene expression through RNA transcript association and interaction with hnRNPs in Drosophila. PLoS Genet. 5. doi:10.1371/journal.pgen.1000670

Pinchot, S.N., Sippel, R.S., Chen, H., 2008. Multi-targeted approach in the treatment of thyroid cancer. Ther. Clin. Risk Manag. doi:R06105226 [pii]

Pokholok, D.K., Harbison, C.T., Levine, S., Cole, M., Hannett, N.M., Lee, T.I., Bell, G.W., Walker, K., Rolfe, P.A., Herbolsheimer, E., Zeitlinger, J., Lewitter, F., Gifford, D.K., Young, R.A., 2005. Genome-wide map of nucleosome acetylation and methylation in yeast. Cell 122, 517–27. doi:10.1016/j.cell.2005.06.026

Popovici, V., Budinska, E., Tejpar, S., Weinrich, S., Estrella, H., Hodgson, G., Van Cutsem, E., Xie, T., Bosman, F.T., Roth, A.D., Delorenzi, M., 2012. Identification of a poor-prognosis BRAF-mutant-like population of patients with colon cancer. J. Clin. Oncol. 30, 1288–95. doi:10.1200/JCO.2011.39.5814

Postiglione, M.P., Parlato, R., Rodriguez-Mallon, A., Rosica, A., Mithbaokar, P., Maresca, M., Marians, R.C., Davies, T.F., Zannini, M.S., De Felice, M., Di Lauro, R., 2002. Role of the thyroid-stimulating hormone receptor signaling in development and differentiation of the thyroid gland. Proc. Natl. Acad. Sci. U. S. A. 99, 15462–7. doi:10.1073/pnas.242328999

Prassas, I., Eissa, A., Poda, G., Diamandis, E.P., 2015. Unleashing the therapeutic potential of human kallikrein-related serine proteases. Nat. Rev. Drug Discov. 14, 183–202. doi:10.1038/nrd4534

Prior, I.A., Hancock, J.F., 2001. Compartmentalization of Ras proteins. J. Cell Sci. 114, 1603–8.

Prior, I.A., Lewis, P.D., Mattos, C., 2012. A comprehensive survey of ras mutations in cancer. Cancer Res. doi:10.1158/0008-5472.CAN-11-2612

Puxeddu, E., Durante, C., Avenia, N., Filetti, S., Russo, D., Schlumberger, M., al., et, Cooper, D.S., al., et, Xing, M., Espinosa, A.V., al., et, Wellbrock, C., al., et, Davies, H., al., et, Moretti, S., al., et, Ciampi, R., al., et, Wan, P.T., al., et, Kimura, E.T., al., et, Melillo, R.M., al., et, Mitsutake, N., al., et, Ugolini, C., al., et, Sedliarou, I., al., et, Kim, T.Y., al., et, Knauf, J.A., al., et, Lee, J.H., al., et, Fugazzola, L., al., et, Kebebew, E., al., et, Trovisco, V., al., et, Adeniran, A.J., al., et, Nikiforova, M.N., al., et, Yamashita, S., Saenko, V., Filetti, S., al., et, Cohen, Y., al., et, Salvatore, G., al., et, Xing, M., al., et, Hayashida, N., al., et, Chung, K.W., al., et, Rowe, L.R., al., et, Sapio, M.R., al., et, Kumagai, A., al., et, Pizzolanti, G., al., et, Tallini, G., Fugazzola, L., al., et, Xu, X., al., et, Puxeddu, E., al., et, Riesco-Eizaguirre, G., al., et, Kim, K.H., al., et, Lee, J.H., al., et, Liu, R.T., al., et, Namba, H., al., et, Jo, Y.S., al., et, Kim, T.Y., al., et, Xing, M., al., et, Lupi, C., al., et, Vasko, V., al., et, Kim, J., al., et, Rodolico, V., al., et, Xing, M., Durante, C., al., et, Groussin, L., Fagin, J.A., Solit, D.B., al., et, Ouyang, B., al., et, Salvatore, G., al., et, Mitsiades, C.S., al., et, Liu, D., al., et, Kim, S., al., et, Roberts, P.J., Der, C.J., Sebolt-Leopold, J.S., English, J.M., Kolch, W., al., et, Mitsutake, N., al., et, Mesa, C., al., et, Palona, I., al., et, Liu, D., al., et, Giordano, T.J., al., et, Frattini, M., al., et, Porra, V., al., et, Hu, S., al., et, Cristofaro, J. Di, al., et, Holt, E., 2003. Clinical implications of BRAF mutation in thyroid carcinoma. Trends Endocrinol. Metab. 19, 138–45. doi:10.1016/j.tem.2007.12.003

Rabes, H.M., Demidchik, E.P., Sidorow, J.D., Lengfelder, E., Beimfohr, C., Hoelzel, D., Klugbauer, S., 2000. Pattern of Radiation-induced RET and NTRK1 Rearrangements in 191 Post-Chernobyl Papillary Thyroid Carcinomas: Biological, Phenotypic, and Clinical Implications. Clin. Cancer Res. 6, 1093–10103.

Radman-Livaja, M., Rando, O.J., 2010. Nucleosome positioning: How is it established, and why does it matter? Dev. Biol. doi:10.1016/j.ydbio.2009.06.012

Raju, I., Kaushal, G.P., Haun, R.S., 2016. Epigenetic regulation of KLK7 gene expression in pancreatic and cervical cancer cells. Biol. Chem. doi:10.1515/hsz-2015-0307

Rakyan, V.K., Down, T.A., Thorne, N.P., Flicek, P., Kulesha, E., Gr??f, S., Tomazou, E.M., B??ckdahl, L., Johnson, N., Herberth, M., Howe, K.L., Jackson, D.K., Miretti, M.M., Fiegler, H., Marioni, J.C., Birney, E., Hubbard, T.J.P., Carter, N.P., Tavar??, S., Beck, S., 2008. An integrated resource for genome-wide identification and analysis of human tissue-specific differentially methylated regions (tDMRs). Genome Res. 18, 1518–1529. doi:10.1101/gr.077479.108

Raman, P., Koenig, R.J., 2014. Pax-8-PPAR-γ fusion protein in thyroid carcinoma. Nat. Rev. Endocrinol. 10, 616–23. doi:10.1038/nrendo.2014.115

Ramani, V.C., Kaushal, G.P., Haun, R.S., 2011. Proteolytic action of kallikrein-related peptidase 7 produces unique active matrix metalloproteinase-9 lacking the C-terminal hemopexin domains. Biochim. Biophys. Acta - Mol. Cell Res. 1813, 1525–1531. doi:10.1016/j.bbamcr.2011.05.007

Raue, F., Frank-Raue, K., 2015. Epidemiology and Clinical Presentation of Medullary Thyroid Carcinoma. Recent

Results Cancer Res 204, 61–90. doi:10.1007/978-3-319-22542-5_3

Real Academia Española, 2014. DICCIONARIO DE LA LENGUA ESPAÑOLA [WWW Document]. El Dicc. la Leng. española. URL http://lema.rae.es/drae/?val=practica

Rebaï, M., Rebaï, A., 2016. Molecular genetics of thyroid cancer. Genet. Res. (Camb). 98, e7. doi:10.1017/S0016672316000057

Rego-Iraeta, A., Pérez-Méndez, L.F., Mantinan, B., Garcia-Mayor, R. V, 2009. Time trends for thyroid cancer in northwestern Spain: true rise in the incidence of micro and larger forms of papillary thyroid carcinoma. Thyroid 19, 333–40. doi:10.1089/thy.2008.0210

Renehan, A.G., Tyson, M., Egger, M., Heller, R.F., Zwahlen, M., 2008. Body-mass index and incidence of cancer: a systematic review and meta-analysis of prospective observational studies. Lancet 371, 569–78. doi:10.1016/S0140-6736(08)60269-X

Rezzónico, J.N., Rezzónico, M., Pusiol, E., Pitoia, F., Niepomniszcze, H., 2009. Increased prevalence of insulin resistance in patients with differentiated thyroid carcinoma. Metab. Syndr. Relat. Disord. 7, 375–380. doi:10.1089/met.2008.0062

Rhee, J.-K., Kim, K., Chae, H., Evans, J., Yan, P., Zhang, B.-T., Gray, J., Spellman, P., Huang, T.H.-M., Nephew, K.P., Kim, S., 2013. Integrated analysis of genome-wide DNA methylation and gene expression profiles in molecular subtypes of breast cancer. Nucleic Acids Res. 41, 8464–74. doi:10.1093/nar/gkt643

Ricarte-Filho, J.C., Ryder, M., Chitale, D.A., Rivera, M., Heguy, A., Ladanyi, M., Janakiraman, M., Solit, D., Knauf, J.A., Tuttle, R.M., Ghossein, R.A., Fagin, J.A., 2009. Mutational Profile of Advanced Primary and Metastatic Radioactive Iodine-Refractory Thyroid Cancers Reveals Distinct Pathogenetic Roles for BRAF, PIK3CA, and AKT1. Cancer Res. 69.

Rinaldi, S., Lise, M., Clavel-Chapelon, F., Boutron-Ruault, M.C., Guillas, G., Overvad, K., Tjønneland, A., Halkjær, J., Lukanova, A., Kaaks, R., Bergmann, M.M., Boeing, H., Trichopoulou, A., Zylis, D., Valanou, E., Palli, D., Agnoli, C., Tumino, R., Polidoro, S., Mattiello, A., Bas Bueno-De-Mesquita, H., Peeters, P.H., Weiderpass, E., Lund, E., Skeie, G., Rodríguez, L., Travier, N., Sánchez, M.J., Amiano, P., Huerta, J.M., Ardanaz, E., Rasmuson, T., Hallmans, G., Almquist, M., Manjer, J., Tsilidis, K.K., Allen, N.E., Khaw, K.T., Wareham, N., Byrnes, G., Romieu, I., Riboli, E., Franceschi, S., 2012. Body size and risk of differentiated thyroid carcinomas: Findings from the EPIC study. Int. J. Cancer 131. doi:10.1002/ijc.27601

Rodrigues, H.G., de Pontes, A.A., Adan, L.F., 2012. Use of molecular markers in samples obtained from preoperative aspiration of thyroid. Endocr J 59, 417–424. doi:10.1507/endocrj.EJ11-0410

Rodriguez, J., Frigola, J., Vendrell, E., Risques, R.-A., Fraga, M.F., Morales, C., Moreno, V., Esteller, M., Capellà, G., Ribas, M., Peinado, M. a, 2006. Chromosomal instability correlates with genome-wide DNA demethylation in human primary colorectal cancers. Cancer Res. 66, 8462–9468. doi:10.1158/0008-5472.CAN-06-0293

Rodríguez-Rodero, S., Fernández, A.F., Fernández-Morera, J.L., Castro-Santos, P., Bayon, G.F., Ferrero, C., Urdinguio, R.G., Gonzalez-Marquez, R., Suarez, C., Fernández-Vega, I., Fresno Forcelledo, M.F., Martínez-Camblor, P., Mancikova, V., Castelblanco, E., Perez, M., Marrón, P.I., Mendiola, M., Hardisson, D., Santisteban, P., Riesco-Eizaguirre, G., Matías-Guiu, X., Carnero, A., Robledo, M., Delgado-Álvarez, E., Menéndez-Torre, E., Fraga, M.F., 2013. DNA methylation signatures identify biologically distinct thyroid cancer subtypes. J. Clin. Endocrinol. Metab. 98, 2811–21. doi:10.1210/jc.2012-3566

Rollins, R.A., Haghighi, F., Edwards, J.R., Das, R., Zhang, M.Q., Ju, J., Bestor, T.H., 2006. Large-scale structure of genomic methylation patterns. Genome Res. 16, 157–163. doi:10.1101/gr.4362006

Roman-Gomez, J., Jimenez-Velasco, A., Agirre, X., Castillejo, J.A., Barrios, M., Andreu, E.J., Prosper, F., Heiniger, A., Torres, A., 2004. The normal epithelial cell-specific 1 (NES1) gene, a candidate tumor suppressor gene on chromosome 19q13.3-4, is downregulated by hypermethylation in acute lymphoblastic leukemia. Leukemia 18, 362–5. doi:10.1038/sj.leu.2403223

Romei, C., Elisei, R., 2012. RET/PTC Translocations and Clinico-Pathological Features in Human Papillary Thyroid Carcinoma. Front. Endocrinol. (Lausanne). 3, 54. doi:10.3389/fendo.2012.00054

Rosai, J., Saxén, E.A., Woolner, L., 1985. Undifferentiated and poorly differentiated carcinoma. Semin. Diagn. Pathol. 2, 123–36.

Rückert, F., Hennig, M., Petraki, C.D., Wehrum, D., Distler, M., Denz, a, Schröder, M., Dawelbait, G., Kalthoff, H., Saeger, H.-D., Diamandis, E.P., Pilarsky, C., Grützmann, R., 2008. Co-expression of KLK6 and KLK10 as prognostic factors for survival in pancreatic ductal adenocarcinoma. Br. J. Cancer 99, 1484–92. doi:10.1038/sj.bjc.6604717

Russo, D., Damante, G., Puxeddu, E., Durante, C., Filetti, S., 2011. REVIEW Epigenetics of thyroid cancer and novel therapeutic targets. J. Mol. Endocrinol. 46, 73–81. doi:10.1530/JME-10-0150

Sadow, P.M., Hunt, J.L., 2011. Update on clinically important variants of papillary thyroid carcinoma. Diagnostic Histopathol. 17, 106–113. doi:10.1016/j.mpdhp.2010.12.005

Saenko, V., Rogounovitch, T., Shimizu-Yoshida, Y., Abrosimov, A., Lushnikov, E., Roumiantsev, P., Matsumoto, N., Nakashima, M., Meirmanov, S., Ohtsuru, A., Namba, H., Tsyb, A., Yamashita, S., 2003. Novel tumorigenic rearrangement, rfp/ret, in a papillary thyroid carcinoma from externally irradiated patient. Mutat. Res. 527, 81–90. doi:10.1016/S0027-5107(03)00056-3

Saini, S., 2016. PSA and beyond: alternative prostate cancer biomarkers. Cell. Oncol. doi:10.1007/s13402-016-0268-6

Saito, K., Kawakami, K., Matsumoto, I., Oda, M., Watanabe, G., Minamoto, T., 2010. Long interspersed nuclear element 1 hypomethylation is a marker of poor prognosis in stage IA non-small cell lung cancer. Clin. Cancer Res. 16, 2418–2426. doi:10.1158/1078-0432.CCR-09-2819

Salas, L.A., Villanueva, C.M., Tajuddin, S.M., Amaral, A.F.S., Fernandez, A.F., Moore, L.E., Carrato, A., Tardón, A., Serra, C., García-Closas, R., Basagaña, X., Rothman, N., Silverman, D.T., Cantor, K.P., Kogevinas, M., Real, F.X., Fraga, M.F., Malats, N., 2014. LINE-1 methylation in granulocyte DNA and trihalomethane exposure is associated with bladder cancer risk. Epigenetics 9, 1532–1539. doi:10.4161/15592294.2014.983377

Salassidis, K., Bruch, J., Zitzelsberger, H., Lengfelder, E., Kellerer, A.M., Bauchinger, M., 2000. Translocation t(10;14)(q11.2:q22.1) fusing the kinetin to the RET gene creates a novel rearranged form (PTC8) of the RET proto-oncogene in radiation-induced childhood papillary thyroid carcinoma. Cancer Res. 60, 2786–9.

Sandoval, J., Esteller, M., 2012. Cancer epigenomics: Beyond genomics. Curr. Opin. Genet. Dev. doi:10.1016/j.gde.2012.02.008

Sandoval, J., Mendez-Gonzalez, J., Nadal, E., Chen, G., Carmona, F.J., Sayols, S., Moran, S., Heyn, H., Vizoso, M., Gomez, A., Sanchez-Cespedes, M., Assenov, Y., Müller, F., Bock, C., Taron, M., Mora, J., Muscarella, L.A., Liloglou, T., Davies, M., Pollan, M., Pajares, M.J., Torre, W., Montuenga, L.M., Brambilla, E., Field, J.K., Roz, L., Lo Iacono, M., Scagliotti, G. V., Rosell, R., Beer, D.G., Esteller, M., 2013. A prognostic DNA methylation signature for stage I non-small-cell lung cancer. J. Clin. Oncol. 31, 4140–4147. doi:10.1200/JCO.2012.48.5516

Sanso, G.E., Domene, H.M., Garcia, R., Pusiol, E., de, M., Roque, M., Ring, A., Perinetti, H., Elsner, B., Iorcansky, S., Barontini, M., 2002. Very early detection of RET proto-oncogene mutation is crucial for preventive thyroidectomy in multiple endocrine neoplasia type 2 children: presence of C-cell malignant disease in asymptomatic carriers. Cancer 94, 323–30. doi:10.1002/cncr.10228

Santin, A.D., Diamandis, E.P., Bellone, S., Marizzoni, M., Bandiera, E., Palmieri, M., Papasakelariou, C., Katsaros, D., Burnett, A., Pecorelli, S., 2006. Overexpression of kallikrein 10 (hK10) in uterine serous papillary carcinomas. Am. J. Obstet. Gynecol. 194, 1296–1302. doi:10.1016/j.ajog.2005.10.794

Santisteban, P., Acebrón, A., Polycarpou-Schwarz, M., Di Lauro, R., 1992. Insulin and insulin-like growth factor I regulate a thyroid-specific nuclear protein that binds to the thyroglobulin promoter. Mol. Endocrinol. 6, 1310–7. doi:10.1210/mend.6.8.1406708

Saxonov, S., Berg, P., Brutlag, D.L., 2005. A genome-wide analysis of CpG dinucleotides in the human genome distinguishes two distinct classes of promoters.

Schagdarsurengin, U., Richter, A.M., Hornung, J., Lange, C., Steinmann, K., Dammann, R.H., 2010. Frequent epigenetic inactivation of RASSF2 in thyroid cancer and functional consequences. Mol. Cancer 9, 264. doi:10.1186/1476-4598-9-264

Scheffzek, K., Ahmadian, M.R., Kabsch, W., Wiesmüller, L., Lautwein, A., Schmitz, F., Wittinghofer, A., 1997. The Ras-RasGAP complex: structural basis for GTPase activation and its loss in oncogenic Ras mutants. Science 277, 333–8.

Schlumberger, M.J., 1998. Papillary and follicular thyroid carcinoma. N. Engl. J. Med. 338, 297–306. doi:10.1056/NEJM199801293380506

Schmid, C.W., Deininger, P.L., 1975. Sequence organization of the human genome. Cell 6, 345–358. doi:10.1016/0092-8674(75)90184-1

Schmid, K.W., 2015. Histopathology of C cells and medullary thyroid carcinoma, in: Recent Results in Cancer Research. pp. 41–60. doi:10.1007/978-3-319-22542-5_2

Schmitt, M., Magdolen, V., Yang, F., Kiechle, M., Bayani, J., Yousef, G.M., Scorilas, A., Diamandis, E.P., Dorn, J., 2013. Emerging clinical importance of the cancer biomarkers kallikrein-related peptidases (KLK) in female and male reproductive organ malignancies. Radiol. Oncol. 47, 319–29. doi:10.2478/raon-2013-0053

Schubbert, S., Shannon, K., Bollag, G., 2007. Hyperactive Ras in developmental disorders and cancer. Nat. Rev. Cancer 7, 295–308. doi:10.1038/nrc2109

Schübeler, D., MacAlpine, D.M., Scalzo, D., Wirbelauer, C., Kooperberg, C., van Leeuwen, F., Gottschling, D.E., O'Neill, L.P., Turner, B.M., Delrow, J., Bell, S.P., Groudine, M., 2004. The histone modification pattern of active genes revealed through genome-wide chromatin analysis of a higher eukaryote. Genes Dev. 18, 1263–71. doi:10.1101/gad.1198204

Schussler, G.C., 2000. The thyroxine-binding proteins. Thyroid 10, 141–9. doi:10.1089/thy.2000.10.141

Schwartzentruber, J., Korshunov, A., Liu, X.-Y., Jones, D.T.W., Pfaff, E., Jacob, K., Sturm, D., Fontebasso, A.M., Quang, D.-A.K., Tönjes, M., Hovestadt, V., Albrecht, S., Kool, M., Nantel, A., Konermann, C., Lindroth, A., Jäger, N., Rausch, T., Ryzhova, M., Korbel, J.O., Hielscher, T., Hauser, P., Garami, M., Klekner, A., Bognar, L., Ebinger, M., Schuhmann, M.U., Scheurlen, W., Pekrun, A., Frühwald, M.C., Roggendorf, W., Kramm, C., Dürken, M., Atkinson, J., Lepage, P., Montpetit, A., Zakrzewska, M., Zakrzewski, K., Liberski, P.P., Dong, Z., Siegel, P., Kulozik, A.E., Zapatka, M., Guha, A., Malkin, D., Felsberg, J., Reifenberger, G., von Deimling, A., Ichimura, K., Collins, V.P., Witt, H., Milde, T., Witt, O., Zhang, C., Castelo-Branco, P., Lichter, P., Faury, D., Tabori, U., Plass, C., Majewski, J., Pfister, S.M., Jabado, N., 2012. Corrigendum: Driver mutations in histone H3.3 and chromatin remodelling genes in paediatric glioblastoma. Nature 484, 130–130. doi:10.1038/nature11026

Scopa, C.D., 2004. Histopathology of Thyroid Tumors. An Overview 3, 100–110.

Sen, S.K., Han, K., Wang, J., Lee, J., Wang, H., Callinan, P.A., Dyer, M., Cordaux, R., Liang, P., Batzer, M.A., 2006. Human genomic deletions mediated by recombination between Alu elements. Am. J. Hum. Genet. 79, 41–53. doi:10.1086/504600

Sharma, S., Kelly, T.K., Jones, P.A., 2010. Epigenetics in cancer. Carcinogenesis 31, 27–36. doi:10.1093/carcin/bgp220

Shaw, J.L. V, Diamandis, E.P., 2007. Distribution of 15 human kallikreins in tissues and biological fluids. Clin. Chem. 53, 1423–1432. doi:10.1373/clinchem.2007.088104

Sheaffer, K.L., Elliott, E.N., Kaestner, K.H., 2016. DNA hypomethylation contributes to genomic instability and intestinal cancer initiation. Cancer Prev. Res. doi:10.1158/1940-6207.CAPR-15-0349

Shen, L., Toyota, M., Kondo, Y., Lin, E., Zhang, L., Guo, Y., Hernandez, N.S., Chen, X., Ahmed, S., Konishi, K., Hamilton, S.R., Issa, J.-P.J., 2007. Integrated genetic and epigenetic analysis identifies three different subclasses of colon cancer. Proc. Natl. Acad. Sci. U. S. A. 104, 18654–9. doi:10.1073/pnas.0704652104

Shigaki, H., Baba, Y., Watanabe, M., Iwagami, S., Miyake, K., Ishimoto, T., Iwatsuki, M., Baba, H., 2012. LINE-1 Hypomethylation in Noncancerous Esophageal Mucosae is Associated with Smoking History. Ann. Surg. Oncol. 19, 4238–4243. doi:10.1245/s10434-012-2488-y

Shigeo Ishikawa, Masahiro Sugimoto, Kenichiro Kitabatake, Ayako Sugano, Marina Nakamura, Miku Kaneko, Sana Ota, Kana Hiwatari, Ayame Enomoto, Tomoyoshi Soga, M.T. and M.L., 2016. Identification of salivary metabolomic biomarkers of oral cancer screening. Sci. Rep. 6.

Shmelkov, S. V., Jun, L., St. Clair, R., McGarrigle, D., Derderian, C.A., Usenko, J.K., Costa, C., Zhang, F., Guo, X., Rafil, S., 2004. Alternative promoters regulate transcription of the gene that encodes stem cell surface protein AC133. Blood 103, 2055–2061. doi:10.1182/blood-2003-06-1881

Shukla, S., Kavak, E., Gregory, M., Imashimizu, M., Shutinoski, B., Kashlev, M., Oberdoerffer, P., Sandberg, R., Oberdoerffer, S., 2011. CTCF-promoted RNA polymerase II pausing links DNA methylation to splicing. Nature 479, 74–9. doi:10.1038/nature10442

Siddiqui, S., White, M.G., Antic, T., Grogan, R.H., Angelos, P., Kaplan, E.L., Cipriani, N.A., 2016. Clinical and Pathologic Predictors of Lymph Node Metastasis and Recurrence in Papillary Thyroid Microcarcinoma. Thyroid 26, 807–815. doi:10.1089/thy.2015.0429

Siegel, R., Miller, K., Jemal, A., 2015. Cancer statistics , 2015 . CA Cancer J Clin 65, 29. doi:10.3322/caac.21254.

Simard, E.P., Ward, E.M., Siegel, R., Jemal, A., 2012. Cancers with increasing incidence trends in the United States: 1999 through 2008. CA. Cancer J. Clin. 62, 118–128. doi:10.3322/caac.20141

Simon, R., Roychowdhury, S., 2013. Implementing personalized cancer genomics in clinical trials. Nat. Rev. Drug Discov. 12, 358–69. doi:10.1038/nrd3979

Slough, C.M., Randolph, G.W., Morrison, D., 2006. Workup of Well-Differentiated Thyroid Carcinoma. Cancer Control 13.

Smallridge, R.C., Chindris, A.M., Asmann, Y.W., Casler, J.D., Serie, D.J., Reddi, H. V., Cradic, K.W., Rivera, M., Grebe, S.K., Necela, B.M., Eberhardt, N.L., Carr, J.M., McIver, B., Copland, J.A., Thompson, E.A., 2014. RNA sequencing identifies multiple fusion transcripts, differentially expressed genes, and reduced expression of immune function genes in BRAF (V600E) mutant vs BRAF wild-type papillary thyroid carcinoma. J. Clin. Endocrinol. Metab. 99. doi:10.1210/jc.2013-2792

Smallridge, R.C., Marlow, L.A., Copland, J.A., 2009. Anaplastic thyroid cancer: molecular pathogenesis and emerging therapies. Endocr. Relat. Cancer 16, 17–44. doi:10.1677/ERC-08-0154

Smanik, P.A., Liu, Q., Furminger, T.L., Ryu, K., Xing, S., Mazzaferri, E.L., Jhiang, S.M., 1996. Cloning of the Human Sodium Iodide Symporter. Biochem. Biophys. Res. Commun. 226, 339–345. doi:10.1006/bbrc.1996.1358

Smith, I.M., Mydlarz, W.K., Mithani, S.K., Califano, J.A., 2007. DNA global hypomethylation in squamous cell head and neck cancer associated with smoking, alcohol consumption and stage. Int. J. Cancer 121, 1724–8. doi:10.1002/ijc.22889

Smith, J.A., Fan, C.Y., Zou, C., Bodenner, D., Kokoska, M.S., 2007. Methylation status of genes in papillary thyroid carcinoma. Arch Otolaryngol Head Neck Surg 133, 1006–1011. doi:10.1001/archotol.133.10.1006

Soares, P., Trovisco, V., Rocha, A.S., Lima, J., Castro, P., Preto, A., Maimo, V., Botelho, T., Seruca, R., Sobrinho-Simos, M., 2003. BRAF mutations and RET/PTC rearrangements are alternative events in the etiopathogenesis of PTC. Oncogene 17, 4578–45780. doi:10.1038/sj.onc.1206706

Sobin, L.H., Gospodarowicz, M.K., Wittekind, C., 2009. TNM classification of malignant tumours, Clinical Oncology.

Sobrinho-Simões, M., Eloy, C., Magalhães, J., Lobo, C., Amaro, T., 2011. Follicular thyroid carcinoma. Mod. Pathol. 24 Suppl 2, S10–S18. doi:10.1038/modpathol.2010.133

Solmonson, A., Mills, E.M., 2016. Uncoupling Proteins and the Molecular Mechanisms of Thyroid Thermogenesis. Endocrinology 157, 455–62. doi:10.1210/en.2015-1803

Sotiropoulou, G., Rogakos, V., Tsetsenis, T., Pampalakis, G., Zafiropoulos, N., Simillides, G., Yiotakis, A., Diamandis, E.P., 2003. Emerging interest in the kallikrein gene family for understanding and diagnosing cancer. Oncol. Res. 13, 381–91.

Soto, J., Rodriguez-Antolin, C., Vallespín, E., De Castro Carpeño, J., Ibanez De Caceres, I., 2016. The impact of next-generation sequencing on the DNA methylation-based translational cancer research. Transl. Res. doi:10.1016/j.trsl.2015.11.003

Spiro, M.J., Gorski, K.M., 1986. Studies on the posttranslational migration and processing of thyroglobulin: use of inhibitors and evaluation of the role of phosphorylation. Endocrinology 119, 1146–58. doi:10.1210/endo-119-3-1146

Stefan, M., Zhang, W., Concepcion, E., Yi, Z., Tomer, Y., 2014. DNA methylation profiles in type 1 diabetes twins point to strong epigenetic effects on etiology. J. Autoimmun. 50, 33–37. doi:10.1016/j.jaut.2013.10.001

Stenson, G., Nilsson, I.-L., Mu, N., Larsson, C., Lundgren, C.I., Juhlin, C.C., Höög, A., Zedenius, J., 2016. Minimally invasive follicular thyroid carcinomas: prognostic factors. Endocrine. doi:10.1007/s12020-016-0876-y

Stephen, J.K., Chitale, D., Narra, V., Chen, K.M., Sawhney, R., Worsham, M.J., 2011. DNA methylation in thyroid tumorigenesis. Cancers (Basel). 3, 1732–1743. doi:10.3390/cancers3021732

Stower, H., 2013. Alternative splicing: Regulating Alu element "exonization." Nat. Rev. Genet. 14, 152–153. doi:10.1038/nrg3428

Strahl, B.D., Allis, C.D., 2000. The language of covalent histone modifications. Nature 403, 41–45. doi:10.1038/47412

Stulak, J.M., Grant, C.S., Farley, D.R., Thompson, G.B., van Heerden, J.A., Hay, I.D., Reading, C.C., Charboneau, J.W., 2006. Value of preoperative ultrasonography in the surgical management of initial and reoperative papillary thyroid cancer. Arch. Surg. 141, 489–94; discussion 494–6. doi:10.1001/archsurg.141.5.489

Sun, W., Lan, X., Wang, Z., Dong, W., He, L., Zhang, T., Zhang, H., 2016. Overexpression of long non-coding RNA NR_036575.1 contributes to the proliferation and migration of papillary thyroid cancer. Med. Oncol. 33, 102. doi:10.1007/s12032-016-0816-y

Suzuki, K., Kawashima, A., Yoshihara, A., Akama, T., Sue, M., Yoshida, A., Kimura, H.J., 2011. Role of thyroglobulin on negative feedback autoregulation of thyroid follicular function and growth. J. Endocrinol. 209, 169–74. doi:10.1530/JOE-10-0486

Suzuki, K., Nakazato, M., Ulianich, L., Mori-Aoki, A., Moriyama, E., Chung, H.K., Pietrarelli, M., Grassadonia, A., Matoba, H., Kohn, L.D., 2000. Thyroglobulin autoregulation of thyroid-specific gene expression and follicular function. Rev. Endocr. Metab. Disord. 1, 217–24.

Suzuki, M., Shiraishi, K., Eguchi, A., Ikeda, K., Mori, T., Yoshimoto, K., Ohba, Y., Yamada, T., Ito, T., Baba, Y., Baba, H., 2013. Aberrant methylation of LINE-1, SLIT2, MAL and IGFBP7 in non-small cell lung cancer. Oncol. Rep. 29, 1308–1314. doi:10.3892/or.2013.2266

Suzuki, M.M., Bird, A., 2008. DNA methylation landscapes: provocative insights from epigenomics. Nat. Rev. Genet. 9, 465–76. doi:10.1038/nrg2341

Swanton, C., 2014. Cancer evolution: the final frontier of precision medicine? Ann. Oncol. 25, 549–551. doi:10.1093/annonc/mdu005

Szinnai, G., Polak, M., Szinnai, G., Vliet, G. Van, Deladoëy, J., Rastogi, M.N., LaFrancchi, S.H., Moreno, J.C., Vijlder, J.J.M. de, Vulsma, T., al., et, Knobel, M., Medeiros-Neto, G., Alm, J., Larrson, A., Zetterstrom, R., Alm, J., Hagenfeldt, L., Larsson, A., al., et, Zoeller, R.T., Rovet, J., Calvo, R., Obregon, M.J., Ona, C.R. de, al., et, Bernal, J., Collaborative, N.E.C.H., Brosco, J.P., Mattingly, M., Sanders, L.M., Grosse, S.D., Vliet, G. Van, Devos, H., Rodd, C., Gagne, N., al., et, Roberts, H.E., Moore, C.A., Fernhoff, P.M., Toublanc, J., Mitchell, M.L., Hsu, H.W., Sahai, I., Group, E.W., al., et, Deladoëy, J., Ruel, J., Giguère, Y., al., et, Harris, K.B., Pass, K.A., Hinton, C.F., Harris, K.B., Borgfeld, L., al., et, Park, J.S., Lin, M., Grosse, S.D., al., et, Mengreli, C., Kanaka-Gantenbein, C., Girginoudis, P., al., et, Corbetta, C., Weber, G., Cortinovis, F., al., et, Gagné, N., Parma, J., Deal, C., al., et, Olivieri, A., Stazi, M.A., Mastoiacovo, P., al., et, Weller, G., O'Rahilly, R., O'Rahilly, R., Müller, F., Shepard, T.H., Andersen, H., Andersen, H.J., Shepard, T.H., Trueba, S.S., Augé, J., Mattei, G., al., et, Szinnai, G., Lacroix, L., Carré, A., al., et, Felice, M. De, Lauro, R. Di, Fagman, H., Nilsson, M., Zorn, A.M., Wells, J.M., Kraus, M.R.C., Grapin-Botton, A., Plachov, D., Chouwhury, K., Walther, C., al., et, Lazzaro, D., Price, M., Felice, M. De, al., et, Zannini, M., Avantaggiato, V., Biffali, E., al., et, Thomas, P.Q., Brown, A., Beddington, R., Parlato, R., Rosica, A., Rodriguez-Mallon, A., al., et, Carré, A., Rachdi, L., Tron, E., al., et, Antonica, F., Kasprzyk, D.F., Opitz, R., al., et, Fagman, H., Grande, M., Edsbagge, J., al., et, Felice, M. De, Ovitt, C., Biffali, E., al., et, Kusakabe, T., Hoshi, N., Kimura, S., Fagman, H., Grande, M., Gritli-Linde, A., al., et, Olin, P., Ekholm, R., Almquist, S., Greenberg, A.H., Czernichow, P., Reba, R.C., al., et, Thorpe-Beeston, G.J., Nicolaides, K.H., Felton, C.V., al., et, Calvo, R.M., Jauniaux, E., Gulbis, B., al., et, Hodges, R.E., Evans, T.C., Bradbury, J.T., al., et, Perry, R., Heinrichs, C., Bourdoux, P., al., et, Deladoëy, J., Vassart, G., Vliet, G. Van, Castanet, M., Polak, M., Bonaïti-Pellié, C., al., et, Léger, J., Marinovic, D., Garel, C., al., et, Xu, P.X., Zheng, W., Leclef, C., al., et, Martinez-Barbera, J.P., Clements, M., Thomas, P., al., et, Manley, N.R., Capecchi, M.R., Manley, N.R., Capecchi, M.R., Westerlund, J., Andersson, L., Carlsson, T., al., et, Kimura, S., Hara, Y., Pineau, T., al., et, Dentice, M., Cordeddu, V., Rosica, A., al., et, Mansouri, A., Chowhury, K., Gruss, P., Abdelhak, S., Kalatzis, V., Heilig, R., al., et, Clifton-Bligh, R.J., Wentworth, J.M., Heinz, P., al., et, Taji, E. Al, Biebermann, H., Limanova, Z., al., et, Ferrara, A.M., Rossi, G., Zampella, E., al., et, Devriendt, K., Vanhole, C., Matthijs, G., al., et, Macchia, P.E., Lapi, P., Krude, H., al., et, Sunthornthepvarakul, T., Gootschalk, M.E., Hayashi, Y., al., et, Ferrara, A.M., Sanctis, L. De, Rossi, G., al., et, Parmentier, M., Libert, F., Maenhaupt, C., al., et, Vassart, G., Dumont, J.E., Smits, G., Campillo, M., Govaerts, C., al., et, Szkudlinski, M.W., Fremont, V., Ronin, C., al., et, Postiglione, M.P., Parlato, R., Rodriguez-Mallon, A., al., et, Lee, S.T., Lee, D.H., Kim, J.Y., al., et, Narumi, S., Muroya, K., Abe, Y., al., et, Chang, W.C., Liao, C.Y., Chen, W.C., al., et, Nicoletti, A., Bal, M., Marco, G. De, al., et, Rapa, A., Monzani, A., Moia, S., al., et, Calebiro, D., Gelmini, G., Cordella, D., al., et, Alberti, L., Proverbio, M.C., Costagliola, S., al., et, Mizuno, H., Kanda, K., Sugiyama, Y., al., et, Tennenbaum-Rakover, Y., Grasberger, H., Mamanasiri, S., al., et, Krude, H., Biebermann, H., Göpel, W., al., et, Congdon, T., Nguyen, L.Q., Nogueira, C.R., al., et, Yuan, Z.F., Mao, H.Q., Luo, Y.F., al., et, Ramos, H.E., Nesi-França, S., Boldarine, V.T., al., et, Cangul, H., Morgan, N.V., Forman, J.R., al., et, Alves, E.A., Cruz, C.M., Pimentel, C.P., al., et, Brust, E., Beltrao, C.B., Chammas, M.C., al., et, Stapleton, P., Weith, A., Urbanek, P., al., et, Magliano, M.P. di, Lauro, R. Di, Zannini, M.S., Meeus, L., Gilbert, B., Rydlewski, C., al., et, Jo, W., Ishizu, K., Fujieda, K., al., et, Narumi, S., Yoshida, A., Muroya, K., al., et, Vilain, C., Rydlewski, C., Duprez, L., al., et, Sanctis, L. De, Corrias, A., Romagnolo, D., al., et, Castanet, M., Leenhardt, L., Léger, J., al., et, Lanzerath, K., Bettendorf, M., Haag, C., al., et, Tonacchera, M., Banco, M.E., Montanelli, L., al., et, Esperante, S.A., Rivolta, C.M., Miravalle, L., al., et, Narumi, S., Muroya, K., Asakura, Y., al., et, Mahjoubi, F., Mohammadi, M.M., Montazeri, M., al., et, Alcantara-Ortigoza, M.A., Angel, A.G., Martinez-Cruz, V., al., et, Liu, S.G., Zhang, S.S., Zhang, L.Q., al., et, Ramos, H.E., Carre, A., Szinnai, G., al., et, Castanet, M., Park, S.M., Smith, A., al., et, Moreno, L.M., Mansilla, M.A., Bullard, S.A., al., et, Dixon, M.J., Marazita, M.L., Beaty, T.H., al., et, Guazzi, S., Price, M., Felice, M. De, al., et, Asmus, F., Horber, V., Pohlenz, J., al., et, Guillot, L., Carre, A., Szinnai, G., al., et, Civitareale, D., Lonigro, R., Sinclair, A.J., al., et, Bohinski, R.J.,

Lauro, R. Di, Whitsett, J.A., Maeda, Y., Dave, V., Whitsett, J.A., Carre, A., Szinnai, G., Castanet, M., al., et, Krude, H., Schutz, B., Bibermann, H., al., et, Willemsen, M.A., Breedveld, G.J., Wouda, S., al., et, Weir, B.A., Woo, M.S., Getz, G., al., et, Winslow, M.M., Dayton, T.L., Verhaak, R., al., et, Gras, D., Jonard, L., Roze, E., al., et, Turbay, D., Wechsler, S.B., Blanchard, K.M., al., et, Buckingham, M., Meilhac, S., Zaffran, S., Schott, J.J., Benson, D.W., Basson, C.T., al., et, Reamon-Buettner, S.M., Borlak, J., Passeri, E., Frigerio, M., Filippis, T. de, al., et, Hermanns, P., Grasberger, H., Refetoff, S., Ohlenz, J., Engelen, K. Van, Mommersteeg, M.T.M., Baars, M.J.H., al., et, Teissier, R., Guillot, L., Carré, A., al., et, Castanet, M., Sura-Trueba, S., Chauty, A., al., et, Amendola, E., Luca, P. De, Macchia, P.E., al., et, Sriphrapradang, C., Tenenbaum-Rakover, J., Weiss, M., al., et, Lado-Abeal, J., Castro-Piedras, I., Palos-Paz, F., al., et, Narumi, S., Muroya, K., Asakura, Y., al., et, Poduri, A., Evrony, G.D., Cai, X., al., et, Gundry, M., Vijg, J., Carré, A., Castanet, M., Sura-Trueba, S., al., et, Redon, R., Ishikawa, S., Fitch, K.R., al., et, Erdogan, F., Larsen, L.A., Zhang, L., al., et, Stankiewicz, P., Lupski, J.R., Conrad, D.F., Bird, C., Blackburne, B., al., et, Thorwarth, A., Mueller, I., Biebermann, H., al., et, Abu-Khudir, R., Paquette, J., Lefort, A., al., et, 2014. Genetics of normal and abnormal thyroid development in humans. Best Pract. Res. Clin. Endocrinol. Metab. 28, 133–50. doi:10.1016/j.beem.2013.08.005

Szymański, Ł., Matak, D., Bartnik, E., Szczylik, C., Czarnecka, A.M., 2016. Thyroid Hormones as Renal Cell Cancer Regulators. J. Signal Transduct. 2016, 1362407. doi:10.1155/2016/1362407

Tahara, T., Yamamoto, E., Madireddi, P., Suzuki, H., Maruyama, R., Chung, W., Garriga, J., Jelinek, J., Yamano, H.O., Sugai, T., Kondo, Y., Toyota, M., Issa, J.P.J., Estécio, M.R.H., 2014. Colorectal carcinomas with CpG island methylator phenotype 1 frequently contain mutations in chromatin regulators. Gastroenterology 146. doi:10.1053/j.gastro.2013.10.060

Tajuddin, S.M., Amaral, A.F.S., Fernández, A.F., Chanock, S., Silverman, D.T., Tardón, A., Carrato, A., García-Closas, M., Jackson, B.P., Toraño, E.G., Márquez, M., Urdinguio, R.G., García-Closas, R., Rothman, N., Kogevinas, M., Real, F.X., Fraga, M.F., Malats, N., Sala, M., Castaño, G., Torà, M., Puente, D., Villanueva, C., Murta-Nascimento, C., Fortuny, J., López, E., Hernández, S., Jaramillo, R., Vellalta, G., Palencia, L., Fermández, F., Amorós, A., Alfaro, A., Carretero, G., Lloreta, J., Serrano, S., Ferrer, L., Gelabert, A., Carles, J., Bielsa, O., Villadiego, K., Cecchini, L., Saladié, J.M., Ibarz, L., Céspedes, M., Serra, C., García, D., Pujadas, J., Hernando, R., Cabezuelo, A., Abad, C., Prera, A., Prat, J., Domènech, M., Badal, J., Malet, J., Rodríguez de Vera, J., Martín, A.I., Taño, J., Cáceres, F., García-López, F., Ull, M., Teruel, A., Andrada, E., Bustos, A., Castillejo, A., Soto, J.L., Guate, J.L., Lanzas, J.M., Velasco, J., Fernández, J.M., Rodríguez, J.J., Herrero, A., Abascal, R., Manzano, C., Miralles, T., Rivas, M., Arguelles, M., Díaz, M., Sánchez, J., González, O., Mateos, A., Frade, V., Asturias, M., Muntañola, P., Pravia, C., Huescar, A.M., Huergo, F., Mosquera, J., Fernandez, A.F., Tardon, A., Garcia-Closas, M., Torano, E.G., Marquez, M., Garcia-Closas, R., Investigators, for the S.B.C.S., 2014. LINE-1 methylation in leukocyte DNA, interaction with phosphatidylethanolamine N-methyltransferase variants and bladder cancer risk. Br J Cancer 110, 2123–2130. doi:10.1038/bjc.2014.67

Takanashi, Y., Honkura, Y., Rodriguez-Vazquez, J.F., Murakami, G., Kawase, T., Katori, Y., 2015. Pyramidal lobe of the thyroid gland and the thyroglossal duct remnant: A study using human fetal sections. Ann. Anat. - Anat. Anzeiger 197, 29–37. doi:10.1016/j.aanat.2014.09.001

Talbert, P.B., Henikoff, S., 2010. Histone variants--ancient wrap artists of the epigenome. Nat Rev Mol Cell Biol 11, 264–275. doi:nrm2861 [pii]\n10.1038/nrm2861

Talieri, M., Alexopoulou, D.K., Scorilas, A., Kypraios, D., Arnogiannaki, N., Devetzi, M., Patsavela, M., Xynopoulos, D., 2011. Expression analysis and clinical evaluation of kallikrein-related peptidase 10 (KLK10) in colorectal cancer. Tumour Biol. 32, 737–44. doi:10.1007/s13277-011-0175-4

Tallini, G., Asa, S.L., 2001. RET oncogene activation in papillary thyroid carcinoma. Adv Anat Pathol 8, 345–354. doi:10.1097/00125480-200111000-00005

Tan, G.H., Gharib, H., 1997. Thyroid incidentalomas: management approaches to nonpalpable nodules discovered incidentally on thyroid imaging. Ann. Intern. Med. 126, 226–31.

Targovnik, H.M., Citterio, C.E., Rivolta, C.M., 2011. Thyroglobulin gene mutations in congenital hypothyroidism. Horm. Res. pædiatrics 75, 311–21. doi:10.1159/000324882

Targovnik, H.M., Esperante, S.A., Rivolta, C.M., 2010. Genetics and phenomics of hypothyroidism and goiter due to thyroglobulin mutations. Mol. Cell. Endocrinol. 322, 44–55. doi:10.1016/j.mce.2010.01.009

Tavares, C., Melo, M., Cameselle Teijeiro, J.M., Soares, P., Sobrinho-Simoes, M., 2015. ENDOCRINE TUMOURS: Genetic predictors of thyroid cancer outcome. Eur J Endocrinol 174, 117–26. doi:10.1530/eje-15-0605

Teijeiro, J.C., Sobrinho-Simoes, M., 2003. Carcinoma papilar de la glándula tiroides Problemas en el diagnóstico y controversias 36, 373–382.

Tong, Q., Xing, S., Jhiang, S.M., 1997. Leucine zipper-mediated dimerization is essential for the PTC1 oncogenic activity. J. Biol. Chem. 272, 9043–7.

Toraño, E.G., Petrus, S., Fernandez, A.F., Fraga, M.F., 2012. Global DNA hypomethylation in cancer: review of validated methods and clinical significance. Clin. Chem. Lab. Med. 50, 1733–42. doi:10.1515/cclm-2011-0902

Toyota, M., Suzuki, H., 2010. Epigenetic drivers of genetic alterations, Advances in Genetics. doi:10.1016/B978-0-12-380866-0.60011-3

Trka, J., Kalinova, M., Hrusak, O., Zuna, J., Krejci, O., Madzo, J., Sedlacek, P., Vavra, V., Michalova, K., Jarosova, M., Stary, J., 2002. Real-time quantitative PCR detection of WT1 gene expression in children with AML: prognostic significance, correlation with disease status and residual disease detection by flow cytometry. Leukemia 16, 1381–9. doi:10.1038/sj.leu.2402512

Tufano, R.P., Noureldine, S.I., Angelos, P., 2015. Incidental

thyroid nodules and thyroid cancer: considerations before determining management. JAMA Otolaryngol. Head Neck Surg. 141, 566–72. doi:10.1001/jamaoto.2015.0647

Tunbridge, W.M., Evered, D.C., Hall, R., Appleton, D., Brewis, M., Clark, F., Evans, J.G., Young, E., Bird, T., Smith, P.A., 1977. The spectrum of thyroid disease in a community: the Whickham survey. Clin. Endocrinol. (Oxf). 7, 481–93.

Van Heuverswyn, B., Leriche, A., Van Sande, J., Dumont, J.E., Vassart, G., 1985. Transcriptional control of thyroglobulin gene expression by cyclic AMP. FEBS Lett. 188, 192–196. doi:10.1016/0014-5793(85)80370-7

Vanderpump, M.P.J., 2011. The epidemiology of thyroid disease. Br. Med. Bull. 99, 39–51. doi:10.1093/bmb/ldr030

Vargas-Uricoechea, H., Bonelo-Perdomo, A., Sierra-Torres, C.H., 2014. Effects of thyroid hormones on the heart. Clínica e Investig. en Arterioscler. 26, 296–309. doi:10.1016/j.arteri.2014.07.003

Varley, K.E., Gertz, J., Bowling, K.M., Parker, S.L., Reddy, T.E., Pauli-Behn, F., Cross, M.K., Williams, B.A., Stamatoyannopoulos, J.A., Crawford, G.E., Absher, D.M., Wold, B.J., Myers, R.M., 2013. Dynamic DNA methylation across diverse human cell lines and tissues. Genome Res. 23, 555–567. doi:10.1101/GR.147942.112

Vasko, V., Ferrand, M., Di Cristofaro, J., Carayon, P., Henry, J.F., De Micco, C., 2003. Specific pattern of RAS oncogene mutations in follicular thyroid tumors. J. Clin. Endocrinol. Metab. 88, 2745–2752. doi:10.1210/jc.2002-021186

Venkataraman, G.M., Yatin, M., Marcinek, R., Ain, K.B., 1999. Restoration of iodide uptake in dedifferentiated thyroid carcinoma: relationship to human Na+/I-symporter gene methylation status. J. Clin. Endocrinol. Metab. 84, 2449–57. doi:10.1210/jcem.84.7.5815

Villabona, C. V, Mohan, V., Arce, K.M., Diacovo, J., Aggarwal, A., Betancourt, J., Amer, H., Jose, T., Desantis, P., Cabral, J., 2016. Utility of Ultrasound vs. Gene Expression Classifier in Thyroid Nodules with Atypia of Undetermined Significance. Endocr Pr. 22, 1199–1203.

Villacorte, M., Delmarcelle, A.-S., Lernoux, M., Bouquet, M., Lemoine, P., Bolsée, J., Umans, L., de Sousa Lopes, S.C., Van Der Smissen, P., Sasaki, T., Bommer, G., Henriet, P., Refetoff, S., Lemaigre, F.P., Zwijsen, A., Courtoy, P.J., Pierreux, C.E., 2016. Thyroid follicle development requires Smad1/5- and endothelial cell-dependent basement membrane assembly. Development 143, 1958–70. doi:10.1242/dev.134171

Vriens, M.R., Suh, I., Moses, W., Kebebew, E., 2009. Clinical features and genetic predisposition to hereditary nonmedullary thyroid cancer. Thyroid 19, 1343–1349. doi:10.1089/thy.2009.1607

Vu-Phan, D., Koenig, R.J., 2014. Genetics and epigenetics of sporadic thyroid cancer. Mol. Cell. Endocrinol. doi:10.1016/j.mce.2013.07.030

Waddington, C.H., 2012. The Epigenotype. Int. J. Epidemiol. 41, 10–13. doi:10.1093/ije/dyr184

Waddington, C.H., 1942. The Epigenotype. Endeavour 1, 18–20. doi:10.1093/ije/dyr184

Walker, B.A., Wardell, C.P., Chiecchio, L., Smith, E.M., Boyd, K.D., Neri, A., Davies, F.E., Ross, F.M., Morgan, G.J., 2011. Aberrant global methylation patterns affect the molecular pathogenesis and prognosis of multiple myeloma. Blood 117, 553–562. doi:10.1182/blood-2010-04-279539

Wan, P.T.C., Garnett, M.J., Roe, S.M., Lee, S., Niculescu-Duvaz, D., Good, V.M., Jones, C.M., Marshall, C.J., Springer, C.J., Barford, D., 2004. Mechanism of Activation of the RAF-ERK Signaling Pathway by Oncogenic Mutations of B-RAF first effector identified downstream of RAS (Avruch et al. Cell 116, 855–867.

Wang, C., Yan, G., Zhang, Y., Jia, X., Bu, P., 2015. Long non-coding RNA MEG3 suppresses migration and invasion of thyroid carcinoma by targeting of Rac1. Neoplasma 62, 541–9. doi:10.4149/neo_2015_065

Wang, Y.Y., Lin, Y.C., Hung, H.C., Tien, W.Y., Shieh, T.Y., 2013. Polymorphisms in Kallikrein7 and 10 genes and oral cancer risks in Taiwan betel quid chewers and smokers. Oral Dis. 19, 824–32. doi:10.1111/odi.12072

Watson, J.D., Crick, F.H.C., 1953. Molecular structure of nucleic acids. Nature. doi:10.1097/BLO.0b013e3181468780

Weber, C.M., Henikoff, S., 2014. Histone variants: dynamic punctuation in transcription. Genes Dev. 28, 672–82. doi:10.1101/gad.238873.114

Weber, F., Teresi, R.E., Broelsch, C.E., Frilling, A., Eng, C., 2006. A limited set of human MicroRNA is deregulated in follicular thyroid carcinoma. J. Clin. Endocrinol. Metab. 91, 3584–91. doi:10.1210/jc.2006-0693

Weisenberger, D.J., Campan, M., Long, T.I., Kim, M., Woods, C., Fiala, E., Ehrlich, M., Laird, P.W., 2005. Analysis of repetitive element DNA methylation by MethyLight. Nucleic Acids Res. 33, 6823–6836. doi:10.1093/nar/gki987

Weisenberger, D.J., Siegmund, K.D., Campan, M., Young, J., Long, T.I., Faasse, M. a, Kang, G.H., Widschwendter, M., Weener, D., Buchanan, D., Koh, H., Simms, L., Barker, M., Leggett, B., Levine, J., Kim, M., French, A.J., Thibodeau, S.N., Jass, J., Haile, R., Laird, P.W., 2006. CpG island methylator phenotype underlies sporadic microsatellite instability and is tightly associated with BRAF mutation in colorectal cancer. Nat. Genet. 38, 787–93. doi:10.1038/ng1834

Weisser, M., Kern, W., Rauhut, S., Schoch, C., Hiddemann, W., Haferlach, T., Schnittger, S., 2005. Prognostic impact of RT-PCR-based quantification of WT1 gene expression during MRD monitoring of acute myeloid leukemia. Leukemia 19, 1416–23. doi:10.1038/sj.leu.2403809

Whitcomb, S.J., Basu, A., Allis, C.D., Bernstein, E., 2007. Polycomb Group proteins: an evolutionary perspective. Trends Genet. 23, 494–502. doi:10.1016/j.tig.2007.08.006

White, M.G., Nagar, S., Aschebrook-Kilfoy, B., Jasmine, F., Kibriya, M.G., Ahsan, H., Angelos, P., Kaplan, E.L., Grogan, R.H., 2016. Epigenetic Alterations and Canonical Pathway Disruption in Papillary Thyroid Cancer: A Genome-wide Methylation Analysis. Ann. Surg. Oncol. 23, 2302–2309. doi:10.1245/s10434-016-5185-4

Whitwam, T., VanBrocklin, M.W., Russo, M.E., Haak, P.T., Bilgili, D., Resau, J.H., Koo, H.-M., Holmen, S.L., 2007. Differential oncogenic potential of activated RAS isoforms in melanocytes. Oncogene 26, 4563–4570. doi:10.1038/sj.onc.1210239

Widschwendter, M., Jiang, G., Woods, C., Müller, H.M., Fiegl, H., Goebel, G., Marth, C., Müller-Holzner, E., Zeimet, A.G., Laird, P.W., Ehrlich, M., 2004. DNA hypomethylation and ovarian cancer biology. Cancer Res. 64, 4472–4480. doi:10.1158/0008-5472.CAN-04-0238

Wilkins, M.H.F., Stokes, A.R., Wilson, H.R., 1953. Molecular structure of deoxypentose nucleic acids. Nature 171, 738–40.

Willem de Groot, J.B., Links, T.P., M Plukker, J.T., M Lips, C.J., W Hofstra, R.M., Oncology JWBdG, S., n.d. RET as a Diagnostic and Therapeutic Target in Sporadic and Hereditary Endocrine Tumors. doi:10.1210/er.2006-0017

Williams, D., 2008. Radiation carcinogenesis: lessons from Chernobyl. Oncogene 27 Suppl 2, S9–18. doi:10.1038/onc.2009.349

Williams, D., 2008. Twenty years' experience with post-Chernobyl thyroid cancer. Best Pract. Res. Clin. Endocrinol. Metab. 22, 1061–1073. doi:10.1016/j.beem.2008.09.020

Willoughby, D.A., Vilalta, A., Oshima, R.G., 2000. An Alu element from the K18 gene confers position-independent expression in transgenic mice. J. Biol. Chem. 275, 759–768. doi:10.1074/jbc.275.2.759

Wirth, E.K., Schweizer, U., Köhrle, J., 2014. Transport of thyroid hormone in brain. Front. Endocrinol. (Lausanne). doi:10.3389/fendo.2014.00098

Wiseman, S.M., Masoudi, H., Niblock, P., Turbin, D., Rajput, A., Hay, J., Bugis, S., Filipenko, D., Huntsman, D., Gilks, B., 2007. Anaplastic thyroid carcinoma: expression profile of targets for therapy offers new insights for disease treatment. Ann Surg Oncol 14, 719–729. doi:10.1245/s10434-006-9178-6

Wu, C., 1980. The 5′ ends of Drosophila heat shock genes in chromatin are hypersensitive to DNase I. Nature 286, 854–860. doi:10.1038/286854a0

Wu, G., Broniscer, A., McEachron, T. a, Lu, C., Paugh, B.S., Becksfort, J., Qu, C., Ding, L., Huether, R., Parker, M., Zhang, J., Gajjar, A., Dyer, M. a, Mullighan, C.G., Gilbertson, R.J., Mardis, E.R., Wilson, R.K., Downing, J.R., Ellison, D.W., Zhang, J., Baker, S.J., 2012. Somatic histone H3 alterations in pediatric diffuse intrinsic pontine gliomas and non-brainstem glioblastomas. Nat. Genet. 44, 251–253. doi:10.1038/ng.1102

Wu, H.-C., John, E.M., Ferris, J.S., Keegan, T.H., Chung, W.K., Andrulis, I., Delgado-Cruzata, L., Kappil, M., Gonzalez, K., Santella, R.M., Terry, M.B., 2011. Global DNA methylation levels in girls with and without a family history of breast cancer. Epigenetics 6, 29–33. doi:10.4161/epi.6.1.13393

Xie, H., Wang, M., Bonaldo Mde, F., Rajaram, V., Stellpflug, W., Smith, C., Arndt, K., Goldman, S., Tomita, T., Soares, M.B., 2010. Epigenomic analysis of Alu repeats in human ependymomas. Proc Natl Acad Sci U S A 107, 6952–6957. doi:0913836107 [pii]\r10.1073/pnas.0913836107

Xing, J., Zhang, Y., Han, K., Salem, A.H., Sen, S.K., Huff, C.D., Zhou, Q., Kirkness, E.F., Levy, S., Batzer, M.A., Jorde, L.B., 2009. Mobile elements create structural variation: Analysis of a complete human genome. Genome Res. 19, 1516–1526. doi:10.1101/gr.091827.109

Xing, M., Alzahrani, A.S., Carson, K.A., Viola, D., Elisei, R., Bendlova, B., Yip, L., Mian, C., Vianello, F., Tuttle, R.M., Robenshtok, E., Fagin, J.A., Puxeddu, E., Fugazzola, L., Czarniecka, A., Jarzab, B., O'Neill, C.J., Sywak, M.S., Lam, A.K., Riesco-Eizaguirre, G., Santisteban, P., Nakayama, H., Tufano, R.P., Pai, S.I., Zeiger, M.A., Westra, W.H., Clark, D.P., Clifton-Bligh, R., Sidransky, D., Ladenson, P.W., Sykorova, V., 2013a. Association between BRAF V600E mutation and mortality in patients with papillary thyroid cancer. JAMA 309, 1493–501. doi:10.1001/jama.2013.3190

Xing, M., Cohen, Y., Mambo, E., Tallini, G., Udelsman, R., Ladenson, P.W., Sidransky, D., 2004. Early Occurrence of RASSF1A Hypermethylation and Its Mutual Exclusion with BRAF Mutation in Thyroid Tumorigenesis. Cancer Res. 64, 1664–1668. doi:10.1158/0008-5472.CAN-03-3242

Xing, M., Haugen, B.R., Schlumberger, M., 2013b. Progress in molecular-based management of differentiated thyroid cancer. Lancet 381, 1058–1069. doi:10.1016/S0140-6736(13)60109-9

Xing, M., Liu, R., Liu, X., Murugan, A.K., Zhu, G., Zeiger, M.A., Pai, S., Bishop, J., 2014. BRAF V600E and TERT promoter mutations cooperatively identify the most aggressive papillary thyroid cancer with highest recurrence. J. Clin. Oncol. 32, 2718–2726. doi:10.1200/JCO.2014.55.5094

Xing, M., Tokumaru, Y., Wu, G., Westra, W.B., Ladenson, P.W., Sidransky, D., 2003a. Hypermethylation of the Pendred syndrome gene SLC26A4 is an early event in thyroid tumorigenesis. Cancer Res. 63, 2312–2315.

Xing, M., Usadel, H., Cohen, Y., Tokumaru, Y., Guo, Z., Westra, W.B., Tong, B.C., Tallini, G., Udelsman, R., Califano, J.A., Ladenson, P.W., Sidransky, D., 2003b. Methylation of the Thyroid-stimulating Hormone Receptor gene in epithelial thyroid tumors: A marker of malignancy and a cause of gene silencing. Cancer Res. 63, 2316–2321.

Xing, M.M., 2007. Minireview: Gene methylation in thyroid tumorigenesis. Endocrinology. doi:10.1210/en.2006-0927

Yachida, S., Jones, S., Bozic, I., Antal, T., Leary, R., Fu, B., Kamiyama, M., Hruban, R.H., Eshleman, J.R., Nowak, M.A., Velculescu, V.E., Kinzler, K.W., Vogelstein, B., Iacobuzio-Donahue, C.A., 2010. Distant metastasis occurs late during the genetic

evolution of pancreatic cancer. Nature 467, 1114–7. doi:10.1038/nature09515

Yamanoi, K., Arai, E., Tian, Y., Takahashi, Y., Miyata, S., Sasaki, H., Chiwaki, F., Ichikawa, H., Sakamoto, H., Kushima, R., Katai, H., Yoshida, T., Sakamoto, M., Kanai, Y., 2015. Epigenetic clustering of gastric carcinomas based on dna methylation profiles at the precancerous stage: Its correlation with tumor aggressiveness and patient outcome. Carcinogenesis 36, 509–520. doi:10.1093/carcin/bgv013

Yang, A.S., Estécio, M.R.H., Doshi, K., Kondo, Y., Tajara, E.H., Issa, J.-P.J., 2004. A simple method for estimating global DNA methylation using bisulfite PCR of repetitive DNA elements. Nucleic Acids Res. 32, e38. doi:10.1093/nar/gnh032

Yates, L.R., Campbell, P.J., 2012. Evolution of the cancer genome. Nat. Rev. Genet. 13, 795–806. doi:10.1038/nrg3317

Yip, L., Farris, C., Kabaker, A.S., Hodak, S.P., Nikiforova, M.N., McCoy, K.L., Stang, M.T., Smith, K.J., Nikiforov, Y.E., Carty, S.E., 2012. Cost impact of molecular testing for indeterminate thyroid nodule fine-needle aspiration biopsies. J. Clin. Endocrinol. Metab. 97, 1905–12. doi:10.1210/jc.2011-3048

Yoon, K.-A., Park, S., Hee Lee, S., Hee Kim, J., Soo Lee, J., 2009. Comparison of Circulating Plasma DNA Levels between Lung Cancer Patients and Healthy Controls. doi:10.2353/jmoldx.2009.080098

You, J.S., Jones, P.A., 2012. Cancer Genetics and Epigenetics: Two Sides of the Same Coin? Cancer Cell. doi:10.1016/j.ccr.2012.06.008

Yousef, G.M., Diamandis, E.P., 2002. Expanded human tissue kallikrein family--a novel panel of cancer biomarkers. Tumour Biol. J. Int. Soc. Oncodevelopmental Biol. Med. 23, 185–192. doi:64027

Yousef, G.M., Diamandis, E.P., 2001. The new human tissue kallikrein gene family: structure, function, and association to disease. Endocr. Rev. 22, 184–204. doi:10.1210/edrv.22.2.0424

Zambudio, A.R., Rodríguez, J., Riquelme, J., Soria, T., Canteras, M., Parrilla, P., 2004. Prospective study of postoperative complications after total thyroidectomy for multinodular goiters by surgeons with experience in endocrine surgery. Ann. Surg. 240, 18–25.

Zavitsanos, P., Amdur, R.J., Drew, P.A., Cusi, K., Werning, J.W., Morris, C.G., 2015. Favorable Outcome of Hurthle Cell Carcinoma of the Thyroid Treated With Total Thyroidectomy, Radioiodine, and Selective Use of External-Beam Radiotherapy. Am. J. Clin. Oncol. doi:10.1097/COC.0000000000000180

Zelic, R., Fiano, V., Grasso, C., Zugna, D., Pettersson, A., Gillio-Tos, A., Merletti, F., Richiardi, L., 2014. Global DNA hypomethylation in prostate cancer development and progression: a systematic review. Prostate Cancer Prostatic Dis. 1–12. doi:10.1038/pcan.2014.45

Zhang, K., Wang, X.Q., Zhou, B., Zhang, L., 2013. The prognostic value of MGMT promoter methylation in Glioblastoma multiforme: A meta-analysis. Fam. Cancer. doi:10.1007/s10689-013-9607-1

Zhang, W., Liu, H.T., 2002. MAPK signal pathways in the regulation of cell proliferation in mammalian cells. Cell Res. 12, 9–18. doi:10.1038/sj.cr.7290105

Zhang, Y., Guo, G.L., Han, X., Zhu, C., Kilfoy, B.A., Zhu, Y., Boyle, P., Zheng, T., 2008. Do polybrominated diphenyl ethers (PBDE) increase the risk of thyroid cancer? Biosci. Hypotheses 1, 195–199. doi:10.1016/j.bihy.2008.06.003

Zhou, H., Hu, H., Lai, M., 2010. Non-coding RNAs and their epigenetic regulatory mechanisms. Biol Cell 102, 645–655. doi:10.1042/BC20100029

Zhou, Q., Chen, J., Feng, J., Wang, J., 2016. Long noncoding RNA PVT1 modulates thyroid cancer cell proliferation by recruiting EZH2 and regulating thyroid-stimulating hormone receptor (TSHR). Tumour Biol. 37, 3105–13. doi:10.1007/s13277-015-4149-9

Zimmermann, M.B., Galetti, V., 2015. Iodine intake as a risk factor for thyroid cancer: a comprehensive review of animal and human studies. Thyroid Res. 8, 8. doi:10.1186/s13044-015-0020-8

Zoghlami, A., Roussel, F., Sabourin, J.C., Kuhn, J.M., Marie, J.P., Dehesdin, D., Choussy, O., 2014. BRAF mutation in papillary thyroid carcinoma: Predictive value for long-term prognosis and radioiodine sensitivity. Eur. Ann. Otorhinolaryngol. Head Neck Dis. 131, 7–13. doi:10.1016/j.anorl.2013.01.004

Zuo, H., Gandhi, M., Edreira, M.M., Hochbaum, D., Nimgaonkar, V.L., Zhang, P., DiPaola, J., Evdokimova, V., Altschuler, D.L., Nikiforov, Y.E., 2010. Downregulation of Rap1GAP through epigenetic silencing and loss of heterozygosity promotes invasion and progression of thyroid tumors. Cancer Res. 70, 1389–1397. doi:10.1158/0008-5472.CAN-09-2812

Anexos

1. Anexo 1

1.1. Características histológicas más relevantes de los tumores de tiroides

Anexo 1.1 : Características más releventes de los tumores de tiorides de acuerdo a su tipo histológico. Extraído de (Xing 2013)

Histología	Origen celular	Prevalencia (%)	Características macroscópicas	Características microscópicas	Agresividad	Referencias
FTA	Folicular	Lesión benigna	– Tamaño variable (de entre 1 a más de 10 cm) – Aspecto gomoso y homogéneo – Rodeado por una cápsula fibrosa – No hay invasión capsular y/o vascular	– Folículos aparentemente normales que contienen coloide – Figuras mitóticas rara vez – Ocasionalmente el citoplasma puede contener gránulos eosinófilos brillantes (células de Hürtle) y pleomorfismo nuclear focal, atípia y gran nucleolo.	– Tumores benignos	– Scopa 2004 – McCherry 2011
PTC	Folicular	80-85	– Tamaño medio de 2-3 cm – Firmes y blancos – Apariencia invasiva – Calcificaciones bastante comunes	– Arquitectura papilar – Características nucleares: – Grande, alargado y superpuesto – Aspecto esmerilado, pálido y/o vacío – Contorno irregular con inclusiones y surcos – Nucleolo pequeño	– WDTC poco agresivo – Supervivencia a los 5 años mayor del 90% – Propensión a la metástasis linfática	– Hunt and Barnes, 2003 – Teijeiro and Sobrinho-Simões, 2003 – Livolsi 2011
FTC	Folicular	10-15	– Rodeados por una cápsula más fina e irregular que la de los FTA – Unicéntricos – Microinvasiones (FTC mínimamente invasivo) o macroinvasiones (FTC invasivo) capsulares y/o vasculares	– Carece de las características nucleares de PTC – La variante de células de ¨Hürtle presenta numerosas y grandes mitocóndrias con nucleolos de cromatina muy densa	– WDTC poco agresivo – Supervivencia a los 5 años mayor del 90% – La invasión vascular aumenta la agresividad – La variante de células de Hürtle es agresiva con tendencia a la metástasis nodal y a distancia	– Schlumberger, 1998 – Scopa 2004 – Sobrinho-Simões et al., 2011 – Bose and Walts, 2012
PDTC	Folicular	4-7	– Tamaño medio superior a 5 cm – Sólidos y no encapsulados – Invasión estratiroidea	– Células pequeñas e hipercromáticas – Nucleolo difuso	– Tumor medianamente desdiferenciado y muy agresivo – Supervivencia a los 5 años del 50% – Metástasis nodal y a distancia – Riesgo de recurrencia	– Bongiovanni et al., 2009 – Kane and Sharma, 2015
ATC	Folicular	2-3	– Tamaño superior a 5 cm – Sólidos y blanquecinos – No encapsulados – Invasión a tejidos adyacentes a la tiroides – Múltiples nódulos en toda la glándula – Suelen presentar áreas hemorrágicas y necróticas	– Las células crecen en racimos sólidos – Células con citología atípica y altamente mitóticas – Células en huso, escamosoas o gigantes según el subtipo histológico – Suelen presentar zonas con histología típica de WDTC	– Tumor totalmente desdiferenciado y extremadamente agresivo – Supervivencia a los 5 años nula – Supervivencia media inferior a 6 meses. – Metastáticos a distancia	– Pinchot et al., 2008 – Khairy, 2009 – Smallridge et al., 2009 – Adeniran and Chhieng, 2016
MTC	Parafolicular	10	Tamaño variable de entre pocos centímetros a varios milímetros. Firme y consistente de color blanquecino o rojo Pueden presentar infiltraciones al tejido sano	– Células fusiformes o poligonales agrupadas en nidos, trabéculas o folículos y separadas por un estroma fibroso – Pueden observarse depósitos de amiloide acelular – Citoplasma repleto de gránulos densos rodeados de membrana	Moderadamente agresivo Propensión a metástasis linfática	– Pacini et al., 2010 – Figlioli et al., 2013 – Schmid, 2015

1.2. Estructura de RAS y RAS mutante

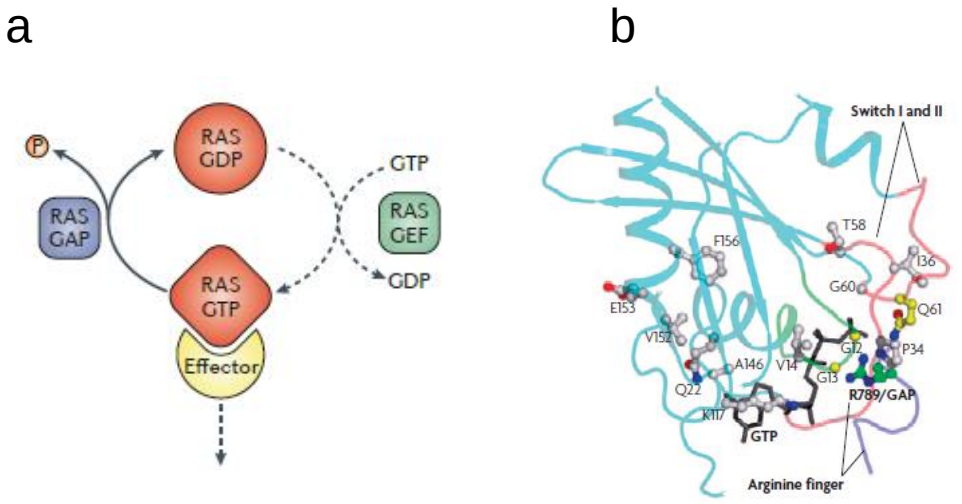

Anexo 1.2 | Estructura de RAS y RAS mutante. (a) La alternancia entre los estados activo e inactivo de RAS depende de su unión de GTP o GDP respectivamente. Los intercambiadores de nucleótidos guanina (GEFs), entre los que se encuentra SOS, permiten el intercambio de GDP por GTP mientras que las proteínas activadoras de GTPasas (GAPs) inducen la hidrólisis de GTP a GDP. Figura extraída de (Cox et al., 2014). **(b)** Mutaciones no sinónimas en G12 o G13 de RAS provocan la sustitución del único aminoácido que carece de cadena lateral, la glicina, lo que conlleva interferencias estéricas de la cadena lateral del nuevo aminoácido con la estructura que adquiere RAS durante la hidrólisis de GTP a GDP. Esto insensibiliza la inactivación de RAS por GAP manteniendo RAS constitutivamente activo. Por otro lado, entre la glutamina 61 (G61) de RAS y la arginina 789 (R789) de GAP se forma un puente de hidrógeno que permite el ataque nucleofílico de una molécula de agua imprescindible durante la hidrólisis de GTP. Mutaciones no sinónimas en este residuo (Q61) impiden la formación de dicho puente de hidrógeno reduciendo la estabilidad de RAS durante la transición de GTP a GDP bloqueando la actividad de la GAP y manteniendo RAS constitutivamente activo (Malumbres and Barbacid, 2003; Scheffzek et al., 1997). Figura extraída de (Schubbert et al., 2007).

1.3. Tipos de translocaciones del gen RET

Tabla A1.3 | Tipos de translocaciones del gen *RET*. Adaptado de (Nikiforova and Nikiforov, 2008; Rabes et al., 2000; Romei and Elisei, 2012; Tallini and Asa, 2001).

Translocación	Genes	Localización cromosómica	Prevalencia (%)	Referencia
RET/PTC1	*CCD6*	Inv10(q11.2;q21)	60-70	(Grieco et al., 1990)
RET/PTC2	*PRKAR1A*	t(10;17)(q11.2;q23)	<5	(Bongarzone et al., 1993)
RET/PTC3	*NCO4*	inv10(q11.2;q10)	15	(Bongarzone et al., 1994)
RET/PTC4	*NCO4*	inv10(q11.2;q10)	raro	(Fugazzola et al., 1996)
RET/PTC6	*TRIM24*	t(7;10)(q11.2;q32)	1.6	(Klugbauer and Rabes, n.d.)
RET/PTC7	*TRIM33*	t(1;10)(p13;q11.2)	1.6	(Klugbauer and Rabes, n.d.)
RET/PTC8	*KTN1*	t(10;14)(q11.2;q22.1)	1-5	(Salassidis et al., 2000)
RET/PTC9	*RFG9*	t(10;18)(q11.2;q21-22)	1-5	(Klugbauer et al., 2000)
ELKS/RET	*ELKS*	t(10;12)(q11.2;p13.3)	1-6	(Nakata et al., 2002)
PCM1/RET	*PCM1*	t(8;10)(p21-22;q11.2)	EUP	(Corvi et al., n.d.)
RFP/RET	*TRIM27*	t(6;10)(p21;q11.2)	EUP	(Saenko et al., 2003)
HOOK3/RET	*HOOK3*	t(8;10)(p11.21;q11.2)	EUP	(Ciampi et al., 2007)

2. Anexo 2

2.1. Formato original del trabajo I

www.impactjournals.com/oncotarget/ Oncotarget, Vol. 7, No. 9

Quantification of Unmethylated Alu (QUAlu): a tool to assess global hypomethylation in routine clinical samples

Raquel Buj[1,2], Izaskun Mallona[1,2], Anna Díez-Villanueva[1,2], Víctor Barrera[1], Dídac Mauricio[2,3,4], Manel Puig-Domingo[2,3,4], Jordi L. Reverter[2,3], Xavier Matias-Guiu[5], Daniel Azuara[6], Jose L. Ramírez[2,7], Sergio Alonso[1,2], Rafael Rosell[2,7], Gabriel Capellà[6], Manuel Perucho[1,2,8], Mercedes Robledo[9,10], Miguel A. Peinado[1,2] and Mireia Jordà[1,2]

[1] Institute of Predictive and Personalized Medicine of Cancer (IMPPC), Badalona, Barcelona, Spain

[2] Germans Trias i Pujol Health Sciences Research Institute (IGTP), Badalona, Barcelona, Spain

[3] Department of Endocrinology and Nutrition, University Hospital Germans Trias i Pujol, Badalona, Barcelona, Spain

[4] ISCIII Center for Biomedical Research on Diabetes and Metabolic Associated Diseases (CIBERDEM), Madrid, Spain

[5] Department of Pathology and Molecular Genetics, University Hospital Arnau de Vilanova and University of Lleida, Biomedical Research Institute of Lleida (IRBLLEIDA), Lleida, Spain

[6] Catalan Institute of Oncology (ICO-IDIBELL), L'Hospitalet de Llobregat, Barcelona, Spain

[7] Catalan Institute of Oncology (ICO), Hospital Germans Trias i Pujol, Badalona, Barcelona, Spain

[8] Catalan Institution for Research and Advanced Studies (ICREA), Barcelona, Spain

[9] Hereditary Endocrine Cancer Group, Spanish National Cancer Research Center (CNIO), Madrid, Spain

[10] ISCIII Center for Biomedical Research on Rare Diseases (CIBERER), Madrid, Spain

***Correspondence to**: Mireia Jordà, **email**: mjorda@imppc.org*

*Correspondence to: Miguel A. Peinado, **email**: map@imppc.org*

Keywords: DNA hypomethylation, Alu repeats, human cancer, biomarker, routine clinical biospecimens

Received: November 23, 2015 ***Accepted***: January 25, 2016 ***Published***: February 07, 2016

ABSTRACT

Hypomethylation of DNA is a hallmark of cancer and its analysis as tumor biomarker has been proposed, but its determination in clinical settings is hampered by lack of standardized methodologies. Here, we present QUAlu (Quantification of Unmethylated Alu), a new technique to estimate the Percentage of UnMethylated Alu (PUMA) as a surrogate for global hypomethylation.

QUAlu consists in the measurement by qPCR of Alu repeats after digestion of genomic DNA with isoschizomers with differential sensitivity to DNA methylation. QUAlu performance has been evaluated for reproducibility, trueness and specificity, and validated by deep sequencing. As a proof of use, QUAlu has been applied to a broad variety of pathological examination specimens covering five cancer types.

Major findings of the preliminary application of QUAlu to clinical samples include: (1) all normal tissues displayed similar PUMA; (2) tumors showed variable PUMA with the highest levels in lung and colon and the lowest in thyroid cancer; (3) stools from colon cancer patients presented higher PUMA than those from control individuals; (4) lung squamous cell carcinomas showed higher PUMA than lung adenocarcinomas, and an increasing hypomethylation trend associated with smoking habits.

In conclusion, QUAlu is a simple and robust method to determine Alu hypomethylation in human biospecimens and may be easily implemented in research and clinical settings.

INTRODUCTION

Extensive evidence describes cancer as a combination of genetic and epigenetic alterations which cooperate at every step of the tumor progression (reviewed in [1]). DNA methylation is the most well-characterized epigenetic mark in mammals and consists in the covalent addition of a methyl group to the cytosine located

within the CpG dinucleotide. It is frequently associated with silenced chromatin and transcriptional repression (reviewed in [2-3]). Among all the epigenetic alterations that delineate cancer genomes, loss of global DNA methylation has been considered a hallmark. Numerous works have demonstrated that DNA hypomethylation is an early and sustained event in tumorigenesis. Besides, it promotes a permissive landscape for cancer development and progression by encouraging chromosomal instability, imprinting loss, aberrant gene expression and transposon activation (reviewed in [2-3]). More importantly, it has been reported a strong association between the degree of DNA hypomethylation and the tumor grade and stage, which has attracted great interest for its potential clinical value, not only in cancer diagnosis and prognosis [4-9], but also as a marker of cancer risk [9-12].

A wide variety of techniques have been designed to measure global DNA methylation, some of which quantify the overall levels of 5-methylcytosine in the genome compared with unmethylated cytosines (e.g. HPLC, immunochemical assay, etc.), while others assess the methylation levels of specific genome compartments (reviewed in [9, 13]). Among the second group, the most widely used methods are those based on repeat elements, as they exhibit a high copy number and are widespread throughout the human genome. Nevertheless, none of them has been established in the clinical practice due in part to technical, economical and time shortcomings, which preclude a standardized alternative.

Here we present a new method, Quantification of Unmethylated Alu (QUAlu), which uses Alu repeats as surrogate reporter of global DNA methylation. Alu repeats are primate-specific transposable elements that belong to the Short Interspersed Elements (SINEs) family and represent the most abundant class of repetitive sequences in the human genome (1.1 million copies per haploid genome) [14]. Alu elements contain up to 25% of the overall CpG sites in the genome (Table 1) and are highly methylated in somatic tissues. Interestingly, they are located in gene-rich regions [15].

QUAlu is a simple and rapid method based on the digestion of genomic DNA with the methylation-sensitive and insensitive isoschizomers *Hpa*II/*Msp*I, the ligation of an adaptor and a qPCR using primers specific for the Alu consensus sequence. We have applied this technique to a broad variety of pathological examination samples including fresh frozen tissues, formalin-fixed paraffin-embedded (FFPE) sections, fine-needle aspiration biopsies (FNAB), stools and liquid biopsies. Our preliminary results underscore the potential clinical utility of the assessment of unmethylated Alu elements by QUAlu.

RESULTS

QUAlu design and technical evaluation

According to the reference human assembly hg19, there are over 28 millions of CpG dinucleotides in the human genome and more than half are located within repeat elements, being Alu elements those containing the highest fraction, namely 25.4% (Table 1). Therefore, we selected Alu elements as the most adequate surrogate reporter of global methylation and developed QUAlu technique, a method to identify unmethylated Alu repeats which shares the quantitative nature of the related technique LUMA [16] and the specificity of QUMA [17]. Fundamentals of QUAlu assay are outlined in Figure 1 and Supplementary Figure S1. QUAlu is based on the different methylation sensitivity of the isoschizomers *Hpa*II/*Msp*I (see Materials and Methods and Supplementary Material), whose recognition site is C/CGG, located in the Alu consensus sequence AACCCGG present in 14.4% of Alu elements (Table 1). Noteworthy, analysis of whole genome bisulfite sequencing data [18] showed that the *Hpa*II/*Msp*I sites embedded in CpG islands may be used as reporters of the overall methylation of these genomic elements [19]. In this regard, we also confirmed that this postulate may be also applied to Alu repeats: more than 90% of the *Hpa*II/*Msp*I sites within the Alu consensus sequence AACCCGG showed concordant methylation levels with the whole Alu sequence (Supplementary Table S4). To determine the virtual representativeness of QUAlu (QUAluome), an electronic qPCR simulation was performed showing a theoretical coverage of 155 878 Alu elements (see Supplementary Material), which corresponded to the 13.65% of the Aluome, with a bias toward amplification of young subfamilies (Supplementary Figure S2).

To assess the linearity of QUAlu, different starting amounts of HCT116 genomic DNA, ranging from 0.3 to 80 ng, were used. As it can be observed in Figure 2A, all quantifications showed excellent linearity ($R^2 > 0.98$ in all cases). Moreover, similar percentages of unmethylated Alu elements were obtained, being the overall average 8.8± 2.2 (Supplementary Figure S3A). The same assay was done with clinical samples from normal tissues of lung, colon and thyroid, obtaining an excellent linearity in all cases (Supplementary Table S5).

The inter-assay repeatability was assessed by analyzing the same HCT116 genomic DNA in 39 independent QUAlu assays. The mean of all the analyses was 9.9% and the standard deviation ±1.6. Furthermore, replicates of tumor and normal clinical samples were measured in different plates confirming that the technique is reproducible ($R^2 = 0.981$) (Figure 2B). Importantly, the feasibility of QUAlu in samples containing partially degraded DNA was verified (Supplementary Material and

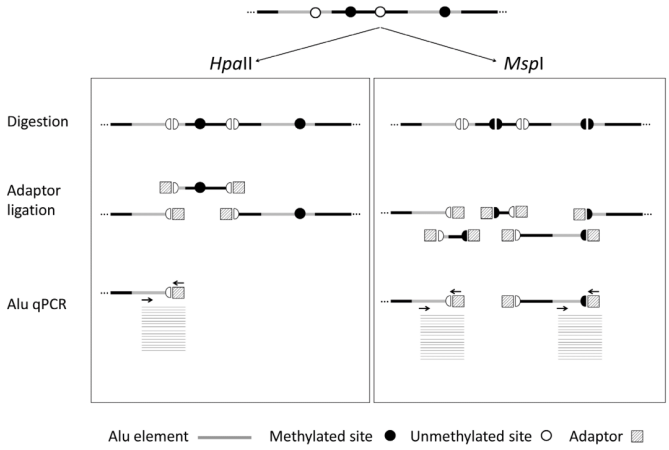

Figure 1: QUAlu technique diagram. Genomic DNA is digested using *Hpa*II and *Msp*I isoschizomers (DNA methylation sensitive and insensitive, respectively), ligated to a synthetic adaptor, and Alu elements are specifically amplified by qPCR in two separated reactions. The ratio between the two reactions gives the percentage of unmethylated Alu elements (PUMA). DNA normalization is performed by parallel amplification of L1PA.

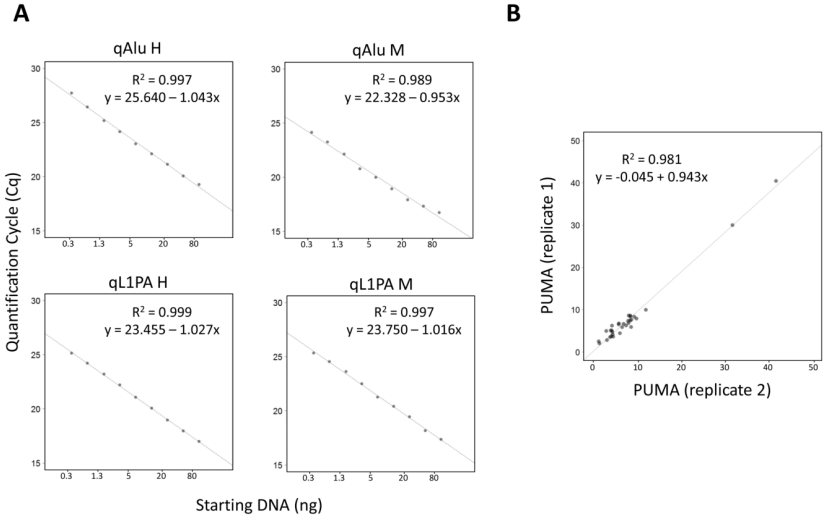

Figure 2: Evaluation of QUAlu technique. A. Standard curves showing the linear range of the different qPCRs performed in a QUAlu assay. HCT116 genomic DNA amounts ranging from 0.3 to 80 ng were used. **B.** Correlation of the percentage of unmethylated Alu elements (PUMA) determined by QUAlu in two independent experiments.

Table 1: Alu repeat content in the human genome and representativeness in the virtual QUAlu [a]

Sequence	No of elements	Base pairs	No of CpGs	No of HpaII/MspI sites	AACCCGG hits[d]	QUAluome[d]
Alu [b]	1,194,734	305,076,148 (9.7%)	7,173,987 (25.4%)	742,725 (32.3%)	172,574 (79.1%)	155,878
LINE [c]	1,498,690	638,481,131 (20.4%)	3,412,416 (12.1%)	155,813 (6.8%)	6,881 (3.2%)	0
CpG islands	28,691	21,842,742 (0,7%)	2,089,537 (7.4%)	270,622 (11.8%)	4,470 (2.1%)	0
Genome	-	~3,200,000,000 (100%)	28,217,009 (100%)	2,297,221 (100%)	218,131 (100%)	0

[a]Data based on GRCh37/hg19 human genome assembly.
[b]RepeatMasker's Alu repFamily members discarding FLAMs and FRAMs.
[c]RepeatMasker's LINE repClass members.
[d]Virtual QUAlu amplicons.

Table 2: Percentage of Unmethylated Alu repeats (PUMA) in different human tissues and tumors

	Thyroid	Prostate	Breast	Colon	Lung
Normal tissue	6.2 ± 1.6 (n = 9)	4.8 ± 2.6 (n=7)	5.6 ± 2.66 (n=14)	6.9 ± 1.9 (n=16)	5.9 ± 2.0 (n=37)
Tumor tissue	8.2 ± 3.1 (n=59)	8.5 ± 8.8 (n=18)	10.0 ± 5.9 (n=20)	14.6 ± 5.2 (n=16)	14.6 ± 8.3 (n=39)
p-value [a]	0.032	0.357	0.002	< 0.001	< 0.001

[a]Normal vs. Tumor, Mann-Whitney U test

Supplementary Figure S3B-S3C).

It is of note that consistent QUAlu results may be achieved with DNA amounts well below one haploid genome. In fact, linear range response was reached with as little as 0.005 pg of DNA per PCR tube (equivalent to 0.002 haploid genomes) (Supplementary Figure S4). The low requirements of QUAlu are due to the multiplex nature of its target (a large pool of more than one hundred thousand Alu repeats), reaching sensitivity detection 4 to 5 orders of magnitude higher than a single copy locus (e.g. promoter region of Digestive organ expansion factor homolog (zebrafish) -*DIEXF*- gene) (Supplementary Figure S4 and Supplementary Material). Noteworthy, the complexity of the QUAlu product is visualized as a broad melting peak for both the *HpaII* and the *MspI* samples, contrasting with the narrower peak of a single PCR product (Supplementary Figure S5).

Finally, the specificity of QUAlu to amplify Alu elements was validated by next-generation sequencing of five QUAlu determinations. The results showed that 97% of the reads (range 96.6-98.1%) obtained from the sequenced samples aligned with Alu repeats (Supplementary Table S6) and confirmed the complex composition of QUAlu product composed of multiple different Alu elements with similar distributions among all the analyzed samples (Supplementary Figure S6).

QUAlu application to fresh frozen human cancer samples

QUAlu technique was applied to analyze the levels of unmethylated Alu elements in different cancer types and their normal counterparts (Table 2 and Supplementary Table S7). Interestingly, the different normal tissue types showed similar values of Percentage of UnMethylated Alu elements (PUMA) (Table 2) (Kruskal Wallis test, p-value = 0.308), being the average PUMA 6.0 ± 2.1 (range 1.8-14.8). However, PUMA showed a broad variation in tumors, ranging from 0.9 to 40.5 (average = 10.7 ± 6.8). Furthermore, important differences were observed between cancer types (Table 2 and Figure 3A) (Kruskal Wallis test, p-value < 0.05), with colon and lung exhibiting 2-3 fold higher levels of unmethylated Alu repeats as compared with thyroid, prostate and breast cancer (Supplementary Tables S7 and S8).

The comparison between normal and tumor samples showed statistically significant differences in most cancer types, except in prostate cancer (Mann-Whitney U test, p-value = 0.357) (Figure 3A and Table 2).

Since there were no differences among normal tissues in the proportion of unmethylated Alu elements, the 99th percentile (PUMA = 12%) was taken as a cut-off value to consider a tumor as hypomethylated. Thus, particular analysis of each tumor type revealed that 62.5% of colon and 64.1% of lung tumors were hypomethylated, while in breast and prostate tumors this figure was 20%

and 16.7%, respectively. Otherwise, only 11.9% of thyroid tumors had percentages of unmethylated Alu elements above the reference value (Supplementary Figure S7). When considering only the matched normal-tumor pairs of all cancer types (n = 81), the difference among them was evident in most cases (paired Mann-Whitney U test p-value<0.001). About one third of colon (5/16) and lung (13/37) tumors displayed a high hypomethylation as compared with the paired normal tissue (fold change greater than 3). Contrarily, this big difference was uncommon in breast (2/14), prostate (1/7) or thyroid (0/7) cancer (Supplementary Tables S7 and S9).

Evaluation of PUMA as biomarker in specific cancers

To estimate the potential value of the percentage of unmethylated Alu elements to discriminate between normal and tumoral tissue we performed ROC analyses (Figure 3B). Area Under the Curve (AUC) values confirmed that PUMA was a good biomarker (AUC > 0.8) for breast, colon and lung cancer, with sensitivities and specificities >80%, except for breast cancer, whose sensitivity reached 92.9% but the specificity was lower

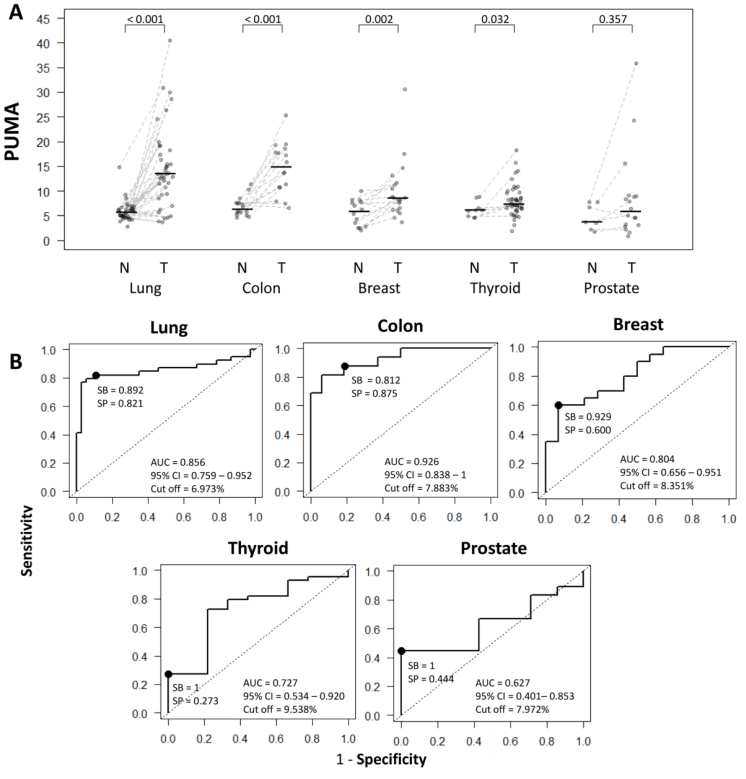

Figure 3: Comparison and diagnostic value of QUAlu among different cancer types. A. PUMA in different cancer types (normal tissue (N) and tumor (T)); the median of each group is represented by a black line. **B**. Receiver Operating Characteristic curves for the diagnosis of lung, colon, breast, thyroid and prostate cancer according to the percentage of unmethylated Alu (PUMA) elements determined by QUAlu.

(60%). Otherwise, for both prostate and thyroid cancer, although the sensitivity reached 100%, the specificity was low (44.4% and 27.3%, respectively). The cut-off values varied from tissue to tissue (Figure 3B), with the lowest levels in lung (6.97) and the highest in thyroid (9.54).

Moreover, to evaluate the clinical value of the QUAlu assay, we performed additional statistical analyses in two cancer types with the highest and the lowest PUMA, namely lung and thyroid cancer.

As described above, lung cancers exhibited high levels of hypomethylated Alu elements, but differences were also detected among lung cancer subtypes. Specifically, lung squamous cell carcinoma showed the highest PUMA (16.8 ± 8.8) compared with lung adenocarcinomas (12.2 ± 6.1) (Mann-Whitney U test *p*-value = 0.001) (Figure 4A and Supplementary Table S10). On the other hand, while no significant differences were observed in PUMA among lung normal tissue from never smokers, former smokers (more than 10 years) and current smokers (Kruskal Wallis test *p*-value >0.05), there was a significant increasing trend (Mann-Whitney U test, *p*-value = 0.006) of lung tumors to become more unmethylated in current smokers compared to former smokers (Figure 4B).

As regard to thyroid cancer, there were no significant differences in the percentage of unmethylated Alu elements in relation to histology subtype (Kruskal Wallis test, *p*-value = 0.231) or genetic alteration (RAS or BRAF mutations) (Kruskal Wallis test *p*-value = 0.147).

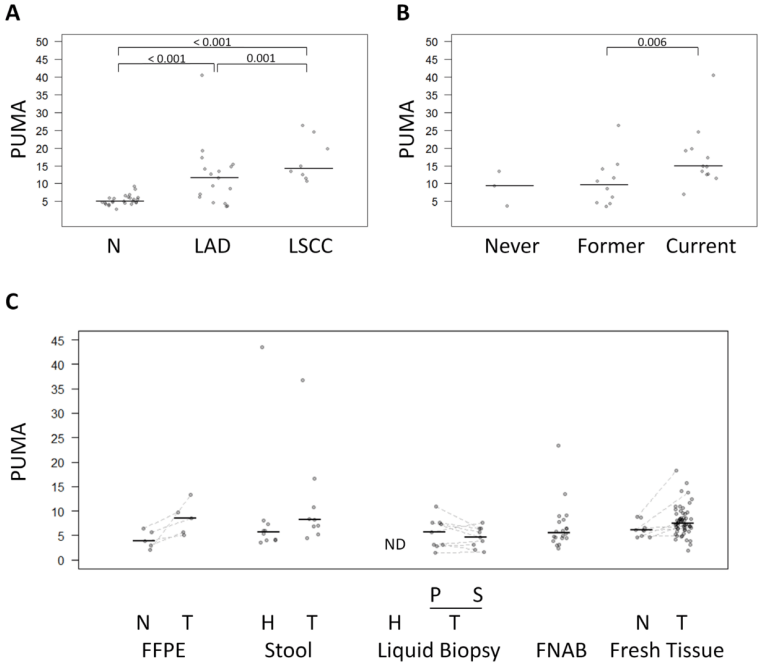

Figure 4: Comparison of QUAlu among different clinical characteristics and sample types. A. PUMA in normal lung tissue, lung adenocarcinoma (LAD) and lung squamous cell carcinoma (LSCC) and **B**. in lung cancer patients according to their smoking habits. **C**. PUMA in different sample types: FFPE (colon cancer patients), stool (healthy donors and colon cancer patients), liquid biopsy (plasma from healthy donors, and plasma and serum from lung cancer patients), FNAB (thyroid goiter patients), fresh tissue (thyroid cancer patients). The median of each group is represented by a black line. Normal (N), tumor (T), healthy donors (H), plasma (P), serum (S), no detectable samples (ND).

QUAlu application to diverse pathological examination biospecimens

Next, we evaluated the applicability of QUAlu to biospecimens obtained in standard pathological procedures often containing low amount of poor quality DNA (FFPE, FNAB, liquid biopsies and stools). Due to the low amount of starting material, DNA was not quantified and 1 ul of the extracted DNA was used for QUAlu analysis (see Supplementary Material). All samples produced detectable levels of amplified Alu elements (qAlu M Cq range: 16 to 30, qAlu H Cq range: 19 to 34) (Supplementary Figure S8), with the exception of plasma samples obtained from healthy individuals and one stool sample from one colon cancer patient.

The low number of samples precluded a robust comparison of the results, but some insightful trends were observed (Figure 4C). FFPE colon tumors showed higher PUMA than the matching normal samples (paired Mann-Whitney U test p-value = 0.062). Moreover, elevated Alu hypomethylation in the stools was more frequent in colon cancer patients than in control individuals (Mann-Whitney U test p-value = 0.079). Interestingly, liquid biopsies produced similar PUMA in plasma and serum from lung cancer patients, but did not amplify in cancer-free controls, which is consistent with the common absence of circulating free DNA in healthy individuals [20].

Finally thyroid goiters FNABs showed a PUMA in the same range than normal tissues with some exceptions: four cases presented a PUMA above 8.8, the highest value in normal thyroid tissue (Figure 4C).

DISCUSSION

Most of human genome is methylated, but in a wide range of pathologies, including cancer, a global DNA hypomethylation occurs affecting in large extent repetitive elements, which constitute ~45% of the genome. Weisenberger et al. [21] demonstrated that the methylation of different repetitive sequences, namely, LINE-1, Alu and satellite 2 (Sat2), significantly correlated with global methylation levels measured by high performance liquid chromatography (HPLC), and proposed the use of these repeats as surrogate reporters of global methylation. LINEs have been broadly used to estimate the global levels of hypomethylation [22-24], but Alu elements display some features that make them more suited for this purpose. Namely, Alu repeats constitute the most abundant retrotransposon and contain 25% of all the CpGs in the human genome. Moreover, due to their prevalent localization in gene-rich regions [15] epigenetic variations in Alu repeats may have direct implications in gene regulation, and by extension, in tumor biology.

Here we present QUAlu, a new technique to measure the levels of DNA unmethylation in Alu repeats, with several features that facilitate a direct implementation in clinical and research settings. These include a 100 fold higher sensitivity than other related methods [25], as accurate determinations can be performed with as little as 300 pg of DNA (corresponding to approximately 150 diploid cells). QUAlu specificity for Alu elements is extremely high, as demonstrated by deep sequencing of its products, where 97% of the reads mapped in Alu repeats.

Moreover, thanks to the calibration with internal controls (L1PA simultaneously with Alu repeats), QUAlu is relatively unaffected by the quantity and quality of the starting material in artificially degraded DNA. Furthermore, we have demonstrated that this technique is amenable to be applied to a broad spectrum of pathological examination specimens routinely collected in clinical settings (frozen tissues, FFPE, liquid biopsies, stools and FNAB). In spite of the low number of samples analyzed, preliminary results are promising, especially for FFPE and stools. Nevertheless, direct applicability of QUAlu in different clinical settings requires the analysis of large series of cases to define the threshold, sensitivities and specificities.

With clinical practice in mind, technical benefits of QUAlu include the small number of steps (digestion-ligation, real time PCR and analysis), the short time required to complete the determination (less than 5 hours from the DNA to the final result, even without automation of the process), and the low cost (about 6.3 US$ per sample, including technician labor).

As mentioned above, several techniques have been developed to estimate global methylation, and many of them target repeat elements as surrogate reporters (reviewed in [9, 13]). While most of these methods may constitute good alternatives to compare global methylation levels among a few samples, their implementation as a clinical tool is not a straightforward approach due to either technical complexity or exquisite sample necessities. QUAlu simplicity and limited equipment requirements facilitate its implementation in most laboratories.

To assess the clinical potential of QUAlu, we determined the extent of Alu hypomethylation in different human cancers by analyzing normal and tumor tissues. In a first analysis we compared the different normal tissues and different individuals, showing that the levels of unmethylated Alu elements were very consistent from tissue to tissue and from individual to individual. This result was in agreement with previous studies analyzing global DNA methylation by MethyLight and HPLC [21] or targeting Alu elements [26-27], but not with other works reporting tissue-associated global methylation differences targeting LINE-1 [28].

Our data suggests that the degree of hypomethylation is variable among different cancer types, with thyroid, prostate and breast cancer exhibiting low levels of hypomethylation, while cancers of colon and lung displayed the highest levels. Chalitchagorn et al.

[28] analyzed LINE-1 methylation using bisulfite based PCR in several cancers, and although they found high levels of hypermethylation in some types (e.g. esophagus cancer), no hypomethylation was observed among the ones analyzed in our study. This might be explained by the low sensitivity of their technique or the low number of samples analyzed.

It is interesting to note that the low-hypomethylation cancer group included hormone-related tissues (thyroid, prostate and breast) with no direct interaction with external factors, while the high-hypomethylation group (colon and lung) was composed by tumors with a high exposure to environmental factors (e.g. diet, air). While we do not know the reason for this association, there are evidences supporting the impact of certain environmental factors (drugs, chemicals, pollutants and other agents) in the deregulation of epigenetic enzymes, which will eventually generate epigenetic changes, including DNA hypomethylation, that may accumulate over the time causing alterations in key cellular processes and promoting cancer [29-30]. Noteworthy, it has been reported that Alu hypomethylation (but not LINE-1 hypomethylation) in esophageal mucosa may reflect an epigenetic field for cancerization in esophageal carcinogenesis [12]. Other alternative explanations may be related with the dynamics of tumor progression in different tumor types and the role of DNA hypomethylation behind specific deregulation of biological pathways, including genomic stability [31-32].

Confirming previous reports [33] we found significant differences in the levels of hypomethylation among the two types of lung cancers considered here. Lung adenocarcinomas, the histological subtype most frequently associated with never-smokers and former smokers, were less hypomethylated than lung squamous cell carcinomas. Many studies have suggested a strong correlation between loss of DNA methylation and smoking habit in cancer patients [34-36], but also in healthy people [37-38]. In this regard, we found a significant increase of hypomethylation in current smokers compared to former smokers, but this trend was not observed in the adjacent normal tissue. This result may indicate different mechanisms of tumor progression in ex-smokers as compared with current smokers.

In summary, we have demonstrated that QUAlu is a feasible approach to analyze global DNA methylation in almost any type of biospecimen routinely collected in ordinary clinical settings. DNA hypomethylation is a hallmark of cancer but, as we have shown, its degree is highly variable. Its determination with a technique as QUAlu may have a broad spectrum of applications including diagnostic and prognostic evaluations.

MATERIALS AND METHODS

Samples

This study included a total of 300 pathological examination samples of different sources: 220 fresh frozen tissue samples (Supplementary Tables S1and S2), 10 FFPE samples, 31 liquid biopsies, 19 stool samples and 20 thyroid goiter FNAB samples. Regarding fresh frozen tissues, 16 colorectal carcinomas and their paired normal adjacent tissues were obtained from Hospital Universitari de Bellvitge (Barcelona, Spain). Forty-four thyroid carcinomas and 9 paired adjacent thyroid tissues were obtained as described in our previous study [39]. DNA of 20 breast carcinomas and 14 paired normal adjacent tissues, 18 prostate carcinomas and 7 paired normal adjacent tissues, and 39 lung carcinomas and 37 normal adjacent tissues were obtained from the Spanish National DNA Bank (BNADN, Salamanca, Spain). Patient characteristics are shown in Supplementary Tables S1 and S2. Five normal and tumoral paired colorectal carcinoma FFPE samples were obtained from Cooperative Human Tissue Network (CHTN). Nine stool samples from colorectal carcinoma patients and 10 from healthy donors were obtained from Hospital Universitari de Bellvitge (Barcelona, Spain). Finally, nine plasma and serum paired lung carcinoma liquid biopsies, 13 plasma liquid biopsies from healthy donors and 20 thyroid goiter FNAB samples were obtained from Hospital Universitari Germans Trias i Pujol (Badalona, Spain). The study was approved by the Hospital Germans Trias i Pujol Ethics Committee. Informed consent was obtained before surgery.

The colorectal carcinoma cell line HCT116 was obtained from the American Type Culture Collection (ATCC) and was authenticated on 3rd March 2014 by using the AmpFLSTR® Identifiler® Plus PCR Amplification Kit (Applied Biosystems). Cells were cultured in D-MEM/F12, supplemented with sodium pyruvate, L-glutamine and 10% fetal bovine serum (Life Technologies, MD, USA) and were maintained at 37ºC in a 5% CO_2 atmosphere. Genomic DNA was isolated using different methods as described in the Supplementary Material.

Human genome sequence data sets

We used the GRCh37/hg19 human genome assembly. Genomic positions of Alu elements, LINE sequences, CpG islands and CpG dinucleotides were retrieved from the UCSC MySQL repository (genome-mysql.cse.ucsc.edu). Motif search was performed with EMBOSS (http://emboss.sourceforge.net/). To count the number of overlapping features (Table 1) we used the BEDTools package (v2.19.1, [40]). For more technical details see Supplementary Material.

Quantification of Unmethylated Alu (QUAlu) assay

The principle underlying this technique is the selective amplification of Alu repeats containing an unmethylated CpG site within the consensus sequence AACCCGG. Briefly, genomic DNA was digested in parallel in two separated tubes with *Hpa*II and *Msp*I methylation-sensitive and -insensitive isoschizomers, respectively, which leave identical sticky ends (C/CGG). Next, a synthetic adaptor was ligated to the digested DNA fragments. Quantification was performed by qPCR using a primer complementary to the chimeric sequence of the adaptor plus the consensus Alu sequence after *HpaII* digestion (AACC + synthetic adaptor) and another one complementary to the Alu consensus sequence and located ~20 nucleotides upstream of the *HpaII* cutting site (Supplementary Figure S1). Thereby, qPCR of *Msp*I digestion (qAlu M) allowed the quantification of all the amplifiable Alu elements (irrespective of the methylation status), while qPCR of *Hpa*II digestion (qAlu H) only quantified the subset of amplifiable Alu elements containing an unmethylated CpG. Thus, the final result corresponded to the fraction of unmethylated Alu elements respect the total number of amplifiable Alu elements calculated according to the equation described below. Furthermore, two specific qPCRs for L1PA (a Long Interspersed Nuclear Element-1, LINE-1 subfamily) were performed to normalize the DNA input for both *Msp*I (qL1PA M) and *Hpa*II digestions (qL1PA H). For more technical details see Supplementary Material.

QUAlu data analysis

Statistical analyses were performed using R version 3.1.0. The Percentage of UnMethylated Alu elements (PUMA) for each sample was assigned according to this equation:

$$PUMA = \frac{\frac{E_{qAlu\,H}^{-Cq_{qAlu\,H}}}{E_{qL1PA\,H}^{-Cq_{qL1PA\,H}}}}{\frac{E_{qAlu\,M}^{-Cq_{qAlu\,M}}}{E_{qL1PA\,M}^{-Cq_{qL1PA\,M}}}} \times 100$$

The relative amount of unmethylated Alu elements (given by qAlu H normalized by the reference sequence qL1PA (qL1PA H)) and the relative amount of total amplifiable Alu elements (given by qAlu M normalized by qL1PA M) were calculated as a ratio of exponential functions in which the base was the qPCR efficiency (E) and the variable was the quantification cycle (Cq). To tackle the qPCR error propagation, permutation tests were done to obtain a final PUMA and its variation using the qPCR R package (v1.4-0, [41]). Mann-Whitney U test and Kruskal Wallis tests were used, as appropriate, to assess the significance among the different groups of samples. Correlation analyses were conducted using two-tailed Kendall tests. The significance level was established at $p<0.05$ for all analyses. Receiver operating characteristic (ROC) curves were generated using the pROC R package (v1.7.3, [42]) to assess the cut-off value that best discriminated between tumor and normal tissue according to the PUMA.

Characterization of QUAlu product by Next Generation Sequencing

To determine the specificity of the technique, the products generated by qAlu H and qAlu M from 5 samples (the colorectal cancer cell line HCT116, a lung squamous carcinoma with its normal matching tissue and a papillary thyroid carcinoma with its normal matching tissue) were sequenced using Ion Torrent technology (Life Technologies). For more technical details see Supplementary Material and Supplementary Table S3.

ACKNOWLEDGMENTS

We thank Mar Muñoz, Esmeralda Castelblanco and Veronica Mancikova for excellent technical support. We also thank all the patients and control donors for making this study possible.

CONFLICTS OF INTEREST

MAP is cofounder and equity holder of Aniling, a biotech company with no interests in this paper. The other authors declare no conflict of interest.

GRANT SUPPORT

RB was supported by a FPI fellowship from Ministerio de Economía y Competitividad. AD-V was supported in part by a contract PTC2011-1091 from Ministerio de Economía y Competitividad. This work was supported by grants from FEDER, the Ministerio de Economía y Competitividad (SAF2011/23638 to MAP), the Instituto de Salud Carlos III (FIS PI11/02421 to JR, FIS PI11/01359 and FIS PI14/00240 to MR, FIS PI14/00308 to MJ, FIS PI12/00511 to MP), and Fundació Olga Torres (to MJ).

Editorial note

This paper has been accepted based in part on peer-review conducted by another journal and the authors' response and revisions as well as expedited peer-review in Oncotarget.

REFERENCES

1. Sandoval J and Esteller M. Cancer epigenomics: beyond genomics. Curr Opin Genet Dev. 2012; 22:50-55.
2. Ehrlich M. DNA hypomethylation in cancer cells. Epigenomics. 2009; 1:239-259.
3. Feinberg AP. Phenotypic plasticity and the epigenetics of human disease. Nature. 2007; 447:433-440.
4. Li J, Huang Q, Zeng F, Li W, He Z, Chen W, Zhu W and Zhang B. The prognostic value of global DNA hypomethylation in cancer: a meta-analysis. PLoS One. 2014; 9:e106290.
5. Fabris S, Bollati V, Agnelli L, Morabito F, Motta V, Cutrona G, Matis S, Grazia Recchia A, Gigliotti V, Gentile M, Deliliers GL, Bertazzi PA, Ferrarini M, Neri A and Baccarelli A. Biological and clinical relevance of quantitative global methylation of repetitive DNA sequences in chronic lymphocytic leukemia. Epigenetics. 2011; 6:188-194.
6. Igarashi S, Suzuki H, Niinuma T, Shimizu H, Nojima M, Iwaki H, Nobuoka T, Nishida T, Miyazaki Y, Takamaru H, Yamamoto E, Yamamoto H, Tokino T, Hasegawa T, Hirata K, Imai K, et al. A Novel Correlation between LINE-1 Hypomethylation and the Malignancy of Gastrointestinal Stromal Tumors. Clin Cancer Res. 2010; 16:5114-5123.
7. Saito K, Kawakami K, Matsumoto I, Oda M, Watanabe G and Minamoto T. Long interspersed nuclear element 1 hypomethylation is a marker of poor prognosis in stage IA non-small cell lung cancer. Clin Cancer Res. 2010; 16:2418-2426.
8. Frigola J, Sole X, Paz MF, Moreno V, Esteller M, Capella G and Peinado MA. Differential DNA hypermethylation and hypomethylation signatures in colorectal cancer. Hum Mol Genet. 2005; 14:319-326.
9. Torano EG, Petrus S, Fernandez AF and Fraga MF. Global DNA hypomethylation in cancer: review of validated methods and clinical significance. Clin Chem Lab Med. 2012; 50:1733-1742.
10. Moore LE, Pfeiffer RM, Poscablo C, Real FX, Kogevinas M, Silverman D, Garcia-Closas R, Chanock S, Tardon A, Serra C, Carrato A, Dosemeci M, Garcia-Closas M, Esteller M, Fraga M, Rothman N, et al. Genomic DNA hypomethylation as a biomarker for bladder cancer susceptibility in the Spanish Bladder Cancer Study: a case-control study. Lancet Oncol. 2008; 9:359-366.
11. Choi JY, James SR, Link PA, McCann SE, Hong CC, Davis W, Nesline MK, Ambrosone CB and Karpf AR. Association between global DNA hypomethylation in leukocytes and risk of breast cancer. Carcinogenesis. 2009.
12. Matsuda Y, Yamashita S, Lee YC, Niwa T, Yoshida T, Gyobu K, Igaki H, Kushima R, Lee S, Wu MS, Osugi H, Suehiro S and Ushijima T. Hypomethylation of Alu repetitive elements in esophageal mucosa, and its potential contribution to the epigenetic field for cancerization. Cancer Causes Control. 2012; 23:865-873.
13. Jorda M and Peinado MA. Methods for DNA methylation analysis and applications in colon cancer. Mutat Res. 2010; 693:84-93.
14. Deininger P. Alu elements: know the SINEs. Genome Biol. 2011; 12:236.
15. Lander ES, Linton LM, Birren B, Nusbaum C, Zody MC, Baldwin J, Devon K, Dewar K, Doyle M, FitzHugh W, Funke R, Gage D, Harris K, Heaford A, Howland J, Kann L, et al. Initial sequencing and analysis of the human genome. Nature. 2001; 409:860-921.
16. Karimi M, Johansson S and Ekstrom TJ. Using LUMA: a Luminometric-based assay for global DNA-methylation. Epigenetics. 2006; 1:45-48.
17. Rodriguez J, Vives L, Jorda M, Morales C, Munoz M, Vendrell E and Peinado MA. Genome-wide tracking of unmethylated DNA Alu repeats in normal and cancer cells. Nucleic Acids Res. 2008; 36:770-784.
18. Lister R, Pelizzola M, Dowen RH, Hawkins RD, Hon G, Tonti-Filippini J, Nery JR, Lee L, Ye Z, Ngo Q-M, Edsall L, Antosiewicz-Bourget J, Stewart R, Ruotti V, Millar AH, Thomson JA, et al. Human DNA methylomes at base resolution show widespread epigenomic differences. Nature. 2009; 462:315-322.
19. Barrera V and Peinado MA. Evaluation of single CpG sites as proxies of CpG island methylation states at the genome scale. Nucleic Acids Res. 2012; 40:11490-11498.
20. Schwarzenbach H, Hoon DS and Pantel K. Cell-free nucleic acids as biomarkers in cancer patients. Nat Rev Cancer. 2011; 11:426-437.
21. Weisenberger DJ, Campan M, Long TI, Kim M, Woods C, Fiala E, Ehrlich M and Laird PW. Analysis of repetitive element DNA methylation by MethyLight. Nucleic Acids Res. 2005; 33:6823-6836.
22. Tajuddin SM, Amaral AF, Fernandez AF, Chanock S, Silverman DT, Tardon A, Carrato A, Garcia-Closas M, Jackson BP, Torano EG, Marquez M, Urdinguio RG, Garcia-Closas R, Rothman N, Kogevinas M, Real FX, et al. LINE-1 methylation in leukocyte DNA, interaction with phosphatidylethanolamine N-methyltransferase variants and bladder cancer risk. Br J Cancer. 2014; 110:2123-2130.
23. Salas LA, Villanueva CM, Tajuddin SM, Amaral AF, Fernandez AF, Moore LE, Carrato A, Tardon A, Serra C, Garcia-Closas R, Basagana X, Rothman N, Silverman DT, Cantor KP, Kogevinas M, Real FX, et al. LINE-1 methylation in granulocyte DNA and trihalomethane exposure is associated with bladder cancer risk. Epigenetics. 2014; 9:1532-1539.
24. Inamura K, Yamauchi M, Nishihara R, Lochhead P, Qian ZR, Kuchiba A, Kim SA, Mima K, Sukawa Y, Jung S, Zhang X, Wu K, Cho E, Chan AT, Meyerhardt JA, Harris CC, et al. Tumor LINE-1 methylation level and microsatellite instability in relation to colorectal cancer prognosis. J Natl Cancer Inst. 2014; 106.

25. Lisanti S, Omar WA, Tomaszewski B, De Prins S, Jacobs G, Koppen G, Mathers JC and Langie SA. Comparison of methods for quantification of global DNA methylation in human cells and tissues. PLoS One. 2013; 8:e79044.
26. Choi SH, Worswick S, Byun HM, Shear T, Soussa JC, Wolff EM, Douer D, Garcia-Manero G, Liang G and Yang AS. Changes in DNA methylation of tandem DNA repeats are different from interspersed repeats in cancer. Int J Cancer. 2009; 125:723-729.
27. Wu HC, Delgado-Cruzata L, Flom JD, Kappil M, Ferris JS, Liao Y, Santella RM and Terry MB. Global methylation profiles in DNA from different blood cell types. Epigenetics. 2011; 6.
28. Chalitchagorn K, Shuangshoti S, Hourpai N, Kongruttanachok N, Tangkijvanich P, Thong-ngam D, Voravud N, Sriuranpong V and Mutirangura A. Distinctive pattern of LINE-1 methylation level in normal tissues and the association with carcinogenesis. Oncogene. 2004; 23:8841-8846.
29. Herceg Z and Vaissiere T. Epigenetic mechanisms and cancer: an interface between the environment and the genome. Epigenetics. 2011; 6:804-819.
30. Mathers JC, Strathdee G and Relton CL. Induction of epigenetic alterations by dietary and other environmental factors. Adv Genet. 2010; 71:3-39.
31. Rodriguez J, Frigola J, Vendrell E, Risques RA, Fraga MF, Morales C, Moreno V, Esteller M, Capella G, Ribas M and Peinado MA. Chromosomal instability correlates with genome-wide DNA demethylation in human primary colorectal cancers. Cancer Res. 2006; 66:8462-9468.
32. Eden A, Gaudet F, Waghmare A and Jaenisch R. Chromosomal instability and tumors promoted by DNA hypomethylation. Science. 2003; 300:455.
33. Suzuki M, Shiraishi K, Eguchi A, Ikeda K, Mori T, Yoshimoto K, Ohba Y, Yamada T, Ito T, Baba Y and Baba H. Aberrant methylation of LINE-1, SLIT2, MAL and IGFBP7 in non-small cell lung cancer. Oncol Rep. 2013; 29:1308-1314.
34. Smith IM, Mydlarz WK, Mithani SK and Califano JA. DNA global hypomethylation in squamous cell head and neck cancer associated with smoking, alcohol consumption and stage. Int J Cancer. 2007; 121:1724-1728.
35. Andreotti G, Karami S, Pfeiffer RM, Hurwitz L, Liao LM, Weinstein SJ, Albanes D, Virtamo J, Silverman DT, Rothman N and Moore LE. LINE1 methylation levels associated with increased bladder cancer risk in pre-diagnostic blood DNA among US (PLCO) and European (ATBC) cohort study participants. Epigenetics. 2014; 9:404-415.
36. Liu F, Killian JK, Yang M, Walker RL, Hong JA, Zhang M, Davis S, Zhang Y, Hussain M, Xi S, Rao M, Meltzer PA and Schrump DS. Epigenomic alterations and gene expression profiles in respiratory epithelia exposed to cigarette smoke condensate. Oncogene. 2010; 29:3650-3664.
37. Shigaki H, Baba Y, Watanabe M, Iwagami S, Miyake K, Ishimoto T, Iwatsuki M and Baba H. LINE-1 hypomethylation in noncancerous esophageal mucosae is associated with smoking history. Ann Surg Oncol. 2012; 19:4238-4243.
38. Tajuddin SM, Amaral AF, Fernandez AF, Rodriguez-Rodero S, Rodriguez RM, Moore LE, Tardon A, Carrato A, Garcia-Closas M, Silverman DT, Jackson BP, Garcia-Closas R, Cook AL, Cantor KP, Chanock S, Kogevinas M, et al. Genetic and non-genetic predictors of LINE-1 methylation in leukocyte DNA. Environ Health Perspect. 2013; 121:650-656.
39. Mancikova V, Buj R, Castelblanco E, Inglada-Perez L, Diez A, de Cubas AA, Curras-Freixes M, Maravall FX, Mauricio D, Matias-Guiu X, Puig-Domingo M, Capel I, Bella MR, Lerma E, Castella E, Reverter JL, et al. DNA methylation profiling of well-differentiated thyroid cancer uncovers markers of recurrence free survival. Int J Cancer. 2014; 135:598-610.
40. Quinlan AR and Hall IM. BEDTools: a flexible suite of utilities for comparing genomic features. Bioinformatics. 2010; 26:841-842.
41. Ritz C and Spiess AN. qpcR: an R package for sigmoidal model selection in quantitative real-time polymerase chain reaction analysis. Bioinformatics. 2008; 24:1549-1551.
42. Robin X, Turck N, Hainard A, Tiberti N, Lisacek F, Sanchez JC and Muller M. pROC: an open-source package for R and S+ to analyze and compare ROC curves. BMC Bioinformatics. 2011; 12:77.

2.2. Material suplementario del trabajo I

Supplementary Methods

Samples

Primary tumors and normal adjacent tissues were snap frozen following surgery and stored at -80ºC. Genomic DNA from thyroid samples was extracted using the DNeasy Blood and Tissue kit (QUIAGEN, Valencia, CA, USA) according to the manufacturer's protocol. Genomic DNA from colon samples was isolated by standard phenol/chloroform protocol. Genomic DNA from breast, prostate and lung samples were obtained from the Spanish National DNA Bank (BNADN, Salamanca, Spain). One 10µm section of FFPE blocks was processed using the E.Z.N.A. FFPE DNA kit (Omega Bio-Tek, Norcross, GA, USA), with a xylene wash to remove paraffin and a final treatment of RNaseA (1 h at 45ºC). DNA from liquid biopsy samples was isolated with QIAamp DNA Blood Mini Kit (QIAGEN), while DNA from stools was extracted with QIAamp DNA Stool Mini Kit (QIAGEN). Genomic DNA from HCT116 cells and thyroid FNAB samples was extracted using the PureLink Genomic DNA Kit (Invitrogen, Carlsbad, CA, USA). Importantly, QUAlu assay was carried out using HCT116 genomic DNA isolated by different methods and no differences were observed in the percentage of unmethylated *Alu* elements (data not shown).

QUAlu protocol

For the standard QUAlu protocol, 2 aliquots consisting of 5 ng of genomic DNA (from fresh frozen tissues and cell lines) or 1uL of unknown concentration genomic DNA (FFPE, liquid biopsies, stools and FNAB samples) were simultaneously digested and ligated in two respective tubes with either 1 U of *Msp*I (International Inc., Burlington, Ontario, Canada) or 1 U of *Hpa*II (Fermentas). For the reaction 2 uL of Tango buffer 10X (Fermentas), 2 U of T4 ligase, 1 uL of T4 ligase buffer 10X (Fermentas), 1 nmol/L of synthetic adaptor (the adaptor sequence is shown below and in Supplementary Fig. S1) and water were added to a final volume of 30 uL. Mixes were incubated for 1 h at 37ºC followed by 2 h at 16ºC. Next, thermal inactivation of the enzymes was performed for 20 min at 65ºC.

	*Msp*I digestion (uL)	*Hpa*II digestion (uL)
Nuclease-free water	24.7	24.7
10X Tango buffer	1	1
10X T4 ligase buffer	2	2
Adaptor (1 nmol/L)	1	1
***Msp*I (10 U/uL)**	0.1	-
***Hpa*II (10 U/uL)**	-	0.1
T4 ligase (5 Weiss U/uL)	0.2	0.2
DNA	1	1
Final Volume	30	30

Real-Time PCR experiments were performed in a LightCycler® 480 Real-Time PCR System with white Multiwell Plate 384 plates (Roche Diagnostics GmbH, Mannheim, Germany). Both *Msp*I and *Hpa*II digestion-ligation mixtures were quantified using a specific *Alu* qPCR and a specific L1PA qPCR. A final volume of 10 uL for each reaction was prepared as follows: 5 uL of LightCycler® 480 SYBR Green I Master (Roche), 1 umol/L forward primer, 1 umol/L reverse primer (see detailed information about primers sequence below) and 1 uL of template from the digestion-ligation mixture diluted 1:20, equivalent to 0.008 ng of DNA.

	qALU (uL)	qL1PA (uL)
Nuclease-free water	3.8	3.8
***Alu* Fw primer (100 nmol/L)**	0.1	-
***Alu* Rv primer (100 nmol/L)**	0.1	-
L1PA Fw primer (100 nmol/L)	-	0.1
L1PA Rv primer (100 nmol/L)	-	0.1
LightCycler® 480 SYBR Green I Master	5	5
Digestion-ligation dilution	1	1
Final Volume	10	10

Each sample was assessed in triplicate. Conditions for amplification were: 10 min at 95ºC, 40 cycles of 10 s at 95ºC and 7 s at 56ºC. The assay ended with a melting-curve program: 15 s at 95ºC, 1 min at 70ºC, then ramping to 95ºC while continuously monitoring fluorescence, and final cooling to 4ºC. Each pair of tumor and normal tissue was analyzed in the same QUAlu assay to minimize technical variation. Furthermore, each QUAlu assay was performed including a negative control without template and two positive controls consisting of two different starting amounts of genomic HCT116 DNA (10 ng and 5 ng). For each primer pair (qAlu and qL1PA) the efficiency value (E) per individual well was calculated by using the amplification curve kinetics (cpD2 method) (Guescini et al., 2008). The efficiency average for each pair of primers in every qPCR plate was used to obtain the percentage of unmethylated *Alu* elements (PUMA).

Determination of *Alu* elements containing the AACCCGG motif

First, data were downloaded from the UCSC MySQL database. Namely, *Alu* elements were retrieved as those elements from the RepeatMasker table (rmsk) (Smit et al., 1996) with repFamily "*Alu*" and repName starting by "*Alu*", to avoid FLAM and FRAM elements. Second, coordinates were transformed into sequence using the bedtools getfasta program (Quinlan and Hall, 2010) using the hg19 reference genome assembly. Third, sequences were scanned for the motif with the EMBOSS program fuzznuc (Rice et al., 2000) without allowing neither mismatches nor gaps. The search covered both the direct and complement strands. We reported the *Alu* elements containing the AACCCGG pattern, not the individual hits. The run counted 173 792 hits on 172 574 different *Alu* elements, as some *Alu* elements have more than a single copy of the motif.

Adaptor and primers design

The complementary oligonucleotides that made up the adaptor (ADP1 5'-AAAGCTCTGA -3' and the 5' phosphorylated ADP2 5'-CGTCAGAGCTTTGCGAAT -3' (Invitrogen) were designed to generate a cohesive end with a 5' CG overhang compatible with the 3' GC overhang produced by the *Hpa*II/*Msp*I digestion (Supplementary Fig. S1). The synthetic adaptor was prepared by incubating two complementary oligonucleotides at 65ºC for 2 minutes, and then cooling to room temperature for 35 minutes.

qAlu primers were specifically designed to amplify *Alu* elements. The reverse primer (qAlu Rv: 5'- ATTCGCAAAGCTCTGACGGGTT -3') was homologous to the synthetic adaptor, but additionally it was extended with the 5'- GGGTT -3' sequence complementary to the consensus *Alu* sequence 5'-AACCC -3' (Supplementary Fig. S1). The forward primer was devised to anneal within an *Alu* consensus sequence located upstream of the *Hpa*II/*Msp*I site. By bioinformatic analysis of the HG19 human genome assembly, we found 172 574 *Alu* repeats perfectly fulfilling QUAlu sequence features (presence of the 5'-AACCCGG -3' sequence containing the CCGG restriction site, see previous section).

To evaluate the adequacy of the design we performed a virtual experiment by digesting the 172 574 *Alu* repeats with *Msp*I (C\CGG) and subsequent concatenation to the ADP2 adaptor at the 3' end. One thousand random sequences of this subset were aligned with ClustalW using the default parameters. Then different *Alu* forward primers were designed and used together with the reverse primer (qAlu Rv) to perform an electronic PCR on the different concatenated *Alu* fragments (Slater and Birney, 2005),

allowing 3 mismatches on the *Alu* forward primer and limiting the generated products from 50 to 200 bp. The selected forward primer (qAlu Fw: 5'- AGCTACTCGGGAGGCTGAG - 3') matched 155 878 amplicons of 58 bp. The set of scripts used to perform this analysis is available at the qualu sourceforge repository (http://sourceforge.net/projects/qalu/). The primers used in qL1PA PCR were designed by Terribas *et al*. (Terribas et al., 2013).

Ion Torrent library preparation, sequencing and analysis

Ion Torrent specific sequences A and P1 (Supplementary Table S3) were fused to QUAlu amplicons following manufacturer's procedures (Ion Amplicon Library Preparation (Fusion Method), Life Technologies). Briefly, 1 uL of qAlu H amplicons and 1 uL of qAlu M amplicons of each sample were used to perform 20 cycles of quantitative PCR (LightCycler® Real-Time PCR System, Roche) with qAlu H and qAlu M primers, as follows: 5 uL of LightCycler® 480 SYBR Green I Master (Roche), 1 umol/L of forward primer and 1 umol/L of reverse primer, in a final volume of 10 uL. Then 1 uL of this product was used to perform 15 additional cycles in the same conditions but using Ion Torrent fusion primers (Supplementary Table S2).

Amplicons were purified (High Pure PCR Product Purification Kit, Roche), analyzed by Bioanalyzer (DNA 1000 assay, Agilent), and the peaks around the expected size were pooled for multiplexed sequencing. Next, Ion SphereTM Particles (ISPs) were prepared accordingly to the Ion PGMTM Template OT2 200 Kit protocol (Life Technologies) using the Ion OneTouchTM 2 System (Life Technologies). Finally, ISPs were sequenced using the Personal Genome Machine® (PGM) System (Ion Torrent, Life Technologies) following the manufacturer's procedures (Ion PGM Hi-Q Sequencing Kit, Life Technologies). Ion Torrent primer sequences (A and P1) were removed from the reads using cutadapt (https://code.google.com/p/cutadapt/).

Effect of DNA degradation on QUAlu performance

HCT116 high quality DNA and aliquots sheared by enzymatic digestion with MseI (NewEngland Biolabs) (2 ug of genomic DNA digested at 37ºC overnight) or by sonication (UCD300 Bioruptor Next Generation System (Diagenode, Seraing, Belgium); 25 and 45 cycles of sonication, 60 sec on / 60 sec off) were analyzed by QUAlu using standard conditions (see above).

Standard curve and relative sensitivity of QUAlu versus a single copy locus

Serial dilutions of HCT116 genomic DNA ranging from 25 ng to 0.005 pg of starting material per PCR tube were analyzed by qAlu M to determine the relative performance of this qPCR against a single copy locus (specifically the promoter region of Digestive organ expansion factor homolog (zebrafish) –DIEXF- gene, HGNC: 28440; accession number NM_0143388). The assay was performed in a LightCycler® 480 Real-Time PCR System with white Multiwell Plate 384 plates (Roche) in a final volume of 10 uL as follows: 5 uL of LightCycler® 480 SYBR Green I Master (Roche), 1 umol/L of DIEXF forward and reverse primers (5'- AACACTAGTGAACGAACT -3' and 5'- AGGAAGTTGTCCAGTCAA -3') and 1 uL of template. DIEXF amplicon length was 181 bp. The qPCR efficiencies per individual well, calculated as previously described, were 2.1 for qAlu M and 1.8 for DIEXF.

Tips and troubleshooting

- Input DNA: for optimal results, the amount of input DNA should be between 0.3 and 80 ng/uL. If input DNA concentration is too low to be quantified or is unknown, you can proceed with 1uL of DNA.

- Adaptor preparation: Incubate 5 uL of ADP1 (100 nmol/L) and 5 uL of ADP2 (100 nmol/L) at 65ºC for 2 minutes and then cool to room temperature for 35 min. Add 990 uL of nuclease-free water and mix thoroughly to obtain 1mL of adaptor (1 nmol/L). Prepare single-use aliquots and store at -20 ºC.

- 10X Tango buffer preparation: thaw commercial buffer following manufacturer's instructions, prepare single-use aliquots and store at -20ºC.

- 10X T4 ligase buffer preparation: thaw commercial buffer following manufacturer's instruction, prepare single-use aliquots and store at -20ºC. Do not defrost 10X T4 ligase buffer aliquots more than twice.

- For best results, use freshly made digestion-ligation in the qPCR. Do not freeze the digestion-ligation. • Always keep the tubes on ice.

- QUAlu is a very sensitive technique, thus always include a negative control (1uL of nuclease-free water instead of DNA) to detect possible contaminations. Negative controls should not amplify before cycle 34. Dismiss samples with quantification cycles similar to the negative control.

- Typical melting curves are shown below and samples with abnormal profiles should be discarded.

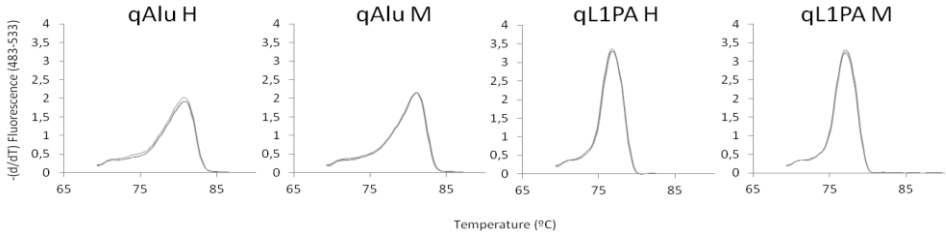

- Although QUAlu works in a wide range of concentrations, accurate comparisons should be performed with samples at similar DNA concentrations. When two samples are in very different ranges, it is recommended to repeat the quantification diluting the most concentrated sample.

- All the qPCRs related to a sample (qAlu for *Hpa*II and for *Msp*I and qL1PA for *Hpa*II and for *Msp*I) should be analyzed in the same plate. All quantitative PCRs should be performed in triplicate.

List of abbreviations

- Quantification of Unmethylated *Alu* (QUAlu)
- qPCR using *Alu* primers of *Msp*I digested DNA (qAlu M)
- qPCR using *Alu* primers of *Hpa*II digested DNA (qAlu H)
- qPCR using L1PA primers of *Msp*I digested DNA (qL1PA M)
- qPCR using L1PA primers of *Hpa*II digested DNA (qL1PA H)
- Percentage of UnMethylated *Alu* elements (PUMA)
- Quantification Cycle (Cq)

Supplementary figures

(a)

Alu consensus sequence:

GGCCGGGCGCGGTGGCTCACGCCTGTAATCCCAGCACTTTGGGAGGCCGAGGCGGGCGGATCACCTGAGGTCAGGAGTTCG
AGACCAGCCGGCCAACACGGTGAAACCCGTCTCTACTAAAAATACAAAAATTAGCGGGCGTGGTGGCGCGCGCCTGTAATC
CCAGCTACTCGGGAGGCTGAGGCAGGAGAATCGCTTGAACCCGGGAGGCGGAGGTTGCAGTGAGCCGAGATCGCGCCACTG
CACTCCAGCCTGGGCGACAGAGCGAGACTCCGTCTC

(b)

QUAlu assay:

MspI/HpaII site: **C/CGG**
Adaptor 1 (ADP1): 5′- AAAGCTCTGA -3′
Adaptor 2 (ADP2): 5′- CGTCAGAGCTTTGCGAAT -3′
qAlu Fw: 5′- AGCTACTCGGGAGGCTGAG -3′
qAlu Rv: 5′- ATTCGCAAAGCTCTGACGGGTT -3′

Genomic DNA around the *Msp*I/*Hpa*II site:

5′- CGCCTGTAATCCCAGCTACTCGGGAGGCTGAGGCAGGAGAATCGCTTGAACCCGGGAGGCGGAG -3′
3′- GCGGACATTAGGGTCGATGAGCCCTCCGACTCCGTCCTCTTAGCGAACTTGGGCCCTCCGCCTC -3′

DNA fragment digested with *Msp*I or *Hpa*II:

5′- CGCCTGTAATCCCAGCTACTCGGGAGGCTGAGGCAGGAGAATCGCTTGAACC -3′
3′- GCGGACATTAGGGTCGATGAGCCCTCCGACTCCGTCCTCTTAGCGAACTTGGGC -5′

Adaptor preparation:

5′- CGTCAGAGCTTTGCGAAT -3′
::::::::::
3′- AGTCTCGAAA -5′

***MspI* or *HpaII* digested DNA ligated to the adaptor:**

5′- CGCCTGTAATCCCAGCTACTCGGGAGGCTGAGGCAGGAGAATCGCTTGAACCCGTCAGAGCTTTGCGAAT -3′
3′- GCGGACATTAGGGTCGATGAGCCCTCCGACTCCGTCCTCTTAGCGAACTTGGGCAGTCTCGAAA -5′

qPCR using Alu consensus primers:

3 -TTGGGCAGTCTCGAAACGCTTA -5′
5′- CGCCTGTAATCCCAGCTACTCGGGAGGCTGAGGCAGGAGAATCGCTTGAACCCGTCAGAGCTTTGCGAAT -3′
3′- GCGGACATTAGGGTCGATGAGCCCTCCGACTCCGTCCTCTTAGCGAACTTGGGCAGTCTCGAAA -5′
5′- AGCTACTCGGGAGGCTGAG -3′

Supplementary Figure S1 | QUAlu digestion and ligation process. (A) The *Alu* consensus sequence was obtained from Weisenberger *et al.* (Weisenberger et al., 2005). **(B)** Scheme of the QUAlu assay with the detailed sequence of adaptor and primers. The sequence of the resulting amplicon is underlined.

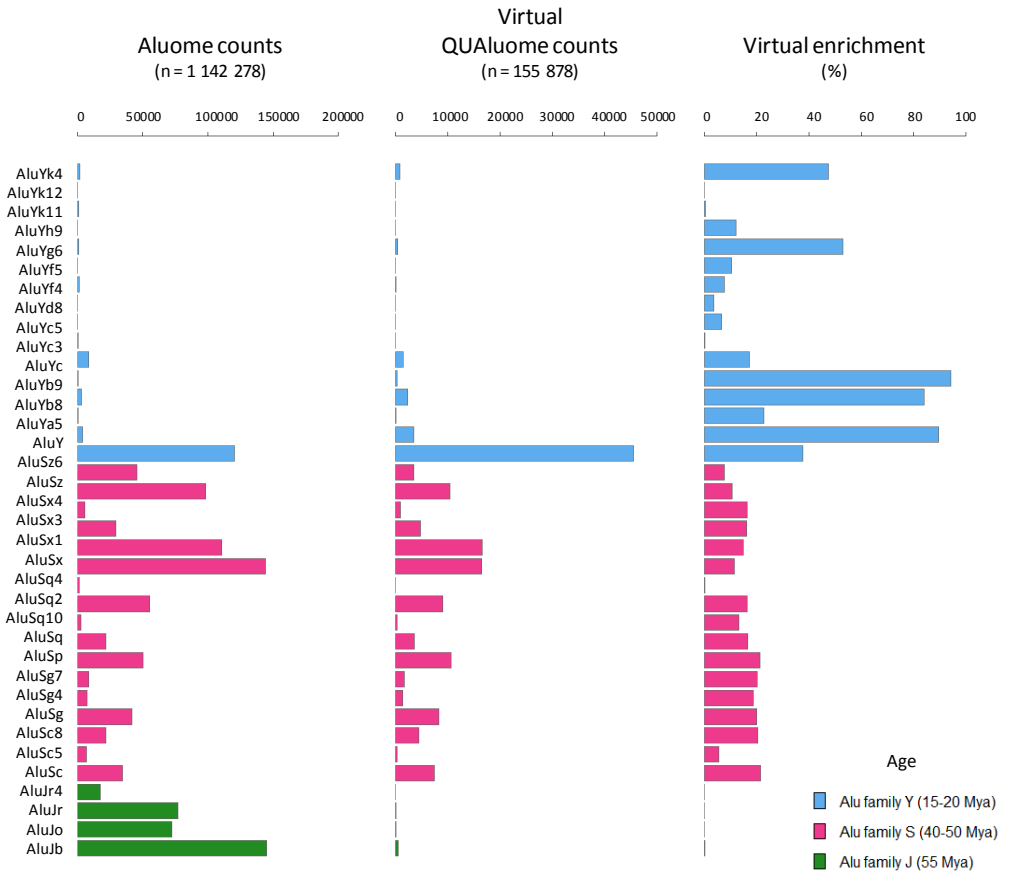

Supplementary Figure S2 | Distribution of *Alu* elements per subfamilies in the different experimental subsets. Absolute number of *Alu* elements within the **(A)** human complete Aluome and **(B)** the virtual QUAluome. **(C)** QUAluome enrichment in comparison to Aluome. Subfamilies classification is according to RepeatMasker (Salter et al., 2000). *Alu* families are sorted from younger to older and subfamilies by alphabetical order. Mya, million years ago.

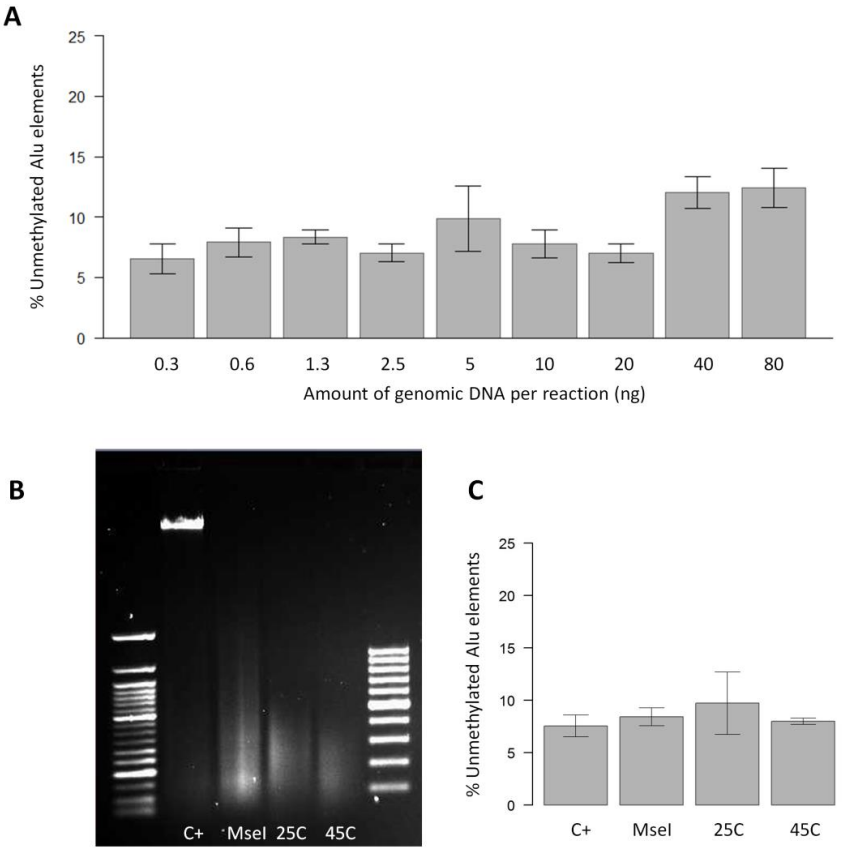

Supplementary Figure S3 | QUAlu performance: linearity of response and Influence of DNA integrity. **(A)** Quantification of the percentage of unmethylated *Alu* elements in the different points of the standard curve used in the linearity assessment. **(B)** Agarose gel (1%) showing different profiles of DNA degradation: non-degraded (C+), digested with *Mse*I, sonicated for 25 (25C) or sonicated for 45 cycles (45C). **(C)** Percentage of unmethylated *Alu* elements assessed by QUAlu in non degraded (C+) and degraded DNA.

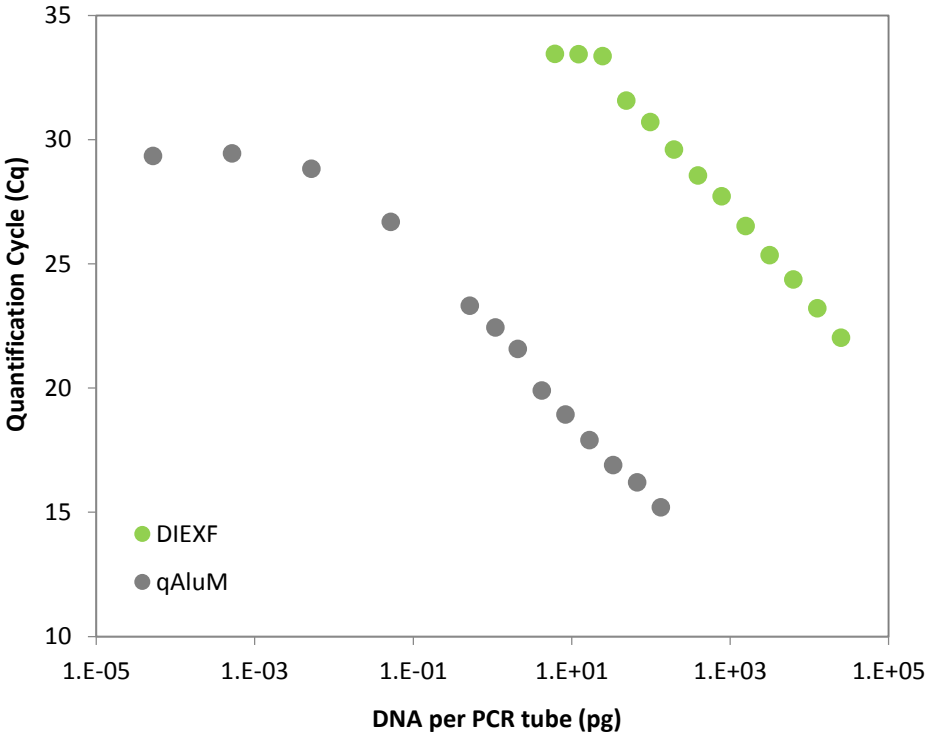

Supplementary Figure S4 | qAlu M (gray) and a single copy locus (promoter region of DIEXF gene) (green) of serial dilutions of genomic DNA. qAlu amplification showed a linear response with dilutions of up to 0.005 pg of HCT116 genomic DNA per tube. DIEXF single locus amplification was linear up to 24 pg of HCT116 genomic DNA per tube.

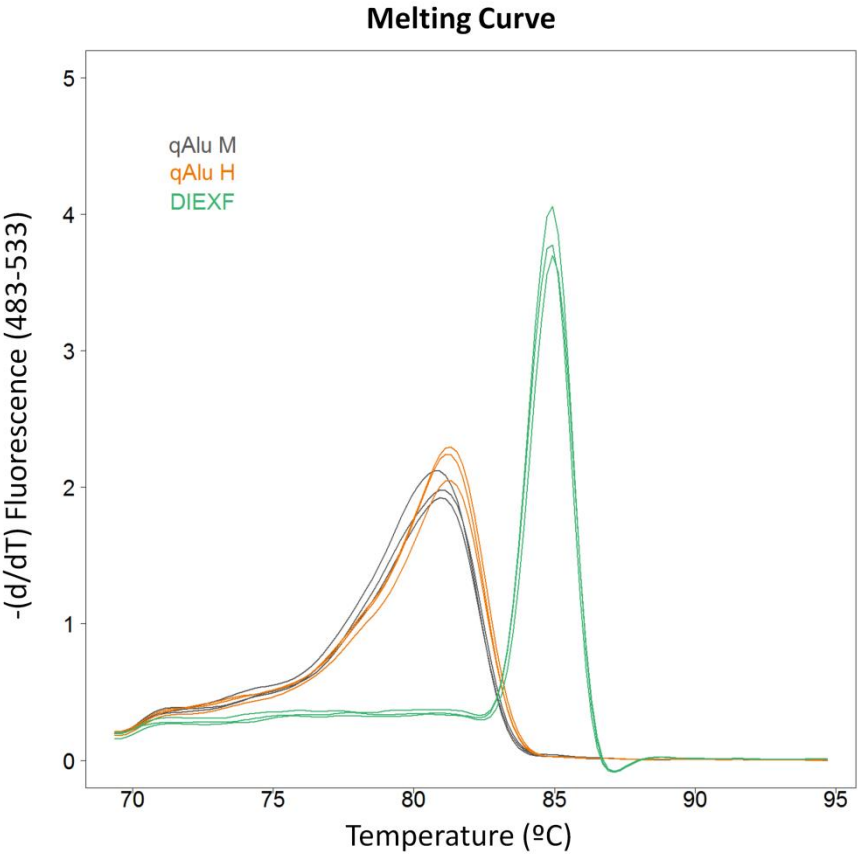

Supplementary Fig 5 | Fluorescence melting peaks of qAlu M, qALu H and DIEXF qPCR in HCT116 genomic DNA. qAlu M: qPCR using the DNA obtained in *Msp*I digested DNA in QUAlu assay. qAlu H: qPCR using the DNA obtained in *Hpa*II digested DNA in QUAlu assay.

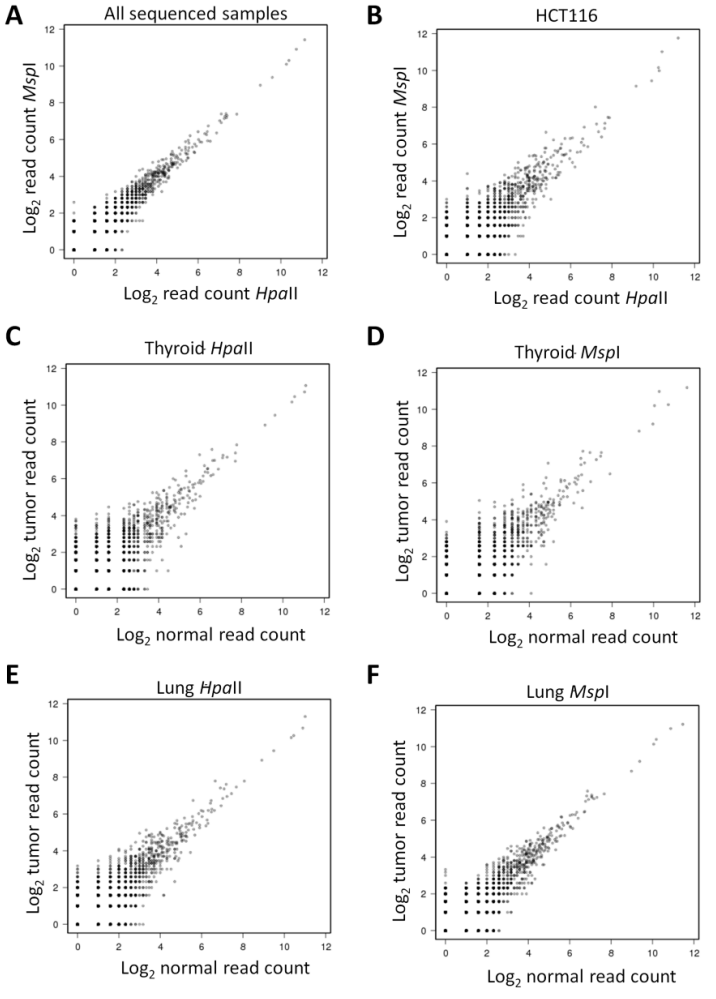

Supplementary Figure S6 | Comparison of Next generation sequencing reads counts for QUAlu product. Each dot corresponds to a unique sequence. **(A)** Comparison between *Hpa*II and *Msp*I digestions data for all samples and **(B)** for HCT116 cell line. **(C-F)** Comparison between normal and tumor for thyroid and lung cancer samples digested with *Hpa*II and *Msp*I. Reads count for each sample and each digestion condition were normalized by the sum of all reads.

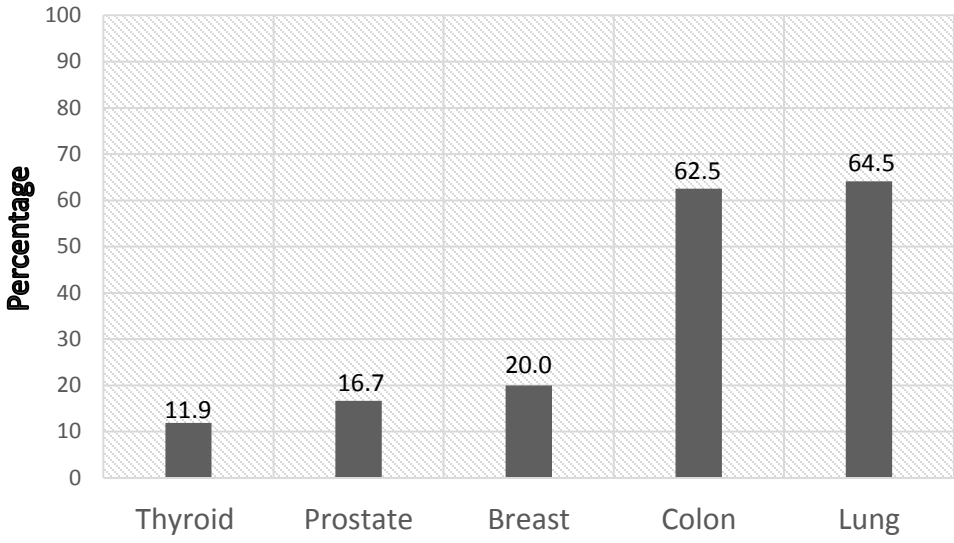

Supplementary Figure S7 | Hypomethylated tumor samples. Fraction of hypomethylated tumor samples (PUMA>12) in five cancer types.

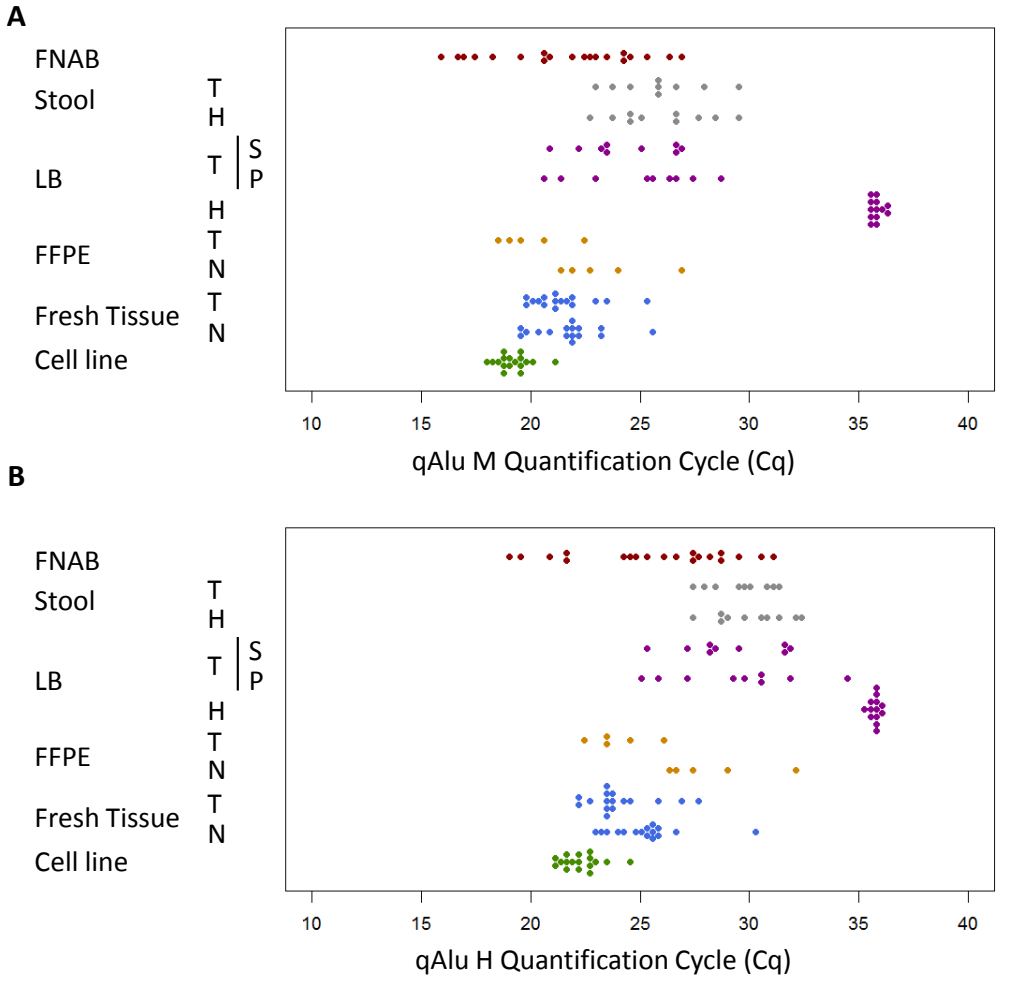

Supplementary Fig 8 | Quantification cycles comparison among different sample types. (A) qAlu M and **(B)** qAlu H quantification cycles from: the colorectal carcinoma cell line HCT116 (Cell Line; considered the reference for high quality genomic DNA); normal (N) and tumor (T) colon fresh tissue; normal (N) and tumor (T) colon FFPE samples; healthy donors plasma (H), lung cancer patients plasma (P) and serum (S) liquid biopsies (LB); healthy donors (H) and colon cancer patients (T) stools; and thyroid goiter FNABs (FNAB).

Supplementary tables

Supplementary tables are at the online version of this paper (Oncotarget. 2016 Mar 1; 7(9): 10536–10546. doi: 10.18632/oncotarget.7233) or at the digital edition of this thesis.

Supplementary references

Guescini M, Sisti D, Rocchi MB, Stocchi L and Stocchi V. A new real-time PCR method to overcome significant quantitative inaccuracy due to slight amplification inhibition. BMC Bioinformatics. 2008; 9:326.

Quinlan AR and Hall IM. BEDTools: a flexible suite of utilities for comparing genomic features. Bioinformatics. 2010; 26(6):841-842.

Rice P, Longden I and Bleasby A. EMBOSS: the

European Molecular Biology Open Software Suite. Trends Genet. 2000; 16(6):276-277.

Slater GS and Birney E. Automated generation of heuristics for biological sequence comparison. BMC Bioinformatics. 2005; 6:31.

Smit A, Hubley R and Green P. RepeatMasker Open-3.0. 1996. Computer program.

Terribas E, Garcia-Linares C, Lazaro C and Serra E. Probe-based quantitative PCR assay for detecting constitutional and somatic deletions in the NF1 gene: application to genetic testing and tumor analysis. Clin Chem. 2013; 59(6):928-937.

Weisenberger DJ, Campan M, Long TI, Kim M, Woods C, Fiala E, Ehrlich M and Laird PW. Analysis of repetitive element DNA methylation by MethyLight. Nucleic Acids Res. 2005; 33(21):6823-6836.

3. Anexo 3

3.1. Formato original del trabajo II

IJC
International Journal of Cancer

DNA methylation profiling of well-differentiated thyroid cancer uncovers markers of recurrence free survival

Veronika Mancikova[1]*, Raquel Buj[2]*, Esmeralda Castelblanco[3], Lucía Inglada-Pérez[1,4], Anna Diez[2], Aguirre A. de Cubas[1], Maria Curras-Freixes[1], Francisco Xavier Maravall[3], Didac Mauricio[5,6,7], Xavier Matias-Guiu[8], Manel Puig-Domingo[5,6,7], Ismael Capel[9], María Rosa Bella[10], Enrique Lerma[11], Eva Castella[12], Jordi Lluis Reverter[5,6,7], Miguel Ángel Peinado[2], Mireia Jorda[2] and Mercedes Robledo[1,4]

[1] Hereditary Endocrine Cancer Group, Spanish National Cancer Research Centre (CNIO), Madrid, Spain
[2] Institute of Predictive and Personalized Medicine of Cancer (IMPPC), Badalona, Barcelona, Spain
[3] Department of Endocrinology and Nutrition, University Hospital Arnau de Vilanova, IRBLLEIDA, Lleida, Spain
[4] ISCIII Center for Biomedical Research on Rare Diseases (CIBERER), Madrid, Spain
[5] Germans Trias i Pujol Health Sciences Research Institute (IGTP), Badalona, Spain
[6] Department of Endocrinology and Nutrition, University Hospital Germans Trias i Pujol, Barcelona, Spain
[7] Department of Medicine, Autonomous University of Barcelona, Barcelona, Spain
[8] Department of Pathology, University Hospital Arnau de Vilanova,University of Lleida, IRBLLEIDA, Lleida, Spain
[9] Department of Endocrinology and Nutrition, Hospital de Sabadell, Sabadell, Spain
[10] Department of Pathology, Hospital de Sabadell, Sabadell, Barcelona, Spain
[11] Department of Pathology, Hospital Santa Creu i Sant Pau, Barcelona, Spain
[12] Department of Pathology, University Hospital Germans Trias i Pujol, Badalona, Spain

Cancer Genetics

Thyroid cancer is a heterogeneous disease with several subtypes characterized by cytological, histological and genetic alterations, but the involvement of epigenetics is not well understood. Here, we investigated the role of aberrant DNA methylation in the development of well-differentiated thyroid tumors. We performed genome-wide DNA methylation profiling in the largest well-differentiated thyroid tumor series reported to date, comprising 83 primary tumors as well as 8 samples of adjacent normal tissue. The epigenetic profiles were closely related to not only tumor histology but also the underlying driver mutation; we found that follicular tumors had higher levels of methylation, which seemed to accumulate in a progressive manner along the tumorigenic process from adenomas to carcinomas. Furthermore, tumors harboring a *BRAF* or *RAS* mutation had a larger number of hypo- or hypermethylation events, respectively. The aberrant methylation of several candidate genes potentially related to thyroid carcinogenesis was validated in an independent series of 52 samples. Furthermore, through the integration of methylation and transcriptional expression data, we identified genes whose expression is associated with the methylation

Key words: well-differentiated thyroid cancer, methylation, *BRAF*, *RAS*, prognostic markers

Abbreviations: *AKT3*: v-akt murine thymoma viral oncogene homolog 3; *BRAF*: v-raf murine sarcoma viral oncogene homolog B1; CIMP: CpG island methylator phenotype; *COL4A2*: collagen type IV alpha 2; *DLEC1*: deleted in lung and esophageal cancer 1; *EI24*: etoposide induced 2.4 mRNA; FA: follicular adenoma; FDR: false discovery rate; FTC: follicular thyroid carcinoma; fvPTC: papillary thyroid carcinoma follicular variant; *KLK10*: kallikrein-related peptidase 10; *NIS*: sodium-iodine symporter; PcG: PolyComb Group; PTC: papillary thyroid carcinoma; *RARβ2*: retinoic acid receptor β2; *RASSF1*: *RAS* association domain family protein 1; *RET*: "rearranged during transfection" protooncogene; RFS: recurrence-free survival; *TIMP3*: tissue inhibitor of metalloproteinase-3; *TSHR*: thyroid-stimulating hormone receptor; *WT1*: Wilms tumor 1

Additional Supporting Information may be found in the online version of this article.

*V.M. and R.B. contributed equally to this work

Grant sponsor: Fondo de Investigaciones Sanitarias; **Grant numbers:** PI11/01359; FIS PI11/02421 and PI11/01354; **Grant sponsor:** The Fundación Mutua Madrileña; **Grant number:** AP2775/2008; **Grant sponsors:** the Comunidad de Madrid S2011/BMD-2328 TIRONET, "la Caixa"/CNIO international PhD programme (V.M. and A.A.d.C.), CIBERER (L.I.-P.) and Spanish Ministry of Economy and Competitiveness (FPI program) (R.B.); **Grant sponsor:** Spanish Ministry of Economy and Competitiveness; **Grant number:** SAF2011/23638; **Grant sponsor:** Fondo de Investigaciones Sanitarias; **Grant number:** PI12/00236 (M.C.); **Grant sponsor:** Technical Support Staff program of the Spanish Ministry of Economy and Competitiveness; **Grant number:** PTA2011-5655-I (A.D.)

DOI: 10.1002/ijc.28703

History: Received 14 Oct 2013; Accepted 19 Dec 2013; Online 31 Dec 2013

Correspondence to: Mercedes Robledo, Spanish National Cancer Center (CNIO), Madrid, Spain, Tel.: +34-917-328-000, Fax: +34-912-246-972, E-mail: mrobledo@cnio.es or Mireia Jorda, Institute of Predictive and Personalized Medicine of Cancer (IMPPC), Badalona, Barcelona, Spain, Tel.: +34-935-543-050, Fax: +34-934-651-472, E-mail: mjorda@imppc.org

Int. J. Cancer: **135**, 598–610 (2014)

status of their promoters. Finally, by integrating clinical follow-up information with methylation levels we propose etoposide-induced 2.4 and Wilms tumor 1 as novel prognostic markers related to recurrence-free survival. This comprehensive study provides insights into the role of DNA methylation in well-differentiated thyroid cancer development and identifies novel markers associated with recurrence-free survival.

What's new?

Follicular cell-derived carcinomas of the thyroid gland, which are the most common endocrine malignancies, are of special interest for molecular research, given their common cellular origin. However, whether epigenetic modifications contribute to the heterogeneous nature of follicular thyroid malignancies remains unclear. Here, genome-wide characterization of DNA methylation patterns of well-differentiated thyroid tumors shows that tumors with distinct subtypes and mutational status have unique methylation profiles, offering insight into the biology underlying the heterogeneity and differential outcomes of thyroid cancers. Novel markers associated with recurrence-free survival were also identified and could be used for patient classification.

Follicular cell-derived carcinoma arises from the main cell population of the thyroid gland and is the most common endocrine malignancy, accounting for more than 95% cases. This general term represents a highly heterogeneous entity composed of a spectrum of differentiation stages, ranging from benign lesions such as follicular adenoma (FA), to well-differentiated but mostly indolent carcinomas such as papillary thyroid carcinoma (PTC) or follicular thyroid carcinoma (FTC), through to undifferentiated, more invasive and lethal human malignancies, such those classified as poorly differentiated thyroid carcinoma and anaplastic thyroid carcinoma. Most well-differentiated carcinomas can be effectively clinically managed and have an excellent prognosis. However, a subset of these tumors behave aggressively, and there is currently no effective treatment for them.[1] As all these malignancies arise from the same cell type, it is of great interest to understand the molecular alterations giving rise to the observed heterogeneity.

Genetics has been shown to play an important role in the development of this disease. The most recurrent point mutations and rearrangements tend to affect the effector genes of the MAPK pathway, such as v-raf murine sarcoma viral oncogene homolog B1 (*BRAF*), the *RAS* family and the "rearranged during transfection" protooncogene *RET*. These early alterations have been shown to be exclusive, subtype-specific and to a certain extent prognostic. Virtually all tumors bearing *RAS* mutations present a follicular pattern of growth (FA, FTC or PTC follicular variant [fvPTC]), while *BRAF* mutations and rearrangements in the *RET* gene are characteristic of PTC.[2] It is widely accepted that *BRAF*-positive tumors tend to have a worse prognosis.[3,4] Conversely, *RAS* mutations are detected among both follicular carcinomas and adenomas, thus having diagnostic value but not prognostic value, and leaving many clinical questions to be answered.

At present, high-throughput techniques are being used to identify altered pathways related to the development of specific tumor types or clinical features. In thyroid cancer, it has been demonstrated that aberrant expression patterns can predict a patient's prognosis.[5] Moreover, these patterns have been closely linked to the presence of particular mutations and shown to be specific to each.[5–7] Although it might be expected that other genomic features such as methylation are also closely related to the particular mutated gene that leads to carcinogenesis, little is known about aberrant epigenetic profiles specific to individual thyroid cancer subtypes. Studies published to date have followed either a strict candidate gene-based approach or have used a limited number of samples.[8] Therefore, the genes identified so far as repressed by aberrant methylation are either involved in thyroid gland function (*e.g.*, thyroid-stimulating hormone receptor [*TSHR*],[9] sodium-iodine symporter [*NIS*][10] or have a tumor suppressor gene function (*e.g.*, tissue inhibitor of metalloproteinase-3 [*TIMP3*], retinoic acid receptor β2 [*RARβ2*],[11,12] *RAS* association domain family protein 1 [*RASSF1*][13]. A global view of genome-wide aberrant methylation in thyroid cancer is still lacking.

In this study, we quantitatively profiled the genome-wide DNA methylation of 83 primary thyroid tumors (18 FA, 18 FTC and 47 PTC) and 8 samples of adjacent normal thyroid tissue using the 27 K Infinium Methylation Array. We identified disease subtype- and mutation-specific DNA methylation patterns and propose novel markers related to recurrence-free survival (RFS). Moreover, by integrating methylation data with mRNA expression, we were able to identify genes whose expression is associated with the methylation status of their promoter regions, thereby adding new insights into thyroid carcinogenesis.

Material and Methods

Sample collection and patient follow-up

One hundred and thirty-two thyroid tumors were snap frozen following surgery at Hospital Sant Pau and Hospital Sabadell in Barcelona (Spain) and at Hospital Arnau de Vilanova in Lleida (Spain), and stored at −80°C. Of these, 83 primary thyroid tumors (42 PTC, 5 fvPTC, 18 FA and 18 FTC) not previously profiled at the genome-wide DNA methylation level[8] were used in the discovery phase of the study, and the remaining 49 tumor samples (24 PTC, 9 fvPTC, 12

FA and 4 FTC) in the replication phase. Sections of each sample were evaluated by a pathologist and, when necessary, non-tumoral tissue was dissected. We studied eight adjacent normal thyroid tissues in the discovery and three in the replication series. At least 80% of the cells were cancerous in all tumor samples, while non-tumor samples had no observable tumor epithelium. Tumors were classified as PTC, fvPTC, FA and FTC according to the criteria proposed by WHO classification of tumors of the endocrine system, by three pathologists with experience on thyroid pathology (XM, MRB and EL). All cases in the PTC group exhibited the typical cytological and architectural features of the classical variant. Strict criteria were used for fvPTC; tumors showed unquestionable cytological features together with a follicular pattern of growth. For FA, presence of capsule and absence of hyperplasic changes in the adjacent thyroid tissue was required. For FTC, obvious evidence of vascular and capsular invasion was also required. Genomic DNA was extracted from all samples using the DNeasy Blood and Tissue kit (QIAGEN) according to the manufacturer's protocol.

The clinical follow-up of the patients was performed by physical examination, neck ultrasonography, simultaneous determination of serum anti-tiroglobulin antibodies with tiroglobulin (basal, or after thyrotropin stimulation by thyroid hormone withdrawal or the administration of recombinant human thyrotropin) and whole-body iodine scanning. If there was a suspicion of local or distant disease, other imaging techniques such as CT, MRI, PET-CT or scintigraphy were used. The frequency and the type of technique used depended on the postoperative staging, which was also used to assess prognosis and to guide adjunctive therapy.

Mutation analysis

All PTCs were screened by Sanger sequencing for *BRAF* mutations at codon 600 in exon 15, while FA, FTC and fvPTC samples were screened for mutations in *H-, N-* and *K-RAS* at mutational hotspots on codons 12 and 13 of exon 2 and codon 61 of exons 3. When available, cDNA from PTC samples was also screened for *RET/PTC1* and *RET/PTC3* rearrangements as previously described.[5]

DNA methylation assay, data processing and data analysis

Briefly, genomic DNA was bisulfite-converted using the EZ DNA Methylation Kit (Zymo Research, Orange, CA) following the manufacturer's recommended procedures. Genome-wide promoter DNA methylation profiling was performed at the Spanish "Centro Nacional de Genotipado (CEGEN-ISCIII)" (www.cegen.org) using the Illumina Infinium HumanMethylation 27K Platform (Illumina, San Diego, CA) as described previously.[14] This assay generates DNA methylation data for 27,578 CpG dinucleotides covering 14,473 unique genes. The raw intensity data were quartile-normalized using the R package, HumMeth27QCReport.[15] For each CpG site, methylation levels were quantified using β-values, which represent the proportion of methylation, calculated as $M/(M + U)$, where M is the methylated probe intensity and U the unmethylated probe intensity. β-Values range from 0 to 1, with 0 being completely unmethylated and 1 being completely methylated. M-Values, defined as $\log_2(M/U)$, were used for statistical analyses; negative values indicate less than 50% methylation and positive values indicate more than 50% methylation.[16] We excluded probes that were detected in less than 95% of the samples (16 probes), probes designed for sequences on either the X or the Y chromosome (1,084 or 7 probes, respectively) as well as probes that potentially hybridized to more than one genomic locus (538 probes). The data discussed in this publication have been deposited in NCBI's Gene Expression Omnibus and are accessible through GEO Series accession number GSE51090 (http://www.ncbi.nlm.nih.gov/geo/query/acc.cgi?acc=GSE51090).

Unsupervised hierarchical clustering was performed using Cluster 3.0 software with "complete linkage" (Pearson correlation, uncentered metrics). The clusters were subsequently visualized using Treeview (http://rana.stanford.edu/software), and Principal Component Analysis (PCA) was performed using R CRAN version 2.15.3 (R, 2013).

Differences in DNA methylation status between normal thyroid tissue and specific subtypes were tested using POMELLO II, applying either a t-test with 200,000 permutations or linear models (limma).[17] To account for multiple hypotheses testing, p-values were adjusted using Benjamini's false discovery rate (FDR) correction. We defined a probe to be hypomethylated or hypermethylated when it displayed a mean M-value difference (ΔM-value) < -1.4 or >1.4, respectively, between a particular tumor group and normal tissue, and had a FDR < 0.05.

Methylation status validation: selection of candidate genes and bisulfite sequencing

Three of the most differentially methylated probes, all with a high fold-change across the experimental groups, were selected for validation. Biological functions were considered as additional criteria to select candidate promoter regions. Technical validation of microarray results was performed using bisulfite sequencing, first in a subset of the original discovery series (comprising 4 FA, 7 FTC, 13 PTC and 8 adjacent normal thyroid tissue samples). The candidate markers were then validated in 52 independent samples (24 PTC, 9 fvPTC, 12 FA, 4 FTC and 3 adjacent normal thyroid tissue samples).

From the bisulfate-treated DNA, at least two independent nested PCRs (for each sequence to be studied) were performed using two sets of primers specifically designed to contain no CpG sites (Supporting Information Table S1). The pooled PCR products were purified (High Pure PCR product Purification Kit, Roche) and analyzed by Sanger sequencing (BigDye Terminator v3.1 Cycle Sequencing Kit, Applied Biosystems). Primary tumors were classified as hyper- or hypomethylated when the studied locus showed an increase or a

Table 1. Summary of the main clinical and pathological characteristics of samples used in this study

Clinical characteristics	Discovery series (n = 83) Number (%)[1]	Replication series (n = 49) Number (%)[1]
Gender		
Male	17 (20.5)	13 (26.5)
Female	66 (79.5)	35 (71.5)
Missing	0 (0)	1 (2.0)
Age		
Median	47	45
Min-max	13–78	20–84
Histology		
PTC	42 (50.6)	24 (49.0)
fvPTC	5 (6.0)	9 (18.4)
FTC	18 (21.7)	4 (8.2)
FA	18 (21.7)	12 (24.4)
NT	8	3
Recurrence[2]		
Yes	14 (21.5)	7 (18.9)
No	47 (72.3)	24 (64.9)
Missing	4 (6.2)	6 (16.2)
Follow-up (months)		
Median	36	46.5
IQR	13.5–84	21–73.25
Mutation		
BRAF^{V600E}	23 (27.7)	13 (26.5)
RAS	13 (15.7)	2 (4.1)
RET/PTC1	3 (3.6)	0 (0)
Negative	44 (53.0)	44 (69.4)

A total of 132 tumor samples and 11 normal adjacent tissues were used in this study, divided in the discovery series (83 tumors and 8 normal thyroid tissues) and replication series (49 tumors and 3 normal samples).
IQR, interquartile range.
[1]The percentage is calculated taking into account only the total number of tumors (normal tissues were not included).
[2]The data on recurrence are only included for the malignant tumors (adenomas were not taken into account).

decrease, respectively, in methylation level of over 20% relative to the average methylation of normal thyroid samples.

Integration of gene expression and DNA methylation

To identify genes whose expression is associated with methylation of their promoters, we assessed correlations between methylation and mRNA expression using two approaches. First, mRNA expression was compared to DNA methylation using the 31 primary thyroid tumors[5] for which data were available. Expression of all the available genes identified as differentially methylated (FDR $<$ 0.05, ΔM-value $>$ |1.4|) was examined in this study. For genes with multiple probes included in the methylation array, the probe with the highest variance was selected, as previously described.[18] Correlation was measured using the Spearman coefficient. Second, we used an independent mRNA expression dataset available from GEO (http://www.ncbi.nlm.nih.gov/geo; GEO data base GSE27155).[6] This database contains both histopathological and genetic information on the samples included. We merged the list of genes with differential methylation (FDR $<$ 0.05, ΔM-value $>$ |1.4|) with that of those identified as differentially expressed (t-test, FDR $<$ 0.05).

Identification of genes whose methylation is of potential prognostic value

To identify methylation changes that could serve as potential prognostic markers, we integrated available clinical follow-up data of 60 patients with the methylation profiles. First, we performed supervised analysis with the POMELO II tool using methylation data for carcinoma samples from individuals free of the disease for at least 5 years and those with recurrence within 5 years after the appearance of the disease. Next, we chose probes with the most significant changes in methylation (FDR $<$ 0.05, ΔM-value $>$ |1.4|), and using SPSS (IBM SPSS Statistics version 19) we conducted an univariate Cox regression analysis to determine the impact of methylation status on RFS. RFS was defined as the time between initial diagnosis and relapse or death by the disease, with observations censored at last follow-up if no event had occurred. p-Values were adjusted using Benjamini's FDR correction.

Results

DNA methylation profiles reflect histology and *RAS*/*BRAF* mutational status in well-differentiated thyroid cancer

The main clinical and pathological characteristics, as well as the somatic tumoral mutation status, of the patients included in the study are summarized in Table 1 (more detailed information is available in Supporting Information Table S2). The prevalence of the mutations found among our samples is similar to that previously described.[2] We excluded probes that appeared to be constitutively unmethylated (M-value $<$ -2.0, corresponding to a β-value $<$0.2; 8,657 probes) or methylated (M-values $>$2.0, corresponding to a β-value $>$0.8; 717 CpGs) in all samples. The vast majority of the unmethylated probes were in CpG islands (97.8%); DAVID functional annotation analysis[19] returned GO terms such as primary metabolic processes (Benjamini–Hochberg-adjusted p-value = 1.8×10^{-18}) and cellular metabolic processes (Benjamini-Hochberg-adjusted p-value = 4.8×10^{-24}) as best hits (Supporting Information Fig. S1), suggesting an enrichment of housekeeping genes. Most of the methylated probes were located at non-CpG islands (63.6%), and no functional enrichment of the genes involved was observed. Further analyses were performed with the remaining 17,274 probes.

An unsupervised hierarchical cluster analysis of the 912 CpGs with standard deviation >1.2 identified two distinct clusters based on histological subtype and the underlying mutation (Fig. 1*a*). More specifically, "cluster 1" was enriched with FTC (p-value < 0.0001) and showed statistically significantly higher levels of methylation when compared to normal tissue samples grouped in "cluster 2" (p-value $= 2.7 \times 10^{-7}$). "Cluster 2" comprised two sub-clusters. "Cluster 2A" consisted of tumors with substantial histological heterogeneity, including, among others, the majority of FA samples (11 out of 18 FA) and all the normal thyroid tissue samples. Of note, the branch lengths between the normal thyroid samples were shorter than those between the tumor samples, indicating greater heterogeneity in methylation profiles among the latter. The tumors grouped in this sub-cluster also showed higher levels of methylation compared to normal tissue (p-value $= 4.6 \times 10^{-3}$). Finally, "cluster 2B" showed a robust methylation profile and comprised 36 tumors, 35 of which were PTCs; this sub-cluster included all those with the $BRAF^{V600E}$ mutation and *RET/PTC1* rearrangement. The methylation levels of samples in "cluster 2B" showed no statistical difference compared with normal tissue samples, suggesting methylation profiles differences between tumors with follicular and papillary growth patterns.

Although no clustering of samples harboring *RAS* mutations was observed using unsupervised analysis, it is noteworthy that those fvPTC bearing a *RAS* mutation were grouped in clusters 1 and 2A, together with *RAS*-FTC and *RAS*-FA, while the only tumor bearing a *BRAF* mutation clustered with *BRAF*-PTC tumors. Therefore, we applied a principal components analysis (PCA) using the 912 CpGs with highest methylation variability, and confirmed the grouping of samples according to their mutational status (Fig. 1*b*). Using publically available data from The Cancer Genome Atlas (TCGA) project (87% of the 912 probes used for the unsupervised analysis were also included in the 450K platform), we were able to confirm the robust clustering of thyroid tumors according to primary mutation, *BRAF versus RAS* (Fig. 1*c*).

Identification of differentially methylated regions in well-differentiated thyroid cancer

We identified 9 hypomethylated probes (9 genes) in FA, 83 (77 genes) in FTC and 53 (51 genes) in PTC. We also observed 89 hypermethylated CpGs (83 genes) in FA, 460 (416 genes) in FTC and 39 (31 genes) in PTC. A Venn diagram analysis revealed that a substantial proportion of differentially methylated regions identified in FA was also altered in FTC. Sixty-nine (83%) hypermethylated and six (67%) hypomethylated probes in FA were also hyper- and hypomethylated, respectively, in FTC (Figs. 2*a* and 2*b* and Supporting Information Fig. S2). Table 2 summarizes the 20 most significant subtype specific probes identified as well as their corresponding $\Delta\beta$-values. An extended list of all differentially methylated probes is listed in Supporting Information Table S3.

After dividing FA and FTC samples according to their mutational status, we assessed associations of individual probes with each of the genetic subgroups. For *RAS*-positive tumors, we identified 72 probes (70 genes) and 203 probes (181 genes) to be hypomethylated in FA and FTC, respectively. Hypermethylated were 263 probes (258 genes) and 454 probes (426 genes) in FA and FTC, respectively. In tumors with no mutations, we identified on one hand 11 hypomethylated probes (11 genes) in FA and 77 (71 genes) in FTC, and on the other hand 105 hypermethylated probes (97 genes) in FA and 587 (528 genes) in FTC (Figs. 2*c* and 2*d* upper and Supporting Information Fig. S2).

After dividing PTC samples according to the genetic alterations they harbored, we identified 126 hypomethylated probes (121 genes) in *BRAF*-positive tumors, 74 (72 genes) in *RAS*-positive tumors and 7 (7 genes) in tumors with no detectable mutations (16 tumors); we found 78 hypermethylated probes (70 genes) in *BRAF*-related tumors, 141 (132 genes) *RAS*-mutated tumors and 84 (78 genes) in tumors with no mutations. No probes were found to be specific to PTC tumors harboring the *RET/PTC1* rearrangement (Figs. 2*c* and 2*d* lower and Supporting Information Fig. S2). All hypo- and hypermethylated genes for each tumor subtype are listed in Supporting Information Table S3.

Furthermore, we aimed to identify the differentially methylated probes specifically associated with mutational status, independently of histology, by separately comparing with normal tissue all *RAS*-tumors, all *BRAF*-tumors and all non-mutated tumors. We obtained 450 probes from these analyses (Supporting Information Table S3) that, when used to perform PCA, resulted in a robust separation of mutated samples into two main groups: *BRAF*-positive samples together with *RET/PTC1* samples and samples harboring *RAS* mutations (Fig. 3).

For all differentially methylated probes identified (both mutation- and subtype-related), we also investigated the genomic context of their location, as it is well-known that hypo- and hypermethylation target different genomic regions in cancer (Supporting Information Fig. S3). We observed that hypermethylation in thyroid tumors occurred preferentially within a CpG island, whereas hypomethylation tended to affect probes outside of CpG islands (p-value < 0.0001). In addition and as previously reported,[20] hypermethylation occurred preferentially at stem cell PolyComb Group (PcG) target genes (p-value < 0.0001), while hypomethylated probes were highly enriched with CpGs that are heavily methylated in Embryonic Stem Cells (p-value < 0.0001).

Validation and replication of differentially methylated loci

We chose the promoter regions of three genes for validation using bisulfite sequencing; hypermethylation of two of them (*COL4A2* and *DLEC1*) was more common in thyroid neoplasias in general than in normal tissues, while hypomethylation

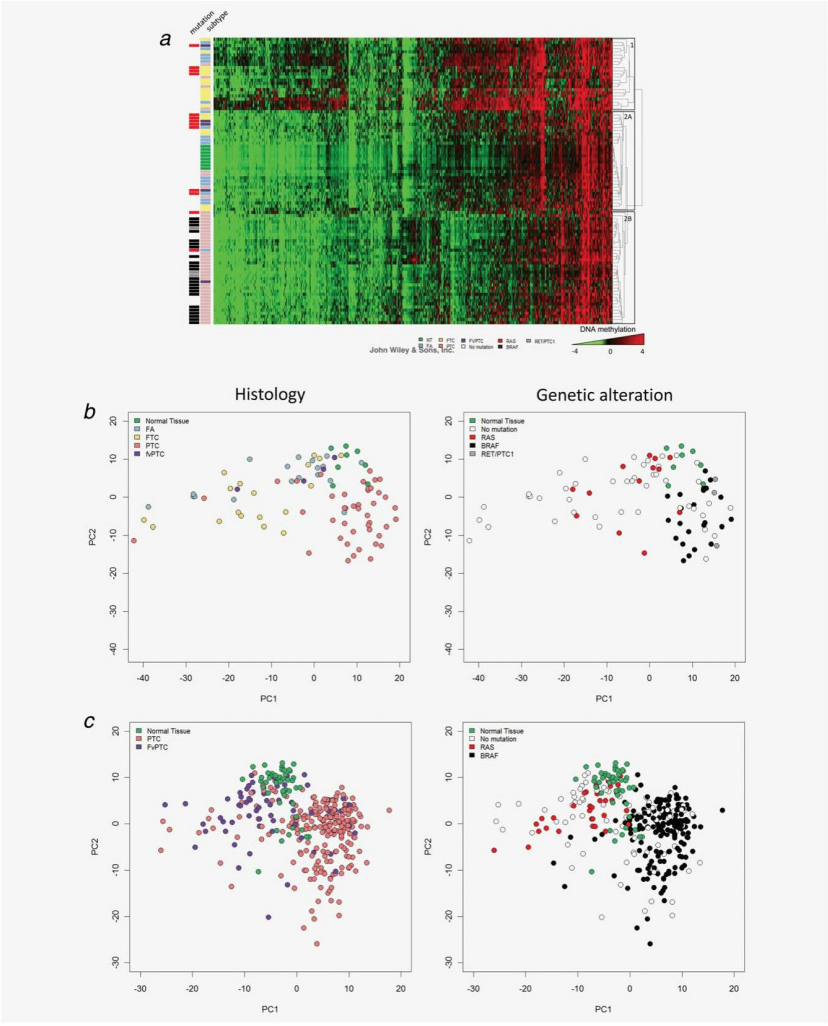

Figure 1. (*a*) Unsupervised hierarchical cluster analysis. Hierarchical cluster analysis of 83 primary thyroid tumors and 8 adjacent normal tissue samples based on the 912 CpGs with the greatest variability (SD > 1.2). The analysis divided the sample set into two main clusters. "Cluster 1" was statistically significantly enriched with FTC samples. In "cluster 2B" the majority of PTC was gathered, while in "cluster 2A" normal tissues, showing a very homogeneous profile, were localized together with the majority of FA. (*b*) Principal component analysis. PCA analysis of 83 primary thyroid tumors and 8 adjacent normal tissue samples based on the 912 CpGs with the greatest variability (SD > 1.2). PCA analysis showed a clear relationship between DNA methylation and histology as well as genetic alterations. The three tumors containing a *RET/PTC* rearrangement group with *BRAF*-positive samples. (*c*) Principal component analysis. PCA analysis using DNA methylation data from the TCGA project (including 304 primary thyroid tumors and 50 adjacent normal tissue samples) based on the same CpGs with the greatest variability (SD > 1.2) identified in our study.

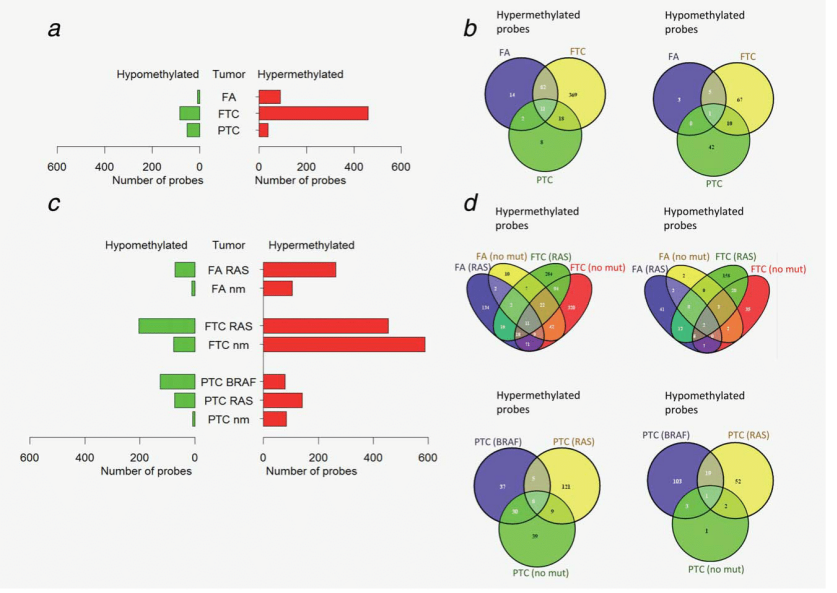

Figure 2. Differentially methylated probes. (*a*) Subtype-specific probes identified using POMELO II based on FDR < 0.05 and ΔM-value $> |1.4|$. (*b*) Venn diagram showing the overlap between the identified subtype-specific hyper- and hypomethylated probes. (*c*) Mutation-specific probes identified using POMELO II and the criteria listed above. (*d*) Venn diagram analysis showing overlap between the identified mutation-specific hypermethylated and hypomethylated probes, respectively.

Cancer Genetics

of *KLK10* was specific to PTC tumors harboring the $BRAF^{V600E}$ mutation. Comparison of quantitative methylation values at these three CpG sites from the HumanMethylation 27K Platform and bisulfite sequencing in 32 samples confirmed the accuracy of the array-based measurement (Supporting Information Fig. S4). The analysis by bisulfite sequencing assessed not only the methylation state of the CpG within the probe but also the flanking CpGs, revealing that the differential methylation affected a larger region (Supporting Information Fig. S4). These results validate the use of the single CpG sites interrogated by Illumina Infinium HumanMethylation 27K Platform as surrogate reporters of regional methylation. In addition, we replicated the findings for the three candidate genes in an independent series of 24 PTC, 9 fvPTC, 12 FA, 4 FTC and 3 normal thyroid tissues (Supporting Information Table S2).

In the discovery series, as measured by the array, *COL4A2* was hypermethylated in 66% of PTC, 21% of FA and in 56% of FTC samples; in the independent replication series hypermethylation was observed in 41% of PTC and 33% of FA samples. The lack of *COL4A2* hypermethylation among FTC samples could be due to the fact that only four samples were available. Conversely, *DLEC1* showed hypermethylation in the discovery series in 23% of PTC, 42% of FA and 56% of FTC samples, compared to 23% of PTC, 8% of FA and 75% of FTC samples in the replication series. In the replication series, we confirmed the *KLK10* hypomethylation in all *BRAF*-positive samples (Supporting Information Fig. S4).

Correlation between DNA methylation and mRNA expression

The integration of methylation and expression data available[5] from 31 thyroid tumors allowed us to examine gene expression levels of a limited number of genes (4,029 genes on both platforms that represent 27.8% of the genes included on the methylation array). We examined the correlation between DNA methylation and mRNA expression in all histological groups where at least five samples were available for the analysis. In PTCs with the $BRAF^{V600E}$ mutation, we observed an inverse correlation with expression for 13.3% (6 out of 45

Table 2. TOP 20 subtype-specific probes for FA, FTC and PTC

Probe ID	Gene ID	FDR	Δ*M*-value	Δβ-value	Chr.	CpG Island
TOP 20 FA-specific probes						
cg06367117	*ALDOC*	2.00E-07	2.71093869	0.3926528	17	TRUE
cg08047457	*RASSF1*	9.00E-07	2.29675986	0.40019958	3	TRUE
cg21554552	*RASSF1*	2.40E-06	2.44631867	0.36554431	3	TRUE
cg17568996	*NFAM1*	2.42E-05	2.25126535	0.33678735	22	FALSE
cg06821120	*RASSF1*	0.0001938	1.7311015	0.33777293	3	TRUE
cg27219973	*GNRHR*	0.0008154	1.54777294	0.2221765	4	FALSE
cg13926569	*PAPSS2*	0.0013162	1.72337985	0.27635483	10	FALSE
cg09606564	*MFAP4*	0.0013598	1.4726875	0.25294503	17	FALSE
cg16393207	*GDPD5*	0.0013598	1.54616899	0.22478436	11	TRUE
cg14129786	*MGMT*	0.0014039	1.66225486	0.22401578	10	TRUE
cg14973995	*TETRAN*	0.0014039	2.07575889	0.30959818	4	TRUE
cg18055007	*DDAH2*	0.0014133	1.88659804	0.25590677	6	TRUE
cg17582777	*EFNA3*	0.0017439	−1.53694597	−0.23233439	1	FALSE
cg05656364	*VAMP8*	0.0021883	−1.55332458	−0.16488351	2	FALSE
cg22995106	*COG4*	0.0022767	1.40257423	0.1805763	16	TRUE
cg15692239	*ALDOC*	0.0022767	2.53820971	0.20161756	17	TRUE
cg21402071	*CHRNB4*	0.0028915	1.82059373	0.20535253	15	FALSE
cg26365553	*MADD*	0.0031854	1.42934142	0.24722019	11	FALSE
cg12783776	*SERPING1*	0.0033165	1.9289042	0.27738869	11	TRUE
TOP 20 FTC-specific probes						
cg21554552	*RASSF1*	7.00E-07	2.98852759	0.45417166	3	TRUE
cg08047457	*RASSF1*	9.00E-07	2.72818463	0.47218605	3	TRUE
cg14679230	*LIPE*	3.80E-06	1.45037569	0.1459732	19	FALSE
cg04972979	*C20orf54*	5.50E-06	1.61451484	0.30256229	20	FALSE
cg16517394	*TNFSF4*	9.60E-06	1.8536169	0.23950413	1	FALSE
cg00804392	*RHOH*	1.11E-05	1.85216994	0.29420054	4	TRUE
cg05467458	*SLC7A9*	1.52E-05	1.70161824	0.28134819	19	FALSE
cg20802392	*CTSK*	1.52E-05	1.98033411	0.27687162	1	TRUE
cg26218269	*MAB21L2*	1.58E-05	1.72450003	0.21028063	4	TRUE
cg06367117	*ALDOC*	1.58E-05	3.13695217	0.45480542	17	TRUE
cg16779976	*BLNK*	1.58E-05	−1.5932182	−0.17493057	10	FALSE
cg04629204	*EXTL1*	1.68E-05	1.4815062	0.24451418	1	FALSE
cg14120436	*GNB5*	2.62E-05	1.59384173	0.20025587	15	FALSE
cg20592700	*WIPI2*	2.62E-05	−1.50386259	−0.13059051	7	TRUE
cg00777121	*RASSF1*	4.72E-05	1.4952662	0.24566678	3	TRUE
cg10861599	*TNFSF4*	4.72E-05	1.57521415	0.19950722	1	FALSE
cg20356482	*FBP2*	5.00E-05	1.40957532	0.20331262	9	TRUE
cg09538582	*KRTHA5*	5.45E-05	1.47233264	0.09209393	17	FALSE
cg20394284	*JAK2*	6.48E-05	1.69088777	0.22587538	9	TRUE
TOP 20 PTC-specific probes						
cg13019092	*PDZK1*	<0.0000001	1.4330228	0.15003065	1	FALSE
cg07763768	*C9orf45*	<0.0000001	1.85389182	0.22681097	9	TRUE
cg02423618	*SPATA8*	<0.0000001	−1.56480549	−0.20065839	15	FALSE

Table 2. TOP 20 subtype-specific probes for FA, FTC and PTC (Continued)

Probe ID	Gene ID	FDR	Δ*M*-value	Δβ-value	Chr.	CpG Island
cg18302652	*IL8*	2.58E-05	−1.69117713	−0.22868075	4	FALSE
cg17568996	*NFAM1*	7.01E-05	1.87197435	0.24967876	22	FALSE
cg24497819	*SELPLG*	0.0001279	−2.22238036	−0.3194521	12	FALSE
cg19385139	*COL4A2*	0.0002352	1.95997347	0.2680565	13	FALSE
cg03001305	*STAT5A*	0.000285	−2.54273891	−0.31643091	17	FALSE
cg15262516	*COL4A2*	0.0004566	1.40539859	0.16244608	13	FALSE
cg04057858	*UNQ9391*	0.0008376	−1.40846284	−0.18092863	8	FALSE
cg02523400	*SERPIND1*	0.0009559	2.57803439	0.31279995	22	FALSE
cg27105123	*EPS8L1*	0.0009877	−1.60910587	−0.23177057	19	FALSE
cg03733371	*LIPH*	0.0012087	−2.5252893	−0.35653317	3	FALSE
cg18752880	*C1QTNF3*	0.0014062	1.47593113	0.26132674	5	FALSE
cg04756629	*LOC400696*	0.0015227	−1.8391597	−0.21467597	19	FALSE
cg12385643	*UGT1A6*	0.0016378	−1.65626606	−0.18292765	2	FALSE
cg12530080	*PMCHL1*	0.0016882	−1.81689239	−0.26447097	5	FALSE
cg18343292	*MS4A7*	0.0016882	−1.49789853	−0.18361614	11	FALSE
cg27009703	*HOXA9*	0.0017272	1.75344159	0.18988395	7	TRUE
cg10236239	*SULT1C2*	0.001969	1.48508253	0.23764054	2	FALSE

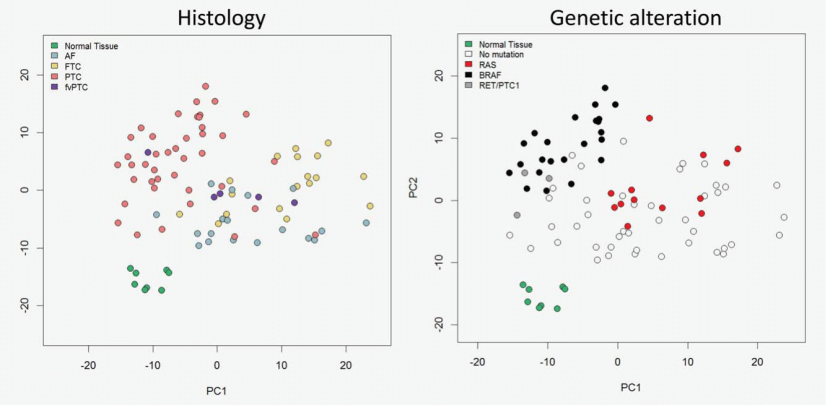

Figure 3. PCA analysis using 450 mutation-specific probes. PCA analysis using 450 probes identified to be differentially methylated in supervised cluster analysis. The probes were identified to be specifically associated with the mutational status and independent of the histology and their usage resulted in a robust separation of samples into two main groups: *BRAF*- and *RET/PTC*-positive tumors and *RAS*-positive tumors.

genes available for integration) of genes with significant changes in methylation. Among FTC, 10.4% (16/153) of genes showed a similar trend, while in the case of FA it was 11.6% (5/43).

Additionally, we identified differentially expressed genes using an mRNA expression data from an independent case series.[6] After comparing these genes with the lists of differentially methylated genes we found that 10% (7 out of 70 differentially methylated genes) and 2.9% (12/416) of the genes hypermethylated in PTC (*BRAF*-related) and FTC, respectively, were down-regulated. Moreover, we found that 20.7% (25/121) of the hypomethylated genes in PTC (*BRAF*-related)

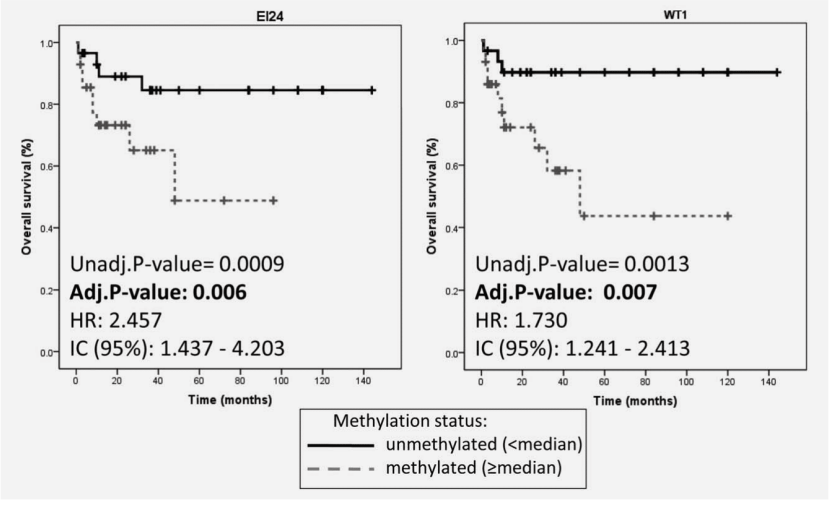

Figure 4. Prognostic value of the methylation status of *EI24* and *WT1* genes. RFS of 60 thyroid cancer patients based on the methylation levels, considered as a continuous variable, of each of the proposed prognostic factors. RFS was defined as the time between initial diagnosis and recurrence or death due to the disease, with follow-up censored at last contact if no event had occurred. The unadjusted *p*-values (Unadj. *p*-value) were obtained from Cox regression analysis, and were corrected for multiple testing (adj. *p*-value, shown in bold).

and 1.9% (1/77) in FTC were up-regulated. We did not, however, find any association between changes in methylation and gene expression in FA.

A substantial portion of the genes whose expression we observed to be inversely correlated with the methylation level of their corresponding promoters has been already described to play a role in the tumorigenic process (*CTSF, KLK10, PHLDA2, RUNX1, TACSTD2, BAALC, CTSF, HMGA1, RASSF2, IMPDH1* and *TNFRSF10C*). Moreover, for *BRAF*-related PTC they also included genes from the MAPK pathway (*MAPK13, DUSP5* and *RAP1GA1*) and genes involved in apoptosis (*LCN2, RIPK1* and *LGALS1*), whereas for FTC we observed a down-regulation by hypermethylation of several genes involved in innate immune response (*C7, SERPING1, TRAF3, PYCARD* and *CFH*). All genes identified in this analysis are listed in Supporting Information Table S4.

Identification of methylation-related prognostic markers

The analysis of 34 samples (PTC and FTC) with available follow-up information identified 32 probes differentially methylated among patients with and without recurrence (Supporting Information Table S3). We performed survival analysis of 60 patients to evaluate the impact of methylation levels of these genes on RFS, obtaining significant associations with risk of recurrence for etoposide induced 2.4 (*EI24*) and Wilms tumor 1 (*WT1*) (Fig. 4). Among all known risk factors associated with poor prognosis (sex, age of onset, mutation in *BRAF*, FTC and tumor size), only the latter showed statistical significance in our study ($p = 0.016$). After including tumor size as a covariable, the association of *EI24* and *WT1* methylation levels with prognosis remained significant ($p = 0.004$; HR = 2.08; CI: 1.262–3.445 and $p = 0.006$; HR = 1.64; IC = 1.149–2.335, respectively); results from the univariate analysis are shown in Figure 4. In addition, the association of *EI24* and *WT1* methylation level with recurrence remained significant in multivariable analysis including separately each of the remaining clinical variables known to be related to poor prognosis.

Discussion

Alterations in DNA methylation have been shown to play a role in tumorigenesis and disease progression in many malignancies, including thyroid cancer. Until recently, technical limitations have restricted methylation studies to the characterization of a handful of candidate loci[9–11,13] and one genome-wide exploratory study, mainly focused on identification of subtype specific methylation patterns.[8] Here, we describe quantitative DNA methylation levels at more than 26,000 loci across 14,000 gene promoters. By assaying the largest collection of thyroid tumors described so far, we were able to not only confirm methylation changes seen in previously published candidate loci studied but also identify novel

recurrent ones. Our results suggested that in thyroid cancer, aberrant methylation targets specific genomic regions, particularly PcG-associated stem cell genes and sequences that are highly methylated in stem cells, which are also commonly epigenetically deregulated in other cancer types.[20] Moreover, according to our results, the methylation patterns in thyroid cancer are specific to the follicular and papillary patterns of growth as well as to the underlying mutational event. Furthermore, by comparing DNA methylation with mRNA expression data, we further confirmed that the relationship between methylation and expression is complex and context-dependent.[21] Finally, by integrating methylation data with clinical information we were able to propose novel prognostic markers in well-differentiated thyroid cancer.

Alterations in DNA methylation have been observed in early cancers and precursor lesions, suggesting that they play an important role in malignant initiation,[20,22,23] and our observations are largely consistent with this hypothesis. It has been proposed that follicular adenoma is a precursor lesion for follicular thyroid carcinoma, as evidenced by both the simultaneous presence of carcinomas in benign lesions and the similarity in the molecular alterations observed in FA and FTC.[24] The few differences in methylation between FA and normal thyroid tissue samples that were also observed in FTC could represent the initiating changes, providing an additional piece of evidence that FA may give rise to FTC, and new insights about the critical steps in follicular cell neoplastic transformation. We also observed a progressive gain of promoter CpG-island hypermethylation between benign- (83 probes) and malignant-stage tumors (460 probes), which confirms previous findings.[20,23]

Although in other cancer types distinct methylation patterns have been found to be associated with the presence of specific mutations,[25–29] to our knowledge, ours is the first study to assess this in thyroid cancer. We observed a robust separation of mutated samples, especially evident for fvPTC, where the mutation apparently was tightly associated with their methylation pattern and subsequent clustering. These findings are consistent with those from a recent genome-wide methylation study in two thyroid cancer cell lines showed they undergo hypermethylation in an important proportion of genes upon the knockdown of *BRAF*.[30] Given that TCGA project's methylation data validated the pattern according to the mutation, it seems reasonable to conclude that methylation pattern is specific to the particular mutation involved in thyroid cancer. However, the biological mechanism explaining this remains unknown, and further experiments are needed.

We found it particularly striking that PTCs had a higher proportion of hypomethylated probes. In cancer, hypomethylation is more prominent in large inter-genic satellite regions and has been related to genomic instability,[31,32] whereas PTC has been described as the thyroid cancer subtype with least structural rearrangements.[33] As the platform used in the study was biased towards gene promoters, it is likely that the observed hypomethylation events on unique sequences could cause increased expression of cancer-promoting genes, rather than genomic instability. An integrative study applying various OMICs approaches to a common series of PTC tumors is required to shed light on the relationship between hypomethylation and genomic instability.

The results for PTC tumors harboring the $BRAF^{V600E}$ mutation specifically caught our attention. The presence of $BRAF^{V600E}$ has been strongly associated with the "CpG island methylator phenotype" (CIMP) in colorectal cancer,[25,28] but it has been suggested that this mutation is not sufficient to induce CIMP in a colorectal cell line.[26] Rather, to promote its oncogenic effects, it requires additional cooperative events, often of an epigenetic nature,[26,34] which bypass the senescence and apoptosis that this mutation induces in cells.[27,35] Importantly, this tumor suppressor mechanism has been recently described in thyroid carcinogenesis[36] even though it remains to be established which events are associated with its impairment. Concomitant activation of v-akt murine thymoma viral oncogene homolog 3 (*AKT3*) was reported to overcome *BRAF*-induced senescence in melanoma cells.[37] Indeed, in our experimental setting, we observed strong *AKT3* promoter hypomethylation (FDR = 6.6×10^{-6}, ΔM-value = −2.26). However, we did not observe a correlation between *AKT3* methylation and expression, probably due to the fact that the corresponding CpG dinucleotide arrayed did not lie within a CpG island. Nevertheless, a tendency towards elevated expression of *AKT3* specifically in PTC has been reported by others.[38] In addition, the over-activation of the mTOR pathway, which is classically regulated through the phosphatidylinositol-3-kinase (PI3K)/AKT pathway, has been recently reported to be strongly associated with *BRAF* mutation-positive PTC.[39] Further studies are necessary to decipher the precise role of *AKT3* in the development of *BRAF*-related thyroid tumors.

In both case series considered, the hypermethylation of the promoter regions of *COL4A2* and *DLEC1* was confirmed in follicular cell-derived tumors, while the hypomethylation of *KLK10* was strongly associated with *BRAF* mutation-positive PTC. *KLK10* is a member of the kallikrein family of genes, which are secreted serine proteases that have been extensively studied in cancer due to their involvement in extracellular matrix degradation as well as their promising role as disease biomarkers.[40] Hypomethylation of *KLK10* has been recently associated with biochemical recurrence in prostate cancer.[41] Conversely, *COL4A2* encodes one of the six subunits of type IV collagen, the major structural component of basement membranes. The C-terminal portion of the protein, known as canstatin, is an inhibitor of angiogenesis and tumor growth.[42] Finally, *DLEC1* is a candidate tumor-suppressor gene, which is commonly deleted in various carcinomas; more importantly, it has been reported to be epigenetically repressed in many tumor types.[43,44]

To gain insights into the functional implications of epigenetic changes, we integrated the DNA methylation data with gene expression profiling data. The integration with an independent series of samples identified a relatively lower

proportion of correlated genes in FTC, and we observed no correlations for FA, which was probably due to the small number of samples included in the original study.[6] Nevertheless, in general, we observed similar proportions of genes showing correlation to those reported in previous studies.[18,25] The products of some of the correlated genes in PTC samples harboring the $BRAF^{V600E}$ mutation were clustered in the MAP kinase cascade, which further confirms the importance of impairment of this pathway in the development of this tumor subtype. In FTC samples, we observed an enrichment of genes involved in innate immunity response mechanisms, known for a long time to promote carcinogenesis.[45]

We found that elevated levels of methylation of at least two genes known to participate in carcinogenesis were associated with increased risk of recurrence of thyroid cancer. Interestingly, both genes, *EI24* and *WT1*, exhibited a significant association with poor prognosis even after adjustment for relevant clinical variables. Although preliminary, the associations of these novel markers with disease recurrence could potentially serve to better stratify patients. Specifically, *EI24* is a putative tumor-suppressor gene, the expression of which is impaired in several types of cancer by either aberrant methylation or deletion.[46] More importantly, this impairment has been found to be associated with tumor invasiveness[46] and poor response to treatment.[47] *WT1* encodes a transcription factor, mutated in a small subset of patients with Wilm's tumors, and whose expression has been suggested to be indicative of minimal residual disease in leukemias.[48,49] Furthermore, its methylation status has been recently proposed to be correlated with time to recurrence in prostate cancer.[50]

To summarize, the assessment of genome-wide DNA methylation profiles in the largest series of well-differentiated thyroid tumors described so far allowed us to identify and replicate distinct epigenetic signatures that reflect the underlying tumor histology as well as the mutation status. Specific aberrant methylation associated with the early development of this disease was found, and DNA methylation events associated with changes in gene expression were identified. We proposed novel prognostic markers, which according to our data are independent of the already established ones.

Acknowledgments

The authors would like to thank Mario Fraga and Agustin Fernández for their invaluable suggestions about methylation data analyses. The authors used data generated by The Cancer Genome Atlas managed by the NCI and NHGRI; information about TCGA can be found at http://cancergenome.nih.gov.

References

1. Kondo T, Ezzat S, Asa SL. Pathogenetic mechanisms in thyroid follicular-cell neoplasia. *Nat Rev Cancer* 2006;6:292–306.
2. Nikiforov YE, Nikiforova MN. Molecular genetics and diagnosis of thyroid cancer. *Nat Rev Endocrinol* 2011;7:569–80.
3. Lupi C, Giannini R, Ugolini C, et al. Association of BRAF V600E mutation with poor clinicopathological outcomes in 500 consecutive cases of papillary thyroid carcinoma. *J Clin Endocrinol Metab* 2007;92:4085–90.
4. Xing M, Westra WH, Tufano RP, et al. BRAF mutation predicts a poorer clinical prognosis for papillary thyroid cancer. *J Clin Endocrinol Metab* 2005;90:6373–9.
5. Montero-Conde C, Martin-Campos JM, Lerma E, et al. Molecular profiling related to poor prognosis in thyroid carcinoma. Combining gene expression data and biological information. *Oncogene* 2008;27:1554–61.
6. Giordano TJ, Kuick R, Thomas DG, et al. Molecular classification of papillary thyroid carcinoma: distinct BRAF, RAS, and RET/PTC mutation-specific gene expression profiles discovered by DNA microarray analysis. *Oncogene* 2005;24:6646–56.
7. Maliszewska A, Leandro-Garcia LJ, Castelblanco E, et al. Differential gene expression of medullary thyroid carcinoma reveals specific markers associated with genetic conditions. *Am J Pathol* 2013;182:350–62.
8. Rodriguez-Rodero S, Fernandez AF, Fernandez-Morera JL, et al. DNA methylation signatures identify biologically distinct thyroid cancer subtypes. *J Clin Endocrinol Metab* 2013;98:2811–21.
9. Xing M, Usadel H, Cohen Y, et al. Methylation of the thyroid-stimulating hormone receptor gene in epithelial thyroid tumors: a marker of malignancy and a cause of gene silencing. *Cancer Res* 2003;63:2316–21.
10. Venkataraman GM, Yatin M, Marcinek R, et al. Restoration of iodide uptake in dedifferentiated thyroid carcinoma: relationship to human Na+/I-symporter gene methylation status. *J Clin Endocrinol Metab* 1999;84:2449–57.
11. Hu S, Liu D, Tufano RP, et al. Association of aberrant methylation of tumor suppressor genes with tumor aggressiveness and BRAF mutation in papillary thyroid cancer. *Int J Cancer* 2006;119:2322–9.
12. Brait M, Loyo M, Rosenbaum E, et al. Correlation between BRAF mutation and promoter methylation of TIMP3, RARbeta2 and RASSF1A in thyroid cancer. *Epigenetics* 2012;7:710–9.
13. Schagdarsurengin U, Gimm O, Hoang-Vu C, et al. Frequent epigenetic silencing of the CpG island promoter of RASSF1A in thyroid carcinoma. *Cancer Res* 2002;62:3698–701.
14. Bibikova M, Le J, Barnes B, et al. Genome-wide DNA methylation profiling using Infinium(R) assay. *Epigenomics* 2009;1:177–200.
15. Mancuso FM, Montfort M, Carreras A, et al. HumMeth27QCReport: an R package for quality control and primary analysis of Illumina Infinium methylation data. *BMC Res Notes* 2011;4:546.
16. Du P, Zhang X, Huang CC, et al. Comparison of Beta-value and M-value methods for quantifying methylation levels by microarray analysis. *BMC Bioinformatics* 2010;11:587.
17. Morrissey ER, Diaz-Uriarte R. Pomelo II: finding differentially expressed genes. *Nucleic Acids Res* 2009;37:W581–6.
18. Selamat SA, Chung BS, Girard L, et al. Genome-scale analysis of DNA methylation in lung adenocarcinoma and integration with mRNA expression. *Genome Res* 2012;22:1197–211.
19. Huang da W, Sherman BT, Lempicki RA. Systematic and integrative analysis of large gene lists using DAVID bioinformatics resources. *Nat Protoc* 2009;4:44–57.
20. Zhuang J, Jones A, Lee SH, et al. The dynamics and prognostic potential of DNA methylation changes at stem cell gene loci in women's cancer. *PLoS Genet* 2012;8:e1002517.
21. Varley KE, Gertz J, Bowling KM, et al. Dynamic DNA methylation across diverse human cell lines and tissues. *Genome Res* 2013;23:555–67.
22. Belinsky SA, Nikula KJ, Palmisano WA, et al. Aberrant methylation of p16(INK4a) is an early event in lung cancer and a potential biomarker for early diagnosis. *Proc Natl Acad Sci USA* 1998;95:11891–6.
23. Fernandez AF, Assenov Y, Martin-Subero JI, et al. A DNA methylation fingerprint of 1628 human samples. *Genome Res* 2012;22:407–19.
24. Arora N, Scognamiglio T, Zhu B, et al. Do benign thyroid nodules have malignant potential? An evidence-based review. *World J Surg* 2008;32:10.
25. Hinoue T, Weisenberger DJ, Lange CP, et al. Genome-scale analysis of aberrant DNA methylation in colorectal cancer. *Genome Res* 2012;22:271–82.
26. Hinoue T, Weisenberger DJ, Pan F, et al. Analysis of the association between CIMP and BRAF in colorectal cancer by DNA methylation profiling. *PLoS One* 2009;4:e8357.
27. Michaloglou C, Vredeveld LC, Soengas MS, et al. BRAFE600-associated senescence-like cell cycle arrest of human naevi. *Nature* 2005;436:720–4.
28. Weisenberger DJ, Siegmund KD, Campan M, et al. CpG island methylator phenotype underlies

sporadic microsatellite instability and is tightly associated with BRAF mutation in colorectal cancer. *Nat Genet* 2006;38:787–93.
29. Shen L, Toyota M, Kondo Y, et al. Integrated genetic and epigenetic analysis identifies three different subclasses of colon cancer. *Proc Natl Acad Sci USA* 2007;104:18654–9.
30. Hou P, Liu D, Xing M. Genome-wide alterations in gene methylation by the BRAF V600E mutation in papillary thyroid cancer cells. *Endocr Relat Cancer* 2011;18:687–97.
31. Li J, Harris RA, Cheung SW, et al. Genomic hypomethylation in the human germline associates with selective structural mutability in the human genome. *PLoS Genet* 2012;8:e1002692.
32. Rodriguez J, Frigola J, Vendrell E, et al. Chromosomal instability correlates with genome-wide DNA demethylation in human primary colorectal cancers. *Cancer Res* 2006;66:8462–9468.
33. Ward LS, Brenta G, Medvedovic M, et al. Studies of allelic loss in thyroid tumors reveal major differences in chromosomal instability between papillary and follicular carcinomas. *J Clin Endocrinol Metab* 1998;83:525–30.
34. Suzuki H, Igarashi S, Nojima M, et al. IGFBP7 is a p53-responsive gene specifically silenced in colorectal cancer with CpG island methylator phenotype. *Carcinogenesis* 2010;31:342–9.
35. Zhu J, Woods D, McMahon M, et al. Senescence of human fibroblasts induced by oncogenic Raf. *Genes Dev* 1998;12:2997–3007.
36. Vizioli MG, Possik PA, Tarantino E, et al. Evidence of oncogene-induced senescence in thyroid carcinogenesis. *Endocr Relat Cancer* 2011;18:743–57.
37. Cheung M, Sharma A, Madhunapantula SV, et al. Akt3 and mutant V600E B-Raf cooperate to promote early melanoma development. *Cancer Res* 2008;68:3429–39.
38. Ringel MD, Hayre N, Saito J, et al. Overexpression and overactivation of Akt in thyroid carcinoma. *Cancer Res* 2001;61:6105–11.
39. Faustino A, Couto JP, Populo H, et al. mTOR pathway overactivation in BRAF mutated papillary thyroid carcinoma. *J Clin Endocrinol Metab* 2012;97:E1139–49.
40. Borgono CA, Diamandis EP. The emerging roles of human tissue kallikreins in cancer. *Nat Rev Cancer* 2004;4:876–90.
41. Olkhov-Mitsel E, Van der Kwast T, Kron KJ, et al. Quantitative DNA methylation analysis of genes coding for kallikrein-related peptidases 6 and 10 as biomarkers for prostate cancer. *Epigenetics* 2012;7:1037–45.
42. Roth JM, Akalu A, Zelmanovich A, et al. Recombinant alpha2(IV)NC1 domain inhibits tumor cell-extracellular matrix interactions, induces cellular senescence, and inhibits tumor growth in vivo. *Am J Pathol* 2005;166:901–11.
43. Seng TJ, Currey N, Cooper WA, et al. DLEC1 and MLH1 promoter methylation are associated with poor prognosis in non-small cell lung carcinoma. *Br J Cancer* 2008;99:375–82.
44. Wang Z, Li L, Su X, et al. Epigenetic silencing of the 3p22 tumor suppressor DLEC1 by promoter CpG methylation in non-Hodgkin and Hodgkin lymphomas. *J Transl Med* 2012;10:209.
45. Dunn GP, Bruce AT, Ikeda H, et al. Cancer immunoediting: from immunosurveillance to tumor escape. *Nat Immunol* 2002;3:991–8.
46. Mazumder Indra D, Mitra S, Singh RK, et al. Inactivation of CHEK1 and EI24 is associated with the development of invasive cervical carcinoma: clinical and prognostic implications. *Int J Cancer* 2011;129:1859–71.
47. Mork CN, Faller DV, Spanjaard RA. Loss of putative tumor suppressor EI24/PIG8 confers resistance to etoposide. *FEBS Lett* 2007;581:5440–4.
48. Trka J, Kalinova M, Hrusak O, et al. Real-time quantitative PCR detection of WT1 gene expression in children with AML: prognostic significance, correlation with disease status and residual disease detection by flow cytometry. *Leukemia* 2002;16:1381–9.
49. Weisser M, Kern W, Rauhut S, et al. Prognostic impact of RT-PCR-based quantification of WT1 gene expression during MRD monitoring of acute myeloid leukemia. *Leukemia* 2005;19:1416–23.
50. Kobayashi Y, Absher DM, Gulzar ZG, et al. DNA methylation profiling reveals novel biomarkers and important roles for DNA methyltransferases in prostate cancer. *Genome Res* 2011;21:1017–27.

3.2. Material suplementario del trabajo II

Supplementary figures

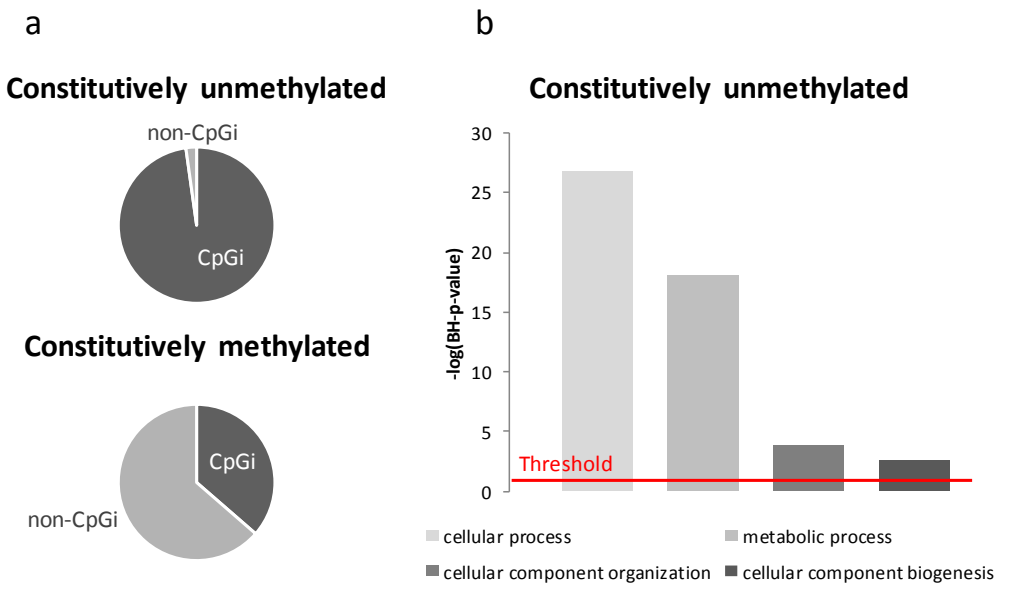

Supplementary Figure S1 | Distribution of constitutively unmethylated and methylated probes. (a) by location with respect to CpG islands; **(b)** in terms of enrichment, by biological process categories from DAVID functional analysis (constitutively unmethylated probes only).

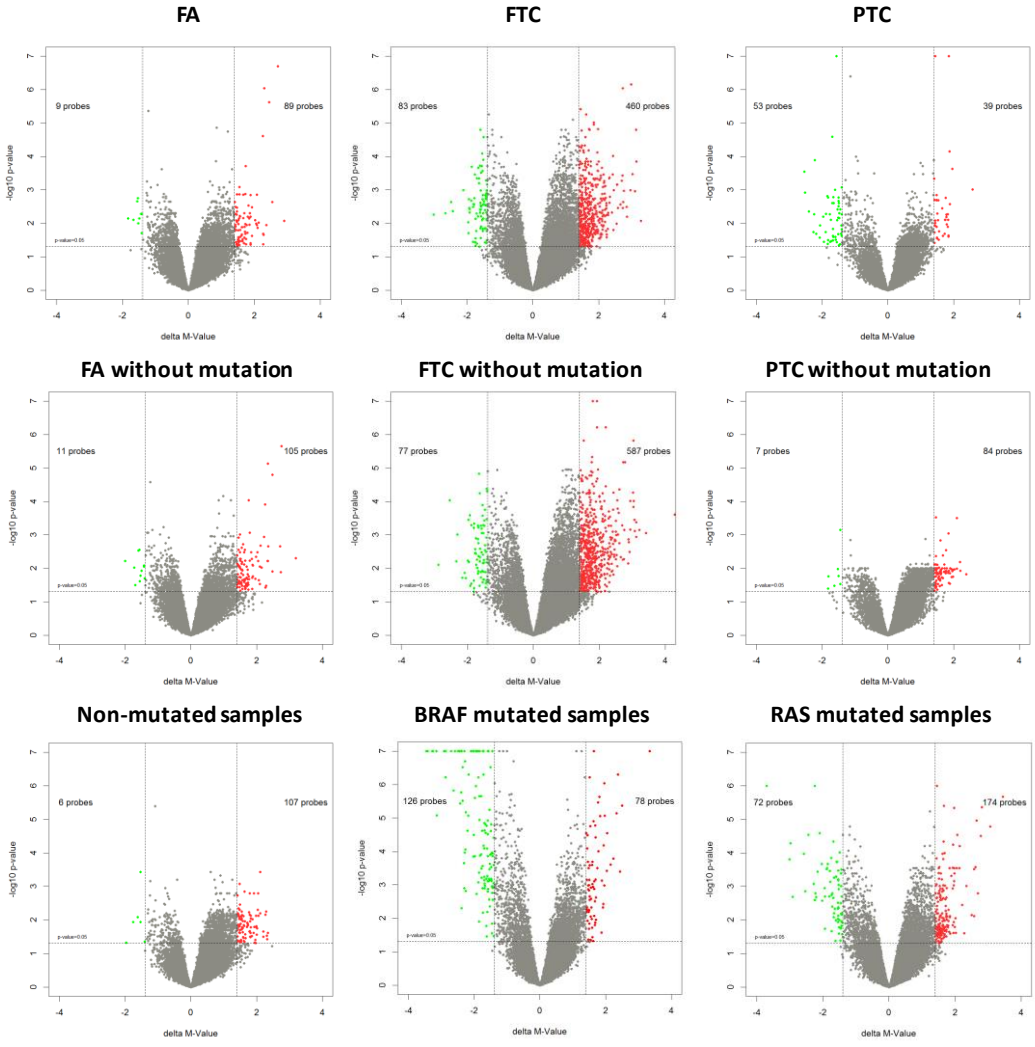

Supplementary Figure S2 | Identification of differentially methylated probes. Volcano plots, from each of the supervised analysis carried out, identifying differentially hypomethylated (green) and hypermethylated (red) probes, defined based on FDR<0.05 and ΔM-value ≥ |1.4|).

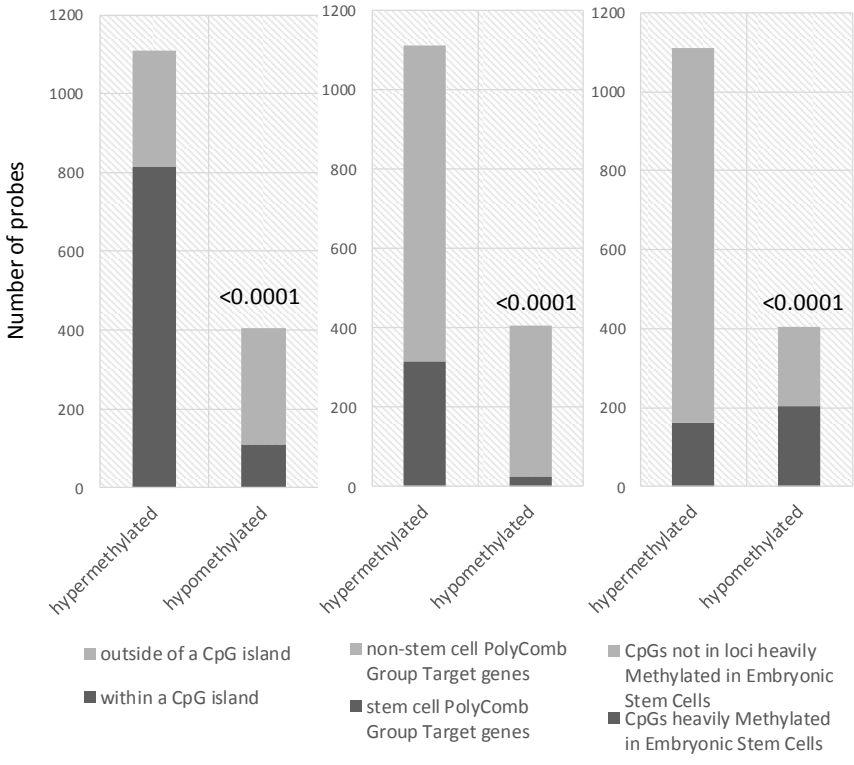

Supplementary Figure S3 | Number of probes hypermethylated and hypomethylated, by location with respect to: CpG islands; type of associated gene targeted by Polycomb Repressive Complex; loci that are heavily methylated in Embryonic Stem Cells.

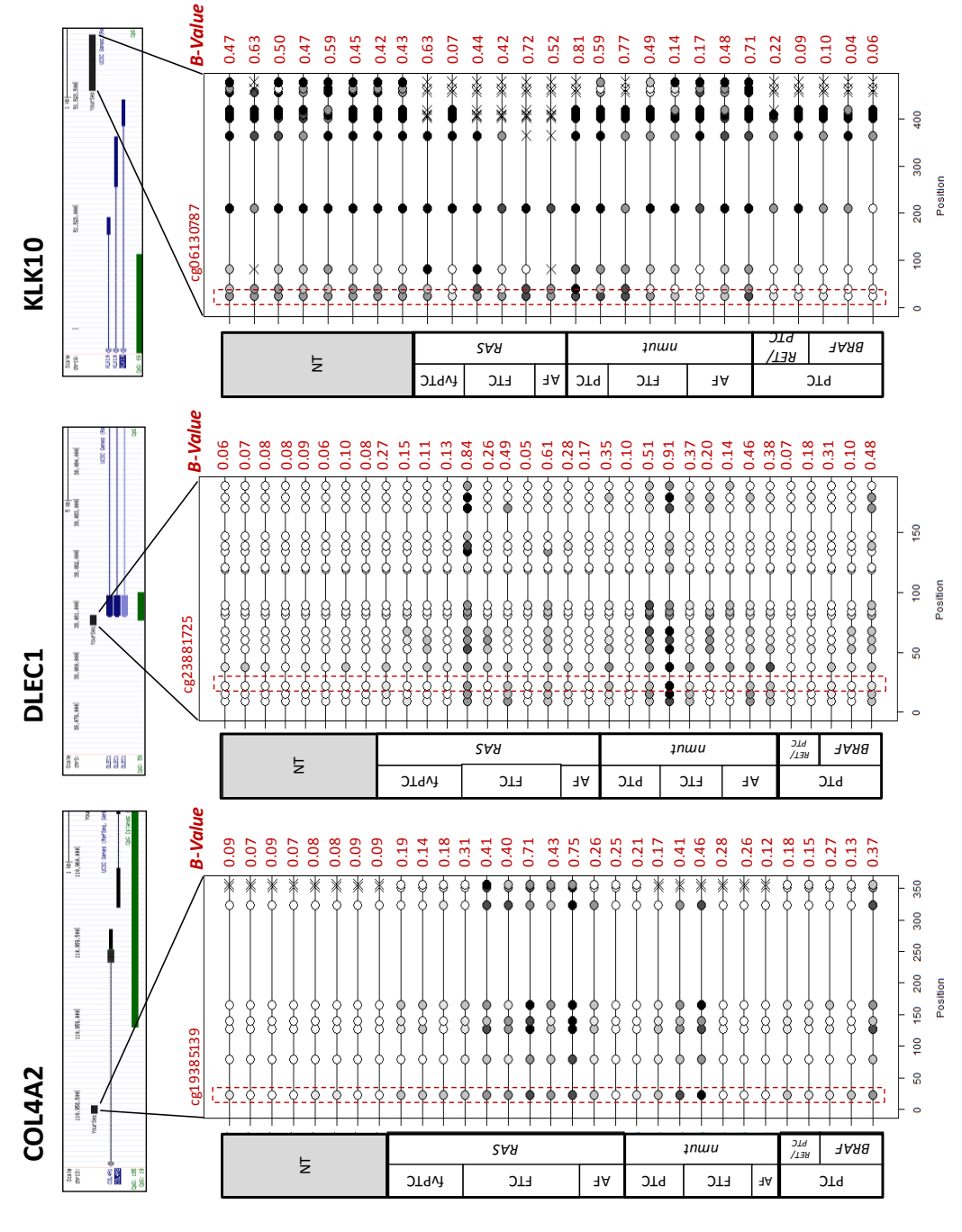
a
COL4A2
DLEC1
KLK10
b
cg19385139
cg23881725
cg06130787
B-Value
0.09 0.07 0.09 0.07 0.08 0.08 0.08 0.09 0.09 0.19 0.14 0.18 0.31 0.41 0.40 0.71 0.43 0.75 0.26 0.25 0.21 0.17 0.41 0.46 0.28 0.26 0.12 0.18 0.15 0.27 0.13 0.37
0.06 0.07 0.08 0.08 0.09 0.06 0.10 0.08 0.27 0.15 0.11 0.13 0.84 0.26 0.49 0.05 0.61 0.28 0.17 0.35 0.10 0.51 0.91 0.37 0.20 0.14 0.46 0.38 0.07 0.18 0.31 0.10 0.48
0.47 0.63 0.50 0.47 0.59 0.45 0.42 0.43 0.63 0.07 0.44 0.42 0.72 0.52 0.81 0.59 0.77 0.49 0.14 0.17 0.48 0.71 0.22 0.09 0.10 0.04 0.06
NT
RAS
mut
BRAF
RET/ PTC
PTC
FTC
AF
fvPTC
pTC
Position
Percentage of methylation
0-4%
5-24%
25-49%
50-74%
75-94%
95-100%

C

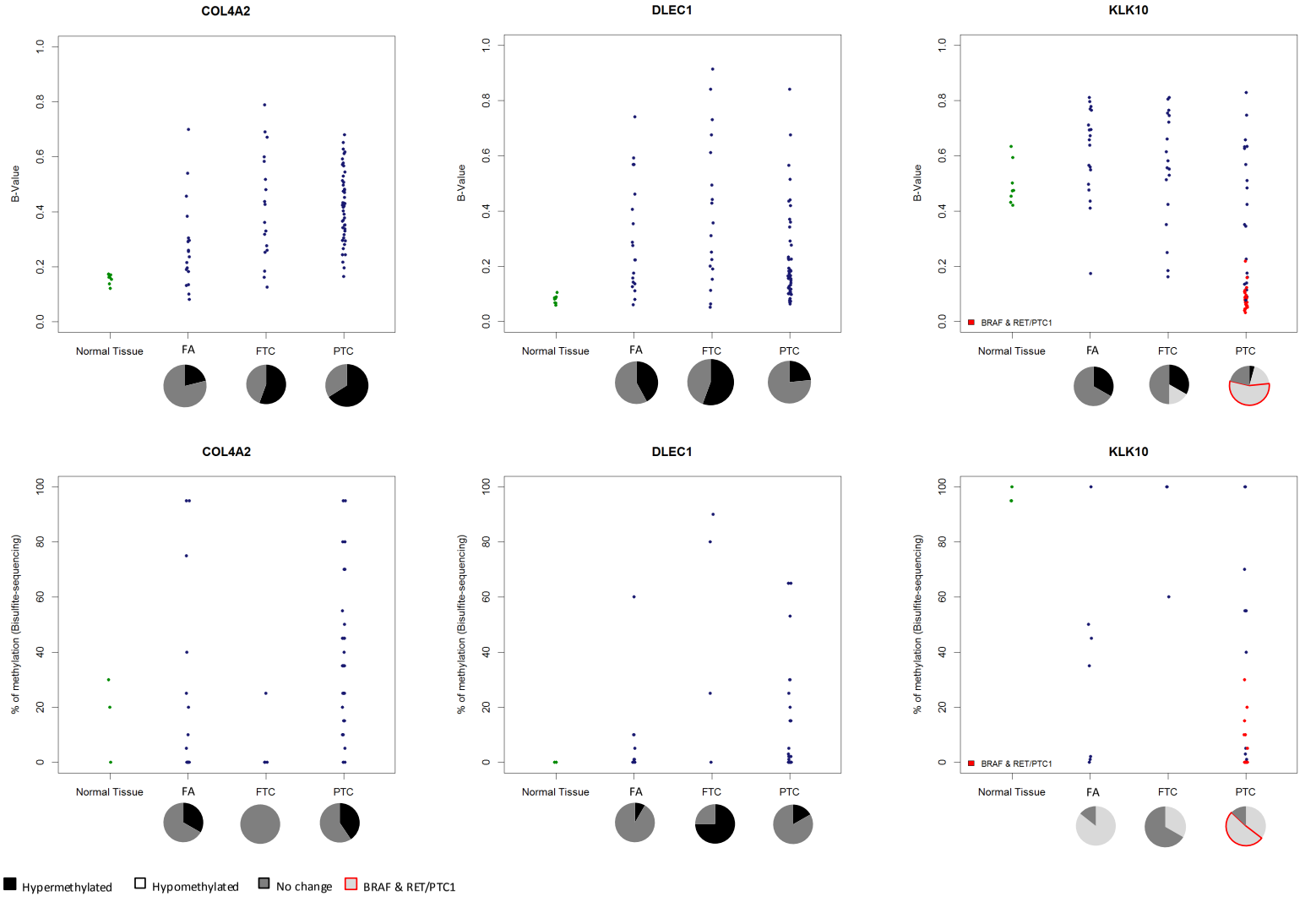
COL4A2
DLEC1
KLK10
B-Value
% of methylation (Bisulfite-sequencing)
Normal Tissue
FA
FTC
PTC
BRAF & RET/PTC1
Hypermethylated
Hypomethylated
No change
BRAF & RET/PTC1

Supplementary Figure S4 | Validation of selected loci. (a) Diagram of the promoter region of the analyzed loci**. (b)** Lollipops displaying the methylation pattern of each locus validated by bisulfite sequencing in different samples. CpGs are represented by circles. The CpG interrogated by the probe of the Illumina Infinium HumanMethylation 27K Platform is marked with a red dotted square and the corresponding beta-value is indicated in red. NT: normal tissue; AF: follicular adenoma; FTC: follicular thyroid carcinoma; PTC: papillary thyroid carcinoma; fvPTC: papillary thyroid carcinoma follicular variant. **(c)** Validation of the identified aberrant methylation events in an independent series. Methylation levels assessed by Beta-values from the methylation array for 47 PTC, 18 FA, 18 FTC and 8 adjacent normal tissue samples are visualized in the upper panel. Methylation levels assessed by bisulfite sequencing in an independent series of 33 PTC, 12 FA, 4 FTC and 3 adjacent normal tissue samples are shown in the lower panel. Pie charts refer to proportion of samples showing aberrant methylation at the selected loci in discovery and replication series.

Supplementary tables

Supplementary tables are at the online version of this paper (Int J Cancer. 2014 Aug 1;135(3):598-610. doi: 10.1002/ijc.28703) or at the digital edition of this thesis

4. Anexo 4

4.1. Material suplementario del trabajo III

Supplementary methods

RNA isolation, reverse transcription and quantitative Polymerase Chain Reaction (RT-qPCR).

Total RNA (kindly provided by Dra. M. Robledo from CNIO, Madrid, Spain) from 7 normal tissues, 3 RAS, 10 *BRAF* and 1 non-mutated thyroid tumor, and 500 ng of each RNA were reverse transcribed (SuperScriptTM III Reverse Transcriptase, Invitrogen) in a final volume of 20 uL following the manufacturer's instructions.

One microliter of 1:2 or 1:10 diluted cDNA was used to analyze the expression of *KLK4*, *KLK6*, *KLK7*, *KLK10* and the reference genes cyclophilin A (*PPIA*) and Pumilio RNA Binding Family Member 1 (*PUM1*) in a LightCycler® 480 Real-Time PCR System with white Multiwell Plate 384 plates (Roche). qPCR was carried out in triplicates in a final volume of 10 uL as follows: 5 uL of LightCycler® 480 SYBR Green I Master (Roche), 1 uM of forward primer and 1 uM of reverse primer (Supplemental Table S1). The thermal cycling conditions were composed of an initial denaturation step of 10 min at 95ºC followed by 40 cycles of 10 seconds at 95ºC, 20 seconds at the corresponding annealing temperature (Supplemental Table S1) and 20 seondsc at 72ºC. The assay ended with a melting-curve program: 15 seconds at 95ºC, 1 min at 70ºC and then ramping to 95ºC while continuously monitoring fluorescence.

The relative quantification to reference genes was calculated with CHAINY tool (http://maplab.cat/chainy/) following the amplification curve kinetics method (cqD2 method) to calculate the qPCR efficiency.

Differential gene expression and clustering analysis

The Log_2(RPKM+1) of the 15 KLK genes was used to perform a gene supervised hierarchical clustering of thyroid cancer from TCGA series. The fold change between tumors and normal tissues, calculated as the difference between Log_2(RPKM+1) mean of tumors and normal tissues) for each KLK gene in 12 different cancer types (THCA, BLCA, BRCA, COAD, HNSC, KIRC, KIRP, KICH, LIHC, LUA, LUSC and PRAD) was used to obtain a gene-supervised hierarchical clustering. Manhattan distance and ward.D2 method

of clustering were used in all analysis. Heatmaps were done with the function heatmap.2 from the gplots R package [v3.0-1, (Warnes et al., 2015)]. Differential gene expression analysis among BRU tumors and BRAF-like, RAS-like and normal tissues groups were carried out using the R Bioconductor package DESeq v1.5 (Anders and Huber, 2010).

Supplementary tables

Supplementary tables are at the digital edition of this thesis.

Supplementary figures

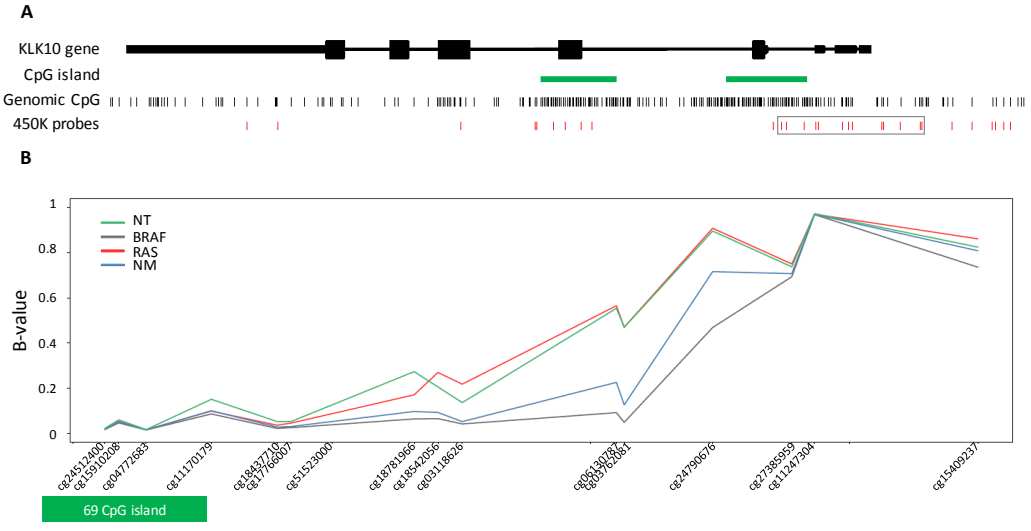

Supplemental Figure S1: DNA methylation within *KLK10* promoter-associated CpGi shore. (A) Diagram of *KLK10* gene region; black bars represent the CpG sites within the region and red bars represent the CpG sites covered by the Infinium HumanMethylation450 array. **(B)** B-values of the CpGs covering part of the *KLK10*-associated 69 CpG island and the corresponding downstream CpG island shore [~3Kb; indicated as a gray box in (A)] for each tumor group from TCGA series. NT: normal tissues, *BRAF*: BRAF mutated tumors, RAS: *HRAS*-, *KRAS*- or *NRAS*-mutated tumors; NM: non-mutated tumors.

A

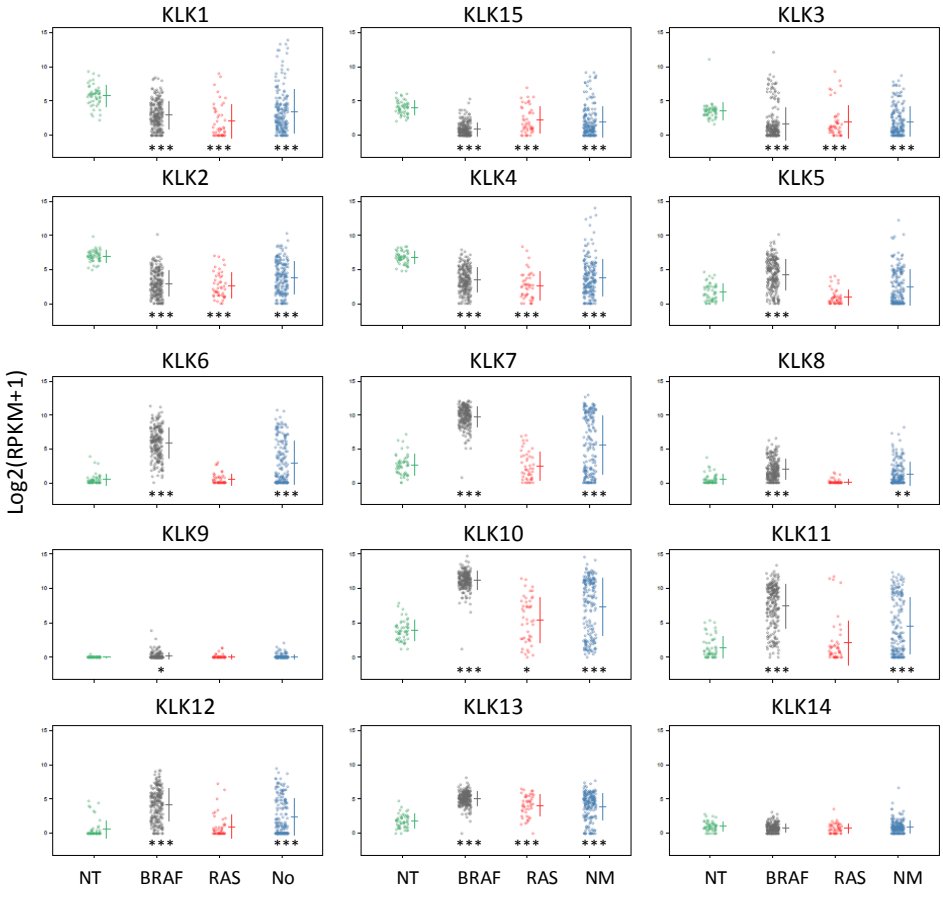
KLK1
KLK15
KLK3
KLK2
KLK4
KLK5
KLK6
KLK7
KLK8
KLK9
KLK10
KLK11
KLK12
KLK13
KLK14
Log2(RPKM+1)
NT
BRAF
RAS
No
NM

B

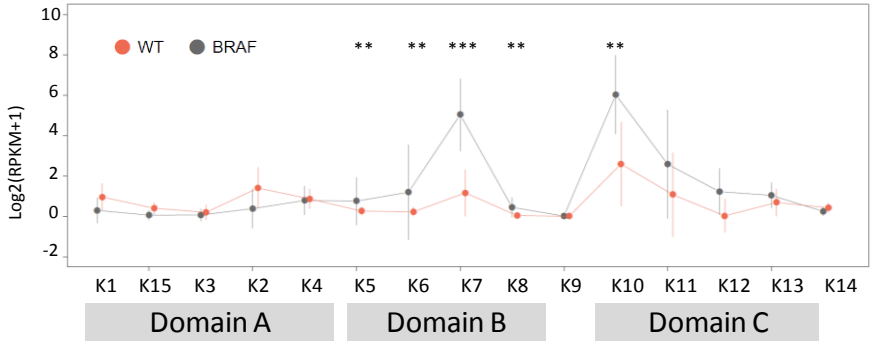
WT
BRAF
Log2(RPKM+1)
K1
K15
K3
K2
K4
K5
K6
K7
K8
K9
K10
K11
K12
K13
K14
Domain A
Domain B
Domain C

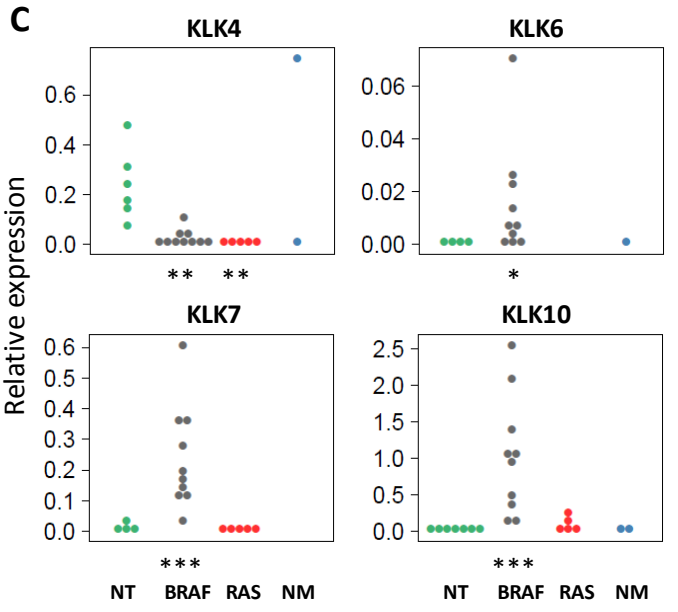

Supplemental Figure S2: Expression of *KLK* genes in PTC according to the mutational state of *BRAF* and *RAS*. (A) Expression level based on RNA-Seq data for each *KLK* gene in TCGA series. Expression level mean, standard deviation and the statistically significance of the comparison between normal tissue and each tumoral group are plotted. **(B)** *KLK* expression profile based on RNA-Seq data of *BRAF* mutated and *BRAF* wild type ($BRAF^{WT}$)PTCs from Smallridge series. The statistically significance of the differential expression between both groups for each *KLK* is plotted. The cluster can be divided in three expression domains (A to C). **(C)** Relative expression of *KLK4*, *KLK6*, *KLK7* and *KLK10* analyzed by RT-qPCR and normalized by Cyclophilin A (*PPIA*) and Pumilio RNA Binding Family Member 1 (*PUM1*) of a subset of samples from Mancikova series. NT: normal tissues, *BRAF*: BRAF mutated tumors, RAS: Ras-mutated tumors; NM: non-mutated tumors.

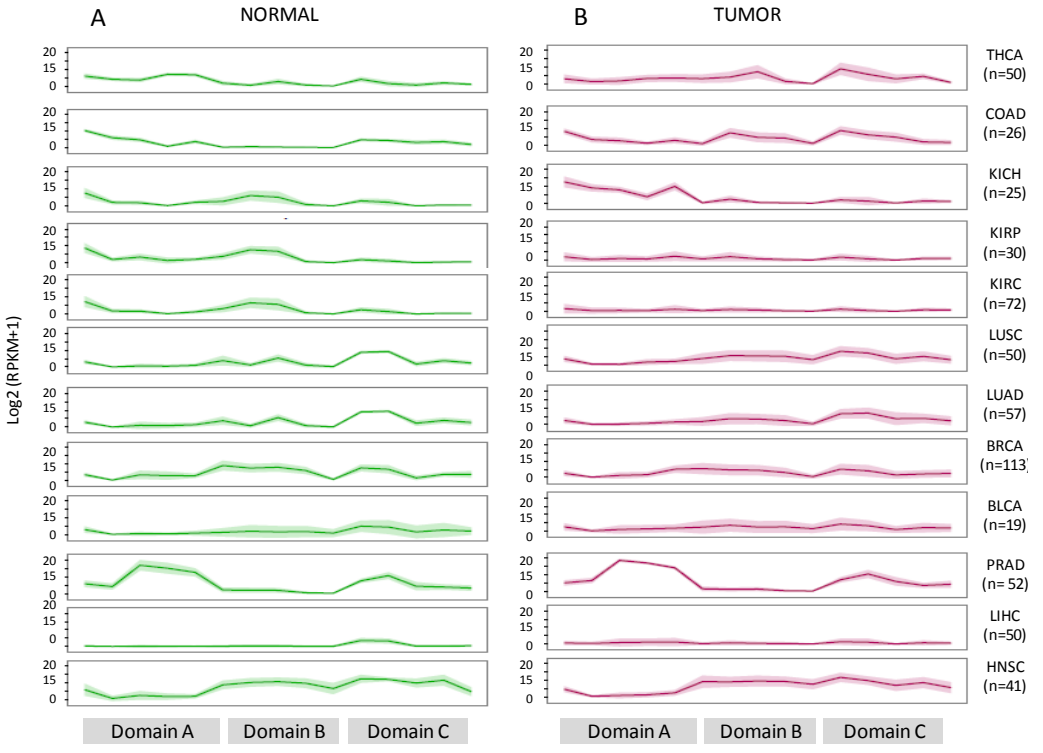

Supplemental Figure S3: *KLK* expression profiles in different cancer types. KLK expression profile based on RNA-Seq data of different cancer types analyzed by TCGA**.** The average of the expression of normal tissues (green) and their paired tumors (red) and the corresponding dispersion (shadowed areas) are represented. In all cases the cluster can be divided in three domains (A to C).

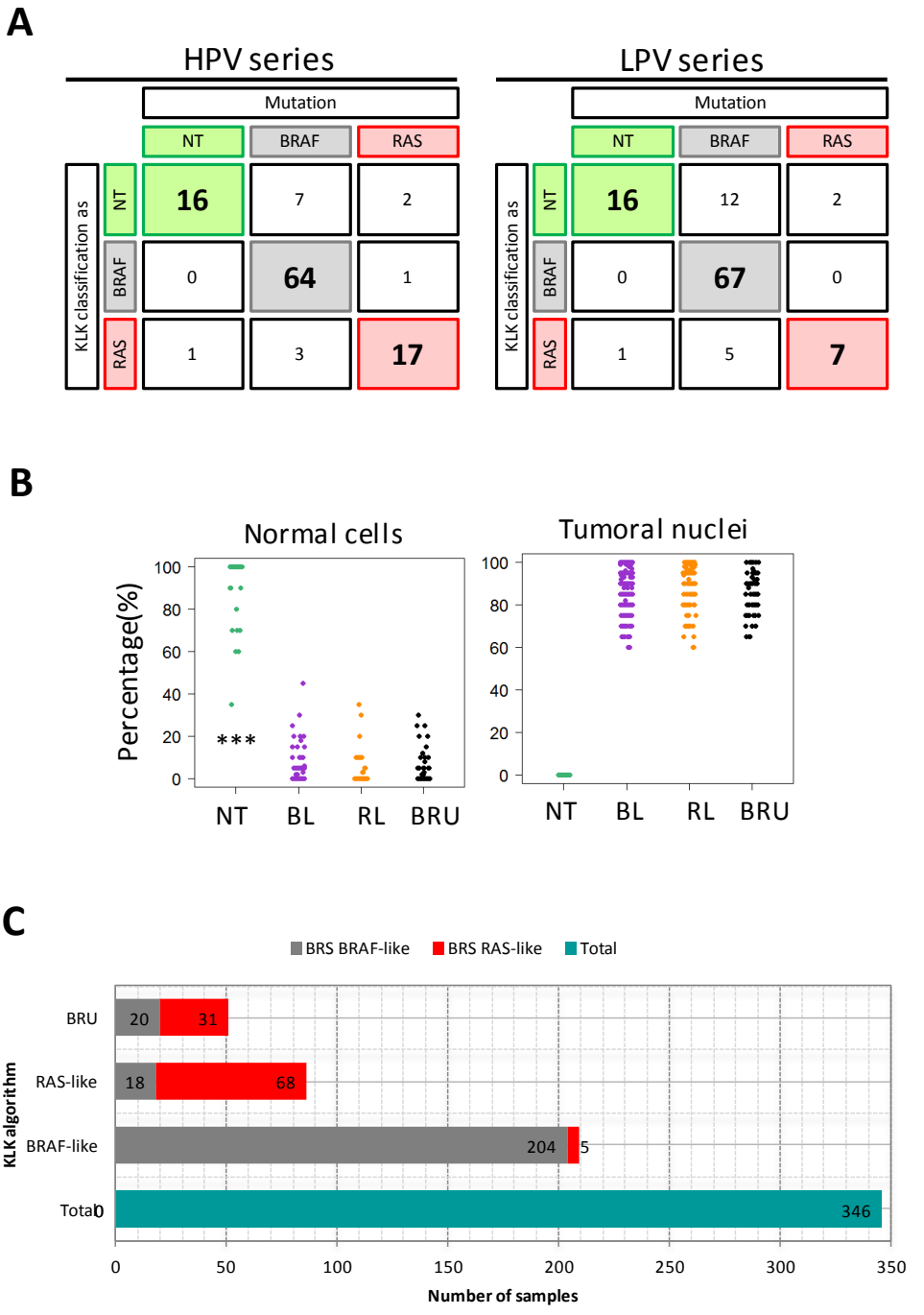

Supplemental Figure S4: KLK Algorithm validation. (A) Confusion matrices for high pure (HP) and low pure (LP) validation series according to KLK algorithm. **(B)** Percentage of normal cells and tumoral nucleis in each considered group: normal tissue (NT), BRAF-like (BL) and RAS-like (RL) tumors. The statistical significance of the differences between BRU and the rest of sample groups is plotted. **(C)** Overlapping between KLK Algorithm and BRS classification from TCGA series (n = 346).

Supplementary tables

Supplementary tables are at the digital form of this thesis

Supplementary references

Anders, S., Huber, W., 2010. Differential expression analysis for sequence count data. Genome Biol. 11, R106. doi:10.1186/gb-2010-11-10-r106

Ritchie, M.E., Phipson, B., Wu, D., Hu, Y., Law, C.W., Shi, W., Smyth, G.K., 2015. Limma powers differential expression analyses for RNA-sequencing and microarray studies. Nucleic Acids Res. 43, e47. doi:10.1093/nar/gkv007

Warnes, G.R., Bolker, B., Bonebakker, L., Gentleman, R., Liaw, W.H.A., Lumley, T., Maechler, M., Magnusson, A., Moeller, S., Schwartz, M., Venables, B., 2015. gplots: Various R Programming Tools for Plotting Data. R Packag. version 2.17.0. 2015. doi:10.1111/j.0022-3646.1997.00569.x